

WMO  
305  
1993

C. 2

**WORLD METEOROLOGICAL ORGANIZATION**

**GUIDE  
ON THE  
GLOBAL DATA-PROCESSING SYSTEM**



**WMO-No. 305**

**Secretariat of the World Meteorological Organization - Geneva - Switzerland  
1993**

**© 1993, World Meteorological Organization**

**ISBN 92-63-13305-0**

**NOTE**

The designations employed and the presentation of material in this publication do not imply the expression of any opinion whatsoever on the part of the Secretariat of the World Meteorological Organization concerning the legal status of any country, territory, city or area, or of its authorities, or concerning the delimitation of its frontiers or boundaries.

TABLE FOR NOTING SUPPLEMENTS RECEIVED

Supplement No.	Dated	Inserted in the publication	
		by	date
✓ 1	Oct. 1999	Zeneba	20-11-03
✓ 2	Sept. 2000	„	„
✓ 3	June 2001	„	„
✓ 4	Aug. 2001		
5			
6			
7			
8			
9			
10			
11			
12			
13			
14			
15			
16			
17			
18			
19			
20			
21			
22			
23			
24			
25			

# WORLD METEOROLOGICAL ORGANIZATION

## GUIDE ON THE GLOBAL DATA-PROCESSING SYSTEM

WMO-No. 305

---

---

Supplement No. 4

August 2001

This supplement contains amendments to Chapter 3, paragraph 3.1.2 and related new Annex 3.A, as approved by CBS-XII.

**Contents:** Replace pages v to vi by new pages v to vi.

**Chapter 3:** Replace pages III.1 and III.2 by new pages III.1 and III.2;  
Add new pages III.31 and III.32.

---

WORLD METEOROLOGICAL ORGANIZATION

# GUIDE ON THE GLOBAL DATA-PROCESSING SYSTEM

WMO-No. 305

---

Supplement No. 3

June 2001

This supplement contains amendments to Chapter 6: Quality control procedures, as approved by CBS-XII.

**Contents:** Replace pages ix to x by new pages ix to x.

**Chapter 6:** Replace pages VI.21 to VI.26 by new pages VI.21 to VI.27.

---

WORLD METEOROLOGICAL ORGANIZATION

# GUIDE ON THE GLOBAL DATA-PROCESSING SYSTEM

WMO-No. 305

---

Supplement No. 2

September 2000

This supplement contains amendments to Chapter 6: Quality control procedures, Table 6.2 and paragraph 6.3.2.1.

**Contents:** Replace pages ix to x by new pages ix to x.

**Chapter 6:** Replace pages VI.5 to VI.23 by new pages VI.5 to VI.26.

---

WORLD METEOROLOGICAL ORGANIZATION

GUIDE ON THE GLOBAL  
DATA-PROCESSING SYSTEM

WMO-No. 305

---

Supplement No. 1

October 1999

This supplement contains amendments to Chapter 6: Quality control procedures, Table 6.2 and paragraph 6.3.2.1.

**Contents:** Replace pages ix and x by new pages ix and x.

**Chapter 6:** Replace pages VI.5 and VI.6 by new pages VI.5 and VI.6;  
Replace pages VI.9–VI.21 by new pages VI.9–VI.23.

---

# CONTENTS

	<i>Page</i>
	xi
Preface .....	xi
Glossary .....	xiii
Chapter 1 PURPOSE AND SCOPE OF THE GLOBAL DATA-PROCESSING SYSTEM (GDPS) .....	I.1
Chapter 2 MAJOR REAL-TIME FUNCTIONS OF WMCs AND RSMCs, INCLUDING THE ROLE OF NMCs.....	II.1
2.1 World Meteorological Centres (WMCs) .....	II.1
2.2 Regional Specialized Meteorological Centres (RSMCs) .....	II.1
2.3 National Meteorological Centres (NMCs).....	II.1
2.3.1 Role of NMCs.....	II.1
2.3.2 Data acquisition at NMCs.....	II.2
2.3.3 Data processing at NMCs.....	II.2
2.3.4 Data-processing systems and telecommunication at NMCs .....	II.2
Chapter 3 METHODS USED IN THE AUTOMATED PROCESSING OF DATA FOR ANALYSIS AND PREDICTION.....	III.1
3.1 General .....	III.1
3.1.1 Criteria for observational data requirements.....	III.1
3.1.2 Data sources.....	III.1
3.1.3 Numerical weather analysis and prognosis as distinct from analysis and prognosis by conventional means .....	III.2
3.1.4 Rationale for automation .....	III.2
3.1.5 The computer and humans .....	III.2
3.1.6 Major functions of an automated weather analysis and prognosis system .....	III.2
3.1.7 Equipment needed to perform major functions at an automated weather analysis and prognosis centre .....	III.3
3.2 Organization and procedures for data collection .....	III.3
3.2.1 Purposes of a data-collection system .....	III.3
3.2.2 Basic types of data-collection systems .....	III.4
3.2.3 Scope and operation of a data-collection system .....	III.4
3.3 Automated data recognition, decoding and correction procedures (data pre-processing) .....	III.4
3.3.1 Recognition of meteorological messages .....	III.4
3.3.2 Decoding of meteorological bulletins.....	III.4
3.3.3 Quality control of the decoded message data and further checking procedures.....	III.5
3.3.4 The sorting and formatting of decoded information .....	III.5
3.4 Methods of numerical weather analyses.....	III.5
3.4.1 Purpose .....	III.5
3.4.2 General structure of a numerical weather analysis scheme.....	III.5
3.4.3 The optimum interpolation technique.....	III.6
3.4.3.1 Three-dimensional variational analysis .....	III.8
3.4.4 Spectral statistical interpolation .....	III.8
3.4.5 Methods of analysis based on successive corrections .....	III.9
3.4.6 Methods of analysis based on functional representation .....	III.9
3.4.7 Handling of asynoptic data (four-dimensional data-assimilation techniques).....	III.10
3.4.8 Initialization .....	III.11
3.4.8.1 Static initialization .....	III.11
3.4.8.2 Normal mode initialization .....	III.11
3.4.8.3 Dynamic initialization.....	III.12
3.4.8.4 Diabatic initialization.....	III.12
3.4.8.5 Combined initialization techniques .....	III.13

	<i>Page</i>
3.5 Numerical weather prediction (NWP) methods .....	III.13
3.5.1 General characteristics of current NWP models .....	III.13
3.5.2 Numerical techniques.....	III.14
3.5.2.1 Vertical coordinate schemes .....	III.14
3.5.2.2 Parameterization schemes.....	III.15
3.5.2.3 Integration schemes.....	III.20
3.6 Methods of deriving and presenting output products.....	III.21
3.6.1 Automatic output of numeric data.....	III.21
3.6.2 Requirements and technical aspects of conversion of information in alphanumeric (GRID/GRAF) and binary (GRIB, BUFR) code .....	III.22
3.6.2.1 System configuration.....	III.22
3.6.2.2 Software .....	III.23
3.7 Utilization of numerical products .....	III.23
3.7.1 Utilization of numerical products for the statistical forecasting of weather parameters.....	III.24
3.7.2 Utilization of numerical products in dynamical forecasting of weather parameters .....	III.24
3.8 Sources of error in numerical prognoses .....	III.24
Annex 3.A Guidelines where action is required to minimize the impact of a loss of observations on the operations of the GDPS .....	III.31

<b>Chapter 4 METHODS USED IN THE MANUAL PROCESSING OF DATA FOR ANALYSIS AND FORECASTING .....</b>	<b>IV.1</b>
4.1 Use of encoded analyses and prognoses .....	IV.1
4.1.1 WMO analysis codes.....	IV.1
4.1.2 Use of WMO analysis codes in data-processing activities .....	IV.1
4.1.2.1 Manual operations.....	IV.1
4.1.2.2 Automated operations .....	IV.1
4.2 Manual analysis of the vertical structure of the atmosphere .....	IV.1
4.2.1 General .....	IV.1
4.2.2 The plotting of thermodynamic diagrams.....	IV.1
4.2.3 The use of thermodynamic diagrams in forecasting .....	IV.2
4.2.4 Wind shear hodographs.....	IV.2
4.2.5 Vertical cross-sections.....	IV.2
4.2.5.1 General .....	IV.2
4.2.5.2 Time cross-sections .....	IV.2
4.2.5.3 Space cross-sections .....	IV.2
4.2.6 Representation of air masses.....	IV.3
4.2.7 The plotting of atmospherics .....	IV.3
4.2.7.1 The plotting model.....	IV.3
4.2.7.2 Rules for plotting the individual elements.....	IV.3
4.2.8 Plotting and analysis of wave conditions .....	IV.3
4.2.8.1 Plotting model.....	IV.3
4.2.8.2 Isopleths of wave heights .....	IV.3
4.2.8.3 Movement of predominant wave trains .....	IV.3
4.2.9 Pressure-change charts.....	IV.3
4.2.10 Tropopause charts .....	IV.4
4.3 Methods of manual analysis and prognosis in extratropical latitudes .....	IV.4
4.3.1 Manual techniques involved in analysis .....	IV.4
4.3.1.1 Requirements for manual analyses .....	IV.4
4.3.1.1.1 Monitoring objectively-produced analyses.....	IV.4
4.3.1.1.2 Use of manual analyses in connection with numerical weather prediction techniques.....	IV.5
4.3.1.1.3 Early provision of analyses .....	IV.5
4.3.1.1.4 Quality control through the manual preparation of analyses.....	IV.5
4.3.1.1.5 Small features .....	IV.5
4.3.1.1.6 Understanding the behaviour of the atmosphere .....	IV.5
4.3.1.2 Analysis techniques .....	IV.5
4.3.1.2.1 Types of analyses .....	IV.6
4.3.1.2.1.1 Isobaric analysis.....	IV.6
4.3.1.2.1.2 Analysis of discontinuities.....	IV.6
4.3.1.2.1.3 Analysis of vertical instability .....	IV.6
4.3.1.2.1.4 Vertical cross-section analysis.....	IV.6
4.3.1.2.1.5 Specialized analyses of individual elements .....	IV.6

	Page
4.3.1.2.1.6 Analysis of satellite data .....	IV.6
4.3.1.2.2 Analysis of surface features .....	IV.7
4.3.1.2.2.1 Frontal analysis.....	IV.7
4.3.1.2.2.2 The pressure field.....	IV.8
4.3.1.2.2.3 Use of numerical forecast products in the preparation of analyses.....	IV.8
4.3.1.2.2.4 Analysis of other features.....	IV.8
4.3.1.2.3 Upper-air analysis techniques .....	IV.8
4.3.1.2.3.1 General considerations .....	IV.8
4.3.1.2.3.2 Principles of analysis.....	IV.10
4.3.1.2.3.3 Other types of upper-air analyses .....	IV.12
4.3.1.2.4 Analysis of satellite information.....	IV.13
4.3.1.2.4.1 Types of satellite and imagery available.....	IV.13
4.3.1.2.4.2 Use of satellite data.....	IV.13
4.3.1.2.4.3 Satellite data and upper-air analyses.....	IV.14
4.3.1.2.4.4 Satellite data in data-sparse areas.....	IV.14
4.3.1.2.5 Analysis of radar information .....	IV.15
4.3.1.2.5.1 General considerations .....	IV.15
4.3.1.2.5.2 Non-coherent radars .....	IV.15
4.3.1.2.5.3 Coherent (Doppler) radars .....	IV.19
4.3.1.2.5.4 Analysis of lightnings .....	IV.20
4.3.1.2.6 Other techniques for the analysis of data .....	IV.20
4.3.2 The human role in modern forecasting techniques.....	IV.22
4.3.2.1 The intervention role of the analyst or forecaster in an automated weather prognosis system....	IV.22
4.3.2.2 The manipulation of numerically produced forecasts .....	IV.23
4.3.2.3 The production of prognoses during periods of computer outage.....	IV.24
4.3.2.4 Manual techniques in the production of very-short-range forecasts (periods of several hours) ...	IV.24
4.3.3 The use of workstations in the forecasting environment.....	IV.24
4.3.3.1 General .....	IV.24
4.3.3.2 Technology .....	IV.24
4.3.3.3 Workstation applications .....	IV.25
4.3.3.4 Design considerations in setting up a workstation-based system .....	IV.32
4.3.3.5 Other considerations .....	IV.32
4.3.3.6 Trends in workstation hardware and software technology .....	IV.33
4.3.3.7 Workstation application trends .....	IV.33
 Chapter 5 METHODS OF ANALYSIS AND FORECASTING IN THE TROPICS .....	 V.1
5.1 Introduction .....	V.1
5.2 Mean structure and circulation of the tropical belt .....	V.1
5.2.1 The intertropical convergence zone (ITCZ) .....	V.1
5.2.2 The monsoon circulation.....	V.4
5.2.3 Energetics of the tropical motion systems .....	V.6
5.2.4 Origin of tropical disturbances .....	V.6
5.2.4.1 Barotropic instability .....	V.6
5.2.4.2 Conditional Instability of the Second Kind (CISK).....	V.7
5.3 Observational database for tropical analysis and forecasting .....	V.7
5.3.1 Some special problems of tropical analyses vis-a-vis observational data .....	V.8
5.4 Tropical wave disturbances .....	V.8
5.4.1 Major characteristics of tropical wave disturbances.....	V.9
5.4.1.1 Four to five-day large-scale (synoptic) waves in the lower and middle troposphere.....	V.9
5.4.1.2 Four to five-day planetary-scale waves in surface pressure .....	V.10
5.4.1.3 Planetary-scale equatorial waves in the upper troposphere and lower stratosphere .....	V.10
5.4.1.3.1 Mixed Rossby-gravity waves .....	V.10
5.4.1.3.2 Kelvin waves .....	V.11
5.4.1.4 Low frequency modes of the tropical troposphere 30- to 50-day oscillation.....	V.12
5.4.1.5 Waves on the inter-annual time scale: quasi-biennial oscillation.....	V.12
5.4.2 Cold surges of Asian winter monsoon .....	V.12
5.5 Tropical synoptic models .....	V.13
5.5.1 Waves.....	V.15
5.5.1.1 Synoptic-scale wave disturbances in the Caribbean.....	V.15

	<i>Page</i>	
5.5.1.2	Synoptic-scale wave disturbances in the Pacific.....	V.17
5.5.1.3	African waves.....	V.17
5.5.2	Vortices .....	V.18
5.5.2.1	Tropical cyclones .....	V.18
5.5.2.1.1	Model of a tropical cyclone .....	V.19
5.5.2.1.1.1	Wind field.....	V.19
5.5.2.1.1.2	Surface pressure distribution.....	V.20
5.5.2.1.1.3	Temperature field.....	V.21
5.5.2.1.1.4	Cloud systems.....	V.21
5.5.2.1.1.5	Dynamics of the inner core and outer region .....	V.22
5.5.2.2	Monsoon depressions .....	V.23
5.5.2.2.1	Monsoon depressions in the Indian region .....	V.23
5.5.2.2.1.1	Characteristic features of monsoon depressions .....	V.23
5.5.2.2.1.2	Synoptic features preceding the formation of monsoon depressions .....	V.25
5.5.2.2.2	Monsoon depressions in the Australian region.....	V.25
5.5.2.3	Mid-tropospheric cyclones.....	V.25
5.5.2.3.1	Subtropical cyclones .....	V.25
5.5.2.3.2	Arabian Sea cyclones.....	V.27
5.5.2.4	Upper-tropospheric cyclones .....	V.28
5.5.2.4.1	North Pacific.....	V.28
5.5.2.4.2	North Atlantic.....	V.29
5.5.2.4.3	Temporal storms of Central America .....	V.30
5.5.2.4.4	Southern hemisphere.....	V.31
5.5.2.5	Lower-tropospheric anticyclones .....	V.31
5.5.3	Linear disturbances.....	V.32
5.5.3.1	Shear lines.....	V.32
5.5.3.2	Asymptotes .....	V.33
5.6	Tropical synoptic analysis techniques.....	V.34
5.6.1	Manual analysis techniques.....	V.34
5.6.1.1	Conventional charts .....	V.35
5.6.1.2	Auxiliary charts.....	V.37
5.6.2	Automated analysis techniques .....	V.37
5.7	Tropical forecasting methods.....	V.37
5.7.1	Approaches to operational weather forecasting.....	V.37
5.7.2	Short-range forecasting techniques.....	V.38
5.7.2.1	Models .....	V.39
5.7.2.2	Extrapolation and interpolation .....	V.39
5.7.2.3	Analogues .....	V.39
5.7.2.4	Climatology .....	V.39
5.7.3	Tropical numerical weather prediction .....	V.39
5.7.3.1	Predictability of tropical weather.....	V.39
5.7.3.2	Operational numerical weather prediction systems and models .....	V.41
5.7.3.3	Extended range prediction.....	V.42
5.7.3.4	Statistical interpretation of NWP output for the prediction of weather elements .....	V.43
5.8	Prediction of tropical cyclones .....	V.43
5.8.1	Tropical cyclone formation.....	V.43
5.8.1.1	Genesis.....	V.43
5.8.1.1.1	Climatological features .....	V.43
5.8.1.1.2	Synoptic features.....	V.44
5.8.1.1.2.1	Low-level cyclonic vorticity.....	V.44
5.8.1.1.2.2	Vertical wind shear .....	V.45
5.8.1.1.2.3	Upper-level divergence .....	V.45
5.8.1.1.2.4	Satellite imagery features .....	V.45
5.8.1.2	Intensity changes.....	V.45
5.8.1.2.1	The role of moist convection .....	V.45
5.8.1.2.2	Role of vorticity .....	V.46
5.8.1.2.3	Environmental interactions .....	V.46
5.8.1.2.4	Upper-level outflow patterns associated with tropical cyclone intensity changes.....	V.47
5.8.1.2.5	Satellite imagery features .....	V.48

	<i>Page</i>
5.8.1.2.6 Intensity and structure change due to landfall .....	V.49
5.8.1.2.7 Transition to extratropical systems.....	V.49
5.8.1.2.8 Relation between inner core and outer region intensify changes .....	V.49
5.8.2 Track forecasting methods .....	V.49
5.8.2.1 Theoretical aspects of tropical cyclone motion .....	V.49
5.8.2.2 Synoptic considerations.....	V.50
5.8.2.3 Analogue models .....	V.54
5.8.2.3.1 Probability ellipses.....	V.54
5.8.2.4 Statistical models.....	V.54
5.8.2.4.1 Simulated analogue models .....	V.54
5.8.2.4.2 Statistical-synoptic models .....	V.55
5.8.2.4.3 Statistical-dynamical models .....	V.56
5.8.3 Cyclone prediction by numerical models.....	V.57
5.8.3.1 Results of tropical cyclone prediction and simulation experiments by numerical models .....	V.57
5.8.3.2 Single-level model: the SANBAR barotropic model .....	V.59
5.8.3.3 Operational NWP models for tropical cyclone prediction: the problem of missing vortex in the initial fields.....	V.59
5.8.3.3.1 National Meteorological Centre, Washington .....	V.60
5.8.3.3.2 European Centre for Medium Range Weather Forecasts (ECMWF), United Kingdom .....	V.60
5.8.3.3.3 United Kingdom Meteorological Office (UKMO) .....	V.61
5.8.3.3.4 Japan Meteorological Agency (JMA) .....	V.61
5.8.4 Tropical cyclone probability forecasts .....	V.62
5.8.5 Verification of tropical cyclone forecasts.....	V.62
5.8.5.1 Measures of track forecast errors .....	V.62
5.8.5.2 Comparison of various objective aids.....	V.63
5.8.6 Storm surge prediction .....	V.65
5.8.6.1 Surge prediction by mathematical models .....	V.65
5.8.6.1.1 Datum.....	V.65
5.8.6.1.2 Initialization.....	V.65
5.8.6.1.3 Storm modelling.....	V.65
5.8.6.1.4 Surge modelling.....	V.66
5.8.6.1.5 Tide surge interactions .....	V.67
5.8.6.1.6 Surge predictions .....	V.67
5.8.6.2 Surge prediction with the help of nomograms.....	V.67
5.9 Mesoscale phenomena in the tropics .....	V.67
5.9.1 Terrain-induced mesoscale systems .....	V.68
5.9.1.1 Sea and land breezes over flat terrain.....	V.68
5.9.1.2 Mountain-valley winds.....	V.68
5.9.1.3 Forced airflow over and around rough terrain .....	V.69
5.9.2 Synoptically-induced mesoscale phenomena .....	V.69
5.9.2.1 Convective storms .....	V.69
5.9.2.1.1 Short-lived single cell storms.....	V.70
5.9.2.1.2 Supercell storms.....	V.70
5.9.2.1.3 Mutticell storms .....	V.70
5.9.2.2 Environmental conditions favourable for the occurrence of convective storms.....	V.71
5.9.2.2.1 Use of a hodograph for the diagnosis of vertical wind shear .....	V.72
5.9.3 Operational diagnostic tools for mesoscale forecasting.....	V.72
5.9.4 Mesoscale forecasting methods .....	V.73
5.9.4.1 Linear extrapolation .....	V.73
5.9.4.2 Conceptual models.....	V.73
5.9.4.3 Rules of thumb .....	V.73
5.9.4.4 Mesoscale climatology .....	V.74
5.9.4.5 Special purpose one-dimensional models.....	V.74
5.9.4.6 Mesoscale numerical weather prediction.....	V.74
Annex 5.A Guidelines for determining the type of cyclone and origin of subtropical cyclones .....	V.86
Annex 5.B Guidelines for estimating the intensity of subtropical cyclones .....	V.86
Annex 5.C Similarities and differences between the Dvorak technique for tropical cyclones (T) and the subtropical cycone (ST) technique.....	V.86

	<i>Page</i>
Chapter 6    QUALITY CONTROL PROCEDURES .....	VI.1
6.1    General description .....	VI.1
6.1.1    Pre-processing checks .....	VI.1
6.1.2    Physical elements .....	VI.1
6.1.3    Building a quality control system.....	VI.1
6.1.4    Flagging .....	VI.1
6.2    Pre-processing checks .....	VI.2
6.2.1    Checks within the telecommunication area.....	VI.2
6.2.1.1    Heading checks.....	VI.2
6.2.1.2    Checking E E reports .....	VI.2
6.2.1.3    Checking the syntax and five-character groups .....	VI.2
6.2.2    Control of the WMO code part.....	VI.3
6.2.2.1    Checking the date and time .....	VI.3
6.2.2.2    Checking the block/station number and the position .....	VI.3
6.2.2.3    Checks during the decoding procedure.....	VI.3
6.2.2.4    Duplicate checks.....	VI.4
6.3    Quality control techniques.....	VI.4
6.3.1    Gross-error limit checks .....	VI.5
6.3.1.1    Limit checks for surface data .....	VI.5
6.3.1.2    Limit checks for upper-air data (TEMP, PILOT, TEMP SHIP, PILOT SHIP) .....	VI.8
6.3.1.3    Limit checks for single level wind and temperature data (aircraft, SATOB).....	VI.9
6.3.1.4    Limit checks for satellite-sounding data (SATEM) .....	VI.9
6.3.2    Internal consistency checks.....	VI.10
6.3.2.1    Consistency checks for surface data .....	VI.10
6.3.2.1.1    In case of indicator $i_x = 1\text{--}4$ .....	VI.10
6.3.2.1.2    In case of indicator $i_x = 5\text{--}7$ .....	VI.13
6.3.2.2    Consistency checks for upper-air data.....	VI.15
6.3.2.2.1    Lapse-rate check of vertical temperature profiles .....	VI.15
6.3.2.2.2    Checking the consistency between significant level data and standard level data .....	VI.16
6.3.2.2.3    Checking the hydrostatic balance between standard level height and standard level temperature data.....	VI.17
6.3.2.2.4    Checking the vertical wind shear.....	VI.21
6.3.3    Time consistency checks.....	VI.21
6.3.3.1    Checking the surface data .....	VI.21
6.3.3.2    GPCC procedures for precipitation quality monitoring.....	VI.22
6.3.3.2.1    Treatment of errors .....	VI.22
6.3.3.3    Checking the positions in consecutive reports.....	VI.23
6.3.3.4    Check against numerical forecasts.....	VI.24
6.3.4    Space/time consistency check.....	VI.25
6.3.4.1    Space consistency or neighbour test.....	VI.25
6.3.4.2    Comparison with analysis .....	VI.25
6.4    Flagging and design of computer programs .....	VI.26
6.4.1    Example of a flagging system .....	VI.26
6.4.2    Design of computer programs .....	VI.26
6.5    Combined quality control .....	VI.27
Chapter 7    NON-REAL-TIME FUNCTIONS OF WMCs, RSMCs AND NMCs .....	VII.1
7.1    Major non-real-time functions of WMCs, RSMCs and NMCs .....	VII.1
7.2    Collection, quality control, storage and retrieval of data in the GDPS.....	VII.1
7.2.1    Collection of data to be stored.....	VII.1
7.2.2    Quality control of data to be stored .....	VII.1
7.3    Data to be stored at each level of the GDPS.....	VII.1
7.4    Media and formats for storage and exchange.....	VII.1
7.5    Classification, cataloguing and exchange of data .....	VII.1
Chapter 8    EXCHANGE OF PERSONNEL ENGAGED IN DATA-PROCESSING ACTIVITIES.....	VIII.1

## PREFACE

At its Extraordinary Session (London, September/October 1990), the Commission for Basic Systems (CBS) agreed that there was a need to update the *Guide on the Global Data-processing System* and approved the proposed table of contents for the new updated edition. The tenth session of the Commission for Basic Systems (Geneva, November 1992) considered and approved the texts for the new Chapters 1, 2, 3, Chapter 4, sections 4.3.1.2.5 and 4.3.3, and Chapter 5, and requested the Secretary-General to arrange for the issuance of a new edition of the *Guide* as soon as possible.

The *Guide on the GDPS* is a reference volume which contains brief descriptions of many methods and techniques used in data processing both in mid- and tropical latitudes. As it would not be possible to include an exhaustive discussion of current methods and techniques, Chapters 3 and 5 contain comprehensive reference lists which the user of the *Guide* should consult for more detailed studies.

The Secretariat was assisted in the preparation of the new edition by Dr N.F. Veltischev (Russian Federation), who drafted Chapter 3 on the methods used in the automated processing of data for analysis and prediction and Chapter 4, section 4.3.1.2.5 on analysis of radar information with a contribution to this section from Mr D. Katsimardos (Greece). Mr H. Allard (Canada) drafted the text for section 4.3.3 on the use of workstations in the forecasting environment and Mr K. Prasad (India) drafted the text for Chapter 5 on methods of analysis and forecasting in the tropics. A review of the draft *Guide* was carried out by the Secretariat and detailed contributions were made by Dr P. Julian (U.S.A.), Dr P. Francis (U.K.), Mr T. Hart (Australia) and Mr S. Cheng (Hong Kong).

The current material in Chapter 4 on methods used in the manual processing of data for analysis and forecasting and Chapters 6, 7 and 8 had only minor editorial changes. The CBS Working Group on the GDPS is keeping the new edition under constant review. Supplements containing new updated materials will be issued periodically as developments take place in data-processing techniques.

I wish to express my sincere thanks on behalf of WMO to all those who have contributed to the writing and editing of this edition of the *Guide*.



(G.O.P. Obasi)  
Secretary-General

S E C R E T A R I A T   N O T E

In accordance with the decision of Eighth Congress (Abridged Report with Resolutions, General Summary, paragraph 3.1.2.15), the unit hectopascal (hPa) has been adopted as the unit of atmospheric pressure for use in both the operational and research work of the Organization. Therefore, whenever the unit millibar (mb) appears in the text of the *Guide on the Global Data-processing System*, it has been replaced by hectopascal (hPa).

## GLOSSARY

*Aliasing* – the process by which a wave's structure is misrepresented by inadequate resolution in a grid array.

*Analysis, numerical, (objective or automatic)* – may be used interchangeably for any of a variety of analysis schemes performed by a programme (software) written for an electronic computer.

*State of the art* – the status or degree of advancement of knowledge and of the application of technology in a given area or for a given subject, such as the degree of advancement in numerical weather prediction.

*Bilinear* – first order function in two dimensions.

*Biquadratic* – second order function in two dimensions.

*Bogus* – usually refers to an observation which has been "manufactured" to assist in an objective analysis scheme (e.g. a bogus TEMP observation).

*Computer* – any machine which can accept data in a presented form, process the data, and supply the results in a specified format. The three main categories are digital, analogue and hybrid computers. They come in many sizes depending on their capacity, complexity and degree of miniaturization. Generally, smaller computers are designated with the prefix "mini" or "micro" to indicate their overall size.

*Conditional Instability of the Second Kind* (CISK) – refers to the active interaction of the large-scale vortex and cloud system which occurs during the amplification of a warm-core pre-tropical storm vortex into a mature tropical storm (e.g. hurricane). The clouds supply the heat energy needed to drive the vortex, and the vortex, by providing low-level water vapour convergence, organizes and maintains the cloud system.

*Correlation function* – overall average of the product of the deviations of quantities from their mean values.

*Differencing schemes* – three ways of contrasting time-differencing schemes when solving a system of several differential equations in an atmospheric model, which describe both fast-moving gravity waves and slower-moving Rossby waves:  
(a) *Implicit* – requiring a matrix inversion for solution; (b) *Semi-implicit* – part explicit, part implicit; (c) *Split-explicit* – separate explicit solutions, usually split into fast-travelling gravity waves and Rossby waves.

*Eigenfunction* – in mathematics, a solution belonging to the characteristic value of a differential or integral equation.

*Grid* – An equally-spaced array or network of points (i.e. grid points) or locations in two- or three-dimensional space at which certain meteorological data are available or at which mathematical operations are performed to produce an analysis or forecast of meteorological parameters (e.g. by use of a numerical model).

*Homogeneity* – used to describe a fluid, solid or gas, having the same physical properties throughout.

*Inviscid* – without frictional effects.

*Isotropic fluid* – a fluid whose local properties are independent of the axes of reference.

*Iterative process* – a process in which exactly the same mathematical procedure is repeated until a convergence criteria is met.

*Linear* – a first-order relation between variables, e.g.  $ax + ay + \dots$

*Mass* – a physical measure of the principal inertial property of a particle of its resistance to change of motion. The gravitational mass of a particle is proportional to the gravitational force acting on it from the Earth and thus is a measure of its weight.

*Momentum* – the product of mass of a particle  $m$  and its velocity  $v$ .

*Monotonic* – a function is monotonic over a given range of an independent variable  $x$  if the derivative  $\partial f / \partial x$  has the same sign throughout the range.

*Non-linear* – all higher-order relations (i.e. other than linear) between variables, e.g.  $ax_1y_1 + ax_2y_2 + \dots$

*Normal mode* – eigenfunctions of a set of linearized differential equations.

*Parameter* – a quantity which may have various values, each fixed within the limits of a stated case, or a quantity representing a statistical population. In meteorology, the term is used to refer to observed or derived weather data (e.g. temperature, pressure-height, vorticity, etc.) or to constants or quantities which represent small-scale processes in the atmosphere (e.g. friction).

*Parameterization* – the use of area-averaged quantities to determine the evolution of sub-grid-scale events in a numerical model.

*Polar singularity* – in spherical coordinate systems, the pole point is undefined since  $1/\cos 90^\circ = 00$  or is undefined.

*Residual difference* – difference between the estimated (e.g. first guess) and true observed value of a meteorological quantity. The Reynolds stress terms are a special case involving residuals.

*Scalar* – any physical quantity whose field can be described by a single numerical value at each point in space. A scalar quantity is distinguished from a vector quantity by the fact that it possesses only magnitude rather than magnitude and direction, e.g. pressure is a scalar and velocity is a vector.

*Truncation error* – an error arising from the approximation of exact differentials with finite differences (e.g. to truncate a Taylor series).

## CHAPTER 1

### **PURPOSE AND SCOPE OF THE GLOBAL DATA-PROCESSING SYSTEM (GDPS)**

The purpose of the Global Data-processing System is to make available to all Members the basic processed data they require both for real-time and non-real-time uses. Real-time uses are operations in which the information must be received and used or processed within at most, a few hours after it is generated. These are concerned mainly with daily processing of basic observational data to produce analyses and prognoses for operational use. Non-real-time uses are those operations which can be carried out over a more extended time period. For these, it is necessary to lay down standard procedures for the storage and retrieval of all types of observational and processed data. The GDPS is made possible through an integrated system of World Meteorological Centres (WMCs), Regional Specialized Meteorological Centres (RSMCs) and National Meteorological Centres (NMCs) equipped to the maximum degree possible with modern facilities, including high-speed computers. The GDPS is a world-wide system composed of national facilities and other processing facilities provided by individual Members and co-ordinated through the direction of the WMO Commission for Basic Systems and its Working Group on the Global Data-processing System. Co-ordination through this working group is confined to the global and regional levels. Other details at the regional and national levels are left to regional associations. The details on the organization of the GDPS are given in Annex IV to the *WMO Technical Regulations*, Volume I (WMO-No. 49).

---

## CHAPTER 2

### MAJOR REAL-TIME FUNCTIONS OF WMCs AND RSMCs, INCLUDING THE ROLE OF NMCs

#### 2.1 World Meteorological Centres (WMCs)

The WMCs should concentrate on the global types of product, primarily describing planetary and large-scale meteorological phenomena. They are intended to be service centres whose products will be available for use by all Members as aids to forecasting and long-range applications.

The real-time functions of the WMCs are given in Volume I of the *Manual on the GDPS* (WMO-No. 485).

WMCs should be prepared to issue products in forms which can be transmitted rapidly with a high concentration of useful information.

In view of the advantages of digital forms of transmission over pictorial forms (from the point of view of efficiency in the GTS and at centres equipped with automatic data-processing facilities), WMCs should be able to convert from one form to another.

Some Members may require special types of products, such as boundary condition data for a number of time steps, to be used by RSMCs/NMCs in their limited area numerical analyses and prognoses. Initially, arrangements for the exchange of such data should be done on a bilateral or multilateral basis.

The primary responsibility for real-time quality control of all observational data rests with the national Meteorological Service from which the observation originated. WMCs should also carry out appropriate quality control of the observational data they receive, in order to ensure the high quality of their analyses and prognoses.

The above functions of the WMCs do not affect the status of any international commitment of the Members concerned for support to shipping and aviation, nor determine the manner in which Members execute these responsibilities. On the contrary, the results of the implementation of the WWW have shown that the GDPS aids Members in meeting such international commitments by making better and more varied products available for use.

#### 2.2 Regional Specialized Meteorological Centres (RSMCs)

The RSMCs are divided into two categories: Regional Specialized Meteorological Centres with geographical specialization and Regional Specialized Meteorological Centres with activity specialization.

The major task of RSMCs with geographical specialization is to meet the requirements of NMCs, located in its area of responsibility — for regional analyses and forecasts — and to co-ordinate their operational functions through the appropriate regional bodies and the Commission for Basic Systems. The real-time functions of the RSMCs with geographical specialization, together with a list of such centres, are given in Volume I of the *Manual on the GDPS*.

The major task of RSMCs with activity specialization is to provide Members with specialized products to cover global and/or regional requirements in the following fields of application: marine meteorology, tropical cyclones, meteorological/environmental hazards, drought monitoring and climate diagnosis. The functions of the RSMCs with activity specialization, together with a list of such centres, are given in Volume I of the *Manual on the GDPS*.

In view of the advantages of digital forms of transmission over pictorial forms (from the point of view of efficiency in the GTS and at centres equipped with automatic data-processing facilities), RSMCs should be able to convert from one form to another for further dissemination within their respective Regions.

The primary responsibility for real-time quality control of all observational data rests with the national Meteorological Service from which the observation originated. RSMCs should also carry out appropriate quality control of the observational data they receive, in order to ensure the high quality of their analyses and prognoses.

#### 2.3 National Meteorological Centres (NMCs)

##### 2.3.1 Role of NMCs

The primary task of an NMC is to provide weather analyses, forecasts and other meteorological information for the area of the country concerned. Members are responsible for the functions of their NMCs. The scope of activities of NMCs may vary widely, depending on the following factors:

- (a) The area over which the responsibilities of a given NMC extends;
- (b) The social and economic activities within the country concerned;
- (c) The possibilities of using WMC and RSMC products for national purposes;
- (d) The possibilities of co-operating with other NMCs;
- (e) The role that an NMC plays, within the national meteorological system of a given country, in providing services to specified users (in large countries these services are usually provided by specialized agencies, while in smaller ones the NMCs may be responsible for issuing a wide range of special service products);
- (f) Some of the NMCs may also function as WMCs and RSMCs in addition to their role as NMCs.

The RSMCs and WMCs do not normally issue weather forecasts for the public and have no direct contact with users. The gap between WMC and RSMC products and users' requirements in a given country should be bridged by the activities of the NMC concerned.

The specific tasks of the NMCs (the real-time functions of NMCs) are given in Volume I of the *Manual on the GDPS*.

Beyond the activities, which in certain countries form part of the tasks of the NMCs, but which are normally considered tasks of WMCs and RSMCs, the NMCs may also be responsible for ensuring:

- (a) That a system of monitoring is in operation for nationally and internationally exchanged meteorological data (see also the Plan for Monitoring the Operation of the World Weather Watch as given in Volume I, Attachment II.14 of the *Manual on the GDPS*);
- (b) That WMC and RSMC products are used to the maximum possible extent and thereby the unnecessary duplication of costs and effort is avoided;
- (c) That large-scale WMC and RSMC products are refined as required on the basis of additional calculations with fine-mesh models;
- (d) That the WMC, RSMC and NMC products available on various scales are expertly interpreted and converted into forms of public or specialized information; and
- (e) That these types of information are distributed efficiently to the general public and to specified users, by establishing and maintaining a suitable servicing system, which may include local consulting bureaux, automated data bank facilities, or quite simple devices, depending on operational requirements.

### 2.3.2 ***Data acquisition at NMCs***

There are three main groups of data which must be acquired by NMCs:

- (a) The first group includes the reports of the meteorological stations within the given country. An internationally agreed selection of these data is to be transmitted for use by other centres via the Global Telecommunication System (GTS). All types of data to be exchanged internationally on the GTS are given in the *Manual on the Global Telecommunication System* (WMO. No. 386);
- (b) The second group comprises the reports of observing stations outside the area of the country. These data, received via the Global Telecommunication System, do not usually provide the area coverage necessary for runs with fine-mesh models. Therefore, special arrangements might be required in order to obtain the necessary data;
- (c) The third group includes the products (analyses and forecasts) of WMCs, RSMCs and other NMCs which are received in alphanumeric (GRID/GRAF), binary (GRIB, BUFR) or in pictorial form. A recent requirement raised by certain NMCs engaged in numerical weather prediction is for receiving boundary conditions originating from large-scale global or hemispheric models which are run at the WMCs and some RSMCs. These data are considered to be necessary for the running of limited-area fine-mesh models. Another way to fulfil this requirement could be through special bilateral or multilateral arrangements for the exchange of boundary-value data.

### 2.3.3 ***Data processing at NMCs***

The data-processing activities fall into two distinct categories. The real-time activities include all tasks in connection with weather analyses and forecasts as well as graphic and alphanumeric presentation of observations and processed information. The non-real-time activities comprise various tasks in connection with climatology, long-range forecasts, research, and the operation of the data-storage and retrieval facilities.

One important aspect of real-time data processing is numerical weather prediction (NWP). It should be stressed, however, that this is not the sole task of a computer centre at an NMC. Moreover, the operations which should be carried out by an NMC require serious consideration, given the availability of NWP products by WMCs, RSMCs and large NMCs. The main reasons which might motivate an NMC to undertake NWP operations are:

- (a) The need for more detailed forecasts, taking into account local influences;
- (b) The desire to obtain some important charts faster than they are available by regional or global telecommunications circuits.

However, these two motivations call for quite different operational facilities. The limited area fine-mesh models used to provide sufficiently detailed forecast charts would generally require substantial computer resources which are not always available at small NMCs.

Personal computers and work stations with a continuously growing power allow, however, to find solutions to most of the data-processing problems in the small NMCs, including the processing of NWP products from the major GDPS centres for deriving new products (e.g. trajectories of air particles) and preparing local weather forecasts with the use of NWP objective interpretation methods. These facilities also permit to solve the problem of product display.

### 2.3.4 ***Data-processing systems and telecommunication at NMCs***

The level of data-processing activities in NMCs can vary substantially depending upon the Members' national requirements, so it is difficult to specify, in a detailed way, the minimum requirements for data-processing facilities in NMCs. It is possible however to identify in broad terms the components of the data-processing system appropriate to meet the requirements of an NMC in a small meteorological service.

An NMC could require automation to assist in the performance of such functions as:

- (a) The real-time monitoring of observations with interactive capability for quality control purposes;
- (b) The preparation and dissemination facilities for worded forecasts;
- (c) The manipulation of data fields from major centres to prepare a range of derived products;
- (d) The operation of simple statistical models using local observations and imported data;
- (e) The interactive processing of real-time and climatological fields in support of short- and medium-range forecasting;
- (f) The preparation of forecast bulletins in an automated or semi-automated fashion using local observations and imported data;
- (g) The development of local weather forecasting techniques;
- (h) The preparation of high quality, hard copy graphical output, including the archival of a limited set of parameters/fields.

Following consideration of the list of functions to be performed in an NMC and taking into account the need to minimize the size and complexity of the data-processing system, the following features for a system meeting both the data-processing and telecommunications requirements can be adopted. The system should have two microcomputer configurations. The microcomputers should have Unix-based operating systems and be joined by a local area network connection. One of these microcomputers should run a communicating and message switching system, while the other should have an applications and graphics package. This separation does not imply, necessarily, a logical separation. The technical advice strongly suggests that the merging of the two general tasks into a single central processing unit operation would result in an unacceptable level of complexity.

The following essential components of the system and their functionality can be identified.

#### *The telecommunication system*

The functional requirements of the telecommunication subsystem should include the collection of observations and grid-point data bulletins from the GTS (and AFTN, as appropriate), the storage of messages in a database, the transmission of observations to the GTS and products on national communications circuits, and the capability for real-time bulletin monitoring.

#### *Graphics and display service*

The purpose of this function is to capture numerical products, observations, and possibly facsimile transmissions from the database for display by the visual display unit and/or printer hardware. A connection between the message handling system and the applications system is necessary not only to effect this capture, but also to allow the display of locally-produced observations for quality control purposes. A certain amount of interactive ability is therefore necessary.

#### *Database considerations*

Central to the design of an effective automated data-processing system is the database.

The telecommunications subsystem database must hold:

- (a) Bulletins of incoming messages;
- (b) Locally generated observations;
- (c) Products for national dissemination;
- (d) Bulletins of locally generated observations for transmission on the GTS.

The applications subsystem database must hold:

- (a) Reports derived from decoded bulletins;
- (b) Fields derived from decoded bulletins;
- (c) Products prepared through the processing of reports and fields.

If possible, the database residing in each computer should be controlled by the same database management system (DBMS), which should be relatively simple so as to minimize computing overheads and facilitate the speed of response of the overall data-processing system.

#### *Training and maintenance*

The training and maintenance aspect implies that systems cannot be implemented and maintained without ongoing software and hardware maintenance. On-site maintenance can only be achieved if operators are thoroughly trained in all aspects of the system. It is therefore recommended that careful attention should be paid to the technology transfer requirements of the data-processing system.

## CHAPTER 3

### METHODS USED IN THE AUTOMATED PROCESSING OF DATA FOR ANALYSIS AND PREDICTION

#### 3.1 General

##### 3.1.1 Criteria for observational data requirements

The observational data requirements and the domain of integration of a numerical weather prediction model depend upon the scale of weather phenomenon to be predicted and the range of the forecast, i.e. short, medium, or long-range.

Several scale classifications of meteorological phenomena have been suggested. One of them, suggested by Orlanski (1975), is as follows (Figure 3.1):

- (a) Microscale (less than two km, for example, tornadoes, dust devils, turbulence);
- (b) Mesoscale (between two km and 2 000 km, for example thunderstorms, cloud clusters, fronts, hurricanes);
- (c) Macroscale (above 2 000 km, for example, baroclinic waves, tidal waves, ultra long waves).

The scale classification given in the *Manual on the GDPS* is as follows:

- (a) Small scale (less than 100 km, for example, thunderstorms, katabatic winds, tornadoes);
- (b) Mesoscale (100–1 000 km, for example, fronts and cloud clusters);
- (c) Large scale (1 000–5 000 km, for example, depressions and anticyclones);
- (d) Planetary scale (more than 5 000 km, for example, long upper-tropospheric waves).

Other scale classifications can also be found in the *Guide on the Global Observing System* (WMO-No. 488).

Output products from the WMCs and RSMCs incorporate large- and planetary-scale features. Forecasting of mesoscale phenomena are handled at the NMC level. The horizontal resolution and frequency of observations called for in the WMO *Technical Regulations* and in the WWW plan are based on operational experience using manual methods of analysis and prognosis. Subsequent theoretical studies have shown these requirements to be of the correct order of magnitude.

##### 3.1.2 Data sources

The majority of data exchanged for purposes of analysis and prognosis continue to be observed at the main synoptic hours (e.g. 0000 UTC, 0600 UTC, 1200 UTC and 1800 UTC). However, the use of asynoptic data from buoys, aircraft and satellites as well as data from the ground based remote sensing systems (radars, wind profilers, lightning location systems) increase continuously. Procedures for the assimilation of synoptic and asynoptic data into operational analysis-prediction system are described in section 3.4. Guidelines where action is required to minimize the impact of a loss of observations on the operations of the GDPS is given in Annex 3.A.

$L_s$	$T_s$	$1 \text{ MONTH}(\beta L_s)^{-1}$	$(f)^{-1}$	$1 \text{ DAY} \left(\frac{g}{\theta} \frac{d\theta}{dz}\right)^{-\frac{1}{2}}$	$\left(\frac{g}{\theta}\right)^{\frac{1}{2}} \cdot \left(\frac{L}{u}\right) \text{ HOUR}$
10 000 KM	Standing waves	Ultra long waves	Tidal waves		
2 000 KM			Baroclinic waves		
200 KM			Fronts and Hurricanes		
20 KM			Nocturnal low-level jet Squall lines Inertial waves Cloud clusters Mtn. & lake disturbances		
2 KM				Thunderstorms I.G.W. C.A.T Urban effects	
200 M				Tornadoes Deep convection Short gravity waves	
20 M				Dust devils Thermals Wakes	
				Plumes Roughness Turbulence	

Figure 3.1 – Scale definitions and different processes with characteristic time and horizontal scales (according to Orlanski, L., 1975).

### 3.1.3 *Numerical weather analysis and prognosis as distinct from analysis and prognosis by conventional means*

Weather analysis and prognosis involve a very large number of data. For practical purposes, these data have to be handled in a relatively short time. Over the years, the volume of data to be handled at weather centres has been ever-increasing.

The reasons for this are the growing demand for more detailed information about actual weather conditions and the fact that the preparation of more detailed forecasts, or forecasts valid for longer periods, requires a very large input of data. However, in general, the time available for the collection, analysis and preparation of forecasts has not increased, and in many countries the demand is such that total preparation time has decreased. Conventional means are no longer sufficient to cope fully with the present operational task in meteorology. While this is true as far as data collection and analysis are concerned, it is even more true in regard to weather prediction by hydrodynamical methods. Here the use of computers is a necessity.

Operational systems of numerical weather analysis and prognosis therefore fulfil a dual function: they speed up the work and perform a computing task far beyond the scope of any conventional means. At present, time numerical weather analysis dominates in the majority of the GDPS centres. For certain operations, however, either manual or interactive, man-machine methods are still required.

### 3.1.4 *Rationale for automation*

When planning the automation of a weather centre, there is always the temptation to automate quickly and completely, simply because the concept of automation is appealing. However, there may be several operations which can be carried out more efficiently by hand (at least in the foreseeable future). A careful analysis of the state of the art in operational meteorology and computer technology needs to be made before reaching a decision on which portions of the operation can or should be automated. An analysis of this type will also be helpful in deciding the type and size of computer(s) to be used. The following criteria will be helpful when deciding on the automation of a centre:

- (a) A greater quantity of useful work will be accomplished through automation of the centre than can be accomplished by the centre's staff without automation. A computer can be programmed to carry out a large number of calculations, mathematical computations and logical operations in a very short time. However, the importance of these calculations to the centre's operation and the effective use of the centre's staff (mathematicians, meteorologists, etc.) must be carefully evaluated before the decision to automate is made;
- (b) Better meteorological products will be produced through automation, for example, more legible products (for analogue facsimile transmission), more accurate products (through use of numerical weather prediction models), or automated products less subject to routine errors in format or content.

### 3.1.5 *The computer and humans*

Automation is often seen as a means of replacing humans in the operation of a weather centre. However, experience will show that the machine and man together can achieve much more in quantity and quality of work than either can alone. No general rules can be put forth on the optimum mixture of humans and computers. Resources (money and labour) and mission requirements vary widely from centre to centre. In general, however, the routine jobs performed by technicians, such as communications or data decoding and plotting, can be performed more efficiently by computers, while the technicians' time can be better spent in operating and programming the computers. Many routine jobs formerly performed by meteorologists can also be done by using computers. Among these are multi-level analyses of pressure, temperature, winds, and humidity. Quantitative interpretation of satellite photographs for sea-level analyses, where sub-synoptic systems are involved, is as yet too detailed, complex and subjective to be performed efficiently by computers. Also, interpretation of prognostic charts of pressure, temperature, wind and humidity from a numerical model to produce a weather forecast can still be done more effectively by a trained and experienced meteorologist. As advances are made in computer technology and numerical weather prediction, more functions of the weather centre may be automated, and the criteria given in section 3.1.4 will have to be re-evaluated.

With the introduction of personal computers, the possibilities for the automation of routine jobs increased enormously, particularly in the fields of data handling and product display. This aspect of human-computer interaction is discussed in detail in section 4.3.3.

### 3.1.6 *Major functions of an automated weather analysis and prognosis system*

- (a) *Data-collection function*, which performs meteorological message recognition and storage;
- (b) *Data preprocessing*, which (within each message) performs meteorological message decoding, error checking, quality control, formatting of data for analysis, and preparation of databases;
- (c) *Four-dimensional data assimilation and objective analysis*, which includes:
  - (i) Preparation of forecast background fields by intermittent or continuous data assimilation;
  - (ii) Multi-level fitting of a mixture of observations (surface and upper-air data obtained by conventional and non-conventional methods) to correct the forecast background field to obtain a grid-point or spectral analysis in a standard coordinate system;
- (d) *Initialization of the forecast model*, to suppress high-frequency inertia-gravity oscillations excited by imbalances in the initial fields;

- (e) *Integration of a prognostic model*, which can be based either on filtered and primitive hydrostatic equations or on non-hydrostatic inelastic and fully compressible equations with the use of a large-mesh or fine-mesh grid, or by the use of a spectral representation;
- (f) *Derivation*, via statistical-dynamic techniques, of specific weather parameters, for example, temperature, cloudiness and visibility, precipitation, etc.;
- (g) *Post-processing*, which includes:
  - (i) Digital meteorological message formatting, for example, observations, wind and temperature forecasts for aviation, GRID/GRAF or GRIB code formatting of meteorological data, and digital to analogue conversion;
  - (ii) Formatting of computer-generated graphical information for presentation on graphical output devices or for digital and facsimile transmissions.

The functions and equipment at an automated centre are shown in Figure 3.2.

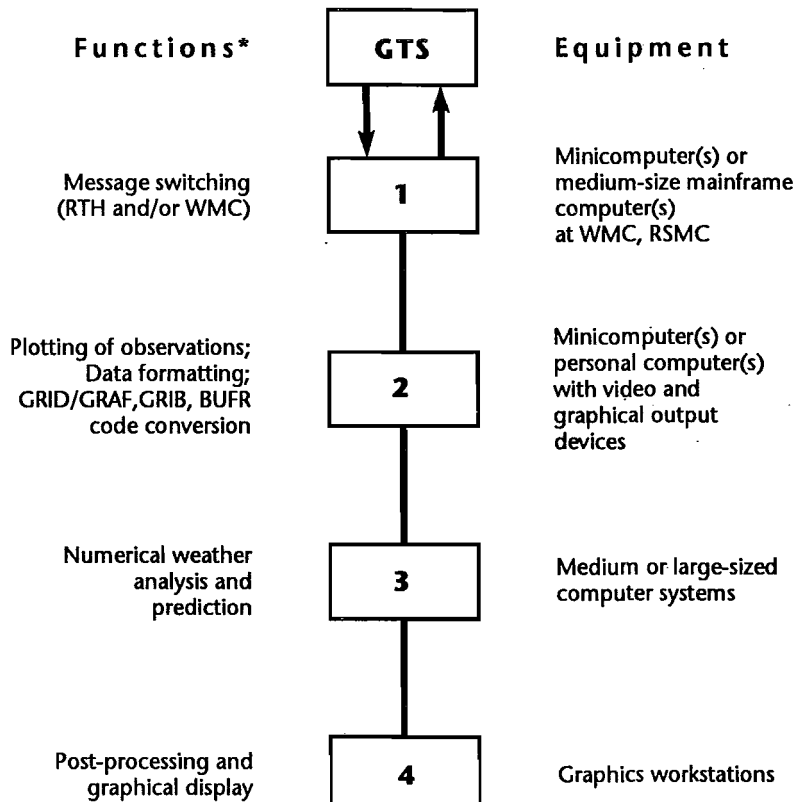


Figure 3.2 – Functions and equipment at an automated WMC, RSMC, or NMC. (\*All functions can be handled by one large computer and there are several combinations of functions and computers).

### 3.1.7 **Equipment needed to perform major functions at an automated weather analysis and prognosis centre**

The actual size of a computer at a centre will depend on local processing and communication needs. General requirements for hardware are:

- (a) Specialized equipment between communication circuits and computers to convert electric signals into digital computer formats;
- (b) A communications computer to handle the data-collection and decoding functions;
- (c) To handle the analysis and prognosis functions within an acceptable time period, another computer is usually required. Speeds for computers currently in use at meteorological centres vary approximately between 10 and 1 000 MFLOPS (million floating point operations per second);
- (d) Special equipment is needed to convert digital computer information into presentations which are suitable for use by meteorologists and other users, for example, a personal computer-based workstation, line printers, electromechanical or electrostatic plotters, etc. (Figure 3.2).

Details are provided in the *Guide on the Automation of Data-processing Centres* (WMO-No. 636).

## 3.2 Organization and procedures for data collection

### 3.2.1 **Purposes of a data-collection system**

The primary purpose of a data-collection system is to support a centre's operational analysis-forecast system. This system will include the preparation of:

- (a) Hemispheric or global analyses and prognoses at the WMCs and some RSMCs;
- (b) Analyses and prognoses for specific areas at an RSMC, and;
- (c) Analyses and prognoses for local or national use at an NMC.

The data-collection system also embraces efforts at centres involving research in support of operations (for example, testing of new operational models or improvements in current operational models). Most often, these data will be similar to the data required for daily operations. However, special storage or handling of the data for research in support of operations may be necessary.

The data-collection system also supports a centre's storage and retrieval system, which furnishes data to the centre itself or to other WMO Members, for various types of studies (for example, climatological, hydrological, agricultural, marine).

### **3.2.2 Basic types of data-collection systems**

- (a) *Automated systems*, in which a communications computer collects all meteorological messages from the GTS and local and national communications circuits (Figure 3.2);
- (b) *Manual systems*, in which all meteorological messages are collected from communications circuits via electromechanical equipment and selected manually for further processing.

Often, a combination of both automated and manual collection methods will be used, particularly at smaller centres. The manual system may be used to provide partial back-up for the automated system in case of computer malfunction or outage.

### **3.2.3 Scope and operation of a data-collection system**

Within a centre, the operation of a data-collection system, the selection of areas of data collection and data cut-off times must be considered together.

The volume and time of receipt of meteorological data required for numerical models can also have an impact on the operation of the data-collection system. For instance:

- (a) A model integrated over a limited area will in general require a greater density of meteorological observations over that area than a global model;
- (b) Some models can be started as soon as the first parts of the TEMP messages have been received, while the start of other models may need to await the later arrival of the complete TEMP messages from a given area. Therefore, data collection is a continuous process with one or more cut-off times from which an analysis-prognosis cycle begins. The cut-off times may generally be the following:
  - (i) An early cut-off time (for example, at observation time plus two hours) for a model integrated over a limited area. This cut-off time might provide data for the principal real-time forecast operation at an RSMC/NMC;
  - (ii) A late cut-off time (for example, at observation time plus four or five hours) for a regional model integrated over a substantial portion of a hemisphere and a global model integrated over the globe. This cut-off time could support a main operational model at an RSMC or a preliminary operational run at a WMC or large RSMC;
  - (iii) A delayed cut-off time (for example, at observation time plus 10 to 12 hours) for a multi-level hemispheric or global analysis and prognosis, which will provide a forecast background field for the next analysis-forecast cycle. The data available at this cut-off time would be useful at a WMC where a significant number of observations from certain areas are not available at the time of the main operational run. This operation might also include a six-hourly update cycle in a four-dimensional assimilation scheme.

## **3.3 Automated data recognition, decoding and correction procedures (data pre-processing)**

The automated procedures in this area carry out a number of separate functions.

### **3.3.1 Recognition of meteorological messages**

All weather data enter the computer directly from communication circuits or are introduced into the computer by means of a magnetic tape or paper tape generated during the data-collection phase. Local and special-purpose data may enter through a keyboard station. The data stream is examined and divided into messages by reference to the standardized message format. Inspection of the abbreviated heading or catalogue number allows recognition of, and separation into, several general data categories for decoding. Minor errors and deviations from the standardized format (for example, erroneous spacing between elements) may be tolerated but rigid adherence to the format is the only guarantee of correct identification. As a general rule, non-adherence to the standard format results in rejection of the message or possibly diversion of the message into a manual editing position. Such messages are normally routed to a teleprinter or an electronic display, where corrections may be made. The corrected messages are then returned to the computer.

### **3.3.2 Decoding of meteorological bulletins**

On the basis of the general data category identified in the recognition phase, the proper decoding program can usually be called. In some cases, however, reference to the text of the bulletin is required. The decoder fulfils two important functions: the specification of the location from which a report is made, and the conversion of a report into database format. The former is accomplished by reference to a directory which relates the encoded station identifier into a geographical location. Reports with invalid station numbers, invalid geographical positions, inconsistent or unreasonable data — a condition which may arise from incorrect encoding or transmission errors — are flagged and are either rejected or directed to an editing position for correction and eventual re-entry into the system.

### 3.3.3 *Quality control of the decoded message data and further checking procedures*

Certain essential phases of quality control should be accomplished at the observing station and by the responsible centres, before transmission via the GTS. The purpose of this quality control and correction is to provide the highest possible reasonable standard of meteorological data before they are distributed to the user. Minimum standards or real-time quality control are given in Volume I, Attachment II-1 to the *Manual on the GDPS*. Methods and rules to be used by the responsible centres are shown separately for surface and upper-air observations and may include:

- (a) Surface observations
  - (i) Consistency in time by comparison with prior observation;
  - (ii) Internal consistency;
  - (iii) Tests against climatological limits;
  - (iv) Tests against physical or absolute limits for quantified parameters;
  - (v) Compliance with WMO code standards (for example, identification, code and format checks).
- (b) Upper-air observations
  - (i) Consistency in the vertical;
  - (ii) Consistency in time;
  - (iii) Tests against statistical limits for quantified parameters;
  - (iv) Tests for physical consistency between related parameters;
  - (v) Tests against absolute limits (for example, wind direction within the range 0-360);
  - (vi) Compliance with WMO code standards (for example, identification, code and format checks).

Efforts must be made to correct all errors and to validate the doubtful data detected by the above methods, both on the source document and or the message to be transmitted, provided that transmission is not delayed. If these efforts cannot be made without causing delay, then the data will be transmitted and corrective action taken at the next stage of quality control. The quality control and data correction procedures applied to data prior to their use in data processing are described in more detail in Chapter 6.

### 3.3.4 *The sorting and formatting of decoded information*

The end product of the preliminary data-processing program is a set of corrected observational data for a certain synoptic hour or for a few (three to six) hours surrounding a synoptic hour, when four-dimensional assimilation methods are used. Within the computer, these data will then be sorted and formatted according to the purpose and scale of analyses for which they are going to be used. Sorting procedures may provide for the rejection of repeated messages as well as for the combination of Parts A and C of separately reported upper-air messages.

The size of the formatted data set will depend on the area from which reports are collected, on the applied cut-off time, and on the quality of the reports.

In operational work, the formatted data sets are used for objective analysis and for compiling bulletins of processed data. The data sets usually remain available in the mass storage of the computer for a certain length of time.

## 3.4 Methods of numerical weather analyses

### 3.4.1 *Purpose*

The fundamental purpose of an automated objective weather analysis is the transformation of meteorological parameters from irregular observational networks to gridded networks for use in numerical analysis and forecast schemes. These meteorological quantities, available at the grid intersections, or in functional or spectral form after the objective analysis is completed, may be used either as input to numerical forecast models, or displayed as synoptic charts of various weather parameters.

As automated analysis schemes use available information systematically, procedures for quality control and meteorological consistency may be built into the system. These procedures include combinations of the manual and automated monitoring of observations as they become available. Most systems also include bogus observations into the database to handle the problem of data sparseness in some regions, particularly the tropical ocean areas.

A final stage is added to standard procedures of analysis when data sets are used to initialize the numerical models. Imbalances between mass and momentum fields excite spurious inertia-gravity oscillations during the forecast. The magnitude of the initial imbalance, therefore, must either be eliminated or reduced prior to the start of numerical forecasts.

The initialization step should also include a technique for overcoming incompatibilities between the numerical model and the analysis scheme. A sophisticated primitive equation model develops its own internally consistent structures which can occur at smaller scales of motion than are resolved by the coarse observational network.

Finally, the analysis scheme and initialization procedure may be included as part of a four-dimensional data-assimilation scheme to handle asynoptic data. The comprehensive discussion of objective analysis can be found in Thiebaux and Pedder (1987) and Daley (1991).

### 3.4.2 *General structure of a numerical weather analysis scheme*

Most operational analysis schemes begin with a first guess for each parameter to be analysed. These initial approximations are located at the grid points and are updated during the analysis by interpolation. The scheme may be two-dimensional using data available on quasi-horizontal surfaces, or three-dimensional using data within a three-dimensional volume of influence.

The first guess grid-point values are usually obtained from a six- or twelve-hour numerical forecast. Geopotential values are obtained directly from the numerical forecast for each grid point at each level to be analysed. Temperatures may be constructed from the predicted values of thickness and the lapse rates. Some models use, however, the inverse technique when the primary variable is temperature and the geopotential is derived from it. Wind components and moisture values are usually obtained directly from numerical forecast or may be obtained by solving some form of dynamic and thermodynamic equation.

After the first guess grid-point values are obtained, the value of the first guess parameter at each observational location is determined. For this task, a simple bilinear, or, at most, a biquadratic, interpolation is performed. The difference between the first guess value and the observed value is then computed:

$$f'_i = F_i - \tilde{F}_i$$

where  $f'_i$  is the difference (or residual) for the  $i$ th observation,  $F_i$  is the observed value, and  $\tilde{F}_i$  is the corresponding guess value of the variable at the same location (Figure 3.3). At this point in the analysis procedure, the observed data may be checked for gross errors. A tolerance that varies with latitude and season is assigned to each variable. Observations are rejected when the value of the residual exceeds the tolerance assigned to it. The tolerances are very liberal, detecting only very obvious errors, thus reducing the risk of rejecting valid reports.

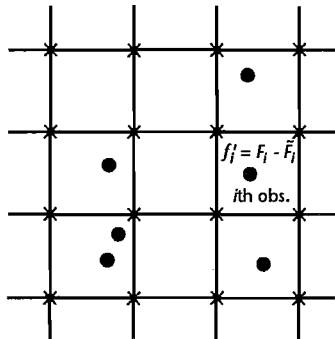


Figure 3.3 – Two-dimensional procedure for obtaining a difference ( $f'_i$ ) between the observed and corresponding guess value at an observation location ( $i$ ). Observation locations are given by (●) and first guess locations (grid points) are given by (x).

Lists of all rejected data may be produced, along with the reason for the rejection. When data are rejected, the monitoring analyst may use existing information to correct the observation, replace the observation with a new report, or substitute bogus values generated by an experienced analyst.

After the observational values have passed quality control checks, an objective numerical analysis scheme updates the first guess values. The updating procedure usually applies pre-calculated weights to the residuals. The manner in which the weights are calculated and applied differs among analysis schemes. Normally, the updating procedure minimizes analysis errors or fits the values of the final analysed field to the observations at each location where data is available.

### 3.4.3 The optimum interpolation technique

The method of optimum interpolation proposed by Eliassen (1954) and later by Gandin (1963, 1969) implies minimization (in the statistical sense) of the mean-square analysis error. The analysed value  $\hat{F}_g$  at each grid point  $g$  is determined by adding a weighted linear sum of the residuals  $f'_i$  to the guess value  $\tilde{F}_g$ :

$$\hat{F}_g = \tilde{F}_g + \sum_{i=1}^n a_i f'_i$$

where  $a_i$  is the weight assigned to the residual of the  $i$ th observation and  $n$  is the number of observations permitted to influence the analysis at grid point  $g$  (Figure 3.4).

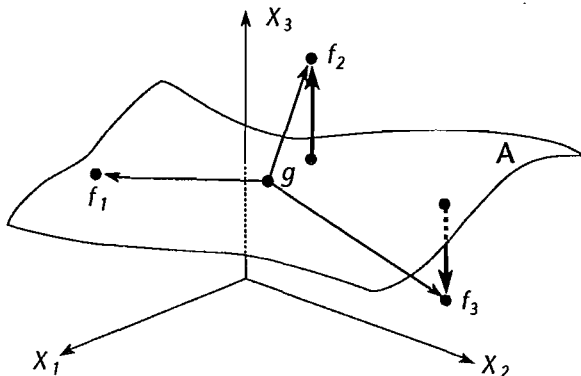


Figure 3.4 – Three-dimensional interpolation to grid point  $g$ , as used in optimum interpolation analysis.  $f_1$ ,  $f_2$  and  $f_3$  are data points (on, above and below the analysis surface  $A$ ) and are connected to  $g$  by position vectors.

The mean-square analysis error  $\overline{E^2}$  at each grid point is given by:

$$\overline{E^2} = \overline{(F_g - \hat{F}_g)^2} = \overline{\left[ F_g - \tilde{F}_g - \sum_{i=1}^n a'_i f'_i \right]^2}$$

where  $F_g$  is the true value of the parameter to be analysed. The statistical optimum interpolation scheme requires that the weights for each grid point be chosen so that the value of  $E^2$  is a minimum. To accomplish this, the expression for  $E^2$  is differentiated partially with respect to each of the  $a_i$  and equated to zero, which yields the following set of  $n$  equations:

$$\sum_{j=1}^n \overline{f'_i f'_j} a'_j = \overline{f'_i f'_g}; \quad i = 1, 2, \dots, n;$$

These linear equations may be solved for the weights  $a'_i$  if the covariances  $\overline{f'_i f'_g}$  and  $\overline{f'_i f'_j}$  can be specified. The quantities are covariances only if the values of  $f'_i$  are zero.

For the computational process it is convenient to express this set of equations in the following normalized form:

$$\sum_{j=1}^n \mu_{ij} a'_j = \mu_{gi}; \quad i = 1, 2, \dots, n;$$

where  $\mu_{ij} = \overline{f'_i f'_j} / (\overline{f'^2} \overline{f'^2})^{1/2}$

$$a'_j = \overline{f'^2} / (\overline{f'^2}) a_j$$

The term  $\mu_{ij}$  is the correlation of the residual at the  $i$ th observational location with that at the  $j$ th location. The term is the correlation between the true residual at the grid point (the quantity to be estimated) and the residual at the  $i$ th observational location. This correlation is a function of location only and depends upon the statistical characteristics of the first guess  $\tilde{F}_g$  as well as the actual field  $F$ . In operational optimum interpolation systems, many simplifying assumptions are made about the nature of the  $\mu$  correlation, and it is represented by an analytical function of the distance between the two locations involved. This assumption implies that the field to be analysed is statistically homogeneous and isotropic which, unfortunately, is not the case with many meteorological parameters. In some mesoscale analyses of meteorological elements near the surface, an anisotropy factor associated with the distribution of land and water is included (Andersson, et al., 1986).

The three-dimensional correlation function is required in optimum interpolation schemes which use observations at levels other than the quasi-horizontal level of the analysis. Three-dimensional correlation functions are approximated by the product of a two-dimensional function of horizontal distance and a one-dimensional function of height difference between the two locations. When the observational error  $\epsilon_i$  is included in the expression for each residual:

$$f'_i = F_i - \tilde{F}_i + \epsilon_i$$

the linear set of optimum interpolation equations becomes:

$$\sum_{j=1}^n (\mu_{ij} + \tau_{ij} \sigma_j + \tau_{ij} \sigma_i + \rho_{ij} \sigma_i \sigma_j) a'_j = \mu_{gi} + \tau_{gi} \sigma_i; \quad i = 1, 2, \dots, n;$$

where  $\tau_{ij} = \overline{f'_i \epsilon_j} / (\overline{f'^2} \overline{\epsilon_j^2})^{1/2}$

$$\rho_{ij} = \overline{\epsilon_i \epsilon_j} / (\overline{\epsilon_i^2} \overline{\epsilon_j^2})^{1/2}$$

$$\sigma_i = (\overline{\epsilon_i^2} / \overline{f'^2})^{1/2}$$

and, as before, the weights  $a'_i$  may be determined provided that the value of the correlation and error variance terms can be specified.

The symbol,  $\tau_{ij}$ , represents the correlation between the true residual at one location and the observational error at another location. This correlation will be non-zero for an observing system that used the same guess field as the analysis scheme. The  $\tau$  correlation is difficult to evaluate and, to date, no one has attempted to determine its structure. All of the operational analysis schemes set the value of  $\tau_{ij}$  uniformly equal to zero.

The correlation  $\rho_{ij}$  is non-zero when the errors between two observations at different locations are correlated. Hollett (1975) has shown that rawinsonde errors in geopotential, temperature, and wind measurements are all correlated vertically to some extent. Errors in satellite temperature measurements from the same orbital pass are usually correlated horizontally (Bergman and Bonner, 1976; Schlatter and Branstator, 1979).

The normalized root-mean-square observational error  $\tau_i$  for each of the observations appears in the equations for determining weights. The observational error is usually a known quantity which has been supplied by the designer of the observing system. It can also be determined by comparison with other observations whose error level is either known or is assumed to be small.

Optimum interpolation as described here may be applied to any scalar field when the correlation and error patterns for that field are known. Geopotential, however, is the only meteorological parameter which nearly meets the restrictive assumptions of homogeneity and isotropy. For this reason, a form of optimum interpolation, termed multivariate analysis (Gandin, 1963), is employed to analyse wind and temperature fields.

Statistical optimization is accomplished in the same manner as univariate optimization, except that the expressions for analysis error in each parameter are minimized simultaneously. A specification of all possible auto- and cross-correlations between the variables analysed is necessary for the determination of the weights.

The wind-field analysis presents a special problem. Calculation of covariances of the wind field is difficult because the wind field is non-isotropic. Usually the geostrophic assumption is used to relate the wind correlations to the height correlations. For example the  $\bar{u}'\bar{z}'$  correlation function becomes:

$$\overline{\bar{u}'\bar{z}'} = -\frac{g}{f_i} \frac{\partial}{\partial y_i} (\overline{\bar{z}_i\bar{z}_i})$$

where the geostrophic relationship has been used. All other correlations involving wind and mass variables, such as  $\overline{\bar{u}'\bar{u}'}$ ,  $\overline{\bar{v}'\bar{v}'}$ ,  $\overline{\bar{v}'\bar{z}'}$ , can be specified in terms of the geopotential correlation function through the geostrophic relationship.

In addition, the correlation function for temperature can be specified in terms of the geopotential correlation through the hydrostatic equation:

$$\overline{T'} = -\frac{g}{R} \frac{\partial z'}{\partial \ln p}$$

where the primed quantities are deviations from the guess field.

A fully three-dimensional multivariate analysis of the mass and momentum field is possible provided that the geopotential correlation functions, error covariances, and observational errors can be specified. However, computer resources usually determine what is done operationally. Lorenc (1981) provides a detailed discussion of a three-dimensional multivariate statistical interpolation method.

#### 3.4.3.1 THREE-DIMENSIONAL VARIATIONAL ANALYSIS

A linear optimum interpolation scheme cannot properly utilize an observed quantity which is related in a non-linear way to the forecast model variables (for example, satellite radiance data to air temperature). One means of coping with the nonlinearity is to use a variational analysis scheme.

Three-dimensional variational analysis is a generalization of optimal interpolation. The analysed fields are chosen so as to minimize a function which measures the deviation from the first guess field and the observations, together with other constraints. The function, sometimes called the cost function, consists of a number of terms, which impose the constraints, and can be written, for example, as follows:

$$J = J(g) + J(o) + J(c) + \dots$$

where  $J(g)$  is a quadratic measure of the difference between the analysis and the first guess field, and involves the covariance matrix of first guess errors;  $J(o)$  is the difference between the analysis and observations, and involves the covariance of observation errors;  $J(c)$  is some measure of the intensity of gravity wave activity, and is included to minimize noise in the forecast. In its simplest form, the variational method reduces to optimum interpolation. However, it is more powerful in its capacity to assimilate non-conventional data types.

#### 3.4.4 Spectral statistical interpolation

The spectral statistical interpolation (SSI) system has recently become operational at the WMC Washington (Parrish and Derber, 1991). The SSI has some similarity to spectral analysis, but differs in the use of background (first guess) and the statistical considerations of optimum interpolation (OI).

The SSI minimizes the same objective function as conventional OI. This function includes analysis increments, forecast error covariance, observational error covariance and a linear transform operator, which converts the analysis variables to the observation type and location.

Compared to the OI analysis there are two principal differences in how SSI approximates the minimum of desired objective function. First, the forecast error is estimated in terms of model (or spectral) variables. In defining the analysis variables, the balanced components of the mass and momentum fields are combined into a single variable. This allows the balance between mass and momentum fields to be implicitly included.

The second principal difference between SSI and OI is that in the former system, all observations are used at once to perform the analysis globally. Because the SSI analysis variables are spectrally defined, the analysis must be solved as a single problem and not approximated locally as is done in OI.

Performing the analysis globally has the advantages of not producing discontinuities in the solution resulting only from data selection and eliminating the need for an expensive procedure of data sorting and selection.

Owing to spectral representation and the linear balance constraint between mass and momentum fields, the SSI result is very different from that which could be produced from OI analysis, for which a mass

observation at the Equator produces no wind correction. Due to the same reasons, the fields resulting from SSI have no need to be initialized.

### 3.4.5 Methods of analysis based on successive corrections

A method proposed by Bergthorsson and Doos (1955) and later modified by Cressman (1960) is flexible and economical in terms of computing resources. This so-called successive correction method is similar to the optimum interpolation method in that weights are applied to observations within a predetermined region of influence surrounding the grid point. However, the weights are specified rather than calculated. To obtain an update to the guess field  $\hat{F}_g$ , the following expression is used:

$$\hat{F}_g = \tilde{F}_g + \sum_{i=1}^n a_i f_i / \sum_{i=1}^n a_i$$

where  $a_i$  are the weights and are usually of the form:

$$\alpha e^{-\beta r^2}, \frac{\alpha}{\beta + \gamma r^4}, \text{ or } \frac{\alpha^2 - r^2}{\alpha^2 + r^2}$$

in which  $r$  is the distance between the observation and the grid point, and the constants  $\alpha$ ,  $\beta$  and  $\gamma$  are determined empirically.

In practice, several scans are carried out, the result from each scan being used as the guess for the next. The weighting function is changed during each scan so that stations at a considerable distance from the grid point have less influence on successive scans, and so that the error control criteria can be made more stringent with each scan. This technique permits the analysis of smaller-scale features during the final scans.

Some improvements in the technique include non-isotropic weighting functions (Marks and Jones, 1977). Meteorological quantities tend to have a higher correlation along the direction of the wind. Hence, the gradient of the wind field can be used to shape the weighting function, elongating it so that the minor axis is in the direction of the gradient.

A similar approach was used by Atkins (1974) in the objective analysis of relative humidity for a fine-mesh model. Here the gradient of the first guess field, obtained from a 12-hour forecast, is used to determine the shape of the weighting function in such a way that elongated features such as fronts in the first guess field are retained in the analysis.

The successive correction technique is flexible and economical. This technique yields excellent results in regions of dense observational data. However, the accuracy of this scheme is poor in regions of sparse or irregularly distributed stations. In addition, it is impossible to incorporate the error structure of the observations as in the optimum interpolation technique.

The disadvantage of most methods of numerical weather analysis is their failure in data-sparse regions, such as the Sahara and the southern Oceans. A recently developed technique may be used with any analysis method to improve the result in these areas. The main idea behind this technique is the updating of the guess field at those grid points that are surrounded by data before updating the guess field at those grid points located in data-sparse regions. The updated grid points may then be used as new stations for the other grid points. The weight of these new grid-point stations should be slightly less than the weight assigned to grid points upgraded with real stations. The grid points should, therefore, be updated according to prescribed priorities:

- (a) The closeness and number of stations surrounding the grid point;
- (b) The number of nearby grid points previously interpolated;
- (c) The closeness to the centre of the domain under analysis.

This technique enables previously interpolated grid points to be used, subject to the aforementioned priorities, as a station for the interpolation of succeeding grid points (Gandin, 1969). The method has achieved promising results in the analysis over the Sahara desert.

### 3.4.6 Methods of analysis based on functional representation

The first scheme for numerical weather analysis was based on the representation of meteorological fields by second-order polynomials (Panofsky, 1949). Since that time, many functional representations have been proposed for purposes of analysis. However, Hough spectral functions (Flattery, 1971) and empirical orthogonal polynomials (Dixon, 1969) have been proposed and used operationally.

All schemes using functional representation minimize analysis error by computing expansion coefficients according to:

$$\overline{E^2} = \left[ F - \sum_{x,y,z} a_{xyz} \phi_{xyz} \right]^2$$

where  $E$  is the root-mean-square analysis error,  $F$  is the analysed field and  $\phi$  represents the function of the spatial coordinates  $x$ ,  $y$ ,  $z$ , which is used to represent the data.

The procedure used to determine the expansion coefficients depends upon the nature of the functions chosen for the representation. The least-squares technique is usually employed to find the set of  $a_{xyz}$  which minimizes the magnitude of  $E$ . The method may solve the coefficient matrix directly, or use an iterative technique

for the solution. When the solution is iterative, a guess set of coefficients is needed to initiate the analysis. These guess coefficients are determined through a decomposition of the first guess field into the functional form that is chosen for the analysis.

Although analysis schemes based upon functional representation are economical in terms of computer resources and yield adequate results in data-sparse regions, schemes of this type do not have the flexibility of other types of objective-analysis methods. The inclusion of observational error structure and magnitude is difficult. In addition, the small-scale features necessary for the initialization of a numerical model are not very well represented by these techniques.

### 3.4.7 Handling of asynoptic data (four-dimensional data-assimilation techniques)

The database currently available to meteorological centres contains observations from many different types of observing stations, including an overwhelming amount of asynoptic satellite data. For the analysis of this huge quantity of data, most large meteorological centres have chosen a technique called four-dimensional data assimilation.

A true four-dimensional assimilation would permit observed data to be inserted into a numerical model whenever the observed report is received at the centre. Primitive equation models interpret new information as local imbalances and respond by producing gravitational oscillations. Therefore, most operational systems are designed to assimilate the observations in a three-step procedure: analysis, initialization, and forecast. The process is repeated every six or twelve hours. Asynoptic data are extrapolated to the nearest analysis time and assigned a proper error depending upon the time and quality of the observation. Some GDPS centres use the continuous data assimilation procedure.

The success of assimilation depends on getting accurate and consistent information into the model. For example, the satellite-derived soundings have been shown to have errors correlated in both space and time and thus gradient information may be more reliable than the absolute values. In this connection, a variational method has been developed to assimilate temperature and moisture gradient information from satellites into a NWP model (Cram and Kaplan, 1985). Discussion of direct use of satellite sounding radiances in numerical weather prediction can be found in Eyre and Lorenc (1989). At present, approaches to assimilation of information from the perspective data sources, such as wind profilers, are being developed. It should also be noted that assimilation of more data from conventional observations (data on clouds, precipitation, visibility, snow depth, surface state) is performed in mesoscale NWP models, in particular (Wright and Golding, 1990).

Four-dimensional analysis has been used extensively within the framework of the conventional synoptic observation system. Weather services have long based their analysis not only on synoptic data for the time of the analysis, but also on the fields predicted from the previous observation hour and valid at the time of the analysis. Consequently, the analysis depends upon past as well as present data, and the added information improves the quality of the analysis. A schematic example of four-dimensional intermittent assimilation is given in Figure 3.5.

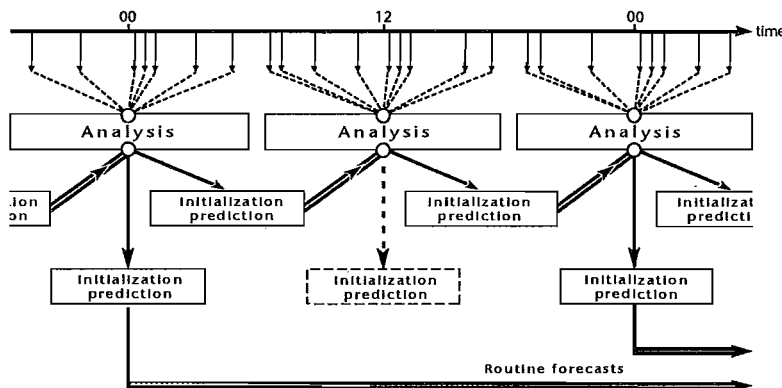


Figure 3.5 – A schematic example of a four-dimensional intermittent assimilation scheme.

Recently, methods allowing explicitly for the variation in time of the analysis variables have been under active investigation (Courtier and Talagrand, 1987, 1990; Pailleux, 1989). A number of different formulations of four-dimensional assimilation are being considered. The evolution of the model variables may be modified or nudged so that they tend towards an observed value at a particular time (the total model evolution is chosen so as to minimize its deviation from a set of observations over a time span). This may be done by a four-dimensional variational analysis using the adjoint equation technique. Here the goal is to find a model trajectory which agrees reasonably with the observations available in an assimilation period ( $T_o, T_f$ ) and also fits the forecast valid at  $T_o$ , the first guess. The trajectory is determined by the vector  $X(o)$  of initial values. To solve this problem, the model must be integrated forward from  $T_o$  in order to compare the model state  $X(t)$  with the observations. Then the adjoint model is integrated backwards to  $T_o$  in order to find the gradient of the cost function with respect to  $X_o$ .

Four-dimensional assimilation schemes are rather expensive in terms of computer resources, as they require several iterations of forward-backward integration, and since the full model trajectory must be stored.

The variational analysis using the adjoint equation technique is a powerful scheme which fully allows for the variation in both space and time of the meteorological parameters, but it involves an assumption that the evolution predicted by the model is exact. That is, model error is not taken into account in the method.

An alternative means of four-dimensional assimilation, based on Kalman filtering, has been suggested (WMO, 1991). In this method, the state of atmosphere is specified by some vector  $X$ . The evolution of  $X$  is governed by a vector difference equation, involving a transition matrix and an error term. Forecast error arises through omission of this term. Observations are related to the true state through a matrix equation with a further error term. The analysis process consists of modifying a forecast by terms proportional to the difference between forecast and observed values. Recursion equations for the model and analysis error covariance matrices can be derived by making reasonable statistical assumptions about the unbiased nature of the model and the observation errors. An expression for the gain matrix, used in the analysis, may also be obtained. It ensures an optimal estimate of the true atmospheric state on the basis of observations. The crucial aspect of Kalman filtering is that forecast error covariance is calculated in a manner consistent with the model dynamics. This method is, however, expensive from a computational point of view.

The three components of the data assimilation system are not independent of one another. Meteorological parameters must be delivered to the numerical model in the coordinate framework of the model, with a prior knowledge of the model's internal dynamics. A specification of the distribution of forecast error is essential because the analysis step uses the model's numerical forecast to obtain the first guess field. Hence, each component of the analysis-initialization-forecast system must be designed with careful consideration of the structure and numerical techniques employed by the other components of the system.

### 3.4.8 Initialization

Initialization is the process of adjusting the data prior to a model integration so that the forecast shows a minimum of noise (the high-frequency transient behavior).

Many initialization procedures have been developed since the introduction of primitive equation models in the late 1950s. The removal of high frequency gravitational modes induced by initial imbalances between the mass and momentum field has been the basis of a considerable amount of research. Bengtsson (1975) has reviewed many of these techniques in which some form of balance between the observed mass and wind field is attempted.

The methods can be classified into two categories: static methods, in which diagnostic constraints are applied to the initial values, and dynamic methods, in which the numerical model itself is integrated forward and backward around the initial time until some form of balance is achieved. A method developed in the 1970s, called non-linear normal mode initialization, contains elements of both the static and dynamic methods. Depending on the exclusion or inclusion of diabatic processes into initialization schemes these will be classified as adiabatic or diabatic. In the first case, the initial state is adjusted to keep the mass and wind fields in balance, while in the second case, the effects of diabatic atmospheric processes are incorporated into an adjustment procedure.

#### 3.4.8.1 STATIC INITIALIZATION

Early static methods were based on a solution of the linear or non-linear balance equation (Houghton and Washington, 1969; Benwell and Bretherton, 1968) which required that the wind field be determined by the mass field at mid-latitudes. However, this technique cannot produce a divergent wind component, which must be included to inhibit the onset of inertia-gravity modes (Phillips, 1960).

An attempt to provide the divergent wind component through a solution of the quasi-geostrophic omega equation for a global scheme was suggested by Houghton, *et al.* (1971). In this experiment, the desired balance between the mass and momentum field was not achieved without severe modification of the initial analysed mass field. However, this scheme was used successfully at the RSMC Bracknell (Benwell and Bretherton, 1968). At the WMC Washington, the Shuman and Hovermale (1968) model was initialized with analysed geopotential heights, with non-divergent winds implicitly balanced through the analysis procedure (Cressman, 1960 and later, Flattery, 1971), and with the divergent wind component from a 12-hour forecast by the same model. However, neither of these schemes yielded a completely satisfactory solution to the problem.

Another static initialization technique based on a variational approach was proposed by Sasaki (1970) and Stephens (1970). Here, the accuracy of the mass and wind field was predetermined and the two fields were permitted to adjust mutually within a balanced constraint. Phillips (1977) added the hydrostatic equation as another constraint to formulate a variational method for baroclinic systems.

#### 3.4.8.2 NORMAL MODE INITIALIZATION

An exceptionally powerful and economic technique for initialization purposes started to be developed in the 1970s.

In many contexts, waves are quasi-linear phenomena. It had been known for a long time that one class of solutions to the linearized primitive equations described internal-gravitational waves. Dickinson and Williamson (1972) used that knowledge to define an initialization scheme which attempted to filter high frequency waves from a model initial condition. They produced a balanced field by projecting the initial fields onto the normal modes and then setting the coefficients of inertia-gravity modes equal to zero. This procedure completely eliminates the growth of high-frequency gravitational oscillations in a linear forecast model because

there is no mechanism in the model for generating these oscillations if the mass and momentum fields are initially in balance. This method has since been called linear normal mode initialization. It was not very successful because spurious oscillations were generated by non-linear interactions during the integration.

Non-linear balance equations were first described in terms of normal modes by Machenhauer (1977) and Baer (1977). Machenhauer considered the prognostic equations for amplitudes of gravitational modes, and showed that with or without initialization, the adiabatic non-linear forcing term has a strong, slowly varying component. This yields a correspondingly slow response, which approximately satisfies a non-linear balance equation expressed in terms of normal mode amplitude and their forcing. He proceeded to show how solutions to this new balance condition could be determined and applied to the initialization problem. Working with a barotropic spectral model, he performed a non-linear normal mode initialization (NNMI) by setting the time tendencies of initial gravity mode coefficients equal to zero rather than the amplitude of the coefficients themselves. Baer applied a Rossby number scaling to the primitive equations, schematically expressed in terms of the normal modes, and explicitly considered the presence of multiple time scales. He showed that asymptotically slow solutions were possible, and that these solutions were characterized by a non-linear balance condition expressed in terms of the normal modes. The non-linear normal mode technique produces a divergent wind component and eliminates gravity wave oscillations.

Since Machenhauer's original work on initialization, several variations for spectral and grid-point models have appeared. Bourke and McGregor (1983) developed a NNMI scheme which only considered explicitly the vertical structures of the modes, resulting in a simpler application of NNMI to limited-area models for which horizontal mode structures were more difficult to determine. Temperton (1988) presented an elegant mathematical demonstration of the equivalence of the Bourke and McGregor method with that of Machenhauer applied to the same model. He termed those schemes which use only the vertical structures as implicit NNMI (INNMI) schemes, contrasted with explicit schemes which require determination of the modes' complete three-dimensional structures.

Many other initialization methods have been developed since the advent of NNMI. A good review can be found in Daley (1981, 1991), Machenhauer (1983) and Errico (1989).

#### 3.4.8.3 DYNAMIC INITIALIZATION

None of the static initialization techniques have been completely successful in eliminating the spurious oscillations in non-linear models. Nevertheless, all of the methods do reduce the amplitude of the unwanted modes to some degree. For a more complete solution, researchers have developed several dynamic initialization techniques in which some form of the numerical model is used for initialization.

In one type of dynamic initialization, the numerical model is integrated forward and backward around the initial time (Nitta and Hovermale, 1969; Miyakoda and Mayer, 1968; Temperton, 1976) with an integration scheme which selectively damps the high-frequency oscillations. The mass and momentum fields are permitted to adjust mutually while the integration about the initial time is in progress. It is also possible to allow the wind field to adjust to the mass field by restoring the mass field during each time step. Another initialization method is possible through scale decomposition in a spectral model where the forcing can proceed in accordance with adjustment theory — wind to mass for long waves and vice versa for short waves.

Temperton (1976) showed that a forward-backward scheme can remove the highest frequency external gravity mode. As the amplitude damping provided by the time integration scheme is only frequency dependent, it becomes virtually impossible to separate the large-scale inertia-gravity modes from the small-scale Rossby modes. Moreover, irreversible processes cannot be incorporated into forward-backward schemes without resorting to the adoption of empirical techniques.

In addition to the disadvantages mentioned above, forward-backward initialization schemes are expensive to implement. Each iteration is equivalent to one mode time-step and many iterations are required to achieve a satisfactory balance. For these reasons, forward-backward schemes have not been used in operational weather-forecast systems.

#### 3.4.8.4 DIABATIC INITIALIZATION

Despite continuous progress made during recent years, numerical weather prediction models are still plagued by a slowness to forecast appropriate amounts of precipitation during the first few hours of integration. This is the so-called "spin-up" problem of condensation and precipitation, which can be defined as the persistence of deficient latent heating during the first few hours of integration.

The frequent exclusion of the existing condensation activity at initial time leaves out a significant heat source affecting the adjustment between the mass and flow fields. Tarbell, *et al.* (1981) found that latent heating dominates this balance in stratiform precipitation of mid-latitude cyclones.

The inclusion of observed latent heat sources with a consistent higher-resolution moisture analysis are critical components in reducing the underestimation of initial divergence. Around 1980, the first numerical weather prediction models incorporating initial latent heating based on the observed precipitation rates (often with re-analysed moisture) were developed. The incorporation of latent heating effects has been carried out in the framework of static (Tarbell, *et al.*, 1981; Salmon and Warner, 1986; Werden, 1988; Turpeinen, *et al.*, 1990) and dynamic (Danard, 1985; Ninomiya and Kurihara, 1987; Wang and Warner, 1988) initializations. The suggested approaches differ in their choice of source for the precipitation measurements and of the feedback method used to link the observations to the model equations. If the dynamic initialization technique is used, then the model

has to be run for a few hours (often ahead of the initial time) to create appropriate heating rates. In static initialization, prescribed latent heating rates are incorporated during the first few time steps of the actual forecast or during the initialization if the NNMI technique is used.

The numerical experiments and operational use of diabatic initializations (Puri and Miller, 1990; Krishnamurti, *et al.*, 1991) showed that they drastically reduce the spin-up giving realistic vertical motions from the very beginning of the integration. The rain rates continued to remain deficient for the first few time steps.

Until now, diabatic initialization has been applied mainly to mesoscale and limited area models, since precipitation rate estimation on the global scale presents more problems than over populated areas, where rain rates can be inferred not only from satellite data, but from radars and rain gauges as well. The problem on the global scale can be partially solved by the use of a model to predict rainfall in the procedure of diabatic initialization (as it is done, for example, in the ECMWF model).

#### 3.4.8.5 COMBINED INITIALIZATION TECHNIQUES

Some combined initialization techniques have been developed recently. A combination of normal mode and dynamic initialization has been used by Sugi (1986). It diminishes the earlier drawbacks of dynamic initialization and permits the incorporation of diabatic processes into the initialization scheme.

The combination of non-linear normal mode initialization with a variational procedure has been suggested by Daley (1978) and extended later by Fillion and Temperton (1989) and Fillion (1991). The major advantage of this approach is that it allows for the mutual adjustment of the wind and mass fields based on the presumed accuracy of the observations, yields a divergent wind component, and eliminates high frequency oscillations from the integration. It also allows the user to adjust, within limits, the wind to mass or vice versa. The variational generalization of the non-linear normal mode technique gives the user much greater control over the adjustment process and allows the optimal use of the data. It is expensive in terms of computer time, but it was shown by Fillion (1991) that a variational extension of implicit normal mode initialization is feasible at a reasonable cost with present day computers.

### 3.5 Numerical weather prediction (NWP) methods

Operational numerical weather prediction is based upon theoretical models of the atmosphere. According to the formulation of momentum, mass conservation and state equations these models may be subdivided into hydrostatic filtered and primitive equation (PE) models and non-hydrostatic models based on anelastic or elastic (fully compressible) equations. The models of the first class are used for simulation of the large-scale atmospheric motions, in which the horizontal scale is much greater than the vertical one. The non-hydrostatic models, taking into account vertical accelerations, are used for simulation of mesoscale atmospheric systems with comparable scales in vertical and horizontal directions. Depending on the inclusion of energy sources (sinks), the models may be classified as diabatic or adiabatic. At present, diabatic hydrostatic PE models dominate in operational NWP, though recently non-hydrostatic models have been introduced into operational practice to prepare more detailed short-range weather predictions over limited areas (Kiselnikova, *et al.*, 1987; Golding, 1990).

In regard to the computational techniques for solving the governing differential equations, the models used may be subdivided into finite-difference and spectral classes. At the present time, the spectral models dominate in the NWP on global and hemispherical scales, while limited area NWP models mostly use finite difference techniques.

#### 3.5.1 General characteristics of current NWP models

Numerical weather prediction has undergone dramatic changes during the past decade to keep pace with the explosion of new computer applications and technologies. Major trends in the development of NWP models are mentioned briefly here. In the field of atmospheric modelling on the large scale, there is a trend to expand from a hemispheric to a global domain with a parallel increase of resolution in both the vertical and horizontal grid. This has been accompanied by the introduction of more sophisticated procedures for parameterizing atmospheric physics. These factors have led to a steady growth in numerical prediction skill. For example, the skill of surface pressure predictions for three days ahead was the same in 1990 as it was 15 years before for one day ahead. The lead time of useful NWP has increased during the last 20 years from three to seven days in the extra-tropical latitudes of the northern hemisphere. Experiments on 30-day extended range predictions have been performed and are continuing in some major GDPS centres.

In the field of numerical weather prediction over limited areas, the tendency has been practically the same as on a global scale, i.e. an increase of spatial resolution (up to 10–15 km in the horizontal grid), and the introduction of more sophisticated physics which permits direct numerical prediction of such meteorological elements as surface wind and temperature, precipitation, and visibility. The tendency emerging here is the development of very fine mesh models covering relatively small regions, providing detailed short-range weather predictions. A change from PE-hydrostatic models to non-hydrostatic models has started in the field of mesoscale weather prediction. Experience in the operational running of very fine mesh models has shown that they provide better short-range predictions of intense atmospheric systems and highly variable meteorological elements, such as clouds and precipitation.

Most large meteorological centres have several numerical models at their disposal to meet the needs of forecasting on different time scales. These are global (hemispheric) and limited area (regional and/or mesoscale).

Medium-range (four to 10 days) numerical predictions are usually produced from global model forecasts. At present, such global models have fairly complete parameterizations of subgrid-scale effects. Already the horizontal resolution of such models is better than 100 km, with as many as 30 layers in the vertical.

Short-range numerical forecasts are produced with a combination of limited-area models and statistical models. The domain size of limited-area models and statistical models varies from the continental scale ( $\approx 10^8 \text{ km}^2$ ) down to the regional (country) scale ( $\approx 10^6 \text{ km}^2$ ) depending upon the range of applications and the available computer resources. Lateral boundary values are either obtained from a previous forecast produced by a large-scale model, or from a forecast made by a model running concurrently. The lateral boundary condition may be one-way interactive whereby no information is passed to the large-scale model, or two-way interactive whereby information is passed back and forth between the two models. The grid of the limited-area model may be fixed relative to the grid of the large-scale model or may move during the integration period. For example, in a limited-area hurricane-track prediction model used at the WMC Washington (Hovermale, *et al.*, 1977), the limited-area grid moves according to the speed and direction of the storm, keeping the position of the storm vortex near the centre of the fine-mesh grid.

The parameterization of subgrid-scale effects is most sophisticated in limited-area models because the meteorological events being predicted have a short life-span and can appear at these scales. The limited-area model is usually run first in the daily or twice daily operational cycle because it provides more timely forecasts for short-range guidance.

Output from limited-area models, in addition to creating the usual synoptic charts, may provide information for statistical models. As numerical models do not always forecast the quantities necessary for a public weather forecast directly, statistical models have been developed to provide objective forecasts of weather elements, such as maximum and minimum temperature, probability of precipitation, and cloud amount. The output from statistical models may appear as completely automated computer-worded forecasts if the computer resources and software are available.

As far as the operational aspects are concerned, models differ in their operational characteristics (time needed for integration, complexity of computation), in the numerical procedures used, and in the output products which become available. Operational schedules demand that the numerical models be reliable, consistent and trouble-free. For this reason, many recently developed parameterization schemes and numerical techniques do not appear in operational models. All new schemes should undergo a trial period before they are implemented operationally.

More detailed information on the nationally- or internationally-developed operational numerical weather prediction systems may be found in the WWW Technical Progress Reports on the Global Data-processing System, which are compiled annually by the WMO Secretariat from national contributions. Normally, these publications contain contributions from about 30 countries and international organizations providing information on the world-wide state of operational NWP.

Information on the state of operational NWP systems in 21 countries and ECMWF in 1991 can be found in the first report of this series (WMO, 1992).

### 3.5.2 Numerical techniques

Strictly speaking, the heading numerical technique would imply a discussion of the methods of discretization and numerical solving of the governing differential equations. However, some additional numerical problems which arise can be discussed, for example, what kind of coordinates to use, and how to handle the physical processes which cannot be resolved by the computational grid. Aside from the purely numerical integration techniques, these important topics will also be discussed below. The following discussion is subdivided into three general headings: vertical coordinate schemes, parameterization schemes, and integration schemes.

#### 3.5.2.1 VERTICAL COORDINATE SCHEMES

Several vertical coordinate techniques are available. It is crucial that the functions or variables chosen for the vertical coordinate be monotonic functions of height above mean sea-level. The transformation from height to any general vertical coordinate is discussed in detail by Kasahara (1974). Some vertical coordinates which have been used are height above mean sea-level, hydrostatic pressure, potential temperature, and sigma — a scaled pressure variable. Mixed coordinate systems have been considered and adopted.

Height and pressure have an advantage over other coordinates because the pressure gradient force is then contained in one term. However, when topographic features are included, height and pressure coordinate surfaces intersect the Earth and cause problems at the lower boundary of the model. Consequently, the terrain requires special lower-boundary conditions to determine horizontal derivatives.

Potential temperature has been used for the vertical coordinate in several numerical models (Eliassen and Raustein, 1968; Bleck, 1974; Uccellini, *et al.*, 1977; Deaven, 1976). The equations governing adiabatic, inviscid, hydrostatically balanced fluid flow become deceptively simple when written in isentropic coordinates. The major advantage of isentropic coordinates occurs because the vertical velocity is a function only of diabatic heating, eliminating the need to compute the dynamic vertical velocity. In addition, the vertical resolution is a function of static stability, giving increased vertical resolution automatically in regions of high static stability.

As with pressure and height surfaces, potential temperature surfaces intersect the Earth causing lower-boundary problems. Also, superadiabatic regions, which occur in thin cloud layers and near the Earth's surface, cannot be mapped into isotropic coordinates. For this reason, primarily, isentropic coordinates have not been used in operational prediction models.

The sigma coordinate, a transformed pressure coordinate, is:

$$\sigma = \frac{p}{p^*} \text{ or } \sigma = \frac{p - p_T}{p^* - p_T}$$

where  $p^*$  represents surface pressure and  $p_T$  is the pressure at the top of the model. This coordinate was suggested by Phillips (1957) to overcome problems caused by intersections of coordinate surfaces with the Earth's surface. This transformation makes the Earth's surface a coordinate surface eliminating coordinate intersections. As coordinate surfaces are no longer horizontal, the pressure gradient force now contains two variables accounting for the slope relative to a pressure surface. These two variables contain hydrostatic components which must be set up so that they are equal and of opposite sign in order to obtain a correct pressure gradient force.

Other representations have been suggested for the vertical coordinate (Washington and Williamson, 1977; Perkey, 1976) making it a function of height similar to the sigma coordinate function of pressure. The same problems in computation of the pressure gradient force nevertheless remain.

As the lower-boundary condition is simplified in transformed coordinate systems, sigma has become the vertical coordinate chosen for most operational prediction models. Special consideration (Brown, 1974) in the calculation of the hydrostatic equation helps reduce errors related to the accuracy of the pressure gradient force. The hydrostatic extraction scheme of Chen, *et al.*, (1987) reduces the errors associated with vertical discretization by formulating the model in terms of deviation from a reference atmosphere.

As a generalization of the sigma vertical coordinate, Mesinger (1984) and Mesinger, *et al.* (1988) proposed the so-called eta coordinate using a step-like mountain representation. In contrast to the sigma coordinate, the coordinate surfaces of the eta coordinate are quasi-horizontal. In addition, the eta coordinate preserves the simplicity of the lower boundary condition of the sigma system. A year's test of a high resolution meso-alpha scale prediction model using this coordinate system showed that it can be used for operational applications (WMO, 1991).

### 3.5.2.2 PARAMETERIZATION SCHEMES

The numerical solution of the hydrodynamic equations on a finite grid places a limit on the scales that can be resolved by using the numerical model. Many boundary-layer processes, such as the exchange of heat, moisture and momentum with the Earth's surface, and convective, radiative and microphysical processes in the free atmosphere, occur on too small a scale to be resolved by the grids of operational prediction models. Grid-point variables in large-scale prediction models are area-averaged quantities. Subgrid scale events must be determined from these area-averaged quantities. This process is called parameterization.

#### *Parameterization of atmospheric turbulence*

Figure 3.6 shows the schematic cross-section of the atmosphere differentiated according to the methods of turbulence representation in the vertical direction. The most universal element of this structure is the surface layer (SL). This layer is particularly characterized by a daytime unstable stratification whose depth can exceed 100 m. The SL thickness decreases to 10 m and less during night-time stable stratification (Wyngaard, 1985). From the view of hydrodynamic representation, the similarity theory is the most commonly used parameterization method for the SL. In contrast, the so-called K-parameterizations dominate over similarity theory in the transitory (or Ekman) layer and in the free atmosphere aloft. The internal layers with their own parameterizations can be identified within the surface layer, as Figure 3.6 shows.

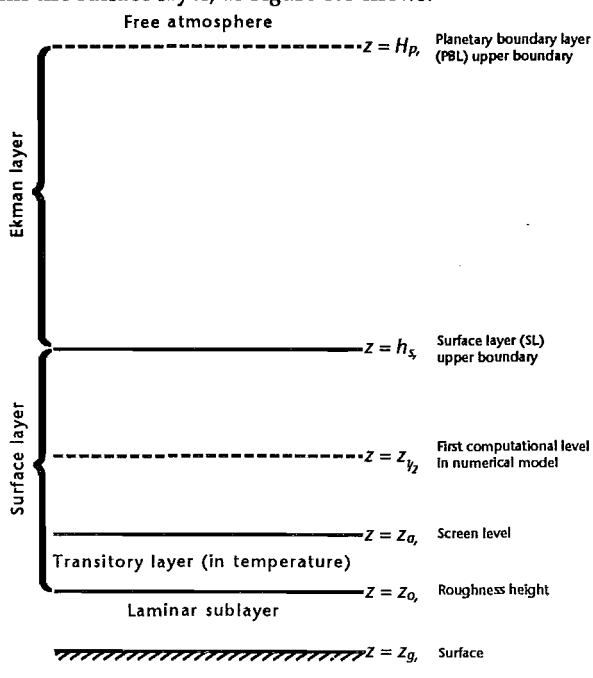


Figure 3.6 – Atmospheric cross-section.

The laminar sublayer, with the domination of molecular viscosity is placed between the ground level  $Z_g$  and the roughness height  $Z_o$ . It is supposed that this sublayer does not affect velocity and pressure distribution. In other words  $U = V = W = O$  and  $p(Z_o) = p(Z_g)$ . The laminar sublayer is accounted for in the temperature and moisture distribution by making use of formulae relating these variables at the  $Z = Z_g$  and  $Z = Z_o$  levels. The laminar sublayer is usually included in more detailed mesoscale models. The need for a relationship between temperature  $T$  and humidity  $q$  at  $Z = Z_o$  and  $Z = Z_g$  is caused by the formulation of heat and moisture budgets at the surface in terms of  $T(Z_g)$  and  $q(Z_g)$  and by the expression of sensible heat and moisture fluxes in the SL, according to similarity theory, in terms of  $T(Z_o)$  and  $q(Z_o)$ . Otherwise the system of equations is unclosed.

The roughness height  $Z = Z_o$  characterizes the terrain aerodynamic properties and varies from 0.001 cm (flat surface) to 1–3 m (urban areas with high buildings). Over sea,  $Z_o$  can be obtained from the Charnock (1955) formula. Over land,  $Z_o$  values can be obtained from tables or diagrams constructed with the use of experimental data.

The reference level  $d$ , called the zero-plane displacement, is introduced additionally to  $Z_o$  in the presence of a tall canopy. This parameter's value depends on the canopy type and can be obtained from tables, diagrams and empirical relations. For tall plants, the  $d$  value is usually confined between 50 and 100 per cent of the full height of the plants and varies from several centimetres (grass) to 20 m (tall forest) (Oke, 1978). Normally,  $d$  is several times larger than  $Z_o$ . On average  $d = 4 Z_o$ . Moreover,  $Z_o$  is counted from the  $Z = d$  level if  $d$  is taken into consideration. The equivalent height ( $Z - d$ ) is used then instead of  $Z$  in relations for universal functions in the computation of surface fluxes. According to Hicks, *et al.* (1979), the zero-plane displacement, like roughness, should be different for each of the momentum, heat and moisture fluxes.

The computation of turbulent fluxes in the surface layer is based, in most operational models, on the Monin-Obukhov (1953, 1954) similarity theory, according to which:

$$\overline{u_i u_3} = -C_D(u^2 + v^2)^{1/2} u_i; \quad C_D = 1/\varphi^2$$

$$\overline{f' u'_3} = C_H(u^2 + v^2)^{1/2} \Delta f; \quad C_H = 1/(\varphi\psi); \quad f = T, q$$

and the scales  $u_*$  (friction velocity),  $T_*$  (temperature flux) and  $q_*$  (moisture flux) are equal to:

$$u_* = K_o (u^2 + v^2)^{1/2}/\varphi$$

$$f_* = K_o \Delta f/\psi, \quad f = T, q$$

Here, the Einstein summation convention for indices is assumed.  $\Delta f$  is a difference between  $f$  values at the  $Z = Z_o$  or  $Z = Z_a$  level, and at a given  $Z$  level, which will be denoted as  $Z_{1/2}$ , while  $\varphi$  and  $\psi$  are the universal functions of the two non-dimensional parameters  $Z_{1/2}/Z_o$  ( $Z_{1/2}/Z_a$  for  $T$ , according to Blackadar, 1979) and  $\zeta$ . At a given  $Z_{1/2}$  the value of the first parameter is obtained directly. The value of the second parameter,  $\zeta = Z_{1/2}/L$  ( $L$  is the Monin-Obukhov length scale) should be found as a solution of the equation:

$$\zeta = R_{l_B} \frac{\varphi^2}{\psi}, \quad R_{l_B} = g Z_{1/2} \Delta T / [(u^2 + v^2) T]$$

where  $u$ ,  $v$  and  $T$  ( $R_{l_B}$  is the bulk Richardson number) are computed at  $Z = Z_{1/2}$ . Different analytic formulations of the  $\varphi$  and  $\psi$  functions can be found in numerous publications.

The original method neglects the contribution of atmospheric water stratification into turbulence generation. Inclusion of this factor transforms the relation for  $\zeta$  as follows:

$$\zeta = R_{l_B}(1+I) \frac{\varphi^2}{\psi}; \quad I = 0.61 q_* T / T_* = 0.61 T \Delta q / \Delta T$$

The approach described above currently dominates the computation of surface eddy fluxes in NWP models.

Parameterizations based on aerodynamic properties are also used in numerical models, such that:

$$\overline{u_i u_3} = -C_D/V/u_i,$$

where  $C_D$  is an empirically determined drag coefficient (Cressman, 1960). This class of parameterizations in the surface layer is economical in terms of storage and computer time. However, no resolution of the boundary layer structure is possible with these techniques. Therefore, important processes such as the turning of the wind towards low pressure near the Earth's surface are neglected.

There is much more variety in both the formulation and approach to turbulence above the surface layer. K-parameterization is, currently, the dominant approach in NWP models. The K-parameterization approach expresses turbulent stresses and fluxes by using exchange coefficients. All K-parameterizations can be divided into three categories: (a) empirical one-dimensional formulations adjusted to experimental data; (b) formulations which can be argued from the three-dimensional system of equations for the second moments; (c) hybrid approaches, i.e. methods of the first category improved by considering equations for second moments and category (b) methods modified heuristically.

Empirical K-parameterizations consider the vertical stresses and fluxes only, suggesting that:

$$\overline{w'f'} = -K \frac{\partial f}{\partial z}$$

One of the comprehensive reviews of these parameterizations has been made by Blackadar (1979).

The eddy exchange coefficient  $K$  in this formula is obtained from the variables included in the NWP model and their derivatives. These are usually relations of the type:

$$K = \ell^2 (u_z^2 + v_z^2)^{1/2} f(R_i)$$

$$R_i = \frac{g}{\theta} \frac{\partial \theta}{\partial z} / (u_z^2 + v_z^2)$$

where  $\theta$  is potential temperature, and  $u$  and  $v$  are wind components. These relations can differ both in the shapes of the  $f$ -function and the turbulence scale  $\ell$ , characterizing the scale of energetically dominating eddies.

A principal disadvantage of the aforementioned approach consists of its one-dimensional nature which discounts the contribution of horizontal gradients (in velocity, temperature and moisture) to turbulence. Meanwhile in many cases (atmospheric fronts, squall lines), horizontal shear is as important as vertical shear. Scale analysis leads to the conclusion that horizontal diffusion becomes important at a grid size of 30 km and less (McBean, *et al.*, 1979).

The adequate simulation of three-dimensional turbulence requires the application of second moment equations. This approach is rather expensive in terms of computer resources and is used mainly in research. It is assumed in this parameterization, that the eddy viscosity coefficient for momentum  $K_m$ , and the exchange coefficients for the scalar variables  $K_f$  are proportional to  $E^{1/2}$  ( $E$  is turbulent kinetic energy):

$$K_m = c_1 \Delta E^{1/2}, \quad K_f = c_f K_m$$

The constant  $\Delta$  is a grid scale. It is similar to the turbulence scale  $\ell$  in the empirical parameterizations and depends on the grid size. The turbulent kinetic energy  $E$  is proportional to the square of the total deformation:

$$E = c^2 \Delta^2 \text{Def}^2, \quad \text{Def}^2 = D_{ij} D_{ij}$$

where  $D_{ij}$  is the deformation tensor. The coefficients  $c$ ,  $c_1$  and  $c_f$  in this parameterization are constant and vary with different models. The above parameterizations are justified if the scale of parameterized eddies lie in the inertial range. This limits the computational grid size to 50–100 m. Therefore more recent studies have been devoted to the development of a generalized method which would be valid for larger spatial scale averaging.

One such generalization consists of the introduction of the full energy evolution equation for subgrid turbulence kinetic energy instead of the diagnostic relation mentioned above. Both this, and the diagnostic parameterization, can be considered as simplified versions of Yamada and Mellor's (1975) level 2.5 turbulence model in the context of the conception of subgrid turbulence. It should be acknowledged that sufficient progress in turbulence parameterizations has been achieved, based on the 2.5-level model and its simplified versions (Yamada, 1983; Holt and Raman, 1988). However, there are still problems to be solved. The 2.5-level model gives relations for all the stresses and fluxes. However its application to horizontal stresses and fluxes is not rigorously justified, because the model neglects most anisotropic effects. Due to the physical anisotropy of turbulence and the large differences in the grid sizes in vertical and horizontal directions, most operational NWP models separate eddy viscosity in the vertical and horizontal planes and treat the vertical viscosity along the aforementioned lines, and horizontal viscosity mainly according to computational considerations. More detailed information on the processes within a boundary layer and their parameterization can be found in Stull (1988), Sorbjan (1989) and Garrat (1992).

#### *Parameterization of convection and microphysics*

The spatial and temporal resolutions of existing NWP models at the present time do not permit the explicit treatment of convective processes and detailed cloud and precipitation microphysics. In reference to clouds and precipitation, the processes are usually separated into two classes: large-scale condensation and consequent cloud and precipitation formation which are resolved by the computational grid, and convective scale clouds and precipitation which are not directly resolved by NWP models.

Though a number of cloud and precipitation models with detailed representation of microphysics have been developed by now, their use requires enormous computational resources because both the number of variables and the computational load increase substantially. In view of this, highly simplified approaches to cloud and precipitation modelling are generally used in large-scale models.

The following major hypotheses are normally used in the modelling of grid-scale clouds and precipitation. The evolution equation is treated for a single moisture variable, which represents both the water vapour and liquid (ice) phases of atmospheric water. The second simplified hypothesis, which is used commonly in prognostic models, postulates that water vapour condensation and cloud water evaporation take place instantly, and that the supersaturation state does not exist. The cloud and precipitation are evaluated diagnostically. In the simplest approach, all excess over saturation is treated as precipitation, which falls out instantly. In most current large-scale NWP models, the process of evaporation of precipitation along its trajectory from the source area to surface is included. A discussion of the approaches to cloud and precipitation representation in NWP models can be found in Sundqvist (1978) and ECMWF (1985).

More sophisticated parameterization procedures have been introduced recently for short-range mesoscale models (Golding, 1984; Veltishchev, *et al.*, 1982). As a result of their coalescence and the evaporation of precipitation in unsaturated areas, the growth processes of the hydrometeor can be accounted for in the simplest way by using a Kessler-type (1969) parameterization. This parameterization involves three processes: the aggregation of small cloud droplets to the sizes when gravitational sedimentation appears, the coagulation of cloud particles with raindrops, and rain evaporation in unsaturated areas.

The original Kessler parameterization allows for clouds and precipitation in the liquid water phase only. It was later extended, and presently there are a number of parameterization schemes which also include cloud and precipitation in the ice phase (Tripoli and Cotton, 1982; Lin, *et al.*, 1983; Rutledge and Hobbs, 1983; Sergeev, 1983). These parameterizations require at least one additional evolution equation for precipitation. Since the demand for computer resources in such parameterizations is rather modest, they are used in some mesoscale operational models.

Convection transforms the spatially-averaged meteorological fields by the vertical transport of heat, moisture and momentum as well as by heating (cooling) occurring due to phase conversions of atmospheric water. It also produces substantial amounts of precipitation, particularly in low latitudes and in the summer in the extra-tropics. The convective processes are highly non-linear and depend on the large-scale flow.

Nevertheless, starting with Smagorinsky's (1956) work, procedures for the approximation of some cumulative convection effects have been developed, and are called cumulus convection parameterization. Cumulus convection parameterization pursues two major purposes: to take into account convective mixing and precipitation, and to prevent unstable stratification in numerical solutions which can cause numerical instability in hydrostatic models.

These parameterizations have been developed for global and regional NWP models with 100 km and larger grids. In such cases, the characteristic horizontal scales of directly resolved motions and of convection are quite different and enable the use of some physical-based hypotheses and suggestions. These include the homogeneity of cumulus clouds inside a computational cell, and the instantaneous character, or *a priori* postulated duration, of convective processes, etc. Such hypotheses together with information on potential convective instability obtained from the prognostic scheme allow the evaluation of an approximate cumulus cloud or cumulus cloud ensemble model, which provides the two above-mentioned purposes.

Two types of cumulus convection parameterizations are currently in use: parameterization of deep convection and of shallow convection. The latter permits parameterization of the convective exchanges in the mixing layer and makes it possible to generate the shallow clouds in the boundary layer which affect the radiative transfer in the lower atmosphere.

Several approaches to cumulus convection parameterization have been suggested by Kuo (1965, 1974), Arakawa and Schubert (1974), Kreitzberg and Perkey (1976), Anthes (1977), Fritsch and Chappell (1980) and Tiedtke, *et al.*, (1988). These studies do not exhaust the very long list of papers devoted to this problem. A useful review of observations and parameterization of convection is presented by Cotton and Anthes (1989).

The application of cumulus convection parameterization in a mesoscale non-hydrostatic NWP model, using 10–15 km grids, is questionable because the governing equations treat the buoyancy force explicitly and more completely than by means of the approximate relations in the common parameterization procedures. Together with parameterizations of the microphysics, the direct computation of convection on a mesoscale can provide a better description of convective precipitation. Taking into account the general trend towards the development of very fine-mesh mesoscale NWP models over limited areas, one can expect that, in the future, direct modelling of convection will be introduced into NWP practice.

#### *Parameterization of radiative transfer*

Radiative energy sources are equally important in both long-range numerical weather prediction and short-range prediction, if the latter is designed to predict weather elements near the surface, and there is a need to model the diurnal cycle.

Usually the radiative source of heat is expressed through the divergence of the resulting radiative flux:

$$\epsilon_r = \frac{1}{\rho c_p} \operatorname{div} \vec{F}$$

where  $\rho$  is density,  $C_p$  is the specific heat capacity at constant pressure, and  $\vec{F}$  is the radiative flux. Taking into account that radiative fluxes vary most substantially in the vertical direction, the problem is usually considered to be one-dimensional, and the above-mentioned expression is reduced to:

$$\epsilon_r = \frac{1}{\rho c_p} \frac{\partial F}{\partial z}$$

where  $F$  is now the radiative flux in the vertical direction.

The real structure of the radiative processes in the atmosphere is very complex and depends upon a number of scattering and absorbing mechanisms on clouds and aerosols, and on optical and geometric features of the ground surface.

At present, so-called line-by-line radiative transfer schemes exist, which take into account the major absorption lines in the spectrum, starting from ultraviolet and ending with far infrared. However, these models are too demanding from a computational point of view, and are used mainly in tests of other parameterizations.

As a rule, NWP models use simplified and highly parameterized algorithms, which are usually based on broad band approximations, with the absorbing and scattering properties of the atmospheric constituents assumed to be known over wide spectral ranges.

Taking into account that the solar and terrestrial spectra effectively do not overlap, the spectrum is separated usually into solar ( $\lambda_1 \leq 4\mu m$ ) and long-wave (infrared,  $\lambda_2 \leq 4\mu m$ ) spectral ranges. In more sophisticated models, several subranges within both the short-wave and long-wave ranges are identified, to take into account in more detail the radiative effects of the most optically-active atmospheric constituents.

The broad band methods of radiative flux computations are based on solving the radiative transfer equations for a plane-parallel scattering and absorbing atmosphere. In NWP practice, two general approaches are used. The first approach (Geleyn and Hollingsworth, 1979; Ritter and Geleyn, 1991) uses a delta two-stream approximation for solving the radiative transfer equations in both solar and long-wave ranges. The second approach uses a two-stream formulation for the computation of short-wave fluxes only, while the long-wave fluxes are computed by using a broad band flux emissivity method (Morcrette and Fouquart, 1986; Morcrette, 1990; Garand, 1983). In the solar radiation region, such major absorbers as H<sub>2</sub>O, O<sub>3</sub>, air molecules (Rayleigh scattering) and clouds are considered. The radiative effects of CO<sub>2</sub>, O<sub>2</sub> and aerosols are also sometimes included. In the thermal radiation region, the emissivities of atmospheric water (in the gaseous, liquid and ice phase), CO<sub>2</sub> and O<sub>3</sub> are considered. In more complicated models, the radiative effects of NO, CH<sub>4</sub>, N<sub>2</sub>O and O<sub>2</sub> are also included.

In order to describe the absorbing properties of the gaseous components in the broad spectral bands, exponential sum fitting techniques are used (Ritter and Geleyn, 1991) when the exponent indices are considered as a number of monochromatic absorption coefficients.

The external parameters in the radiative flux parameterizations are provided partly by the NWP models. These model-produced parameters could be air temperature, pressure, atmospheric water (in gaseous, liquid and ice phase), and aerosols. The remaining external parameters, associated with the concentration of different atmospheric gases, are usually taken from climatological data.

In current radiative transfer parameterizations, a major difference exists in the treatment of atmospheric water because the choice of parameterization technique depends strongly on the output provided by the dynamical part of the NWP model. If the NWP model provides its radiative code with only the percentage cloud cover, then the transmission of radiation in the cloud layer is adjusted by using a coefficient depending on the cloud percentage (Garand, 1983). Then solar optical properties are also fixed. If the model provides data on the cloud water (ice) and precipitation water (ice) content together with information on the effective radii of hydrometeors, then the extinction and backscattering coefficients depending on these atmospheric water parameters are introduced into the computational algorithms (Veltishcheva and Iljin, 1989). Information on the currently used radiation codes can be found in WMO/ICSU (1984), WMO (1988), Mokhov and Petukhov (1988) and in the NWP Progress reports published annually by the WMO Secretariat. Some useful review on radiative processes and their parameterization can be found in Stephens (1984), Fouquart (1988) and Harshvardhan (1991).

#### *Parameterization of surface processes*

Many studies have shown that numerical weather prediction models are very sensitive to the parameterization of the surface exchange processes at the atmosphere-land boundary. The development of a daytime planetary boundary layer is strongly dependent upon the parameterized surface sensible and latent heat fluxes. The convective precipitation over land is also sensitive to the soil-moisture/surface-evaporation parameterization. In this connection, surface processes are now included in most operational NWP models. The exchange of heat and moisture at the air-surface interface is accomplished by the use of balance equations. Moisture and heat transfer within the upper soil layer is also included in some operational models. The actual pattern of heat and moisture transfer in the vegetation, snow cover and soil is quite complicated, and therefore parameterizations that account only for the "bulk" effects of the land surface are commonly used in NWP models. The following major land surface properties and processes are considered in modern NWP models:

- (a) The surface albedo, which depends on the surface type (the spatial and temporal variability of the surface albedo is introduced through the inclusion of ice, snow and vegetation into the parameterization scheme); and
- (b) Evaporation from the surface, which includes evapotranspiration from the plants and takes account of the soil water content.

The latter is updated through the computation of a water budget which, in addition to evaporation, includes precipitation, runoff, and water infiltration into the soil. Recent studies into the parameterization of land surface processes in NWP models can be found in ECMWF (1988). The approaches to the inclusion of vegetation into the parameterization of surface processes can be found in Deardorff (1978), Chen (1984), Dickinson, *et al.*, (1986) and Wetzel and Chang (1987).

#### *Parameterization of terrain effects*

Besides direct representation of orography in the  $\sigma$  or other orographic coordinate systems, parameterization of gravity wave drag exists in the majority of NWP models. Inclusion of this drag, exerted by the

integral effect of the gravity waves generated by topography, allows a more realistic simulation of the airflow over mountainous terrain. The details on parameterization of gravity wave drag can be found in Palmer, *et al.*, (1986) and Miller and Palmer (1987).

### 3.5.2.3 INTEGRATION SCHEMES

The equations for numerical weather prediction are differential equations in space and time. The initial conditions must be specified functions of the spatial coordinates to enable computation of spatial derivatives. One method of representing meteorological fields is to associate the value of each quantity with a point in space. This is the standard grid-point representation. Another method, having some appealing mathematical properties, uses a set of values in which each is associated with a specified function of the spatial coordinates. This is the now popular spectral representation. Both representations, however, are only tables of numbers.

The spatial coordinates chosen for the representation may be the usual spherical Earth coordinates,  $\varphi$  latitude and  $\lambda$  longitude, or a specified transformation mapping the sphere onto a simpler rectangular coordinate system. Two common transformations for numerical prediction purposes are the polar stereographic and Mercator's projections. Most hemispheric prediction models use the polar stereographic projection, and models designed for tropical application use Mercator's projections. Neither of these coordinate systems contains the polar singularity present in spherical coordinates.

When a grid-point representation is chosen, the partial differentials are approximated with finite differences in space and time. The number of schemes available is almost limitless. Kurihara (1965) and Lilly (1965) have examined a large number of possible differencing schemes. Probably the most widely used approximation for the evaluation of the first derivative is the centred difference:

$$\frac{\Delta F}{\Delta \chi_i} = \frac{1}{2\Delta \chi} [F_{i+1} - F_{i-1}]$$

which, when combined with a centred difference in time:

$$\frac{F_i^{t+1} - F_i^{t-1}}{2\Delta t} = \frac{\Delta F^t}{\Delta \chi_i}$$

becomes the commonly called leap-frog scheme. Any scheme similar in form to the leap-frog scheme can be solved explicitly with a two-step marching process in which the spatial differences are calculated first and then the quantities are advanced forward in time. Time filtering is normally used to dampen the oscillations produced by the leap-frog scheme. The Asselin (1972) frequency filter is commonly applied for this purpose.

All differencing schemes have some undesirable property because they are approximations. Truncation error, common to all finite differences, is one such property. The term originated from the derivation of finite differences from truncated Taylor's series. Hence, the magnitude of the error is given by the first term truncated from the series. In general, higher-order schemes reduce the truncation error. In addition, long waves have less truncation error than short waves.

Another problem associated with grid-point methods arises from finite representation. Non-linear instability (Phillips, 1959) caused by aliasing and amplitudes generated in wave numbers unresolvable by the grid, leads to exponential growth in non-linear numerical systems. Non-linear instability is controlled either by designing the system so that the undesirable waves are not generated or by removing them from the solution through filtering or smoothing.

One popular method of filtering is the addition of a viscosity term to damp small-scale waves (Smagorinsky, *et al.*, 1965; Kasahara and Washington, 1967; Shuman and Hovermale, 1968). However, Merilees (1975) has shown that these terms tend to overdamp the meteorological waves.

The value of the time step is limited in explicit schemes by the Courant-Friedrichs-Levy (1928) criterion:

$$\frac{c\Delta t}{\Delta \chi} \leq 1$$

where  $c$  is the phase speed of the fastest travelling wave permitted by the system of equations. Split explicit schemes have been developed to overcome this restriction (Mesinger and Arakawa, 1976). Here, the fast-travelling gravity waves are treated separately, permitting a longer time step for the calculation of the meteorological waves.

Other differencing schemes have been devised, for reasons of economy, to permit longer time steps. One class of schemes, termed implicit, has good stability properties. For example:

$$\frac{F_i^{t+1} - F_i^t}{\Delta t} = \frac{\Delta F^{t+1}}{\Delta \chi_i}$$

is stable for all time steps and is implicit because of the appearance of  $\Delta F^{t+1}/\Delta \chi_i$  on the right of the equation. The semi-implicit technique, proposed by Marchuk (1964) and used by Kwizak and Robert (1971), Bourke (1974) and Hoskins and Simmons (1975) — in which only the linearized gravity wave terms are time-averaged — has permitted lengthening the time step by a factor of three without seriously damaging the meteorological solution.

The advection process is very important in NWP models, not only because it accounts for a large part of local tendencies for many atmospheric fields, but also because it is related to the stability, accuracy and

computational efficiency of the numerical methods that are used in these models. In order to remain stable, conventional Eulerian advection must satisfy the above-mentioned Courant-Friedrichs-Levy (CFL) condition, which restricts the size of the time step that can be used in conjunction with a given spatial resolution and advecting wind.

To avoid this restriction, a semi-Lagrangian integration scheme has been introduced and used in different studies since the end of the 1950s. The idea of the method can be illustrated by considering the equation governing simple advection in the  $x$  direction by a wind field  $u$ :

$$\frac{\partial F}{\partial t} + u \frac{\partial F}{\partial x} = 0$$

In the semi-Lagrangian formulation, this equation is written in the form of a total derivative following the motion:

$$\frac{d}{dt} F[x(t), t] = 0$$

In a centred scheme it is approximated as:

$$\frac{F[x(t + \Delta t), t + \Delta t] - F[x(t - \Delta t), t - \Delta t]}{2\Delta t} = 0$$

Choosing the locations at the forecast time to correspond to grid points  $x_j$  and letting  $d_j$  represent the displacements during one time step leads to:

$$F(x_j, t + \Delta t) = F(x_j - d_j, t - \Delta t)$$

where:

$$d_j = \Delta t u (x_j - d_j, t)$$

The implicit equation for displacements  $d_j$  is generally solved iteratively and involves interpolating the  $u$  field since  $x_j - d_j$  will usually lie between grid points. Having found  $d_j$ , the required  $F(x_j, t + \Delta t)$  value can be obtained.

The introduction of the semi-Lagrangian formulation of the advective terms permits an increase in the time step (roughly three to six times those permitted by the CFL criterion for the corresponding Eulerian models), without reducing the accuracy of the forecasts. In this connection, semi-Lagrangian schemes are being introduced widely into both finite-difference and spectral NWP models. Details of the implementation of semi-Lagrangian schemes for solving primitive equations can be found in Robert (1981), Robert, *et al.*, (1985) and Ritchie (1987).

Since the birth of the transform method (Orszag, 1970) to convert from wave to grid space, it has been possible to represent the horizontal variation of quantities on a sphere with truncated series of spherical harmonics in numerical models. The transform technique implies a one-to-one relationship between spectral coefficients and grid-point quantities and provides an economical transformation back-and-forth from wave space to grid points.

The spectral formulation has several advantages over finite-difference grid-point models. The solution of the Helmholtz equation can be reduced to a simple multiplication of coefficients because spherical harmonics are eigenfunctions of the Laplacian equation and are orthogonal over the sphere (Merilees, 1976). The contribution of non-linear terms to the tendency of individual harmonics is obtained by the grid transform. Finally, and most important for operational purposes, the spectral technique, is economical in terms of computational time.

The construction of limited-area models with spectral methods is difficult because spectral techniques depend upon representation by periodic functions. Orszag (1972) has developed pseudo-spectral techniques which permit the inclusion of boundary conditions. Since that time, several operational spectral limited-area models have been developed (Segami and Tatsumi, 1989; Tanguay, *et al.*, 1990). At present, the spectral formulation dominates in the global NWP models. In regards to limited area models, both finite-difference and spectral formulations are used.

With the introduction of prognostic equations for atmospheric water into the governing equation systems used in NWP, the need for numerical schemes to guarantee the non-negative values of such variables as cloud water and precipitation in the process of numerical integration is enhanced. The number of such monotonic schemes has been developed recently and incorporated into NWP models.

### 3.6 Methods of deriving and presenting output products

#### 3.6.1 Automatic output of numeric data

In a large centre, several thousand numeric bulletins or products may be generated automatically every 24 hours. In some cases, these messages are transmitted from the main processing computer system, where the analysis and forecast data fields at grid points are stored. However, an increasing number of messages are encoded in the central processor and then sent for storage and transmission to a communications computer. These messages contain meteorological data of many types which are then exchanged and decoded by means of the communications computer systems of each centre.

Grid-point data are in most cases intended to undergo additional processing either with a computer or manually, in order to restore the data fields for a variety of purposes, such as flight planning for long-haul international aviation, convenience of pictorial display, verification statistics and the like. For computer-to-computer exchanges, GRID, GRAF, GRIB, and BUFR codes are used. However, some centres are not equipped to handle processed data in digital form. For these reasons, data fields are still required to be presented and transmitted as the coordinates of field isopleth, as an alternative to a digital code, or in a pictorial format, when the latter is not practicable.

### **3.6.2 Requirements and technical aspects of conversion of information in alphanumerical (GRID/GRAF) and binary (GRIB, BUFR) code**

At the present time, certain branches of the Main Telecommunication Network of the GTS are already heavily loaded because of the excessive distribution of meteorological products in analogue form. The continued significant increase in alphanumeric traffic, caused by new programs, and the increasing exchange of numerical analyses and forecasts in GRID/GRAF code form will necessitate a decrease in the transmission of data in analogue form. Most of the products now distributed in pictorial form could be transmitted without difficulty in digital form. Furthermore, it should be kept in mind that some 50-100 GRID/GRAF code messages can be transmitted in the time required for the transmission of one map in pictorial form.

The implementation of the X.25 protocol opened new possibilities for the distribution of meteorological products in binary form. The use of the binary codes BUFR and GRIB allow a substantial increase in the volume of information transmitted through the GTS. At the present time, telecommunication links with X.25 protocol facilities exist between major GDPS centres and one can expect that the implementation of this technology will spread in the future.

The transfer from analogue to alphanumeric or binary distribution of NWP products implies, however, that a conversion must take place either at the RSMC level, when forwarding the products to national centres which do not have conversion equipment, or at the NMC level if the required equipment is available there. As the conversion process is highly dependent on the specific requirements of the users and is related to the map projection and scale, area, representation and parameters to be superimposed, it seems logical to perform the conversion at the NMCs whenever possible.

There are still at present many national centres which do not have the capability to receive data in alphanumeric or binary form nor the equipment to convert the grid point fields in pictorial forms. In view of the fact that many WMO Members are likely to acquire equipment to receive and convert data from binary/alphanumeric to pictorial form over the next few years, some guidelines for necessary systems to be acquired are given below.

#### **3.6.2.1 SYSTEM CONFIGURATION**

It should be noted that the GRIB (gridded binary) code exchange should be performed over error-controlled medium or higher-speed circuits. It is also considered that if a large amount of data need to be acquired in GRID/GRAF (alphanumeric) code, then both medium-speed lines and error-controlled circuits may be required because of the relatively large amount of data to be transmitted and the software problems caused by erroneous messages. Therefore, a centre planning to initiate large-scale conversion of alphanumeric data into pictorial form must be already equipped with a telecommunication computer system with interface to error-controlled medium-speed circuit. Nevertheless, a centre receiving a limited amount of GRID data on a low-speed line may wish to convert this information into pictorial form.

It is recommended that conversion functions be performed separately from the telecommunication functions (reception or transmission of data). The system performing these functions should have at least two mini/microcomputer configurations. The telecommunications will be handled by a mini or microcomputer. The conversion function is considered a part of the graphical applications. The graphics will be handled by another special mini/microcomputer system connected, on-line (for example a LAN) or off-line by a magnetic device, to the telecommunication system depending on data volume and time constraint. It should be noted that many other solutions are possible apart from those described above.

Regarding the graphical equipment required for the production of meteorological maps, two types of plotters can be distinguished:

- (a) Pen plotters which draw continuous lines with one or several pens of different colours on pre-printed maps;
- (b) Electrostatic plotters which produce maps by printing small black dots, as controlled by the software, with a resolution of 100 dots/inch or more on specially prepared paper.

In both cases, on-line (direct connection to the computer) or off-line (data transfer via magnetic device) connections are possible. However, in the case of a mini/microcomputer, an on-line connection is clearly preferable. An off-line connection is quite acceptable in the case of a major computer installation, in particular for a pen plotter which in any case requires a significant amount of operator intervention.

When deciding if a pen plotter or an electrostatic plotter is to be acquired, the following aspects should be taken into account:

- (a) The price of an electrostatic plotter is normally lower than the price of a comparable pen-plotter system;
- (b) The electrostatic system produces maps significantly faster than a pen plotter. On the other hand, the determination of the data controlling the plotters is considerably more time-consuming for the electrostatic plotter, in particular if the resolution of the plotter is very high (more than 100 dots/inch);

- (c) The reliability of the best electrostatic plotters is very high (in the order of 3 000 hours of mean time between failures) as compared with pen plotters. A duplication of the electrostatic equipment is therefore perhaps not necessary, whilst a pen plotter normally needs a back-up solution;
- (d) The use of pre-printed backgrounds and ballpoint or ink pens normally make the pen plotter more attractive if the maps are to be processed further by meteorologists. This is particularly true if other than isoline maps (surface and upper-air plotting, vertical TEMPs, etc.) are to be produced by the system.

If the aim is to have a conversion system with a minimum amount of operator intervention, then the recommended solution is a mini/microcomputer-controlled electrostatic plotter with the computer being connected on-line to the telecommunication system (and the plotter on-line to the minicomputer). It should also be noted that such a system could easily be expanded to distribute maps automatically on facsimile circuits because of the logical similarity between the two systems.

In many cases, a computer-controlled system for the conversion of GRIB, BUFR, GRID/GRAF code data into pictorial form and the subsequent automatic distribution of this information on facsimile circuit could be the preferred solution. This requires fairly small hardware enhancements as compared with a system producing meteorological maps locally using an electrostatic plotter. Due to the logical similarity of the two types of map output, virtually no software modifications are required.

At present, the visualization technique based on personal computers has been introduced in most of the equipped centres. Personal computers, accompanied by an A-3 format laser printer can serve as suitable hardware for the visual display and preparation of hard copies of meteorological charts, bulletins and other products. Details of processing and visualization of the products with the use of PC-based workstations are described in Chapter 4.

### 3.6.2.2 SOFTWARE

The software required for the conversion of data in alphanumeric form into maps is naturally dependent on the hardware configuration of the centre in question (and in particular the visualization equipment available) and is also related to the special requirements of the users of the products. However, the following basic components of the software are more or less identical for all installations of this type:

- (a) A general-purpose plotting package with features such as lines of different thicknesses, scaling of arrays, data lines and axes, character and number plotting, etc. (this is a package used by many other sub-routines and is quite practical in general plotting applications not directly related to meteorological maps);
- (b) Identification (possibly performed at the telecommunications level) and decoding of WMO BUFR, GRIB, GRID/GRAF code messages produced by various centres (this will either be a fairly general package for decoding virtually any kind of WMO numerical code messages or, more probably, if a relatively small computer is to be used, special versions of the decoding package provided for each producing centre);
- (c) Interpolation, including conversion from one map projection to another (this will usually include conversion from latitude-longitude grids to polar-stereographic grids, depending on what is used by the originating and receiving centres);
- (d) Grid-to-isoline computations (in the case of a pen plotter, this will be the production of vectors from grid-point data. In the case of an electrostatic plotter, this will be the determination of black and white dots either by direct interpolation from grid point values or from vectors determined as an intermediate result);
- (e) Background generation (this is normally of interest only in the case of an electrostatic plotter, where a fairly general background package is needed, but could also in some cases be used for a pen plotter system).

For other meteorological applications, packages producing plotted charts from the corresponding SYNOP messages, upper-air plotted charts or vertical cross-sections from the TEMP and PILOT reports, etc., might also be of interest.

A higher level of sophistication in product visualization can be achieved with the use of graphical displays on personal computers. The use of colours and graphics (including three-dimensional graphics), together with the possibility of animating a series of static images, makes this approach a powerful tool for data analysis. Details on this subject are given in Chapter 4.

### 3.7 Utilization of numerical products

Though great progress has been achieved in numerical weather prediction in recent decades, most of the success has been in the prediction of large-scale features of the atmosphere. Small-scale features, those of a few tens of kilometres in extent, and surface (or near-surface) weather variables — such as temperature, height and amount of clouds, precipitation, visibility and wind — are often not predicted directly by large-scale numerical models, and when they are, the accuracy may be fairly low. To decrease the deficiencies inherent in the large-scale NWP models, statistical or dynamical interpretation methods are applied to NWP products, which enable the generation of information that is directly not obtainable, or the correction of parameters given by NWP models. These aspects of NWP interpretation are discussed below.

### 3.7.1 *Utilization of numerical products for the statistical forecasting of weather parameters*

Statistical relationships are usually much stronger between forecast and currently measured variables than between forecasts and time-lagged variables. Therefore, the statistical technique should rely on the numerical product for its input in many applications. When the objective forecasting system is inherently statistical in nature and depends for its input on data from numerical prediction models, it is said to be an interpretative system, since it is interpreting the numerical model.

The methods used for developing statistical forecasting systems range from simple scatter plots to sophisticated statistical models which require significant computer resources. Some examples include regression, regression estimation of event probabilities (Miller, 1964), discriminant analysis (Miller, 1962), logic model (Brelsford and Jones, 1967), adaptive logic (Glahn, 1964) and canonical correlation (Glahn, 1968). In every application, there is a predictand (perhaps more than one) which is the variable to be forecast or estimated. Also, there is always at least one predictor that is used to estimate the predictand. The predictors can be determined in three ways:

- (a) The classical method where all of the predictors are current observations;
- (b) The perfect prog (PP) method (Klein, 1969), where actual observations are used to derive the prediction equation, but the predictors are generated by a numerical model;
- (c) The model output statistics (MOS) method (Glahn and Lowry, 1972), which uses values from numerical models to derive the prediction equation which is then applied to predictors obtained from the same model. A more detailed description of the MOS method can also be found in ECMWF (1978).

We shall discuss here only methods (b) and (c) because method (a) is not relevant to the use of NWP products.

Each method has its advantages and disadvantages. The MOS technique is popular because it corrects biases produced by the model. The disadvantage of the MOS technique is that a large data set from the model must be accumulated to derive statistically-sound prediction equations, and that these relationships must be rederived whenever a major model change occurs. The most recent discussion on NWP products statistical interpretation can be found in Glahn, *et al.*, (1991). Since there is no proven advantage of one method over the other, both PP and MOS techniques are used in practice at meteorological centres. Sometimes MOS- and PP-based systems are run in parallel and rule-based systems are developed to combine the MOS and PP forecasts to produce the final product. Post-treatment techniques based on past performance of the forecast are used in some centres. These are applied to improve the final product, to decrease bias, and to increase the sharpness, reliability and skill score of the forecasts prepared by the PP method, because, in this case, it takes on some of the desirable attributes of a MOS system. To minimize the adverse effects of frequent modifications in NWP models on the MOS system, one approach is to use data from several months of coincident runs of both an old and new dynamical model to generate covariance matrices that represent a longer developmental sample of the new model. These matrices are produced from a short coincident sample of old and new model output, as well as a long sample of the old model output. These enhanced matrices are then used to develop the forecast relationships.

At present, statistical forecasts based on NWP products are used widely in both the medium and short ranges. The output from global NWP models are used mainly for preparing day-to-day forecasts of temperature and precipitation with a lead time of up to 10 days. In the short range, a variety of NWP-based statistical forecasts are prepared. Among them are maximum/minimum temperature at the screen level, precipitation amount, surface wind, visibility, sunshine duration, cloud amount and the height of cloud base, fog, probability of thunderstorms and severe storms.

### 3.7.2 *Utilization of numerical products in dynamical forecasting of weather parameters*

NWP products are also used in a number of deterministic models which serve two major purposes: to obtain new parameters which are not produced directly by NWP models, and to improve the quality of prediction of some meteorological parameters which are not predicted satisfactorily due to limited resolution and/or physics of the large-scale NWP model. Among examples of the first type include models of air pollution transport at different time and space scales, models for wave and storm-surge prediction, and other applied models.

Among examples of the second type, the dominant case is a one-dimensional planetary boundary model designed to produce screen level temperature and humidity, surface wind and detailed vertical distribution of meteorological parameters in the atmospheric boundary layer, locally adapted to measurement stations.

NWP products are also used as time-dependent boundary conditions for limited area models nested into the computational domain of a model covering a larger area. At the present time, there are a number of such limited area models on a regional scale. Very fine-mesh mesoscale models are being introduced progressively into the operational cycles of meteorological centres, so the demand for NWP products generated from the larger-scale models is being increased.

## 3.8 Sources of error in numerical prognoses

The sources of error are usually studied by means of numerical experiments. There are two major types of errors. Errors of the first type can be classified as purely computational. They arise due to inevitable truncations in the finite-difference representation of derivatives in the governing equations. This type of error is studied usually by comparing numerical and analytical solutions for some idealized flows, when analytical solutions are available.

Errors of the second type are associated with errors in initial and boundary conditions, and with deficiencies in the physical part of NWP models. Errors in the specification of the system's initial condition seriously

affect the skill of NWP models. Without going into details related to the general problems of hydrodynamic instability and the predictability of atmospheric processes, we shall point out a general tendency, which is justified by theoretical considerations. This is that the errors in the initial conditions do not amplify rapidly if the atmospheric state is quasi-steady. In the case of a transitory situation, when fast changes take place in the spatial structure of atmospheric fields, errors in the initial state strongly affect the numerical weather prediction. More details on the general aspects of predictability and the predictabilities at the different scales of atmospheric motions can be found in Lorenz (1969, 1986), Carnevale and Holloway (1982), Anthes (1984), Anthes, *et al.*, (1985) and James (1990).

In the limited area models, an additional source of error arises at the lateral boundaries because the time-dependent boundary conditions provided by predictions from a larger-scale model can have some errors. With time, these errors propagate into the computational domain and strongly affect the resulting solution since the prediction within a limited area converges with the boundary problem as the time integration period is increased.

The simplified formulation of many physical processes introduces a number of errors, which are evaluated normally by conducting a series of numerical experiments that isolate the contribution of the different physical processes to the obtained solutions (forecasts). There are a variety of such experiments, which show, that inadequate treatment of practically all physical processes causes errors in NWP (WMO, 1988; Bourke, *et al.*, 1991).

At present all meteorological centres producing NWP run verification modules which are included in the operational cycle. The results of such verifications are published annually in the WWW Technical Progress Report on the Global Data-processing System.

#### REFERENCES

- Andersson, E., N. Gustafsson, L. Meuller and G. Omstedt, 1986: SMHI PROMIS-Rapporter. *PROMIS-Report No. 1*.
- Anthes, R. A., 1977: A cumulus parameterization scheme utilizing a one-dimensional cloud model. *Monthly Weather Review*, 105, pp. 270–286.
- Anthes, R. A., 1984: The general question of predictability. *Lecture for AMS intensive course on mesoscale meteorology and forecasting*, 9–20 July 1984, Boulder, Colorado.
- Anthes, R. A., H. L. Kuo, A. P. Baumhefner, R. Errico and T. W. Bettge, 1985: Predictability of mesoscale atmospheric motions. *Advances in Geophysics*, 28 B, pp. 159–202.
- Arakawa, A. and W. H. Schubert, 1974: Interaction of a cumulus cloud ensemble with the large-scale environment, Part 1. *Journal of the Atmospheric Sciences*, 31, pp. 674–701.
- Asselin, R., 1972: Frequency filter for time integration. *Monthly Weather Review*, 100, pp. 487–490.
- Atkins, M. Y., 1974: The objective analysis of relative humidity. *Tellus*, 26, pp. 663–671.
- Baer, F., 1977: Adjustment of initial conditions required to suppress gravity oscillations in nonlinear flows. *Contributions to Atmospheric Physics*, 50, pp. 350–366.
- Bengtsson, L. O., 1975: Four-dimensional assimilation of meteorological observations. *WMO/ICSU GARP Publications Series*, No. 15.
- Benwell, G. R. and F. P. Bretherton, 1968: A pressure oscillation in a ten-level atmospheric model. *Quarterly Journal of the Royal Meteorological Society*, 94, pp. 123–131.
- Bergman, K. H. and W. D. Bonner, 1976: Analysis error as a function of observational density of satellite temperature soundings with spatially correlated errors. *Monthly Weather Review*, 104, pp. 1308–1316.
- Bergthorsson, P. and B. R. Doos, 1955: Numerical weather map analysis. *Tellus*, 7, pp. 329–340.
- Blackadar, A. K., 1979: High-resolution models of planetary boundary layer. *Advances in Environmental Science and Engineering*, 1, pp. 50–85.
- Bleck, R., 1974: Short-range prediction in isentropic coordinates with filtered and unfiltered numerical models. *Monthly Weather Review*, 102, pp. 813–829.
- Bourke, W. P., 1974: A multi-level spectral model: Formulation of hemispheric integrations. *Monthly Weather Review*, 102, pp. 687–701.
- Bourke, W. P. and J. C. McGregor, 1983: A non-linear vertical mode initialization scheme for a limited area prediction model. *Monthly Weather Review*, 111, pp. 2285–2297.
- Bourke, W. P., R. A. Mullenmeister, K. Arpe, D. Baumhefner, P. Caplan, J. L. Kinter, S. F. Milton, W. E. Stern and M. Sugi, 1991: Systematic errors in extended range predictions. CAS/JSC Working Group on Numerical Experimentation, *Report No. 16*, WMO/TD-No 444.
- Brelsford, W. M. and R. H. Jones, 1967: Estimating probabilities. *Monthly Weather Review*, 95, pp. 570–576.
- Brown, J. A., 1974: On vertical differencing in the sigma system. *Office Note 92*, NMC, Washington, D.C.
- Carnevale, G. F. and G. Holloway, 1982: Information decay and the predictability of turbulent flows. *Journal of Fluid Mechanics*, 116, pp. 115–121.
- Charnock, H., 1955: Wind stress on a water surface. *Quarterly Journal of the Royal Meteorological Society*, 81, pp. 639–640.
- Chen, J., 1984: Uncoupled multi-layer model for the transfer of sensible and latent heat flux densities from vegetation. *Boundary Layer Meteorology*, 28, pp. 213–226.
- Chen, J. B., J. Liren and W. L. Wu, 1987: Design and test of an improved scheme for global spectral model with reduction of truncation error. *Advances in Atmospheric Sciences*, 4, pp. 156–168.
- Cotton, W. R. and R. A. Anthes, 1989: *Storm and Cloud Dynamics*. Academic Press, New York.
- Courant, R., K. O. Friedrichs and H. Lewy, 1928: Über die partiellen Differenzengleichungen der mathematischen Physik. *Mathematisch Annalen*, 100, pp. 32–74.

- Courtier, P. and O. Talagrand, 1987: Variational assimilation of meteorological observations with the adjoint vorticity equation, Part II: Numerical results. *Quarterly Journal of the Royal Meteorological Society*, 113, pp. 1329–1347.
- Courtier, P. and O. Talagrand, 1990: Variational assimilation of meteorological observations with the direct and adjoint shallow water equations. *Tellus*, 42A, pp. 531–549.
- Cram, J. M. and M. L. Kaplan, 1985: Variational assimilation of VAS data into a mesoscale model: Assimilation method and sensitivity experiments. *Monthly Weather Review*, 10, pp. 367–374.
- Cressman, G. P., 1960: Improved terrain effects in barotropic forecasts. *Monthly Weather Review*, 88, pp. 327–342.
- Daley, R., 1978: Variational non-linear normal mode initialization. *Tellus*, 30, pp. 201–218.
- Daley, R., 1981: Normal mode initialization. *Reviews of Geophysics and Space Physics*, 19, pp. 450–468.
- Daley, R., 1991: *Atmospheric Data Analysis*. Cambridge University Press, Cambridge.
- Danard, M., 1985: On the use of satellite estimates of precipitation in initial analyses for numerical weather prediction. *Atmosphere-Ocean*, 23, pp. 23–42.
- Deardorff, J. W., 1978: Efficient prediction of ground surface temperature and moisture with inclusion of a layer of vegetation. *Journal of Geophysical Research*, 83, pp. 1889–1903.
- Deaven, D. G., 1976: A solution for boundary problems in isentropic coordinate models. *Journal of the Atmospheric Sciences*, 33, pp. 1702–1713.
- Dickinson, R. E. and D. L. Williamson, 1972: Free oscillations of a discrete stratified fluid with application to numerical weather prediction. *Journal of the Atmospheric Sciences*, 29, pp. 623–640.
- Dickinson, R. E., A. Henderson-Sellers, P. J. Kennedy and M. F. Wilson, 1986: Biosphere-atmosphere transfer scheme (BATS) for the NCAR Community Climate Model. *NCAR Technical Note*, NCAR/TN-275.
- Dixon, R., 1969: Orthogonal polynomials as a basis for objective analysis. Meteorological Office, *Scientific Paper No. 30*. H.M.S.O., London.
- Eliassen, A., 1954: Provisional report on calculation of spatial covariance and auto-correlation of the pressure field. *Report No. 5*, Videnskaps-Academiets Institutt for Vaer-Og Klimaforskning.
- Eliassen, A. and E. Raustein, 1968: A numerical integration experiment with model atmosphere based on isentropic coordinates. *Meteorologiske Annaler*, 5, pp. 45–63.
- Errico, R. M., 1989: Theory and application of nonlinear normal mode initialization. *NCAR Technical Note*, NCAR/TN-344+1A.
- European Centre for Medium Range Weather Forecasts, 1978: *Seminars 1978: The interpretation and use of large-scale numerical forecast products*.
- European Centre for Medium Range Weather Forecasts, 1985: *Proceedings of the workshop on cloud cover parameterization in numerical models*, 26–28 November 1984.
- European Centre for Medium Range Weather Forecasts, 1988: *Proceedings of the workshop on parameterization of fluxes over land surface*, 24–28 October 1988.
- Eyre, J. R. and A. C. Lorenc, 1989: Direct use of satellite sounding radiances in numerical weather prediction. *Meteorological Magazine*, 118, pp. 13–16.
- Fillion, L. and C. Temperton, 1989: Variational implicit normal mode initialization. *Monthly Weather Review*, 117, pp. 2219–2229.
- Fillion, L., 1991: Variational implicit normal mode initialization on the sphere. *Monthly Weather Review*, 119, pp. 562–631.
- Flattery, T. W., 1971: Spectral models for global analysis and forecasting. *Technical Report No. 242*, Air Weather Service, U.S. Air Force, pp. 42–54.
- Fouquart, Y., 1988: Radiative transfer in climate models: In: *Physically-based Modelling and Simulation of Climate and Climatic Change*, Part 1 (M. E. Schlesinger, ed.). Kluwer Academic Publishers, Dordrecht.
- Fritsch, J. M. and C. F. Chappell, 1980: Numerical prediction of convectively driven pressure systems, Part 1: Convective parameterization. *Journal of the Atmospheric Sciences*, 37, pp. 1722–1733.
- Gandin, L. S., 1963: *Objective Analysis of Meteorological Fields*. Gidrometeoizdat, Leningrad.
- Gandin, L. S., 1969: Objective analysis. *Lectures on numerical short-range weather prediction*. WMO Regional Training Seminar, Moscow, 1965. Gidrometeoizdat, Leningrad, pp. 633–677.
- Garand, L., 1983: Some improvements and complements to the IR emissivity algorithm including a parametrization of the absorption in the continuum region. *Journal of the Atmospheric Sciences*, 40, pp. 230–244.
- Garrat, J. R., 1992: *The Atmospheric Boundary Layer*. Cambridge University Press, Cambridge (In press).
- Geleyn, J. F. and A. Hollingsworth, 1979: An economical analytical method for the computation of the interaction between scattering and line absorption of radiation. *Contributions to Atmospheric Physics*, 50, pp. 1–16.
- Glahn, H. R., 1964: An application of adaptive logic to meteorological prediction. *Journal of Applied Meteorology*, 3, pp. 718–725.
- Glahn, H. R., 1968: Canonical correlation and its relationship to discriminant analysis and multiple regression. *Journal of the Atmospheric Sciences*, 25, pp. 23–31.
- Glahn, H. R. and D. A. Lowry, 1972: The use of model output statistics (MOS) in objective weather forecasting. *Journal of Applied Meteorology*, 11, pp. 1203–1211.
- Glahn, H. R., A. H. Murphy, L. J. Wilson and J. S. Jensenius, Jr., 1991: *Lectures on the interpretation of NWP products in terms of local weather phenomena and their verification*. WMO Training Workshop, WMO/TD No. 421.
- Golding, B. W., 1984: The Meteorological Office mesoscale model: its current status. *Meteorological Magazine*, 113, pp. 289–302.

- Golding, B. W., 1987: The U.K. Meteorological Office mesoscale model. *Boundary Layer Meteorology*, 41, pp. 97–108.
- Golding, B. W., 1990: The Meteorological Office mesoscale model. *Meteorological Magazine*, 119, pp. 81–86.
- Harshvardhan, 1991: Atmospheric radiation. *Review of Geophysics*, Supplement of Volume, 29, pp. 56–58.
- Hicks, B. B., G. D. Hess and M. L. Wesley, 1979: Analysis of flux-profile relationships above tall vegetation: An alternative view. *Quarterly Journal of the Royal Meteorological Society*, 105, pp. 1074–1077.
- Hollet, S. R., 1975: *Three-dimensional spatial correlations of PE forecast errors*. M.S. Thesis, Department of Meteorology, McGill University, Montreal.
- Holt, T. and S. Raman, 1988: A review and comparative evaluation of multilevel boundary layer parameteorizations for the first-order and turbulent kinetic energy closure schemes. *Review of Geophysics*, 26, pp. 761–780.
- Hoskins, B. J. and A. J. Simmons, 1975: A multi-layer spectral model and semi-implicit method. *Quarterly Journal of the Royal Meteorological Society*, 101, pp. 637–655.
- Houghton, D. and W. M. Washington, 1969: On global initialization of the primitive equations, Part I. *Journal of Applied Meteorology*, 8, pp. 726–737.
- Houghton, D., D. G. Baumhefner and W. M. Washington, 1971: On global initialization of primitive equations, Part II: The divergent component of the horizontal wind. *Journal of Applied Meteorology*, 10, pp. 626–634.
- Hovermale, J. B., D. G. Marks and S. H. Scolnik, 1977: Operational analysis and prediction with the movable fine mesh system at the National Meteorological Centre. *Proceedings of the seventh technical exchange conference*, El Paso, Atmospheric Science Laboratory, White Sands, New Mexico.
- James, I. N., 1990: Order and chaos up in the air. *Nature*, Vol. 348, No. 6299, pp. 283–284.
- Kasahara, A. and W. M. Washington, 1967: NCAR global general circulation model of the atmosphere. *Monthly Weather Review* 95, pp. 384–402.
- Kasahara, A., 1974: Various vertical coordinate systems used for numerical weather prediction. *Monthly Weather Review*, 102, pp. 509–522.
- Kessler, E., 1969: On the distribution and continuity of water substance in atmospheric circulations. *Meteorological Monographs*, 10, No. 32, American Meteorological Society, Boston.
- Kiselnikova, V. Z., E. M. Pekelis, D. Ya. Pressman, N. F. Veltishchev and A. A. Zhelnin, 1987: Development of mesoscale models for weather elements prediction. WMO, *PSMP Report Series No. 23*.
- Klein, W. H., 1969: The computer's role in weather forecasting. *Weatherwise*, 22, pp. 195–218.
- Kreitzberg, C. W. and D. J. Perkey, 1976: Release of potential instability, Part 1: A sequential plume model within a hydrostatic primitive equation model. *Journal of the Atmospheric Sciences*, 33, pp. 456–475.
- Krishnamurti, T. N., J. Xue, H. S. Bedi, K. Ingles and D. Ocsterhof, 1991: Physical initialization for numerical weather prediction over the tropics. *Tellus*, 43 A-B, pp. 53–81.
- Kuo, H. L., 1965: On formation and intensification of tropical cyclones through latent heat release by cumulus convection. *Journal of the Atmospheric Sciences*, 22, pp. 40–63.
- Kuo, H. L., 1974: Further studies of the parameterization of the influence of cumulus convection on large-scale flow. *Journal of the Atmospheric Sciences*, 31, pp. 1232–1240.
- Kurihara, V., 1965: On the use of implicit and iterative methods for the time integration of the wave equation. *Monthly Weather Review*, 93, pp. 33–46.
- Kwizak, M. and A. J. Robert, 1971: A semi-implicit scheme for grid point atmospheric models of the primitive equations. *Monthly Weather Review*, 99, 32–36.
- Lilly, D. K., 1965: On the computational stability of numerical solutions of time-dependent nonlinear geophysical fluid dynamics problems. *Monthly Weather Review*, 93, pp. 11–26.
- Lin, V. L., R. D. Farley and H. D. Orville, 1983: Bulk parameterization of the snow field in a cloud model. *Journal of Climate and Applied Meteorology*, 22, pp. 1065–1092.
- Lorenc, A. C., 1981: A global three-dimensional multivariate statistical interpolation scheme. *Monthly Weather Review*, 109, pp. 701–721.
- Lorenz, E. N., 1969: The predictability of a flow which possesses many scales of motion. *Tellus*, 21, pp. 289–307.
- Lorenz, E. N., 1986: Atmospheric predictability: do we have a mathematical theory? *Extended abstracts of papers of the international symposium on short- and medium-range numerical weather prediction*, WMO/IVGG, 4–8 August 1986, Tokyo, WMO/TD-No. 114, pp. 539–541.
- Machenauer, B., 1977: On the dynamics of gravity oscillations in a shallow water model with application to normal mode initialization. *Contributions to Atmospheric Physics*, 50, pp. 253–271.
- Machenauer, B., 1983: Fundamentals of nonlinear normal mode initialization. The interaction between objective analysis and initialization (R. Daley, J. Derome and D. Williamson, eds.), *NCAR Technical Note NCAR/TN-204+PROC*.
- Marchuk, G. I., 1964: A new approach to the numerical solution of differential equations of atmospheric processes. *Technical Note No. 66*, WMO-No. 162, TP. 79, pp. 212–226.
- Marks, D. G. and R. V. Jones, 1977: An operational analysis scheme on isentropic surfaces. *Proceedings of the third AMS conference on numerical weather prediction*, Omaha, Nebraska, pp. 192–202.
- McBean, G. A., K. Bernhardt, S. Bodin, Z. Litynska, A. P. van Ulden and J. C. Wyngaard, with contribution from B. R. Kerman, J. D. Reid, Z. Serbjan, J. L. Wolmsley and G. A. McBean (ed.) 1979: The planetary boundary layer. WMO, *Technical Note No. 165*, WMO-No. 530.

- McFarlane, N. A., 1987: The effects of orographically excited gravity wave drag on the general circulation of the lower stratosphere and troposphere. *Journal of the Atmospheric Sciences*, 44, pp. 1775–1800.
- Merilees, P. E., 1975: The effect of grid resolution on the instability of a simple baroclinic model. *Monthly Weather Review*, 103, pp. 101–104.
- Merilees, P. E., 1976: The equations of motion in spectral form. *Journal of the Atmospheric Sciences*, 25, pp. 736–743.
- Mesinger, F. and A. Arakawa, 1976: Numerical methods used in atmospheric models. *WMO/GARP Publications Series*, Vol. I.
- Mesinger, F., 1984: A blocking technique for mountains in atmosphere models. *Rivista di Meteorologia Aeronautica*, 44, pp. 195–202.
- Mesinger, F., Z. I. Janjic, S. Nickovic, D. Gavrilov and D. G. Deaven, 1988: The step-mountain co-ordinate model: Description and performance for cases of Alpine lee cyclogenesis and for a case of an Appalachian redevelopment. *Monthly Weather Review*, 116, pp. 1493–1518.
- Miller, R. G., 1962: Statistical prediction by discriminant analysis. *Meteorological Monographs*, 4, 25.
- Miller, R. G., 1964: Regression estimation of event probabilities. *Technical Report No. I*, Contract CWG-10704, The Travellers Research Centre, Inc., Hartford, Connecticut.
- Miller, R. G. and T. N. Palmer, 1987: Orographic gravity-wave drag: Its parameterization and influence in general circulation and numerical weather prediction models. *Seminar on observation, theory and modelling of orographic effects*, ECMWF, 15–19 September 1986, Vol. 1, pp. 283–333.
- Miyakoda, K. and R. W. Mayer, 1968: Method of initialization for dynamic weather forecasting. *Tellus*, 20, pp. 115–128.
- Mokhov, I. I. and Y. K. Petukhov, 1988: *Cloudiness radiation interaction in the general circulation models, weather prediction and climate*. Soviet Cloudiness and Radiation Climatology Programme. Moscow.
- Monin, A. S. and A. M. Obukhov, 1953: Dimensionless characteristics of turbulence in the atmospheric surface layer. *Doklady Akademii Nauk SSSR*, 93, pp. 223–226.
- Monin, A. S. and A. M. Obukhov, 1954: Fundamental laws of turbulent exchange in the atmospheric surface layer. *Trudy Geofizicheskii Institut, Akademii Nauk SSSR*, No. 24 (151), pp. 163–187.
- Morcrette, J. J. and X. Fouquart, 1986: The overlapping of cloud layer in short-wave radiation parameterizations. *Journal of the Atmospheric Sciences*, 43, pp. 321–328.
- Morcrette, J. J., 1990: Impact of changes to the radiation transfer parameterizations plus cloud optical properties in the ECMWF model. *Monthly Weather Review*, 118, pp. 847–873.
- Ninomiya, K. and K. Kurihara, 1987: Forecast experiment in a long-lived mesoscale convective system in Baiu frontal zone. *Journal of the Meteorological Society of Japan*, 65, pp. 885–889.
- Nitta, T. and J. B. Hovmöller, 1969: A technique of objective analysis and initialization for the primitive forecast equations. *Monthly Weather Review*, 97, pp. 652–658.
- Oke T. R., 1978: *Boundary Layer Climates*. Methuen and Co. Ltd., London.
- Orlanski, L., 1975: A rationale subdivision of scales for atmospheric processes. *Bulletin of the American Meteorological Society*, 56, pp. 520–527.
- Orszag, S. A., 1970: Transform method for the calculation of vector-coupled sums: Application to the spectral form of the vorticity equation. *Journal of the Atmospheric Sciences*, 27, pp. 890–895.
- Orszag, S. A., 1972: Comparison of pseudospectral and spectral approximations. *Studies in Applied Mathematics*, 51, pp. 253–259.
- Pailleux, J., 1989: Design of a variational analysis: Organization and scientific points. *ECMWF Technical Memorandum No. 50*.
- Palmer, T. N., G. J. Shutt and R. Swinbank, 1986: Alleviation of a systematic westerly bias in general circulation and numerical weather prediction models through an orographic gravity wave drag parameterization. *Quarterly Journal of the Royal Meteorological Society*, 112, pp. 101–1039.
- Panofsky, H. A., 1949: Objective weather map analysis. *Journal of Meteorology*, 6, pp. 386–392.
- Parrish, D. E. and J. C. Derber, 1991: The National Meteorological Centre's spectral statistical interpolation analysis system. *NMC Office Note No. 379*, Washington, D.C.
- Perkey, D. J., 1976: A description and preliminary results from a fine-mesh model for forecasting quantitative precipitation. *Monthly Weather Review*, 104, pp. 1513–1526.
- Phillips, N. A., 1957: A coordinate system having some special advantage for numerical forecasting. *Journal of Meteorology*, 14, pp. 184–185.
- Phillips, N. A., 1959: An example of nonlinear computational instability. In: *The Atmosphere and the Sea in Motion* (B. Bolin, ed.), Rockefeller Press, New York.
- Phillips, N. A., 1960: On the problem of initial data for the primitive equations. *Tellus*, 12, pp. 121–126.
- Phillips, N. A., 1977: Variational analysis in pressure coordinates. *Office Note 134*, National Meteorological Centre, Washington D.C.
- Puri, K. and J. J. Miller, 1990: The use of satellite data in the specification of convective heating for diabatic initialization and moisture adjustment in numerical prediction models. *Monthly Weather Review*, 118, pp. 67–93.
- Ritchie, H., 1987: Semi-Lagrangian advection on a Gaussian grid. *Monthly Weather Review*, 115, pp. 608–619.
- Ritter, B. and J. F. Geleyn, 1992: A comprehensive radiation scheme for numerical weather prediction models with potential applications in climate simulations. *Monthly Weather Review*, 120, pp. 303–325.
- Robert, A., 1981: A stable numerical integration scheme for the primitive meteorological equations. *Atmosphere-Ocean*, 19, pp. 35–46.

- Robert, A., T. L. Yee and H. Ritchie, 1985: A semi-Lagrangian and semi-implicit numerical integration scheme for multilevel atmospheric models. *Monthly Weather Review*, 113, pp. 388–394.
- Rutledge, S. A. and P. V. Hobbs, 1983: Mesoscale and microscale structure and organization of clouds and precipitation in mid-latitude cyclones. VIII: A model for the “seeder-feeder” process in warm-frontal rainbands. *Journal of the Atmospheric Sciences*, 40, pp. 1185–1206.
- Salmon, E. M. and T. T. Warner, 1986: Short-term numerical precipitation forecasts initialized using a diagnosed divergent-wind component. *Monthly Weather Review*, 114, pp. 2122–2132.
- Sasaki, Y., 1970: Some basic formalism in numerical variational analysis. *Monthly Weather Review*, 98, pp. 875–883.
- Schlatter, T. W. and G. W. Branstator, 1979: Estimation of errors in Nimbus-6 temperature profiles and their spatial correlation. *Monthly Weather Review*, 107, pp. 1402–1413.
- Segami, A. and V. Tatsumi, 1989: Operational mesoscale weather prediction with Japan spectral model. *Journal of the Meteorological Society of Japan*, 67, pp. 907–924.
- Sergeev, B. N., 1983: Numerical modelling of atmospheric front and associated clouds and precipitation. *Meteorologiya i Gidrologiya*, No. 4, pp. 21–29.
- Shuman, F. G. and J. B. Hovermale, 1968: An operational six-layer primitive equations model. *Journal of Applied Meteorology*, 7, pp. 525–547.
- Smagorinsky, J., 1956: On the inclusion of moist adiabatic processes in numerical prediction models. *Berichte des Deutschen Wetterdienstes*, 5, pp. 82–90.
- Smagorinsky, J., S. Manabe and J. L. Holloway, 1965: Numerical results from a nine-level general circulation model of the atmosphere. *Monthly Weather Review*, 93, pp. 727–768.
- Soderman, D. and L. Winberg, 1980: Conversion of grid-point data into meteorological maps with a mini-computer system. WMO, *WWW Planning Report No. 37*.
- Sorbjan, Z., 1989: *Structure of Atmospheric Boundary Layer*. Prentice-Hall, Englewood Cliffs.
- Stephens, G. L., 1984: The parameterization of radiation for numerical weather prediction and climate models. *Monthly Weather Review*, 112, pp. 826–867.
- Stephens, J. J., 1970: Variational initialization with the balance equation. *Journal of Applied Meteorology*, 9, pp. 732–739.
- Stull, R. B., 1988: *An Introduction to Boundary Layer Meteorology*. Kluwer Academic Publishers, Dordrecht.
- Sugi, M., 1986: Dynamic normal mode initialization. *Journal of the Meteorological Society of Japan*, Ser. II, Vol. 64, pp. 623–636.
- Sundqvist, H., 1978: A parameterization scheme for non-convective condensation including prediction of cloud water content. *Quarterly Journal of the Royal Meteorological Society*, 104, pp. 677–690.
- Talagrand, O. and R. Courtier, 1987: Variational assimilation of meteorological observations with the adjoint vorticity equation, Part I: Theory. *Quarterly Journal of the Royal Meteorological Society*, 113, pp. 1313–1328.
- Tanguay, M., A. Robert and R. Laprise, 1990: A semi-implicit semi-Lagrangian fully compressible regional forecast model. *Monthly Weather Review*, 118, pp. 1970–1980.
- Tarbell, T. C., T. T. Warner and R. A. Anthes, 1981: An example of the initialization of the divergent wind component in a mesoscale model. *Monthly Weather Review*, 109, pp. 77–95.
- Temperton C., 1976: Dynamic initialization for barotropic and multilevel models. *Quarterly Journal of the Royal Meteorological Society*, 102, pp. 297–311.
- Temperton, C., 1988: Implicit normal mode initialization. *Monthly Weather Review*, 116, pp. 1013–1031.
- Thiebaux, J. and M. Pedder, 1987: *Spatial Objective Analysis*. Academic Press, New York.
- Tiedtke, M., W. A. Heckley and J. Slingo, 1988: Tropical forecasting at ECMWF: The influence of physical parameterization of the mean structure of forecasts and analyses. *Quarterly Journal of the Royal Meteorological Society*, 114, pp. 639–664.
- Tripoli, G. J. and W. R. Cotton, 1982: The Colorado State University three-dimensional cloud/mesoscale model—1982, Part I: General theoretical framework and sensitivity experiments. *Journal des Recherches Atmosphériques*, 16, pp. 185–219.
- Turpeinen, O. M., L. Garand, R. Benoit and M. Roch, 1990: Diabatic initialization of the Canadian regional finite-element (RFE) model using satellite data, Part I: Methodology and application to a winter storm. *Monthly Weather Review*, 118, pp. 1381–1395.
- Uccellini, L. W., D. R. Johnson and R. E. Schlesinger, 1977: An isentropic and sigma coordinate hybrid numerical model. Isentropic numerical models — Results on model development for zonally averaged and secondary circulation. *Report to the National Science Foundation*, University of Wisconsin, Madison, Wisconsin, pp. 177–254.
- Veltishchev, N. F., A. A. Zhelnin, V. Z. Kiselnikova, Y. M. Pekelis and D. Ja. Pressman, 1982: Mesoscale weather forecasting. *Meteorologiya i Gidrologiya*, No. 4, pp. 5–15.
- Veltishcheva, N. S. and V. O. Iljin, 1989: Numerical temperature and precipitation prediction over the fine-mesh with incorporation of urban effect. *Meteorologiya i Gidrologiya*, No. 2, pp. 21–30.
- Wang, W. and T. T. Warner, 1988: Use of four-dimensional data assimilation by Newtonian relaxation and latent-heat forcing to improve a mesoscale-model precipitation forecast. *Monthly Weather Review*, 116, pp. 2593–2613.
- Washington, W. and D. L. Williamson, 1977: A description of the NCAR global circulation models. *Methods in Comparative Physics No. 17: General circulation models of the atmosphere*, Academic Press, New York.
- Werden, W., 1988: The diabatic ECMWF normal mode initialization scheme. *Beiträge zur Physik der Atmosphäre*, 61, pp. 274–302.

- Wetzel, R. J. and J.-T. Chang, 1987: Concerning the relationship between evapotranspiration and soil moisture. *Journal of Climate and Applied Meteorology*, 26, pp. 18–27.
- World Meteorological Organization/International Council of Scientific Unions, 1972: *Parameterization of sub-grid-scale processes*. Global Atmospheric Research Programme, Series No. 8.
- World Meteorological Organization/International Council of Scientific Unions, 1984: The intercomparison of radiation codes in climate models (ICRCCM). *Report of the Meeting*, 15–18 August 1984, Frascati, WCRP-93, WMO/TD No. 28.
- World Meteorological Organization, 1986: *Manual on the Global Telecommunication System*, WMO-No. 386.
- World Meteorological Organization, 1988: *Workshop on systematic errors in models of the atmosphere*, 19–23 September 1988, Toronto, CAS/SCC Report No. 12, WMO/TD No. 273.
- World Meteorological Organization, 1990: *Preprints of the international symposium on assimilation of observations in meteorology and oceanography*, 9–13 July 1990, Clermont-Ferrand.
- World Meteorological Organization, 1990: Radiation and climate: Intercomparison of radiation codes in climate models (ICRCCM). *Report of the Workshop*, 15–17 August 1988, Paris, WCRP-39, WMO/TD No. 371.
- World Meteorological Organization, 1991: Numerical weather prediction progress report for 1990. *Technical document*, Research and Development Programme, NWPP Report Series, No. 17, WMO/TD No. 403.
- World Meteorological Organization, 1992: *Manual on the Global Data-processing System*, WMO-No. 485.
- World Meteorological Organization, 1992: 1991 WWW Technical Progress Report on the Global Data-Processing System. GDPS TP Report Series, No. 1, WMO/TD No. 491.
- Wright, B. J. and B. W. Golding, 1990: The interactive mesoscale initialization. *Meteorological Magazine*, 119, pp. 234–244.
- Wyngaard, J. C., 1985: Structure of the planetary boundary layer and implications for its modelling. *Journal of Climate and Applied Meteorology*, 24, pp. 1113–1142.
- Yamada, T. and G. L. Mellor, 1975: A simulation of the Wangara atmospheric boundary layer data. *Journal of the Atmospheric Sciences*, 32, pp. 2309–2329.
- Yamada, T., 1983: Simulations of nocturnal drainage flows by a q-1 turbulence closure model. *Journal of the Atmospheric Sciences*, 40, pp. 91–106.

## ANNEX 3.A

**GUIDELINES WHERE ACTION IS REQUIRED TO MINIMIZE THE IMPACT OF A LOSS OF OBSERVATIONS ON THE OPERATIONS OF THE GDPS**

1. The guidelines are based on experience with the shutdown of the OMEGA system and the action taken on year 2000 compliance. The action proposed addresses the various phases into which such problems can be divided.
2. While the guidelines focus on the loss of observations, they could just as well apply to maximizing the impact of positive changes in the GOS. Such situations may arise as part of a planned programme change such as targeted observations, special observing period data or implementation of a new observing platform. A need for information on a coordinated basis is also required in such situations to allow the data-processing system to both cope with, and optimally use, such new observations.

**Alerting**

3. The change in the observing systems may be known in advance or it may be unplanned.

For known changes:

- (a) Operators should provide notification to WMO following the current procedures where these are specified;
- (b) Otherwise information should be provided giving adequate notice through means such as:
  - (i) Official advice from the Secretary-General to NMHSs;
  - (ii) Notification through the technical commissions, in particular CBS and CIMO;
  - (iii) Use of specialist groups established for particular observation types (e.g. satellite soundings);
  - (iv) A data user's e-mail news group.

Unplanned changes:

- (a) Lead Centres should maintain reliable monitoring procedures to detect any problems;
- (b) RTHs should identify any communications problem restricting the flow of data;
- (c) Lead Centres should alert data providers (if necessary) through designated contact points (such as the Technical Coordinator of the AMDAR Panel). The WMO Secretariat may be able to assist in identifying relevant contact points.

4. Problems should be detectable with the quantity and quality monitoring systems established within CBS. Although many centres carry out data monitoring, the Lead Centres responsible for particular observation types should alert the operators and user community to a potential problem, particularly if the loss is due to a change in quality rather than to a loss of the observations itself (such changes may be due to changes in calibration of satellite instruments which may not be apparent to all users). For the NHMSs, this alerting can be through designated points of contact. The established network of focal points for data quality monitoring was not established for this purpose but may be suitable. This network needs to be updated regularly.

**Assessment of the problem**

5. In order to assess the problem:

- (a) Define the nature of the problem:
  - (i) Collect authoritative information from operating agencies;
  - (ii) Obtain guidance from relevant technical experts within CBS or other Commissions;
- (b) Obtain information on the scope of the problem and the timing of planned changes:
  - (i) Range of users and programmes likely to be affected;
  - (ii) Geographical extent;
  - (iii) Duration of the problem (if temporary);
- (c) Assess the likely impact on a range of users:
  - (i) NWP;
  - (ii) General use of the observations in the operations of NMHSs such as forecasting and climate or marine services;
  - (iii) Other WMO Programmes especially GCOS, hydrology, GAW;
  - (iv) Other WMO commitments e.g. UN/OCHA, GCOS, IPCC, and the Montreal Protocol.

6. The WMO system should act as an advocate for the broad range of its Members and users and be aware of the sensitivities of NHMSs and programmes to data losses.

7. For NWP, the impact can be based on surveys of previous observation impact studies and the work of organizations such as NAOS, COSNA, and EUCOS, the CBS OPAG/IOS and the OPAG/DPFS expert team. These studies can be used as the basis for an extrapolation to the current observation problem.

8. The assessment of the problem needs to be a collective effort. However, suitable individuals to initiate and coordinate action may be the chairpersons of the OPAGs on IOS or DPFS, or if the problem is confined to within one or two Regions, the appropriate RA chairperson of the regional Working Groups on Planning and Implementation of the World Weather Watch.

### **Problem prevention where possible**

9. This includes, for example, to make submissions to data providers to influence decisions.  
 10. Expert and representative impact assessments provide an authoritative basis for such submissions. This strategy was used unsuccessfully in the case of the OMEGA system, but is being used to preserve the microwave frequencies allocated for meteorological and remote-sensing purposes. It may also be used to make representations to NMHSs on planned closures of particularly valuable observing stations through:

- (a) Dissemination of information to highlight the impact of the loss of observations;
- (b) Form alliances with other users affected (e.g. radioastronomy in the case of microwave frequencies).

Responsibility for such tasks is best suited to the Secretariat.

### **Investigate mitigation strategies**

11. This includes:

- (a) Preserve maximum components possible of the observation: In the case of the OMEGA system, for example, WMO advocated the continuation of soundings for temperature and humidity even if wind observations were not possible;
- (b) Assist in implementing replacement systems: In the case of soundings from NOAA-11, for example, an informal group worked by e-mail with NOAA/NESDIS to facilitate the implementation of the new message type for soundings from NOAA-15 through message decoding and testing, feedback on errors and sharing information among the user community. The process was assisted by a responsive attitude and helpful advice from NESDIS;
- (c) Use alternative sources of data: This may be a longer strategy as in the future composite GOS, but there may be short-term possibilities such as use of AMDAR ascent and descent profiles for radiosonde flights. CBS can assist by providing information and training in such possibilities;
- (d) Establish back-up systems (e.g. satellites);
- (e) Build-in redundancy in the GOS: This may also be a longer strategy for the future composite GOS.

The responsibility for such task is best suited to CBS.

### **Finding and allocating resources to ameliorate the problem**

12. This could range from funding for particular observation types to relocation of back-up satellites. The impact statements referred to above may be used in developing priorities for the allocation of funding. Other criteria may be:

- (a) Effectiveness in ameliorating the problem;
- (b) Reliability;
- (c) Meeting of functional requirements (e.g. reaching 5 hPa for GUAN radiosondes);
- (d) Quality (e.g. as assessed through the Lead Centre monitoring);
- (e) Long-term continuity (especially for GCOS);
- (f) Support for multiple programmes;
- (g) Unique characteristics.

The responsibility for such task is best suited to Members.

### **Monitoring the problem**

13. This includes:

- (a) Assessing the extent of the problem and comparisons with projections;
- (b) Fine-tuning and adaptation of responses where possible.

### **Post-event review**

14. After the event, conduct a review to record any lessons learnt and document any procedures for future events.

The responsibility for such task is best suited to CBS.

### **Administrative aspects**

15. This second point worked successfully in the case of the termination of the OMEGA system. The team made recommendations to alleviate the problem and to assign priorities for use of the available funding for installation of alternative (GPS) radiosondes, for example:

- (a) Utilize existing formal and informal groups within CBS and WMO in general (CIMO, CAS, CCI);
- (b) If the problem is of a significant scale, establish a task team to analyse the problem, share existing information and develop expert advice.

## CHAPTER 4

# METHODS USED IN THE MANUAL PROCESSING OF DATA FOR ANALYSIS AND FORECASTING

### 4.1 Use of encoded analyses and prognoses 4.1.1 WMO analysis codes

There are four WMO codes, listed in detail in Volume I of the *Manual on Codes* (WMO-No. 306), which can be used to encode various types of meteorological data, analyses and forecasts, namely:

- (a) FM 45-IV IAC — Analysis in full form which provides for the manual coding of surface and upper-air analyses and prognoses by the location of individual elements, such as pressure centres, fronts, isobars, height contours, winds, tropopause waves, etc. This code form is no longer widely used in meteorological operations;
- (b) FM 46-IV IAC FLEET — Analysis in abbreviated form which was designed to be used for marine operations in reporting analyses and prognoses of sea-level pressure systems, fronts, etc., as well as sea-surface waves and temperatures. This code is still used by some marine interests;
- (c) FM 47-IX Ext. GRID — Processed data in the form of grid-point values, which was developed for use in both manual and computer encoding of the meteorological data field in grid-point form. However, experience has shown that the complexity of the code form has made its use practically impossible in manual operations and discouraged its use in all but the largest automated WWW centres;
- (d) FM 49-IX Ext. GRAF — Processed data in the form of grid-point values (abbreviated code form) which was developed to encourage use of the GRID code form in manual operations as well as at small computer centres (e.g. NMCs). The GRAF code is a simplified version of the GRID code in which each bulletin will contain data for one parameter at one level or pressure surface. To further simplify the use of the GRAF code, section 2 (grid geometry) and section 4 (check sums) of the GRID code are omitted in the abbreviated version.

### 4.1.2 Use of WMO analysis codes in data-processing activities 4.1.2.1 MANUAL OPERATIONS

In those WMO Regions where there are many manually-operated centres, it is recommended that meteorological analysis and prognoses be exchanged, as far as possible, by using FM 49-IX Ext. GRAF. Certain charts, such as surface analyses with plotted data, and charts prepared for use in the ICAO Area Forecast System will have to be exchanged by analogue facsimile. To receive analyses and prognoses from outside the Region (e.g. from a WMC or RMC), it may be necessary to make bilateral or multilateral agreements with an automated centre in or outside the Region to convert these products from grid-point to pictorial form, as described in section 3.6.2.

### 4.1.2.2 AUTOMATED OPERATIONS

In those WMO Regions where automated centres predominate, it is recommended that most meteorological analyses and prognoses be exchanged using the GRID/GRAF codes. Centres should be equipped with hardware/software systems for converting grid products into pictorial form (see section 3.6.2). Certain charts, such as aviation forecasts, which are not suited for encoding and exchanging in grid-point form may continue to be exchanged in pictorial form. Requirements for the exchange of products in grid-point form within each WMO Region, should be co-ordinated on a regional, or at least multilateral, basis so as to avoid unnecessary duplication of products and excessive load on telecommunications circuits.

### 4.2 Manual analysis of the vertical structure of the atmosphere 4.2.1 General

This section summarizes manual methods for the plotting and analysis of thermodynamic and wind shear hodographs, the plotting and analysis of vertical cross-sections and the plotting of atmospherics and pressure changes in both tropical and extratropical regions.

### 4.2.2 The plotting of thermodynamic diagrams

The data used for plotting thermodynamic diagrams are obtained from radiosonde, aircraft dropsondes and satellite vertical-temperature sounding reports.

The name and indicator number of the station or the geographical coordinates of the point as well as the time at which the report was made are entered on each diagram.

The pressure-temperature curve should always be drawn, the points being joined by straight lines.

The representation of humidity should preferably be by means of dew-point temperatures, though wet-bulb temperatures may be used. The legend on the chart should state clearly which element is entered. The dew-point temperatures (or wet-bulb temperatures) may be joined by broken straight lines.

If more than one sounding is entered on the same diagram, the curves should be distinguished one from the other by employing different symbols for the plots of temperature and dew point (or wet-bulb temperature) or additionally, when a polychromatic system is in use, by joining the points by lines of different colours.

Additional information, such as the heights of certain levels, the thicknesses of layers of the atmosphere, winds, cloud details, etc. may be entered on the diagram, preferably in the form of an inset table.

There are several types of thermodynamic charts which are in use in Meteorological Services. Among these are:

- (a) T-log p diagram;
- (b) Stüve or pseudo-adiabatic diagram;
- (c) Tephigram; and
- (d) Herlofson's skew T-log p diagram.

More detailed information on the theoretical basis, structure and use of these diagrams can be found in Stüve (1927), Berry, Bollay and Beers (1945), Herlofson (1947), Defrise (1948), Saucier (1955) and Pettersen (1956).

#### 4.2.3 *The use of thermodynamic diagrams in forecasting*

Thermodynamic diagrams are used in operational forecasting to analyse the stability of the atmosphere for forecasting thunderstorms and other types of severe weather, to analyse (and predict) the height of low clouds, to forecast the onset or termination of fog conditions, and to predict the maximum afternoon temperature and many other conditions connected with the general vertical structure of temperature and humidity in the atmosphere. More information on the use of thermodynamic diagrams in analysis and forecasting can be found in Berry, Bollay and Beers (1945).

#### 4.2.4 *Wind shear hodographs*

Wind data derived from observations made by pilot balloons, radiosondes, etc. may be plotted on a polar diagram to obtain wind shears and other information.

The diagram consists of a series of equidistant concentric circles labelled in suitable steps of wind speed. From the centre of these circles radii are drawn, usually at intervals of ten degrees and labelled from 10° to 360°.

On the diagram, wind at any height may be represented by a point at the intersection of the appropriate radius for direction and the appropriate circle for speed. The height of the observation should be entered alongside the point in decametres or tens of millibars with the letter S denoting the observation at the surface. This operation is carried out for successive altitudes and the plotted points are joined by a series of straight lines. The curve so obtained is called a hodograph.

If more than one sounding is entered on the same diagram, they should be distinguished one from the other by using different symbols for the plots of the wind data, or additionally, when a polychromatic system is in use, by joining the plotted points by lines of different colours.

For each hodograph the diagram should bear the time at which the observation was made and the name and indicator number or the geographical coordinates of the station at which the observation was made.

Use of the hodograph for single-station analysis and forecasting is given by Oliver and Oliver (1945).

#### 4.2.5 *Vertical cross-sections*

##### 4.2.5.1 *GENERAL*

Vertical cross-sections of the atmosphere are produced in two main forms:

- (a) *Time cross-sections*, which refer to soundings made above a single station over a period of time. In this case the base or abscissa of the diagram represents time on a suitable linear scale and the ordinate represents altitude, preferably on a linear scale;
- (b) *Space cross-sections*, which refer to conditions in a vertical plane at a specific time. The base or abscissa of the diagram represents distance along the horizontal on the same scale or a multiple or simple fraction of the scale of the basic synoptic chart in use. The ordinate represents altitude, preferably on a linear scale.

##### 4.2.5.2 *TIME CROSS-SECTIONS*

For each time of observation a line is drawn on the diagram at right angles to the base line intersecting the altitude or pressure lines. On this line, for simplicity called the vertical line, data are plotted for each level at which observations are available. A large number of derived parameters, such as potential temperature, virtual temperature, and specific volume, may be required on cross-section diagrams for detailed analysis techniques.

##### 4.2.5.3 *SPACE CROSS-SECTIONS*

For each station for which a sounding is available along the line of the section, a vertical line is drawn on the diagram at the appropriate position on the base line. Observations are then plotted on the diagram in the same manner as for time cross-sections.

The analysis of cross-section diagrams may be carried out in various ways. It may include the demarcation of the frontal surfaces, tropopause or areas of cloud, as well as the drawing of one or more of a number of isopleths such as isotherms, isentropes or isotachs. On every cross-section diagram the legend should give a complete explanation of the items included in the analysis. A more thorough discussion of cross-section analysis is found in Saucier (1955).

#### 4.2.6 Representation of air masses

A description of air-mass symbols and the techniques for representing air masses on synoptic charts will not be discussed in this guide. Information on classifications and depictions on synoptic charts is provided by Saucier (1955) and Pettersen (1956).

#### 4.2.7 The plotting of atmospherics

##### 4.2.7.1 THE PLOTTING MODEL

The plotting model for representing atmospherics on surface charts is:



##### 4.2.7.2 RULES FOR PLOTTING THE INDIVIDUAL ELEMENTS

**GG** Time of observation

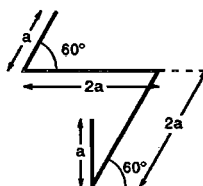
This is entered as given in the report.

**A<sub>i</sub>** The repetition rate of the atmospherics

This is plotted by means of sloping lines added to the basic symbol. The following table shows the complete symbol to be plotted for each value of A<sub>i</sub>.

	0	1	3	5	7	9
<b>A<sub>i</sub></b>	✓	✓	✓	✓	✓	✓

The dimensions of the symbols for A<sub>i</sub> are shown in the following diagram:



The recommended length for 2a is 1 cm.

**a<sub>i</sub>** Distribution of atmospherics

This is not shown in the model but it is used as follows:

If a<sub>i</sub> is reported as zero, there is an isolated point of atmospherics and the symbol for A<sub>i</sub> is plotted so that the bottom point is at the position given.

If a<sub>i</sub> is reported as 4, the atmospherics are occurring within the area enclosed by lines joining the successive position points given in the message and the symbol given by A<sub>i</sub> is plotted inside it.

If a<sub>i</sub> is reported as 6, the atmospherics lie along the line joining the successive position groups and the symbol for A<sub>i</sub> is plotted in the middle, at one end or at both ends of the line.

#### 4.2.8 Plotting and analysis of wave conditions

##### 4.2.8.1 PLOTTING MODEL

Procedures for plotting individual elements of wave conditions are given in Volume, I Attachment II.4 of the *Manual on the GDPS*.

##### 4.2.8.2 ISOPOLETHS OF WAVE HEIGHTS

Isopleths of wave heights should be drawn at intervals of one metre or multiples or sub-multiples thereof, a solid line being used for sea waves and a broken line for swell waves. Areas of confused direction are indicated by dots in a line, thus .....

##### 4.2.8.3 MOVEMENT OF PREDOMINANT WAVE TRAINS

Large arrows with solid shafts are entered on the charts to indicate the directions in which the predominant sea wave trains are moving. Large arrows with broken shafts are entered to show the directions in which the predominant swell wave trains are moving.

##### 4.2.9 Pressure-change charts

Isallobars on charts for three-hour pressure changes should be drawn for intervals of one hectopascal; on those for 12 hours and 24 hours the intervals may be 5 hPa.

If a single colour is used, the zero change line should be thicker than the other lines and the lines with negative values may be dashed.

If a polychromatic system is employed, black or purple is recommended for the zero line, blue for the lines of positive change, and red for those showing negative change.

In both systems, the values of the change lines will be clearly labelled, preceded by the appropriate positive or negative sign.

The centres of isallobaric highs should be marked by a plus sign and the centres of isallobaric lows by a minus sign. Earlier positions of centres, with the corresponding time to the nearest hour UTC entered above the centre, may be connected by an arrow, the head of which terminates at the position point of the current centre.

#### 4.2.10 *Tropopause charts*

Suggested intervals for isopleths showing the contours of the tropopause are as follows:

- (a) If altitudes of the tropopause are used: 1 000 m but with additional isopleths at intervals of 500 m when the spacing is wide or irregular;
- (b) If pressure values of the tropopause are used: 50 hPa but with additional isopleths at intervals of 25 hPa when the spacing is wide or irregular.

On occasion, tropopauses at two or more levels may be in existence over the same area of the chart. Two or more sets of intersecting lines may then have to be drawn to give a complete representation of the tropopause field.

### 4.3 Methods of manual analysis and prognosis in extratropical latitudes

The role of computers and humans was already discussed previously. This section summarizes the various techniques which are used by man in the work of analysis and prognosis at the present time. Analyses and prognoses prepared by numerical methods are now readily available either from a computer system within a centre or from external sources via facsimile or the use of GRID/GRAF-code products from other centres. As these become more sophisticated and achieve accuracy there is a period of transition during which many of the time-honoured traditional methods give way to new techniques when numerical products play an increasingly important role. Thus the emphasis in these paragraphs is placed on the new manual techniques being evolved to obtain the best value from the data and the computer products now available. Traditional methods will certainly be mentioned, but if more details are required on such methods, recourse should be made to the many standard textbooks on the subject. This section is divided into two main parts:

- (a) Manual techniques involved in analysis;
- (b) The human role in modern forecasting techniques.

#### 4.3.1 *Manual techniques involved in analysis*

The object of analysis is the determination and depiction of space and time variations of significant meteorological parameters with a view to facilitating the forecasting of those parameters, that is their determination at a future time. An essential characteristic of manual analysis is the recognition of structure and the use of structural concepts or structural models, for example depressions, anticyclones, troughs, ridges, fronts, instability lines, and so forth. An analysis must be conceived as a four-dimensional activity (three dimension being in space and the fourth dimension being time). Practical considerations, however, limit the process to the use of displays in two dimensions, for example surface and upper-air contour charts, supplemented by one-dimensional representations, such as aerological diagrams. The sequence in time of these displays is a recognized method of ensuring historical continuity, while hydrostatic and dynamical consistency are necessary constraints for the achievement of meaningful results. An analysis of meteorological variables specifies an initial state, that is the atmospheric state at some fixed time, but the diagnosis of this initial state requires the use of analyses from earlier times, and also the recognition of continuity principles and theoretical ideas based on the known behaviour of structural models. The following aspects of the problems of analysis will be discussed:

- (a) Requirements for manual analyses;
- (b) Analysis techniques.

##### 4.3.1.1 REQUIREMENTS FOR MANUAL ANALYSES

Numerical methods have now enabled the analysis of meteorological variables to be made by machine, and fields depicting the spacial distribution of such variables can be produced in almost any format required. Thus analyses of all the usual fields required are now produced by computer methods at larger meteorological centres and many such analyses are available for use by other centres (either via facsimile or GRID/GRAF data). Requirements for undertaking manual analyses at a particular centre will depend on whether computer facilities are available or not. However, requirements for manual analysis can arise from the need:

- (a) To monitor objectively produced analyses;
- (b) To ensure that the best possible analyses are available for numerical weather prediction techniques;
- (c) To provide analyses earlier than they would otherwise be available;
- (d) To carry out quality control of data;
- (e) To analyse small features;
- (f) To provide the day-to-day means for forecasters and analysts to understand the evolution of the atmosphere.

###### 4.3.1.1.1 *MONITORING OBJECTIVELY-PRODUCED ANALYSES*

When numerical techniques are used for the production of analyses it is necessary to prepare manual analyses of certain fields and features in order to assess the quality of the numerical products. As techniques to produce analyses by numerical methods improve, monitoring requirements will tend to diminish, if not disappear

altogether. The degree of monitoring will depend on the availability of staff and the quality of the analyses produced by the numerical methods. At a large centre where numerical weather prediction techniques are employed, other considerations may apply. These are discussed below.

#### **4.3.1.1.2 USE OF MANUAL ANALYSES IN CONNECTION WITH NUMERICAL WEATHER PREDICTION TECHNIQUES**

At a large centre which produces numerical weather prediction products, it is of considerable importance to ensure that the background fields for the time of the new analyses are as good as possible. Such background fields are usually in the form of 12-hour forecasts based on an analysis of the data for the previous 12 hours. Since the forecasts cannot be expected to be accurate if the analyses on which they are based are poor, considerable effort is required to ensure that the 12-hour forecasts are as accurate as possible. This usually involves carrying out analyses by hand, but using computer products in the process. The analyses held in the computer are then adjusted as necessary before the final 12-hour forecast is run prior to the arrival of the new data. The rationale for this approach and the techniques involved are discussed below.

#### **4.3.1.1.3 EARLY PROVISION OF ANALYSES**

At a large centre with automated facilities it is not possible to obtain an analysed chart by objective means until a certain period of time has elapsed after the observation time. The reason for this is that it is unproductive to carry out the analysis program before the majority of data are available. However, it is possible to obtain plotted charts in the interim period (sometimes referred to as "quick-look" charts). Although the data plotted will not be complete, it is possible to sketch analyses which may be of considerable value in the preparation of forecasts which have to be issued prior to the arrival of machine-analysed charts.

At smaller centres the need for manual analysis is even more pressing since analyses via facsimile or the utilization of GRID/GRAF-code products arrive quite late. This is because the analyses have to be prepared first at the main centre (computed and prepared in a suitable form for transmission) and then further time is required to issue the analyses via the appropriate telecommunications network. Thus in a small office there is usually a greater requirement for the use of manual techniques in the analysis of data which are available in alphanumeric form, especially those data relating to the immediate area near the centre or the country in which the centre is located.

#### **4.3.1.1.4 QUALITY CONTROL THROUGH THE MANUAL PREPARATION OF ANALYSES**

Automated global data-processing centres carry out quality control procedures (see Chapter 6). Such computerized techniques can, however, be complemented by manual quality control techniques resulting from the manual analysis of data. Such quality control depends upon the skill of the analyst in detecting subtle errors in data which evade the normal automated quality control tests. Manual analysis techniques can frequently highlight data which are erroneous but which evade the automated quality control tests. If left untouched in the computer, such data may result in significant errors in the numerically produced forecasts.

#### **4.3.1.1.5 SMALL FEATURES**

Analyses prepared by objective methods are usually for large areas. The numerical techniques involved in numerical analysis programs make use of a grid of points (see paragraph 3.4.2). Features which are in the order of, or smaller than, the spacing of the grid points cannot be analysed satisfactorily by numerical methods. Such analyses are best made by using manual methods.

#### **4.3.1.1.6 UNDERSTANDING THE BEHAVIOUR OF THE ATMOSPHERE**

The construction of well-drawn hand analyses is an art as well as a skill. The analyst also needs to have an appreciation of the atmosphere. When constructing an analysis, the analyst will take into account continuity in time and in space. In the construction of constant-level or constant-pressure charts the analyst is required to keep in mind the basic physical and thermodynamic behaviour of the atmosphere. When manual analyses are not prepared, but numerical products are accepted, there is nothing to draw the attention of the analyst to these aspects since vertical and horizontal stability will have been ensured while continuity in space and time will have been included automatically. Thus there is a possibility that forecasters will no longer examine the observations in detail and no longer appreciate the works of the atmosphere as before. There may be a tendency to accept machine products since they are now so good. It is by continually working with observations that gives a forecaster much of his background ability to know the atmosphere. This knowledge in turn assists his or her interpretation of the forecast even if produced numerically. Thus it may be considered worthwhile to retain manual analysis to some extent within an office, to ensure that forecasters are still able to work with basic observations. These skills are important in an office in which there are forecasters who have to issue forecasts of weather (as opposed to forecast fields, for example the forecast mean sea-level pressure field). In an office merely concerned with the production of analysed fields and forecast fields there is probably little, if any, need for manual analysis techniques to be maintained except perhaps from the necessity to monitor the machine analyses.

#### **4.3.1.2 ANALYSIS TECHNIQUES**

Modern analysis techniques incorporate many of the time-honoured traditional techniques, but also utilize the many aids now available, such as the provision of fields analysed by numerical methods. The various techniques will be discussed under the following headings:

- (a) Types of analysis;
- (b) Analysis of surface features;
- (c) Upper-air analysis techniques;
- (d) Analysis of satellite information;
- (e) Other techniques for the analysis of data.

#### 4.3.1.2.1 TYPES OF ANALYSES

The analyses required at a meteorological centre include:

- (a) Isobaric analysis;
- (b) Discontinuities;
- (c) Vertical instability;
- (d) Cross-sections;
- (e) Specialized analyses of individual elements;
- (f) Satellite data.

##### 4.3.1.2.1.1 ISOBARIC ANALYSIS

The depiction of atmospheric variables at different pressure levels constitutes the basic framework of analysis. These levels include the surface (or 1 000 hPa), 850, 700, 500, 300, 200 and 100 hPa, and the data being plotted for 0000 and 1200 UTC. Additionally, there may be special needs for charts at other levels, for example at 400 and 250 hPa, and at the higher levels of 50, 30 and 10 hPa, and above. The 1 000/500 hPa thickness chart plays a fundamental role in depicting the mean temperature state of the lower troposphere and in ensuring hydrostatic consistency between the surface and 500 hPa levels.

It is advantageous to depict more than one set of isopleths on the chart for any particular isobaric surface, for example 500 hPa contours and surface isobars and/or surface frontal analysis. In this way, details of vertical structure are emphasized and an appreciation of the thermal advection field is afforded. This follows from the evident relationship between the surface and upper patterns. This aspect of analysis, in which the emphasis is on the large-scale distribution of meteorological parameters, must be supplemented by the analysis of features on a smaller scale.

##### 4.3.1.2.1.2 ANALYSIS OF DISCONTINUITIES

The analysis of smaller-scale features or discontinuities comprises:

- (a) Frontal analysis, three-dimensional in character, but depicted on the surface chart;
- (b) Inversions, identified from aerological diagrams;
- (c) Advection discontinuities, particularly in sub-tropical areas;
- (d) Tropopause characteristics, identified from aerological diagrams;
- (e) Jet streams, from upper-wind ascents, in relation to tropopause analysis;
- (f) Trowals (Canadian practice) defined as a trough of warm air aloft;
- (g) Squall lines, instability lines, and pressure jumps;
- (h) Shear lines (upper-air).

The importance of the analysis of discontinuities derives from their close association with features of weather, that is with three-dimensional, dynamical and physical processes.

##### 4.3.1.2.1.3 ANALYSIS OF VERTICAL INSTABILITY

Vertical instability, that is hydrostatic instability, plays an obvious part in many weather processes. Its analysis is, therefore, of considerable importance particularly in subtropical areas where it may play a dominant role, for example in upper cold lows and troughs. In assessing liability to instability, the direct use of aerological diagrams is essential and regard should be paid to the distribution of humidity and its possible modification. At an RMC, the depiction of vertical stability over extensive areas is achieved by the use of a stability chart on which the values of a stability parameter, for example the Showalter Index or Boyden Index, are depicted as isopleths. Reports of atmospherics (SFLOC) are particularly useful in data-sparse areas and their distribution in space and time may be depicted with advantage.

##### 4.3.1.2.1.4 VERTICAL CROSS-SECTION ANALYSIS

The use of cross-section analysis techniques to depict the distribution of one or more parameters in the vertical is an auxiliary aid. The horizontal axis of such cross-sections may depict variations in space, that is along a particular line or axis, or variations in time. Further details are discussed in sections 4.2.5 and 4.3.1.2.6.

##### 4.3.1.2.1.5 SPECIALIZED ANALYSES OF INDIVIDUAL ELEMENTS

Individual meteorological elements may be analysed separately, for example wind hodograph analysis and isotach analysis.

For particular elements, for example visibility, cloud and precipitation, isochrones may be constructed to emphasize variations in space and time particularly of the leading edges of such phenomena.

##### 4.3.1.2.1.6 ANALYSIS OF SATELLITE DATA

Satellite data are now available at most centres. The use of such data is discussed fully in section 4.3.1.2.4.

#### 4.3.1.2.2 ANALYSIS OF SURFACE FEATURES

In meteorology, the well-analysed surface weather map or synoptic chart is a basic aid from which a forecaster is able to start to build up an understanding of the state of the atmosphere at a given time. The word synoptic means viewed together. A surface synoptic chart is a snapshot of weather observations which are made from ground level or from ships at sea. It is the skilful analysis of these observations which constitutes a firm foundation upon which all forecasters of the weather must ultimately depend.

The individual surface observations are not entirely confined to a point on the Earth's surface. The observations of the state of the sky give a great deal of information about the upper levels of the atmosphere, while those of the state of the weather and, in particular, the visibility can provide information on conditions within a range extending a considerable distance from the point at which the observation is made.

The actual observations which are made and which are available include instrumental or measured observations, such as the barometric pressure, temperature, wind speed and direction, visibility (sometimes measured and sometimes estimated) and height of the base of low cloud, as well as visual observations, which include the types of clouds in the sky, the total amount of sky covered by clouds, and the present and past states of the weather.

The analysis of a surface (mean sea-level) synoptic chart may be divided into two major basic steps. These are:

- (a) Frontal or air-mass analysis;
- (b) Construction of the mean sea-level pressure field.

After these two steps have been satisfactorily accomplished there are a number of secondary steps which may be taken in order to extract the maximum amount of information from the data available. For example, the isallobaric pattern may be drawn in selected areas on the chart. It may also be useful to depict areas of precipitation, freezing precipitation, thunderstorm activity and fog on the chart, using various colours.

The two main steps of the analysis of the mean sea-level synoptic chart mentioned above need not be taken rigidly in the order shown. Although there is no hard-and-fast rule, many analysts will find it convenient to decide where the main air-mass boundaries are and to place the fronts in those areas of the chart of immediate interest before attempting to construct the isobars. Such areas of interest are usually the extratropical areas and areas in the vicinity of the analysis centre. The exact shape of the isobars is determined to a considerable extent by the position of the fronts. The pressure pattern may give valuable information regarding the position of a front, but this assistance from the isobar shape is best used to settle an otherwise inconclusive argument rather than to serve as a primary reason for the identification of a front.

##### 4.3.1.2.2.1 FRONTAL ANALYSIS

Continuity in frontal analysis is of paramount importance. It is therefore essential for the analyst to have at least one, and preferably two or more, consecutive synoptic charts beside him relating to previous synoptic hours when carrying out a frontal and air-mass analysis. When making decisions on the passage of fronts through particular synoptic stations, it is sometimes more valuable to compare observations 24 hours apart, thus cutting out the diurnal factor.

Fronts should relate to the large-scale thermal field and it is good practice to ensure that the fronts depicted in the analysis are related to the broad-scale thermal field characterizing the lower troposphere. The 1 000/500 hPa thickness analysis is a useful one in this context since it depicts the mean temperature of the atmosphere below 500 hPa.

Fronts can be considered as discontinuities in the thermal advection field. The frontal passage at any particular station may be recognized from discontinuities evident in the autographic record. On small-scale charts, these observations are not generally available and it is desirable to be able to identify or recognize frontal positions from the relation of the flow to the thermal field. Fronts determine sharp changes in the advective process. A cold front is usually followed by the strong advection of cold air, known as cold advection, while a warm front is necessarily preceded by a zone of strong warm advection. Occlusions mark the transition between zones of warm and cold advection.

Fronts at the surface are associated with maximum low-level velocity convergence and are marked by discontinuous cyclonic shear of the geostrophic wind.

Fronts should be related to the properties of air masses. The analysis of air mass properties, formerly considered of unique significance, is still of use in everyday practice, since fronts are associated with the strong non-linearity occurring in such zones. Those individual elements of greatest importance include:

- (a) Temperature, in particular potential temperature;
- (b) Dew point;
- (c) Cloud;
- (d) Visibility.

Numerically produced products may assist in the placement of fronts. This is an area where numerically produced products can be of considerable use and guidance.

The analysis of the 1 000/500 hPa thickness field, the 850 hPa wet-bulb potential temperature and other fields of potential temperature can provide useful guidance on the positioning of fronts, especially the large-scale thermodynamic features in the atmosphere. In this connection, it is strongly recommended that on small-scale charts (1:15 million, 1:20 million, 1:30 million) fronts are only included in the analysis if they are indeed large-scale features consistent with the broad thermal structure of the atmosphere. The use of satellite pictures in frontal analysis is discussed in section 4.3.1.2.4.

#### 4.3.1.2.2.2 THE PRESSURE FIELD

After the major frontal systems have been identified, isobars should be sketched in. Preliminary work involves sketching some of the key isobars (say at 8 or 10 hPa intervals) and then completing the detail when these key isobars fit the data reasonably well. Continuity should be maintained from the previous analysis. There are two ways of achieving this continuity. The time-honoured traditional method is to place the analysis for the previous synoptic hour underneath the chart being analysed on a light table. With the availability of computer forecast products, however, continuity can be catered for by using a six- or 12-hour forecast chart as the basis for the analysis, adjusting the isobars as necessary. Even if this latter method is used it is recommended that the analysis be compared with the previous one before finalizing the fine detail.

The main features of the pressure field include:

- (a) The anticyclone;
- (b) The ridge of high pressure;
- (c) Frontal wave depressions in various stages of development;
- (d) The occluded-depression vortices in which the occlusion often no longer extends into the low pressure centre;
- (e) The polar depression;
- (f) The tropical depression;
- (g) The thermal or heat low;
- (h) The orographic or lee depression;
- (i) The trough of low pressure.

In addition to the areas of high and low pressure, the pattern may take the form of a col or saddle-shaped feature which connects adjacent high and low pressure systems. In summer, there may be little pressure gradient over areas of the analysis. In these areas the pressure field is called flat or slack.

Over high ground, barometric pressures are normally reduced to mean sea-level. However, if the altitude of the station is high, the reduction process introduces significant errors with the result that the pressure value at the station cannot compare with neighbouring low-level stations. Thus in drawing isobars over a large plateau or over an area of high ground there will be a discontinuity between the sea-level pressures and those reduced to a higher level. In such instances, care must be taken to ensure the regularity of the pattern. It may be useful to draw such high-level patterns with dashed lines, for example, in a different manner from the main sea-level pattern. When there is a high mountain range (for example, the Alps), sea-level isobars on either side of the range may not be continuous. The effect is particularly pronounced if there is a marked difference in air temperature between the two sides of the range. On these occasions, it may be desirable to omit the isobars over the high ground or to draw them discontinuously rather than imply fictitious curvatures in the isobars over the adjacent lowlands.

#### 4.3.1.2.2.3 USE OF NUMERICAL FORECAST PRODUCTS IN THE PREPARATION OF ANALYSES

Numerical forecast products can be useful in the preparation of analyses. A 12-hour forecast from a numerical weather prediction model can be used in preference to the previous synoptic chart to provide a useful first guess field. The analyst does not then mentally have to move features forward by six or 12 hours since the computer has already done this task in computing its forecast. The job of the analyst becomes an adjustment of the 12-hour forecast in light of the new data available. Keeping in mind that this background first guess field is a forecast, the analyst must complete the job by ensuring continuity with the previous analyses available. Such techniques are particularly valuable when analysing the pressure fields over areas of sparse data. Useful assistance can also be obtained in connection with the movement of fronts by studying the various fields which can be associated with fronts, such as humidity fields, wet-bulb potential temperature fields, and so forth. A careful appraisal of the computer movement of such fields in relation to the analysis of the previous 12 hours can be a useful means of making decisions on frontal positions in the absence of other data at the new time of analysis.

#### 4.3.1.2.2.4 ANALYSIS OF OTHER FEATURES

The analysis of isallobars, humidity fields, cloud, wind speed, temperature fields, areas of significant types of weather and so forth should be related to the overall pressure and frontal analysis. It should be said that the necessity for such analyses will depend on local requirements.

#### 4.3.1.2.3 UPPER-AIR ANALYSIS TECHNIQUES

##### 4.3.1.2.3.1 GENERAL CONSIDERATIONS

Since weather occupies three dimensions in space, no study of it is complete without the inclusion of the vertical structure of the atmosphere. Observations of temperature, humidity, pressure and wind in the free atmosphere are recorded regularly at a number of land and ocean stations, but the number of these stations is small compared with the number of stations taking surface observations. This is largely due to the cost of maintaining upper-air stations, particularly over the ocean. Fortunately, irregularities in the spatial distribution of the values of the temperature, humidity and wind are not as great in the upper air as at the surface. It is therefore of the utmost importance in the analysis of upper-air charts to ensure that no observation is neglected unless there are good grounds for considering it to be grossly inaccurate. This is not meant to imply that all observations should be accepted as exact. A critical weighting of the various items of information is essential for sound analysis. The importance of continuity from one level to another and from one time to another in upper-air analysis

cannot be over-stressed. Over the oceans it is quite possible for an important feature on one chart to apparently be lost 12 hours later in the area between simultaneous soundings made many hundreds of kilometres apart. It is absolutely essential that any feature clearly portrayed on one chart should not be neglected at higher or lower levels or dropped from subsequent charts without very good reason.

The traditional observations plotted on upper-air charts are mainly instrumental and, with the exception of wind, are measured by an instrument (radiosonde) remote from the station. There are various types of radiosonde and unfortunately the accuracy of types or even of models within types is not uniform. The inaccuracies fall broadly into two groups: systematic errors characteristic of the design of the radiosonde and the techniques employed in its operation, and non-systematic errors which occur during a particular ascent. Irregularities of the former group are frequently noticed at national boundaries at the higher levels (mainly 200 hPa and above) and arise largely from radiation effects on the radiosondes. This effect is most marked at high levels during daytime, and it is to be noted that such instrumental errors are generally a function of height, so that if an error is found or suspected at one level it must be allowed for at other levels in the same ascent. A non-systematic error on any ascent may or may not affect the accuracy of the information for a level other than that at which it occurs, depending on the nature of the error and on the technique used for the calculation of the results of the soundings. The errors of radiosondes can be assessed on an operational day-to-day basis by careful analysis of the 100 hPa level.

There are now other sources of data besides the traditional observations described in the paragraph above. These sources include imagery (visible and infrared) and radiance measurements from satellites, and reliable observations of wind from aircraft. Photographs from satellites in orbit may be used to locate systems in the upper air as well as at the surface, while those from geostationary satellites enable cloud movements to be measured and hence wind at the cloud height to be derived (SATOB). Satellite measurements of atmospheric infrared radiances at various wavelengths enable estimates to be made of temperatures at a number of levels in the atmosphere and can be used for the calculation of thickness values (SATEM) which in turn can be used to provide estimates of the geopotential height of various geopotential surfaces. Such data fill large gaps in the network of observations, but they vary in quality and must be checked carefully before use. Winds reported by aircraft are almost invariably measured by Doppler radar or inertial navigation systems and provide a very valuable and reliable source of data for the higher levels, in particular the 300 hPa level. Such observations have compensated in some measure for the reduction in the ocean weather station networks and, although the observations are restricted in general to the main air routes, they provide an excellent and hitherto unavailable opportunity for detailed analysis of the wind field at levels near that of the jet stream. It is therefore of vital importance that such aircraft data be exchanged regionally and globally in real time. In general, wind observations are transmitted during flight over sparsely populated areas, the data then being introduced into the global telecommunications system. However, there is a tendency to require the transmission of the data during flight over data-sparse areas which are not always the same as sparsely populated areas. When flying over areas where transmission of weather data in flight is not a requirement, the aircrrew usually enter the wind observations on a special in-flight reporting form and deposit this in a central place for subsequent collection by staff from the Meteorological Service. Every effort should be made to ensure that the information is entered into the global telecommunications system as quickly as possible. An aircraft-to-satellite data relay system (ASDAR) was used during the First GARP Global Experiment (FGGE) to provide wind and temperature data. This scheme was very successful and new techniques are being developed to provide an improved operational system for use in the future. Features of the newly developed system will enable two temperature and wind data profiles to be obtained from aircraft every 7.5 minutes during flight and more frequently on ascent and descent, thus providing the possibility of obtaining data similar to those from radiosondes at many of the major airports.

The upper-air observations enumerated above can be plotted in a variety of ways. One way is to plot the observations on charts depicting a particular surface, each chart having observations for a particular height or level plotted on it. Such charts fall into two groups: those portraying the variations of pressure over surfaces of constant height above mean sea-level, and those showing the variation of height over levels of constant pressure. Mean sea-level pressure analyses and forecasts are examples of the former type, but when preparing upper-air analyses it is more convenient in practice to use surfaces of constant pressure (contour analyses). Such a system for the upper-level fields has the advantage that one geostrophic wind scale can be used for all levels and this scale can also be applied to the thickness isopleths giving a simple determination of the thermal wind. Furthermore, isopleths on isobaric surfaces are lines of constant potential temperature.

Another way of making use of upper-air data is to plot the data on vertical cross-sections of the atmosphere. Two methods of analysis, isentropic analysis and frontal contour analysis, are valuable techniques.

The upper-air charts commonly required at an operational meteorological centre include constant pressure charts for the levels 1 000, 850, 700, 600, 300, 250, 200 and 100 hPa. Charts at levels above this, up to 10 hPa, are also drawn at some centres, but mainly for research purposes.

A further set of charts of considerable use to upper-air analysts and forecasters are the thickness charts. On these charts are plotted the thicknesses of the column of air between two chosen pressure levels and, in addition, the vector differences between the winds at the two pressure levels. The isopleths of equal thickness are drawn at standard intervals, as in the case of upper-air analyses. The interval varies at different centres but is

usually in the order of 40, 50 or 60 gpm. The most frequently used thickness charts are for the layers 1 000/500 hPa, 1 000/850 hPa and 1 000/700 hPa. For some aviation purposes, charts are drawn at the level of the maximum wind. These are usually combined with tropopause analyses.

Contour analyses at levels from 1 000 hPa up to 100 hPa and of various thickness patterns are now carried out on a routine basis by computers, and the larger centres issue their output for use by other centres. At a centre with automatic facilities, it may still, however, be necessary for manual analyses to be drawn, both as a check on the computer products and as a basis for amendment of the computed patterns if they are not efficient in some way. The computer analyses are based upon:

- (a) A background field, the 12-hour prognosis based upon the previous analysis;
- (b) The observations.

Quality control is applied to the observations (see Chapter 6), and the procedure, however comprehensive, must be rigid but not too exacting. Thus observations may be accepted which are in error, or some which are correct may be rejected. The forecaster may, on the basis of his or her examination and analysis of the data, intervene to remove any observations which are considered to be in error or to re-insert those flagged by automatic quality control techniques as possibly in error and which are believed by the analyst to be correct. Intervention may also be made to amend the contour or thickness pattern in areas where it is felt that the computer analyses could be improved, for example, where data are sparse and the analysis relies heavily on the background field, or where a fairly intense synoptic system may not have been adequately represented. The intervention consists of the insertion of bogus observations which, it is hoped, will lead to a better computer analysis. It is also possible to intervene directly on the field in question by means of direct intervention schemes using a visual-display unit and light-pen input.

#### 4.3.1.2.3.2 PRINCIPLES OF ANALYSIS

The basic principle of the analysis of upper-air data is the drawing of contours to fit the reported heights, using the observed winds to estimate the direction and magnitude of the slope of the isobaric surface, that is the orientation and spacing of the contours. In practice, the analysis is complicated by the presence of errors in both the heights and the winds and by the fact that, although the geostrophic wind approximation is reasonable over much of the chart, there are areas where the ageostrophic component of the wind may be significant.

The traditional method of upper-air analysis was to take the mean sea-level analysis as the starting point. Contour analyses of the upper levels were constructed using analyses of the thicknesses of different layers from the surface (1000 hPa level) and applying gridding techniques. Thus vertical consistency was ensured and use was made of the analysis with the most data, the mean sea-level analysis.

In the last few years the increasing availability of aircraft data in the vicinity of the 300 and 250 hPa constant-pressure surface, as well as the interpretation of satellite imagery in diagnosing upper features and the use of radiance data from satellites have made the analysis of the 300 hPa level possible without the need for a gridding process from the surface. Thus it is now more practical to analyse the 100 hPa level to assess radiosonde errors, make the appropriate corrections to the 300 hPa radiosonde data and then analyse the 300 hPa level directly. The 250 hPa and 200 hPa levels can then be analysed in relation to the 300 and 100 hPa levels. The same principles of continuity of features must be maintained in the drawing of upper-air charts as in the construction of surface analyses. Data at levels of up to 500 hPa can be analysed with reference to the surface features, with gridding techniques only being used over the ocean and other data-sparse areas. The 500 hPa analysis may need adjustment when compared with the 300 hPa analysis.

Errors in radiosonde reported values lead to errors in the computed geopotential heights, which generally increase with height. In the upper troposphere and the stratosphere, a large part of the error is a result of solar radiation falling on the instrument. The total error is composed of systematic and random errors. Random errors cannot be spotted unless there is a fairly close network of stations. Systematic errors would not have a great effect on the analysis if all the sondes had the same systematic error, but this is not the case and it is only too obvious to the analyst of the 100 hPa charts that allowance must be made for the various kinds of radiosonde in use. It is also useful to know whether or not a solar-radiation correction has been applied before transmission. Information on the types of radiosonde in use is given in the WMO *Catalogue of Radiosondes in Use by Members*, which is published as Report No. 11 of the Commission for Instruments and Methods of Observation. This report is re-issued at irregular intervals. It is possible to determine, on a rough basis, corrections to be applied to the various groups of sondes to bring their heights into better agreement. To do this it is necessary to choose one group of sondes as a standard and select charts when, according to reported winds, the airflow is relatively simple with slack gradients. It is then possible to calculate the gradients from the wind reports and to establish contour heights over the chart in terms of the standard sonde heights. The systematic errors of sondes in the various geographical groups (mainly national) according to the solar elevation can then be determined. A considerable number of occasions must be taken in order to eliminate random errors. The systematic errors thus found can be applied as corrections to future reports during analysis (or by additional plotting). The scheme provides valuable information in undertaking manual analysis, and can also be adapted in the use of computer techniques.

These corrections are best found at 100 hPa but they also apply to some extent to 200 and 300 hPa. Hawson and Caton (1961) suggest that after having established the error at 100 hPa, the following corrections should be applied to the lower-level observations:

<i>Level</i>	<i>Correction related to the error at 100 hPa</i>
200 hPa	60 per cent
300 hPa	35 per cent
500 hPa	10 per cent

These same percentages can also be applied as rough corrections to individual anomalous soundings if it is believed that the abnormality noted increases progressively with height. It will be appreciated that any change in radiosonde type, or in method of obtaining results will result in systematic errors becoming obsolete without warning. Such values need to be kept up to date, a task which is feasible at a centre with automatic facilities.

Where there is a dense network of reporting stations, as in Europe and North America, a compromise of the majority of winds and heights is not difficult to attain and erroneous data can usually be detected fairly easily. However, over the sea, and in other areas where the observations are far apart, each station's report must be examined critically. If an erroneous observation is incorporated in the analysis it may well introduce errors over a large area and consequent errors in the forecast over even wider areas. It is essential to make use of all possible checks, such as continuity in time and in the vertical, and of the reasonableness of the analysis in comparison with climatological limits and known patterns. The maintenance of displays showing successive observations from isolated stations and the close scrutiny of such displayed information in relation to the overall analysis cannot be stressed too highly.

Errors in reported winds should also be kept in mind. These errors arise from two sources. One is the random error of the range, bearing and elevation readings of the radar, the error increasing only slowly with height. The other source of error which should be borne in mind is when, as a result of the geopotential height error, the reported wind does not correspond to the height of the required pressure level. This error may be important in regions of strong vertical wind shear.

Reports of wind determined by aircraft are a valuable help in the analysis of the 300 and 250 hPa contour patterns. Although the associated contour heights are not available, contour gradients may be derived on the contour charts from the observed winds. Normally this is done by showing that the geostrophic relationship holds and relating the derived pattern to any available radiosonde data. Adjustments may be made, for example for curvature and to improve the fit, if necessary. The pattern has to be merged to fit the analysis over areas where height data are available.

In a large centre where numerically produced analyses are available, preliminary analyses may need to be drawn using manual procedures. Such preliminary analyses may have been prepared using either the 12-hour forecasts as the first guess field or the traditional continuity methods using the previous analysis as the guide for the new analysis. Any further work of manual analysis should, however, include the numerically produced analyses to as great an extent as possible. Centres should, therefore, make the best possible use of computers, with their ability to process large quantities of data rapidly, and of humans, with their ability to exercise judgement based on experience and complex logical processes. The computer takes as a background field the 12-hour forecast based on the analyses at the last main synoptic hour, usually 12 hours earlier. The background field is then modified by the new data. In regions where data are plentiful the new analysis is based mainly on the data, but where data are sparse, the background field is hardly changed. The data, before incorporation in the analysis, undergo quality control in the computer and those which are in error according to certain fixed criteria are rejected. The human analyst also examines the data to see whether:

- (a) Any observations that contain errors can be corrected, perhaps after a detailed examination of the ascent or after comparison with neighbouring observations;
- (b) Any good observations have been rejected;
- (c) Any poor observations have been accepted.

Faults detected during the computer quality control procedure can be corrected by intervention, although there is still room for human error of judgement in deciding how the observational data should be treated. The intervention consists in re-inserting good or corrected observations.

In some areas where there are few observations at the time of analysis, the analyst may have some idea of developments from intermediate data or from other sources (aircraft, satellite data, and so forth), and here the background field may be amended by the insertion of bogus observations in an attempt to influence the way the machine will produce its analysis.

Analyses for the various levels should be carried out in several stages. The analyst should:

- (a) Correct the 100 hPa heights for known systematic errors;
- (b) Analyse the 100 hPa level placing emphasis on wind speeds and using the contour heights corrected as in (a) above as an overall guide. The final analysis should fit the wind field;
- (c) Note the differences that exist between the analysed height and the reported contour height;
- (d) Apply 60 per cent of this correction to the 200 hPa heights, 35 per cent to the 300 hPa heights, and 10 per cent to the 500 hPa heights;
- (e) Analyse the 300 hPa chart using the aircraft winds and any SATEM data available;
- (f) Analyse the 250 and 200 hPa levels using the 300 hPa analysis as a guide;
- (g) Convert the mean sea-level pressure analysis into a 1 000 hPa contour chart using a standard empirical relationship taking account of surface temperature values;

- (h) Draw the lower levels up to the 500 hPa level with regard to the 1 000 hPa features, gridding over data-sparse areas, if necessary;
- (i) Compare the 500 hPa analysis with that for 300 hPa and adjust, as appropriate.

Such a scheme includes the following features: the value of the 100 hPa analysis to detect sonde errors in geopotential height, the relatively good data coverage at 300 hPa, and the basic mean sea-level analysis with its good data coverage.

When computer-produced analyses are available, the further analysis of upper-air charts is carried out using a somewhat different process. The computer analyses can be used as first guess fields and the human analyst then adjusts this first guess field as necessary. In areas where considerable adjustment is required, efforts need to be made to discover why the two analyses are so divergent. Such a situation may be due to several reasons:

- (a) Lack of data;
- (b) Poor quality data;
- (c) Incorrect data not detected during the normal quality control procedures.

If appropriate, action must then be taken to remove any offending data in the machine analysis or to take measures to ensure the improvement of the analyses held in the computer. The analysis of jet streams and of the tropopause are dealt with below.

#### 4.3.1.2.3.3 OTHER TYPES OF UPPER-AIR ANALYSES

Two types of upper-air analyses, namely the analysis of jet streams and the analysis of tropopause data, will be described here. There are other less common techniques, such as isentropic analysis and trajectory analysis, which are discussed later.

The analysis of the jet stream is of considerable importance and no set of upper-air charts for middle latitudes, extending to the tropopause, can be considered complete unless some attention is given to this feature. The jet stream is defined as a strong narrow current concentrated along the quasi-horizontal axis in the upper atmosphere, characterized by strong vertical and lateral wind shears and featuring one or more velocity maxima. The vertical wind shear is in the order of 10–20 knots per thousand metres, while the lateral shear is about 18 knots per hundred nautical miles and an arbitrary lower limit of 60 knots is assigned to the speed of the wind of the core.

On a constant-pressure chart, the presence of the jet stream is indicated by a belt of more or less closely packed contours lying along the belt of strong wind. The belt may be hundreds or thousands of kilometres long, it is usually curved, and may have a few simple branches. In middle latitudes, the jet streams are often at about 300/250 hPa so that the standard level at which these jets are most marked is usually 300 hPa. In the case of sub-tropical jet streams, the 200 hPa chart is more useful since the cores are found mainly at about that level. However, these jets are also usually well marked at 300 hPa. It is therefore usual to mark the jet streams on the 300 hPa chart first and then to proceed upwards and downwards. Jets as defined above are not normally found below 500 hPa. The core of the jet is rarely coincident with the standard level so that, in general, no chart will portray the maximum wind. It is therefore sometimes convenient to have a maximum wind chart irrespective of level. Another point to remember is that the axes of the various isobaric cross-sections of a jet are not vertically above one another, but are often progressively displaced towards the tropospheric warm air both above and below the core.

The remarkable wind shears of the jet streams are perhaps best shown in vertical cross-sections perpendicular to the axis of the core. On contour charts, the close packing of the contours along the quasi-horizontal section of the jet does not indicate directly to the eye either the location of the jet axis or the wind strengths and shears. These latter features are brought out in a much more prominent manner if isotachs are drawn on the chart. For such purposes, the isotachs can be drawn at intervals of say 20 knots, and, where possible, to fit the actual wind reported. On such charts, the jet axis is usually indicated by a double or thick line with the actual value of the velocity maximum along it inserted at appropriate places. Over the continents of Europe and North America, the network of upper-air observations is sufficient to allow fairly accurate placing of the jet axis and isotachs on each chart almost on wind reports alone. Over the oceans, the paucity of data makes such recognition impossible and one must then resort to more indirect methods of analysing the chart. Once again continuity in time and space becomes of the utmost importance and every observation must be given full weight unless very definite evidence deems otherwise.

In the placing of jet streams over the oceans, the relation of the jets to the surface frontal system should be borne in mind. In middle latitudes, the jet streams usually exist in close association with a strong thermal gradient of well-marked fronts and, although the core of the jet will lie in the warm air a little below the tropopause, the slope of the frontal surface is such that the core actually lies well to the cold side of the surface-front position. In fact, an approximate rule is that the core lies vertically above the position of the frontal surface at 500 hPa. It should be noted, however, that the sub-tropical jets are not so related to frontal features and that, when their meanderings are sufficiently large to bring them or branches of them northward, no attempt should be made to tie them to surface fronts. Similarly, branches of middle latitudes sometimes occur which cross surface cold fronts to the rear of a depression.

The analysis of the tropopause is facilitated by the fact that the potential temperature at the tropopause does not change greatly over 24 hours. Strict application of the WMO definition of the tropopause may occasionally result in misleading reports which could, in particular, omit the lower tropopause. Continuity from previous charts should help to indicate when this has happened and recourse to the individual ascents may

be necessary to obtain the true value for the analysis. Tropopause funnels or lows may cause some difficulties in analysis as they are often relatively small and may not be indicated directly by the observations on a particular chart. If they extend below the 300 hPa level they are normally aligned vertically with warm centres of the 300/200 hPa thickness patterns. On the other hand, tropopause domes or highs are usually aligned with warm areas in the 500/300 hPa thickness patterns. Tropopause contour gradients often show little slope over large areas, and the gradient is concentrated into narrow bands of tropopause breaks which are, in general, associated with both the sub-tropical jet stream and the polar-front jet stream.

#### 4.3.1.2.4 ANALYSIS OF SATELLITE INFORMATION

A considerable amount of information is available from satellites and the analysis of such information is a necessary part of any analysis technique. Much of the information is readily analysed by numerical methods, but the interpretation of the pictorial information and certain derived data, such as winds, forms an essential part of manual techniques of analysis. The section on detailed aspects of various types of analysis includes the use of satellite data, but the purpose of this present section is to review the information available and how it can be used in general terms.

##### 4.3.1.2.4.1 TYPES OF SATELLITE AND IMAGERY AVAILABLE

There are two basic types of satellite:

- (a) Geostationary; and
- (b) Polar-orbiting.

A geostationary satellite is located over the Equator and can provide a view of the atmosphere at frequent intervals. Thus, visible and infrared imagery are available. Valuable information can be derived from this imagery, for example winds can be deduced for the lower atmosphere (using elements of low cloud such as cumulus-type clouds) and for the upper part of the atmosphere (using elements of high cloud). Other types of information can be obtained, such as observations of the water vapour of the middle atmosphere.

The polar-orbiting satellites take photographs looking down through the atmosphere, the photographs, being in the visible and infrared spectrum. These satellites also measure radiances from which vertical profiles of temperature can be deduced. Geopotential heights of pressure surfaces at an array of points on the surface of the Earth can be calculated using these data. Although more suitable for use in numerical analysis techniques, such radiance data can also be used in manual techniques.

The imagery, on the other hand, is of considerable value in manual techniques and is used less easily in numerical methods. Colour enhancement techniques, however, are being used in the interpretation of imagery, more details of which are given in the section dealing with the production of short-period weather forecasts.

##### 4.3.1.2.4.2 USE OF SATELLITE DATA

As already mentioned, there are two types of imagery — in the visible and in the infrared spectrum. When using the pictures, analysts must be fully aware of the information conveyed by the two types of imagery. The pictures taken in the visible spectrum provide a view of the clouds as they would appear to an observer looking down. Since high clouds are usually thin they have a certain amount of transparency, while lower rain-bearing clouds are thick and dense. Such features are apparent in the visible-light imagery received. Infrared imagery, however, is a measure of the temperature radiated from the radiating surface which is viewed. The colder the temperature the whiter the image on monochrome photographs. Enhanced imagery in colour could give considerably more detail. However, high clouds, which are rather transparent on visible pictures, thus enabling low clouds below to appear on the imagery, are not transparent to infrared wavelengths. The top of the high clouds form a cold radiating surface and this appears very white on the imagery. This does not allow any cloud (radiating surfaces) to be viewed below the highest level of cloud (the highest radiating surface).

If the visible and infrared pictures can be viewed as a pair, the information on one complements the other. For example, a large area of white on the infrared picture in a position where no white can be seen on the visible picture implies a thin veil of cirrus clouds. However, in the case of cumulonimbus clouds, the anvil cirrus will show up clearly on the infrared picture, while the lower parts of the cloud will appear as a white mass on the visible picture. The two pieces of information taken together confirm the presence of cumulonimbus clouds.

Since temperature is represented on the infrared pictures, deductions can be made about clouds in the atmosphere. For example, if over the dark grey colour of the sea a patch of darker colour is observed this could be a patch of warmer water or, in certain circumstances, it could be the top of a layer of stratus, the top of the stratus being warmer than the sea surface owing to an inversion in the lower part of the atmosphere. This example merely highlights the amount of potential information which is available in the infrared pictures and the need for correct interpretation.

The placement of surface features must be done with considerable care and thought if pictures in the infrared are available only. Inexperienced analysts tend to move fronts forward too quickly when they have to analyse only the night-time infrared imagery, since it is sometimes forgotten that the apparent mass of cloud is cirrus which is shearing well ahead of the surface features in the strong upper flow.

As the analysis must fit all the traditional observations (unless they are found to be in error) so must it also fit the imagery received from satellites. Features on the satellite pictures should be supported by features on the analysis. Thus an area of cloud on the pictures may be linked with a weak trough in the surface patterns, or an area of medium cloud might be associated with a short-wave feature on the upper-air chart. It is not correct to

attempt to place a feature on the surface chart for every feature on the satellite imagery. The atmosphere must be considered in depth. The inclination to place frontal features on surface charts for every band of cloud should be resisted. The placement of fronts must be considered very carefully, keeping in mind that a front is a thermal feature and must be supported by evidence other than satellite imagery. For example, a frontal system must be compatible with the 1 000/500 hPa thickness pattern and must also be supported by patterns such as the computed surface and 850 hPa wet-bulb potential temperature pattern (a good means of depicting the presence of surface fronts).

Some cloud features may be insignificant in that they are not tied to any specific dynamical feature at the current time but have persisted through a period when they were associated with a significant feature on the chart. Other cloud features may be representative of the general air mass, for example in unstable showery air streams in temperate latitudes. Bands of clouds can often be detected within the general instability cloud. Such bands do not always represent readily detectable features on the synoptic scale, but can well be a formation of mesoscale features. The successful interpretation of these features on the satellite pictures can help improve the forecast information for short periods of time.

There are now sophisticated computer-oriented methods of colour enhancing satellite pictures. Such computerization should be considered as a valuable aid since the products made available are well suited to provide assistance in analysing and forecasting that need to be tackled manually.

#### 4.3.1.2.4.3 SATELLITE DATA AND UPPER-AIR ANALYSES

Photographs of the Earth's surface and clouds are transmitted from geostationary satellites at regular intervals, for example every 15 minutes. The displacement of a given cloud element over the interval between the time of any two photographs may be used to determine the wind speed at the cloud height over that interval. There is usually some uncertainty about the cloud height, although a reasonable idea can often be obtained from the infrared photographs. There may also at times be errors and uncertainties arising from the development of the cloud. The area covered by each satellite is restricted both in latitude and longitude. Data are not available at latitudes higher than about 40–45°, but all longitudes are covered at any one time. Nevertheless, the data help to fill what are normally large gaps between the routine radiosonde and radar-wind ascents. Such derived winds are calculated at some centres and are exchanged on the Global Telecommunication System in the form of SATOBs.

Observations from satellites also indirectly provide a considerable amount of geopotential height information. The satellite's observations of infrared radiation from the atmosphere enable temperatures to be estimated at a number of levels in the atmosphere and, from these temperatures and the corresponding pressures, thickness values for a number of layers can be derived. The algebraic addition of these thicknesses to the geopotential height of the 1 000 hPa level then provides geopotential heights for the constant-pressure surface related to the thickness values used. Thus considerable emphasis is placed on the assumption that the 1 000 hPa surface is as close to the truth as possible. The method is analogous to the old traditional method of gridding all levels from the surface using partial thicknesses (1 000/850, 850/700, 700/500 hPa and so forth). Satellite data are most readily interpreted over the sea in cloud-free regions and, in these cases, provide a valuable addition to the forecaster's sources of data. It should be noted, however, that uncertainties do exist, and some data may not be usable. Regular checks are necessary and these are usually carried out using radiosonde data at 100 hPa.

Satellite photographs can also be used to detect features at the upper-air levels or to confirm the presence of such features. The main principle in the use of the satellite pictures is that ascending motion leads to cloud and descending motion is associated with relatively cloud-free air. Thus, between a trough and a ridge in the upper westerlies there is usually an upward vertical component leading to a good deal of cloud. Conversely, in the flow from a ridge axis to the trough there is descending motion with only small amounts of cloud, mainly cumuliform. The boundaries of the cloudy air are related to the ridge and trough line in a way which depends upon the characteristics of the feature. In a broad, flat ridge the downward motion to the east of the ridge line is quite gradual and clouds may extend some distance beyond it, whereas if the ridge is strongly curved there will be a sharp cloud edge near the ridge line.

A trough axis may often be located where it crosses a frontal cloud band. Sinking air to the west of the trough causes the middle and high clouds to dissipate, leaving only a narrow band of clouds, while to the east the cloud band is broader, more solid and of greater vertical extent.

Since the more extensive cloud bands extend roughly from a trough axis to a ridge line, an approximate idea of the amplitude of the flow may be gained from the latitudinal extent of the cloud band. If the cloud band is quasi-linear, then the direction of the contour lines is roughly along the band. There may be vortices on the poleward side of the flow representing short-wave, rapidly moving disturbances. There may also be cloud vortices or spirals, particularly in a large-amplitude flow, which indicate closed circulations, such as old occluded depressions or cut-off lows, the centre of the cloud spiral being generally coincident with the circulation centre.

#### 4.3.1.2.4.4 SATELLITE DATA IN DATA-SPARSE AREAS

In data-sparse areas such as the southern oceans, satellite information is the only information which is available to the analyst. The use of the radiance data from satellites has already been described. Surface features can often be identified from the imagery resulting in a more realistic surface pattern. Research using manual and computer techniques can be carried out to relate satellite imagery received daily to various upper-air features. If such investigations are carried out over areas where data are available then the reverse process can be used over data-sparse areas enabling features in the upper-flow pattern to be drawn with some confidence.

Another technique in the use of satellite data is to create pseudo-observations. This technique is used in the southern hemisphere.

#### 4.3.1.2.5 ANALYSIS OF RADAR INFORMATION

##### 4.3.1.2.5.1 GENERAL CONSIDERATIONS

Weather radar information represents an important and valuable supplement to the surface, upper-air networks and satellite observation by giving the meteorologist the possibility of looking electronically far beyond the visual horizon and to evaluate what is detected in terms that are appropriate to synoptic and local uses.

Over the past 40 years, meteorological radars have been the most important tool available to the meteorological community for providing short-term forecasts of mesoscale weather events. This is due fundamentally to two factors. The first is that radars have been able to produce semi-quantitative measurements of precipitation and of storm features over large areas from a single point. The second is that there is no tool now available that provides volumetric coverage encompassing a region of several hundreds of kilometres in diameter with a resolution in the order of a kilometre or two. Complete volumetric scanning is available within a matter of minutes. The construction of composites from several radars (the formation of radar networks) allow the use of radar data not only on the local scale, but on the synoptic scale as well.

The existing meteorological radars can be divided into two general classes: non-coherent (conventional) radars, and coherent (Doppler) radars. Conventional radars just measure the reflectivity of hydrometeors, while the Doppler radars provide additional information on the radial velocity of hydrometeors and turbulence characteristics. Explanations of basic physics, which is the basis for observations from conventional and Doppler radars, will be given in the following paragraphs.

In the past two decades, new technological developments have produced dramatic progress in the development of the Doppler radar as an observing tool. Networks of Doppler radars are being introduced at the present time by some national Hydrometeorological Services.

The availability of high-speed and low-cost processing and display systems for real-time analysis permits easy and rapid access to the large volume of data produced by modern radars.

One major technological change in the next generation of meteorological radars will be that many, and possibly most radars, will possess Doppler capability. Some will have polarization diversity capability. However, the next generation of radars will differ most from their predecessors in their use of state of the art digital signal processing and modern quantitative real-time displays.

Taking into account these major tendencies in the development of radar meteorology and the fact that non-coherent radars are still operational in the national Hydrometeorological Services, the following paragraphs describe the use of data from both non-coherent and coherent (Doppler) radars in weather analysis.

##### 4.3.1.2.5.2 NON-COHERENT RADARS

###### *General information*

The radar measurements of clouds and precipitation are based on the scattering of electromagnetic waves by airborne particles. The power of backscattering depends on the size of the particle and on the material of which it is composed. The backscattering properties of the cloud and precipitation particles are often characterized mostly by reflectivity (or reflectivity factor) Z. In the case of non-coherent radars this is the only measured parameter.

Most weather radars operate in a 3–10 cm range. The advantage of a 3 cm wavelength lies principally in the compactness of the equipment since the areal dimensions for a given beam-width decrease with the wavelength. The big disadvantage of this wavelength lies in the attenuation by water and ice particles. The advantage of a 10 cm wavelength lies in the practical absence of attenuation. Equipment is, however, bulky and very expensive in this case if one wants to achieve a high spatial resolution. Wavelengths of 5–6 cm provide a useful compromise between attenuation and beam-width difficulties. Since there is no special advantage in some particular wavelength, the 5–10 cm range is used in most radars.

While interpreting radar observations it should be remembered that there are several limitations which are pertinent to radar data. Since the radar beam diverges or spreads, the energy is distributed over a larger and larger area as the distance from the transmitter increases. Thus, only a very small portion of the transmitted power is intercepted by a small target. This loss of energy due to beam divergency is defined as range attenuation.

The signal received from a target diminishes at a rate directly proportional to the fourth power of the range of a target. However, if a precipitation area is of uniform reflecting properties through its cross-section and if it completely fills the beam, then the total power received by the radar decreases at a rate directly proportional to the square of the range. For example, a precipitation area observed at 150 km, which fills the beam, returns a signal several thousand times as strong as the one received from a target which partially fills the beam. Range attenuation of echo signal depends upon the relationship between the amount of precipitation filling the beam and the distance from the target.

When radio energy passes through a distribution of drops, some of the energy is scattered and some is absorbed by the hydrometeors. Short waves and large water drops result in the greatest signal attenuation.

An outbound signal suffers attenuation as it advances through precipitation and the returning pulse is also attenuated in the precipitation along the return path. If a line of thunderstorms is so intense that

practically all of the power in the beam is lost by attenuation, then there is little or no energy left to be reflected from targets beyond the precipitation area. Targets beyond a heavy, extensive precipitation area appear less bright than they ordinarily would be and, in some cases, they may not show on the scopes at all.

This is why precipitation is estimated usually not over the whole range of the radar, but within a radius of 150–200 km. Furthermore, reflectivity depends upon the dielectric constant. Therefore, ice targets have reflectivities about five times lower than water spheres of the same size. In this connection, the range of the location of clouds and precipitation in winter is decreased. In stratiform precipitation, partially melted snowflakes give rise to an enhanced return, the so-called bright-band, and are likely to result in overestimates of the rainfall rate. At low elevation angles, the backscattering from the ground, the so-called ground clutter, can affect the observations.

At modern computerized radars, the corrections to the signal are performed automatically and processed data are presented in a digital form. More detailed information on weather radars and their use in weather analysis can be found in Battan (1959), WMO (1966), Stepanenko (1973), Doviak and Zrnic (1984) and Bryl'jov, et al. (1986).

#### *Retrieval of precipitation*

A conventional radar, which is capable of measuring only one parameter — reflectivity — is quite limited in providing accurate quantitative estimates of precipitation. This limitation results from the complex nature of even the most simple clouds. Warm clouds, for example, require a two and perhaps a three parameter distribution to describe the local distribution of drop sizes. Mixed phase clouds are even much more complex. This is why a single measurement of reflectivity can provide just a crude estimate of precipitation.

If the scattering particles are spheroids and if their diameters are small compared to the wavelength (i.e. Rayleigh scattering takes place), then:

$$Z = \frac{1}{\Delta V} \sum_i D_i^6$$

where  $Z$  is the reflectivity factor,  $D_i$  is the drop diameter, and  $\Delta V$  is the unit volume. Since characteristic values of  $Z$  in the atmosphere differ by several orders, radar meteorology uses normally the logarithmic scale  $\text{dBZ} = 10 \log Z$  (where  $Z$  is in  $\text{mm}^{-6}/\text{m}^3$ ). In precipitation, dBZ ranges from 0 to more than 60 dBZ.

In order to derive a rainfall rate  $R$  some drop size distribution must be assumed. If a Marshall-Palmer raindrop size distribution is assumed:

$$N(D) = N_0 \exp(-3.67 D/D_0)$$

where  $N_0 = 8000 \text{ m}^{-3} \text{ mm}^{-1}$  and constant, and  $D_0$  depends upon the rain rate and is equivalent to a median drop size. When combining the above two equations it is possible to obtain:

$$Z = AR^b,$$

where  $A = 200$  and  $b = 1.6$ .

If  $N_0$  deviates substantially from this value then the rainfall rate predicted from the  $Z$ - $R$  relation is likely to be in error. Comparisons of  $R$  and reflectivities  $Z$  computed from the  $N(D)$  — measured by disdrometer (Richards and Crozier, 1983) — showed that for different distributions giving the same  $Z$  value, the rainfall rate can differ by as much as four times. Nevertheless, the type of relation in equation  $Z$  is used in most of the cases for quasi-quantitative estimates of precipitation. The values of  $A$  and  $b$  vary widely. In practice, radar data are calibrated against relatively dense pluviographic network and empirical  $Z$ - $R$  relationships are used for a particular radar over a particular area. Some authors indicate that the accuracy in precipitation estimates can be gained to use the simple classification of precipitation (drizzle, widespread precipitation, and showers). The accuracy of precipitation measurements is increased also with the growth of a time-integration interval.

While analysing radar precipitation, one should remember that these data reflect the precipitation at some layer usually between 500 m and 1 000 m above ground level. In most cases, evaporation in the lower 500 m layer does not cause serious depletion of precipitation. In extreme cases of very hot and dry boundary layer, there could be of course some noticeable depletion.

Summing up the above considerations, it is possible to conclude that conventional radars provide rather semi-quantitative information on precipitation. The advantage of radar data is that they have high spatial resolution and are areal by their nature. This unique quality should be used by combining radar observations with conventional precipitation observations while preparing the precipitation analysis over limited areas.

To make precipitation estimates more accurate, the measurement technique for horizontal and vertical polarizations was tested recently and gave encouraging results. The dual-polarization measurements are not yet widely in operation, but due to their potential we shall briefly discuss this approach to the precipitation measurement.

Linear dual polarization radars measure the difference in the reflectivity ( $Z_{DR}$ ) of precipitation with horizontally ( $Z_H$ ) and vertically ( $Z_V$ ) polarized radiation.  $Z_{DR}$  is defined as:

$$Z_{DR} = 10 \log (Z_H/Z_V)$$

When measuring precipitation drop sizes it is assumed that the shape of drops is oblate spheroids with nearly vertical axes, with larger drops having greater oblateness. The horizontal axes of these spheroids are

larger than the vertical ones. Since the backscattering cross-section is greater for incident radiation polarized along the major axis of the spheroid than it is for the orthogonal direction, the ratio of the two orthogonal signals is a measure of the oblateness and therefore of the size of the drops. If the differential reflectivity is measured in addition to  $Z_H$  then it is possible to derive both  $N_0$  and  $D_0$ , or in principle to fit the observations to any generalized two parameter raindrop size distribution. Once  $N_0$  and  $D_0$  for exponential distribution have been derived, a rainfall rate may be calculated since the terminal velocity of the drops is known. Results so far indicate that rainfall rate can be measured by this method with a RMS error of about 15 per cent over large areas (Ulbrich and Atlas, 1984).

The  $Z_{DR}$  measurement also gives information on the phase of hydrometeors. Positive values of  $Z_{DR}$  suggest that hydrometeors are oriented in the horizontal plane, values near zero suggest either no preferred direction of orientation or no deformity, and negative values indicate particles aligned along the vertical. Typical  $Z_{DR}$  values are in the range  $+5 = +3$  dBZ in rain. Values near zero can be interpreted as hail imbedded in a region of rain. Negative values of  $Z_{DR}$  are assumed to be from ice forms that have their long dimensions oriented vertically. More details on the use of polarization radar measurements for estimates of precipitation can be found in the papers published as part of the proceedings of Nowcasting II (European Space Agency, 1984).

#### *Interpretation of radar echoes*

Radar reflectivities are also used directly for the identification of different mesoscale systems associated with the hydrometeor formation. The fact that radar echo is proportional to the hydrometeor diameter is used for the identification of cloud type. Thunderstorms, which contain a moderate number of large water drops, give a brighter echo than stratiform clouds containing a large number of relatively small drops. In general, rain gives a brighter echo than snow, since water particles scatter about five times the radar energy of snow crystals of the same size and shape. The echo brightness from dry hail is also about one fifth of that on rain. Hailstones and snowflakes covered with water reflect signals as if they were entirely composed of water. These characteristics of radar echo, together with information on its geometry, are used in the interpretation of radar reflectivity and identification of weather systems from radar data.

More details on the interpretation of radar echo can be found in Doviak and Zrnic (1984), Brylsov, et al. (1986) and Collier (1989). A brief extract of the literature on the use of radar data in weather analysis is presented below.

If the radar is not computerized, then radar data are visualized most commonly with the use of a plan position indicator (PPI), range position indicator (RPI) and range height indicator (RHI). The first two indicators enable to study the horizontal structure of radar echo, while the latter provides information on the vertical structure along selected radii of particular interest.

In the case of a computerized radar, the original signal can be interpolated into some regular three-dimensional grid (for example, into a Cartesian grid), and the radar data are visualized along the chosen horizontal and vertical planes. The observations from several computerized radars are merged automatically into a radar map, for example, into a radar precipitation map.

Precipitation echoes are divided into convective and stratiform. Quite often, convective- and stratiform-type echoes are observed simultaneously on the PPI, RPI and RHI at various levels of brightness, which also differ by their pattern. The major characteristics of convective-and stratiform-type echoes will be described below.

#### *Convective-type echoes*

These echoes are most commonly associated with isolated thunderstorm activity, cold fronts squall lines, and occasionally warm and occluded fronts. The edges of these echoes are usually well defined. They are normally the brightest echoes observed due to the strong signals which are returned to the receiver. These echoes are often detectable at distances of over 300 km because of the great heights to which they extend. They may occur individually, in groups, or in solid or broken lines.

Echoes associated with air mass thunderstorms and showers are usually isolated or widely scattered with large spaces between them. At times, convective-type echoes may appear as groups of individual echoes in various stages of development. These echoes tend to form, grow and dissipate rapidly.

Perhaps the most striking on PPI-scope displays are those echoes associated with cold fronts and squall lines. The radar does not detect the actual pressure front itself but detects the associated precipitation. Scattered echoes are normally observed first at long ranges due to hydrometeors in the upper portions of the tallest thunderstorms. As the front approaches, more and more precipitation is observed at successively lower levels and the original cells may appear to increase in size and intensity. On radars with wide horizontal beams this effect may also be due to an increase in the azimuth.

One of the main things to remember about convective echoes is that they are usually associated with severe turbulence.

#### *Stratiform-type echoes*

Radar echoes from precipitation associated with stratiform clouds, when seen on the PPI presentation, have a diffuse appearance with ill-defined edges and are usually of quite uniform intensity. These echoes cannot usually be detected at great ranges (e.g. beyond 150 km) because of the relatively low rainfall rates usually associated with such precipitation and because of the relatively small vertical extent of the echoes

giving the greatest received power. This latter effect is clearly demonstrated when the echoes are examined in the vertical cross-section using RHI equipment.

#### *Combination of convective and stratiform echoes*

Most often a combination of the two basic types of echoes is observed. However, it is usually easy to isolate convective echoes. Combinations of these two types of echoes occur during most all-weather conditions, such as with cold and warm fronts, occlusions, isolated air mass type, thunderstorms and orographic precipitation.

#### *Thunderstorms*

This echo is a special type of convective echo. It should be emphasized that unless lightning echoes are observed, there is no obvious way of distinguishing between an echo from a thunderstorm and that from a heavy shower. In general, if the echo is of exceptional intensity or if the top of the echo extends to great heights (for example, heights at which the temperature is probably below -4°C), there is a high probability that the echo is from a thunderstorm.

#### *Hurricanes or typhoons*

Echoes from these storms are usually distinctive in appearance but it must be remembered that attenuation of heavy precipitation associated with these storms may modify considerably the precipitation pattern in some sectors. The first manifestation of a disturbance may be the observance of echoes from squalls that are moving in a direction opposite to that usually prevailing in the area. As the storm develops, the circulation of echoes around a centre becomes complete. The character of the echoes associated with these tropical cyclones varies according to their position relative to the centre. In the periphery of the storm the echoes are convective and cellular in nature, sharp-edged and of high intensity. Any thunderstorms and tornadoes which occur with tropical storms usually occur with these cells and in general the associated weather is squally. These echoes, which move with the storm circulation, have great vertical extent and have been observed as far away as 600 km from the storm centre. Sometimes a relatively echo-free area of some 80 km is observed passing towards the centre of the storm from these outer convective cells, followed by a large area of intense echo with more stable characteristics. Rainfall is very heavy and thunderstorms are usually absent in this rain shield area. If the gain of the radar is reduced, a spirally-banded structure of the echo lines is observed. Further towards the centre, beyond the rain shield mass, a cellular echo structure is often observed. These echoes are arranged in definite spiral bands and surround the eye of the storm. The individual cells and the spiral bands themselves rotate around the centre in an anti-clockwise direction (northern hemisphere).

#### *Tornadoes and waterspouts*

Most tornadoes derive from extremely violent thunderstorms of great vertical development, but on rare occasions they are observed with stratiform clouds and without associated precipitation or radar echo. The following echo features are taken to be indicative of a severe local storm that may be a tornado:

- (a) Unusually great vertical extent (echo top exceeds the reported tropopause);
- (b) An echo which moves to the right (looking downwind) of the direction of other nearby echoes;
- (c) When two echoes merge into one;
- (d) When an echo has a hook shape characteristic for the mesocyclone at upper levels.

Echoes from waterspouts have been observed at short ranges (6–10 km) on the PPI. The echoes are intense and circular in shape and show no other pattern. They are essentially a very low-level phenomenon which is difficult to distinguish on a conventional radar.

#### *Hail*

Hail of damaging size is most common in continental areas of temperate latitudes and is associated with violent convection. The radar echoes which have been positively identified as associated with hail have shown the sharp-edged high-intensity echoes characteristic of precipitation arising from convection.

Studies have shown a strong relationship between radar reflectivity and hail. These same studies have also shown a strong correlation between echo height and occurrence of hail. An echo whose top is higher than the tropopause has a high probability of containing hail.

#### *Snow*

Echoes from snow are fuzzy and diffuse. Because dry ice crystals are much poorer reflectors of radio energy than water drops and because the equivalent precipitation rate of snow reaching the ground is often low, dry snow is not seen to as great a range as rain. Echoes from snow showers are usually of higher intensity than those from more widespread snow but the edges are still diffuse.

#### *Duststorms and sandstorms*

Features of a thunderstorm — such as squall, rise in pressure and fall in temperature after its passage — can be recognized in a duststorm. The cumulonimbus clouds associated with the duststorm can have large water particles and even hail aloft. Hence, occurrence of a duststorm can be inferred from a radar when echoes are observed over arid regions.

### *Echoes ascribed to phenomena not associated with precipitation*

Apart from precipitation, other phenomena can be the cause of an echo received by a radar station. Such phenomena are smoke, insects and birds. Also angel echoes, due to refractive index discontinuities, and anomalous propagation, due to gradients of radio refractive index, should be taken into account by meteorologists who are dealing with the interpretation of the radar data.

#### 4.3.1.2.5.3 COHERENT (DOPPLER) RADARS

##### *General information*

The invention of a powerful klystron amplifier in the 1950s enabled the construction of transmitters providing high phase coherence of transmitted pulses, which are absolutely necessary to measure the velocity of the moving target. The phase coherence of the radar signal assumes that the time interval between the wave crests for the successive transmitted pulses is either constant or is known. The transmitted pulse, interacting with a target, induce the forced molecular oscillation in parallel with the temporal changes in electric and magnetic fields. If the target is either at rest or moves along the plane at a constant range, then its molecules oscillate with the transmitted frequency. If the drop moves towards the transmitter at velocity  $v$ , then the frequency of molecule oscillations is increased by  $v/\lambda$ , where  $\lambda$  is the transmitted wavelength. The oscillating molecules create the electromagnetic field by themselves, which irradiates outward. When the transmitter and receiver are collocated, the value of the Doppler shift of the phase is given by:

$$f_d = -2 v_r / \lambda$$

where  $v_r$  is the radial component of velocity, which is positive when the target moves outward of radar. The factor 2 in the equation appears because the frequency increases in two stages. At first the frequency of electric oscillations increases by  $v_r/\lambda$  within the target, and then the frequency of its oscillations in the direction of the receiver increases by the same value. By knowing the Doppler shift  $f_d$  and the wavelength of the transmitted signal, it is possible to obtain the radial velocity from the above-mentioned equation. In the case of C-band radars, the major targets are hydrometeors. These radars measure, strictly speaking, the radial velocity of hydrometeors and some other impurities (for example, insects at ranges close to the radar), and not air velocity. Therefore, some additional hypotheses are used to convert hydrometeor movements into air speed.

The parameters of meteorological value which are measured by Doppler radars are reflectivity factor  $Z$ , mean, reflectivity-weighted radial velocity,  $v_r$  (m/s), and standard deviation of Doppler spectrum  $\delta_v$  (m/s). Reflectivity characterizes the zero moment of the Doppler spectrum. It is obtained when the radar operates in the amplitude (non-Doppler) mode. This parameter was already discussed above in the section on non-coherent radars. The last two parameters ( $v_r$  and  $\delta_v$ ) are obtained when the radar operates in the Doppler mode.

##### *Retrieval of airflow characteristics*

As was mentioned above, the C-band or S-band Doppler radars measure the radial velocity of hydrometeors. Theoretically, this radial velocity includes all three components of particle motion in the Cartesian coordinate. In the limited case of vertical viewing, the radial component will reflect the vertical velocity of hydrometeors. At the other limit (horizontal viewing), radial velocity will represent horizontal components of motion.

In order to retrieve the wind scans with a low antenna, an elevation angle is used. In this case, vertical velocities of the backscattering particles do not contribute significantly to the radial velocity and it is assumed that radial velocity represents wind components. In other words, it is assumed that the hydrometeors follow the horizontal velocity of the wind.

Wind velocity and direction from the single Doppler radar measurements can be calculated only in the case of horizontally-homogeneous flow. This approach was introduced by Lhermitte and Atlas (1961) and then was further developed by several authors. Comparisons of retrieved wind with that obtained from conventional observations performed by different authors showed that data on the airflow of reasonably good quality can be obtained even from single Doppler radars.

More accurate velocity of the wind can be retrieved from dual Doppler radars. In this case, there is no need to use additional hypotheses on horizontal homogeneity of the flow, but this method is more expensive and, at present, it is used mainly in research.

The second measured characteristic, the standard deviation of a Doppler spectrum, is a measure of the wind shear and small-scale flow fluctuations within a measured volume. Therefore, it is used as an estimation of turbulence.

##### *Interpretation of Doppler radar data*

The corrected and processed radar observations in a Doppler mode can be displayed at velocity-azimuth display (VAD) for their visual interpretation. The radial velocities at these displays range normally from -50 to +50 m/s and are represented in pseudocolours. From the visual representation of radial velocities one can estimate the existence of the zones of strong convergence (or divergence) of the flow. Together with reflectivity data, information on the airflow can be used for identification of intense weather systems, such as gust fronts and downbursts.

Operational interpretation of radar data, and especially of Doppler radar data, requires quite a bit of practice, where the data displaying techniques can play an important role. Section 4.3.3 provides a discussion on the use of workstations.

The details on the use of Doppler radar data in weather analysis can be found in Doviak and Zrnic (1984) and in papers presented at the Nowcasting symposia (European Space Agency, 1984, 1987).

#### 4.3.1.2.5.4 ANALYSIS OF LIGHTNINGS

The technique of measuring the radiated electromagnetic fields to determine the direction of lightnings has been known since the beginning of this century. However, it was not until the mid-1970s that it was possible to use this knowledge to detect thunderstorms on a large scale. Increased insight into the nature of lightning and the development of fast computers were important factors leading to the invention of a real-time lightning location system.

At present, extensive networks of lightning location systems are operating in many parts of the world and are used in weather analysis and forecasting. Only vertical lightnings produce radiation fields which can be detected correctly by the lightning location systems. Therefore, not all flashes are registered by these systems.

Historically, the first network was the so-called magnetic direction-finding (MDF) system. Flash fixing errors depended on network geometry, but for a large network of well-sited direction-flying (DF) stations, 1–2 km accuracy was achievable near the network centre, and 6–8 km near the outer edges. Stations had to be connected in a relatively dense network with separations of 100–200 km or so, depending on detailed requirements.

More recently, the time of arrival (TOA) system has been developed for locating cloud-to-ground lightning strokes. The precise time that lightning touches the ground is monitored to sub-microsecond accuracy at several receiver sites simultaneously. Knowing that lightning travels only a few hundred metres in that time allows precise calculations to determine the accurate stroke location.

The lightning position and tracking system (LPATS) consists of four major components: antennas, receivers, central analyzer, and an interactive graphic map display terminal. A typical LPATS network with receiver spacing of 200 to 300 km needs only five receivers to achieve complete coverage with high detection efficiency over a 720 000 km<sup>2</sup> area. A six-receiver network will adequately cover 1.5 million km<sup>2</sup>. Each receiver in a given network is synchronized to a common timing reference sources such as a TV/radio earth station, a TV broadcast station, or a LORAN-C navigation signal.

Each of the ground stroke detection stations is connected via a communication link to a central analyzer (CA) facility. When ground stroke occurs, the emitted electromagnetic pulse is detected by each listening station. Each station then samples its internal synchronized clock and records the exact time of detection at a particular station. That information is relayed to the CA, where a calculation of the stroke location is made. For a three-station solution, the CA solves a complex spherical hyperbolic explicit non-iterative equations necessary for stroke location and outputs the data in both latitude and longitude. The lightning stroke location accuracy is better than 1 km over the entire area.

Lightning stroke data are converted from their analogue form into a digital format. During this digitization process, the lightning stroke is also examined to determine parameters, such as positive or negative polarity, the time at which the peak occurs, and the value of the peak amplitude of the stroke. The digitized information is relayed to the interactive PC-based visualization system. These data may include the number of strokes over a given area during a given time interval, and the geographical location of strokes at different times. The lightning stroke data are displayed in colour-coded ranges and provide information on the intensity of thunderstorm activity (the number of strokes during the fixed time interval) and on the displacement of lightning cores.

By having this information on a map with a geographical grid and major terrain features, such as coast lines, lakes and rivers, the forecaster can analyse the evolution of thunderstorm activities in both space and time. In combination with radar and satellite data, lightning stroke monitoring provides additional information on the intensity of thunderstorm activity, the expected movement of lightning zones, and their development or decline.

More information on lightning location systems and their use in weather analysis and short-range weather prediction can be found in Bent and Lyons (1984), Browning (1989), Christensen and Nilsson (1984), Lee (1986a, b) and Maier, *et al.* (1983).

#### 4.3.1.2.6 OTHER TECHNIQUES FOR THE ANALYSIS OF DATA

Other analysis techniques are used to depict various features in the atmosphere which are not obvious from the usual isobaric or constant-pressure level chart. The analysis of mesoscale features demands manual techniques since such features are usually in the order of, or less than, the spacing between grid points used for numerical analysis purposes (see section 3.4.2).

The most common representation of the atmosphere at a locality is by means of a plotted upper-air diagram. The diagram can be analysed and data can be derived. The derived data are then used to produce analyses over an area. Useful analyses include the distribution of humidity or the dew-point depression, stability indices, values of potential temperature and wet-bulb potential temperature at different levels, freezing levels, probability of snow and so forth. All of these analyses are best carried out by using computer methods since they are time consuming and laborious. Small centres wishing to have such information should request its provision on the Global Telecommunication System by larger centres, which are able to include the appropriate analysis programs in their computer.

Several specialized types of analysis, which may be valuable from time to time and which can be undertaken manually, include:

- (a) Vertical cross-sections;
- (b) Air trajectories;
- (c) Frontal contour charts;
- (d) Hodograph analysis;
- (e) Isentropic analysis.

Vertical cross-sections can be a valuable aid in obtaining a three-dimensional picture of the synoptic situation. It is rarely practicable to produce vertical cross-sections as a routine, but their occasional production is most helpful in gaining an insight into the vertical structure of fronts and jet streams. Investigations into selective synoptic situations are often aided by the construction of cross-sections. They can also be useful when examining synoptic situations under operational conditions. The most useful form of cross-section charts is one which is graduated using a logarithmic scale of pressure for the vertical axis and a suitable scale of distance for the horizontal axis. The horizontal axis along which the section is to be drawn should be chosen so as to lie close to as many ascents as possible and be roughly perpendicular to a front if that is the main feature of interest. Many different types of features can be examined, for example the analysis of temperature, humidity and wind, to mention just a few. A variant of the vertical cross-section which is sometimes useful is the time-section. In this, the vertical axis represents height or pressure on a logarithmic scale and the horizontal axis refers to time instead of distance. The technique of time-section analysis is more valuable in tropical regions or other areas of sparse data and in temperate latitudes with adequate networks, but even in temperate latitudes the occasional preparation of a time-section can be instructive, in that it displays graphically the continuity of the changes that are taking place in the atmosphere. A simpler type of vertical time cross-section is the actual plotting of observations on a horizontal axis for particular stations. The sequence of observations goes from left to right across the sheet and as many as ten to fifteen observations can be placed in the vertical. Three cross-sections can be examined visually and any rapid and unexpected changes in the various values observed can be quickly detected and decisions can be taken as to whether the changes are real or represent erroneous data. Such a pictorial representation of observations can be useful, for example, over the North Atlantic where the observations from weather ships, Iceland and the Azores can be a valuable supplement to manual quality control of the numerically-produced contour analyses.

The preparation of air trajectories can be useful on many occasions. When a large number of trajectories are required it is best to invoke the use of computerized methods, but when trajectories are only required occasionally, especially at smaller centres, simple techniques can be used to produce satisfactory approximations to trajectories. The trajectories can be obtained as follows. Let us suppose that the charts are available at six-hour intervals, for example, 0600, 1200 UTC, etc. and that trajectories commencing at 0600 UTC are required. It is then assumed that the 0600 UTC chart is typical of the air motion during the period 0600 to 0900 UTC, the 1200 UTC refers to 0900 to 1500 UTC and so on. The position of the parcel of air at 0900 UTC is found by measuring the distance that was travelled in three hours along the streamline or the contour according to the wind speed in that region. If the wind speed is changing or the streamlines are rather curved it may be necessary to proceed in hourly steps. Since specially drawn streamline charts will not usually be available, the contours on constant-pressure charts can normally be used in high latitudes as streamlines. If there is evidence that the winds depart from the pressure pattern significantly, some account should be taken of this, possibly by sketching some streamlines in the area concerned. Wind speeds can be obtained from the geostrophic wind or, if curvature is likely to be important, from the gradient wind. Trajectories are normally calculated using actual synoptic charts. However, it is often necessary to know where a particular mass of air will be in the future. To prepare the trajectories, a similar procedure is used by using the current chart and the forecast charts which are available for the levels of interest.

Frontal contour charts are a method of depicting the three-dimensional structure of frontal surfaces. The frontal contour chart consists of a base map on which a series of lines are drawn showing a position of the intersection of the frontal surface with selected pressure surfaces. Contours for the standard levels, namely 1 000, 850, 700, 500 and 300 hPa, will normally be drawn and these may often be usefully supplemented by 600 and 400 hPa contours. The upper boundary of the frontal zone, that is the lower limit of the warm air mass, is usually taken as defining the frontal surface. The upper-air diagrams for all relevant upper-air ascents should first be examined and the upper limit of the frontal zone should be determined on each. Where the front is well marked this will not be difficult. There will be a much more stable area in the frontal zone than in the warm air above. Wet-bulb potential temperature is one of the best air-mass markers, and the wet-bulb potential temperature in the warm air near the front should be noted. This value can be expected to be roughly the same on each ascent in the same air mass. This fact can be used to ensure that the same front has been selected on each ascent and also to help locate the frontal boundary on ascents where the change in lapse-rate is not well marked. The effect of latitude and land and sea surfaces will, however, tend to introduce gradual spatial changes in the wet-bulb potential temperature representative of the air mass. The values of the pressure at the frontal boundary and the wet-bulb potential temperature at this level should be plotted on the base chart for each upper-air ascent that intersects the frontal surface. Such a chart may be found useful from time to time and manual techniques can be used to prepare it. At a centre with computational facilities, a suitable program should be arranged to produce the charts automatically, if the charts are required on a regular basis.

Hodograph analysis can be of considerable value on an operational forecasting bench. The hodograph is merely a polar diagram depicting the winds observed during an ascent from a particular station. The diagram can be constructed very easily and quickly from the observations of upper winds and can be extremely

useful in detecting warm and cold air advection. The diagram can also be used to indicate the possibility of wave formation on cold fronts and its use in conjunction with satellite pictures can be highly valuable when making decisions about systems in data-sparse areas.

An isentropic chart shows the state of the atmosphere on a surface of constant potential temperature. Except for non-adiabatic processes such as condensation or radiation, air particles will remain on an isentropic surface. The motions of the air masses can be followed on the chart if they can be identified by some other conservative parameter. Absolute humidity, which is a fairly conservative parameter, is used for this purpose and the movement of the moisture pattern is charted. The level chosen for the analysis will usually be as low as possible so as to include a large range of humidity values, but such that it is above the friction layer. Although these analyses may be of value on an operational forecast bench they are used mainly for research purposes. In operational work some forecasters find that the charts can be prepared for a limited area quite quickly and can be of value in forecasting convective activity which can be highly dependent on the moisture pattern. However, convection, with its associated condensation and precipitation, is not an adiabatic process and introduces a non-conservative element into the analysis.

#### 4.3.2 *The human role in modern forecasting techniques*

The human role in modern forecasting techniques depends on the type of centre at which the work is being carried out. At small centres, where much of the work depends on the receipt of products from larger centres, the human role is basically an interpretative one. The forecaster has to interpret the forecast products in light of local conditions and local knowledge. Access to alphanumeric data for a later time will also enable the forecaster at such a centre to update the forecast products available which have, of course, been based on earlier data. A thorough knowledge of what products are available, what they depict, and how they have been prepared will enhance their value considerably when in the hands of an experienced local forecaster. It is possible that the automation of data-processing facilities at the centre has provided the forecasting staff with facilities which enable specialist charts or data to be called at will and hard copy printed, if necessary. Again, the optimum value of such facilities can only be achieved if staff are thoroughly conversant with the facilities which are available. Thus, the forecaster at a small centre with forecast products available from larger centres should concentrate on the meteorology of the situation rather than attempting to interpret the large-scale prognoses provided. The manual forecasting of synoptic features should therefore be confined to the smaller or mesoscale features within the overall large-scale forecast pattern. It is now generally accepted that the computer-based forecasts of the general overall low pattern for periods of two or more days ahead give a good overall indication of the atmospheric developments to be expected. However, the forecast models are often unable to deal with the details in the large-scale development. There is therefore considerable scope for local forecasters to develop skills using the valuable output from the larger centres. The interpretation of the weather associated with prognostic charts is by no means a routine activity and demands a high degree of meteorological understanding. Much effort is still required in order to achieve the degree of skill for forecasts of weather at different localities, for specialized customers and for the general public, which can be matched with that achieved for the forecast products produced from the larger computerized centres with access to numerical weather prediction products.

The human role at a centre with access to large computing facilities ranges from the interpretive role discussed above to a role which can influence the output of the computer and can adapt the final computer forecast products before they are issued for use outside the centre.

The remainder of this section will cover some of the manual techniques which may be found useful in connection with the preparation of numerical weather prediction products and the possible manipulation of the output products before their issue by the centre. Reference will also be made to manual techniques in the production of very-short-range forecasts (for the next few hours) and a few comments will be given on procedures to be used should the computer become inoperative for a period of time. First, however, it will be useful to examine the procedures involved in the preparation of computer forecasts and the involvement of humans in the process.

##### 4.3.2.1 THE INTERVENTION ROLE OF THE ANALYST OR FORECASTER IN AN AUTOMATED WEATHER PROGNOSIS SYSTEM

The human role in obtaining numerical weather prediction products varies from centre to centre and depends to some extent on the numerical models which are used. Some general guidelines are given in this section on the intervention role of the analyst or forecaster in the automated production of forecasts.

The major functions of an automatic weather analysis and prognosis system are listed in Section 3.1.6. Since the quality of a computer prognosis depends upon the quality of the analysis, the point at which any major manual efforts in the forecast process can usefully be made is at the pre-analysis stage. Thus, human intervention is most profitably made in the data-collection function and in the pre-analysis function. The preparation of the numerical forecast consists of several steps. The first step is the analysis of data and this is achieved by using the newly arrived data and a background field based on a 12-hour forecast made on the analysis of data prepared 12 hours previously. Following the computation of the analysis fields the computer then calculates the expected values of the meteorological variables at set times in the future. In this sequence, there are two periods during which humans can intervene usefully:

- (a) In the preparation of analysis fields prior to the preparation of the new background field (12-hour forecast fields) observations;
- (b) Monitoring the incoming data so as to ensure that no errors occur in the analysis prior to the forecast run.

If quality control procedures built into the automated system were perfect and dealt with every eventuality, the human role would be unnecessary. However, procedures are far from perfect and are unable to match the overall appraisal of a set of data plotted on a chart or an experienced analyst or forecaster. It must be acknowledged that quality control procedures are becoming more sophisticated and, at larger centres with considerable computer power, a balance has to be struck between the cost of the human role in relation to the improvement gained in output products. Once this balance point has been reached the human role may have to be eliminated and the consequent loss of human skills and techniques, such as chart analysis, must be accepted.

The use of manual techniques is only justified if it is assumed that the quality of forecast output products is higher when human intervention is used. This human role is basically a monitoring technique to ensure that rogue data are not allowed to ruin the analyses. Such monitoring is only practical if plotted data are actually analysed. Erroneous data which have not already been indicated by the usual quality control procedures can then be removed and suspect data which have been flagged by the computer can be assessed. In areas of sparse data, suitable bogus data can be invented so as to ensure that analyses do not suffer due to lack of data. The preliminary analysis of surface data and several key upper levels will facilitate this monitoring activity. The time available for monitoring is usually short, since it is desirable to run the preliminary forecast programs quite early in the overall sequence. It is normal practice to run the forecast program at the end of the period of time when a certain percentage of data can be assumed to be available. Safeguards must be built into the system such that data cannot be used for the analysis program that have not been monitored by the analyst or forecaster. This applies to data which arrived in the few minutes between the analyst or the forecaster giving the go-ahead for the analysis program to proceed and the actual run of the program itself. Intervention techniques can be achieved by the provision of suitable programs allowing data to be examined, corrected, or rejected at a terminal close to the chart-drawing bench. Programs must be easy to operate, instructions should be clear, and all the eventualities should be covered.

When the first set of analyses from the computer are available they have to be checked carefully for inconsistencies. After examination of the analyses, reasons must be found for any inconsistency that occurs. Erroneous data should then be detected and eliminated before the final forecast run is made. Monitoring can only be usefully achieved if the analyst or forecaster carries out the monitoring in a practical manner through the manual analysis of plotted data.

In the period between the main forecast run and the preparation of the background fields for the next set of data, efforts can be made to ensure that the analyses held in the computer are good and free from serious error. For example, late data need to be assessed since such data, if incorrect, could ruin a previously good analysis, thereby setting the scene for poor 12-hour forecasts and hence poor background fields.

It is useful for forecasters using the operational forecast products to undertake the intervention duties from time to time since it improves their understanding of the forecast model as a whole. The importance of different types of intervention can be assessed and the forecaster becomes more aware of the reliance of the forecast products on the initial analysis.

#### 4.3.2.2 THE MANIPULATION OF NUMERICALLY PRODUCED FORECASTS

When the output forecast products are received from the computer they can be dealt with in two ways:

- (a) They can be issued without modification observations;
- (b) They can be modified in the light of human experience — the man-machine mix.

As numerical models become more sophisticated, modification is becoming less desirable since the overall skill of the forecast products is improving. Prognoses of upper-air features produced at the larger centres are in general acceptable for direct issue. Machine forecasts for the surface pattern can, however, still benefit from human manipulation. The amount of manipulation must be dependent on the computer program. A forecaster may know, for example, that in certain situations the computer model fails to develop particular features. Appreciation of such facts can lead to useful manipulation of the surface forecast fields. Forecasters need to develop an understanding of the type of output related to the synoptic situation and to the initial data available. For example, the knowledge that the data available for analysis was poor should alert the forecaster to the need for more attention to the forecast products than would have been the case had the data available been good and plentiful.

Forecasters have to interpret the forecast products and produce weather forecasts, and the surface prognosis is usually the vehicle by which such an interpretation is made. Although the larger computer numerical weather prediction models can predict rainfall, careful appraisal needs to be made of the results. It is also of importance to relate areas of weather with the recognized features, such as depressions and fronts on the analyses. The objective forecasts of frontal systems is useful but forecasters do need to ensure that the interpretation of the forecast parameters in terms of fronts is correct and that continuity with the analyses at the surface and the upper atmosphere is maintained. The assessment of forecast products can be an exacting task since a thorough knowledge of atmospheric physics and the capabilities of the computer model is essential.

The development of skills required for the useful manual manipulation of machine-produced forecasts requires the constant use of computer products by skilled synopticians. Careful appraisal of the output of the machine products and qualitative verification of the products should be carried out, since such verification assists in building up the confidence of forecasters to modify the computer output.

#### 4.3.2.3 THE PRODUCTION OF PROGNOSSES DURING PERIODS OF COMPUTER OUTAGE

Contingency plans need to be made for the production of prognoses when computer outages occur. Such plans will entail a certain amount of human manipulation of data. If the whole forecast run is missed, manual techniques may have to be employed so as to utilize forecast charts from the last available forecast run as backup charts for issue of the new prognoses. For example, if an outage occurs in the order of 12 hours, then 36-hour prognoses from the last available forecast run could be used as a basis for 24-hour prognoses, but such backup charts would require some adjustment in the light of the later data received. This adjustment can only be achieved if the appropriate manual techniques are developed at the centre. For periods of outage exceeding 12 hours, the value of backup charts decreases rapidly. For these lengthy outages, human involvement must be increased if prognoses are to be issued. It is unlikely that two large centres would have serious outages at the same time, and forecast charts from another centre can be used as convenient backup for the preparation of prognoses. To have to fall back completely on manual techniques for the production of the prognoses is therefore unlikely.

Any manual intervention in the issue of prognoses demands knowledge of the physics of the atmosphere and, to this end, full use should be made of the available data and analyses from other centres. The preparation of additional manual analysis of the raw data is also likely to provide valuable assistance when considerable manual input is required to prepare backup forecast data for issue as prognoses.

Forecasters should therefore prepare themselves continually for such emergencies by trying to understand the atmosphere and its developments and by falling back on some of the traditional theoretical methods of obtaining explanations as to why a development occurs. In this way, forecasters will be in a better position to modify computer forecasts especially in those instances when the computer demands a high degree of manual input into the forecasting process.

#### 4.3.2.4 MANUAL TECHNIQUES IN THE PRODUCTION OF VERY-SHORT-RANGE FORECASTS (PERIODS OF SEVERAL HOURS)

The production of very-short-range forecasts for periods of several hours involves the use of highly specialized techniques. This type of forecasting is sometimes referred to as nowcasting. Considerable use is made of satellite data and radar information in conjunction with rain-gauge data.

### 4.3.3 *The use of workstations in the forecasting environment*

#### 4.3.3.1 GENERAL

There are no universal rules to design the perfect workstation for meteorological purposes. This chapter focuses on methodologies available today to those who wish to use a workstation in their operational environment. It is important to try always to match the appropriate technology to the task while keeping the whole process within feasible and justifiable costs. Quantification of both processor power and memory configuration are deliberately avoided because of the very fast changes taking place in the workstation industry.

Since the early 1970s, workstations have been evolving on the leading edge of electronics and microcomputers. Workstations have advanced a long way since the first vector graphic tubes and primitive raster display devices. Today, commercially available products are more powerful and open up new horizons and possibilities.

Workstations are only beginning to be used in a truly operational mode with applications emerging from both the meteorological centres and commercial developers.

There are many commercial packages available today which may satisfy the operational needs of a meteorological centre. The following are a few examples:

- (a) AMIGAS (Control Data Corporation): Is a complete hardware/software solution for the ingestion, display and management of meteorological data;
- (b) METPRO (General Sciences Corporation): Uses off-the-shelf hardware and software components integrated with application software to ingest and display meteorological data and to generate products from various meteorological data types.

Other commercial packages are available and should be explored before a final one is chosen. Many major national centres have developed their own flavour of workstation package. The following set of workstation applications are typical to fulfil most operational needs:

- (a) Raster image display, animation, presentation tools;
- (b) Field contouring, overlay (with satellite imagery);
- (c) Grid point calculator;
- (d) Meteogram of weather elements over time;
- (e) Verification application;
- (f) Model diagnostic tool;
- (g) Production monitoring and control tools;
- (h) Graphical editing tool;
- (i) Bogus data entry tool.

#### 4.3.3.2 TECHNOLOGY

Workstations which are available on the market today give a very wide spectrum of performance and options, thus complicating the selection process. It is crucially important to match the workstations to specifications of their immediate environment, including file servers, mainframes and specific issues related to networks.

Software standards will ensure diminishing costs of maintenance for the future. As an operating system, UNIX has certainly made its mark as the standard for workstations. The X WINDOWS system developed

by the Massachusetts Institute of Technology is also a common base for application development. One choice that remains to be made by the developer, and which may influence the choice of hardware platform, is the graphical user interface (GUI). The GUI defines the look and feel of applications as well as the standards for the various mechanisms in the operation of the user interface.

#### 4.3.3.3 WORKSTATION APPLICATIONS

- (a) *Research and Development:* The development of graphical packages for workstations has often been driven by the requirements of the research and development community whose needs are driven by innovation, scientific progress and new technology. More sophisticated tools are constantly being developed to analyse and explore new types of data, to manipulate increasing amounts of meteorological information, and to better understand weather phenomena at finer spatial and time scales;
- (b) *Operations:* Operational staff must interact efficiently and effectively with meteorological data (observations, numerical models, statistical products, etc...) in real time. Particular attention should be given to hardware reliability and performance, application hardness, network access, and backup procedures for hardware and communications. In some cases, the task of production control may be performed by the operational meteorologist. He/she should then be supplied with appropriate workstation tools and applications to simplify this task;
- (c) *Network and systems management:* In large organizations, this function is assigned to a specialized group. In smaller installations, this function could also be a part of the production control system, as long as it can be kept at a user-friendly level. Network and systems management applications are now widely available commercially, which monitor and detect communication problems and assist in network and system configuration.

##### *Data types*

- (a) *Observations:* Most workstation applications will require access to many types of observations, such as from surface and aerological stations, wind profilers, ships and aircraft, radar, lightning detectors, remote sensors and climatological archives;
- (b) *Numerical analysis:* To assist the meteorologist in his work, access to numerical products is essential. The WMO supported GRIB format is recommended for data exchange and is widely used in meteorological applications. In the case of an objective analysis, it may be necessary to have an interactive interface to provide some bogus data to supplement or to correct an analysis;
- (c) *Numerical forecasts:* In some cases, different models are used in the process of creating a forecast. Tools are needed to help the meteorologist navigate through these fields efficiently. Again GRIB is the recommended format to use. Many international meteorological centres can now transmit model output in GRIB format;
- (d) *Satellite imagery:* Workstations are now recognized as being indispensable for the manipulation of satellite imagery. Imagery should be stored in such a fashion that extraction is possible at various resolutions and that the creation of animation loops is facilitated. It should also be stored in a format permitting its use in conjunction with other data types;
- (e) *Radar data:* Radar data is one of the best tools for short-term forecasting of severe meteorological phenomena (potentially saving human lives). For those having access to radar information, a great deal of detailed information can be extracted from radar data using a real-time workstation interface.

##### *Basic applications*

- (a) *Graphics display:* Raster or vector image display is a basic function on a meteorological workstation. It will ease the transition from working on paper to working more with soft copies (Figure 4.1);
- (b) *Animation:* An application to animate images is usually required. It should allow building a list of images, editing the ordering, and displaying any image in the list. It is also desirable to control the speed of animation. More advanced applications would have multiple windows for simultaneous animation (Figure 4.2);
- (c) *Imagery interpretation:* The user should be able to control the colour enhancement of the image to help reveal or highlight specific features of the imagery. The ability to zoom in on any area and to pan over the image is also required;
- (d) *Comparison of model output:* The workstation should allow the meteorologist to compare different numerical models. This again necessitates an application permitting the display of various products in multiple windows;
- (e) *Time series:* This type of application gives a very precise view of the model output over the period of the forecast. One or more meteorological parameters can be displayed, for example, on a vertical time cross-section for a given location;
- (f) *Meteograms of weather elements:* Presenting various weather elements over a period of time for a given location can be done by using meteograms. The interface for this application should allow to choose the location and to vary the numerical model or source of input being used;

- (g) *Vertical profiles:* Tools to display radiosonde data can be fairly sophisticated if they include functionality, such as diagnostics, to indicate the potential for severe meteorological situations. Interaction with the raw data and seeing the effects of data modification can be a very helpful tool for short-range forecasts;
- (h) *Production control/monitoring:* Applications of this type can be as simple as reporting the completion of executed jobs or as complicated as monitoring the load and availability of a national wide area network. These applications generally use a network diagram graphically displayed on the screen with colour-coded states for networks and processes (Figure 4.3). Alarms, either visual or audio, are also incorporated to alert the user in case of a failure or abnormal situation (for example, if a computer program does not terminate successfully);
- (i) *Graphical editing:* Interactive graphical drawing can accelerate the work of a user if the application is well designed. Adding, modifying or deleting graphical objects are vital functions of a complete system. Object types include fields, lines, clouds, fronts, meteorological symbols, text, arrows, labels, etc. Editing options, including changing the shape of an object or an option itself — such as colour or thickness — or moving an object on the screen, are desirable (Figure 4.4);
- (j) *Radar display and analysis:* The classical display system for radar data interpretation permits viewing of the horizontal cross-section of the atmosphere using representations, such as constant altitude position plan indicator (CAPPI) or plan position indicator (PPI). It includes facilities for animation, zooming and panning as well as interfaces for colour enhancement and data filtering. More sophisticated systems can produce vertical cross-sections and categorization analysis. With the advent of Doppler radars, more and more types of data-processed outputs are available on the workstation for rapid visual analysis (Figure 4.5). Most of them are used in the operational detection of summer severe weather phenomena (mesocyclones, gust fronts, microbursts, wind shear, etc...). Also, audio or video alarms can alert the meteorologist when predetermined thresholds are reached.

#### *More advanced applications*

- (a) *Presentation/publication tools:* In order to exchange information in a printed format and to combine text with graphics for publications or for training purposes, a desktop publishing application is required. For presentations, either an easily used system for producing slides or one for projecting images directly from the workstation is needed. If colour is used on the workstation, it will be difficult to present the same information without colour prints or colour slides. Various solutions are available on the market today and the prices usually vary depending on the resolution of the devices;
- (b) *Overlay of fields and imagery:* An application with the capability of contouring a field interactively (Figure 4.6) and overlaying it with other contoured fields or satellite imagery (remapped) is possible on the newer generation of workstations. The addition of a calculator to perform algebraic functions on grid point fields and display the results is very useful for specific user needs (Figure 4.7). The ability to create macros and to record the actions of a user for future replay are essential features in an operational context;
- (c) *Generator of worded forecasts:* As improvements are made to numerical models and resolution is increased, it becomes feasible to generate automatically-worded forecasts based on direct model output and statistics. Such a system requires an interface that allows the forecaster to modify the input data when required. A workstation is well suited for such an application (Figure 4.8);
- (d) *Bogus data input and preview:* To enhance the flexibility of a numerical analysis system, it is desirable to be able to supplement observations with subjective input. In the case of communication problems or in sparse data areas, data could be injected into the analysis by using such a process. A good system would allow data entry (on multiple levels simultaneously, if necessary) in an overlay environment with station plotting. The application would ultimately give a preview of the effects of the bogus data in a graphical form by contouring the new analysis and displaying it to the user;
- (e) *Vertical space cross-sections:* A cross-sectional view of the atmosphere is a very useful tool in meteorology. This type of application is most useful if it includes control of vertical resolution and easy control of the positioning of the cross section. Access to complete observational data, numerical analysis, and forecast fields is required to feed this type of application. Tools to vary the actual fields or weather elements to be used must be made as simple as possible because of the complexity of the data being displayed;
- (f) *Environmental emergency response:* This type of application supplies the user with a means of launching, for example, a model simulating the transport of pollutants (Figure 4.9). When results become available, the user can view them with appropriate tools in a graphical format over the region of interest. In the case of environmental emergencies, the user must have many redundant communication facilities to ensure that he/she can forward the valuable information to its destination;
- (g) *Geographical information systems:* On a workstation, the geographical information systems will provide high resolution data on various types of information, such as topography, geography, political boundaries, population, and vegetation among other variables on a geographical background. More sophisticated packages will permit zooming-in on a chosen area of data.

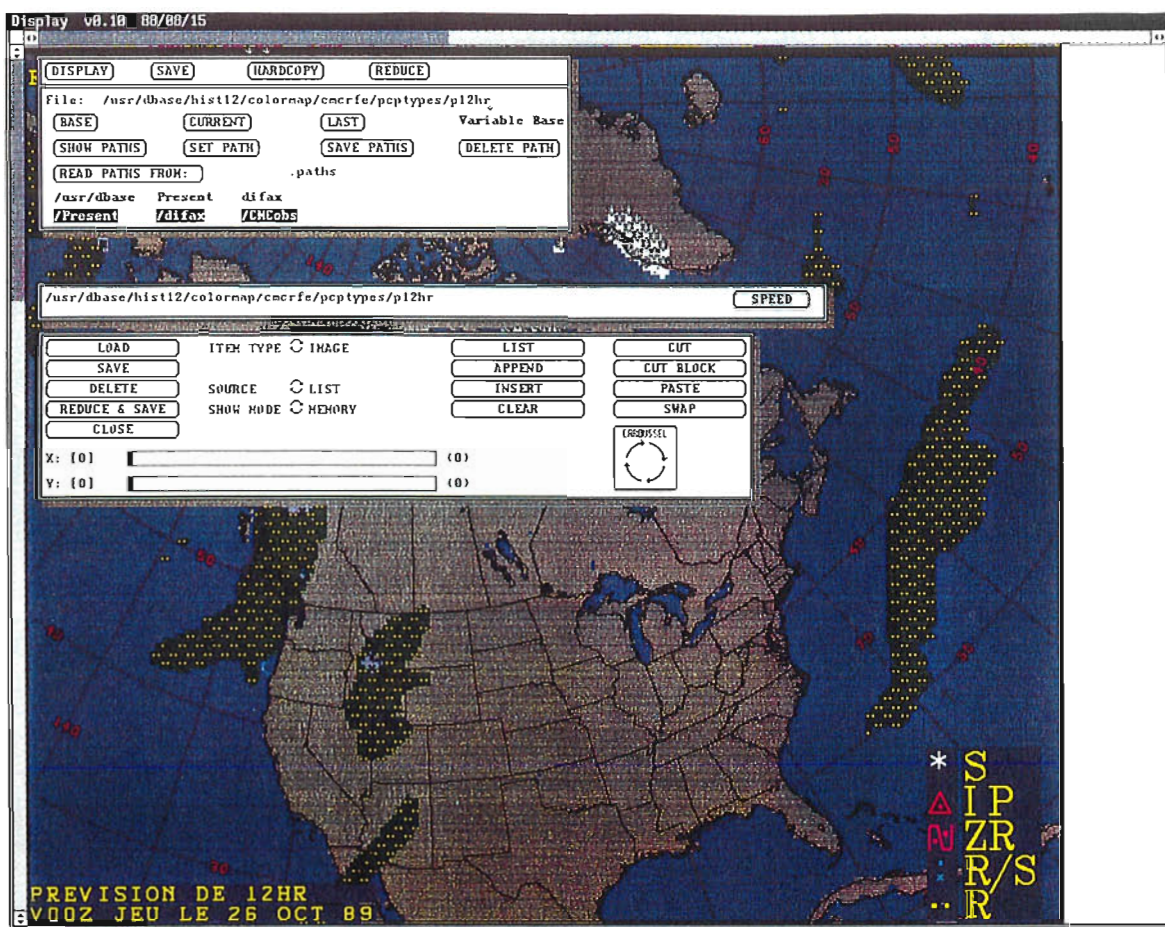
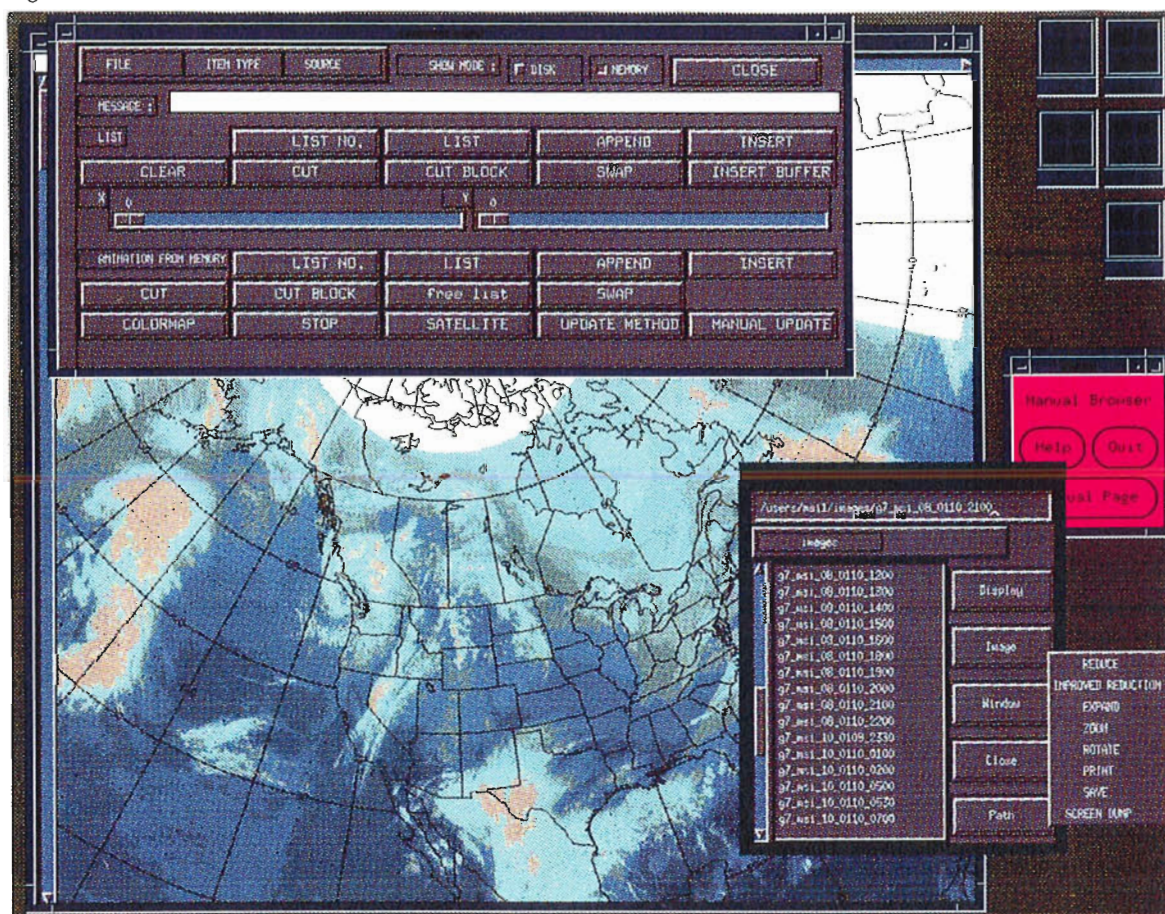


Figure 4.1 (see legends on page E)  
Figure 4.2



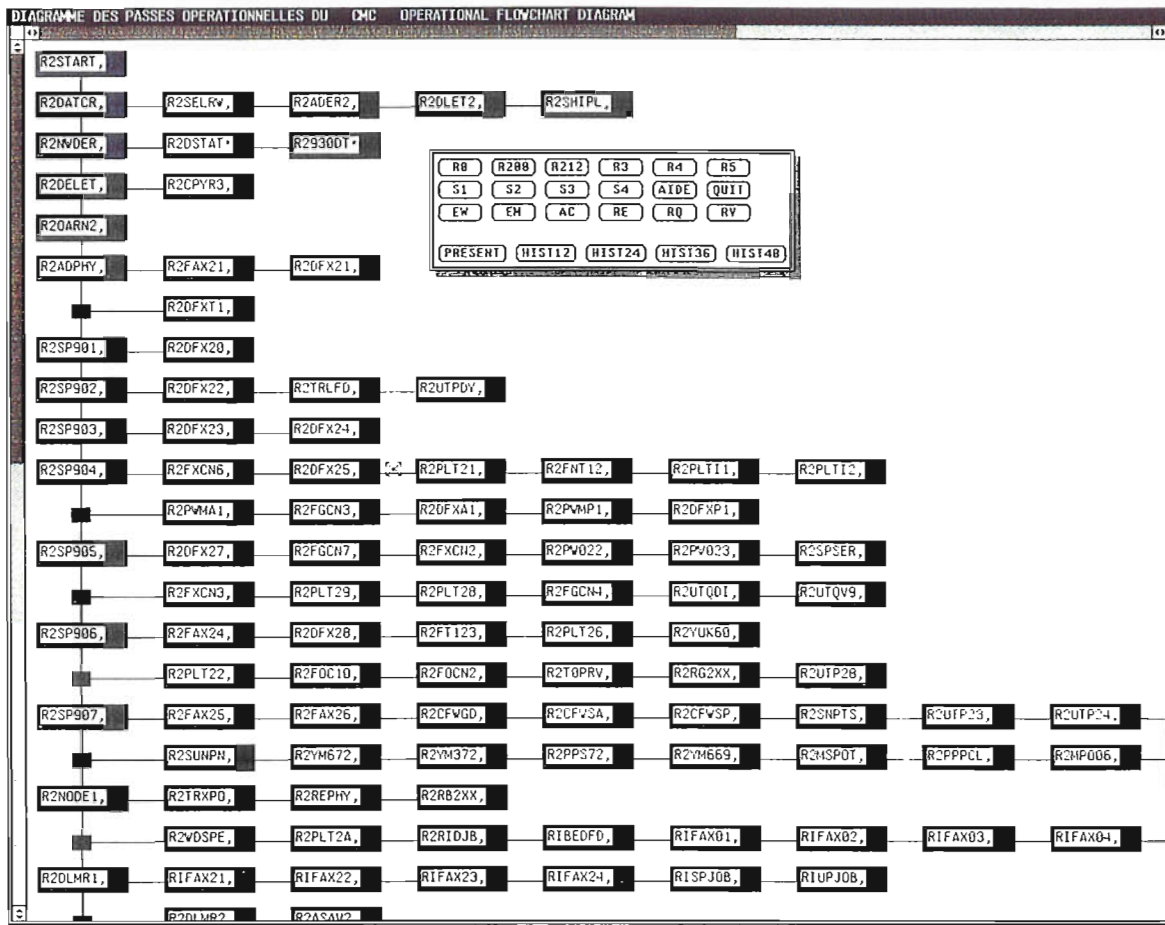
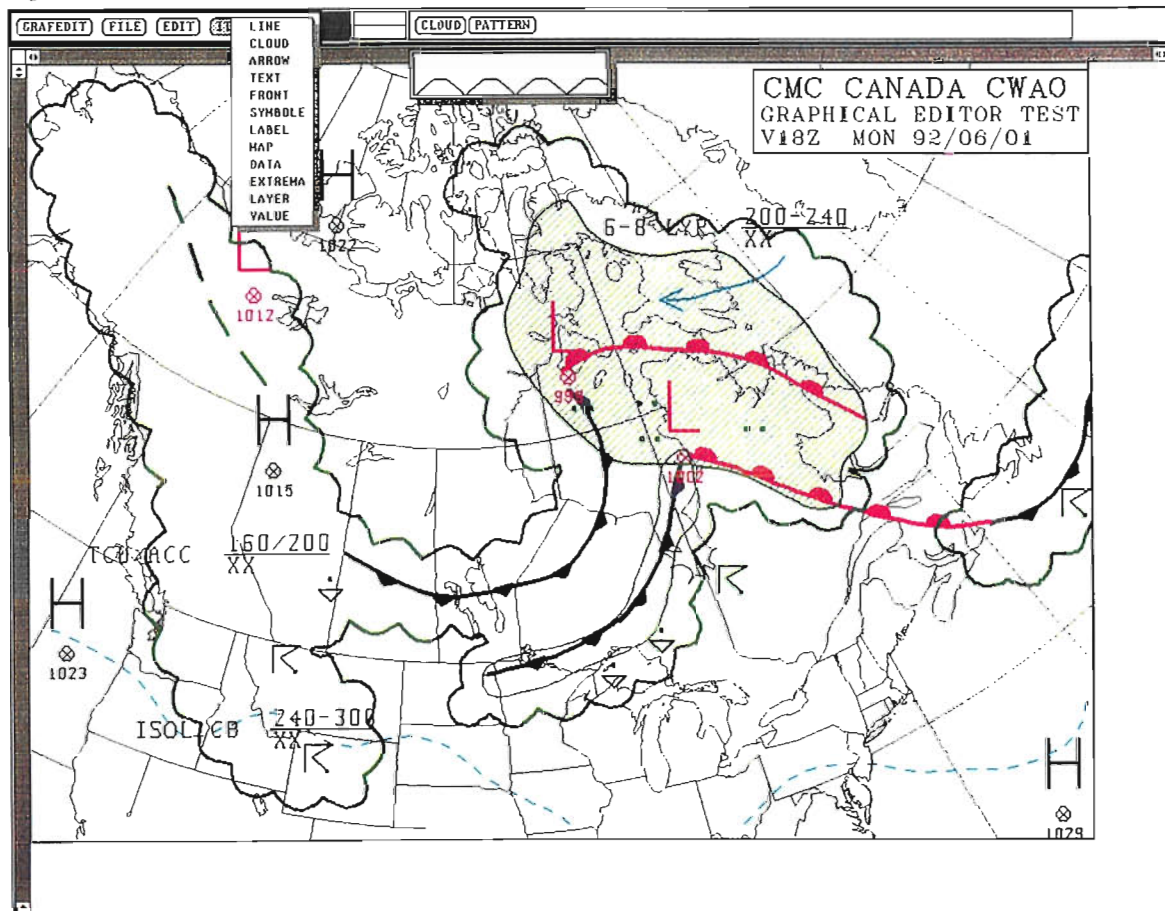


Figure 4.3

Figure 4.4



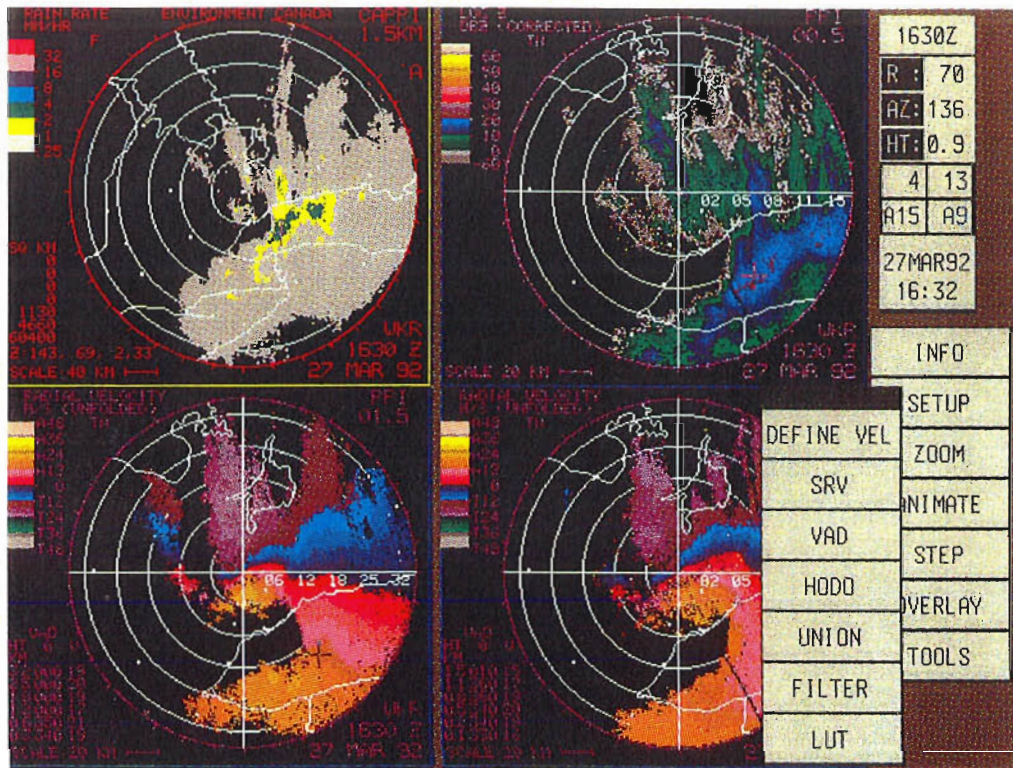
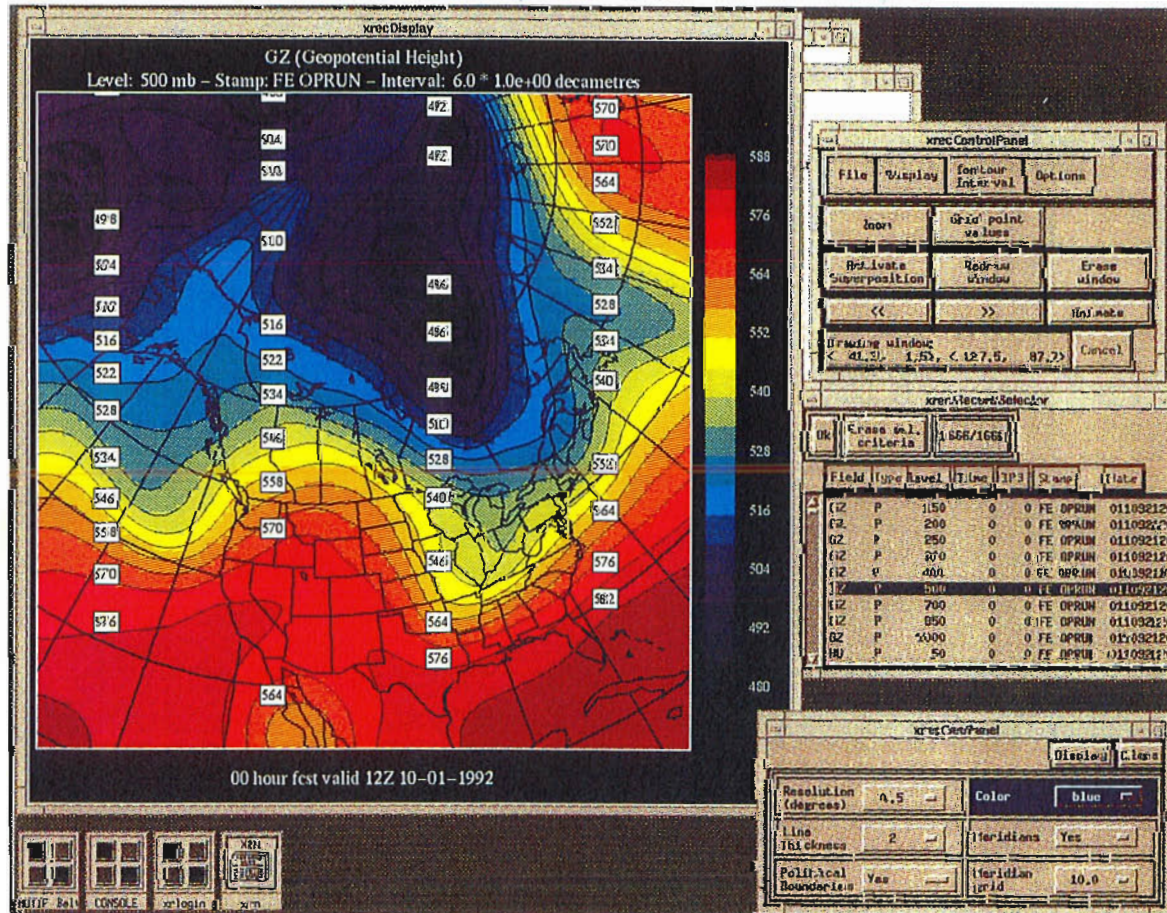


Figure 4.5

Figure 4.6



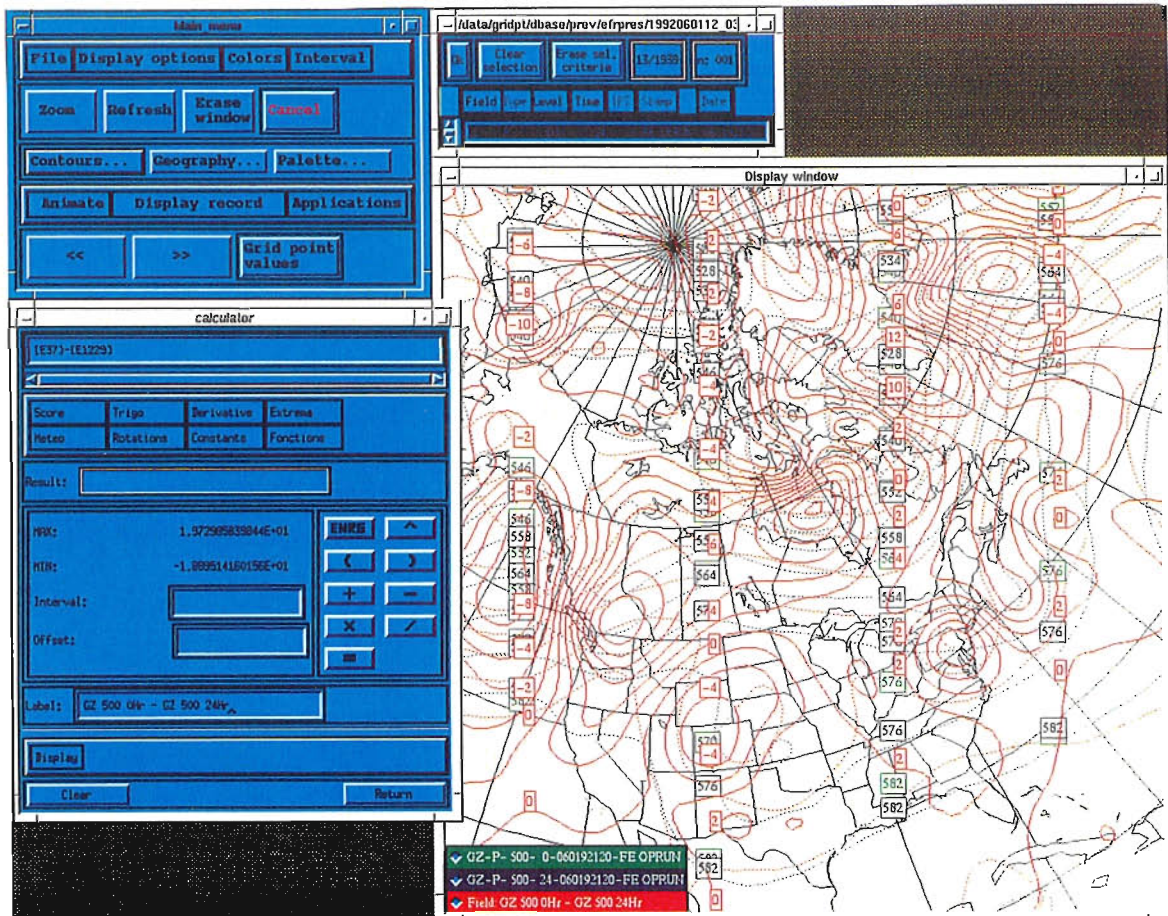
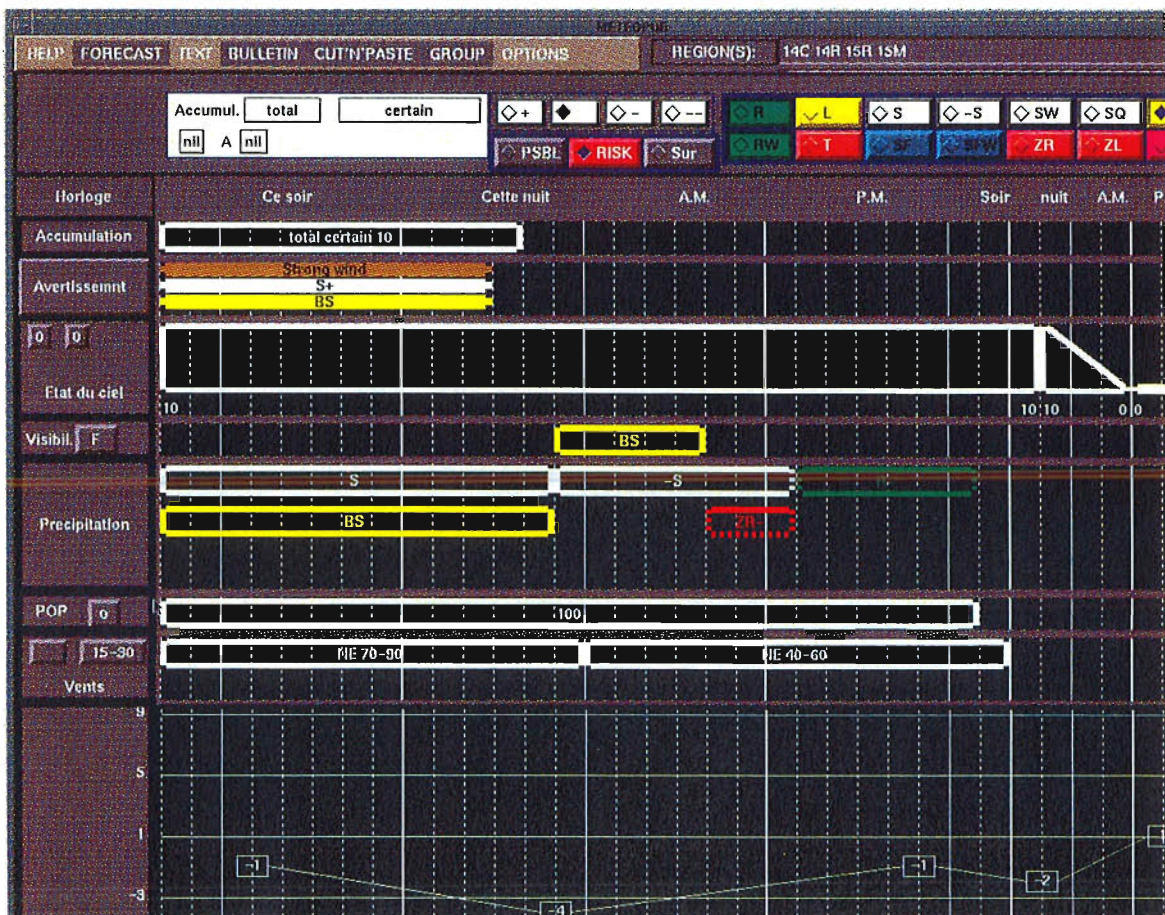


Figure 4.7

Figure 4.8



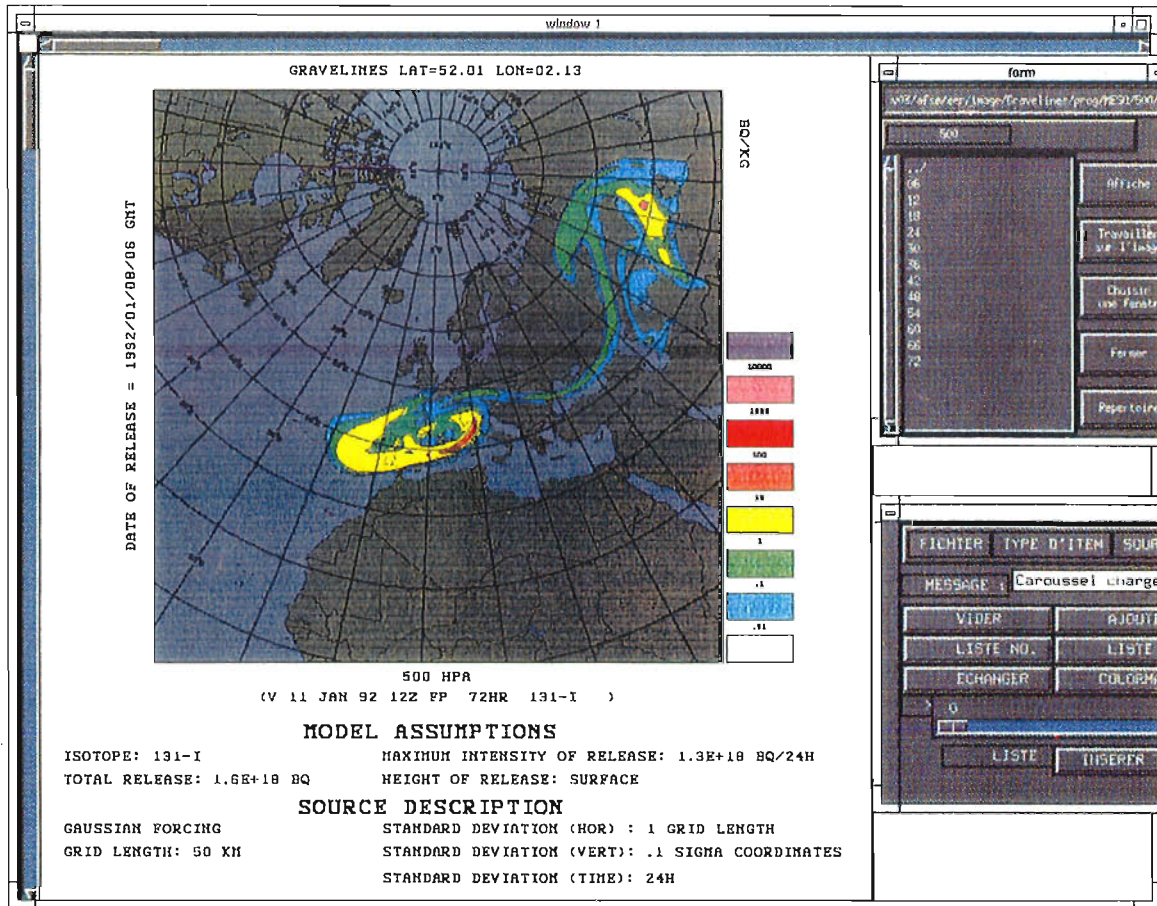


Figure 4.9

**Figure 4.1** — Example of a raster image display application. Here the user is presented with a file selector interface (top) as well as an interface permitting list editing (bottom). Displayed on the screen is a 12-hour precipitation-type forecast.

**Figure 4.2** — Example of an animation application. The file selector interface shown (bottom right) gives the list of available GOES images and the list of options in image manipulation, such as zoom, reduction, rotation, paper printing and others. The animation panel (top) gives various options, such as list editing, control over the images in the memory or in the list, colour map selection, window control, screen control, pan control, and many others. In the display window, we see a GOES satellite image remapped to a polar stereographic projection.

**Figure 4.3** — Example of a production control application. The user interface shown in the centre is used to select the production run of interest. Each box on the diagram represents a process. The colour of the box is representative of the state of the process and it changes colour with each progression. When a problem is detected with one of the processes, the box representing that process turns red and an audible alarm is started.

**Figure 4.4** — Example of a graphical editing application. To simplify the use of this application, the menu window was deliberately restricted to the top portion of the screen and temporary pop-up menus were used to complete the interface. Here the ITEM menu is shown in its active mode giving the complete list of drawing types possible with this application. This example of a significant weather chart is intended to show the capabilities of graphical editing. Note that it would be possible to conform to ICAO standards.

**Figure 4.5** — Example of a radar data analysis application. This is an example of an operational radar data display system. Radar data is analysed and sent to the weather centre in a user-friendly format. The user selects the four image types he wants to see, out of a dozen different products, using a series of pop-up menus. Here, the top left image corresponds to a 1.5 km CAPPI of the rain rate and the right image is a low elevation angle of the reflectivity. The bottom images correspond to the Doppler radial wind velocities at different elevation angles (PPI). A wide range of applications can quickly be chosen by the user (animation, zooming, overlay, etc.) as well as special products which can automatically detect dangerous meteorological areas (gust fronts, microbursts, mesocyclones, etc.).

**Figure 4.6** — Example of a field contouring application. On the right part of the screen, three menu panels are shown: the control panel (top) gives a general access to all the features and options of the application, the record selector panel (centre) gives the choice of model output fields to be contoured and the geography control panel (bottom) gives the user flexible display options. Shown in the display window is a zero-hour 500 hPa height contour field.

**Figure 4.7** — Example of a grid calculator application. This grid calculator menu (centre) contains the basic calculator keys as well as trigonometric, derivatives and special functions. The file selector menu is used with the calculator to select the fields. The bottom panel is a colour legend of the displayed fields. On this example, we see (in red continuous) the resulting geopotential height difference between the zero-hour 500 hPa forecast (in red dashes) and the 24-hour 500 hPa forecast (in purple dashes).

**Figure 4.8** — Example of a worded forecast generator interface. The interface permits the entry and edition of weather element forecasts. The X-axis depicts time and the Y-axis depicts various weather elements, such as wind, precipitation and temperature. The upper part of the interface gives access to qualifiers to give more precision to the forecast. Once the forecast is graphically satisfactory to the user, the automatic text will be generated. The process can be a totally manual operation as well as a computer-generated weather element-based application.

**Figure 4.9** — Example of an environmental emergency response interface. The graphic in the display window shows a 72-hour forecast of a simulated radio active plume at 500 hPa. The concentration levels are colour coded in Becquerels per kilogram of air.

#### 4.3.3.4 DESIGN CONSIDERATIONS IN SETTING UP A WORKSTATION-BASED SYSTEM

The major limiting factor of the size and performance of a workstation-based system is the operating budget of a centre. The cost of post-installation maintenance, including system software upgrades and hardware maintenance, is a very important factor in the decision process.

- (a) Improvements in services must be evaluated to justify the cost of the initial purchase. The savings may come from various sources, as for example:
  - (i) Increased efficiency in human resources utilization;
  - (ii) Reducing the use of paper in the work place;
  - (iii) Generating new products without increasing staff;
- (b) In some cases, the improvements may be instrumental in saving priceless human lives;
- (c) The impact on the speed of delivery of the actual products coming from meteorological operations is a factor in the cost-benefit analysis;
- (d) In the process of evaluating costs, the quality and quantity of workstations needed is an important factor. Some work positions may require two or more workstations to do the job. Other functions may require fully configured workstations with maximum memory and graphics accelerator options;
- (e) The system must be analysed as a whole to evaluate the mass storage needs to supply all of the data that may be needed by the workstation applications, and to hold the software to run the applications. Any need to access previous data should be considered in evaluating disk space. The speed of access can be different for different applications, for example previous data could be stored on slow access devices (optical disk or less expensive disk drives) and real-time data could be on fast access hard disks;
- (f) Applications tend to grow and be integrated together creating a greater need for internal memory. Insufficient memory causes a swapping situation which slows down the workstation and the user. Users also like to open multiple applications, thus simultaneously increasing even further the need for memory;
- (g) A platform should be defined by the type of application that it will serve. A workstation destined to run animation loops of high resolution images does not have the same requirements as one destined to do contouring and overlay of various meteorological fields. Appropriate benchmarks should be established to evaluate the performance of individual platforms;
- (h) The manufacturer's compliance to industry standards is of great importance in the choice of a workstation. The degree of compliance will determine the ease of migration to a future platform;
- (i) The choice of network technology must reflect the requirements for data transfer from the file server to the workstation. The number of workstations on a network may also be a factor. A mixed configuration may be the solution, if for example a very high speed fiber optic link is needed between a file server and a mainframe or a dedicated ETHERNET trunk is needed for ingesting satellite data and a database application.

#### 4.3.3.5 OTHER CONSIDERATIONS

##### *Impacts on working methodology*

The arrival of workstations in the operational environment has a significant impact on the working methodology. Resistance to change is usually very high and is even greater when people have to go through a learning process before they can use a tool. A general recommendation is to let the users explore and comment on the functionality of the workstation in a prototype mode. Having the users participate in the design phase as early as possible will increase the chances of success. A short turnaround time between requests for modifications and modifications themselves is a key in this process.

##### *Revision of staff deployment*

Some consideration must be given to the impact that workstations may have on individuals. Some jobs might be eliminated or redefined completely. Preliminary impact analysis studies should be carried out to determine the positions that will be modified and to find alternative tasks or prepare retraining programmes for those directly affected by the changes.

##### *Ergonomics*

The working conditions are not to be neglected as the performance of an individual could be diminished. Seemingly minor details such as furniture, interface design, ambient lighting, heat dissipation, keyboard and mouse access, radiation, and noise level (coming from the cooling fans of a workstation) should all be addressed.

##### *Maintenance and contingency*

Although workstation technology is usually extremely reliable, maintenance and contingency plans must be set up to ensure the continuity of the services. The more the applications migrate to the workstations, the more the production system becomes dependent on these workstations. It is highly recommended, therefore, to have a complete backup system for critical components.

### *Implementation issues*

The transitional period is critical and should not be executed in a limited time frame. Gradual change-over is more effective. The prototype approach, using user feedback to adjust the final applications and set-up, probably works best. It is essential that users be trained before the arrival of the workstation on their desk. Training could be done on a very broad basis depending on the users' responsibility. For example, a user doing network administration will need to have a solid UNIX background plus comprehensive communications knowledge. Knowledge of a simple text editor such as "vi" is also necessary for most users as well as an understanding of the behaviour of the whole system. A good understanding of the network also helps the users to grasp how to best accomplish their tasks within this environment.

### *Life cycle expectancy*

The life cycle of workstation applications greatly depends on their popularity and on the rate of progress in technology. More powerful workstations will allow the development of previously unimagined applications. These improved applications may impact adversely on the use of previous applications. Sometimes, standardization and revision of graphical libraries will necessitate the rewriting of an improved version of an application, so that in fact this application will enjoy a longer life.

## 4.3.3.6 TRENDS IN WORKSTATION HARDWARE AND SOFTWARE TECHNOLOGY

### *Hardware trends*

The concept of distributing processes amongst a network of processors of various speeds and capacities, and even amongst various vendors, is available on the market today. Commercial database software is evolving towards networks of distributed shared databases, where data could be spread over various machines of various types and could appear to the user as a single database. An example of the use of this technology is the naval environmental operational nowcasting system (NEONS) of the U.S. Naval Oceanographic and Atmospheric Research Laboratory. The data management concept behind NEONS promotes easy access to multiple data types and portability of data using commercial database software. The fast growing industry of massively parallel computers is also bound to drive changes in the workstation market.

### *Communications*

The communication bandwidth is often a limitation to what users would like to be able to do in real time. Advances in communications technology now promise substantial jumps in bandwidth as well as changes in transmission media. The advent of wireless networks, with bandwidths available today only through optical fibre networks, is close at hand.

### *Software standards*

New standards are emerging in the graphics world, with X WINDOWS certainly being a good example. A new standard is now appearing for three-dimensional graphics within the X WINDOWS package called PEX (PHIGS Extension to X), which will open up even more horizons for future applications. The use of X WINDOWS for application development is now a proven method to ensure maximum transportability of an application. This permits easy migration to bigger and faster systems as they become available and make more efficient use of development resources, in avoiding laborious conversion activities.

## 4.3.3.7 WORKSTATION APPLICATION TRENDS

### *Three- and four-dimensional visualization*

Up to now, most of the workstation applications that were used in a forecasting environment were two-dimensional applications of the kind described in section 4.3.3.3. As the cost of workstations is dropping and their abilities are growing, three- and four-dimensional visualization (three dimension plus time) are generating great interest and new possibilities. In an operational context, hardware requirements for four-dimensional visualization are greater in all aspects. It is easy to generate animation sequences which would overload a network, exceed the physical memory of the workstation and be so time consuming that operational deadlines would not be met.

A variety of public domain and commercial packages are available for three- and four-dimensional visualization. Most of these packages give control over the elements to be viewed, the time steps, the colour of the elements, and the angle and location of the viewer. Other available features include volume rendering, texture mapping, rotation and translation, image slicing, shading, multiple light sources, specularity, and transparency. In meteorology, the interest is focused on three-dimensional scalar fields, such as thermodynamic and water variables, charge, vector components, etc. and three-dimensional vector fields, such as velocity and vorticity. One good application example is the comparison of thunderstorm fields synthesized from Doppler observations with numerically simulated fields to help verify model simulation of thunderstorm evolution.

### *Video animation*

Video animation is one of the most progressive areas of workstation application development. It is being used by the scientific community to show the results of research, for example, the impact of global warming, the evolution of the ozone hole, or cloud formation. It is primarily used for public education or for scientific communication and seminars. In the near future, it is foreseeable that video animation will be created

operationally to depict the daily weather. However, before it can be operationally, it will require the development of high performance user - friendly tools, and significant financial and human resources will be needed. In addition, professional quality video equipment is mandatory to serve broadcast news agencies and public television. Examples of future applications in operational meteorology include:

- (a) *Severe weather depiction tools*: This application would enable the user to visualize the development of convective clouds from the output of simulation models at a much finer scale than is currently available by using volume rendering combined with animated ribbons to depict the airflow within the model. Precipitation could be displayed as a transparent object and also animated or toggled on and off. This visualization application could help a forecaster evaluate more precisely the strength of a storm and its track. The user will interact with various variables, such as the geographical area, the vertical profile of the initial state of the local atmosphere, and the forecasted meteorological fields for the period under review. Replacing the traditional tools that look at vertical profile data will allow the user to integrate all of the available data. Satellite data, such as special sensor microwave/imager (SSM/I), combined with numerical model output and data from higher resolution analysis, will permit the development of flexible applications to diagnose severe weather;
- (b) *Aviation tools*: It is anticipated that new tools will be developed to assist in-flight planning. For example, an application could be developed to help precisely locate clouds, turbulence, icing, and winds. This real-time system could actually show a pilot an animation sequence of the weather forecast for his current flight path. With the help of artificial intelligence, systems will be able to suggest safer alternatives to help a pilot or controller in decision-making processes. The revised flight plan would generate a new set of animation data to be viewed by the user. This kind of system will only be possible if the airline companies invest in the needed technology to transfer the information while the planes are airborne;
- (c) *TV products for public dissemination*: The evolving tools available to the operational meteorologist will inevitably increase productivity. The information thus generated will be more effectively delivered by using state of the art technology to package the final products into sequences of movie (or cartoon) animation. Highly specialized commercial applications will most likely satisfy this need as computer aided design (CAD) applications converge with advanced commercial packages of visualizing software to form powerful systems. The system will need to be able to generate, in a rather automated fashion, a complete television weather forecast sequence for a given city. The forecaster would have the role of reviewing and fine-tuning the product.

#### REFERENCES

- Battan, L. J., 1959: *Radar Meteorology*, University of Chicago Press, Chicago.
- Bent, R. B. and W. A. Lyons, 1984: Theoretical evaluations and initial experiences of LPATS (lightning position and tracking system) to monitor lightning ground strikes using a time-of-arrival (TOA) technique. *Seventh international conference on atmospheric electricity*, Albany, American Meteorological Society, pp. 317-324.
- Berry, F. A., E. Bollay and N. R. Beers, 1945: Thermodynamic diagrams and calculations. In: *Handbook of Meteorology*, Section V, McGraw-Hill Book Co., New York, pp. 361-371.
- Browning, K. A., 1989: The database and physical basis of mesoscale forecasting: Mesoscale forecasting and its applications. *Lectures presented at the fortieth session of the WMO Executive Council*, 1-20 June 1989, Geneva, WMO-No. 712.
- Bryllov, G. B., et al., 1986: *Radar Characteristics of Clouds and Precipitation*, Leningrad, Gidrometeoizdat.
- Christensen, U. and L. G. Nilsson, 1984: A lightning detection system in Sweden. *Proceedings of the second international symposium on nowcasting (Nowcasting II)*, 3-7 September 1984, Norrköping, Sweden, pp. 213-218.
- Collier, C. J., 1989: *Applications of Weather Radar Systems. A Guide to Uses of Radar Data in Meteorology and Hydrology*. Ellis Horwood Ltd., Chichester.
- Defrise, P., 1948: *Contribution à une étude comparative des diagrammes aérologiques*, Institut Royal Météorologique de Belgique, Miscellanéis, Fasc. XXXIII.
- Doviak, R. J. and D. S. Zrnic, 1984: *Doppler Radar and Weather Observation*, Academic Press, New York.
- European Space Agency, 1984: Mesoscale observations and very-short-range weather forecasting. *Proceedings of the second international symposium on nowcasting (Nowcasting II)*, 3-7 September 1984, Norrköping, Sweden, Esa-Sp 208.
- European Space Agency, 1987: Mesoscale analysis and forecasting incorporating 'nowcasting'. *Proceedings of an international symposium on mesoscale analysis and forecasting*, 17-19 August 1987, Vancouver, Esa-Sp 282.
- Hawson, C. L. and P. G. F. Caton, 1961: A synoptic method for the international comparison of geopotential observations. *Meteorological Magazine*, 90, pp. 336-344.
- Herlofson, N., 1947: The T-log p diagram with skew coordinate axes. *Meteorologiske Annaler* (Oslo), Norwegian Meteorological Institute, Band 2, No. 10, pp. 311-342.
- Lee, A. C. L., 1986a: An experimental study of the remote location of lightning flashes using a VLF arrival time difference technique. *Quarterly Journal of the Royal Meteorological Society*, Vol. 112, No. 471, pp. 203-229.

- Lee, A. C. L., 1986b: An operational system for the remote location of lightning flashes using a VLF arrival time difference technique. *Journal of Atmospheric and Oceanic Technology*, Vol. 3, No. 4, pp. 630–642.
- Lhermitte, R. M. and D. Atlas, 1961: Precipitation motion by pulse Doppler radar. *Proceedings of the ninth weather radar conference*, 23–26 October 1961, Kansas City, Missouri, pp. 218–223.
- Maier, M. W., et al., 1983: Locating cloud-to-ground lightning with wideband magnetic direction finders. *Fifth symposium on meteorological observations and instrumentation*, 11–15 April 1983, Toronto, pp. 497–504.
- Oliver, V. J. and M. B. Oliver, 1945: Weather analysis from single-station data. In: *Handbook of Meteorology* (F. A. Berry, E. Bollay and N. R. Beers, eds.), McGraw-Hill Book Co., New York, pp. 858–879.
- Petterssen, S., 1956: *Weather Analysis and Forecasting*. Vol. II (second ed.), McGraw-Hill Book Co., New York, pp. 35–63.
- Richards, W. G. and C. L. Crozier, 1983: Precipitation measurement with a C-band weather radar in southern Ontario. *Atmosphere-Ocean*, Vol. 21, No. 2, pp. 125–137.
- Saucier, W. J., 1955: *Principles of Meteorological Analysis*. University of Chicago Press, Chicago.
- Stepanenko, V. D., 1973: *Radar in Meteorology*, Leningrad, Gidrometeoizdat.
- Stüve, G., 1927: Potentielle und pseudopotentielle Temperatur. *Beiträge zur Physik der freien Atmosphäre*, XIII, pp. 218–233.
- Ulbrich, C. W. and D. Atlas, 1984: Assessment of the contribution of differential polarization to improved rainfall measurements, *Radio Science*, 19, pp. 49–57.
- World Meteorological Organization, 1966: *Use of ground-based radar in meteorology*. Technical Note No. 78, WMO-No. 193, TP. 99.
-

## CHAPTER 5

### METHODS OF ANALYSIS AND FORECASTING IN THE TROPICS

#### 5.1 Introduction

The tropics, from a meteorological point of view, generally represent the region between the axes of the subtropical highs in the two hemispheres. The dividing line between the easterlies and westerlies in the middle troposphere is taken to demarcate the boundary between the tropics and the extratropics. The meridional extent of the tropics undergoes seasonal variations consequent upon the migration of the sun, and, therefore, the zone of maximum heating, northward and southward. For practical purposes, the tropics are generally taken to comprise the region between 30°N and 30°S.

The tropics have a great importance in the global circulation due to the fact that they comprise almost half the surface of the earth in which the atmosphere gains both angular momentum from the earth's surface and heat energy in excess of what is required to offset heat loss due to outgoing long-wave radiation. The excess energy received in the tropics is transported poleward to provide for the net loss of radiational energy in the extratropical latitudes. Within the tropics, the excess of realized energy is transported poleward mainly by the mean (Hadley) circulation. The strong Hadley circulation is the dominant factor in the zonally-averaged circulation of the tropics. Further poleward, it is the eddies which assume greater importance and account for most of the energy export from the tropics into the extratropical latitudes. On a mean annual basis, there is a net heating in the tropics and transport from the Equatorial belt to higher latitudes of both hemispheres.

There is a constant interaction taking place between the tropical weather systems and the extratropical ones. The wave disturbances in the tropics are affected in both their movement and intensification by the middle latitude troughs. Riehl (1950) observed that troughs in the middle latitude westerlies often extended from very high to very low latitudes and suggested that poleward flow of heat from the tropics must take place in the restricted regions of these troughs. This shows that the tropical and extratropical circulations are intimately connected with each other and cannot be considered in isolation. In order to study the interactions between the tropical and extratropical circulation systems it becomes necessary to extend the tropical weather analyses to much higher latitudes of up to 50 degrees or so in both hemispheres. Furthermore, inter-hemispheric interactions and cross-equatorial flows also necessitate extension of tropical weather charts to encompass parts of both hemispheres.

This chapter deals with the following methods of analysis and forecasting in the tropics. Section 5.2 describes the general characteristics of the mean structure and circulation of the tropical belt. Section 5.3 gives brief information about the observational database available for tropical analysis and forecasting. Brief characteristics of various tropical wave disturbances are outlined in section 5.4. Section 5.5 deals with different kinds of tropical synoptic models including waves and vortices. The tropical synoptic analysis techniques are mentioned in section 5.6. Section 5.7 discusses the tropical forecasting methods, which include the numerical weather prediction techniques in current operational practices. Section 5.8 deals with prediction of tropical cyclones, verification of track forecasting methods, and storm surge prediction, among others. Lastly, section 5.9 describes various mesoscale phenomena in the tropics. The mesoscale phenomena discussed in this section are, however, common to both tropics and extratropics. It was considered useful to deal with them in some detail here.

#### 5.2 Mean structure and circulation of the tropical belt

In order to gain an understanding of the tropical disturbances for their analysis and forecasting it is first necessary to look at the general circulation of the tropical belt, the energetics involved in the formation and growth of tropical disturbances, and the origin of tropical synoptic disturbances. The main features of the tropical circulation are the subtropical highs, the trade wind belts on their equatorward sides and the zones where the trades meet in the equatorial low pressure belt, the intertropical convergence zone (ITCZ) — known variously as intertropical front (ITF) — and the equatorial front and trade confluence (TC). The ITCZ plays a dominant role in the synoptic scale disturbance activity in the tropics and is the seat of formation of most of the tropical disturbances. Some of these disturbances later develop into tropical depressions and cyclones if they are located sufficiently away from the Equator.

A very large area of the tropical belt is covered by the monsoon circulation encompassing the longitudes of the Indian Ocean and west Pacific. This is the dominant region of atmospheric latent heating. A variety of synoptic disturbances are generated in the monsoon region. Apart from the tropical cyclones and depressions which populate the west Pacific region, the north Indian Ocean (Bay of Bengal and Arabian Sea) is known to have an existence of monsoon depressions and midtropospheric cyclones. These systems account for a major share of the total rainfall in the region.

Some important characteristics of the ITCZ and the monsoon circulation are described below.

##### 5.2.1 *The intertropical convergence zone (ITCZ)*

The terminology used to delineate the zone separating the northern and southern hemisphere flow has had a varied history. Originally the term intertropical front (ITF) was used to indicate a narrow zone in the

lower troposphere in which the air from the summer and winter hemispheres moved equatorward and, for continuity considerations, was forced to rise and move poleward, thereby transporting heat towards the middle latitudes in the upper troposphere. However, to avoid confusion with the frontal systems of the middle latitudes the name was changed to the intertropical convergence zone (ITCZ). The ITCZ is associated with an elongated zone of low pressure and cyclonic wind shear near the Equator.

More recently, data from weather satellites reveal that bands of maximum cloudiness do not always coincide with the axis of lowest pressure. It was also noticed that on many occasions there was more than one convergence (cloud band) zone, and more than one trough of low pressure. Consequently, Ramage (1971) suggested "near equatorial troughs" and "near equatorial convergence lines" as alternatives to ITCZ. However, a numerical study done by Pike (1971) supports the presence of a single ITCZ. According to Hubert, *et al.* (1969), satellite data show that the double ITCZ occurs quite infrequently, despite longitudinal variation, and is an important feature of the ITCZ.

The ITCZ is centred away from the Equator and this fact is reflected in the dry zone along the Equator in the mean satellite cloud brightness photographs (Holton, 1979). When analysing the data from the International Indian Ocean Expedition (IIOE), Sadler (1969) also observed a maximum of cloudiness on both sides of the Equator between three and 10 degrees latitude in both hemispheres. The Equator, on the other hand, was relatively cloud-free for most of the year.

The ITCZ undergoes seasonal variations in regard to its geographical location. It remains close to the geographical Equator in predominantly oceanic longitudes such as the Atlantic and Pacific Oceans showing only slight seasonal variations. In the longitudes covered by large continents, on the other hand, such as the Asian continent, the ITCZ undergoes a strong seasonal migration. In around half the equatorial belt comprising the eastern Pacific and Atlantic Oceans and west Africa, the ITCZ lies north of the Equator throughout the year. The ITCZ is persistent and well defined over the Pacific and Atlantic between about 5°N and 10°N latitudes, and occasionally appears in the Pacific between 5°S and 10°S. A large migration of ITCZ takes place in the longitudes of east Africa, Asia and Australia. In the Indian Ocean area, the cloud maximum associated with ITCZ moves north in the eastern parts in the month of May. Between June and August, the cloud maximum covers the summer monsoon region of Asia, but from September onwards it again moves south to a position near the Equator. The onset of summer monsoon over Asia is believed to be associated with the northward movement of the ITCZ. However, the relation between periodic shifts of the ITCZ and planetary scale motions, such as the summer monsoon, is not well understood because of insufficient upper-air data. It is not clear, for example, whether the onset of the summer monsoon is the result of a disturbance originating over the equatorial ITCZ, nor is it clear whether the ITCZ loses its identity when the monsoon is fully established over Asia. In these regions, the trades originating in the winter hemisphere turn around crossing the Equator and become westerlies in the summer hemisphere.

There is a direct relationship between the position of the ITCZ, the tropical convection and the sea surface temperature (SST). The tropical circulation and rainfall regime are closely related to the annual cycle of surface temperature, which for most of the tropics, is SST. Even though the annual cycle in tropical SST is relatively small, tropical convection is quite sensitive to these differences.

The time-averaged convective precipitation shows an organized coherent rainfall pattern associated with the ITCZ. A good index of the time-averaged precipitation variability in deep tropics and hence the position of ITCZ is provided by the satellite measured outgoing long-wave radiation (OLR). Low values of OLR indicate deep convection and heavy precipitation, while high values indicate the reverse. There is a notable coincidence between the SST maximum, the OLR minimum, and the zonally averaged low-level convergence belt of the Hadley circulation (Rasmusson, 1990). Specifically, the tropical oceanic regions of OLR less than 240 W/m<sup>2</sup> lie mostly within the 28°C SST isotherm. Figure 5.1 shows the mean OLR fields for the two solstice seasons. Experience shows that areas in the tropics where time-averaged OLR is less than 240 W/m<sup>2</sup> generally correspond with regions of mean upward motion and heavy convective rainfall. One large scale OLR minimum (precipitation maximum) is located over Africa, and another over South America/Central America. Both migrate north-south with the high sun season. The third and the most extensive area is centred over the land areas and adjacent warm waters of the east Asian and Australian monsoon regions, with eastward extensions along the ITCZ north of the Equator, and the South Pacific convergence zone in the south-west Pacific. The three regions of heavy precipitation implied by the OLR pattern mark the primary upward branches of the time-averaged direct thermal circulations of the tropics.

The structure of the ITCZ has been studied by Estoque (1975) over the central region of the tropical North Atlantic and North Pacific Oceans from observations collected during the Atlantic Trade Wind Experiment (ATEX) and the Line Island Experiment (LIE), from ISMEX-73 data over the north Indian Ocean by Godbole and Ghosh (1975), and over the GARP Atlantic Tropical Experiment (GATE) area of the Atlantic Ocean by Estoque and Douglas (1978). From these studies it emerges that the ITCZ is associated with warm and dry air some distance away on either side of its location. Estoque has proposed a model for the synoptic scale structure of ITCZ over mid-oceanic regions of the Atlantic and Pacific Oceans. According to his model, the ITCZ system forms a vertical circulation cell with rising motion taking place in the central convergence zone and compensatory descending motion in the vicinity on both sides of the ascending core, resulting in warming and drying of the air. Kumar and Sethumadhavan (1980) presented results of their study of the ITCZ structure from data gathered during MONEX-79. They observed that ITCZ had a cold core structure in the lower levels. An important finding from their study is that there is the absence of any significant warming in the higher levels

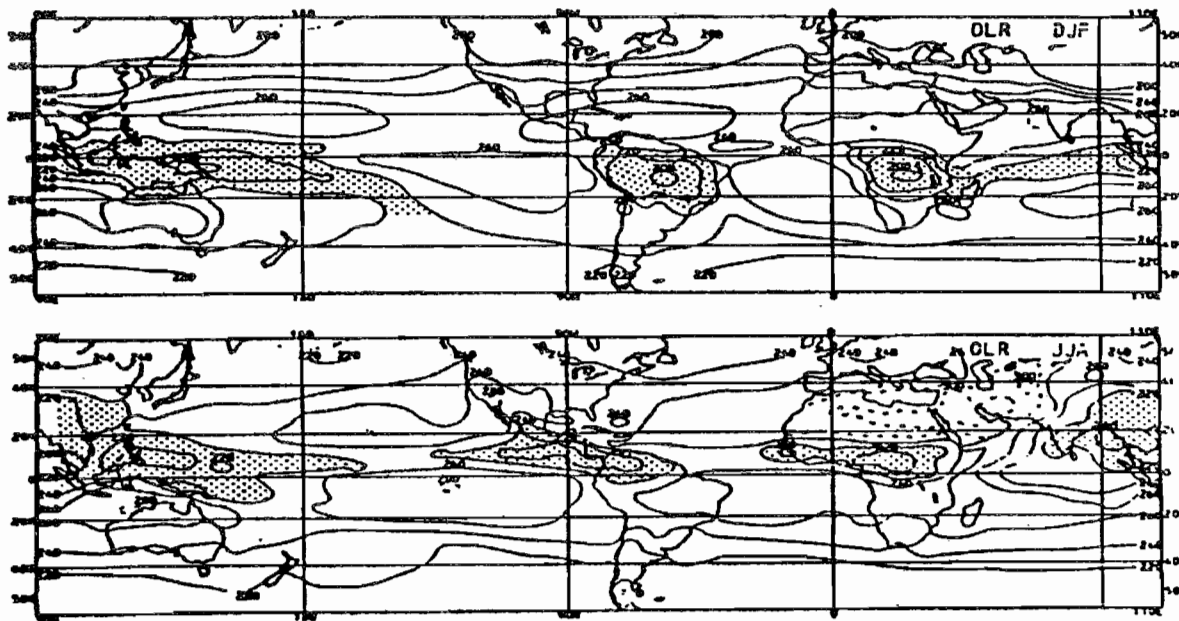


Figure 5.1 — Mean OLR for December–February (upper) and June–August (lower). Areas where OLR is less than  $240 \text{ W/m}^2$  are stippled. Contour interval:  $20 \text{ W/m}^2$  (After Rasmusson, 1990).

over the region of ITCZ. Similar results were noted in respect of the temperature field by Estoque and Douglas (1978) over the GATE ITCZ. This is rather intriguing in view of the fact that heavy convection is taking place in the ITCZ cloud zone, which should result in warming of the middle and upper troposphere. This suggests that the conditional instability of the second kind (CISK), being a primary mechanism for the maintenance of ITCZ, is ruled out.

In the wind field an important observation is the presence of a low-level jet in the vicinity of the ITCZ. Snitkovsky (1973) found such a jet with a wind speed of  $25 \text{ m s}^{-1}$  along  $150^\circ\text{W}$ . A similar jet was also found in the study by Kumar and Sethumadhavan (1980) over the Indian Ocean area based on analysis of MONEX-79 data, where the maximum winds were located between 400 and 800 km south of the surface position of ITCZ and in the 950–750 hPa layer. Katz (1972) analysed the wind field over the Indian Ocean. His results suggest convergence below six kilometres over the ITCZ with a compensating field of divergence aloft.

Very few observations are available at present to determine the moisture balance in the equatorial zone. There is evidence to suggest that within the ITCZ, precipitation greatly exceeds evaporation from the ocean surface. It is believed that much of the upward transfer of moisture is achieved by convergence within the trade winds from both hemispheres. This results in heavy convective cloudiness. Recent observations, particularly satellite photographs, have shown that ITCZ is a narrow zonal band of vigorous cumulus convection. ITCZ is usually composed of a number of distinct cloud clusters, with scales in the order of a few hundred kilometres, which are separated by regions of clear sky. The latent heat released by precipitation is an important driving mechanism for this process.

The cloud clusters observed along the ITCZ are the manifestations of precipitation zones associated with weak wave disturbances which propagate westward along the ITCZ. The time-longitude sections of daily satellite pictures constructed by Chang (1970) and presented in Figure 5.2, show these waves very clearly. Well defined bands of cloudiness are seen to slope from right to left down the page. This slope of the cloud lines implies a westward propagation speed of about  $8\text{--}10 \text{ m s}^{-1}$ . The longitudinal separation of the cloud bands is about  $3000\text{--}4000 \text{ km}$ , corresponding to a period range of about 4.5 days for this type of disturbance. Snitkovsky (1973) also found wave disturbances embedded in the ITCZ, while Kruzhkova and Kryzhanovskaya (1971) found preferred zones on the ITCZ which favoured cyclogenesis. Over parts of west Africa and the eastern Pacific, cyclogenesis was favoured in all seasons. In January, on the other hand, the favoured regions were to the south of India and the southern Pacific, while in July, the North Pacific Ocean was more favourable for cyclogenesis.

Charney (1970) proposed that the ITCZ represents a balance between vertical motion generated by convergence within the planetary boundary layer and the availability of moisture. He showed that a tropical atmosphere was unstable for a disturbance running parallel to the Equator. The growth rate of such a disturbance reached a maximum at about  $10^\circ$  latitude away from the Equator, but vanished directly above the Equator. Charney's work thus explains why cloud maxima are observed some distance away from the Equator, while the Equator remains free of clouds. Manabe, *et al.* (1974) and Pike (1971) were able to demonstrate by modelling experiments that the location of the ITCZ was mainly determined by the distribution of sea-surface temperature. While theoretical work on the mechanics of the ITCZ is in progress, recent observations have tended to emphasize the importance of sea-surface temperature in tropical circulations.

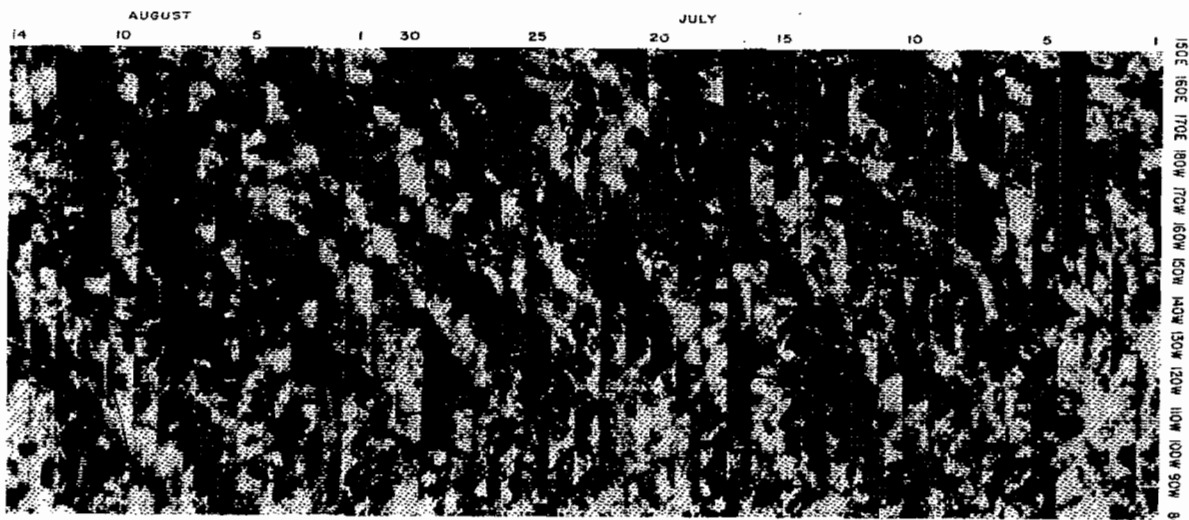


Figure 5.2 — Time-longitude sections of satellite photographs for the period 1 July–14 August 1967 in the 5–10°N latitude band of the Pacific. The westward progression of the cloud clusters is indicated by the bands of cloudiness sloping down the page from right to left (After Chang, 1970, as presented in Holton, 1979).

### **5.2.2      *The monsoon circulation***

Monsoons are a system of seasonal winds which affect many parts of Asia, Africa, Indonesia and northern Australia. The name derives from the Arabic root word 'Mausam' which simply means season, but in meteorological terms it has come to mean the seasonal reversal of winds (Rao, 1976). The name was first used to describe the system of winds over the Arabian Sea where the winds blew for six months from the north-east, and for the remaining six months from a south-westerly direction.

The monsoon winds are most pronounced in the summer season in either hemisphere, that is, during the months of July and August in the northern hemisphere and during January and February in the southern hemisphere. During July, the trade winds from the southern hemisphere move into the northern hemisphere towards India, south-east Asia and parts of eastern Africa. The Asian summer monsoon may be considered to be an extension of the southern trades of the southern hemisphere which, on crossing the Equator, are deflected by the Earth's rotation and, as a consequence, approach the land mass from a south-westerly direction. In January, the north-east trades move southwards towards eastern Africa and north-east Australia. This is known as the winter or north-east monsoon. In India, the period from October to December is also known as the north-east monsoon, as the prevailing winds over the Indian peninsular region and adjoining seas are northeasterlies.

In broad terms, the principal monsoon regions comprise those areas of the Earth which come under the influence of large-scale air movements from a colder to a warmer hemisphere.

To make the definition more objective, Ramage (1971), extending the earlier work of Khromov (1957), added the following criteria for monsoon regions:

- (a) The prevailing wind direction should shift by at least 120 degrees between January and July;
  - (b) The average frequency of prevailing wind directions in January and July should exceed 40 per cent;
  - (c) The mean resultant winds in at least one of the months should exceed  $3 \text{ m s}^{-1}$ ;
  - (d) There should be fewer than one cyclone-anticyclone alteration every two years in either month in a five degree latitude/longitude grid.

The last definition was added to ensure that the seasonal changes in wind direction reflect the replacement of a persistent circulation system by a reverse and equally persistent system. This change should not be merely indicative of a change in the track of moving circulations.

While a precise definition, if at all possible, is a matter of choice, it should be noted that, according to Ramage's definition, the deserts of the Sahara would be monsoonal, even though the rainfall there is quite different from, say, north-east India within the same monsoon region. The former hardly receives rain, while the latter has the heaviest monsoon rain in the world.

Large-scale differential heating between land and ocean is a primary force of the monsoon. This pattern of differential heating results in a much greater annual variation of temperature over land areas compared with the adjoining seas where these are contiguously placed. This causes an excess of pressure over the continents in winter and a deficit in summer. The end result is a marked seasonal shift in the system of winds which constitute the monsoon. The most conspicuous example of this seasonal wind system is the Indian Ocean area, which is land-locked to its north by the vast Asian continent. Such a phenomenon is not observed in the Pacific and Atlantic Oceans, which are open to their north. The differential heating between the land and the ocean causes the pressure and potential temperature surfaces to intersect. Available potential energy thus becomes available for conversion into kinetic energy (Das, 1986). The conversion of available potential energy to kinetic energy is achieved through overturnings of the atmosphere in the x-p plane (Walker circulation) and the y-p plane (Hadley circulation), which dominate the monsoon circulation. As the sun begins to move into

the summer hemisphere, the deviation of isobaric surfaces and potential temperature surfaces begin to increase until a state is reached when available potential energy generated by differential heating is balanced by the conversion to kinetic energy of monsoon winds.

The north-south migration of the monsoon system is controlled by the evolution of the differential heating. Normally a net heating over Indonesia and the equatorial western Pacific Ocean, and a net cooling over northern China and Siberia constitute this differential heating during the winter months. During the northern summer months, on the other hand, an axis of net heating extends near 20°N from the northern Bay of Bengal to the Indochina peninsula. The net cooling is along 30°S, which extends from the Mascarene Islands to western Australia (Johnson, *et al.*, 1987). A principal axis of the annual cycle of the monsoon may be defined following the region of maximum monthly mean rainfall. According to Krishnamurti (1985), this rainbelt migrates from Indonesia to the foothills of the Himalayas between January and August and makes its return between September and December. This axis exhibits considerable inter-annual variability in its position and intensity. During the years of the *El Niño* phenomenon, an eastward and equatorward shift of the net heating region is a major part of the inter-annual variability.

The main elements of the large-scale circulations for the winter and summer monsoons are shown in Figure 5.3. There are basic similarities in the winter and summer monsoon systems. The winter monsoon is dominated by a strong surface anticyclone over Siberia and northern China. The southward movement of cold air mass takes place from this anticyclone in the form of a broad anticyclonic sweep which moves across the China-Pacific-South-East Asia region as a north-east monsoon. The air current converges into the equatorial trough in the south Indian Ocean. The southward-moving colder air is balanced by northward-moving warmer air in the upper troposphere. The upper tropospheric air moving northward is deflected to the right (eastward) by Coriolis force to become the subtropical westerly jet stream over Asia and Japan. This is the broad structure of the north-east monsoon of the northern winter. The Siberian high of the winter monsoon system has its counterpart in the Mascarene high of the summer monsoon, which is located in the southern Indian Ocean. The air mass originating from the Mascarene high moves initially as south-easterly trade winds in the southern hemisphere, which, on crossing the Equator, turn south-west and converge into the monsoon trough present over the Asia-Pacific region. The upper tropospheric air mass moves south in this case and gets deflected to the right (westward) to become the tropical easterly jet stream. Thus the Siberian high of the winter component has somewhat of an analogous role to that of the Mascarene high of the summer monsoon. The cross-equatorial flow and the low-level jet of the northern summer flows are analogous to the low-level north-east monsoon flow and the strong winter surges, known as cold surges, along the eastern coast of Asia. The monsoon troughs are regions of heavy rains in both the systems. A warm troposphere extends vertically above the monsoon trough in both systems. In the upper troposphere the Tibetan high pressure cell of the summer monsoon has its counterpart in the western Pacific upper anticyclone of the winter monsoon. The upper tropospheric monsoon circulation includes two jet streams, the tropical easterly jet stream on the southern flank of the Tibetan high near 10°N and 150 hPa during the summer, and the subtropical westerly jet on the northern flank of the western Pacific anticyclone near 30°N and 200 hPa during the winter.

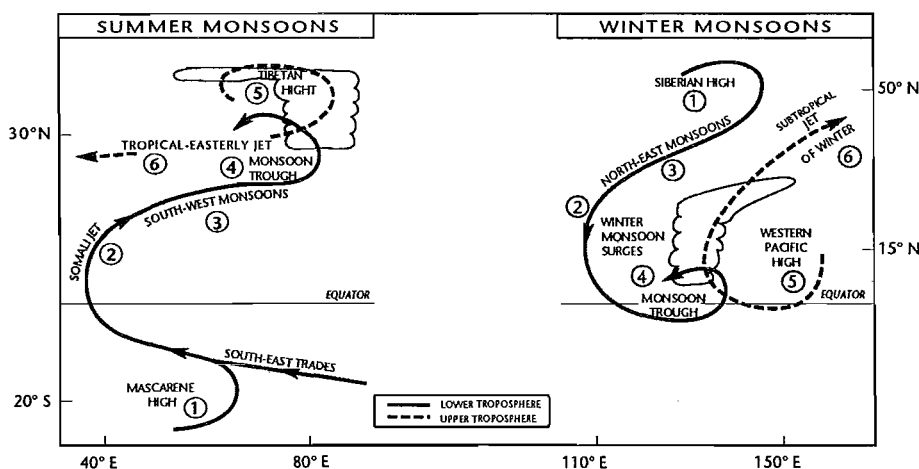


Figure 5.3 — Elements of the summer and the winter monsoon systems (After Krishnamurti, 1990).

The winter monsoon of the northern hemisphere has its extension into the southern hemisphere, which is observed as the summer monsoon of Australia and often referred to as the Australian north-west monsoon (Das, 1986; McBride, 1984). The Australian north-west monsoon bears many similarities to the summer monsoon of the northern hemisphere. It is characterized by a monsoonal equatorial trough in the lower troposphere and accompanying low-latitude westerly winds. Overlying this trough, there is a 200 hPa anticyclonic system similar to the summer monsoon of the northern hemisphere. The tropical parts of northern Australia receive a substantial part of their rainfall in the six-month period between November and April.

Another regional component of the global monsoon circulation is the west African monsoon. In July, a counter-clockwise circulation associated with an anticyclone to the south of the Equator generates a maritime south-easterly wind which, on crossing the Equator, approaches the western part of Africa as a broad south-westerly current. This is the summer monsoon.

On the other hand, along the low lands of western Africa, air from the northern anticyclone over Siberia brings in north-eastern trades which are usually dry and have a high dust load. This is known as Harmattan. A characteristic feature of the Harmattan is the high frequency of dust haze with low precipitation.

### 5.2.3 *Energetics of the tropical motion systems*

It is a well known fact that, outside the tropics, the primary energy source for synoptic disturbances is the available zonal potential energy associated with the strong latitudinal temperature gradients. The development of synoptic disturbances takes place through the conversion of potential energy into kinetic energy. In the tropics, by contrast, since the temperature gradients are very weak, the storage of available potential energy is very small. Therefore, in the tropics, particularly in the equatorial latitudes, latent heat release appears to be the primary energy source for the generation and growth of tropical synoptic disturbances. Observations indicate that most of this latent heat release in the tropics occurs in the convective cloud systems rather than during the large-scale forced ascent. This energy is then transferred to synoptic scales through strong interaction between the cumulus scale convection and large-scale circulations, in which the cumulus scale circulations are embedded. The large-scale motion provides moisture for the convection and the cumulus cells act to provide a large-scale heat source. Because of the special nature of this driving force, as well as the smallness of the Coriolis parameter, large-scale equatorial motion systems have certain distinctive characteristic features which are quite different from those of mid-latitude systems (Holton, 1979). Whereas the middle latitudes are dominated by a westerly current increasing with height (baroclinic environment), the tropics have largely a barotropic environment. Holton (1979) has shown from scaling considerations that, in the absence of condensation heating, tropical motions in which the vertical scale is comparable to the scale height of the atmosphere must be barotropic. Such disturbances cannot convert potential energy into kinetic energy.

The mechanism for the development of the tropical disturbances can be examined with the help of thermodynamic equations. According to Holton the approximate thermodynamic energy equation for a pseudo-adiabatic process is given by:

$$w \frac{\partial \ln \theta / \partial z}{\partial} = - (L_c / C_p T) \cdot (dq_s / dt)$$

where  $w$  is the vertical velocity,  $\theta$  the potential temperature,  $L_c$  the latent heat of condensation,  $C_p$  the specific heat at constant pressure,  $T$  the absolute temperature, and  $q_s$  the saturation value of specific humidity. The above equation requires that the vertical motion be proportional to the diabatic heating. The maximum large-scale vertical velocities, therefore, occur in the convection zones. By continuity, this implies a low-level convergence and upper-level divergence in the convection zones. Given that the absolute vorticity is positive (negative) in the northern (southern) hemisphere disturbances, the cyclonic vorticity is generated in the lower levels and the anticyclonic vorticity in the upper levels in accordance with the divergence term of the simplified vorticity equation:

$$\frac{\partial \zeta}{\partial t} = - V \cdot \nabla \zeta - \beta v - (\zeta + f) V \cdot V$$

The mass velocity adjustment process will then tend to generate a low pressure trough in the lower levels and a high pressure ridge in the higher levels.

### 5.2.4 *Origin of tropical disturbances*

Some tropical disturbances may have their origin as mid-latitude baroclinic waves, which move equatorward and gradually assume tropical characteristics. However, most of the tropical disturbances originate within the tropics. Baroclinic instability, which is the main development mechanism in extratropical developments, cannot account for the tropical disturbances' formation in general because of the source of available potential energy being very weak, except in some selected regions, such as north Africa and the Indian subcontinent.

There are two possible mechanisms which have found acceptance in the initiation of tropical disturbances:

- (a) Barotropic instability of the mean flow arising due to lateral shear;
- (b) Conditional instability of the second kind (CISK) associated with organized convection driven by moisture convergence in the boundary layer.

Combined barotropic-baroclinic instability is also found to operate in some particular regions where the flow is characterized by both lateral and vertical shears.

#### 5.2.4.1 **BAROTROPIC INSTABILITY**

According to the scale analysis of tropical motion systems, in the absence of condensation the vertical motions must be small in the tropics. A first approximation of the flow is governed by the barotropic vorticity equation:

$$d(\zeta + f) / dt = 0$$

Through a linearized perturbation analysis of the above equation, where an assumption is made that the flow consists of a small barotropic perturbation superimposed on a zonal current which depends only on latitude, Holton has shown that a necessary condition for barotropic instability is that the gradient of absolute vorticity of the mean current must vanish somewhere in the region, that is,

$$\beta - d^2 \bar{U} / dy^2 = 0$$

where  $\bar{U}$  is the mean flow depending only on latitude.

Thus the mechanism for barotropic instability operates in regions characterized by strong lateral shears in the flow. Examples of two such prominent areas are the African mid-tropospheric jet (650–700 hPa) and the low-level jet (850 hPa) over the Arabian Sea during the south-west monsoon season. The development of African waves is considered to be due, primarily, to the barotropic instability associated with the middle-level jet. Although barotropic instability provides a satisfactory mechanism for the generation of African waves, and may also play a role in other parts of the tropics, it is to be noted that barotropically unstable disturbances can be maintained only if the shear of the mean zonal flow remains unstable so that the waves can extract energy from the mean flow. The barotropic instability is peculiar to the development processes in the tropics only. The mechanism operates in the mid-latitude jet streams also, although in the middle latitudes, baroclinic instability plays a more important role.

#### 5.2.4.2 CONDITIONAL INSTABILITY OF THE SECOND KIND (CISK)

As already mentioned earlier, the release of latent heat of condensation in cumulus convection is the primary energy source for the maintenance of finite-amplitude equatorial wave disturbances. This could be released in a conditionally-unstable saturated atmosphere with a super moist-adiabatic lapse rate ( $\partial\theta_e/\partial z < 0$ , where  $\theta_e$  is the equivalent potential temperature of a saturated atmosphere). However, numerous theoretical studies have shown that conditional instability produces maximum growth rates for motions on the scales of individual cumulus clouds. Therefore, ordinary conditional instability cannot explain the synoptic scale developments. Moreover, the mean tropical atmosphere is not saturated even in the planetary boundary layer. A parcel has to undergo a considerable degree of forced ascent before it becomes positively buoyant. For the forced ascent to occur in an organized manner, low-level convergence is a must. The cumulus convection and the large-scale motion have therefore to interact and support each other. The cumulus supplies the heat necessary to drive the large-scale disturbance, and the large-scale disturbance produces the moisture convergence necessary to develop the cumulus convection. This process of interaction between the cumulus convection and a large-scale perturbation, if it leads to unstable growth of the large scale, is known as the conditional instability of the second kind (CISK).

### 5.3 Observational database for tropical analysis and forecasting

The observational data requirements for weather analyses, forecasts and warnings by manual and automated procedures are met by the WWW Global Observing System (GOS). The GOS is a composite system consisting of the surface-based sub-system — which includes the regional basic synoptic network of surface and upper-air stations, other observational networks of stations on land and sea, and aircraft meteorological observations — and the satellite sub-system, which includes near-polar-orbiting and geostationary meteorological satellites. At present, there are about 10 000 land stations, 7 000 ships and buoys at sea and 3 000 aircraft. In the space-based sub-system there are at least four polar orbiting and five geostationary satellites. The total volume of data generated by all these systems amounts to approximately eight million alphanumeric characters daily. This observational data volumes are expected to reach 20 million characters per day by the end of the century (WMO, 1987a). The GOS in the tropics, however, suffers from serious deficiencies. While there are natural deficiencies due to large parts of the tropics covered with oceans, there are some areas where the level of implementation of the observing network is rather poor. The overall level of implementation for the surface and upper-air observational programme is about 89 per cent for surface observations and 82 per cent for upper-air observations, while for Africa, the level of implementation is 77 per cent for surface observations and only 48 per cent for upper-air observations. In addition, there are major gaps in the regular supply of conventional upper-air observations in many parts of the world, particularly in Africa and Latin America. In some cases observations are not available to the global system because of local communication problems.

The present day database consists of a wide variety of data coming from the conventional and nonconventional sources. Radiosondes/rawinsondes are the only conventional data sources which give us a detailed and reliable three-dimensional structure of the atmosphere. The continents in the northern hemisphere are well covered and the reception is generally good. However, within the tropics the coverage is poor with the exceptions of Central America, the Caribbean, India and Australia. Most of Africa and South America and practically the entire oceanic areas are very sparse. Though the satellite temperature sounding data (SATEMs) are available to us in plenty and provide a good coverage of mass observational data over the tropical oceans, their utility in the tropics is found to be of limited value because of the quality of SATEMs being too low (Heckley, 1990).

The observational data that are usually made available for manual and automated analyses are:

- (a) Surface observations from land stations (SYNOP) and sea stations (SHIP);
- (b) Drifting buoys (BUOY);
- (c) Radiosonde/rawinsonde (TEMP/TEMP SHIP);
- (d) Wind sounding data from PILOT/PILOT SHIP balloons;
- (e) Satellite cloud motion vectors (SATOB);
- (f) Aircraft reports (AIREP, CODAR, ASDAR). The SYNOP and TEMP network is less dense in the tropics than in the northern hemisphere extratropics. The situation is worse in the southern hemisphere. AIREPs are very few over most of the tropical belt. There is a fairly good coverage of SATOBs, but unfortunately they suffer from the inherent deficiency that these are available for only two levels at the most. SATOBs, however, continue to be an important data source for tropical analysis.

Apart from these quantitative observations, a qualitative observation which is particularly useful in the tropical analysis is the satellite imagery. The cloud patterns observed in the satellite imagery are an extremely useful aid in identifying the nature of tropical disturbances forming in the data-sparse oceanic regions. As in most occasions, the conventional and even non-conventional data are completely absent in such areas, and satellite imageries often provide the first clue about development of tropical disturbances, such as tropical cyclones. The tropical analysts have also to make use of bogus and pseudo observations, which are manufactured in some special situations to capture the disturbances in the initial analysis in automated data assimilation systems for NWP forecasts. With the current scientific and technological advances new remote-sensing techniques are emerging which will greatly enhance the level of GOS during the next decade, particularly in the tropical context. Satellites are expected to provide data at 50 km resolution. Scatterometer wind estimates will provide surface wind data over the oceans with a horizontal resolution of 100 kms (Anderson, *et al.*, 1987). This will be a good data source over the oceans. The new observing systems include a network of automated weather stations, wind profilers, Doppler radar, automated aircraft reporting system, automated shipboard aerological programme (ASAP), etc. in order to increase the spatial and time resolution of the composite observing system. Automatic stations will be provided with microprocessors for quality control of data and formatting. Surface-based remote-sensing techniques will be introduced into the GOS. These will include more advanced radar systems and associated techniques including Doppler and horizontal polarization radars, vertical profiling radars, and sodars. A number of ships will be equipped with highly automated upper-air sounding facilities (ASAP). Simple drifting buoys, deployed outside the main shipping routes will supply important sea-level parameters from the data void surface areas of the oceans. Upper-air temperature and wind data at cruising levels will be supplied by the ASDAR system. Satellites will carry new sensing equipment such as radar altimeters, microwave scatterometers, synoptic aperture radar, etc.

### 5.3.1 *Some special problems of tropical analyses vis-a-vis observational data*

An inherent difficulty in the tropics arises due to the nature of tropical flow variability, poor mass-wind balance relationships and small temperature perturbations. The climatological variance of the flow in the tropics is much smaller than in mid-latitudes. The tropical flow is characterized by very large scales of motion of 30–40 day periods. There also exist small-scale transient disturbances with periods of three to seven days embedded with the large-scale systems. The low climatological variance of the tropical flow implies that the observational errors which might be considered small in the extratropics are large in the tropics in relation to the climatological variability (Heckley, 1990). This poses problems for quality control procedures in the NWP data assimilation systems. Added to this, the short-range forecasts in the tropics, which are used as first guess in objective analysis and are used for controlling the bad observations, compound the problem. The main reason for poor short-range forecasts and hence poor first guess in the tropics is the fact that diabatic forcings are a predominant factor in tropical modelling. These processes are not yet well understood.

Systematic biases in some types of observations, for example in the satellite derived fields, also pose special problems in tropical analysis. It has been demonstrated that the SATOBs are biased towards slow wind speeds (Heckley, 1990). This is attributed to the fact that the clouds are not simply advected by the environmental flow at the cloud level, as pointed out by Kallberg (1985). SATOBs, being in large amounts in the tropics, have a predominating influence on the analysis which tends to be biased towards them. This ultimately affects the model forecasts which may retain this bias towards low wind speeds. In addition, the model may have its own bias (given an unbiased initial state) towards low wind speeds (model climate drift). This phenomenon creates problems of quality control of observation minus first guess' residuals which are used for analysis. The SATOBs would appear to be more accurate to the first guess than the TEMP and AIREPs, which are in reality more accurate.

Another serious problem is that of humidity observations in the tropics, which are too inadequate to match the spatial variations in the humidity field. The humidity analysis is all too important in the tropics as the diabatic processes in tropical models are very sensitive to the initial humidity field. The importance of diabatic processes in tropical modelling has been stressed earlier. The humidity observations play a crucial role for an accurate prediction of tropical disturbances. As against this the humidity observations are less important in the extratropics where the dynamical forcings are dominating. Bengtsson (1985) cites an interesting example in this context where the ECMWF model ran operationally for a period of several months in 1980 with a programming error such that the humidity observations were not used. This was not noticed since the model was able to generate its own humidity field and produce realistic precipitation forecasts.

The unrepresentativeness of the observations is another source of error. This arises due to the analysis and forecast systems' inability to represent certain real atmospheric phenomena. These may be either due to deficiencies in model formulation or model resolution. For example, a radiosonde measurement may be quite accurate. The observation may, however, contain those scales of atmospheric motion that a forecast model or a human analyst is unable to resolve. Thus the observation, though highly accurate, may be unrepresentative. The error assigned to each observation (observational error) must take this into account. This aspect is important for defining the error ratios for optimum interpolation analysis. Such error assignments are based largely on experience, assimilation studies, and to some extent, on guesswork.

### 5.4 Tropical wave disturbances

Several types of wave disturbances have been discovered in the tropics from time to time. A general understanding of the character of these disturbances is required in the context of short-, medium- and long-range forecasting. Wave disturbances were first recognized during the 1940s soon after upper-air observations became

available from the tropical oceans. A systematic study of tropical disturbances began in the 1960s with the implementation of upper-air sounding network in the western and central Pacific. The launch of polar orbiting and geostationary satellites in the 1960s contributed to the understanding of tropical circulation systems in a small measure. Our understanding of the structure and evolution of synoptic scale features was greatly enhanced following the launch of the first geosynchronous satellite on 6 December 1966. Geosynchronous satellite data, together with outgoing long-wave radiation (OLR) data, provided a comprehensive picture of the synoptic cloud clusters. Carlson (1969a, b) made the first detailed study of African waves propagating westward across west Africa and the tropical Atlantic Ocean. The GARP Atlantic Tropical Experiment (GATE), conducted in 1974, provided a useful wealth of observations for the study of those disturbances.

In his review of early synoptic investigations of tropical disturbances, Riehl (1954) described two types of westward propagating waves. One in the lower troposphere with a wavelength of 1 500–2 000 km and the other in the upper troposphere with a wavelength of 3 000–5 000 km. Both have phase speeds of around 6° of longitude per day, which means a frequency of three to four days for the low-level waves and about seven days for the upper-level waves. Riehl placed major emphasis on the low-level waves, which he believed to be largely responsible for the day-to-day weather changes over extensive regions of the tropical oceans. Because these take the form of undulations in a prevailing easterly current, he referred to them as waves in the easterlies, or easterly waves. He observed that in a typical easterly wave, an interval of disturbed weather, marked by enhanced shower activity, cool surface and lower tropospheric temperatures, sets in with the passage of the wave trough and lasts about a day, coinciding with a period of southerly winds (northern hemisphere) and rising barometric pressure. Because of the hydrostatic effect of cool temperatures to the east of the wave troughs, Riehl argued that the wave axes must tilt eastward with height in the lower troposphere, in agreement with observations.

Easterly waves were first observed in the Caribbean area between 15° and 20° N (Riehl, 1945). In Riehl's analyses the waves are depicted with maximum intensity in the equatorial trough zone, between 5° and 10°N. They do not usually extend across the Equator or in the subtropics. The waves are believed to amplify as they move westward. In an independent study of the Pacific disturbances, Palmer (1952) postulated a wave model, based on observations made in the Marshall Island area of the central Pacific during the late 1940s when atomic weapons were being tested in that region. His model was basically similar to the easterly wave except for the fact that it places maximum wave amplitude on the Equator. Hence it has become known as equatorial wave model. Palmer's equatorial wave model has a typical wavelength of 15° longitude and an average westward propagation speed of 10 to 15 knots. These waves were felt to be characteristic of the central Pacific Ocean between longitudes of 160° E and 150° W.

The early wave model studies obviously suffered from many limitations due to:

- (a) Sparseness of data — spacing between stations too large to resolve the waves;
- (b) Grouping of stations limited in longitudinal extent to reveal any long-wave disturbances which might be present;
- (c) Inadequate theoretical framework to explain the observed behaviour of the disturbances;
- (d) Case study approach to synoptic analysis being too time consuming to allow extensive surveys of wave activity necessary to produce meaningful statistics on the contribution of waves to the general circulation.

These difficulties were overcome to a large extent with the availability of satellite imageries, theoretical studies, and special observational programmes, like Line Island experiments, etc. Power spectrum analysis was adopted as an alternative to the case study approach in processing sparse tropical data, which proved to be a very powerful tool and helped in the identification of several types of waves in the troposphere and stratosphere. Various studies on the spectrum and cross spectrum analysis of station time series data in the tropical Pacific were carried out. A review of the findings of these studies is contained in Wallace (1971). The prominent features which emerged from these investigations are as follows:

- (a) The lower tropospheric meridional wind component shows a recurrent tendency for spectral peaks in the four- to five-day range. This is in close agreement with the synoptic evidence of the existence of such waves in Riehl's study;
- (b) There is some support for Riehl's finding that the upper tropospheric waves have a predominant period of about a week;
- (c) There is a large amount of kinetic energy associated with disturbances of periods >>10 days. This is particularly true of zonal component.

The chief characteristics of the tropical wave disturbances as brought out by the power spectrum analysis in the Pacific region are described in the following subsections and are based on Wallace (1969), Wallace (1971) and Holton (1979).

#### 5.4.1 *Major characteristics of tropical wave disturbances*

##### 5.4.1.1 FOUR- TO FIVE-DAY LARGE-SCALE (SYNOPTIC) WAVES IN THE LOWER AND MIDDLE TROPOSPHERE

The distinguishing features of these waves are:

- (a) The meridional component of wind in the lower troposphere has a tendency for spectral peaks in the four- to five-day range, and is most prominent at the equatorial stations;
- (b) Maximum amplitude in the meridional component  $v$  and vertical velocity  $w$  occurs at 5–10° latitude, which corresponds to the position of the ITCZ;
- (c) These waves propagate westward, with a speed slightly in excess of the mean easterly flow;

- (d) They have a longitudinal wavelength in the order of 3 000 km indicating a phase propagation of  $8 \text{ m s}^{-1}$ ;
- (e) These waves are confined to the lower and middle troposphere.

At times when these waves are active they produce fluctuations in the relative humidity field with peak values occurring just to the east or near the trough line in the streamline field. Thus in many respects these disturbances resemble the classical model of an easterly wave.

The existence of wave disturbances with wavelength of 3 000–4 000 km, propagation speed of  $8\text{--}10 \text{ m s}^{-1}$  and period range of 4.5 days in the ITCZ were also later discovered by Chang (1970) through an analysis of the time-longitude sections of daily satellite pictures (see section 5.2.1).

Some evidence of the existence of four- to five-day waves in the larger wavelengths of 8 000 to 10 000 km has been suggested by Yanai and Murakami (1970). They proposed that when those stations that lie within a few degrees of the Equator are considered separately, the computed wavelength of the four- to five-day disturbances in the lower troposphere is in the order of 8 000–10 000 km. This led them to suggest that these might be the low-level reflections of the mixed Rossby-gravity modes of the upper troposphere, which are discussed later.

#### 5.4.1.2 FOUR- TO FIVE-DAY PLANETARY-SCALE WAVES IN SURFACE PRESSURE

Within the four- to five-day frequency band there is also evidence of a planetary-scale oscillation in the surface pressure with amplitude in the order of 1 hPa at the Equator (Wallace and Chang, 1969; Brier and Simpson, 1969). This oscillation in surface pressure is obviously related to the westward propagating waves whose principal component has a horizontal scale of zonal wave number 1. This implies a phase speed of  $100 \text{ m s}^{-1}$ . The amplitude appears to increase slowly with latitude. Wallace and Chang suggested that they might be the tropical manifestations of the retrograde planetary waves of the middle latitudes. Their possible relation to fluctuations in wind and precipitation has not yet been explored (Wallace, 1971).

#### 5.4.1.3 PLANETARY-SCALE EQUATORIAL WAVES IN THE UPPER TROPOSPHERE AND LOWER STRATOSPHERE

##### 5.4.1.3.1 MIXED ROSSBY-GRAVITY WAVES

Fluctuations in the meridional wind component with four- to five-day periods and zonal wavelengths of the order of 10 000 km at the stratospheric levels were first noted by Yanai and Maruyama (1966). Subsequently they also discovered fluctuations in the zonal wind component and temperature. A detailed analysis of these waves led Maruyama (1967) to suggest that these waves may be the mixed Rossby-gravity waves, so called because these types of waves behave as a gravity wave at low zonal wave numbers and as a quasi-geostrophic Rossby at high zonal wave numbers. These waves are also referred to as Yanai waves or Yanai and Maruyama waves. The main features of these waves are summarized below:

- (a) Horizontal wavelengths are in the order of 10 000 km (zonal wave number 4) in the lower stratosphere and vertical wavelengths are in the order of six km. The waves have periods of four- to five-days;
- (b) Horizontal distribution is described by mixed Rossby-gravity mode, as shown in Figure 5.4. The oscillation in  $v$  has maximum amplitude at the Equator, while those in  $w$ ,  $T$  and  $\Phi$  have maximum amplitude near  $5\text{--}10^\circ$  latitude and vanish at the Equator;

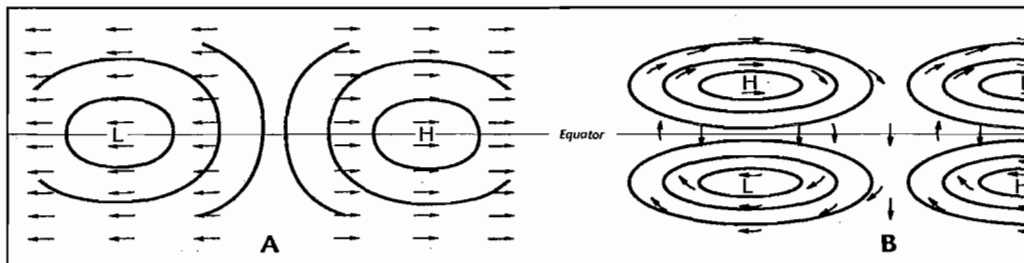


Figure 5.4 — Velocity and pressure distribution in the horizontal plane for (a) Kelvin waves; and (b) mixed Rossby-gravity waves (Adapted from Holton, 1979).

- (c) The amplitude of the zonal meridional wind component fluctuations is in the order of  $2\text{--}3 \text{ m s}^{-1}$ . Propagation is westward in the horizontal at a rate of about  $20 \text{ m s}^{-1}$  (Holton, 1979);
- (d) There is a strong vertical phase propagation upward in the lower troposphere and downward at the tropopause level and above. A downward phase propagation implies that these waves carry wave energy upward and they are forced from below. Therefore these waves must have their origin in the troposphere. Unlike other types of disturbances, this wave extends to stratospheric levels where it causes a strong upward flux of easterly momentum and wave energy (Yanai and Hayashi, 1969);
- (e) The observed phase relationships between various parameters are such that the wind vector at any given point in the northern hemisphere rotates clockwise as the wave passes and the maximum temperature occurs at the time of maximum southerly wind. The reverse is true for a point in the southern hemisphere;
- (f) The waves have a distribution of pressure and zonal velocity which is antisymmetric about the Equator and has a distribution of meridional velocity which is symmetric. The waves appear to have significant amplitude only within about  $20^\circ$  of the Equator. This mode is most easily identified in the meridional wind component, since the oscillation in  $v$  has maximum amplitude at the Equator.

In a study of the equatorially-trapped\* waves at the 200 hPa level and their association with meridional wave energy flux and cloud activity with 1967 and 1972 data, Zangvil and Yanai (1981), and Lu and Yanai (1984) established a linkage between the upper tropospheric mixed Rossby-gravity waves and cloud activity in the ITCZ. Zangvil and Yanai found that the major cloud activity along the sea surface temperature maximum in the tropics seems to be modulated with the space and time scales of the mixed Rossby-gravity waves. From an analysis of the cross-spectral density between satellite cloud brightness data and 200 hPa divergence for westward moving waves at 5° N for the summers of 1967 and 1972, Lu and Yanai found that in 1967 there was a significant cross-spectral density between the brightness and divergence at a period of about five days and wave number 4 (corresponding to mixed Rossby-gravity mode), whereas in 1972 there was no such peak at these scales. The years 1967 and 1972 were two contrasting good monsoon and bad monsoon years, respectively. They went on to suggest that this phenomenon could be explained by the fact that cumulus convection responds to the upper tropospheric divergence associated with the mixed Rossby-gravity waves, and participates in the energy cycle of the wave through condensation heat.

Lu and Yanai (1984) also concluded that the lower stratospheric equatorially-trapped waves have roots in the upper troposphere and that the westward moving roots are associated with the meridional convergence of wave energy flux. The latter finding strongly suggests that these westward moving waves are excited by the pressure work due to middle-latitude disturbances, i.e. the lateral forcing. Earlier, in a similar finding Zangvil and Yanai (1980) also suggested that there is a pronounced equatorward flux of wave energy accompanying westward moving waves with zonal wave number 4 in the period range of five days.

#### 5.4.1.3.2 KELVIN WAVES

Soon after the discovery of four- to five-day oscillations, Wallace and Kousky (1968) noted a large 10- to 15-day period oscillation in the zonal wind. There was no evidence of any related fluctuation in the meridional wind component. This is called atmospheric Kelvin wave, so called because of its resemblance to the shallow water gravity wave which propagates along the coastal boundary and has no velocity component normal to the boundary. In the atmospheric case, the Equator plays the same role as the coast line (Lindzen and Holton, 1968). Holton (1979) suggested that the Kelvin waves have periods in the range of 12 to 20 days and appear to be primarily of zonal wave number 1 (that is, one wavelength spans 360° longitude). The following are some of the main characteristics of Kelvin waves:

- (a) Horizontal wavelength: 20 000 km (zonal wave number 1); vertical wavelength: six km; period: 12 to 20 days; phase propagation: eastward and downward. The corresponding phase speeds of these waves relative to the ground is in the range of 30 m s<sup>-1</sup>;
- (b) The amplitude of the fluctuation in zonal wind component is 8–12 m s<sup>-1</sup>; no fluctuation in meridional wind component;
- (c) The waves produce distinct temperature fluctuations. Warmest temperatures precede the maximum westerly winds by 1/4 cycle;
- (d) The Kelvin wave has a distribution of pressure and zonal velocity which is symmetric around the Equator;
- (e) The wave amplitude is large at the Equator and decays to about half the maximum value at 10° latitude. The waves have significant amplitude only within about 20° of the Equator.

In some of the later observational and modelling studies, the existence of equatorial waves (Kelvin and mixed Rossby-gravity modes) of larger periods was also pointed out. From a spectral analysis of FGGE III B data Maruyama (1982) found a predominant peak at the period of 36 days for an eastward moving wave in zonal wind component and geopotential at 200 hPa with frequency of wave number 1. The oscillations of the two parameters were nearly in phase with each other, which was indicative of the existence of a Kelvin wave. Parker (1973) found Kelvin waves in the layer near the tropopause by analysing upper-air data of some tropical stations. The period range was 25–45 days.

At present, it appears that both the Kelvin waves and mixed Rossby-gravity waves are excited by oscillations in the large-scale convective heating pattern in the equatorial troposphere. This aspect has also been examined through modelling studies. In a pioneering study, Lau and Peng (1987) proposed the excitement of equatorially-trapped waves over warm oceans where the cumulus convection, via the well known CISK mechanism, provides positive feedback. An equatorial heat source excites a Kelvin wave propagating to its east and a Rossby-gravity wave to its west. The propagating Kelvin wave has its maximum wave CISK heating along the Equator, whereas the mixed Rossby-gravity wave has its maximum heating near roughly 12° N. Over the equatorial Indian Ocean and the Pacific Ocean, warm sea surface temperatures contribute to the maintenance of Kelvin waves.

Although these waves do not contain much energy compared to typical tropospheric disturbances, they are the predominant disturbances of the equatorial stratosphere, and through their vertical energy and momentum transport, play a crucial role in the general circulation of the atmosphere (Holton, 1979).

---

\*The planetary scale waves are generally trapped (that is, they cannot propagate energy vertically) unless the frequency of the wave is greater than the Coriolis frequency. In middle latitudes the waves with periods in the range of several days are generally not able to propagate significantly into the stratosphere. However, as the Equator is approached, the Coriolis frequency allows these waves to become untrapped and propagate vertically (Holton, 1979).

#### 5.4.1.4 LOW FREQUENCY MODES OF THE TROPICAL TROPOSPHERE 30- TO 50-DAY OSCILLATION

Quasi-periodic variations in tropical winds and surface pressure with 40–50 days were first reported by Madden and Julian (1971, 1972) using a continuous ten-year record of daily radiosonde data at Canton Island. They found amplitudes in the order of  $5 \text{ m s}^{-1}$  in zonal wind and 0.7 hPa in surface pressure. The zonal wind exhibited out of phase fluctuations at 850 and 200 hPa, with a node in the 700 to 400 hPa layer. Positive surface pressure anomalies were accompanied by positive zonal wind anomalies at low levels and cool temperature anomalies throughout the depth of the troposphere. They recognized that the oscillation was a global scale phenomenon which influenced much of the tropical troposphere. Madden and Julian (1972) described the oscillation as a poleward and eastward propagating disturbance with a zonal wave number 1 structure which seemed to modulate the convection in the tropical Pacific. This disturbance is also referred to as the Madden Julian oscillation.

The 30–50 day oscillation has been extensively studied in the perspective of the Asian summer monsoon. The importance of this oscillation in this context was first emphasized by Yasunari (1981) who noted zonally-oriented cloud lines that propagated meridionally from the equatorial latitudes to the Himalayas. Krishnamurti and Subrahmanyam (1982) identified distinct motion systems on these time scales. At the 850 hPa surface, a train of zonally-oriented troughs and ridges were shown to exhibit, a near-steady meridional propagation. The meridional scale of this system is around 3 000 km and its meridional phase speed is roughly  $1^\circ$  latitude per day. The troughs were associated with rising motions and clouds while the ridges were essentially cloud free. The phenomena of onset, active and break monsoon appeared to be related to the passage of these low-frequency systems. The meridionally-moving troughs and ridges tend to form near the Equator, amplify as they arrive at around  $10^\circ\text{N}$  and finally appear to dissipate as they arrive near the Himalayas (Krishnamurti, 1990).

From a global perspective, Krishnamurti and Gadgil (1985), Krishnamurti, *et al.* (1985) and Lorenc (1984) have examined various aspects of the 30–50 day oscillations over the globe during the First GARP Global Experiment (FGGE) years. Krishnamurti and Gadgil found that the amplitude of the oscillations on the 30–50 day time scale were not only dominant over the region of the summer monsoon but also at higher latitudes near  $50^\circ\text{N}$  and  $50^\circ\text{S}$  near the 200 hPa level. The wind oscillation on the time scale of 30–50 days are prominent over the monsoon regions as well as over the middle latitudes. The per cent variance on this time scale (in relation to all other time scales) over the middle latitudes is quite small compared to the tropics. The tropical oscillations on this time scale seem to be strongly related to tropical convection.

A major observational finding on the 30–50 day time scale relevant to the monsoon are the divergent motions on the planetary scale. Using empirical orthogonal functions to represent the temporal behaviour of the divergent wind, Lorenc (1984) identified a planetary-scale wave (mostly zonal wave number 1) that propagates from west to east in roughly 30–50 days. He also noted that this wave can be identified nearly all year round. Krishnamurti, *et al.* (1985) further examined this phenomenon with the help of a 200 hPa velocity potential field and found that nearly the entire year the 30–50 day waves (with maximum amplitude around zonal wave number 1) propagate eastward with regularity. This oscillation has been hypothesized by Anderson (1984) to be a consequence of modulation of convection within the Hadley cell circulation. The 40–50 day period corresponds roughly to the time required for an air parcel to complete a circuit through the Hadley cell.

#### 5.4.1.5 WAVES ON THE INTER-ANNUAL TIME SCALE: QUASI-BIENNIAL OSCILLATION

An entirely new feature of tropical variability, the stratospheric quasi-biennial oscillation (QBO) was discovered in the early 1960s by Reed (1960). An explanation of the phenomenon was provided a few years later by Lindzen and Holton (Lindzen, 1968). The QBO also known as 26-month oscillation refers to the oscillations in the zonal wind regime of the equatorial stratosphere, where the easterly and westerly wind regimes alternate with a quasi-biennial periodicity.

The observed features of the QBO include:

- (a) Zonally symmetric easterly and westerly wind regimes alternate regularly with a period varying from about 24 to 30 months;
- (b) Successive regimes first appear above 30 km and propagate downward at a rate of one km per month;
- (c) The downward propagation occurs without loss of amplitude between 30 and 23 km, but there is a rapid attenuation below 23 km;
- (d) The oscillation is symmetric about the Equator with maximum amplitude of about  $20 \text{ m s}^{-1}$ , and a half width of about  $12^\circ$  latitude;
- (e) Amplitude decreases with increasing latitude and becomes very small around  $30^\circ$  latitude (Holton, 1979).

#### 5.4.2 Cold surges of Asian winter monsoon

During the northern hemisphere winter, the strong surface cooling and the formation of an intense anticyclone (the Siberian High) over the Asian continent, together with the warm ocean surface and active convection over the equatorial maritime continent (Ramage, 1971), set up an intense circulation system — the northern winter monsoon. In the lower troposphere, north-easterly flow from the Siberian High penetrates southward into the near-equatorial troughs leading to enhanced convection. In the upper troposphere, strong divergent outflow originates from the South China Sea (Krishnamurti, *et al.*, 1973). Part of the divergent flow subsides over a broad area over Asia with maximum convergence centered over northern China, and a part stretches along the

Equator in both directions to form the east-west circulation (Chang and Lau, 1980). Most of the heavy rainfall over the maritime continent are due to tropical depressions developing in the lower troposphere near-equatorial trough. The surface north-easterly flow has a very pronounced fluctuation, called the cold surge, that is generally associated with middle latitude synoptic systems. Following the passage of a cold front over China, the Siberian high pressure system intensifies and the divergent outflow brings a strong surface north-east flow southward and cooling can occur as far south as the Equator (Chang and Lau, 1980; Ramage, 1971).

Despite the fact that vigorous tropical storms are extremely rare over Malaysia, Indonesia and the South China Sea, considerable weather fluctuations do occur. The periods of dry spell can often last 10 to 20 days while 24-hour rainfall amounts of 20 to 50 centimeters associated with a tropical depression are not uncommon. During a dry spell, tropical depressions do not penetrate westward from central Pacific. Cold surges are generally weak and do not extend into the South China Sea. During the active monsoon period, the convective activity associated with a tropical depression is often enhanced greatly when there is also a strong cold surge from the north (Cheang and Krishnamurti, 1980).

While the cold surges are the most prominent phenomena during the winter monsoon and have received considerable attention, the moderation of the cold surges and the tropical convection between the dry spells and the active monsoon period also plays an important part in the monsoon circulation. The cold surges have been observed to exhibit fluctuations on the synoptic time scales at a three- to five-day range as also on a 10–20 day range. Pan (1984), through a power spectrum analysis of FGGE level III B data, inferred that the 10–20 day mode is the dominant mode in the low pass filtered 500–1 000 hPa thickness field. Pan observed that the slower changing mode of the cold surges is directly related to the lower tropospheric north-south thermal gradient between the Asian continent and the South China Sea. When the north-south thermal gradient in the lower troposphere over Siberia and northern China intensifies, increases in pressure gradient reach the South China Sea, low-level cold air penetrates south into central and southern China, subtropical jet stream intensifies, and upper tropospheric equatorial outflow increases, perhaps due to increases in tropical convective activity. While most of the changes occur almost simultaneously, the return flow of the local Hadley circulation from the tropics lags cooling by several days (Pan, 1984). When the lower tropospheric north-south thermal gradient slackens, the Siberian high pressure system weakens, and the subtropical jet stream intensity decreases. Tsay and Wang (1981) show that directly prior to and following a severe equatorward penetrating surge, the kinetic energy of zonal wave numbers 3 and 6 have large variations between 30 and 70°N. About two to three days prior to the surge, the kinetic energy of wave number 3 grows strongly in the 50–70°N latitude band. The wave number 6 kinetic energy grows very strongly between 30–50°N starting one to two days prior to the surge. Joung and Hitchman (1982) investigated the existence of longer mid-latitude wave propagation prior to severe eastward penetrating surges (moving over Korea). They identified a rapidly moving wave train over the Atlantic Ocean about eight days prior to the surge, moving toward the surge region. Shaffer, *et al.* (1984) examined the role of mid-latitude long-wave forcing on equatorial penetrating surges. They observed that three to five days prior to the surge, one or more of the mid-latitude long waves amplifies, with a phase such that a northerly flow component ensues over the Himalaya mountains and Tibetan Highlands. This long wave intensification forces amplification of a pre-existing wave or genesis of a shorter response wave (surge wave) in the lee of the Himalayas due to conservation of potential vorticity. This response wave in the lee of the Himalayas gives ideal dynamic support for intensification/initiation of the cold surge. The deepening trough in the lee enhances upper-level horizontal convergence and dynamically intensifies the quasi-stationary surface anticyclone in north central China. At the same time, the amplifying surge wave provides upper-level support for cyclogenesis over the western Pacific Ocean. Thus the ideal dynamic response to an amplifying surge wave may strongly intensify the surface pressure gradient along the China coast and the resultant surge of cold air.

## 5.5 Tropical synoptic models

The structure of synoptic disturbances depends much on the structure of basic current in different regions of the tropics. Structures of basic current are very dissimilar in different parts of the tropics (Palmen and Newton, 1969). Riehl (1950) observed that this fact is reflected in a greater variety in the character of synoptic disturbances in the tropics than in higher latitudes. According to Riehl any four types of vertical wind profiles (Figure 5.5) are found in various regions of the tropics at various times. Over most of the trade wind region in winter the circulation is characterized by lower level easterlies overlaid by westerlies in the upper levels (curve *c*). In summer, the average baroclinicity in the trade wind region is weaker with either profile (*a*) or (*b*) observed in the trades depending on whether the meridional temperature gradient is directed equatorward or poleward at various places and times. Profile (*d*) is characteristic of the region affected by monsoons.

Due to the marked variations in the structure of the basic currents in the tropics in different regions, there is a greater variety of tropical disturbances. Several areas of the tropics experience major weather-producing systems that are associated with synoptic scale wave disturbances. The tropical Atlantic, central Africa, eastern and western Pacific Oceans are known for the maximum frequency of development of these waves. These waves occur in the easterly trade winds of the tropics and are known as easterly waves. The kinds of disturbances vary with geographical location and season, depending largely upon the regional basic current structure. For example, the easterly waves develop, according to Riehl, only when the easterly current is at least six to eight km deep. For this and other reasons they are common in subtropical latitudes only in summer and in particular longitudes — generally westward of subtropical highs, in the western Atlantic and mid-Pacific, and mainly in the northern hemisphere (Palmen and Newton, 1969). Riehl made a pioneering study of the easterly waves in the Caribbean

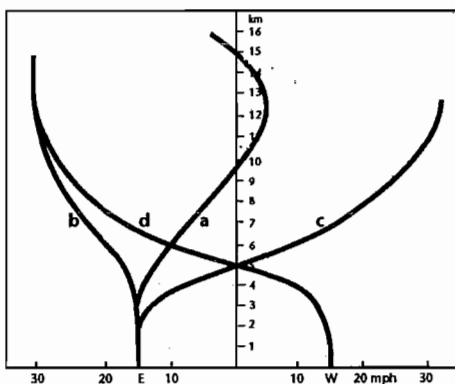


Figure 5.5 — Schematic representation of types of vertical profiles of the zonal wind in low latitudes (After Riehl, 1950, as presented in Palmen and Newton, 1969).

area and presented a classical model of these waves. These low-level tropical wave disturbances embedded in the trade easterlies develop in many parts of the tropical regions. These disturbances form initially as perturbations with weak amplitudes and gradually intensify into organized wave-type circulations during their westward propagation. Some of these waves are the progenitors of tropical depressions and cyclones in the Atlantic and Pacific Oceans. Not all waves, however, have the ideal Riehl's easterly wave type structure. Their structural characteristics, wavelength, amplitude, speed of movement and frequency differ from region to region. The structure is influenced by the basic environment. For instance the structure of the waves in the Pacific undergoes a systematic change as they travel westward. The wave axis, which tilts eastward with height in the eastern sector, becomes vertical in the central region and acquires an opposite tilt in the west. This change of wave structure is believed to be caused by the variation with longitude of the vertical shear of the basic current (Cadet, 1990).

Many waves in the low-level easterlies are reflections of upper-level cyclones. A wave may reach maximum amplitude in the low or middle troposphere or may be a reflection of upper tropospheric features (cold low or equatorial extension of a mid-latitude trough).

The importance of the easterly waves, especially with respect to tropical cyclone forecasting, was first recognized by Dunn (1940), who observed a series of falling and rising pressure (isallobaric centres) moving from east to west across the islands of the Caribbean Sea (Dunn and Miller, 1964). However, in later studies a considerable amount of controversy existed among tropical meteorologists concerning easterly waves with respect to their importance in the development of tropical storms (cyclones). Arnold (1966), Fett (1966), and others infer such development from easterly waves. Sadler (1967a), however, maintained that all tropical cyclones form initially in a shear zone between two currents flowing in opposite directions. Riehl (1945) found that isallobaric centres were accompanied by westward moving wave-like oscillations in the basic easterly flow of the lower troposphere. Recently, several studies have been conducted to identify the character of easterly waves in different regions of the tropics.

The results of time-longitude section and power spectral analysis of the meridional component  $v$  of the horizontal wind, discussed by Cadet (1990), bring out some interesting features of the synoptic scale tropical wave disturbances such as:

- (a) Westward propagating disturbances exist in the region from west Africa to central Atlantic ( $0-60^{\circ}\text{W}$ ) having a period of about three to four days. This kind of disturbance corresponds to African waves. The disturbance appears to originate in central Africa near  $30^{\circ}\text{E}$ , has a maximum amplitude near the west coast of Africa ( $15^{\circ}\text{W}$ ), and weakens as it propagates westward in the Atlantic Ocean and becomes absent over South America ( $60^{\circ}\text{W}-80^{\circ}\text{W}$ );
- (b) In the eastern Pacific region, another westward moving disturbance with periods of four to six days appears. Some of these disturbances propagate further west of the international date line;
- (c) Disturbances with large amplitudes move westward with a period of 5.7 days in the western Pacific region between  $120^{\circ}\text{E}$  and  $170^{\circ}\text{E}$ . The westward phase speed of the disturbances in the western Pacific is slower than those in the central and eastern Pacific. No systematic phase propagation is found in the Indian Ocean region ( $50^{\circ}\text{E}-100^{\circ}\text{E}$ ) and period variations longer than 10 days dominate in this region;
- (d) In the equatorial region between  $15^{\circ}\text{N}$  and  $15^{\circ}\text{S}$ , the disturbances have larger amplitudes over the northern latitudes than over the southern latitudes.

Most of the disturbances have many features in common. These features may be condensed and pictorialized in the form of a model although such disturbances may differ among themselves from one situation to another. These models of synoptic disturbances are important from the forecasting point of view. The development of these models took place at its peak just before World War II. A renewed interest in these models was generated with the availability of conventional data (specially at upper levels and remotely-sensed satellite data).

In view of differences in the features of wave disturbances in different regions of the tropics, the models of these disturbances will be described by region in the subsequent sections.

A wide variety of vortex disturbances also exist in the tropics, which have their origin either in a wave disturbance or develop independently. In addition to the above main disturbances there are linear disturbances, shear lines and asymptotes, which also produce significant amounts of weather activity in different parts of the tropics. Each of these disturbances will be dealt with separately.

### 5.5.1 Waves\*

#### 5.5.1.1 SYNOPTIC-SCALE WAVE DISTURBANCES IN THE CARIBBEAN

The easterly waves of the Caribbean region are the most extensively studied wave disturbances. Their main characteristics are as follows:

- (a) The wave extends through the depth of the troposphere reaching its maximum intensity in the layer between 700 and 500 hPa. The trough axis slopes eastward with height. This implies that as the wave moves westward, the upper part arrives at a station later than the lower part. Figure 5.6 shows an east-west section through an easterly wave. The composite analysis of GATE data in the Caribbean region revealed the existence of a moderate eastward tilt of the trough axis up to 700 hPa, with a strong westward tilt above. Shapiro (1986) analysed the three-dimensional structure of a series of easterly waves in the area during July 1975. In contrast to the classical model presented by Riehl, he found a westward tilt of the trough axis with height. In particular both the vorticity and meridional velocity consistently evidenced a near 90° phase shift at 200 hPa relative to the lower troposphere. The influence of the basic environment on wave structure has been studied by Holton (1971) and Shapiro, *et al.* (1988). Holton developed a simple model to analyse the structure of linear forced wave disturbances in the presence of vertical shear of the mean zonal wind. In the case of a mean wind with westerly shear from the surface up to about 12 km, solutions indicated a surface trough to the west of the heating maximum and an eastward tilt with height in agreement with the classical wave model. With an easterly shear in the basic wind profile, the trough axis tilted westward with height. Shapiro concluded that the eastward tilt of the trough axis in the classical picture of the Caribbean easterly wave is not a simple consequence of the vertical profile of the mean zonal wind. The latitude of the disturbance may be an important factor. For example, with a westerly shear in the lower and middle troposphere, a westward tilt above 700 hPa is found at the latitude of maximum heating when centred at 19°N. An eastward tilt is favoured below 400 hPa when the heating is more to the south, near 9°N. In that case the westward phase shift occurs over a narrow layer near the level of maximum heating;

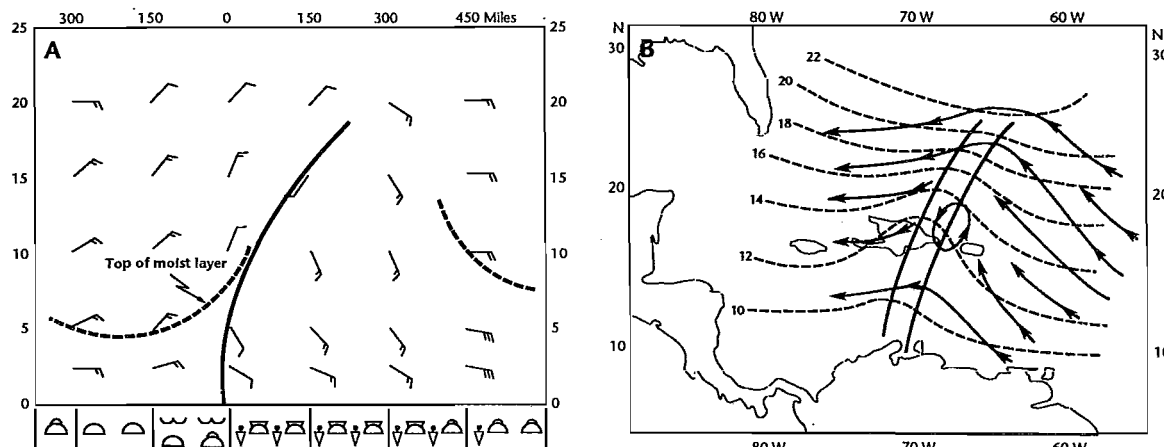


Figure 5.6 — Model of an easterly wave (a) east-west section through the wave; (b) 10 000–15 000 ft. streamlines (solid lines) and surface isobars (dashed lines). Trough line at the surface and 10 000–15 000 ft. denoted by solid lines (After Riehl, 1945, as presented in Atkinson, 1971).

- (b) The waves move westward at average speeds of 10 to 15 knots. When the waves move slower than the basic current in the lower levels and faster than the basic current in the upper levels, the area west of the wave troughs is characterized by subsidence and fair weather, while areas of convergence and disturbed weather occur east of the trough. Riehl (1967) presented a case study where the wave actually moved faster than the basic current in which it was embedded. In this case convergence occurred west of the wave axis increasing in strength as one approached the axis. The cloud pattern across the wave was observed to vary considerably;
- (c) The westward motion of a non-developing easterly wave is a fairly complex problem. Estimates of the various terms of the vorticity equation are generally used to determine which of these contribute to a positive tendency of vorticity west of the surface trough which will make the disturbance to move westwards. Positive vorticity advection contributes most significantly to this local increase of vorticity ahead of the surface trough. This effect is somewhat counteracted by the divergence term of the vorticity equation;

\* This section is taken from Cadet (1990) and Atkinson (1971).

- (d) The temperature and moisture distribution in an easterly wave are shown in Figure 5.7. The isotherms in this time section are shown as a departure of the observed temperature from a tropical standard atmosphere. There is a cold core to the east of the wave trough and a warm core to the west in low levels. In the higher levels between 500 and 250 hPa, a reversal in the thermal anomaly structure may be noted. The colder temperatures in the lower levels behind the wave trough are maintained by a combination of several factors, such as being cut off from insolation due to heavy clouding, evaporation from falling rain, and adiabatic cooling due to ascending motions in the convergent sector. Krishnamurti and Kanamitsu (1973) looked at the maintenance of the cold core of 1 or 2°C, which exists within an easterly wave, especially in the Caribbean region where they maintain a thermal structure in a near steady state. Some numerical experiments conducted by them with and without convection and radiation temperature gradients showed that the cold core is primarily maintained by ascending motions in the region of the boundary layer of the weather active portion of the wave. Ascending motions arising due to frictional convergence and heating aloft account for adiabatic cooling. Thus the cold core is not merely an advective phenomenon that translates from east to west but it is maintained by dynamic and thermodynamic processes. The warm anomaly above is attributed to the effects of cumulus convection. The depth of the moist layer rises as the trough is approached from west to east and is at the maximum east of the wave trough;

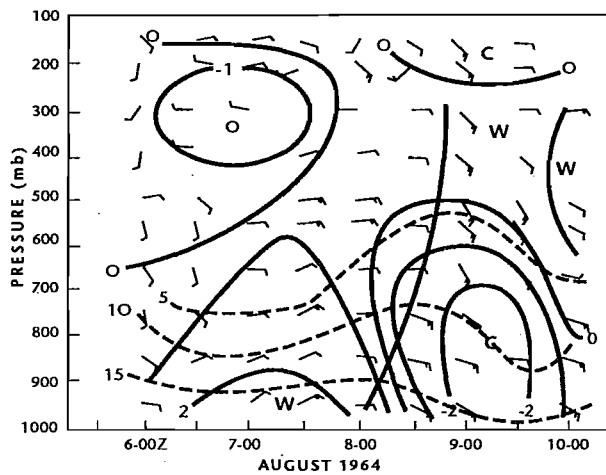


Figure 5.7 — A vertical time section showing winds (knots), temperature C (solid lines) and specific humidity (dashed line) g/kg (After Riehl, 1967, as presented in Cadet, 1990).

- (e) Frank (1969) proposed a cloud pattern structure associated with easterly waves. He called it an inverted-V formation because of its appearance. Figure 5.8 shows an idealized (model) inverted-V pattern, resembling a nested series of upside-down Vs. This type of pattern appears to be best defined in the eastern and central North Atlantic. As the wave approaches the Antilles, the clouds associated with it frequently disappear or become less distinct. This inverted V-model has been documented by using satellite imagery and conventional data sources. Merritt (1964) also reveals that the cloud distribution most frequently related to perturbations in the low-level easterlies has a vortical appearance which seems to be associated with cyclonic vortices in the mid-troposphere;

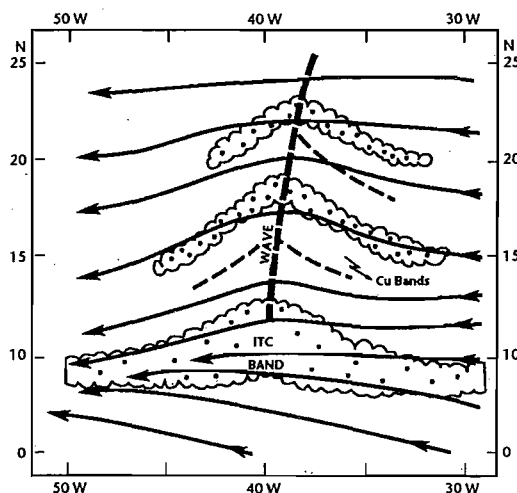


Figure 5.8 — Model of the inverted V cloud pattern (stippled areas) and associated lower-tropospheric flow (After Frank, 1969, as presented in Atkinson, 1971).

- (f) Evidence generally indicates that the barotropic mechanism may be the most important mechanism during the initial formative stage of Atlantic waves. However, after the initial development has taken place, the disturbances loose energy to local zonal flows indicating that the barotropic mechanism is not important in the maintenance of the waves and the role of convection is perhaps more important. In a study of a westward propagating easterly waves of 1961, Krishnamurti and Kanamitsu (1973) found that the transformation of eddy available potential energy into eddy kinetic energy is an important mechanism for the maintenance of easterly waves. This mechanism seems to operate in the following manner: ascending motion occurs at the wave axis and to its rear. Over this region a warm core is present near the 500 hPa surface. Subsidence occurs all around and ahead of the wave axis. The net result of this ascent of relatively warm moist air and descent of relatively colder and dry air is that the generation of eddy kinetic energy occurs from the eddy available potential energy. The above results of Krishnamurti and Kanamitsu are, however, based not on observations but on numerical experiments which may have their own limitations.

#### 5.5.1.2 SYNOPTIC-SCALE WAVE DISTURBANCES IN THE PACIFIC

The eastern and western sectors of the Pacific Ocean are both populated by wave disturbances in the easterlies. Easterly waves over the eastern Pacific Ocean have been studied by Tai and Ogura (1987). The properties of these waves are summarized below:

- (a) The average wavelength of easterly waves over the western Pacific is about 3 500–4 000 km. The waves travel westward at an average speed of 7° longitude per day, that is about  $9 \text{ m s}^{-1}$ . Meridional wind fluctuations are the strongest near 800 hPa ( $3\text{--}4 \text{ m s}^{-1}$ ) and 175 hPa ( $2\text{--}3 \text{ m s}^{-1}$ ). The fluctuations in the upper and lower levels are nearly out of phase. Temperature fluctuations are  $1^\circ\text{C}$  or less with cold anomalies in lower levels in the region just behind the trough and in the upper troposphere above the trough. There is a region of warm anomaly in between. The vertical motion appears everywhere except in the vicinity of the low-level ridge. Convergence predominates at low levels in the waves. The level of nondivergence varies between 500 to 300 hPa. The region of strong divergence is centered at 175 hPa above the low-level trough zone;
- (b) The average wavelength of easterly waves over the eastern Pacific is in the order of 3 000–3 500 km with a period of four to six days and a speed of propagation of  $5\text{--}7 \text{ m s}^{-1}$ . The maximum wave amplitude is about  $4 \text{ m s}^{-1}$ . A secondary maximum in the upper level, as in the case of the western Pacific waves, is not found. The waves possess a cold core in the lower level with warm anomalies above it;
- (c) The structure of the waves in the Pacific undergoes a systematic change as they travel westward. The wave axis tilts eastward with height in the eastern sector, becomes vertical in the central region and acquires an opposite tilt in the western sector. This behaviour of the waves is attributed to the longitudinal variation of the vertical shear of the basic current.

#### 5.5.1.3 AFRICAN WAVES

During northern summer, waves originate over north Africa and propagate westward. These waves travel westward and sometimes develop into tropical cyclones over the Atlantic Ocean or the Caribbean. They owe their existence to a mid-tropospheric jet stream which develops in the area at the 700–650 hPa level, centred near  $16^\circ\text{N}$  (Figure 5.9). The jet is caused by thermal wind due to strong temperature gradients in the lower troposphere between the equator and  $25^\circ\text{N}$ , which develop in response to intense solar heating over the Sahara desert with cold and moist air to the south. Synoptic-scale disturbances are observed to form in the cyclonic shear zone south of this jet core. The barotropic and baroclinic instability associated with this jet provides the energy source for the development of these waves.

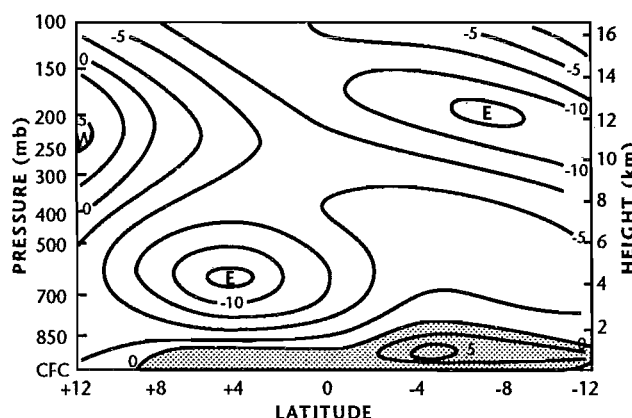


Figure 5.9 — The mean zonal wind distribution in northern Africa ( $30^\circ\text{W}$  to  $10^\circ\text{E}$  longitude) for the period 23 August to 19 September 1974. Latitude is shown relative to latitude of maximum disturbance amplitude at 700 hPa (about  $12^\circ\text{N}$ ). The contour interval is  $2.5 \text{ m s}^{-1}$  (After Reed, *et al.*, 1977, as presented in Holton, 1979).

The existence of African waves was suggested as early as the 1930s. Satellite data provided further insight into the structure of these waves. Burpee (1972) made a pioneering study of African waves. Various studies followed, such as Reed, *et al.* (1977), Thompson, *et al.* (1979), Norquist, *et al.* (1977), Albignat and Reed (1980) and Estoque (1982). On the basis of these studies, the following main features of African waves may be summarized:

- (a) The waves have an average wavelength of 2 500 km and the westward propagation speed is about  $8 \text{ m s}^{-1}$ , implying a period of about three to five days. The disturbances have horizontal velocity perturbations which reach their maximum amplitude at the 650 hPa level;
- (b) The wave axis has a pronounced north-east/south-west tilt in the vicinity of 700 hPa. This implies a strong northward transport of westerly momentum and a conversion of zonal kinetic energy into eddy kinetic energy. In the vicinity of the disturbance path (around  $10^\circ\text{N}$ ), the wave axis is essentially vertical below 700 hPa and slopes westward above. In the region of the strongest baroclinicity to the north of the path, it slopes eastward with a height in the easterly shear zone below 700 hPa, thus suggesting that baroclinic wave growth occurs in this region;
- (c) The disturbances are cold cored below 650 hPa, warm cored between 650 hPa and 250 hPa, and cold cored at the higher levels. The vorticity is largest ( $3 \times 10^{-5} \text{ sec}^{-1}$ ) at 650 hPa. The largest anticyclonic vorticity is observed in the upper troposphere centred well to the north of the lower level cyclonic vorticity centre;
- (d) The largest temperature fluctuations occur at 850 hPa in the region of strong temperature contrast north of the disturbance track. Negative correlation between the temperature and the meridional wind component exists indicating a conversion of zonal to eddy available potential energy;
- (e) The strongest upward motion occurs at 700 hPa in advance of the trough. Upward motion is correlated with warm temperature anomalies in the baroclinic zone around 850 hPa and near 300 hPa, suggesting thereby that the waves are maintained, at least in part, by a baroclinic energy conversion;
- (f) The waves originate over central Africa as a consequence of joint barotropic-baroclinic instability. In the early stages of the waves, convection is unorganized and latent heat release plays little part in wave development. As the waves progress westward, convection becomes better organized, so that over western Africa the condensation heating becomes a dominant factor in their growth and sustenance.

### 5.5.2 Vortices

At least three distinctly different kinds of cyclonic vortices, which are of significant size and strength, exist in the tropical latitudes. The most common and the most important ones are the warm core tropical cyclones. Tropical cyclones occur in a nearly barotropic basic current and acquire their warm core due to the release of latent condensation heat. Their maximum intensity is in the lower troposphere and the intensity decreases with height due to warm core. The second type of cyclonic vortices, observed over India in the summer monsoon season, are the cold core disturbances in baroclinic current with basic westerlies in the lower levels and easterlies in the upper levels. These are monsoon depressions which again have their maximum intensity in the lower troposphere and which typically slope south-westward with height. The third type are the cold core mid-tropospheric cyclones, which occur in subtropical latitudes and resemble in some respects a mid-latitude cyclone. These have their maximum intensity in the middle tropospheric levels. Examples of mid-tropospheric cyclones are the subtropical cyclones, occurring in the Pacific, and the Arabian Sea cyclones of the monsoon season.

The other types of vortices which exist in the tropics are the upper tropospheric cyclones over the tropical oceans during the warm season, and the lower tropospheric anticyclones.

The major characteristics of the models of each of these vortices are described below.

#### 5.5.2.1 TROPICAL CYCLONES

The tropical cyclones are the most impressive phenomena of the tropical regions because of their destructive potential and their large influence on human activities.

The tropical cyclones are intense vortical storms which develop over the tropical oceans in regions of very warm sea surface temperature. These storms go by different names in different ocean basins, such as hurricanes in the Atlantic and eastern Pacific, typhoons in the western Pacific and China Sea, and cyclones in the north Indian Ocean area. The classification of tropical cyclones is also different in different regions of the world. The United States Meteorological Services use the classification system as given below:

- (a) Tropical depression: A weak tropical cyclone with a definite closed surface circulation, one or more closed surface isobars, and highest sustained wind speeds less than 34 knots ( $17 \text{ m s}^{-1}$ );
- (b) Tropical storm: A tropical cyclone with closed isobars and highest sustained wind speeds of 34 to 63 knots ( $17\text{--}32 \text{ m s}^{-1}$ ), inclusive;
- (c) Typhoon/hurricane: A tropical cyclone with highest sustained winds of 64 knots ( $33 \text{ m s}^{-1}$ ) or more.

In Japan any tropical cyclone with winds of 34 knots or greater is called a typhoon. In India the terms depression, deep depression, cyclonic storm, severe cyclonic storm, and severe cyclonic storm with a core of hurricane winds are used for threshold values of wind speeds of 17–27 knots, 28–33 knots, 34–47 knots, 48–63 knots and 64 knots and above, respectively. The classification supertyphoon is applied to those storms reaching an intensity of 130 knots ( $67 \text{ m s}^{-1}$ ) (Askue and Cheng Shang Lee, 1984).

Statistics indicate that about 80 tropical cyclones are observed on the globe per year (Gray, 1981) where the maximum sustained (1-min mean) surface winds exceed  $20\text{--}25 \text{ m s}^{-1}$ . Nearly one-half to two-thirds of these eventually reach hurricane strength. The western North Pacific and South China Sea experience the maximum frequency of tropical cyclone development and are the only areas where tropical storms can form in any month of the year (most commonly from July to October). The frequency of cyclone formation appears to be the greatest when the monsoon trough is north of its normal position or extends farther eastward than normal. During the period from September to December the monsoon trough occasionally extends eastward to  $180^\circ$  longitude or beyond, enhancing the potential of cyclone formation over the region of the Marshall Islands. Tropical cyclone formation in the South China Sea reaches a maximum during the autumn transitional season when the monsoon trough is oriented east-to-west across that area.

The eastern North Pacific ranks second only to the western North Pacific in terms of the average number of tropical storms per year. Almost all storms in this area occur between June and October, with more than 50 per cent occurring during August and September. Once formed, most of these storms move to the west or north-west over cooler waters and into regions with a strong vertical wind shear — two important factors which are believed to inhibit further development and, in fact, dissipate these systems.

Cyclones also form over the eastern North Atlantic which has many features similar to the eastern North Pacific region. However, an important difference is that cyclones in the eastern North Atlantic originate over land in the shear zone over Africa but not at the surface level. The shear zone slopes equatorward from a mean location of  $20^\circ\text{N}\text{--}25^\circ\text{N}$  near the surface to  $10^\circ\text{N}\text{--}15^\circ\text{N}$  at the 700 hPa level. The extremely dry air at the surface shear zone position is not conducive to vortex formation, and vortices tend to form further south where moisture is available throughout a deep atmospheric layer. Therefore, cyclones over Africa are most intense between 850 and 700 hPa and do not generally have an associated surface wind vortex until they reach the coast of western Africa.

In the southern hemisphere, low-level cyclonic vortices form in the monsoon trough, which extends eastward from Africa to about  $180^\circ$  longitude. In these areas, vortex formation generally occurs during the period from November to the end of May and is most common from January to the end of March. Tropical cyclones generally do not occur in either the eastern South Pacific or the South Atlantic regions.

#### 5.5.2.1.1 MODEL OF A TROPICAL CYCLONE

The model of a mature tropical cyclone can be described in terms of its well defined characteristics of wind field, surface pressure distribution, temperature field, cloud systems, and dynamics of the inner core and outer region.

##### 5.5.2.1.1.1 WIND FIELD

The structure of wind field in a tropical cyclone can be examined with the help of a momentum equation expressed in terms of a cylindrical coordinate system. If it is assumed that the radial acceleration is zero (radial component of wind is constant), then in the absence of friction the momentum equation (Holland, 1985) takes the form:

$$V^2/r + fV - 1/r \cdot \partial p / \partial r = 0$$

The above is the gradient wind equation in which the centrifugal force  $V^2/r$ , the Coriolis force  $fV$  and the pressure gradient force  $-1/r \cdot \partial p / \partial r$  are in balance. The nature of flow can be further investigated by defining a non-dimensional scaling parameter:

$$R_o = (V^2/r) / fV = V/ft$$

which is the ratio of the centrifugal to Coriolis acceleration. This is known as the Rossby number. For small values of the Rossby number (centrifugal acceleration negligibly smaller than Coriolis acceleration), the flow is nearly geostrophic.

In tropical cyclones, the horizontal scale of the region where convection is strong is typically about 100 km in radius. The maximum tangential wind speed in the tropical storms ranges typically from  $50\text{--}100 \text{ m s}^{-1}$ . For such high velocities and relatively small scales the centrifugal force term cannot be neglected compared to the Coriolis force. Thus, to a first approximation the radial force balance in a steady-state hurricane satisfies the gradient wind relationship, not the geostrophic balance. In the core region, however, high wind speeds combined with the small radius of curvature result in a centrifugal acceleration  $V^2/r$  that is much larger than the Coriolis acceleration  $fV$ . Therefore, the Coriolis acceleration can be neglected and the flow is said to be in cyclostrophic balance. For very large values of  $R_o$  (greater than 50) cyclostrophic balance occurs. Motion on the hurricane scale remains in hydrostatic balance although motion in the individual cumulus towers is not in hydrostatic equilibrium.

The low-level horizontal circulation field in mature tropical cyclones can be divided into three distinct regions:

- (a) The outer portion which extends from the storm periphery inward to the region of maximum winds. In this region the wind speeds increase towards the centre;
- (b) The region of maximum winds which surrounds the eye is the most outstanding characteristic of the mature tropical cyclones. This region, which measures 10 to 20 kilometres in width, coincides with the wall cloud surrounding the eye and is known as eye wall. This is the innermost convective ring of a tropical cyclone. The most violent convection and heaviest rainfall in the storm are usually associated with the wall cloud as the low-level convergence and upward

vertical motion are the strongest here. The eye wall region is characterized by maximum pressure gradients and strongest winds. There is cyclonic shear inward and anticyclonic shear outward. The temperature increases rapidly while the dew point decreases inward, due to subsiding motion in the eye. The highest dew point values are observed on the radius of maximum tangential winds;

- (c) The eye is the innermost portion of the storm in which the wind speed diminishes rapidly with decreasing distance toward the centre. The size of the eye, as determined by the radius of the eye wall cloud, varies from case to case and also with time within the same storm. The eye radius can vary from less than 20 km in small intense storms to as great as 60 to 80 km in very large storms. Based on 46 aircraft penetration reports, Jordon (1952) found that an eye diameter varied between 13 and 140 km, with no clear relation to central pressure. In most cases, the eye becomes smaller as the cyclone deepens, and larger as it weakens, but the opposite is often true (Palmen and Newton 1969). The circulation of intense tropical cyclones extends upward to around 14 to 15 km (close to the tropical tropopause). Since the storms are warm core, the cyclonic circulation decreases with height. The vertical shear is, however, small reaching up to about 6 km.

The formation of the eye and the eye wall cloud can be explained by the principle of conservation of absolute angular momentum, which is defined as:

$$M_r = V_\theta \cdot r + f/2 \cdot r^2$$

where  $V_\theta$  is the tangential velocity. As the air flows inward, its tangential velocity increases in order for  $M_r$  to be conserved.

The inflowing air cannot enter the central part of a hurricane because, with the tangential velocity achieved by close approach to the centre, the centrifugal force would be so great that the air parcel could not be forced further inward by the radial pressure gradient. With the conservation of angular momentum,  $V_\theta$  would become infinite as a low-level streamline approaches the centre. The total kinetic energy that can be gained by the current is limited by the available pressure drop and therefore cannot increase indefinitely. In other words, the converging currents cannot penetrate a certain minimum radius  $r$  and must turn upward and eventually outward at higher levels, since the radial pressure gradient decreases with elevation. The surface of revolution defined by this streamline is identical with the wall of the eye (Palmen and Newton, 1969).

The vertical circulation of the tropical cyclones may also be divided into three layers:

- (a) The lowest layer from the surface to about 3 km is called the inflow layer since it contains a pronounced component of motion toward the storm centre. Most of this flow occurs below one kilometre in the planetary boundary layer;
- (b) In the middle layer from about 3 to 7.6 km, the flow is mostly tangential with little or no radial motion;
- (c) The outflow layer extends from 7.6 km to the top of the storm, with the maximum outflow in mature storms occurring near 12 km.

The wind field around the centre of the storm is usually asymmetrical with the strongest azimuthal winds occurring to the right of the direction of movement. The azimuthal maximum tends to be located towards the right front quadrant. Several separate wind maxima may be present. The pattern of azimuthal wind is reversed in the southern hemisphere storms so that the maxima occur in the left front quadrant (Sheets and Holland, 1981). The strongest winds occur near the centre in the eye wall. The maximum wind belt tilt outward with height. In the upper troposphere a cyclonic-outflow is seen. The horizontal extent of the cyclonic circulation in the upper troposphere is much smaller than in the lower levels and is surrounded by anticyclonic flow. The outflow in the upper troposphere is reflected by cirrus bands in the satellite pictures.

The relative vorticity near the centre is in the order of  $10^{-3} \text{ s}^{-1}$ , which is 100 times the value at the formative stage. The corresponding rotation rate is 10 times faster than the rotation rate of the earth (Kurihara, 1985).

The vertical motion fields indicate that strong upward motion is confined largely to the vicinity of the core region. The outer region is subsident with bands of only weak upward motion. In particular, there is an area of subsidence with a radius of around  $4\text{--}6^\circ$  latitude that is associated with the clear area that surrounds most of the cyclones.

To summarize, the three-dimensional wind structure of tropical storms consists of air flowing into the storm through the inflow layer, rising primarily in the eye wall cloud and the other rainbands, and finally flowing outward from the storm top and sinking some distance away. A small sinking motion also occurs inside the eye of the cyclone.

#### 5.5.2.1.1.2 SURFACE PRESSURE DISTRIBUTION

Pressure is lowest in the eye. The central pressure defect may vary from as low as 6 hPa (T Number 2.5 of Dvorak's classification) to as great as 140 hPa (T Number 8.0). The lowest central pressure of 870 hPa observed so far is in the case of typhoon Tip in the north-west Pacific on 12 October 1979 with an estimated maximum surface wind of  $85 \text{ m s}^{-1}$  (Kurihara, 1985). The lowest pressure recorded in the northern Indian Ocean is 919 hPa, which was the case of the False Point cyclone that struck Orissa in eastern India in September 1885, although the lowest estimated central pressure in this region is 911 hPa, which was the case of the November 1977

cyclone that hit Andhra Pradesh in India (Mandal, 1990). Both these systems occurred in the eastern coast of the Bay of Bengal. The strongest pressure gradients occur in the eye wall region. The normal pressure gradients observed in the case of an average storm is 2.5 hPa/km (Riehl, 1979). Mandal (1990) reported the case of the Bay of Bengal cyclone of 3 June 1982, which hit Orissa, where the observed pressure gradient was about 13 hPa/km. This is rather high for a storm having an intensity of 100 knots as the maximum wind speed. This suggests that the pressure gradients in individual storms could be very large. Outside the eye wall the pressure gradients are weak.

#### 5.5.2.1.1.3 TEMPERATURE FIELD

Intense tropical cyclones are warm core direct atmospheric circulations in which the warm air rises and the cold air sinks. The heat energy is converted to potential energy and potential energy to kinetic energy. The magnitude of temperature fluctuations in tropical cyclones can be estimated by scaling arguments applied to the motion equation. The relationship between the radial temperature gradient and the vertical shear of the tangential wind is given by:

$$\partial V / \partial z^* \cdot (f + 2V/r) = R/H \cdot \partial T / \partial r$$

where  $z^* = -H \ln(p/p_0)$  is the vertical coordinate in the log-pressure coordinate system,  $H = RT_0/g$  is the standard scale height of the atmosphere,  $V$  is the gradient wind velocity,  $T$  is the absolute temperature,  $f$  is the Coriolis parameter, and  $r$  is the radial distance from the axis of the storm. The cyclonic flow in a cyclone decreases rapidly with height from its maximum values in the lower troposphere. Thus the boundary layer  $\partial V / \partial z^* < 0$ , which by the above equation implies that  $\partial T / \partial r < 0$ , and the temperature maximum must occur at the centre of the storm. This is consistent with the observation that tropical cyclones are warm core systems. This fact is necessary if the cumulus heating is to generate kinetic energy.

If we let the vertical scale of the system be equal to the scale height  $H$ , the tangential velocity scale be  $U \approx 50 \text{ m s}^{-1}$ , the horizontal scale be  $L \approx 100 \text{ km}$ , and assume that  $f \approx 5 \times 10^{-5} \text{ s}^{-1}$ , then we find from the foregoing equation that the radial temperature fluctuation must have a magnitude:

$$\Delta T \approx LH/R \cdot (U/H)(f+2U/L) \approx 10^\circ\text{C}$$

According to the data relating the mean eye temperature and distribution of surface central pressure, presented by Palmen and Newton (1969) and based on Jordan (1958), the moderate tropical cyclones with central pressure in the range 998–980 hPa occur at a surface temperature of 25.2°C and the most intense cyclones with central surface pressure in the range 901–883 hPa occur at a surface temperature of 27.1°C. Thus there is a difference of only 2°C in the surface temperature corresponding to the weakest and the most intense cyclones. Higher up, the eye temperature increases with decreasing surface pressure from hydrostatic considerations.

The primary energy source of tropical cyclones is the release of latent condensation heat, which occurs in the eye wall and the spiral rain bands. In a typical thermal structure, a tropical cyclone has a narrow warm core in the lower troposphere, which reaches a maximum width and magnitude in the upper troposphere of near 250 hPa, and where temperatures of 10°C or more above normal may occur. The maximum horizontal temperature gradients are observed in the vicinity of the maximum wind belt and are concentrated in a narrow band extending from the inner edge of the eye wall out to the exterior of the wall cloud. The maximum temperature gradients are observed in the mid-troposphere. Little gradient is observed within the eye itself, especially in the lower levels. Outside the eye wall, the temperature anomalies in the lower troposphere are slightly below normal. The ultimate heat source of these storms is provided by the warm low-latitude sea-surface temperatures in the major formation areas. In these areas, the addition of sensible heat and moisture to the surface air as it spirals inward balances the adiabatic cooling due to pressure decrease so that the sea-level temperatures remain nearly isothermal.

#### 5.5.2.1.1.4 CLOUD SYSTEMS

The major convective cloud systems (rain bands) in tropical storms have a banded structure as shown by radar echo patterns and satellite photographs. The upward motion in the storms is concentrated in these rain bands, and especially in the clouds surrounding the eye wall where updrafts of 10 to 25 knots have been observed. These bands often form logarithmic spirals that curve inward towards the centre. The importance of rain bands lies in the fact that large intensity changes can result from contraction and reformation of concentric, convective rings around the eye (Willoughby, *et al.*, 1982). The structural changes in rain bands are therefore important from the forecasting point of view. The vertical heat transport and conversion of potential energy to kinetic energy occurs primarily in the rain bands. Enhancement techniques in satellite pictures are used to project the brighter areas which are caused by tall cumulonimbi penetrating the cirrus shield and thus identify the location of major rain bands. The maximum height of cumulonimbi are related to the storm intensity. It is not uncommon for those maximum heights to exceed 15 km especially in the wall cloud.

Apart from the core region rain bands, there are outer region rain bands which are most commonly found in a large-scale convective region that originates in equatorial regions and extends around the eastern side of tropical cyclones. This convective region is often referred to as feeder band by forecasters because of the belief that it provides a conduit for moist tropical air to spiral into the core region. These rain bands may originate as much as 2 000–3 000 km away from the core and can produce severe weather conditions, such as strong winds and heavy rainfall. The bands are observed to move with the cyclone.

### 5.5.2.1.1.5 DYNAMICS OF THE INNER CORE AND OUTER REGION

In a tropical cyclone, there are considerable changes in the dynamical properties from the outer to the core region and from the lower to the upper troposphere, which are outlined below (based on Holland, 1985):

- (a) Within a tropical cyclone, the atmosphere is almost always statically stable so that dry vertical displacements will be resisted. The property of static stability can be expressed in terms of Brunt-Väisälä frequency, which is defined as:

$$N^2 = g \partial \ln \theta / \partial z$$

which represents the degree of resistance to vertical motion for static stability  $N^2 >> 0$ . The conditional instability in an intense cyclone, on the other hand, varies from stable in the eye and weakly unstable in the eye wall, to normal tropical instability in the outer region. There is very little variation in static stability with radius;

- (b) There are large horizontal variations in the inertial frequency  $I$ , the Rossby number  $R_o$  and the rotational Froude number  $F_R$  from the core region to the outer region. The inertial frequency is a measure of resistance to horizontal displacements and is a function of the radial gradient of angular momentum. It is defined as:

$$\begin{aligned} I^2 &= 1/r^2 \partial M_a^2 / \partial r \\ \text{or } I^2 &= (f_0 + \zeta) (f_0 + 2v/r) \end{aligned}$$

For  $I^2 = 0$ , the absolute angular momentum  $M_a$  is constant with the radius. A parcel that is displaced horizontally will stay in gradient wind balance, which is a state of neutral equilibrium to horizontal displacements. If  $I^2 \neq 0$ , any horizontal movement will produce a gradient wind imbalance and radial acceleration. For  $I^2 < 0$ , the absolute angular momentum will be decreasing with the radius and the acceleration will be in the direction of the displacement, which will result in an unstable, growing circulation (inertial instability). For  $I^2 > 0$ , the acceleration will oppose the initial displacement and induce a stable oscillation with frequency  $I$ . The inertial and static stabilities place constraints on radial and vertical motion in a tropical cyclone.

The rotational Froude number  $F_R$  is defined by:

$$F_R = L^2 / L_R^2$$

where  $L$  is the characteristic length scale for the region of interest and  $L_R$  is the Rossby radius of deformation given by:

$$L_R = NH/I$$

where  $NH$  is the speed of the internal gravity mode of interest ( $H$  is the relevant scale height). The rotational Froude number provides an objective indicator of the efficiency of wind and mass adjustments to imposed perturbations.

The core region is characterized by high inertial stability and rotational Froude number flow and is dominated by convective processes. Due to high values of  $F_R$ , the winds tend to adjust to mass field perturbations, such as those associated with cumulus convection. A strong resistance to radial motions (large inertial stability) leads to a tendency towards axial symmetry in the core and only a very small part of the total storm angular momentum is needed for quite large wind accelerations.

The core region of a mature tropical cyclone typically extends three to six times the radius of maximum winds from the cyclone centre. The actual dimensions can vary from as little as 20–30 km in a small cyclone to a few hundred kms in large cyclones.

Strong upward motion in tropical cyclones is largely confined to the vicinity of the core region. The outer region is largely subsident with bands of only weak upward motion. In particular, there is an area of subsidence around 4–6° latitude radius that is associated with the clear area that surrounds most cyclones (Holland, 1985);

- (c) In addition to the horizontal variations, there is a substantial vertical wind shear, with upper tropospheric anticyclonic flow overlying the lower, cyclonic wind regime. The depth and strength of this anticyclonic flow increase with radius. As a result, there is considerable vertical variation in inertial stability, which is strongest near 900 hPa and weakest in the upper troposphere. Similar vertical variations occur in the other scaling parameters.

If frictional effects are also considered, a tropical cyclone may be considered to consist of five distinct regimes: the boundary layer, the core regime, the interaction envelope regime, the outer regime, and the anticyclonic outflow regime.

The interaction envelope regime provides the buffer zone between the environmentally-dominated outer regime and the more convectively-dominated core. The outer flow regime contains the main tropical cyclone volume and is characterized by low Rossby and rotational Froude numbers, and also by low inertial instability. In the outer regime, the mass field preferentially adjusts to wind field perturbations due to angular momentum imports from the environment. The radial motion is not unduly restricted in this regime and the flow tends to be asymmetric.

### 5.5.2.2 MONSOON DEPRESSIONS

Monsoon depressions are intense tropical disturbances in which a perturbation in the pressure and wind field is very large compared to easterly waves and cloud cluster systems of the Atlantic and the Pacific Oceans, but less than in a tropical cyclone. Monsoon depressions are one of the most important synoptic scale disturbances which form periodically on the quasi-stationary monsoon circulation prevailing over the Indian region during the south-west monsoon season of June to September. A planetary scale monsoon trough, which extends from the west coast of Africa to the Pacific coast of Asia, is the most prominent feature of the monsoon circulation. Monsoon depressions are also observed over the Australian region during the north-west monsoon period.

#### 5.5.2.2.1 MONSOON DEPRESSIONS IN THE INDIAN REGION

The depressions form over the Bay of Bengal, east Arabian Sea and even over land (called land depressions), but the Bay of Bengal has the maximum frequency of formation (over 80 per cent of the total) and the Arabian Sea has the smallest (less than 10 per cent).

In India, a system is called a depression if the wind speed in its circulation is 17–27 knots, and a deep depression if the wind speed is 28–33 knots. Weaker systems with winds less than 17 knots are called lows.

The zone of formation is in the head of the Bay of Bengal during July and August and over the central Bay during June and September. During these months, this zone is a favourable region for cyclogenesis. The average frequency of formation over the Bay of Bengal is two per month. Monsoon depressions form over the warm surface of the Bay of Bengal within the moist environment of the monsoon air and move in a west or north-west direction along the monsoon trough towards the warmer and drier environment of the heat low system which exists over western India and Pakistan.

Monsoon depressions are the most significant rain bearing systems of the south-west monsoon season over India, although, according to a study by Mooley (1973), the contribution of the depression-associated rainfall to the total seasonal rainfall is rather small, being only about 11–16 per cent in the areas covered by their tracks. Also, there is not much relationship between the number of monsoon depressions and the monsoon rainfall in a year.

Even though the contribution of monsoon depressions to the total rainfall is small if we only take into consideration the rainfall within their direct field, they contribute significantly if we consider that the formation of monsoon depressions is accompanied by the activation of the monsoon trough system and by the strengthening of monsoon flow two to three days prior to the formation of the depression and two to three days after its passage, when the monsoon trough remains active. Furthermore, weaker systems, which classify as low pressure areas but which behave like depressions, also make a significant contribution. The monsoon depressions assume greater importance due to the following characteristics:

- (a) The passage of a monsoon depression distributes rainfall over a wide area;
- (b) Movement of a monsoon depression in quick succession and their stagnation/slow speed may cause floods in some areas;
- (c) The onset of a monsoon is often associated with the formation and movement of a monsoon depression;
- (d) Prolonged dry spells may be broken by the development of a depression.

The first detailed study of monsoon depressions with an attempt to model this phenomenon was made by Krishnamurti, *et al.* (1975, 1976) in a series of two papers. Sikka (1977) provides a review of the studies on life history, structure, and movement of monsoon depressions. One component of the Monsoon Experiment-1979 (MONEX) was devoted to the study of monsoon depressions especially during their formation stage (Douglas, 1987). Some of the recent studies concerning the synoptic and dynamical structure of depressions include Sarker and Choudhury (1988), Prasad, *et al.* (1990), Warner and Grumm (1984) and Mandal, *et al.* (1987).

#### 5.5.2.2.1.1 CHARACTERISTIC FEATURES OF MONSOON DEPRESSIONS

- (a) The synoptic-scale monsoon depressions with a central pressure of around 992 hPa propagate westward with a speed of roughly  $5^{\circ}$  longitude per day. These depressions are similar to those over the tropical Atlantic and Pacific Oceans, many of which are known to become typhoons. These depressions, however, do not intensify into tropical storms since they form very close to land and move inland soon after their formation, thus having a very short life over the sea. Secondly, very strong vertical wind shears (low-level westerlies and upper-level easterlies), which are a feature of the monsoon circulation in this area, may be a strong inhibiting factor in their further development (Krishnamurti, *et al.*, 1975);
- (b) The surface pressure geometry of monsoon depressions is usually 2–3 closed isobars at a 2 hPa interval. They are often elliptical in shape and elongated in the east-west direction with the major axis being  $5.5^{\circ}$  longitude and a minor axis of about  $4.5^{\circ}$  latitude (Rao, 1976);
- (c) The cyclonic circulation of a depression extends up to 1 000 km in the horizontal and up to 9 km in the vertical. It has a horizontal wavelength of about 2 000 km. In the composite structure (Krishnamurti, *et al.*, 1975), maximum cyclonic components are found at the levels between 0.9 to 1.5 km (with a speed of  $15 \text{ m s}^{-1}$ ) at a distance of 300–400 km from the centre. The cyclonic vorticity gains in strength reaching a height of up to about 800 hPa and decreases above, reversing its sign in the upper troposphere. The zone of maximum cyclonic vorticity lies

- in the south-west sector of the depression. The normal absolute vorticity field in the lower troposphere associated with the monsoon depression is about  $7 \times 10^{-5} \text{ s}^{-1}$ . To the south of the depression, there is superposition of westerlies of the planetary-scale monsoon flows and the flows associated with the depression. In this region, strongest winds (50 knots) may occur (Krishnamurti, *et al.*, 1975);
- (d) The depression centre is found to slope in the vertical to the south-west or west of the sea level centre. Individual cases of deep depressions show little tilt in the vertical at least up to 500 hPa (Sikka, 1977). Prasad, *et al.* (1990) have also found that during the intense stage of a depression there is no tilt in the vertical;
  - (e) The rainfall distribution associated with monsoon depressions usually has a maximum of rainfall in the south-west quadrant. Pisharoty and Asnani (1957) found that in those cases moving west to north-west on any particular morning, heavy rainfall ( $>>7.5 \text{ cm}$  in the preceding 24 hours) extends to about 500 km ahead and 500 km behind the depression centre. This area has a width of about 400 km lying almost entirely to the south of the track. Thus, heavy rainfall over the subsequent 24 hours on a particular day is distributed up to a distance of about 1 000 km ahead of the depression centre on that day. The zone of maximum rainfall is found to shift north-west and then north-east with the depression changing path from north-west to north and then to north-east. Generally 24-hourly accumulated rainfall in association with a depression is 10–20 cm and isolated falls exceeding 30 cm in 24 hours are not uncommon;
  - (f) Monsoon depressions have a cold core structure below the middle levels and warm temperature anomalies above. The thermal amplitude of the monsoon depression is largest near 800 hPa (about 2–3°C). A pronounced warm core ahead of the moving depression arises primarily from the low-level warm advection of desert air west of the depression. The cold core is pronounced below 600 hPa and there is a reversal of thermal structure above that level. Near 400 hPa the amplitude is small, only 1 to 1.5°C. The correlation of vertical velocity and temperature  $W'T'$  and of convective heating and temperature  $H'T'$  are important for the conversion of eddy available potential energy into eddy kinetic energy and the generation of eddy available potential energy from convection, respectively;
  - (g) Douglas (1987) studied the evolution of different terms of the vorticity equation. The divergence term (generation of vorticity by convergence) is positive throughout a deep layer from the surface up to 500 hPa. The horizontal advection term is negative in the lower/middle troposphere, thus indicating that lower values of relative vorticity are being advected into the domain from the north. The two other terms (vertical advection of vorticity and generation by horizontal gradients of vertical motion in the presence of vertical shear) are insignificant below 700 hPa. In the middle atmosphere, the divergence and horizontal advection terms are small and the others cancel out. The net tendency is small. In the upper troposphere, strong divergence tends to diminish rapidly the vorticity. There is a strong vertical import from below because both vertical gradient of vorticity and upward motion  $w$  are large at 300 hPa. Thus in the rain area, cyclonic vorticity increases below 550 hPa and decreases above this level. The transport of vorticity between the two levels is accomplished by cumulus convection;
  - (h) Many attempts have been made to explain the formation process of monsoon depressions. A synoptic-cum-dynamical explanation was offered by Koteswaram and George (1960) and Koteswaram and Bhaskar Rao (1963), whereby, following Petterson's theory of development applied originally to extratropical cyclones, they suggested that development of a monsoon depression over the northern Bay of Bengal takes place when an area of positive vorticity advection ahead of a westward moving easterly wave trough in the upper troposphere gets superimposed on the pre-existing monsoon trough which swings into the Bay prior to the formation of a depression. The movement of the upper tropospheric trough could be traced farther eastward to the Pacific. In some cases, the trough may be induced due to an extratropical system (Prasad and Krishna Rao, 1974). Later, theoretical approaches sought to explain the formation of monsoon depressions through the barotropic-baroclinic-CISK dynamics (Sikka and Gadgil, 1975; Shukla, 1976; Krishnamurti, *et al.*, 1976). These studies point out that in the early stages of development, barotropic dynamics play a significant role as the barotropic instability criterion  $\beta - \partial U / \partial y^2$ . The later stage of development as well as the maintenance of the depression are intimately related to the baroclinic and CISK dynamics in which the energy supplied by the release of latent heat of condensation becomes the major energy source for the depression. Using as case study a depression that occurred in August 1968, Krishnamurti, *et al.* (1976) have shown that the condition for the combined barotropic-baroclinic instability (the meridional gradient of potential vorticity vanishing somewhere in the domain) was also satisfied. Through a series of numerical experiments and energy exchange computations, the authors find that in the absence of baroclinic effects the flows are barotropically stable. However, if the baroclinic effects are incorporated, the flows gradually become barotropically unstable. The role of bottom topography and cumulus convection, as incorporated in their experiment by a primitive equation model, was highlighted. They concluded that the cumulus convective heating generates eddy available potential energy releasing heat at appropriate levels above the cold core of the

- depression, where a slight warm core is present. Here the rising of relatively warm air contributes significantly to the generation of eddy kinetic energy of the depression. The main result that comes out of their study is that the disturbance is primarily driven by cumulus convection;
- (i) Monsoon depressions are embedded in a highly sheared environmental flow. Their characteristic cloud pattern is a shear pattern in which dense overcast gets displaced in the direction of vertical shear in the layer in which the convection is embedded. Satellite signatures of monsoon depressions have been studied by Srinivasan, *et al.* (1971) and Choudhury, *et al.* (1985). The shear pattern cloud features of a monsoon depression are similar to those observed in weak stages of tropical cyclones (Dvorak, 1975) in which the dense overcast is always seen displaced down shear from the low-level centre.

#### 5.5.2.2.1.2 SYNOPTIC FEATURES PRECEDING THE FORMATION OF MONSOON DEPRESSIONS

The following synoptic features generally precede the formation of monsoon depressions and are considered favourable for cyclogenesis (Sikka, 1977):

- (a) The pressure drops in the northern Bay of Bengal without any significant fall or rise in other parts of the monsoon trough. This drop in pressure occurs either *in situ* or in association with the movement of a low pressure area from the east which may be the remnant of a typhoon. Low pressure areas moving from the east account for only about 20 per cent of the total number of formations in the season. On most of the occasions these westward propagating lows can only be seen in the 24-hour pressure change field;
- (b) The strengthening of the monsoon current over peninsular India and the central Bay of Bengal to over  $20 \text{ m s}^{-1}$ , which is thought to be associated with a fresh surge of cross-equatorial air. This increases the cyclonic wind shear in the northern Bay;
- (c) The formation of the initial centre of cyclonic circulation in the lower and middle troposphere (800 to 600 hPa), and its intensification and gradual descent to sea level;
- (d) The increase in the moisture content of the air within the middle troposphere (700-500 hPa) over the northern Bay of Bengal;
- (e) The increase in rainfall activity over the Bay islands and coastal regions of Burma, Bangladesh, Orissa and western Bengal;
- (f) The increased divergence in the upper troposphere over the northern Bay of Bengal as evidenced by diffusione of the flow at 200 hPa, downstream increase of easterlies/north-easterlies from Bangladesh to western Bengal, westward migration of perturbations in the upper tropospheric easterlies over western Bengal, and favourable shift in the position of seasonal anticyclonic circulation over the Tibetan region. However, on several occasions a mere visual examination of the routinely analysed upper-tropospheric charts may prove rather disappointing to suggest the presence of these features;
- (g) The persistence of a quasi-circular bright cloud mass (diameter 4–5 degrees) which is usually located to the south of the surface centre of the low pressure area in the initial stage of formation;
- (h) The eastward movement of a north-south trough in the lower troposphere lying over Orissa and Bihar towards the northern Bay resulting in the formation of a depression.

#### 5.5.2.2 MONSOON DEPRESSIONS IN THE AUSTRALIAN REGION

No precise definition of a monsoon depression exists in the Australian region, but in essence this is a cyclonic circulation located over land, within the monsoon shear line, and with maximum intensity in the lower tropospheric levels 850–700 hPa (McBride, 1984). Davidson and Holland (1987) also point out that there is no detailed climatology or precise definition of these depressions in the Australian region. However, they are warm-cored in the middle and upper troposphere in their formative stages. Monsoon depressions occasionally have low-level winds as strong as  $30 \text{ m s}^{-1}$  or greater, and even when located in the middle of the continent they can have a spiral rain band structure similar to that of tropical cyclones (McBride, 1984). The large-scale structure of a depression is very similar to that of a tropical cyclone (McBride and Keenan, 1982; Love and Garden, 1983). In many cases the monsoon depressions are transformed from a tropical cyclone as the latter crosses a coastline (McBride and Keenan, 1982). During their early development stage, both types of systems often show very similar spatial arrangements of curved mesoscale cloud lines.

#### 5.5.2.3 MID-TROPOSPHERIC CYCLONES

In certain tropical regions and seasons, cyclones reach their greatest intensity in the mid-troposphere. Atkinson (1971) discusses these systems in terms of two primary classes, namely subtropical cyclones — which occur over the eastern portion of the North Pacific and the North Atlantic Oceans during the cool season — and Arabian Sea cyclones, which occur near the west coast of India during the south-west monsoon season.

#### 5.5.2.3.1 SUBTROPICAL CYCLONES

Simpson (1952) showed these systems to be a major circulation feature of the subtropics during the cool season. He studied 76 of these systems, known as Kona storms in the Hawaiian Islands, which originate

when a closed upper-level low in the subtropics becomes cut-off from the main stream of the upper-level westerlies. Simpson identified two sources of these storms. Approximately two-thirds develop from occluded cyclones which become trapped at low latitudes by the blocking action of a warm high, and the remaining one-third result from the baroclinic development of cut-off lows in the mid and upper troposphere, which gradually extend their circulation to the surface. A major source of subtropical cyclones is also the decaying tropical cyclones, which have moved into the subtropical latitudes. Once formed, subtropical cyclones appear to have the same general structure and behaviour, regardless of its source.

In the Pacific, subtropical cyclones generally occur at a latitude of 15°N to 35°N and at longitudes between 175°E and 140°W, while similar systems were found by Simpson over the North Atlantic at a latitude of 15°N to 35°N and at longitudes between 30°W and 60°W, and which occurred most frequently between November and January. Based on the Pacific storms, Simpson developed composite models of these systems which included wind and precipitation distributions. These models exhibit the following characteristics:

- (a) The maximum wind speed and precipitation occur in the east quadrant of the storm at a distance of 200 to 500 miles from the centre, depending on the size of the storm;
- (b) With the exception of the few subtropical cyclones, which develop tropical cyclone characteristics, the central core of the storms (within 100 miles of the centre) is a region of weak pressure gradients and light winds;
- (c) In their final stages, these systems generally move into an area that is favourable to frontogenesis and regenerate as a wave cyclone;
- (d) Occasionally, due to the release of latent heat near the storm centre, they acquire the warm core characteristics of tropical storms before recurring and becoming absorbed in the polar westerlies;
- (e) Ramage (1961) also studied the wind and weather patterns associated with subtropical cyclones. Using conventional data and early TIROS satellite imagery, Ramage showed that the strongest winds, steepest pressure gradients, and greatest convergence occur at mid-tropospheric levels (between 600 and 400 hPa). Maximum horizontal convergence occurs near the 600 hPa level, thus resulting in general upward (vertical) motion above this level and sinking motion beneath it, except for the near-surface layer. The storm eye appears to be rather large with scattered clouds and little weather. Areas of significant weather are located between 100 and 300 miles of the centre, while beyond 300 miles only scattered clouds are evident;
- (f) A major difference between the Simpson (1952) and Ramage (1961) models is the distribution of weather about the storm centre. In the former, maximum precipitation falls east of the centre, while in the latter the weather is much more symmetrically distributed with respect to the storm centre. Ramage explained this difference by stating that Simpson did not differentiate between true subtropical cyclones, which are completely cut-off from the polar westerlies, and large-amplitude troughs in the polar westerlies, where the bad weather is generally concentrated east of the trough axis. Ramage also found that these systems are very persistent, lasting up to several weeks, and are mainly absorbed by large-amplitude troughs in the polar westerlies rather than simply decaying as a result of energy deprivation or frictional effects.

In a later study, Hebert (1973) discussed two types of severe subtropical cyclones accompanied by winds of gale force or greater, namely:

- (a) A cold low aloft with circulation extending to surface layers and maximum sustained winds (of gale force or storm strength) generally occurring at a radius of about 100 miles or more from the pressure centre. These systems sometimes undergo a transition and become tropical storms or hurricanes;
- (b) A mesoscale cyclone originating near an old front with maximum sustained winds of gale or storm strength and a radius of maximum winds generally less than 300 miles, the entire circulation sometimes encompassing an area initially less than 100 miles in diameter.

These marine cyclones may vary in structure from cold to warm core, are generally short-lived, and may ultimately evolve into major hurricanes or extratropical wave cyclones. The latter type were originally called neutercanes, but are currently classified as a subdivision of the broader category of subtropical cyclones.

These systems generally develop in a baroclinic environment and may or may not be most intense at mid-tropospheric levels. Part of the problem faced by the operational forecaster is how to categorize, classify and finally forecast the motion and intensity of these systems. In the past, conventional (ship) data, which may have indicated the presence of a low pressure centre in an area which otherwise had the appearance of being under the influence of a ridge of high pressure, tended to be ignored. Frequently, there were no other nearby observations to confirm the existence of such a low. Observations were therefore taken as either indicative of a transient condition and not likely to continue, or as communications transmission errors unless or until other information confirmed the earlier report(s).

The advent of satellite data, especially data from geostationary platforms, showed that these observations were frequently associated with areas of disturbed weather and therefore unlikely to be related to communications errors. Subsequently, Herbert and Poteat (1975) developed a technique to classify these systems based on available satellite data. The goals of their study included using the cloud features associated with subtropical cyclones in order to:

- (a) Differentiate between subtropical cyclones and tropical cyclones in the formative stages (winds of less than gale-force strength);

- (b) Estimate the intensity of subtropical cyclones; and
- (c) Develop criteria which would mesh with the Dvorak (1973) technique if and when these systems exhibited tropical characteristics.

Although their technique was developed for the North Atlantic, its basic features may be applicable to other tropical regions. They however caution the reader: "... as with all studies about tropical and subtropical weather, the relationship between the basic cloud features and observed winds and pressures for those specific areas should be determined from regional data". Guidelines extracted from the paper by Herbert and Poteat (1975) are given in Annexes 5.A to 5.C.

#### 5.5.2.3.2 ARABIAN SEA CYCLONES

These systems, which are the major producers of precipitation along the west coast of India, develop between 700 and 500 hPa in the monsoon trough, which lies across the north-west Arabian Sea during the period of the south-west monsoon season. Miller and Keshavamurthy (1968) discussed the characteristics of these systems based on the completion of a detailed study on data collected during the International Indian Ocean Expedition (IIOE). These data included conventional surface and upper-air observations, research aircraft reports and satellite observations. Wind, pressure, temperature, moisture and weather distributions associated with selected cyclones were composited with respect to the daily 500 hPa cyclone centre positions, which were used as the centre of a movable coordinate frame of reference. Some important characteristics of these systems are given below:

- (a) A composite kinematic analysis for the near surface (500–900 m) and the 600 hPa levels (Figure 5.10) shows that the only evidence of a surface disturbance is a weak trough near the coast, while at 600 hPa, a cyclone centre is well developed. The region of greatest vertical-cloud development and most severe weather is found slightly west of the cyclone centre;

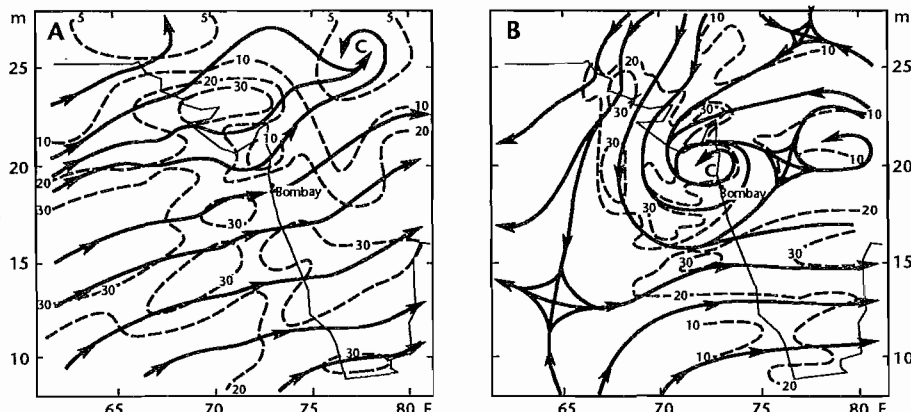


Figure 5.10 — Composite analyses for (a) a near-surface layer (500–900 metres); and (b) the 600 hPa level showing a well developed mid-tropospheric cyclone over western India during July 1963 (Adapted by Atkinson, 1971, from Miller and Keshavamurthy, 1968).

- (b) The thermal structure of these cyclones shows a warm anomaly above the middle levels and a cold anomaly below;
- (c) The maximum value of the absolute vorticity of these systems occurs near the 600 hPa level, with a vertical tilt of the vorticity maximum towards the west in an east-west cross-section and towards the south in a north-south cross-section;
- (d) In the middle levels, the area west of the cyclone centre is characterized by rising motions, while sinking motions prevail to the east due primarily to warm air advection to the west from land areas and cold air advection to the east from oceanic regions. The diurnal variation in vertical velocities is pronounced, probably as a result of the diurnal changes in both wind direction and speed. Krishnamurti and Hawkins (1970) used a five-level diagnostic model to study the structure and energetics of these mid-tropospheric cyclones over southern Asia. Their model, which included a parameterization of cumulus-scale convection and its role in the maintenance of these cyclones, can be used to explain the dynamics associated with the location of the most severe weather west of the cyclone's centre.

The cumulus- and synoptic-scale motions play the following dual roles in the maintenance of these cyclones:

- (a) Both scales contribute to a net warming of the air above the cyclone (diabatic warming by the cumulus-scale motion and adiabatic warming by the synoptic-scale descent);
- (b) The scales oppose each other in the transformation of eddy available potential energy into eddy kinetic energy (cumulus-scale motions cause a net generation of kinetic energy while synoptic-scale transform kinetic energy into potential energy).

Thus, these mid-tropospheric cyclones cannot be maintained as steady-state systems without cumulus convection because synoptic-scale energy conversions, friction, and energy export will feed on and soon destroy their available kinetic energy.

#### 5.5.2.4 UPPER-TROPOSPHERIC CYCLONES

There is evidence of another broad class of disturbances that does not fit any of the above models. These are upper tropospheric cold-core vortices that occur in association with tropical upper-tropospheric troughs over the north-west Pacific and the Atlantic. The mid-Pacific trough is a persistent climatological feature of North Pacific summer circulation extending from Alaska south-westward to Indonesia at 200 hPa. Aspliden, *et al.* (1965–67) have shown evidence of a similar feature in the North Atlantic. These troughs are bounded by ridge lines to the north and south. The mean configuration of 200 hPa ridge and trough lines during August over the northern hemisphere, as proposed by Sadler (1964), is shown in Figure 5.11. It is in these cold troughs that upper-tropospheric cyclones form, occasionally building downward to lower-tropospheric levels, and infrequently producing tropical storms.

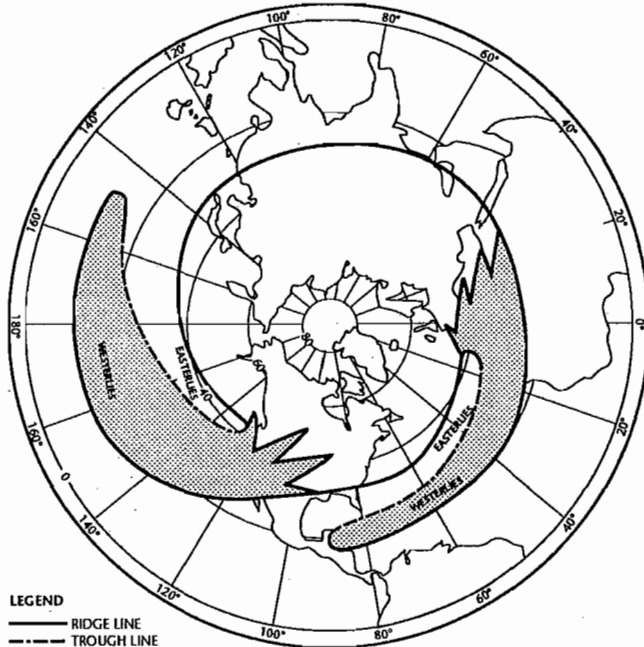


Figure 5.11 — The mean configuration of 200 hPa ridge and trough lines over the northern hemisphere during August (As proposed by Sadler, 1964, and reported by Atkinson, 1971).

These systems are most clearly defined in the upper troposphere with maximum amplitude near 200 hPa. Up to this level, the amplitude increases monotonically with height. The troughs (or cold lows) are colder than their surroundings, with the largest temperature anomalies near the 300 hPa level. The low centres are generally cloud free and show evidence of subsidence. Cloudiness, when it occurs, is confined to outer periphery of the lows.

These disturbances have been observed to move in either direction, but within the subtropical belt they usually track westward at about 5–6° longitude per day. Some are initiated by incursion of cold mid-latitude troughs into the tropics, while others develop *in situ*. Precipitation is associated only with stronger systems which extend through the entire troposphere.

A brief discussion of these cyclones in different regions is given below.

##### 5.5.2.4.1 NORTH PACIFIC

Sadler (1967b) made detailed synoptic studies of upper-tropospheric cyclones over this region. During a ten-day period in 1964, he tracked a series of these systems as they moved westward across the Pacific along the upper trough (using conventional data, aircraft reports and satellite pictures). Several of these upper-level systems developed downwards to the surface over the western portion of the North Pacific and were casually related to observed tropical storm formation. These studies documented the movement and influence of upper-tropospheric vortices on the formation of tropical storms over the region. Upper-level vortices were reflected as induced waves in the trade wind easterlies. During the process of transformation from a cold-core to a warm-core cyclone, the decay of the upper-level circulation was linked to slow advective warming as the system migrated westward into a region of much warmer upper-tropospheric temperatures, with some additional warming through the release of the latent heat of condensation by deep convective processes associated with the cold low.

Sadler's three-dimensional model for the circulation and cloud patterns associated with moderate to strong upper-tropospheric cyclones, which have penetrated downwards from the 200 hPa level towards the surface, is illustrated in Figure 5.12, whereby (a) shows that the vortex has penetrated through the 700 hPa level and is reflected at the surface as an induced trough, and (b) clearly illustrates that the vortex has penetrated to the surface level. The latter is generally restricted to the western portion of the North Pacific since colder sea-surface temperatures and a strong trade-wind inversion tend to inhibit surface vortex development further east. The surface circulation, which develops as a result of this process, will essentially be a function of the areal extent,

intensity and penetration depth of the upper-level cyclone. In some cases, the upper system may only be reflected at the surface as a wind speed minimum with no directional change, whereas in other cases there may be no indication of the upper system at the surface.

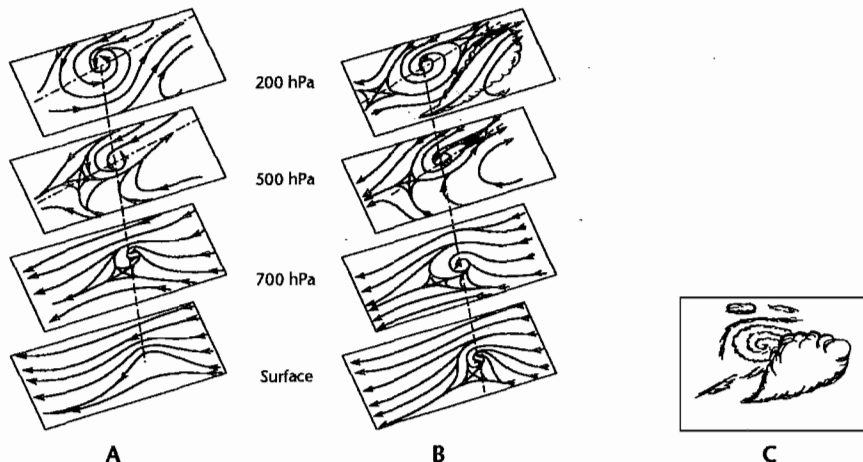


Figure 5.12 — A three-dimensional model of upper-tropospheric cyclones which have penetrated downward to (a) the 700 hPa level and (b) the surface level. Inset (c) depicts their typical satellite-observed cloud distribution (After Sadler, 1967b, as presented by Atkinson, 1971).

Surface systems appear to move westward (at about five degrees longitude per day) in conjunction with their associated upper-level cyclones. However, in some cases, especially during the transitional seasons in the Hawaiian Islands region, the upper cyclones move eastward, resulting in the induced surface trough or vortex moving upstream against the low-level easterly flow.

The clouds associated with upper cyclones depend on the penetration intensity, geographic location and the slope of the system. Figure 5.12 (c) shows a typical cloud pattern associated with the circulations modelled in both (a) and (b). The low-level convergence and major cloud features are in the eastern portion of the surface system, and because of the system's slope, are under a region of upper-level divergence. The vortex cloud pattern, which one can observe from the satellite photos, appears to best fit the circulation pattern near the 700 hPa level.

Vortices, which eventually develop into tropical storms, acquire the characteristic spiral (band) cloud pattern. Sadler (1967b) emphasized that "the appearance of the cloud systems as viewed by satellite is highly variable due to the variable character of the upper circulation systems and of the lower tropospheric thermal structure". Major cloud systems, however, may generally be observed south of the upper-trough line. If not directly associated with an upper cyclone, they may extend or even be removed a considerable distance from the trough, but they are generally confined to the region of westerly flow between the trough and upper-ridge line to the south.

#### 5.5.2.4.2 NORTH ATLANTIC

Aspliden, *et al.* (1965–67) studied the synoptic systems over the North Atlantic area using surface and 200 hPa data and satellite photos. They found the upper-tropospheric trough to be a major circulation feature during the warm season over this region. Generally speaking, their investigation showed that 200 hPa level cyclones located east of 50°W longitude move eastward, while those found west of 50°W longitude move westward. In the central portions of the Atlantic, there appeared to be a tendency for the cyclones to execute loops rather than to move systematically along any given direction or track. These cyclones move at speeds ranging from 0.1 to 5° latitude per day, over typical life spans of 2–31 days. While no cases of tropical storm development from upper-level cyclones were observed during the period of this study, the authors did note upper cyclones apparently reflected at the surface by wave-like perturbations in the easterly flow over the north-west portion of the region. Other studies, however, have indicated that these upper-level cyclones can, on rare occasions, initiate tropical storm developments over the North Atlantic.

Frank (1970) documented the distribution of weather associated with cold upper-tropospheric lows in the North Atlantic region. Using conventional data, he correlated the vertical depth of the layer influenced by a low with the accompanying weather pattern. Lows were designated as either wet or dry depending on the amount of associated weather. On the basis of this study, Frank developed a model (Figure 5.13) of the cloud distribution around upper-level cold lows by averaging the satellite-derived cloud cover in two-degree latitude-longitude grid squares surrounding the low for 13 cold-low cases. Within the central one-degree square, the mean cloud cover was only 0.1, while a well-marked ring of maximum cloudiness (shown by a heavy dashed line in Figure 5.13, encircled the centre at a mean radius of about 145 miles. The cloudiness around these lows was observed to be asymmetric, with the greatest concentration of clouds to the east of the low centre (persistently high with a mean of 0.8 and a range of 0.6 to 1.0 observed in the individual cases examined). Except for the cloud tongue extending southward, the mean diameter of the outer edge of the associated cold-low cloudiness was approximately 600 miles. This model, where the cloud-free central core is surrounded by a

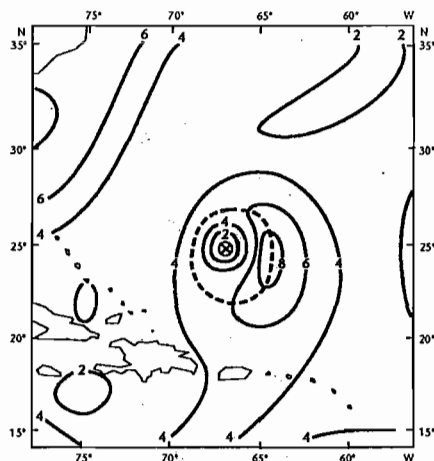


Figure 5.13 — Composite mean cloudiness (in tenths) derived from 13 cases of wet cold lows in the North Atlantic during the period 1961–1966 (After Frank, 1970, as presented by Atkinson, 1971).

cloudiness maximum, suggests the presence of direct circulation (cold air sinking and warm air rising), accompanied by a conversion of potential energy to kinetic energy. Therefore, these upper-level cold lows may be self-sustaining, thus not requiring an outside energy source.

In another study, Carlson (1967) compiled composite data (wind, height, temperature, moisture, vertical velocity, clouds and weather) for a six-day period during October 1965 associated with a steady-state cold low over the eastern Caribbean Sea (Figure 5.14). He observed that the vortex extended to between 500 and 700 hPa as closed circulation. At 700 hPa, a pronounced trough was present, while at the surface, only a weak easterly trough was evident. In the cloud and weather distribution with the low, the main cloud shield was located east of the upper low and trough. The region of significant convection occupied only a small fraction of the total area, with fair weather cumulus and a few towering cumulus clouds persisting west of the upper trough.

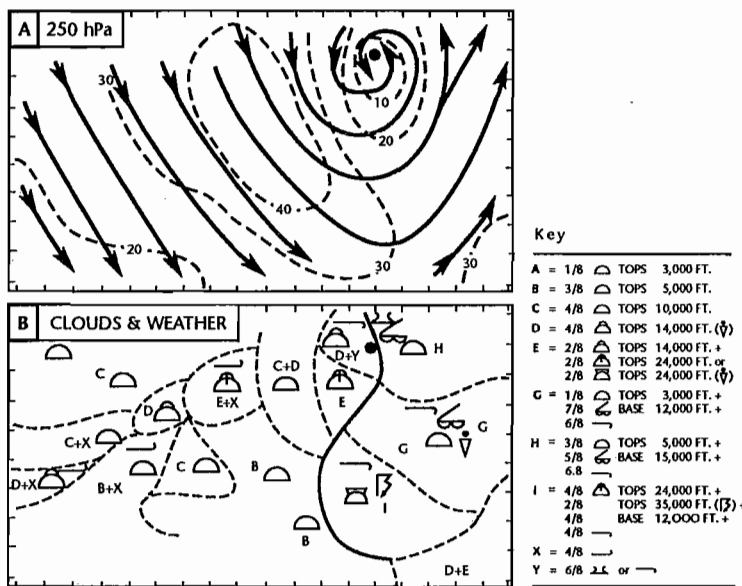


Figure 5.14 — (a) Composite 250 hPa circulation; and (b) cloudiness/weather pattern during a six-day period associated with an upper cold low in the Caribbean during October 1965. Tick marks around the border 1° latitude or longitude. The main cloud shield is enclosed by the scalloped border and the region of significant convection by the stippled area, "I" (After Carlson, 1967, as presented by Atkinson, 1971).

#### 5.5.2.4.3 TEMPORAL STORMS OF CENTRAL AMERICA

These are systems related to upper-tropospheric cyclones, occurring in the eastern North Pacific near and over Central America (from June to November, but most commonly during July and August). The rainfall and cloud cover produced by these storms are similar to those associated with hurricanes. However, the low-level winds associated with temporal storms are relatively weak.

Pallmann (1968) developed a model of low-tropospheric contour patterns and weather distribution associated with these systems (Figure 5.15). This model shows extensive areas of altostratus clouds on the east side of the system with embedded cumulonimbus and continuous rain over the north-eastern quadrant. Since these storms often remain quasi-stationary for periods of many days, they can produce catastrophic rainfall amounts and major flooding in Central America, where the orographic effects serve to enhance the precipitation and create more of a flood potential.

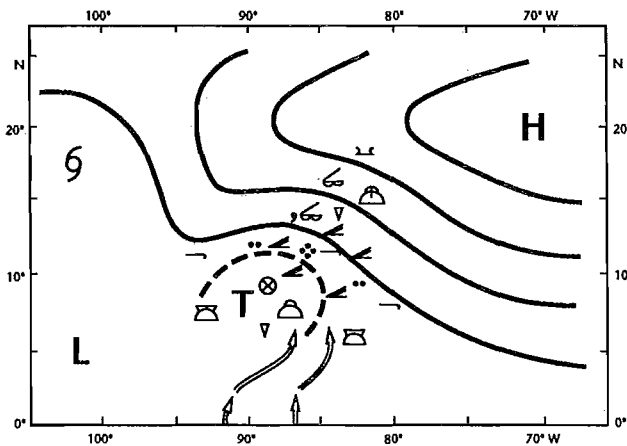


Figure 5.15 — Model of the low-tropospheric contour and weather patterns of a temporal storm (After Pallmann, 1968, as presented by Atkinson, 1971).

#### 5.5.2.4.4 SOUTHERN HEMISPHERE

Cyclones develop during the warm season in the tropical upper-tropospheric trough over the South Pacific. As in the northern hemisphere's tropical oceanic region, these upper cyclones occasionally trigger off tropical storm developments. Since the low-level monsoon trough in the South Pacific seldom extends east of 180° longitude, it seems likely that most cases of infrequent tropical storm development east of the International Date Line result from upper-tropospheric cyclones.

#### 5.5.2.5 LOWER-TROPOSPHERIC ANTICYCLONES

These systems occur mostly in regions and seasons when the monsoon trough is displaced by more than about ten degrees latitude from the Equator (LaSeur, 1964). Near-global coverage with geosynchronous satellites provides the meteorologist with an important data source which is needed to investigate the low-latitude dynamics of such systems. Winds at several levels can be derived from cloud motions by examining successive satellite photos (Hubert and Whitney, 1971; Young, *et al.*, 1972; Bradford, *et al.*, 1975; Novak and Young, 1976; Borneman, 1978). An example of the combined use of satellite and conventional data sources to derive a model of migratory equatorial anticyclones in the eastern North Pacific area (after Fujita, *et al.*, 1969) is shown in Figure 5.16. During the pushing stage, a large-scale flow from the southern hemisphere pushes northward, producing a curved band of intertropical cloudiness, which may be pushed as far as 1 000 km to the north. The formation of tropical storms along the zone in which air from the northern and southern hemispheres begin interacting with large horizontal wind shear and cyclonic relative vorticity is often observed.

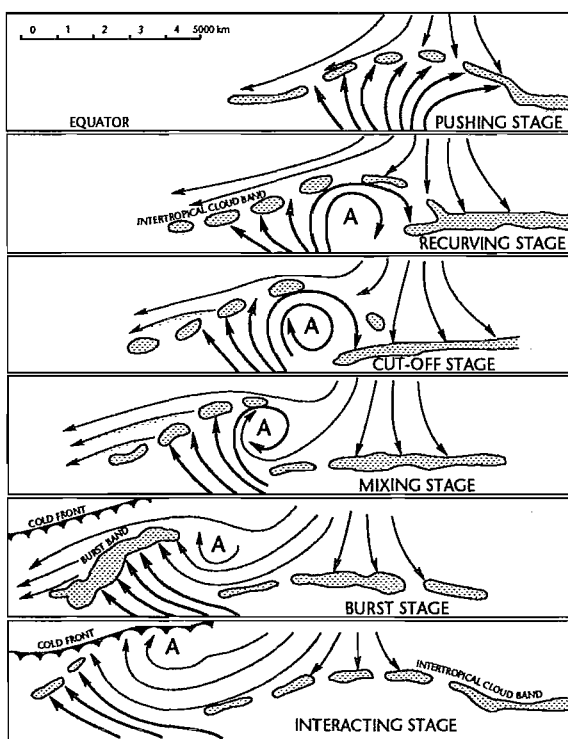


Figure 5.16 — Model of the six stages of equatorial anticyclones in the eastern North Pacific (After Fujita, *et al.*, 1969, as presented in Atkinson, 1971).

Within one to three days the flow from the southern hemisphere gains sufficient anticyclonic relative vorticity for the flow to start returning southwards — this begins the recurring stage — and the intertropical cloud band shows little change. Tropical depressions formed during the pushing stage tend to move out from the region of the tropical cloud band. After a day or so, the equatorial anticyclone is characterized by a closed circulation — called the cut-off stage — and the circulation centre is completely encircled by air from the southern hemisphere.

When a break in the intertropical cloud band occurs, the northern hemisphere trades flow to the south of the anticyclone, and the mixing stage takes place. Northern trades and southern hemisphere flow mix around the periphery of the anticyclone.

When a significant amount of northern trade air has been transported through the southern sectors of the equatorial anticyclone, the system begins to migrate towards the west/north-west. At the same time, the southern hemisphere flow continues to push the cloud band along the leading edge of the anticyclone. This joint push by both the northern trades and the southern hemisphere flow often results in a very intense convergence zone characterized by cyclonic vorticity. An intense band of intertropical cloudiness located in this region is called the burst band. This process is also known as the burst stage, and may last for one or two days. After this period, the burst band disintegrates into small fragments or isolated cloud clusters.

After the burst band has disintegrated, the south or south-easterly flow to the south of the equatorial anticyclone centre continues to be intense. This anticyclonic flow is still strong enough to prevent the south-easterly movement of a mid-latitude cold front and, subsequently, a wave development takes place along the front (the interacting stage). The entire life cyclone examined in the above model covers a time frame of about two weeks.

Fujita, *et al.* (1969) suggest that the development of these anticyclones is related to the cold sea-surface temperatures in the eastern Pacific equatorial areas. An analogous, but less pronounced, equatorial water temperature minimum is found over the eastern Atlantic during summer in the northern hemisphere. This may produce similar near-equatorial anticyclones in that region.

### 5.5.3 *Linear disturbances*

A linear disturbance is a synoptic scale system in which the vorticity or divergence (convergence), or both, tend to be concentrated in a zone whose length is much greater than its width (LaSeur, 1964). There are essentially two classes of disturbances which are recognized in the tropics, namely:

- (a) *Shear lines*: Narrow zones across which there is an abrupt change in the horizontal wind component parallel to these lines, most commonly used to refer to lines of cyclonic shear, such as the monsoon and upper tropospheric troughs. Shear lines can also be associated with the remnants of old frontal zones which have reached the barotropic environment of the tropics;
- (b) *Asymptotes*: Lines or curves of streamline convergence and divergence where streamlines are defined as a series of curves tangent to the wind throughout an instantaneous flow pattern. Asymptotes may also be observed independently within regions of relatively uniform directional flow but they are more typically associated with tropical vortices.

#### 5.5.3.1 SHEAR LINES

Shear lines are lines or narrow zones across which there is an abrupt change in the horizontal wind component parallel to these lines. In simple terms, they are lines of maximum horizontal wind shear.

When mid-latitude baroclinic systems (fronts) penetrate into the quasi-barotropic tropical regions, they are often difficult to track, especially over oceanic regions, by using conventional data. The standard methods of frontal analysis, that is, looking for discontinuities in the temperature, humidity and wind fields across the frontal zone, frequently fail to produce acceptable frontal positions once these systems have entered the tropics. Temperature and humidity (dew point) differences become very small or even completely obliterated as the two different air masses mix and become modified and more homogeneous. Only a slight wind shift may be evident along the frontal zone or shear line which, in many instances, may fail to indicate the frontal position properly.

Satellite imagery may be of special assistance to the analyst, providing some continuity and often identifiable cloud patterns to help locate these frontal positions in shear lines when more conventional data prove inadequate. Here again, we look to the development of a model to aid our analysis and understanding of these systems.

A particular model of identifiable cloud features associated with shear lines (fronts) in the tropics shows that the leading edge of these systems may be marked by a pronounced line of convection. A series of convective lines oriented parallel to the shear line or front and wind may occur on the poleward side of the main line or band. The average cloud tops associated with these systems are generally in the range of 10 000 to 15 000 ft (about 3 to 4.5 km), but low ceilings and heavy rainfall along the line may cause poor terminal weather conditions, especially in the vicinity of land masses which tend to produce marked orographic effects. The model by Palmer, *et al.* (1955) of the surface streamline/isotach pattern associated with a shear line (actually a remnant of a cold front) over a tropical oceanic area (the central Pacific) is shown in Figure 5.17. In this model, slight increases in wind speed and changes in direction are evident just north of the shear line.

When surface cold fronts penetrate the tropics to low latitudes over continental areas during the cold season, surface temperature, dew point, and wind discontinuities can often be maintained due to the repeated nocturnal radiational cooling in the clear, dry, polar air mass. In some regions, topographical features aid in the equatorward penetration of the polar air masses. For example, the Rocky Mountains of North America act to funnel cold air southwards over the Central Plains region of the United States and across the Gulf of Mexico. As a result, cold fronts called northerns or Tehuantepecers frequently affect Central America, bringing heavy rains to the up-slope regions and fohns on the lee slopes.

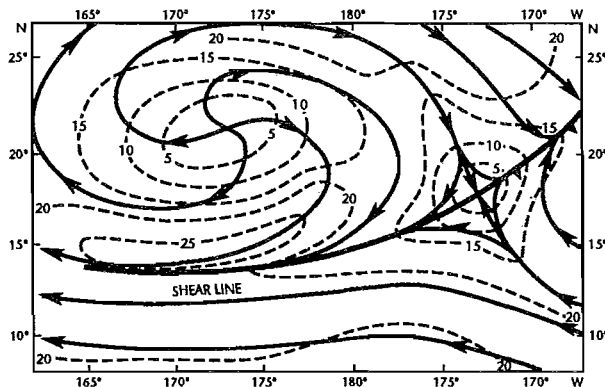


Figure 5.17 — Model of the surface streamline/isotach pattern associated with a shear line over a tropical oceanic area (After Palmer, *et al.*, 1955, as presented in Atkinson, 1971).

Tropical upper-tropospheric troughs and low tropospheric monsoon troughs can also be classified as shear lines or zones. Since these features frequently contain a series of cyclonic vortices, the vorticity and divergence values along these troughs will vary considerably. On some occasions, these systems are characterized by elongated directional wind shear lines with associated elongated vorticity and divergence patterns and may therefore be categorized as linear disturbances. Most of the significant weather near the upper-tropospheric troughs is associated with these cyclonic vortices along the trough lines. Near the low tropospheric monsoon troughs, however, there can be considerable cloudiness and rainfall even when pronounced cyclonic vortices are not evident. Furthermore, there is often a minimum of cloudiness in the monsoon trough line over tropical oceanic regions, with most of the cloudiness located on either side of the trough. Heaviest activity and precipitation are found on the equatorward side of the trough in the low-level westerly flow. Over some tropical continental areas, this monsoon trough line cloud minimum may be obscured by local topographical effects.

#### 5.5.3.2 ASYMPTOTES

These are horizontal lines along which horizontal confluence or diffluence of the airflow occurs. If mass confluence takes place in a plane near the Earth's surface, the incoming air rises at the confluence line (confluent asymptote) and, as a result, these lines are frequently associated with convective clouds. Conversely, if mass divergence takes place, the air near the surface spreads out, away from the line, and subsidence from aloft takes place along the diffluent asymptote.

Significant weather in the tropics is frequently associated with asymptotes of confluence (the rate at which adjacent flow converges along an axis-oriented normal to the flow at the point in question) in the lower troposphere, but the asymptotes are not associated with frontal discontinuities. These features sometimes produce extremely heavy rainstorms and extensive flooding. Palmer, *et al.* (1955) have presented several examples of lines of convective weather along asymptotes of confluence over the central Pacific. Figure 5.18(a) depicts one of these examples. The northern line of towering cumulus clouds is associated with a cold front which has penetrated to low latitudes, while the southern line of active weather between latitudes 5°N and 10°N is associated with a confluent asymptote in the tropical easterly flow. Low-level cyclones usually have one or more asymptotes of confluence merging into the circulation centre, while anticyclones are usually accompanied by asymptotes of diffluence. The location of asymptotes associated with vortices and cold fronts (shear lines) can be forecast with

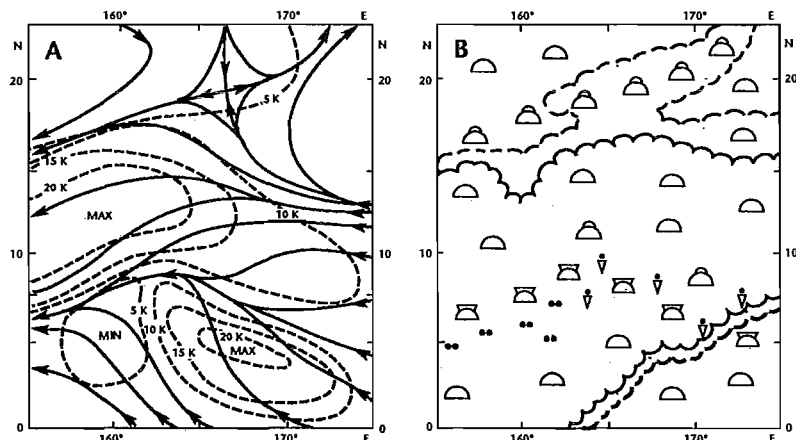


Figure 5.18 — (a) Streamline/isotach analysis for the 1500 ft. (457 m) level; and (b) weather distribution associated with confluent asymptote in the North Pacific on 6 April 1954. The innermost scalloped lines outline the region of broken to overcast high clouds and the outer broken scalloped line depict limits of scattered high clouds. Cloud forms and weather are indicated by standard notations (After Palmer, *et al.*, 1955, as adapted by Atkinson, 1971).

some degree of skill from continuity considerations of past vortex or frontal movements. On the other hand, asymptotes which occur independently and are not associated with vortices or fronts within the tropical air mass, although useful for explaining current weather, are extremely difficult to forecast in terms of formation, movement or dissipation (Atkinson, 1971).

## 5.6 Tropical synoptic analysis techniques

In synoptic meteorology, analysis is defined as a detailed study of the state of the atmosphere based on actual observations, usually including a separation of the entity into its component patterns and involving the drawing of families of isopleths for various elements. Thus the analysis of synoptic charts may consist, for example, of the drawing and the interpretation of the patterns of wind, pressure, pressure change, temperature, humidity, clouds and hydrometeors, all based on actual observations made simultaneously.

While this definition holds true for synoptic-scale analyses at both tropical and extratropical latitudes, it is clear that some synoptic analysis techniques have been more successful, and therefore more useful over certain regions of the globe than others. At mid and high latitudes, for example, "air mass contrasts are (generally) large and pressure patterns well defined. In the tropics proper there is really only one air mass, and the usually weak pressure patterns do differ significantly from the field of motion" (Saucier, 1955).

Problems associated with the measurement, collection, transmission, coding/decoding, accuracy, representativeness, and, often, paucity of meteorological data over tropical regions are discussed in detail by Atkinson (1971). It suffices to say that, the meteorologist working with tropical atmosphere — where synoptic-scale thermal, pressure and density gradients are usually small and diurnal variations large — must make use of analysis techniques which have either been adapted from extratropical models for the tropics or developed specifically for the tropics. The availability of satellite data has helped provide the meteorologist with valuable information at several levels over the otherwise data-void tropical regions. In the remainder of this section, tropical synoptic analysis will be discussed briefly in terms of manual analysis techniques and automated analysis techniques.

### 5.6.1 Manual analysis techniques

Although automated analysis products have recently become popular, practicable and available in many countries, manual analysis techniques are still used universally throughout the tropics.

In general, the levels which appear to be best suited for relating circulation features to existing weather patterns in the tropics, which is the main goal of such analyses, are a near-surface level, which is relatively free of frictional effects, and a level in the upper troposphere. In most tropical areas, the gradient level, which depicts the friction-free flow at about 3 000 ft (915 m) above the surface, and the 200 or 250 hPa level are suitable choices for the basic charts to be analysed. Gradient level data can be obtained from RAWINS, PIBALS, ship reports, ATOLL (analysis of the tropical oceanic lower level) winds, and satellite derived low-level winds. Data at the 200 hPa level are available from RAWIN, PIBALS, aircraft reports at suitable levels, and especially from high-level satellite-derived winds, which are of extreme importance over the otherwise data-void tropical oceanic regions.

Surface analysis of the plotted area includes, but is not limited to:

- (a) Defining the isobaric (pressure) pattern and synoptic-scale systems (highs, lows, tropical/easterly waves, shear lines, troughs, and fronts);
- (b) Determining 24 hour pressure changes; and
- (c) Delineating regions of precipitation, haze, fog, and significant cloudiness.

Recommended analysis procedures for completing the surface/gradient level charts are described in detail by Atkinson (1971) and Saucier (1955).

Streamline/isotach analyses of the wind field at various levels are perhaps the most common type of manual analysis found in the tropics. A basic model for this analysis technique is shown in Figure 5.19. The streamline/isotach analysis technique is especially useful in the tropics in view of the absence of well-defined pressure with a height-wind relationship at low latitudes.

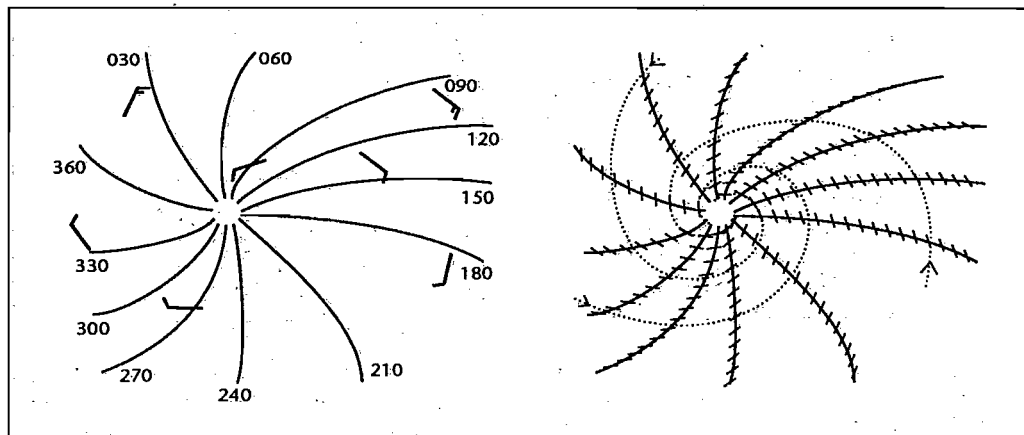


Figure 5.19 — A simple model of the streamline isotach analysis technique (After Dugdale, 1977).

Streamlines, lines whose tangent at any point in a fluid are parallel to the instantaneous velocity of the fluid at the point, are represented by continuous curves with arrowheads placed in such a manner that the wind direction may be inferred by interpolation at any given point on the chart. In a steady state flow, the streamlines coincide with the trajectories of the fluid particles. Otherwise, streamline patterns change with time. A two-dimensional, wind-vector field, usually the horizontal components of the wind vector, is completely specified by combining both streamlines and isotachs (isolines which connect points of equal wind speed).

Streamline analysis contains the following main features:

- (a) Circulations (cyclonic or anticyclonic);
- (b) Asymptotes;
- (c) Singular points;
- (d) Neutral points;
- (e) Waves

Cyclonic (or anticyclonic) circulations (vortices) are often represented by regions of cyclonic (or anti-cyclonic) flow in the streamline analysis pattern. Asymptotes are lines along which, generally, two neighbouring streamlines tend to converge or diverge. Singular points are points into which more than one streamline can be drawn or about which the streamline form a closed curve. Neutral points are points at which two asymptotes, one representing confluence and the other diffluence, intersect each other (singular points associated with cols). Finally, waves are depicted as sinusoidal configuration of parallel streamlines.

A complete analysis of the streamline/isotach pattern is extremely valuable in evaluating the kinetic properties of the explaining current weather conditions and, subsequently, for developing accurate weather forecasts in the tropics. One should remember that the spacing between two consecutive (adjacent) streamlines is not a measure of wind strength, nor does the streamline analysis alone completely define the horizontal wind field. Isotach analysis must be combined with the streamline analysis for this purpose.

The following types of charts are used in manual analysis.

#### 5.6.1.1 CONVENTIONAL CHARTS

Cross-sectional analyses have been used in both extratropical and tropical regions to illustrate and analyse the structure of the atmosphere along a vertical plane. The coordinates of a simple vertical space cross-section are the height above sea level along the ordinate, and a suitable horizontal spatial scale along the abscissa. In a synoptic cross-section (Saucier, 1955), the vertical reference scale is pressure, corresponding to the vertical reference of rawin/radiosonde data. The height scale may be converted to a pressure scale by either:

- (a) Using the pressure-height relationship in a standard atmosphere, where the vertical scale of the chart is linear in height and approximately logarithmic in pressure; or
- (b) Making the ordinate scale equal to the logarithm of the pressure, decreasing as height increases upward.

This type of vertical space cross-section provides an effective link between thermodynamic sounding diagrams and synoptic charts. As such, the vertical space cross-section is used to represent the distribution of various meteorological elements at a number of selected stations at a given point in time. Daily vertical space cross-sections along heavily traveled air routes, for example, are useful in briefing pilots.

Vertical time cross-sections have been found extremely useful in delineating and tracking tropical disturbances (waves, vortices, etc.). These charts are similar to the vertical space cross-section discussed above, except that they provide a depiction of the selected meteorological elements at a single station over a given period of time. In vertical space cross-section, the time is fixed. The ordinate scale is height (above sea-level) or some function of pressure (almost linear in height) and the abscissa is time. Figure 5.20 shows an example of a vertical time cross-section. Sounding and surface data are entered on these charts at the appropriate level above the station along the vertical line corresponding to the time of the observation. The result is a pictorial scheme which represents the time sequence of meteorological events at the station in question.

In the tropics, where disturbances generally move from east to west, vertical time cross-sections are usually plotted with time increasing to the right, so that circulation systems/features (troughs, ridges, waves, vortices) appear as they would on horizontal synoptic charts. In addition to providing an excellent data source for locating these tropical systems, these charts afford the analyst with an opportunity of examining the continuity in plotted meteorological elements during the time intervals between synoptic charts and in the space intervals between analysis levels. The reader is again reminded that these charts are designed to be used with and not as a substitute for, other diagnostic charts and/or data sources.

Checkerboard diagrams have been used to plot hourly weather observations (Atkinson, 1971). A standard checkerboard has 24 boxes in each row so that all the hourly observations at a given station can be plotted. In addition to their use as a means of rapid and frequent updating of the current station weather, this chart provides a valuable climatological aid for analysis and forecasting purposes. Local diurnal weather patterns (convection, showers, fog, cloudiness) can be readily referenced with the aid of this simple diagnostic technique.

Other supplementary or auxiliary charts, such as horizontal and vertical wind shear charts, rainfall analysis charts, nephanalyses, radar cloud-motion charts, etc., are in use at various stations throughout the tropics. In addition, analysts and forecasters, especially in the tropics, should be encouraged to develop other suitable means of portraying the current state of the atmosphere in order to serve their individual (station) analysis/forecast requirements.

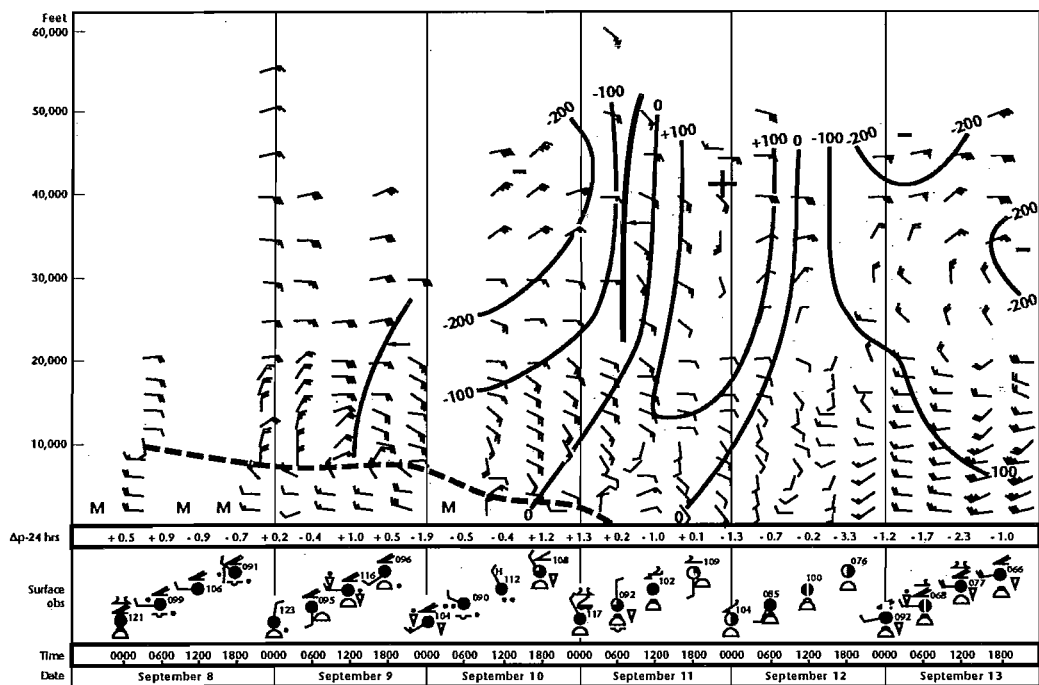


Figure 5.20 — An example of a vertical time cross-section. The heavy dashed line denotes the location of the equatorial trough (After Riehl, 1954).

Aerological diagrams are used in tropical analysis to infer atmospheric stability. It may be difficult to draw inferences from a single rawin/radiosonde ascent because these systems only sample a limited width of the atmosphere. It is worth noting that sub-synoptic-scale phenomena often make sounding data unrepresentative of the larger-scale environmental conditions. In effect, this means that thermodynamic or aerological diagrams are generally not as useful for tropical analysis purposes as they are for frontal, air-mass, cloud, and stability analyses in higher latitudes (Atkinson, 1971). However, these diagrams do provide some useful information for analysis and forecasting purposes. Perhaps the most important meteorological element that can be analysed with tropical soundings is the vertical distribution and time changes of moisture. Vertical temperature profiles tend to provide less information over the tropics equatorward of 20° latitude, where there is little daily variation in temperature from the mean, except with regard to changes in the layer affected by surface heating and cooling. Another exception is the temperature variation found in lower tropospheric levels due to daily changes in the height and/or intensity of the subtropical (trade) inversion.

While different charts are more useful than, or simply preferred to others, in general, aerological or thermodynamic diagrams are useful for illustrating the variations in the primary meteorological variables with height, and also for displaying certain hydrostatic and stability properties of the sounding data. The ordinate of these charts is usually some simple function of pressure, but is often approximately a true height scale. Temperature is usually displayed linearly along the abscissa. Each complete chart generally contains at least five sets of lines:

- (a) Isobars;
  - (b) Isotherms;
  - (c) Dry adiabats;
  - (d) Pseudo-adiabats; and
  - (e) Saturation moisture lines.

They represent transformations of the  $\alpha$  (specific volume),  $-p$  (pressure) or Clapeyron diagram.

In addition to the skew T-log p and the tephigram, which are used in the United States, the United Kingdom and Canada, other thermodynamic diagrams available or in current use include:

- (a) The emagram, which is formed by rotating the isotherms of the  $\alpha$ - $p$  diagram into a vertical position;
  - (b) The Stüve or pseudo-adiabatic diagram, which is popular in the United States because of its simplicity, and similarity with the emagram;
  - (c) The Refsdal aerogram, which has coordinates of  $\log T$ ,  $-T$ ;
  - (d) Bellamy's pastagram, which is a true thermodynamic chart based on the United States standard atmosphere. It is similar to the skew T-log p diagram, except for its upper portion, which is actually an emagram.

The selection of any individual chart for use in a tropical analysis should be based on the following three principles:

- (a) Its accuracy and adaptability for thermodynamic computations (particularly pressure height and stability evaluations);
  - (b) The geometric simplicity of the diagram, as related to the ease with which atmospheric soundings can be plotted and visually interpreted, and to its adaptation as a reference model for mentally picturing various atmospheric processes;
  - (c) The degree to which it differentiates humidity and thermal stratification in a sounding (Saucier, 1955).

Forecasters must make use of all available techniques. The automated and manual plots/analyses discussed here are designed to be employed as part of an integrated set of available techniques and strategies.

#### 5.6.1.2 AUXILIARY CHARTS

These charts fall into two major categories, namely, those produced by an automated objective analysis procedure and the more conventional charts which are produced by plotting and analysing the data manually. Regardless of how they are produced, auxiliary charts complement the products that we have already described (both manually plotted/analysed and objectively-produced analyses). Together, they provide the basis for the type of diagnostic reasoning needed by the operational meteorologist who is faced with the responsibility of predicting environmental conditions at some future time and place, or over some area, based largely on current, and past, observed conditions.

#### 5.6.2 Automated analysis techniques

Improvements in applied mathematical modelling techniques, coupled with advances in computer hardware/software technology, have had a very large impact on the number and type of products now available to meteorologists. The use of automated tropical analysis programs should continue to expand in the future as more and higher quality data become available and weather communications continue to become more sophisticated.

At present, automated analyses over the tropics are provided by several systems of the global data assimilation, numerical analysis and prediction. Recently more detailed numerical analyses in the tropics have been developed in conjunction with regional numerical weather predictions.

It should be noted that due to more sparse observational networks over the tropics and due to smaller spatial scales of tropical weather systems generated to a large extent by convective processes, the numerical analyses over the tropics are still of poorer quality than those in the extratropical latitudes, particularly in the Northern hemisphere.

The methods of numerical analysis in the tropics do not differ principally from those used in the extratropics.

A complete discussion of the methods of numerical weather analysis as well as the rationale for the automation of weather analysis and prognoses, and the major functions of an automated weather analysis and prognosis system are discussed in Chapter 3. In most cases, computerized products have been implemented at large meteorological centres in order to process copious amounts of meteorological data more effectively in relatively short periods of time.

### 5.7 Tropical forecasting methods

#### 5.7.1 Approaches to operational weather forecasting

There are broadly two approaches to operational weather forecasting:

- (a) *Subjective approach* — also known as the synoptic approach — is one in which a human forecaster attempts to predict future changes in the state of the atmosphere from its initial state taking into consideration both his theoretical knowledge and his experience of the evolution of weather situations in the past. The synoptic method of short-range forecasting involves a subjective assessment of the evolution and projection of the weather systems into the near future from the study of surface and upper-air weather charts. The success of the forecast depends upon the skill and experience of the forecaster;
- (b) *Objective approach* (numerical weather prediction), in which the known physical laws are used to describe the changes in the state of the atmosphere. Equations expressing the physical changes in the atmosphere are formulated and solved by numerical methods. The input needed for numerical weather prediction are the state of the atmosphere at an initial time, and the physical laws which govern the changes of that state. Numerical weather prediction is, therefore, described as an initial-value problem. The physical laws applied are based on the conservation of mass, momentum, energy, water vapour, and other gaseous and aerosol material in the atmosphere.

In practice, the application of numerical weather prediction models for weather forecasting has some inherent difficulties mainly because of two reasons. Firstly, it is never possible to define perfectly the initial state of the atmosphere due to the lack of adequate observational data. Secondly, a precise mathematical formulation of the physical laws governing the changes in the atmosphere is a complex problem and exact analytical solutions of these equations are not possible due to the non-linearities involved. The model equations have to be solved through computer-oriented numerical techniques. This itself is not an easily tractable problem. The numerical solutions are dependent to a great extent on the choice of boundary conditions and finite differencing methods which have to be designed carefully so as to ensure stable and realistic solutions. Notwithstanding these inherent limitations, the numerical weather prediction approach has reached a high level of sophistication with advancements in observing technology on one side and computing technology on the other. It has been increasingly possible now to make the horizontal and vertical resolution of the models finer and to incorporate into them a variety of physical processes of the actual atmosphere, with the result that the models have shown vast improvement in their forecast skill over the years.

The operational weather forecasts are classified into the following ranges:

- (a) Short range: Periods up to 72 hours (three days), which include:

- (i) Nowcasting: 0-2 hours (current weather);
- (ii) Very-short-range: 0-12 hours;
- (b) Medium-range: Periods beyond three days and up to 10 days;
- (c) Long-range: Beyond 10 days, a few weeks to a month, or a season or even beyond.

### 5.7.2 *Short-range forecasting techniques*

Atkinson (1971) indicates that some forecast skill can be shown by utilizing careful analyses and extrapolation of existing circulation and weather patterns modified for diurnal and topographical effects. The use of a systematic approach is suggested, including an integrated use of all available data, such as circulation and cloud prognostic charts, climatological aids, local-forecast studies, stability indices, radar, and satellite data.

A good starting point for preparing short-range forecasts is the consideration of circulation and cloud prognostic charts which are prepared from the latest available synoptic analysis, kinematic analysis (stream-line and isotachs), and satellite imagery (photos and derived data). Cloud prognostic charts should be prepared by consideration of climatology and recent nephanalyses prepared from satellite and other data sources (Atkinson, 1971). This analysis should outline regions of active convection and can be placed directly on satellite photos and/or synoptic chart in order to facilitate the extrapolation of moving circulation systems cloud features. Orographically-induced cloudiness, climatological (diurnal) effects and empirical relationships between circulation features and cloud patterns should also be taken into account.

Chang (1970) indicates that direct extrapolation of cloud systems in trade-wind regions may be useful as a forecasting technique. Systems moving into areas of cooler (warmer) sea-surface temperatures often decrease (increase) in intensity. Intensity changes in tropical cloud systems may also be related to interactions between upper- and lower-tropospheric systems. Frank (1969) showed that there is often a rapid increase in convection associated with westward-propagating cloud systems in the North Atlantic as they move under the region of a south-westerly flow aloft east of the upper trough. These cloud systems tend to decrease in intensity as they move west of the upper trough.

The importance of a thorough knowledge of tropical climatology cannot be over-emphasized. The forecaster should prepare or utilize conditional climatological summaries, which provide information, in probabilistic terms, on various categories of meteorological events occurring at various future time periods, based on the value of the initial category of the selected events. Typical examples include structuring conditional climatological summaries for ceiling, visibility, precipitation (occurrences and amounts), cloud cover, and any meteorological element or event which can be separated into distinct categories.

We have already noted that diurnal pressure and temperature changes are normally much larger than inter-diurnal changes at most tropical stations. Therefore, data displaying the mean values of these parameters at various hours during the day or on a monthly or seasonal basis become useful for forecasting purposes. Such tables can be prepared initially on a monthly basis, using hourly departures from the mean monthly pressure or temperature values. These data can then be combined and/or stratified into homogeneous samples on, for example, a seasonal basis.

The diurnal variation of other weather parameters can also be tabulated, or displayed pictorially with the use of a checkerboard, for forecasting purposes. These tabulations should include the hourly percentage frequency of occurrence for such parameters as ceiling, visibility, rainfall, thunderstorms, fog, wind speed and direction, and other parameters of local interest and importance. A knowledge of this aspect of climatology helps to keep the forecasted parameter within reasonable limits and provides guidance on the most likely occurrence times for the various parameters. In addition, this type of climatological information is useful for defining a reasonable range for each parameter, against which actual observations may be checked for errors.

Local forecast studies should be encouraged. If carefully planned and prepared, these studies can be of immense value to the tropical forecaster. In this way, meteorologists will learn how to make use of all available data sources to develop the empirical relationships which best suit their forecasting needs.

Atmospheric stability computations can be developed by using any of a number of aerograms. Several stability indices (SI) should be investigated by the forecaster and empirically related to significant tropical weather features as potentially useful in forecasting. SIs which are commonly in use, but which are now always useful in the tropics, include the Showalter SI, the lifted index, the total totals index (including vertical totals and cross totals indices), Fawbush-Miller SI, and the K value index. A description of these indices is given by Atkinson (1971). Further details on the use of climatology as an aid to forecasting in the tropics is found in Vasic (1977) and Giraud (1977).

A somewhat more extensive approach has been taken by Chelam (1977) who discusses forecasting techniques for western Africa and by Obasi (1977) who presents forecasting techniques in eastern Africa. Chelam, in describing qualitative forecasting techniques, limits his discussion to those techniques which do not necessarily require a dense data network on either a space or time-scale. Therefore, his comments may provide a valuable insight to tropical forecasters who are frequently deprived of the luxury of a dense data network.

Chelam's paper addresses the forecast problems associated with the elements of wind, temperature, humidity, visibility, precipitation, tropical disturbances, dust/haze, west African disturbance lines (squall lines), orographic influences, other synoptic scale systems in the west African region, and items of general interest over the tropics, such as the easterly jet stream, Hadley circulations and monsoon rainfall.

Obasi (1977) discusses forecasting techniques utilized in the east African region. Obasi briefly states the nature of the problems encountered in tropical analysis and then presents a description of several primary

models (the duct, bridge and drift) which can be employed to visualize or conceptualize tropical flow patterns. Five so-called secondary models have been developed by modifying the primary models mentioned above. These are the diamond, the displaced duct, the shear drift, the zonal gradient drift, and the step. Obasi describes these conceptual flow models in some detail. His discussion with respect to the practical considerations required when dealing with a paucity of data, and the need to compile composite data (including data available for non-synoptic times), should be of specific interest to all tropical meteorologists/forecasters who have had to face similar problems.

The following sub-sections describe the methods that are generally used for short-range forecasting.

#### 5.7.2.1 MODELS

The examination of sequences of weather charts covering long periods shows that the weather does not change in a completely random way. If it did, then forecasting would be impossible. It has been found that there is a tendency for certain changes to follow each other in a fairly orderly succession. There are times when a whole set of changes are observed on many separate occasions with only minor differences between one occasion and the next. As an example, there is the sequence of stages in the life history of a tropical cyclone. Although individual cyclones have their own peculiarities, they all have certain properties in common which can be combined into a typical model and which are of immense help in forecasting. This concept of a synoptic model was mentioned earlier.

In former days, before the three-dimensional ideas of air masses and frontal zones were introduced, the only models available were those relating to pressure systems. Attempts were made to relate all weather to a small number of typical isobaric patterns (lows, highs, troughs, ridges, cols, secondaries, etc.). Even today, this relationship of weather and pressure is perpetuated in operational weather forecast practices. However an inherent danger of using models for synoptic forecasting is that these models essentially describe some of the more usual features of the weather. It goes without saying that such descriptions specifically exclude unusual features and it is when the unusual occurs that a standard model breaks down. No single model can therefore be used successfully on every occasion, and a skilled meteorologist is one who is familiar with many models and who uses them all on appropriate occasions.

#### 5.7.2.2 EXTRAPOLATION AND INTERPOLATION

A very useful and widely practiced technique of forecasting is to predict the movement of existing weather by extrapolating the trends of the immediate past forward into the future. Careful analysis of a sequence of charts gives the velocities and accelerations of key features, such as pressure centres, fronts and trough lines. The motion of these features can then be extended into the future on the assumption that changes will continue to occur in a similar way. In general, this will not of course be absolutely true, but for short-period forecasts of up to 12 hours ahead, this is an excellent method of forecasting.

#### 5.7.2.3 ANALOGUES

One way of forecasting future developments that are likely to follow a particular situation is to search for similar situations (or analogues) in the past and see what happened then. The enormous variety of synoptic patterns makes it impossible to compare the present exactly with some past occasion, particularly since the comparison should really be a three-dimensional one. Even if only an approximate similarity is sought, records covering several decades are required. This in itself leads to a complex system of classifying the charts and a colossal labour is involved in any search. The method can really only be used in conjunction with an electronic computer.

#### 5.7.2.4 CLIMATOLOGY

Climatology is the study of the average, or mean weather conditions over a period and the variations of actual daily weather about this mean. There are two broad aspects of the subject, the first is statistical and the second is physical. In the first place, climatology is concerned with summarizing various aspects of the climate in a convenient way. This includes working out frequencies of occurrences, computing mean values and various measures of scatter about the mean, and estimating the significance of departures from the mean. In day-to-day forecasting, this sort of information is of little direct use but it is essential for a forecaster to have in the back of his mind, say, the normal temperature for the time of year and the extreme limits beyond which it is unlikely to go.

### 5.7.3 *Tropical numerical weather prediction*

#### 5.7.3.1 PREDICTABILITY OF TROPICAL WEATHER

Most of the NWP modelling effort has remained concentrated in the extratropical regions due to the existence of a reasonable satisfactory theory of the middle latitude atmospheric dynamics and the availability of a better data coverage. On the other hand, the progress in understanding the dynamics of the tropical circulation has been rather slow. Due to several factors, the predictability of day-to-day weather in the tropics in the short- and medium-range has remained low. The shorter predictability of tropics may be attributed to the following four main factors:

- (a) Relatively poor observational coverage in the tropics and difficulty in defining the accurate initial fields;

- (b) Weak mass-motion coupling and the absence of a sound dynamical framework to define the tropical motion systems uniquely;
- (c) The dominance of physical forcings over the dynamical forcings;
- (d) The lack of full understanding of the interactions between the cumulus-scale and the large-scale motions and inadequate representation of the convective processes in the tropical numerical models.

These characteristics contribute to relatively large errors in analyses and forecasts.

Predictability is usually referred to as the ratio of RMS error to the climatological standard deviation, which is the saturation value of errors. If this ratio is greater than 1.0 there is no skill in the forecast in terms of RMS error. Predictability or the period of useful forecasts is therefore defined as the number of days the RMS error remains below the climatological standard deviation (standard deviation of the day-to-day fluctuations).

It is reasonably well established that the prediction of instantaneous weather patterns too much in advance is impossible. There are clear indications that there is an inherent theoretical limit to determining the predictability of the atmosphere of up to a few weeks. While this is the case for instantaneous weather patterns, there are clear indications (Shukla, 1984; Miyakoda, *et al.*, 1983) that the predictability for time averages (five, 10, or 30 days) is longer, particularly in the tropics (Bengtsson, 1985). According to Shukla (1985) the limit of deterministic predictability for the tropics is only three to five days compared to two to three weeks for the mid-latitudes. Kanamitsu (1985) has shown with the use of ECMWF model that predictability in the tropics is much less (about two days) than that in the extratropics (five to seven days). The low predictability in the tropics is due to the fact that the standard deviation of the day-to-day fluctuations (the saturation value of errors) is much smaller in the tropics and that the instabilities associated with the growth of tropical disturbances are driven by moist convection, leading to larger growth rates than those of the dynamical instabilities of the mid-latitudes, which are driven by horizontal or vertical wind shear. Shukla has further shown that although the root mean square (rms) error of forecasts is quite small in the tropics, the ratio of rms error to standard deviation is more than 0.5 within one to five days, whereas it takes about five to 12 days to reach that value for the mid-latitudes. These conclusions are based on an assumption of an idealized, initial error field over the whole globe. In reality, the observational network over the tropics is worse than that over the mid-latitudes, and the prospects for deterministic prediction of day-to-day weather in the tropics appear to be dim. Shukla observed that the prospects for predicting space-time averages, on the other hand, are good. Partly because of smaller day-to-day variability in the tropics, and partly because of strong influence of boundary conditions, the space-time averages are more predictable in the tropics than in the mid-latitudes.

In a first study ever of the predictability of different scales separately, Smagorinsky (1969) concluded that the larger scales are more predictable than the smaller scales. In this context, Shukla (1985) observed that in the case of 40–60°N latitude for 500 hPa, predictability of the planetary scales (wave numbers 0–4) was more than four weeks compared to about two weeks for synoptic scales (wave numbers 5–12). For wave numbers 13–36, predictability was only a few days. The higher predictability of the planetary scale waves is due to the higher values of their amplitude and variability.

The mean (systematic) errors account for a very large part of the total error in the tropics, that is 80–90 per cent for height, 60–80 per cent for temperature, 50–70 per cent for the zonal component of wind, and 30–50 per cent for the meridional component, in the forecast range of 24 to 168 hours (Kanamitsu, 1985). In comparison, the percentage of mean error to total rms error in the extratropics is 20–30 per cent for all variables. It is, therefore, clear that if one could somehow remove these very large systematic errors, the tropical predictions would dramatically improve. This is a considerable advantage of the tropical modelling and holds promise for improvements in forecasting with improved understanding and better representation of physical processes in the tropical models.

Inadequacies of the current parameterization techniques rapidly degrade the motion field, which in turn produce more unrealistic heating fields. Kanamitsu (1985) demonstrated a strong sensitivity of systematic errors of the ECMWF model to prescribed profiles and distributions of diabatic heating in the tropics. Studies carried out with FGGE data in respect of the numerical weather prediction of the onset of a monsoon in 1979 (Krishnamurti, 1985) have also demonstrated a strong sensitivity of the onset of monsoons to the various cumulus parameterization procedures. The cumulus parameterization is therefore a problematic area in tropical modelling and needs a concerted effort. A solution to this problem may enhance the predictability of the tropics to a great extent.

Despite the inherent shortcomings of NWP in the tropics, as described above, much progress has been made in recent years in the development of numerical weather prediction models for low latitudes. The degree of sophistication of regional and global models has evolved considerably. The need to predict severe weather events has led to the development of high-resolution models with a comprehensive treatment of physical processes. This has been made possible by the availability of a much enhanced level of global observations and much faster computers. This has had a definite impact on the skill of numerical weather prediction models. It has been possible in recent years to improve the physical parameterization schemes substantially. Initialization schemes have been designed such that divergent motions retain important information on the Hadley- and Walker-type vertical circulations. Physical initialization procedures have been devised to include initial rainfall rates derived from a mix of satellite radiance and rain gauge data to improve the initial humidity field.

Many recent studies on the semi-Lagrangian semi-implicit version of the regional models have led to the accurate treatment of non-linear advection and the use of long-time steps. Not only have the regional models

evolved, but the global models are also evolving rapidly towards fine horizontal resolutions. The global models have the advantage that they have no problems of lateral boundary conditions. The performance of high resolution global models has reached a level where they can even be used as mesoscale models of quasi-static type. Mesoscale global models have shown remarkable skill in handling the entire life cycle of tropical cyclones. Several mesoscale regional models have emerged in recent years that deal with the prediction of heavy rainfall. A brief summary of some of these models is given by Krishnamurti, *et al.* (1990).

### 5.7.3.2 OPERATIONAL NUMERICAL WEATHER PREDICTION SYSTEMS AND MODELS

The present day operational weather prediction systems run with a four-dimensional data assimilation procedure. In this procedure, a forecast model is run continuously and model variables are corrected or updated from time to time by inserting the latest observations. In this way, the model fields are nudged towards observations. Observations can be inserted at, or around, the observation time in a continuous manner, or can be collected together and inserted intermittently at fixed intervals of, say every six hours. The former procedure is known as continuous data assimilation, and the latter, as intermittent data assimilation. Intermittent data assimilation is employed in most of the NWP operational systems, for example in the Bureau of Meteorological Research Centre in Australia, the European Centre for Medium Range Weather Forecasts (ECMWF) in the United Kingdom, and the National Meteorological Centre (NMC) in Washington. The United Kingdom Meteorological Office uses the continuous data assimilation procedure (Lorenc, *et al.*, 1991). A natural extension to the techniques is the four-dimensional variational assimilation. In this procedure, a repeated integration is carried out with modified initial states to find the model trajectory (forecast) which best fits the observations and/or other constraints. The techniques for modifying the initial state involves the use of the adjoint of the forecast model, followed by sophisticated (and expensive) minimization procedures. More details on the procedure adopted for data assimilation are found in section 3.4.

Depending on the requirements, there are various types of models used for numerical weather prediction, namely the scales of atmospheric motion to be resolved by the model and the time range for which forecasts are required. The scales of atmospheric motion systems and the relevant prediction models found in WMO (1987a) are listed in Table 5.1.

Barotropic and the single level primitive equation models represent a very useful starting point for numerical weather prediction in the tropics. Further details on these models are presented by Yap (1987).

Table 5.1  
Tropical systems and relevant prediction models

<i>Scale of the system</i>	<i>System</i>	<i>Model</i>	<i>Range of forecast</i>
Planetary scale (5 000 km)	Monsoon Hadley cell Walker cell ITCZ	Global	Long range Medium range
Large scale (1 000–5 000 km)	Monsoon depression Easterly wave	Global Fine-mesh, limited area	Medium range Short range
Mesoscale (100–1 000 km)	Tropical cyclone Squall lines Cloud cluster	Fine-mesh, limited area (movable area)	Short range Very-short range
Small scale (100 km)	Thunderstorm Sea breeze	Boundary layer and mesoscale models	Very-short range Nowcasting

At present, numerical weather prediction in the tropics is based mainly on multi-level primitive equation models. They can be separated into two major groups: global models, where the tropics constitute the part of computational domain, and limited area NWP models designed particularly for the tropical belt or for some region within the tropics. In the latter case, the time-dependent boundary values are supplied by global forecasts. The governing equations, numerical methods and parameterizations of physical processes in the models oriented to the weather prediction in the tropics do not differ principally from those used on a global scale or on a regional scale in the extratropics. Krishnamurti, *et al.* (1990) provide a description of a semi-Lagrangian semi-implicit version of high resolution tropical prediction model, which shows good skill in the circulation forecasts. In an earlier paper, Krishnamurti, *et al.* (1988) reported on tropical storm prediction with a global spectral model of T170 resolution. This kind of model handled the entire life cycle of typhoon Hope in August 1979, which made a landfall near Hong Kong. More details on recent tendencies in the development of NWP are found in section 3.5.

### 5.7.3.3 EXTENDED RANGE PREDICTION

The types of forecasts attempted in the medium- and long-range time scales, also known as extended range predictions cannot be as detailed as the short-range forecasts. While the short- and medium-range forecasts are intended to provide information about day-to-day weather, the long-range forecasts are structured in terms of tendencies or departures of selected meteorological parameters, such as above or below normal temperature or precipitation over a given region during a specified time period.

Until recently, the methods used in extended range predictions were based on statistical and analogue approaches. However, in recent times, numerical weather prediction models have established their utility in extended range forecasting and climate simulations. Substantial improvements have taken place in our ability to predict at least the larger scales of motion, mainly due to a considerable increase in meteorological observations, and a substantial increase in computing power and the resulting model development.

In the analogue approach, charts with the monthly mean temperature and pressure pattern together with charts of anomalies, or differences from normal, are prepared for extended range predictions. These charts and the sequence of synoptic weather types during the month form the basic description of the previous months' weather. A search is then made for any similar months in earlier years, which bear a close resemblance to the month immediately preceding — the expectation being that their sequels will give some indication of the likely character of the month immediately ahead.

In statistical methods, the predictand-predictor relationships form the basis of long-range forecasts. A large number of predictors are tested for their correlation with the predictand and a few highly correlated variables are selected to construct the regression equation.

The numerical weather prediction approach to extended range forecasting is simply to integrate the differential equations of a general circulation model (GCM) in time, using a small time step, and to project the solutions to 10 days, one month or one season ahead, or even beyond. The time step, as in the case of usual NWP models, is as small as five to 30 minutes depending on the time-differencing scheme employed. The small time step is taken so as to treat the physics and particularly the advection terms in the hydrodynamic and thermodynamic equations as accurately as possible and thereby avoid the use of any statistical, mechanistic, or vastly simplified models in the basic framework. The empirical relations or constants are limited to a minimum. The medium-range forecasts that cover about 10 days and the long-range forecasts that cover the range beyond two weeks are not much different in most of the basic formulations. However, the degree of importance of each term in the equation changes, particularly in the areas of hydrological cycle, in some of the sub-grid-scale processes, and in the lower boundary conditions. The last aspect eventually requires an air-sea model that expands the dimension of complexity to a considerable extent.

One significant difference between medium- and long-range forecasts is that the stochasticity becomes increasingly dominant as the time range is extended. Any small uncertainty at the initial time grows due to the inherent dynamic characteristics, and in the monthly time range the uncertainty develops to a sizable amount. In this respect, it is desirable to modify the basic equations beforehand to the so-called stochastic-dynamic model. However no efficient methods exist for computations in stochastic-dynamic type models, and the original GCM equations continue to be used (Miyakoda and Sirutis, 1985).

The models used for medium- and long-range forecasting are normally based on a set of primitive equations in the sigma coordinate system. The models have to cover the global domain. Most of the models have a spectral formulation because of certain advantages that this type of formulation offers, though grid point models are also used. The governing equations are the usual momentum, thermodynamic, and conservation equations mapped to a spherical geometry. The physical processes important in medium-range time scales include hydrological cycles, radiation-cloud feedback processes, moist convection, planetary boundary layer processes, and surface energy fluxes. Bengtsson (1985) gives a description of the dynamical and physical aspects of a medium-range weather prediction model. Bengtsson has observed that the medium-range forecasts are sensitive to the initial specification of soil moisture and sea-surface temperature, particularly in the tropics. The effect of snow cover has not yet been evaluated on the medium-range time scales, but may be of local or regional importance. ECMWF introduced values of snow and soil moisture (estimated from synoptic observations) in the operational forecast models and noticed a minor improvement in the forecast skill (Bengtsson, 1985).

In respect of tropical forecasts, the indication from both subjective and objective assessments is that there are serious deficiencies in the parameterization of convection, and a substantial effort to understand and correct these deficiencies is necessary. Forecast experiments reported by Bengtsson and Simmons (1983) have shown a great sensitivity to the parameterization of moist convection. The incorporation of physical forcing in the initialization has been demonstrated to improve the forecasts in the tropics.

In the context of long-range forecasting, there are two important influences which have to be considered, the internal atmospheric dynamics, and the external boundary forcings. There is an increasing amount of evidence that internal dynamics are indeed essential for the simulation of variability on a monthly time scale. The seasonal forecasts, if possible, can only be obtained by taking into account the effect of external forcings associated with the anomalies of sea-surface temperature, soil moisture, and snow/ice cover (Shukla, 1984). A most impressive example was the 1982–1983 *El Niño* and Southern Oscillation event which exerted an undisputable influence on the gross weather around the globe. This brings out the importance of tropical dynamics and air-sea coupling.

### 5.7.3.4 STATISTICAL INTERPRETATION OF NWP OUTPUT FOR THE PREDICTION OF WEATHER ELEMENTS

At present, the behaviour of synoptic-scale atmospheric systems are accurately predicted one to three days ahead by operational numerical weather prediction models. However, some of the actual weather elements are not predicted as the physical variables of the numerical models. Therefore, the interpretation of numerical predictions, i.e., forecasting weather from the pressure, height, temperature and wind fields forecasted by the numerical model, is a major problem for local weather forecasters.

In order to utilize the numerical products given by a forecast model, several statistical methods have been developed for the computation of forecasts of weather elements. Details of the statistical interpretation methods are discussed in Chapter 3.

## 5.8 Prediction of tropical cyclones\*

This section deals with the synoptic (including satellite features), and statistical and numerical weather prediction techniques of cyclone prediction and looks at various forecast methods (i.e. the verification of tropical cyclone forecasts). A review is made of various prediction techniques designed for forecasting both tropical cyclone intensity and movement.

### 5.8.1 Tropical cyclone formation

Tropical cyclones develop from initial convective disturbances known as cloud clusters or mesoscale convective complexes. As they evolve from a loosely-organized state into mature, intense storms, they pass through several characteristic stages. The very initial stage is sometimes referred to as a tropical disturbance, which is defined as a region of organized convection with a diameter of 200–600 km and having a non-frontal migratory character (Elsberry, 1985). The next three stages of storm development correspond to tropical depressions, tropical storms and typhoons/hurricanes, as defined in section 5.5.2.1. Frank (1985) suggests the following terms to describe the various stages of development of a tropical cyclone:

- (a) Genesis: Transition from a disturbance to a depression, the initial formation of a rotational circulation with a scale of a few hundred km;
- (b) Development: Transition from tropical depression to tropical storm; and
- (c) Intensification: The evolution from tropical storm to hurricane (mature cyclone).

Various considerations go into the forecasting of tropical cyclone genesis and development. The very first consideration is the climatology of cyclone formation in a given region. Climatology acts more as a constraint, that is, for example to know whether or not tropical cyclones have occurred previously in a given region. However, climatology does not provide any general guidelines on the actual genesis or future development/intensification of the disturbance. The genesis, development and intensification are basically related to the synoptic environmental influences. There are distinct cloud features associated with cyclone formation which are observed in satellite imagers.

The climatological, synoptic and satellite cloud imagery features associated with cyclone formation form the basis for synoptic methods of forecasting tropical cyclones. These features are described in the following sub-sections.

#### 5.8.1.1 GENESIS

##### 5.8.1.1.1 CLIMATOLOGICAL FEATURES

Tropical cyclones form over limited areas of the ocean basins, and are highly seasonal. This obviously means that there are specific environmental conditions for the genesis of tropical cyclones, and their further development and intensification. The climatological frequency of genesis is related to six factors, namely:

- (a) A warm and deep oceanic mixed layer (with sea-surface temperature of at least 26.5°C);
- (b) Above average middle level moisture;
- (c) Conditional instability through a deep layer;
- (d) Above-average low-level vorticity;
- (e) Weak vertical shear of horizontal wind;
- (f) A location at least a few degrees poleward of the Equator (i.e. a significant value of planetary vorticity).

McBride (1981a, b) and McBride and Zehr (1981) found that while the thermodynamic conditions necessary for tropical cyclone genesis are commonly satisfied, the formation usually does not occur until a pre-existing convective disturbance moves into a large-scale region with above-average cyclonic vorticity at low levels and anticyclonic vorticity at upper levels. Genesis usually occurs along the line of zero vertical wind shear between regions with stronger shears with opposite signs on either side. McBride found that this circulation pattern was described well by a parameter derived by subtracting the 200 hPa relative vorticity (averaged from 0–6° latitude radius) from the mean 850 hPa vorticity. Lee (1986) found that pre-cyclone cloud clusters had stronger middle- and lower-level cyclonic circulations from 2–8° latitude radius and larger inward eddy fluxes of momentum in the middle levels when compared to non-developing clusters.

Gray (1979) defined a genesis parameter as a product of terms containing functions of the above six parameters, given by:

---

\* Material for this section is drawn from the publication *A Global View of Tropical Cyclones*, which contains the proceedings of the International Workshop on Tropical Cyclones, Bangkok, Thailand, 25 November–5 December 1985.

$$P = f(\zeta_r + 5) \cdot \{1/(s_z + 3)\} \cdot (\partial\theta_e/\partial p + 5) \cdot (E) \cdot \{(\bar{RH} - 40)/30\}$$

where  $f$  is the Coriolis parameter,  $\zeta_r$  is relative vorticity,  $s_z$  is the vertical wind shear between 850 and 200 hPa,  $\partial\theta_e/\partial p$  is the lapse rate of equivalent potential temperature between 950 and 500 hPa, and  $E$  is an ocean energy parameter.

The genesis parameter is the product of three thermal factors and three dynamic factors. The six parameters considered above are, however, not independent. In the tropics, regions of high sea-surface temperatures are invariably correlated with conditional instability due to weak horizontal temperature gradients in the middle levels. High humidities in the middle levels also tend to occur in regions with warm waters. Virtually all areas with deep convection are associated with mean ascending motion and are moist aloft. The relative vorticity and Coriolis parameter can be combined into the absolute vorticity. Thus the large-scale climatological parameters associated with tropical cyclone formation may be summarized as:

- (a) Warm sea-surface temperatures coupled with a deep oceanic mixed layer;
- (b) Significant values of absolute vorticity in the lower troposphere;
- (c) Weak vertical wind shear directly over the pre-storm disturbance;
- (d) Mean upward motion and high middle level humidity.

Gray (1975) hypothesized that the cyclones form only during periods when these conditions are perturbed to values above their regional climatological means. He computed some critical values of the genesis parameter for a tropical depression to develop into a tropical storm for the Pacific and Atlantic Oceans. The average values of  $P$  for the two ocean basins are 73 U and 48 U, respectively, where  $U = 10^{-8}$  Cal K s<sup>-1</sup> cm<sup>-3</sup>. Mandal, *et al.* (1987) have computed similar genesis parameters in the case of a developing and a non-developing cyclone in the north Indian Ocean. They found an average value of 83.5 U as the critical value of the genesis parameter for development of a tropical cyclone in this area. Their results indicate that the critical value of  $P$  is larger in the northern Indian Ocean as compared to the Pacific and Atlantic Oceans.

The need for sea-surface temperatures greater than 26.5°C and a deep lower-level moist layer arise since the genesis and development stages are sensitive to surface evaporation, which are directly related to the sea-surface temperature. Higher sea-surface temperatures also favour latent instability and deep convection. A deep oceanic mixed layer is necessary to prevent the storm from cooling the surface waters through vertical mixing. However, except during the early and late periods of tropical cyclone seasons, and near the poleward borders of preferred regions of development, these two synoptic criteria are almost always present when there is a pre-existing disturbance. The establishment of the warm core necessary for a concentrated pressure fall and cyclogenesis is more dependent on dynamic rather than thermodynamic criteria.

#### 5.8.1.1.2 SYNOPTIC FEATURES

##### 5.8.1.1.2.1 LOW-LEVEL CYCLONIC VORTICITY

An important synoptic scale feature required for tropical cyclone genesis is a pre-existing disturbance with cyclonic vorticity containing abundant deep convection. Riehl (1954) pointed out the need for a pre-existing disturbance for a cyclone to develop. This cyclonic vorticity is required to produce the moisture convergence needed for net tropospheric warming.

McBride and Gray (1980) and Lee (1986) have shown that pre-cyclone disturbances have mean upward velocities of 100 hPa/day or more averaged over a four degree square area. The type of pre-existing disturbance constitutes one of the major regional differences in the initial development of a tropical cyclone. The synoptic weather patterns which lead to the formation of the pre-existing disturbance also vary from region to region. Once the cyclone has formed, however, there is basically little difference in the requirements for intensification (Gray, 1968). Most cyclones form in the shear zone between monsoons — usually cross equatorial westerlies and the trade easterlies (Sadler, 1967a). The enhancement of the flow on either side of this monsoon trough increases the low-level relative vorticity and makes conditions more favourable for genesis. The westerlies on the equatorial side may increase due to cold surges from the winter hemisphere, which raise the pressure at the Equator and lead to stronger pressure gradients and westerly flow along the Equator. Examples of interactions between long waves in the southern hemisphere and equatorial westerlies in the western North Pacific during the northern hemisphere summer were shown by He and Yang (1981).

The easterly flow on the poleward side of the monsoon trough can increase as a result of the intensification of the subtropical ridge. Strong and deep trades on the equatorward side of the subtropical ridge are an indicator of potential for cyclone genesis in the western North and South Pacific.

Gray (1968) estimated that about 80 per cent of all tropical cyclones originate in or just poleward of the ITCZ or monsoon trough. Most of the remainder form from disturbances embedded in an easterly trade wind flow, many of them in association with the tropical upper tropospheric trough (TUTT) (Sadler, 1976, 1978). Sadler showed that westward-moving intense cyclonic vortices in the TUTT lead to the initiation and intensification of typhoons in the western North Pacific. Shimuzu (1982) reported the formation of typhoon Ellis in June 1979 in association with a westward-moving upper-tropospheric cyclonic vortex in TUTT in the western North Pacific. A small fraction (3–5 per cent) form in subtropical regions near stagnant frontal zones or east of upper-level troughs. These so-called baroclinic systems are a special forecast problem in the western North Atlantic and North Pacific Oceans, where the fronts encounter warm waters at relatively high poleward locations compared to the southern hemisphere. Low-level surges from the opposite hemisphere can often play an important role in tropical cyclogenesis.

#### 5.8.1.1.2.2 VERTICAL WIND SHEAR

Weak vertical wind shear is necessary in order to protect the warm core from ventilation effects (drying or cooling). Strong vertical shear between the horizontal lower-level and upper-level flows is perhaps the single most important inhibitor of warm core development. The numerical experiments carried out in recent years (Kurihara and Tuleya, 1981, 1982; Tuleya and Kurihara, 1981, 1982, 1984) have established that low-level vorticity and vertical coupling between the lower and upper troposphere were important factors in cyclone genesis. The vertical coupling was favoured by weak vertical wind shear or a regime in which easterlies increase with height. Genesis is inhibited when westerlies increase with height, which agrees with observations. Tropical cyclones rarely form in regions exhibiting westerly shear with height. Such westerly shears occur in the trade wind regimes equatorward of the tropical upper tropospheric troughs, and in north-west Australia during the north-west monsoon flow period. Westerly shear associated with the passage of mid-latitude troughs that extend into the tropics is also thought to inhibit cyclone genesis.

#### 5.8.1.1.2.3 UPPER-LEVEL DIVERGENCE

A large area of anticyclonic vorticity at upper levels enables the disturbance to establish a suitable outflow mechanism for mass divergence (Erickson, 1977). A critical factor in tropical cyclone development, and perhaps in genesis, is the establishment of one or more upper-tropospheric outflow jets (Sadler, 1978). These jets are usually located in the north-east and south-west quadrants of northern hemisphere cyclones with the reverse pattern in the southern hemisphere. In the northern hemisphere, the jet in the north-east quadrant represents a linking of the anticyclonic outflow with the subtropical jet stream, the tropical upper tropospheric trough, or a penetrating trough from the mid-latitude westerlies. An adjacent upper-level cold low may also provide the necessary mechanism for enhancing the outflow. The south-west quadrant jet may represent an interaction between the cyclone and the tropical easterly jet, but it is often related to the presence of a strong upper-level anticyclone in the winter hemisphere.

#### 5.8.1.1.2.4 SATELLITE IMAGERY FEATURES

By far, the techniques most commonly used for monitoring and predicting the genesis and development of tropical cyclones involve the use of satellite imagery. This is the only available data source in many regions, and the least expensive to exploit in most of them. Most centres use some variation of pattern recognition technique developed by Dvorak (1975, 1984). The usual signs of cyclone genesis as seen in cloud imageries are:

- (a) The first sign of genesis that is detectable in satellite imagery is curvature of cloud band;
- (b) The presence of deep convection in curved bands, a circulation centre (marked by surrounding curved cloud bands) and persistence of these two features for at least 12 hours. Considerable variability, however, exists among the cloud patterns associated with individual pre-cyclone disturbances. Charts showing typical scenarios are generally used;
- (c) In the Atlantic and east Pacific, indications of cyclogenesis are often detectable one or two days prior to the initial stage of formation. The first sign in such cases is that the cloud cluster becomes elongated with a straightening of its northern boundary and an intensification of the convection;
- (d) As the disturbance intensifies, the major convective band becomes stronger and increasingly curved around the circulation centre.

The advent of geostationary satellites has made it possible for countries equipped with the appropriate data receiving and processing systems to compute cloud-motion vectors, or satellite winds, primarily at the cirrus and cumulus cloud-base levels. Several investigators have used these data (Erickson, 1974; Rodgers, *et al.*, 1977) to compute divergence, vorticity, vertical shear of the horizontal wind, and other properties of the fluid (atmosphere). This information can be applied, using synoptic techniques, to the study and forecasting of tropical cyclone development. Erickson (1977) and Arnold (1977), for example, have dealt with observed differences between developing and non-developing tropical disturbances, primarily of the western North Pacific ITCZ type. The results of these studies, based on satellite data alone, can be of use to tropical meteorologists.

#### 5.8.1.2 INTENSITY CHANGES

Intensity changes occur mainly in the core region of a cyclone. In relation to other regions, the core has very high values of the Rossby and Froude numbers, and of inertial stability parameters and is constrained to a comparatively small area with weak angular momentum (see section 5.5.2.1.1.5). Tropical cyclone intensity change is accomplished by a co-operative interaction between the convective and cyclone scales that is influenced by thermodynamical and dynamical interactions with the underlying surface and with the surrounding environment. The environmental influences can both aid and inhibit intensification. The roles of these interactions are discussed below.

#### 5.8.1.2.1 THE ROLE OF MOIST CONVECTION

The latent heat release in moist convection was recognized as a major factor in tropical cyclone intensification by Riehl (1954). The first quantitative specification of a co-operative interaction between the convective and cyclone scales came in the concept of conditional instability of the second kind (CISK), introduced by Charney and Eliassen (1964) and Ooyama (1964). This early theory described a linear scale-interaction process

in which frictional convergence of moisture by the large-scale circulation enhanced the cumulus convection, which in turn intensified the large-scale system, and so on. Such small-amplitude, linear interactions are now known to be too simplistic for tropical cyclone development, and the term CISK has come to be interpreted in the wider sense of the development of a large-scale disturbance by an unstable interaction with the embedded mesoscale convection.

The convection has a considerable impact on the intensity changes in tropical cyclones due to high inertial stability and rotational Froude number flow.

Usually in the tropics, absolute vorticity is small due to small values of the Coriolis parameter. Thus the Rossby radius of deformation (see section 5.5.2.1.1.5), which is the ratio of the gravity wave speed and the inertial frequency (or stability), is very large (often thousands of kilometres) for circulations with large-scale height. This quantity is an indication of the spatial domain over which gravity waves must extend before inertial effects become important. Since cloud clusters are much smaller than these values of  $L_R$ , they are very inefficient at converting latent heat release to warming, which is responsible for the decrease of the surface pressures and the increase of the rotational circulation. The energy from the diabatic heating gets dispersed radially by gravity waves over a scale comparable with  $L_R$  and little perturbation of the rotational flow is observed at radii much smaller than  $L_R$ .

However, in the core region of the tropical cyclone, the relative vorticity is unusually large, hence inertial stability is high and the radius of Rossby deformation is small. As a result, the clusters become more efficient in converting latent heat to warming.

Cyclone intensification appears to depend not on the amount of deep convection occurring within the cyclone system as a whole but rather on the amount of deep convection and the resulting magnitude of the in-up-and-out mass circulation which takes place within the system's central 0–1° or 0–2° radius core (Chen and Gray, 1984).

Tropical cyclones that develop an intense warm eye while unstable moist convection is maintained in the near vicinity are most capable of further intensification (Holland, 1985). For example, Dvorak (1984) shows that deep convection clouds with cold tops are associated with continued intensification. Merrill (1985) compared composites of intensifying typhoons (of similar intensity) in the western North Pacific. Since the temperatures were nearly the same in the lower troposphere, the two types of typhoons contained no significant differences in sea-surface temperatures. But the substantial upper-tropospheric temperature differences indicate that the intensifying typhoon composite is much more convectively unstable (outside the unresolved eye region) than the non-intensifying composite. There are several processes by which a cool upper troposphere can be established through environmental interactions.

#### 5.8.1.2.2 ROLE OF VORTICITY

As mentioned previously, the above normal low-level vorticity is a major factor in determining whether cyclogenesis will take place out of a cloud cluster. The low-level vorticity has two effects: (a) As the vorticity increases, the inertial frequency  $I$  increases, and the Rossby radius of deformation  $L_R$  decreases, which reduces the scale of response and increases the efficiency of conversion of latent heat release to warming. The warming, in turn, decreases the surface pressure and increases the rotational circulation; (b) As the surface rotation increases, frictional convergence (or Ekman pumping) increases the magnitude of the low-level inflow. The low-level inflow of mature tropical cyclones is maintained largely by this frictional convergence.

Once a cloud cluster forms a well-developed vortex with a distinct radius of maximum winds (RMW), the dynamical properties of the air within and outside of the RMW become very different. Inside the RMW, high relative vorticity exists since both the shear and the curvature terms make a positive contribution to vorticity. Outside the RMW, the relative vorticity is typically very small since the shear term is negative. In terms of the above arguments, the high vorticity region inside the RMW is much more efficient at converting the latent heat release to warming and increased rotational flow than is the outer region. Low-level frictional convergence near the vorticity maximum just inside the RMW tends to concentrate the latent heating in that area. This heating lowers the core pressure, strengthens the radial pressure gradient and the rotational flow, contracts the vortex, and enhances the frictional convergence. This, in turn, leads to enhanced convection and so forth. This classical mode of tropical storm intensification is widely accepted as a reasonable explanation of how a tropical storm intensifies into a mature cyclone. However, it does not explain the genesis of a tropical storm from a pre-storm disturbance, since convergence in early stages is primarily due to imbalances between the wind and pressure fields caused by latent heat release and/or non-linear advective processes and not to the small frictional convergence in the weak system.

#### 5.8.1.2.3 ENVIRONMENTAL INTERACTIONS

Tropical cyclones interact with adjacent weather systems to produce intensity changes. Examples include low-level wind surges in the trade wind easterlies or monsoon westerlies, an impinging upper tropospheric trough, with associated outflow jet development, a shearing-off by the imposition of upper-tropospheric westerlies, a development of forced secondary circulations by the collapse of a cold low in the upper troposphere, and the advection of cold or dry air into the cyclone core. Such interactions form the basis for most of the empirical rules for forecasting cyclone intensity changes. Three particular types of interactions, which are associated with rapid intensification or sustained development to a very intense system, are discussed below:

- (a) The first type of interaction seems to occur mainly in the North Atlantic basin. The interaction commences with a cold upper-tropospheric low and a tropical cyclone coming into close proximity by either *in situ* development or relative movement. A sudden filling of the cold low has been observed to be associated with the development of a strong outflow from the cyclone and the rapid intensification into an intense hurricane (Simpson and Riehl, 1981). Riehl suggested that this is due to a spontaneous collapse of the cold pool associated with an upper-tropospheric low. A solenoidal circulation is then generated with subsiding cold air in the low and rising warm air in the cyclone. The original potential energy is converted into kinetic energy of the overturning solenoid, a secondary circulation. According to Riehl, the cyclone then intensifies by a low-level import and upper-level export of angular momentum;
- (b) The second type of interaction involves the development of a strong outflow channel to the westerlies as an upper-level trough approaches or develops to the west of the tropical cyclone. This is a major mechanism in regions such as Australia and the South Pacific Ocean, where tropical cyclones normally develop in close proximity to the subtropical westerly flow in the upper troposphere;
- (c) The third type of interaction is largely a western North Pacific phenomenon in which the cyclone moves into an advantageous position relative to the tropical upper-tropospheric trough. Sadler (1967b, 1978) noted that this sequence of events is normally associated with the intensification of the cyclone and suggested that the underlying mechanism was the establishment of two outflow channels to the north-east and south-west.

#### 5.8.1.2.4 *UPPER-LEVEL OUTFLOW PATTERNS ASSOCIATED WITH TROPICAL CYCLONE INTENSITY CHANGES*

In a detailed study of a number of cyclones formed during the FGGE period in six ocean basins of the globe, Chen and Gray (1984) identified distinct upper-level outflow patterns associated with tropical cyclone intensification. Their study is based on the fact that if a tropical cyclone's outflow circulation is concentrated into narrow channels, there can result an important influence on the storm's inner core intensification. The authors define storm outflow according to the number of observable and concentrated outflow channels as single outflow channel, double outflow channel, and no defined outflow channel.

Each pattern is further divided into three or four sub-patterns according to the relative position of the 200 hPa anticyclone centre and the outflow channel directions resulting in poleward or equatorward outflow or both. The double channel outflow pattern has two upper-level outflow channels, one poleward and one equatorward. The double outflow channels often lead to rapid and very deep cyclone development. An example of double outflow channel is given in Figure 5.21, as observed in the case of typhoon Owen in the north-west Pacific on 25 September 1979. In this pattern, the tropical cyclone is located in the central region of the upper anticyclone. The central maximum wind speed of Owen increased from 45 knots on 24 September to 110 knots on 26 September, apparently due to this double outflow channel pattern. Another example cited by the authors is that of typhoon Tip, which also had a strong double outflow channel during its period of rapid development.

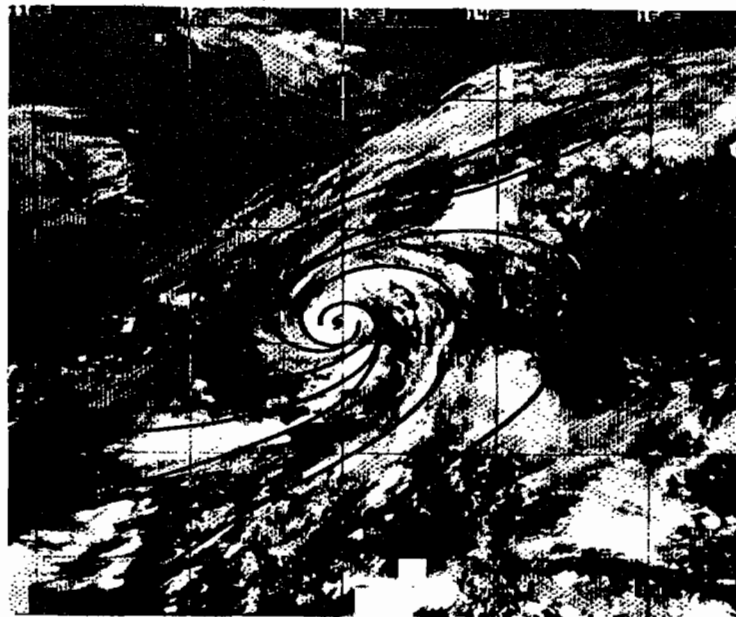


Figure 5.21 — Satellite photograph of Typhoon Owen showing double outflow channel on 25 September 1979 (Adapted from Chen and Gray, 1984).

When flows around an upper anticyclone are not linked up to a recognizable outflow channel it is called a non-outflow pattern. Non-recognizable patterns represent about 20 per cent of the cyclone intensification cases. The peripheries of non-outflow patterns are often feathery with short lateral cirrus lines. These cloud patterns indicate that the upper-level divergence is still strong but it is not organized into recognizable high speed outflow channels.

Statistical analysis of the intensification rates of the FGGE year tropical cyclone cases showed that double channel outflows are most favourable for rapid intensification. For single channel outflow patterns, tropical cyclones with centres located either to the west or to the east of a 200 hPa anticyclone are most favourable for deepest intensification rates rather than centre location.

An upper-level anticyclone on one side of the Equator can have a profound influence on the direction and magnitude of the equatorial outflow channel of a tropical cyclone of the opposite hemisphere. This is particularly the case when an intensifying equatorial southern hemisphere anticyclone moves westward and approaches the same longitude of a northern hemispheric tropical cyclone. The equatorward outflow channel of the tropical cyclone in this type of situation will be strengthened. A very rapid intensification of the cyclone often results. These upper-level cross hemisphere influences appear to be most prevalent for cyclone intensification in the north-eastern and north-western Pacific. Chen and Gray observed that when the storm's outer 4–8° radius 200 hPa outflow was concentrated in narrow and strong channels (as opposed to uniform and weaker outflow channels), the general conditions necessary for inner core cyclone concentration of deep convection were met.

#### 5.8.1.2.5 SATELLITE IMAGERY FEATURES

The technique developed by Dvorak (1975) is probably the best known and most widely used aid for forecasting tropical cyclone intensity changes.

The technique, which offers a systematic approach in estimating tropical cyclone intensities with satellite imagery data has shown good operational consistency in the field over a protracted period of time. These procedures and rules are designed to be used by meteorological analysts as a guide in complex situations, thereby attempting to achieve consistency in estimates by analysts dealing with the same data sets and resources.

Dvorak describes a method for determining tropical cyclone intensities from satellite-enhanced infrared (EIR) imagery. The paper is written with the needs of an operational meteorological analyst in mind, and contains a step by step list of procedures which have been designed to ensure consistency among analysts in obtaining estimates of tropical cyclone intensity. This model also includes ideas which increase the simplicity and objectivity of the analysis, while taking advantage of EIR/geostationary satellite data (available 24 hours a day). By utilizing the cloud features of a tropical cyclone or disturbance and its past history, estimates of its intensity can be made in an operational mode. The cloud features and past history (cloud pattern evolution) are used in conjunction with an empirical model of tropical cyclone development in the analysis. Guidance and constraints are provided by the model for use during periods when cloud patterns associated with such disturbances are in a state of flux and are, therefore, difficult to interpret. Adjustments in the cloud feature/intensity relationship are provided for in the model when such adjustments are indicated.

The cloud features observed in satellite imagery which relate to the intensity of a tropical disturbance are those which describe the cloud system centre and the dense overcast which surrounds the centre. EIR imagery provides discrete boundaries for measuring the features as well as an objective measure of their vertical depth. EIR imagery thus increases the objectivity of the analysis beyond that possible with visible pictures alone. Arnold (1977) examined numerous cyclones of all sizes and strengths. He concluded that the single most important result of the analysis of satellite pictures was the extreme variability of cloudiness on a diurnal, day-to-day and cyclone-to-cyclone basis. This variability was present in the amounts of deep convection, cirrus coverage and banding features of tropical cyclones. His study considered nine different stratifications of satellite data against various cyclone parameters, including pre-depression versus typhoon stage, slow- versus fast-moving systems, directional differences, rapid deepening versus steady typhoons, past and present cloudiness versus intensity, and equatorial versus trade-wind disturbances. He concluded that there was little hope of trying to relate the amount of cloudiness associated with an individual cyclone to any of the nine parameters he considered.

There is some controversy concerning the accuracy of the Dvorak technique in operational applications. Since tropical cyclones typically evolve through characteristic life cycles, one question is whether the satellite imagery has a prognostic skill beyond simply applying regional climatology to knowledge of existing intensity. The accuracies of intensity estimates are difficult to assess due to the lack of independent verification data in most regions. For the present, however, Dvorak's methods remain perhaps the most useful satellite techniques for forecasting intensity changes associated with tropical cyclones.

Rodgers (1984) suggested the use of visible and infrared spin scan radiometer atmospheric sounder (VAS) measurements of two meteorological parameters — upper- and middle-tropospheric thickness, and precipitable water — in tropical cyclone forecasting. He observed that the horizontal gradients and temporal changes in the upper- and middle-tropospheric thickness, and precipitable water are likely to indicate the environmental circulation patterns that may affect the motion or intensification of tropical cyclones, such as tropical upper-tropospheric trough and baroclinic troughs in the westerlies.

One of the mechanisms, as proposed by Gray (1979) is that the tropical cyclone formation and intensification may occur in regions where a lower tropospheric cyclone vortex is superimposed under a limited area (approximately 200 km radius) of dynamically-forced upper-tropospheric subsidence. This subsidence is caused by the upper-tropospheric convergence of the outflows from adjacent deep convective cells and environmental flow. Rodgers gave examples where this kind of subsidence can be recognized from the VAS data which may cause intensification of a tropical cyclone. This could be a useful aid in monitoring and forecasting tropical cyclone intensity and motion changes.

### 5.8.1.2.6 INTENSITY AND STRUCTURE CHANGE DUE TO LANDFALL

Tropical cyclones are known to change their intensity and structure on moving inland (landfall). Following landfall, a rapid decay and possible transition to another type of system occurs. In some cases, cyclones that have moved inland and weakened re-emerge into the sea to intensify again. The weakening of cyclones after crossing land is primarily caused by the loss of surface energy fluxes, particularly in the form of latent heat. The increased frictional dissipation at the surface also produces a stronger inflow, more rapid adiabatic cooling, and a boundary layer stabilization. Moist convection is then reduced and the cyclone rapidly fills. The region of maximum winds also typically expands outward and pressure outside the core region may drop slightly.

Over flat land, the boundary layer stabilization can cause the mid-tropospheric circulation to become uncoupled from the surface. Local downburst-type severe gusts may occur as this air mixes down into the boundary layer. Tornadoes may occur as convection twists the horizontal vorticity associated with the high vertical wind shear into the vertical. The cyclone also may re-organize and maintain this mid-tropospheric organization for a number of days. If supplied by a moist tropical air stream, such systems can produce heavy flooding over the land.

Large mountains will cause considerable disruption of the lower-tropospheric circulation of the cyclone. Very severe local effects are observed in mountainous terrain, including considerable gustiness and very heavy rainfall and flooding locally. Rapid depletion of the atmospheric moisture supply by heavy rainfall combined with dry down slope air flowing into the cyclone centre can result in more rapid decay.

### 5.8.1.2.7 TRANSITION TO EXTRATROPICAL SYSTEMS

The tropical cyclones change their intensity and structure after moving into higher latitudes, due to encountering strong vertical wind shears in the subtropical westerly flow. The cyclones may decay, transform to extratropical systems, or cause some form of baroclinic development, such as wave development on a frontal zone. Such structure changes may sometimes occur quite rapidly, and extratropical transition can be one of the most difficult events to forecast. The following structure changes may occur due to extratropical transition:

- (a) The temperature and moisture fields develop distinct asymmetries;
- (b) The organized core region convection becomes disrupted and disappears;
- (c) The circulation in the middle and upper levels is disrupted and weakens;
- (d) The precipitation shifts towards the front east quadrant;
- (e) Dry, cold air intrudes into the circulation from the front;
- (f) The area of gale force winds broadens.

### 5.8.1.2.8 RELATION BETWEEN INNER CORE AND OUTER REGION INTENSITY CHANGES

Merrill (1984) and Weatherford and Gray (1988) showed that there is a good relation between outer core wind strength and size. However, both size and outer core wind strength, and their changes, are only poorly correlated with core intensity and changes. Tropical cyclones may undergo considerable changes in either core intensity or outer core wind strength, while the other mode remains essentially constant (Holland, 1985). Weatherford and Gray (1984) cite some examples of typhoon cases illustrating the above point. In the case of supertyphoon Wynne in 1980 they observed that during the period from tropical depression to tropical storm, a simultaneous strengthening of the outer wind strength and intensification of core took place. But from the period of the initial typhoon stage, the cyclone's inner core intensification to supertyphoon stage occurred without a significant change in the outer wind strength. Then the outer winds strengthened for a couple of days without changing the inner core intensity. In the decaying stage, Wynne's inner core intensity decreased dramatically while maintaining the same outer wind strength. In another example, supertyphoon Mac in 1982 showed far more rapid inner core intensification than outer region strengthening. As Mac's inner core weakened, however, its outer region strength continued to increase. The authors reported a number of cases which experience few changes in their inner core intensity but large changes in their outer wind strength.

## 5.8.2 Track forecasting methods

The tropical cyclone motion is the end result of a complex interaction of external and internal influences on several horizontal scales. The first order external effect is environmental steering. However, this steering varies in space and time. Changes in the large-scale circulation and adjacent synoptic systems may also affect steering. Internal effects include storm scale influences and the non-linear interaction between the vortex circulation and the environment. In order to understand the role of various factors affecting the tropical cyclone motion, it will be good to have a look at its theoretical aspects.

### 5.8.2.1 THEORETICAL ASPECTS OF TROPICAL CYCLONE MOTION

While considering the dynamic track prediction methods it will be useful to examine briefly the theoretical aspects of tropical cyclone motion. This can be done by referring to the vorticity equation:

$$\frac{\partial \zeta}{\partial t} = -V \cdot \nabla \zeta - \beta v - (\zeta + f) V \cdot V$$

where the terms have their usual meaning. A cyclone moves in response to the vorticity tendency and will be displaced towards (away from) the region with maximum cyclonic (anticyclonic) vorticity tendency. It is seen from the above equation that there are three terms contributing to the vorticity tendency: vorticity advection, the so-called beta-drift, and divergence.

The contribution to vorticity tendency from the vorticity advection term comes in two ways — within the storm field due to asymmetry in the vorticity pattern, and uniform advection of the vortex by large-scale flow (environmental steering). The beta-drift term contributes to the vorticity tendency with positive (negative) tendencies in the northern hemisphere to the west (east) of the centre, i.e. the southward flow to the west advects higher values of planetary vorticity into this region, and the cyclone will tend to move westward into the region of increasing vorticity. The linear beta-effect introduces a secondary circulation by positive-negative vorticity tendency dipole (Holland, 1985). The secondary circulation with a cyclonic rotation to the west and anti-cyclonic rotation to the east of the vortex centre passes directly through the inner core and advects the centre towards the north. According to this interpretation, a north-westward displacement would result from the combination of this northward component and westward propagation due to the  $\beta v$  term. This explains the fact that the cyclones tend to move poleward and westward even in the absence of basic flow.

When non-linear advection processes are included, the flow associated with inner core circulation advects vorticity with cyclonic (anticyclonic) vorticity tendency on the poleward (equatorward) side. The initial effect of adding a non-linear advection term is a poleward translation. An adjustment due to the linear  $\beta$  term leads to a north-westward track in a steady state.

The size and shape of the meridional wind profile would have an influence on the displacement. In a large-size storm in which there are stronger winds at large radii, a larger meridional component will lead to a larger contribution by the  $\beta v$  term, which must be balanced by the horizontal advection term in a steady state. This adjustment process involves a distortion of vorticity pattern that leads to advection by the vortex circulation. Chan and Williams (1987) demonstrate that a vortex with this type of profile will have a north-westward displacement that is nearly twice that of a profile in which the meridional winds are weak at large radii. On the other hand, increasing the wind speeds near the centre of the vortex (increased intensity) does not change significantly the direction or speed of displacement. Some observational studies suggest that more intense tropical cyclones do have larger meridional components.

The contribution due to the divergence term emanates from the storm-scale influences which may result from latent heat release and warming. It is physically plausible that an asymmetric distribution of latent heat release will lead to a deflection of a low pressure centre toward the region of strongest warming. Further details on the theory of tropical cyclone motion are found in Elsberry (1985).

### 5.8.2.2 SYNOPTIC CONSIDERATIONS

#### *Environmental steering*

The most important consideration which goes into synoptic forecasting of tropical cyclone motion is the identification of environmental steering. In many early studies, the tropical cyclone was considered to move as a point vortex in a uniform non-interacting fluid flow. The dynamics of this uniform advection of the vortex is contained in the first term of the right-hand side of the vorticity equation considered above. According to the steering concept, tropical cyclones tend to move with the speed and direction of the deep-layer environmental flow. However, there is some controversy as to the best atmospheric level or layer that primarily determines the tropical cyclone motion. Recent studies, Neumann (1979) and Pike (1985) demonstrate that the tropical cyclone displacements have a higher correlation with the flow at mid-tropospheric levels. Neumann also indicates that a somewhat better performance can be obtained from a mass-weighted deep layer flow. Sanders, *et al.* (1980) demonstrated that an excellent estimate of the deep-layer mean flow can be obtained by using only three levels (850, 500 and 250 hPa). However, omission of the 500 hPa level results in considerable degradation in the estimate.

#### *Surface geostrophic steering*

A relative straight forward method which utilizes the surface-pressure chart and 24-hour surface-pressure changes is the surface geostrophic steering concept. It is used in conjunction with more sophisticated techniques and observing systems to obtain the current value of the tropical cyclone's motion (vital to analogue, statistical and dynamical techniques alike), and to assess the performance of shorter-range objective forecasts against the current synoptic situation.

This technique obtains both the zonal and meridional components of motion by measuring the pressure gradient across the storm. The pressure gradient must be measured from outside the tropical cyclone's circulation (usually from the first anticyclonically curved isobar or col outside the cyclone). The influence of the large north-south change in the Coriolis parameter on the geostrophic computation at low latitudes requires that the zonal component be computed as the difference of components measured north and south of the cyclone centre (WMO, 1979, Figure 3-8).

The basic assumption in this technique is that the air mass of the environment steering the cyclone is homogeneous. Since, even in the tropics, this is not a very good assumption, a modification to the steering is used, which is based on the estimated mean temperature difference across the cyclone for some selected thickness of the atmosphere. Where upper-air temperature data are available, it is convenient to determine the temperature difference required to correspond to the surface isobar interval being used in the analysis over the region of interest. In the absence of upper-air temperature data, the past and present motion of the cyclone or satellite pictures can provide some information about the temperature field. It follows that when the cyclone steers to the right of the geostrophic motion indicated for a homogeneous environment, cooler air is in advance, while steering to the left indicates warmer air is in advance. Evidence of troughs and ridges may be inferred from satellite cloud distributions and may be related to the presence of cold and warm air, respectively.

### *Use of pressure change and departure fields*

Pressure changes during the previous six to 12 hours (corrected for diurnal variations) have been used by several meteorological services to forecast tropical cyclone intensification and direction of movement. Pressure tendency charts — based on such corrected pressure changes, particularly at island and coastal stations — sometimes provide useful indications of the direction of movement, including recurvature of an approaching tropical cyclone. Pressure changes can also be helpful for short-range predictions at critical times. They can be used to determine landfall/no landfall forecasts, or assist in evaluating track changes during an approaching landfall situation.

It is also important for the forecaster to recognize the outer limit of the tropical cyclone circulation. Pressure changes inside the circulation reflect the cyclone's movement during the past few hours, while pressure changes outside the cyclone's circulation often indicate future changes in motion. When there are large pressure changes outside the circulation, their effect is to turn the cyclone at a right angle to the line connecting the isalobaric centre and the cyclone centre (WMO, 1979, Figure 3-11).

At lower latitudes, even a relatively small pressure change south-east or south-west of the centre (in the northern hemisphere) without a compensating pressure change opposite it may cause a significant directional change in the cyclone's motion. This is reflected in the geostrophic steering concept as a consequence of the large effect of the Coriolis parameter at low latitudes. The slower the tropical cyclone is moving, the more pronounced will be the change in direction — even for a pressure change of as small as 1 hPa.

The main advantage of the surface geostrophic steering concept is that it essentially only requires a current surface-pressure analysis and, therefore, can be used when no other aids are available. The use of pressure (height) changes in conjunction with the computation of present motion gives the forecaster an added dimension beyond pure persistence. In addition, it can help prevent forecast errors based on misinterpretation of centre fix data, which may imply radical departures from the previous smoothed track.

The major disadvantage of this technique lies in its sensitivity to inaccuracies in the surface or upper-air analyses which are usually drawn over data-sparse areas. Furthermore, the sensitivity of the computations to the Coriolis effect at lower latitudes can lead to large forecast errors for small (1 hPa) analysis errors. While pressure and height changes help in determining directional and speed changes, their magnitudes and movement relative to the tropical cyclone make the timing of these changes rather difficult.

### *Persistence*

A persistence forecast essentially assumes that the integrated effect of all the forces which have steered the tropical cyclone during some past time period will remain nearly constant, or at least predominate during some future period. Persistence is usually taken as the "smoothed" motion of the tropical cyclone during the previous 12- or 24-hour period. The resulting persistence forecast is then simply given by a linear extrapolation of this past motion for the following 12 to 24 hours. A higher order persistence can be made by taking both directional and speed changes during the past 24 hours into account. Higher order persistence forecasts are often difficult to make under operational conditions because of uncertainties in current and past cyclone positions.

When only a limited number of past centre positions are available, the forecaster must be cautious not to describe the cyclone motion by simply connecting these fixes with used film loops derived from geostationary satellites to detect and document oscillatory motions of tropical cyclones. An examination of land-based radar photos has also shown this type of motion. These motions are related to the interaction of the dynamics of the cyclone centre with the steering current. Tropical-cyclone eye diameters and positioning errors are usually of the same order (15 to 100 km). Therefore, these factors should be weighed in assessing whether the smoothed track extension should be to the left, through, or to the right of the present location. Unless there is strong evidence to the contrary, every effort should be made to fit all position locations so as to minimize directional and speed changes (that is, to maintain continuity).

Nearly all tropical cyclone prediction techniques include a persistence aspect. The main advantage of a persistence forecast is its inherent simplicity. These forecasts tend to perform best where and when the climatological frequency of occurrence is high. The advantage of persistence over climatology lies in its usefulness during anomalous movements at higher latitudes, especially if second-order effects are considered in the latter. Forecast verifications and variance reductions for statistical screening techniques, however, point out the rapid decrease in the skill of persistence forecasts beyond 12 hours. Experiments at the National Hurricane Center (Neumann, 1983) document the considerable improvements in short-range prediction that could result from improved initial motion vectors.

### *Climatology*

These forecasts make use of the temporal and spatial repetitiveness of tropical cyclone tracks produced by the synoptic scale patterns which steer the cyclones. Depending on the sample size, the resultant direction and mean scalar speed of motion can be obtained for latitude/longitude squares of as small as  $2.5^\circ$  and time periods of as short as five days. To make a track prediction, the climatological vectors at the appropriate locations are multiplied by the time interval and the displacements are added to the present latitude and longitude. The climatological forecast then moves the cyclone in the resultant direction at the mean scalar speed for the given location (latitude/longitude) and time of year. Forecasts can be modified if the cyclone moves to a position with different mean values during the forecast period.

Climatological forecasts of tropical cyclone motion show good skill where and when the frequency of occurrence is high. They do not perform as well at higher latitudes or when anomalous synoptic patterns exist. The recognition of the latter fact is an aid in itself. Tropical cyclone forecasters must be aware of regional climatology in order to be able to distinguish between normal and anomalous situations. A climatological forecast must be regarded as a "no-skill" forecast, since the only information included is the present storm location. A combination of persistence plus climatology may be expected to provide an improvement over separate techniques.

#### *Persistence plus climatology*

First described by Bell (1962), these forecasts are useful in many tropical cyclone forecast centres in the eastern hemisphere. Simply stated, if  $P$  is persistence, and  $C$  is climatology, the forecast is expressed in terms of a weighted model such that  $nP + mC$ , where  $n$  and  $m$  are weighting factors (frequently equal in weight). An alternative could be a blend that weighs persistence higher early in the forecast and climatology higher at longer ranges, say at 72 hours. Here, the persistence vector is obtained by linearly extrapolating the smoothed past 12-hour motion. The climatology vector is based on the regional climatology for the current tropical cyclone location and the time of the season. The forecast position, usually for 24 hours ahead, is then given by the mid-point connecting the two positions (obtained from plotting the appropriate values on a mercator chart).

The use of higher order  $P + C$  forecasts would be analogous to the examples given separately for persistence and climatology. The main advantage of either a first- or second-order equal weighting of persistence plus climatology, often called a 1/2 ( $P + C$ ) forecast because each factor is equal to 1/2, is its availability. This type of forecast can be prepared as soon as the current tropical cyclone location is determined. Other weightings and stratifications are possible, and may be useful, but require additional computations. Some disadvantages of this technique are its decreasing utility at higher latitudes, primarily due to recurvature, and insufficient climatology, and the presence of bimodal direction in some areas.

#### *Influence of large-scale and synoptic-scale circulation features on tropical cyclone motion*

The basic current that steers tropical cyclones may undergo fluctuations during the life cycle of the cyclone and affect its movement, due to several reasons. Some of the main influences are the following:

- (a) When the tropical cyclone is within the easterlies, the strength of the basic current is governed by the pressure gradient between the subtropical high and the equatorial trough. Strengthening of the subtropical high or shifts in the location or amplitude of the equatorial trough may produce surges in the trade winds. Spectral analyses of winds in the tropics reveal periodicities on time scales of 10–15 days and 40–50 days. These periodicities are associated with large-scale atmospheric motions which may cause subtle changes in the basic current that depend on the phase of the fluctuation;
- (b) In the western North Pacific where tropical cyclones can occur in all months of the year, the large-scale circulations are quite different during the Asian summer monsoon and the winter monsoon periods. During the summer monsoon, the upper tropospheric circulation is generally dominated by the Tibetan high. If this high is stationary, the upper-level trough over east Asia between the Tibetan high and the subtropical high over the western Pacific may deflect a tropical cyclone to the north and prevent landfall over China. If the Tibetan high is displaced eastward and merges with the subtropical high, the tropical cyclone will tend to be steered westward into China. Other re-arrangements of middle- and high-latitude systems can also affect the environment of western North Pacific tropical cyclones;
- (c) During the winter monsoon period, the basic current that steers western North Pacific tropical cyclones may be changed by several large-scale effects. A stationary east Asia blocking high that is generally near 50–70°N and 110–150°E leads to branching of the high-latitude westerly jet. One effect downstream of the block is a weakening of the subtropical high and of the westward steering component for the tropical cyclones, which may then have a more northward track. The blocking high is also favourable for the development of a long-wave trough in the west. A high-amplitude trough that extends into the subtropics is also favourable for northward movement and recurvature of storms. Because the blocking high and trough system is quasi-stationary, the tendency for more northerly tracks may be persistent. A westward extension of the subtropical anticyclone, on the other hand, would favour a more westward track of the tropical cyclones into the coast of China;
- (d) Adjacent synoptic-scale circulations can have marked influences on the tropical cyclone steering current. The approach of a mid-latitude trough creates one of the most difficult tropical cyclone forecast situations. If the trough amplitude is sufficiently large, the steering current will be shifted toward the pole and recurvature, with the possibility of greatly accelerated motion, is likely;
- (e) In an analysis of the Bay of Bengal cyclones, Srinivasan and Ramamurthy (1973) established a correlation between the position of the cyclones relative to the upper tropospheric ridge at 200–150 hPa, which dominate the large-scale circulation in these levels. The main conclusions, which may be applicable to other regions include:
  - (i) When the storm is well to the south of the subtropical ridge line, the storm movement is in a westerly to west-north-westerly direction. Farther south the storm is from the ridge

- line, and it is more likely to take a west/west-north-westerly track. The storm should be at least 3–4° latitude south of the ridge line;
- (ii) If the storm is within 3° of the ridge line, it is likely to take a generally northerly track than a westerly track. The storm may move slowly and may even remain stationary;
  - (iii) When the storm crosses over to the north of the ridge line, the movement gets an easterly component. Satellite-derived upper winds are useful in delineating the 200–150 hPa-level flow patterns over the sea areas and fixing the location of the subtropical ridge line in an objective fashion;
- (f) Interactions between two adjacently located tropical cyclones can cause unusual tracks that rotate about an intermediate point (Fujiwhara effect). The Fujiwhara effect has been found to be dominant if the separation distance between the two cyclones is less than about 6° latitude. As the separation distance increases from 7 to 15° latitude, the environmental steering effect becomes progressively more important than the Fujiwhara effect. Dong and Neumann (1983) found that most binary tropical cyclones situated in or near the intertropical convergence zone (ITCZ) in the western North Pacific had a counter-clockwise rotation;
- (g) Tropical cyclones which form in association with tropical upper troposphere lows may have an erratic movement because of a weak steering current that includes both low-level easterlies and upper-level westerlies. The interaction of an existing tropical cyclone with an upper tropospheric low can also cause deflections in the cyclone path;
- (h) Adjustments in the position of ITCZ may also affect tropical cyclone steering. Poleward displacement of the equatorial trough will intensify the north-easterly trades. If a strong equatorial anticyclone forms within the equatorial buffer zone and moves poleward to a position about 10° latitude from the Equator, the basic current in the lower latitudes will change from easterlies to westerlies. This situation may induce a sudden shift to a poleward or even eastward tropical cyclone track. Thus the tropical cyclone forecaster must be aware of cross-equatorial influences as well as subtropical and mid-latitude effects;
- (i) The Asian winter monsoon cold surges can also interact locally with the tropical cyclone circulations. The low-level cold surge may affect the direction, as the intensity of the cold and dry air is swept into the tropical cyclone circulation. An upper-level westerly jet may cause a rapid translation toward the north-east and east;
- (j) Sometimes the cirrus canopy of a tropical cyclone may be sheared off and leaves a weakened cyclonic circulation at low levels. If this shearing off occurs at night, the infrared imagery may reveal only the rapid translation of the cirrus canopy. Only when the visual imagery is available after daylight will it become evident that the low-level circulation remained behind. This type of situation may pose a difficult forecast problem and needs to be handled carefully.

#### *Satellite features*

Given the paucity of conventional observations in the tropics, satellite interpretation can be one of the most important analysis tools. Dvorak (1984) provides many examples of synoptic scale circulations revealed in the satellite visible or infrared imagery that subsequently affect the tropical cyclone track. For example, changes in the orientation of the clouds, along the poleward edge of the system provide a clue to forecasting recurvature as the tropical cyclone interacts with a mid-latitude trough. The water vapour imagery also provides additional information on upper-level features that may impact on tropical cyclone motion. Dvorak found that most north-westward moving storms turned northward when a cyclonically curving moisture boundary approached the storm from the north-west, and the moisture/cloud pattern built northward. Storms were observed to turn westward when a significant dissipation in the moisture/cloud pattern occurred north of the storm centre. Thus, the remotely-sensed data can reveal synoptic-scale changes that may not be observed by other data sources.

Studies utilizing satellite pictures have attempted to relate past changes in the cloud features associated with tropical cyclones to future changes in the direction of movement. A study by Fett and Brand (1975), for example, considers six identifiable cloud patterns and extrapolates the rotation of one or several of these features during the previous 24 hours to obtain the directional change in motion during the next 24 hours. Fett and Brand found that the western North Pacific cyclones tend to move toward the right following a clockwise rotation of the minor cloud features in time.

In a similar study, Lajoie and Nicholls (1974) used cloud features of the currently available satellite picture to obtain the succeeding 12-hour directional change. The primary feature used in this study was the first outer cloud band beyond the central cloud mass. Tropical cyclones were observed to change frequently their direction of motion to one given by a line connecting the centre of the cyclone to the most developed cumulonimbus cluster at, or near, the downstream end (in a cyclonic sense of the inflow current) of the outer cloud band and away from a sector devoid of cumulonimbus clusters.

The satellite imagery features are a useful aid to track prediction in data-sparse areas. They provide guidance in detecting sharp directional changes in tropical cyclone motion, which other techniques may not be able to predict with a good deal of skill.

Another aid in determining the direction of tropical cyclone motion is the extension of cloudiness. This corresponds to the depiction of the warm, moist tongue or thickness steering used in other techniques. Cloudiness often extends in advance of the direction of movement of these systems.

### 5.8.2.3 ANALOGUE MODELS

The basic philosophy of analogue models is that a given storm will move with the mean speed and direction of all storms that occurred in that region within some time interval centred on the current day. This may be thought of as another type of climatological prediction.

The technique aims at identifying an acceptable analogue in terms of the space/time tolerances or other specified conditions. The analogue process attempts to select historical storms which are temporally and spatially similar to the current storm. Analogue candidates are usually selected on the basis of such factors as time of the year, initial storm motion (direction and speed), and the position of the analogue storm relative to the current storm (latitude/longitude). Selected analogue tracks, translated to a common origin and combined with persistence, form the basis of the final forecast. A complicating factor in the selection of analogues may exist when more than one of the family of storms is associated with a given area and time of year. A prerequisite for the development and operational use of an analogue model is the availability of archived storm track data. Long series of data are available for most of the ocean basins except the north-east Pacific, where adequate data do not exist prior to the early 1960s.

Automated techniques for the selection of analogues have been developed for the Atlantic by Hope and Neumann (1970), for the western North Pacific by Jarrell and Somevill (1970), for the eastern North Pacific by Jarrell, *et al.* (1975), and for Australia by Annette (1978).

The analogue techniques also include a persistence aspect. In the hurricane analogue (HURRAN) scheme developed by Neumann and Hope (1972), each selected analogue is translated to the position of the existing storm and starts at the heading and speed of the current storm. In the first 36 hours of the forecast, a linear adjustment is made to the heading and speed. At 12 hours, the displacement is 2/3 due to persistence and 1/3 due to the movement of the analogue storm. The analogue models are simple and, if properly used, provide a useful guidance as a first guess in operational cyclone track predictions.

Two disadvantages of the analogue model are that it is not always possible to find enough number of analogues and it is expensive to search the entire historical sample each time to extract analogues. An advantage is that the probability ellipses associated with this technique provide useful information to the forecaster about likely error characteristics.

Temporal and spatial analyses of tropical cyclone tracks show that they tend to be repetitive and to be associated with identifiable and likewise repetitive patterns. Analogue models capitalize on the ability to identify families of storm tracks. By using a series of computer programs, the analogue method associates a current storm with its parent track, thus allowing inferences to be made about the future behaviour of the storm. At least conceptually, the analogue method has been used (in a subjective sense) by forecasters for a number of decades. The objective and routine operational uses of the method were precluded by the vast amount of data which formerly had to be processed manually. The availability and use of high speed computer systems at many tropical cyclone warning centres at present provide a means of rapidly archiving, retrieving, screening and processing large number of historical storm track data.

### 5.8.2.3.1 PROBABILITY ELLIPSES

When analogue forecasts are presented to the user in terms of probability ellipses, the most probable track, as a function of time, is given as the centroid of these ellipses. Less likely tracks are suggested by the size, shape and orientation of the elliptical bounds. When the orientation of the ellipses are along — rather than perpendicular — to the track, forecast problems can be expected to be related mainly to the speed rather than the direction of motion. These ellipses actually represent the projection of a three-dimensional bivariate normal surface on a two-dimensional plane.

When the bivariate normal distribution (probability density function) is integrated over a circular area, one can obtain the probability of a storm being within the given area at a given time. This can also be interpreted as the probability of a storm being within some given distance of a specific location (a city, for example) during the forecast period. Note, however, that there are many areas where the assumption of bivariate normality does not hold, for example, where local topography influences storm tracks or large land masses cause divergent storm tracks, which are best described by a bimodal rather than a unimodal bivariate normal distribution (Crutcher and Joiner, 1977).

### 5.8.2.4 STATISTICAL MODELS

Statistical models are based mainly on the use of regression techniques. There are three types of statistical regression models developed for cyclone track prediction: models which use climatology and persistence only as predictors (simulated analogue models), models which include, but are not limited to, predictors derived from observed synoptic data (classical and/or statistical-synoptic models), and models which include, but are not limited to, predictors derived from numerically predicted fields (statistical-dynamical models). Each of these models is briefly discussed below.

#### 5.8.2.4.1 SIMULATED ANALOGUE MODELS

A class of simple regression equation models for the prediction of tropical cyclone motion are called simulated analogue models. These models explicitly use climatology and persistence, and exclude all current synoptic data in their prediction equations, thus closely resembling analogue models. The predictors used by simulated analogue models are identical to those used by purely analogue models but are used in a

different sense to derive the equations directly. A characteristic of analogue models is the representation of forecast tracks in the form of probability ellipses depicting most probable tracks. Simulated analogue models also provide this capability.

The variance-reducing potential of simulated analogue models is derived from seven basic predictors, including the Julian day number, initial latitude, initial longitude, average meridional speed during the previous 12 hours, average zonal speed during the previous 12 hours, average meridional speed during the previous 24 hours, and average zonal speed during the previous 24 hours.

If available, the wind speed or central pressure (measure of storm intensity) may be included as an eighth basic predictor. Non-linear trends in the data can be accounted for by the inclusion of the products and cross-products of the basic predictors as additional predictors. The only restriction here is that the additional number of predictors generated are commensurate with the sample size. The principal advantage of this method is its simplicity, and regression equations can readily be solved with small computer systems or desk-type calculators, while analogue models require the processing of a large amount of historical storm-track data each time the program is activated. Moreover, simulated analogue models always produce a forecast, even when purely analogue models fail to do so (such as when anomalous situations occur). A small disadvantage is that the storm must have existed 24 hours before the persistence predictors may be calculated. A statistical combination of climatology and persistence (CLIPER) was developed for the Atlantic region by Neumann (1972). This has been extended to other basins, for example, for the south Indian Ocean by Neumann and Randrianarison (1976), for the eastern North Pacific by Neumann and Leftwich (1977), and for the north Indian Ocean by Neumann and Mandal (1977). A similar technique has been developed for the western North Pacific by Xu and Neumann (1985). Predictors such as the present latitude and longitude, and the components of recent motion and intensity of the storm are used. Least squares fitting of basic predictors and various polynomial combinations is used in CLIPER to derive regression equations for latitudinal/longitudinal displacements in 12-hour increments. Thus this technique makes use of the climatology of past tropical cyclone tracks and the persistence components of the present storm to generate a forecast.

#### 5.8.2.4.2 STATISTICAL-SYNOPTIC MODELS

The statistical-synoptic models incorporate predictors obtained from current or recently observed synoptic data. Some early examples of statistical-synoptic models are the north Indian Ocean by Kumar and Prasad (1973), NHC67 by Miller, *et al.* (1968), NHC72 for the North Atlantic by Neumann, *et al.* (1972), and EPHC77 for the eastern Pacific by Leftwich and Neumann (1977). Later examples include TOPEND (Keenan and Woodcock, 1981), AUSTCYC (Kuuse, 1979), and other statistical techniques (Keenan, 1984) for use in Australia. All of these models use observations of predictand and predictor at the current time, and  $t$  (and possibly at 12 hours prior to  $t$ ) to forecast values of the predictant at  $t+h$  hours, where  $h$  is 72 hours.

Predictors used in the models are selected from climatology and persistence as well as from one or more of the current and 24-hour old 1 000, 700 and 500 hPa height fields. For example the Atlantic NHC72 model uses the output from the simulated analogue CLIPER model as a single predictor containing all of the attributes of climatology and persistence. Storm-centred movable grids are generally used to represent the data fields, and predictors are selected systematically using the stepwise screening regression process. The size of the grid selected to represent a synoptic data field depends on the length of the forecast period. Models, which limit the forecast projection to 24 hours, can use a grid of 600 nautical miles extending outward from the storm, while models which attempt to forecast over 72 hours should use a larger grid system. In the larger grid systems, grid-spacings of 300 nautical miles are typical. However, models developed for smaller grids may benefit from a finer grid-spacing of, for example, 150 nautical miles. A nested grid system, where coarseness increases with distance from the storm, has not, as yet, been used in statistical models for the prediction of tropical cyclone motion.

If sufficient development data are available, it is desirable to stratify the various synoptic patterns and then to develop separate sets of regression equations which represent different synoptic patterns. As stated above, the NHC67 model stratifies according to whether the storm is initially located north or south of latitude 30°N, with an additional sub-stratification which depends on the storm's speed, and the NHC72 model stratifies on the basis of the storm's initial motion. The importance of proper stratification was further illustrated by Woodcock (1980) who demonstrated that multiple regression-based forecasts derived separately for different synoptic situations (analogue) provided better predictions than did a single set which did not distinguish among synoptic situations. Since tropical cyclone motion has been shown to be closely related to environmental influences and since environmental influences on cyclones south of the subtropical ridge are quite different from those north of the ridge, regression forecasts for predicting tropical cyclone motion should produce better results if the data are properly stratified with respect to the ridge prior to the development of the regression equation. While stratification conceptually improves with the performance of a given model, extreme care must be taken to avoid drastic reductions in the sample sizes.

Pike (1984) has carried out a comparison of the utility of various thickness and height data in statistical motion prediction. Fifty-six possible data fields pertaining to all mandatory levels, all possible thickness layers bounded by them, and the tropospheric mean were considered. The author found that the deep-layer mean (1 000–100 hPa) height field, calculated as  $H = 75H_{1000} + 150H_{850} + 175H_{700} + 150H_{500} + 100H_{400} + 75H_{300} + 50H_{250} + 50H_{200} + 50H_{150} + 25H_{100}/900$ , where  $H_p$  is the height at pressure  $p$ , produced the most accurate forecasts, followed by the mid-tropospheric 700 and 500 hPa heights. Considerably large average errors are produced

by height fields near sea level and near the tropopause. Most of the thickness fields yield larger vector errors than do the height fields. These results are on expected lines, since tropical cyclones are steered by winds associated with height gradients than by thermal winds associated with thickness gradients.

Matsumoto (1984) suggested a three-way stratification based on the position of the tropical cyclone relative to the 500 hPa ridge. The south-of-ridge category comprises all cyclones that never recurve. North-of-ridge category contains all storms that remain north of the ridge line throughout their lifetime. The on-the-ridge category is comprised of the track segments of recurring cyclones between 24 hours before and 24 hours after the recurvature point. The dependent set used to develop the regression equations includes all Atlantic tropical cyclones from 1946–1978. There are 16 potential forecast predictors derived from a 500 hPa height and 24-hour pressure change, and 500 and 200 hPa geostrophic wind and wind change. The method produced significant improvement in tropical cyclone track forecast.

Methods based on empirical orthogonal functions (EOF) have been proposed for stratification of data (Peak and Elsberry, 1986). Shaffer and Elsberry (1982) have demonstrated that information regarding the large-scale flow about the tropical cyclone may be provided by EOF analysis. The basic technique is to represent the environmental flow as a linear combination of principal components derived from the synoptic fields of a large number of cases. The synoptic information for any particular case may be efficiently represented by the coefficients of a few EOFs, which greatly reduce the data storage requirements.

Peak and Elsberry (1986) used discriminant analysis to develop a prediction method which would better forecast storm motion that deviates significantly from the mean cross-track (CT) and along-track (AT) values. In the discriminant analysis, classification functions are derived to predict in which group (left, straight, or right for the cross-track component and slow, constant or fast for the along-track component) the future cyclone path is most likely to occur. A similar method has been applied by Keenan (1986) based on past track and current synoptic data to estimate probabilities for the zonal and meridional motion components to be in the above average, average or below average categories. The discriminant analysis results were found to be encouraging. The schemes utilize predictors based on persistence and an empirical orthogonal function representation of the synoptic forcing.

One problem encountered in statistical modelling is the production of a "stair step", or otherwise unrealistic forecast track. Although statistically sound, such tracks are frequently produced because of the practice of forecasting the storm's track in 12-hourly time steps, where each segment of the forecast (each 12-hour step) is more or less independent of the other segments. To avoid this problem, the same predictors can be used for each time step for each component of motion, or the forecast for time  $t + h$  (hours) could be made a function of the forecast for the  $t + h + 12$  (hours).

#### 5.8.2.4.3 STATISTICAL-DYNAMICAL MODELS

The upper echelon of statistical models for the prediction of tropical cyclone motion is considered to be those models which derive a portion of the variance reduction from predictors taken from the output of a numerical prediction model. Such models can also derive a portion of their forecast skill from other sources such as climatology, persistence, or currently observed synoptic data. Conceptually, statistical-dynamical models are very appealing in that they combine the advantages of both the statistical and dynamical approaches to tropical cyclone prediction.

The use of model output statistic (MOS) is perhaps the most effective means of introducing numerically forecast data into a statistical prediction framework. The MOS concept (Klein and Glahn, 1974) essentially involves the direct introduction of the output of a numerical model, in both the developmental and operational modes, into a statistical model. From a practical point of view, there are problems involved in using this approach over the data-void areas of the tropics, where data samples are frequently not available as required to ensure adequate statistical significance. Until MOS models are developed for all appropriate tropical cyclone basins, interim approaches to using the statistical-dynamical methods have been undertaken. One of these alternative or substitute approaches is referred to as the perfect prog method (PPM). Another is known as the simulated MOS (SMOS) approach. Both methods, which are considered to be less adequate than the direct MOS approach, have been described in detail by Neumann and Lawrence (1975).

Allen (1984) describe a MOS technique, known as the CYCLOPS objective steering model output statistics (COSMOS) used in forecasting the movement of tropical cyclones in the north-western Pacific. The technique interprets forecasts based on smoothed geostrophic steering flow at various levels to provide 24-, 48-, and 72-hour forecast positions. The process that the model uses in arriving at a 72-hour forecast position consists of three steps: pattern recognition, predictor selection, and application of a bias to the prediction. Input to COSMOS consists of the current position six hours prior, and a 72-hour forecast position from CYCLOPS in the unmodified prognostic modes at the 850, 700, and 500 hPa levels.

Various statistical-dynamical models have been developed at the National Hurricane Center, which have been in operation from time to time. The NHC73 model developed by Neumann and Lawrence (1975) for the Atlantic area, which uses both the perfect-prog and SMOS approaches, shows considerable promise. The model includes the following predictors: output from the CLIPER model, current 1 000, 700, 500 hPa height fields, and 24-, 36-, and 48-hour height predictions from the National Meteorological Centre prediction model. The NHC83 model was introduced for the 1983 hurricane season. Based on a number of evaluation criteria such as timeliness, availability, overall utility, and minimum error, NHC83, through the 1988 hurricane season, has outperformed other models in use at NHC by a rather wide margin (Neumann and McAdie, 1991). Accordingly, this type of

model has a good skill. However, long-term operational use of the model has disclosed certain design weaknesses, which need to be improved. Neumann and McAdie have developed an improved version of the NHC83 model, the NHC90, which, according to the authors, is expected to outperform NHC83. Further details of this model are found in Neumann and McAdie (1991).

### 5.8.3 *Cyclone prediction by numerical models*

Historically speaking, the development of operational dynamical tropical cyclone prediction techniques by numerical models has failed to keep pace with that of statistical methods. While this development lag is to some extent still true, recent advances in the accuracy of numerical models suggest that the gap is closing rapidly. In principle, it is possible to formulate a numerical model, initialize it with observed data, and integrate the time-dependent hydrodynamic equations numerically for a suitable time period in order to obtain the desired forecast. This procedure is, in fact, followed every day at forecast centres around the world. However, when it is applied to the tropics, and specifically to the tropical cyclone forecast problem, certain difficulties arise.

First, tropical cyclones occur most frequently over the data-sparse regions of the tropical oceans, where an accurate specification of the initial state of the atmosphere is especially difficult. Secondly, the high-wind region of a tropical cyclone is small when compared to synoptic-scale systems. This fact alone makes it impractical to resolve the details of the vortex using a single mesh or grid length. Thirdly, the dynamics of the tropical atmosphere and the interaction of a tropical cyclone with its surrounding environment are not as well understood as the circulation regimes found at middle latitudes.

Recent technological advances and the use of ingenious numerical methods or schemes have solved some of these problems. The problem of scale size has been partially solved by the development of faster computers, capable of handling the vast amount of data required by a multi-level large area, fine-mesh numerical model. The so-called nested grids have been employed to resolve the structure of tropical cyclones with a fine-mesh grid, centred on the storm and nested within a large grid which is used to define the storm's environment adequately. The smaller (fine) grid is moved, or relocated, as the storm traverses the large stationary grid. Programmes such as the Global Atlantic Tropical Experiment (GATE), which focus on the problems of understanding the dynamics of the tropical atmosphere and the interaction of tropical weather systems/disturbances with their environments, should serve to improve our diagnostic and predictive skills in relation to these phenomena.

Unlike statistical models, the dynamical/numerical models do not depend on a statistical relationship such as that between a current storm and its historical analogues. Since one might expect the reliability of this type of scheme (dynamical/numerical) to be more independent of the details of a storm's past behaviour — as opposed to the statistical approach — the future course of a given storm should be implicitly predicted through proper integration of the equations of motion. Although the above statement undoubtedly suffers from oversimplification, dynamical models are, at least in part, developed and utilized as an integral part of the forecaster's skills, supplementing the guidance provided by statistical models and perhaps being more useful in situations where the latter prove most frail (for example, when a storm behaves erratically, such as stalling, looping, oscillating, or otherwise exhibiting significant departures from the norm).

In recent years, several studies with much advanced multilevel primitive equation (PE) models, regional and global, have been carried out in tropical cyclone intensity and track prediction and simulation, especially at the European Centre for Medium Range Weather Forecasts, the United Kingdom Meteorological Office, the Bureau of Meteorological Research Centre, Australia, the Geophysical Fluid Dynamics Laboratory, Princeton, the National Meteorological Centre, Washington, and the Japan Meteorological Agency, Tokyo. These studies have amply demonstrated the capability of current numerical models in handling tropical cyclones. The models, while providing reasonable forecasts of the genesis, intensification and movement of cyclones, do not, however, have the capability to resolve their core structure and the inner rain area. This is due to the fact that the finest resolution operational models currently available have a horizontal grid resolution in the order of 50–100 km, which could at best resolve the outer structure of the systems. Furthermore, the vertical motions in the cumulus bands in tropical cyclones are essentially nonhydrostatic, whereas the models are usually constructed on hydrostatic assumption. In order to resolve the core structure adequately, one needs to design models of five to 10 km horizontal resolution and which are based on nonhydrostatic formulations. At the same time, the model should have a domain which extends over several thousand kilometres. Currently, it is feasible to use computationally only a small limited area with a grid spacing of tens of kilometres.

#### 5.8.3.1 RESULTS OF TROPICAL CYCLONE PREDICTION AND SIMULATION EXPERIMENTS BY NUMERICAL MODELS

In a first such study, Bengtsson, *et al.* (1982) described intense hurricane-type vortices which developed in many ECMWF operational grid-point model forecasts of 1980 around the fourth day of their forecasts. Although in some cases, the model storms appeared similar to actual storms, there were several cases where spurious cyclogenesis occurred. The model exhibited a definite bias for the number of north-west Pacific storms. The authors felt that this was attributable to the relatively high sea-surface temperatures used in the model which were required to enhance the transport of moisture upward from the boundary layer. Since 1980, major improvements have been incorporated in the formulation of the surface-layer physics at the ECMWF.

Dell'Osso and Bengtsson (1985), in a later study discussed the relative merits of two models by carrying out three-day forecasts of supertyphoon Tip in 1979. Tip was a major supertyphoon that year. The two models were the ECMWF operational global grid-point model, and a limited-area version (ELAM) of this same model. The global model output was used to provide boundary conditions for ELAM. ELAM's grid resolution was around 57

km, as compared to roughly 208 km for the global model. The most striking aspect of ELAM was its ability to provide a reasonable track forecast. The track of the typhoon in the global model run was somewhat poorer. It appeared from this study that model resolution had a significant impact on the accuracy of track forecasts. Such an increase in skill may in part be due to the simulation of the mesoscale typhoon structure on the finer grid. The typhoon's cross-sectional structure was much more realistic in the ELAM forecasts. The ELAM storm exhibited realistic tangential velocity, a smaller radius of maximum wind, a stronger warm core, and a steeper surface pressure gradient compared to the global model. Another remarkable aspect of the ELAM forecast was the prediction of very realistic-looking spiral precipitation bands, whose location corresponded closely with those seen on satellite photographs. In this study, the authors demonstrated that, beginning with large-scale data, sufficiently high resolution models can simulate, with reasonable accuracy, the development, structure, and motion of a tropical cyclone. However, the model's need for time to develop the mesoscale structure from the large-scale data contributes substantially to errors in the track forecast.

Heckley, *et al.* (1987) described two forecasts of hurricane Elena starting on 31 August 1985. These were made with a global spectral model at a resolution of T106 waves (triangular truncation). The passage of this storm along the northern Gulf of Mexico was of interest here. One of the forecasts was an operational forecast while the other used an experimental version of the operational global spectral model. The only difference in these two experiments was in the parameterization of cumulus convection. The operational model utilized a version of Kuo's parameterization scheme (Kuo, 1974) for deep convection. The experimental model used a lagged adjustment scheme (Betts, 1986; Betts and Miller, 1986) for its parameterization of deep and shallow convection. The operational forecast was somewhat poor and carried the storm roughly 200 km to the south of the Louisiana coast, whereas the experimental forecast showed a landfall very close to the reported location on the Louisiana coast.

Krishnamurti, *et al.* (1988) have reported results of prediction experiments of several major hurricanes/typhoons in the Atlantic/Pacific region with a high resolution global spectral model. The cases examined are those of hurricane Fredericks (1979), hurricane David (1979), typhoon Hope (1979), and typhoon Abby (1983). The spectral model utilizes the transform method for the calculation of non-linear and physical processes. The physical processes include the parameterization of the planetary boundary layer, deep and shallow cumulus convection, radiative processes (including cloud feedback processes, diurnal change and surface energy balance) and large-scale condensation. Envelope orography is used to represent steep mountains globally. Ocean temperatures are prescribed from a preceding 10-day averaged data set for the storm periods. Sensitivity of the storm forecasts to horizontal and vertical resolutions, data sets and representation of physical processes were examined. The experiments showed useful skill of the high resolution global model in track prediction. The position errors at the end of three days in these experiments were in the order of 200 to 300 km, which compared very well with the best estimates of operational forecasts provided by statistical or movable nested grid models. The high resolution model produced a reasonable steering flow, which is important for cyclone motion. The sensitivity experiments carried out on data density, model resolution and physical parameterization processes brought out the following important results:

- (a) A major difference in the quality of forecasts appeared when the model was run with high density FGGE IIIB data sets as against operational FGGE IIIA data with short cut-off time sets of NMC Washington, which highlights the importance of data coverage in the tropics;
- (b) A modified Kuo's scheme for cumulus parameterization yielded successful results in the prediction of formation and motion of a monsoon onset vortex (a typical storm) in the Arabian Sea off the south-west coast of India in June 1979;
- (c) The role of radiative processes is important in a reasonable prediction of subtropical highs. This had an impact on the successful forecast of the recurvature of typhoon Abby in August 1983. The predicted motion of Abby in 24 and 48 hours had a good closeness of fit with the best track positions, the error being around 1° latitude. The prediction of subtropical highs, which is very sensitive to the radiative forcing, contributed to an improved prediction of the high and the attendant steering flow;
- (d) Marked improvements in the track forecasts by increasing the resolution from T21 to T106;
- (e) A major factor is the improved resolution in the planetary boundary layer. The surface fluxes in the constant flux layer are markedly enhanced by an improved vertical resolution near the earth's surface. The hurricane maintenance is particularly sensitive to the latent heat flux;
- (f) The global model with the highest resolution of T106 used in their study was able to resolve maximum winds of only 35–40 m s<sup>-1</sup>, which were underestimated by a factor of 2, while the central pressure was overestimated.

The model could not resolve the inner rain area of the storm, which was located within 100 km of the storm centre. Resolution of the model had to be further refined in order to resolve the inner rain area. However, global spectral models become computationally expensive beyond the resolution of around T170. Furthermore, the transform method starts losing its computational advantage when compared to very high resolution grid point models for scales of less than 100 km. The answer lies in designing stretched spectral models which provide higher resolution locally. In another experiment with a mesoscale multilevel regional primitive equation model of the landfall of an intense tropical cyclone in the Bay of Bengal during May 1979, Krishnamurti, *et al.* (1990) showed the effectiveness of the model in the accurate prediction of the landfall. The predicted motion field showed very little error in the first 72 hours. The predicted track was remarkably close to the observed track.

In yet another sensitivity experiment Krishnamurti, *et al.* (1990) used the Australian Monsoon Experiment (AMEX) data sets to initialize tropical storms Irma and Connie, which formed in the Australian region during the AMEX special observing period. Incorporation of the additional AMEX data had a very substantial impact on the initial conditions. Additional data improved the location of the middle-level cyclone, strengthened the horizontal wind shear across the low-level monsoon trough, enhanced the curvature and outflow jet of the tropical upper tropospheric trough, made the vorticity at all levels over the genesis area cyclonic, strengthened the low-level convergence over the genesis area, and enhanced the mid- to low-level moisture. All these features led the regional forecast model to generate a tropical cyclone with attendant mesoscale structure in the correct location and with correct temporal evolution in both the cases of Irma and Connie. However, the movement of these systems was not well forecast. The reason attributed was a gradual contamination of the large-scale steering influenced by the inadequacies in the physical processes. The authors observed that accurate representation of the four-dimensional structure of convective heating was important for track prediction.

In the control experiments without inclusion of AMEX data, the forecasts of motion and strength of the storms were reported to be extremely poor and the model failed to predict cyclogenesis. Without proper data the weak vertical motions, relatively weak low-level cyclonic vorticity, and a small Coriolis parameter in the initial fields resulted in inefficient convective heating and slow adjustment between the mass field, the divergent wind component, and the rotational wind component. This not only adversely influenced the motion directly (via the divergence term in the vorticity equation) but also indirectly by degrading the large-scale (rotational) steering flow. The importance of adequate data coverage is thus again brought out.

Several single- and multi-level models have been developed for cyclone track prediction purposes. These are briefly described below.

#### 5.8.3.2 SINGLE-LEVEL MODEL: THE SANBAR BAROTROPIC MODEL

SANBAR is a filtered barotropic prediction model which uses winds averaged with respect to mass through the troposphere. The model, originally developed by Sanders and Burpee (1968) and later modified by Pike (1972), essentially predicts tropical cyclone motion by the tracking of minimum stream function and maximum vorticity centres. The pressure-depth over which the initial wind observations are averaged is the 1 000–100 hPa layer. These winds are objectively estimated from the automated 200 hPa and low-level analyses. Both observed and estimated winds form the basis of an objective analysis, which produces a wind field specified at the grid points. Once the initial winds are specified — their non-divergent components are obtained by relaxation of the stream function in the interior of the grid — and the boundary conditions are specified, the simple barotropic vorticity equation is used to predict the movement or track of the stream function minima and the vorticity maxima. The basic dynamical framework of this model is a simplified form of vorticity equation averaged over the depth of the troposphere:

$$\frac{\partial \zeta}{\partial t} = -V \cdot \nabla \eta - V' \cdot \nabla \eta' + \phi(\omega_1 000 - \omega_{100})$$

where  $\eta$  is the absolute vorticity, and  $V$  and  $\eta'$  denote the deviations of winds and vorticities from the vertical averages.

Since the details of the wind structure of a storm's vortex are unavailable and unresolved by the model grid, the storm is replaced by an idealized, symmetrically circular vortex. In the original SANBAR model, this idealized vortex was subtracted from the observational and estimated wind data within the influence region before the objective analysis was performed, and then added on again. This led to a discrepancy between the initial storm motion computed by the model and the actual storm motion observed. In statistical models, short-term forecast motion is invariably highly correlated with current motion. Since the forecaster usually has a reasonable estimate of the current storm motion at forecast time, it was felt that this information could be advantageously incorporated into the SANBAR model (Pike, 1972). Pike's modification resulted in much improved forecasts of direction, especially during the first 24 hours, but too slow a speed bias remained. Sanders, *et al.* (1975) found that this bias was largely the result of:

- (a) Truncation error in the finite difference analogue of stream function  $\psi$ , and the prediction equation calculations resulted in underestimated phase speeds, especially for short wavelengths;
- (b) Relaxation of  $\psi$ , a steering flow which was too weak. These problems were later corrected.

De las Alas and Guzman (1976) used a similar, but simpler model to predict typhoon tracks in the vicinity of the Philippines. Their model employs a relaxation of the non-divergent barotropic vorticity to compute  $\psi$ . The track of the typhoon is computed by following the trajectory of a point representing the initial surface position of the vortex centre as it is advected by the large-scale wind field. Initial experiments with this model on a small number of cases have produced encouraging results.

#### 5.8.3.3 OPERATIONAL NWP MODELS FOR TROPICAL CYCLONE PREDICTION: THE PROBLEM OF MISSING VORTEX IN THE INITIAL FIELDS

The operational numerical prediction of tropical cyclones is fraught with special types of problems primarily because of the fact that the initial structure of a storm cannot be resolved due to lack of observations in the storm field. The storms form in data sparse oceanic regions where observations are not adequate to resolve even the large-scale environmental flow. In some cases, even if observations in the vicinity of a storm are available, quality control checks on the observation-first guess residuals may prevent these data from entering the analysis system. Puri and Lonnberg (1991) suggested using high-resolution structure functions and modification of the analysis scheme to accept data in the vicinity of the storm. Because of these deficiencies in the analysis, the

forecasts produced by the models may be in large error. The correct representation of the storm vortex in the initial gridded fields has therefore received much attention in the recent past. Procedures have been developed to construct an idealized vortex in the storm location based on current information about the size and intensity of the observed storm that are usually inferred from satellite data and synoptic analysis (Mathur, 1991; Andersson and Hollingsworth, 1988; Prasad, 1990). The idealized vortex is either merged with the objectively analysed fields or pseudo (bogus) observations are generated from the idealized structure, which enter the data assimilation system as if they are real observations. Several schemes have been suggested to produce the idealized vortex. A large number of studies with operational numerical models on cyclone track and intensity prediction with bogus vortex introduced in the initialized fields, have shown that these predictions improve very substantially. The success of these experiments has prompted some of the major NWP centres running global models to introduce bogus vortices on a world-wide basis in their operational data assimilation systems. The data on cyclone parameters required for this purpose are likely to be available on GTS on a regular basis. The procedures for generating bogus vortices in some of the centres are briefly outlined in the following paragraphs.

#### 5.8.3.3.1 NATIONAL METEOROLOGICAL CENTRE, WASHINGTON

The operational hurricane prediction model of NMC, Washington is a quasi-Lagrangian model (QLM) based on primitive equations with high horizontal (40 km) and vertical (16 levels) resolution. The model includes parameterization of principal physical and dynamical processes that affect the motion and development of a hurricane (Mathur, 1991).

The prescription of a bogus vortex is based on the storm's central pressure  $p_c$ , the pressure of the outermost closed isobar  $p_b$  and its distance  $R$  (size) from the centre. These three parameters ( $p_b, p_c, R$ ) together with the location of the storm centre are derived from the synoptic analysis of the National Hurricane Center (NHC). The surface pressure  $p_{sfc}(r)$  at a radius  $r$  in the idealized symmetric vortex is obtained from the relation:

$$\begin{aligned} p_{sfc}(r) &= p_{max} - [\Delta P \exp(-x^2)]/(1 + ax^2)^{1/2}; \quad r < R \\ p_{sfc}(r) &= p_b; \quad r \leq R \end{aligned}$$

where  $x = r/R$ ,  $a$  is specified, and the other two constants  $p_{max}$  and  $\Delta P$  are evaluated from the conditions  $p_{sfc}(0)=p_c$  and  $p_{sfc}(R)=p_b$ . The winds at pressure levels are specified in the following manner. First, the wind  $v_g(r)$  at 1 000 hPa is obtained from the gradient wind law:

$$V_g^2/r + f_c v_g - \partial\phi/\partial r = 0$$

where  $f_c$  is the Coriolis parameter at the latitude of the storm centre. The geopotential  $\phi$  at 1 000 hPa is obtained from the approximate relation  $\phi_{1000} = 8[p_{sfc}(r)-1 000]$ . A set of horizontal and vertical functions is used to derive the winds at the higher levels. The functions are chosen so that the wind structure resembles that typically observed in the hurricanes. The geopotentials at the interior grid points are obtained from the wind field with the use of gradient wind relation. Potential temperature is found from the use of hydrostatic equation.

The vertical column at the vortex centre is specified to be nearly saturated. Somewhat lower values of relative humidity (RH) are specified at  $R$ . The convective precipitation rate depends on the RH distribution. Since this rate is expected to be smaller in a weaker storm, the RH values are reduced by a factor of  $0.85+0.015(p_b-p_c)$  for an initial disturbance with  $p_b-p_c < 10$  hPa.

The symmetric fields so obtained are projected on the QLM grid. The vortex fields are merged with the gridded data derived from the NMC's operational global aviation (AVN) analysis, using the relation:

$$X = w \cdot X_v + (1-w)X_a$$

where  $X$  is one of the variables  $u, v, \theta, q$  and  $p_{sfc}$  and the subscripts  $v'$  and  $a'$  denote a field in the vortex and analysis, respectively. The weight  $w$  is given by:

$$\begin{aligned} w &= \cos(\pi r/2R); \quad r < R \\ &= 0 \text{ otherwise} \end{aligned}$$

Several case studies with the QLM have shown that the inclusion into the analysis of an idealized vortex of the same size and intensity as the observed storm generally leads to a better forecast of a storm's structure and track compared to forecasts without the idealized vortex. During the 1988 and 1989 hurricane season, the QLM forecasts of landfall compared well with the NHC83 forecast. However, over the open oceans, the NHC83 performs better than the QLM.

A major modification of the QLM initial conditions was carried out beginning with the 1990 hurricane season. Based on a storm's current motion, a steering current was imposed over the storm area using a secondary circulation (a generalized dipole). The procedure for specifying the dipole is discussed in Mathur (1991). The mean forecast track errors from the QLM, CLIPER and NHC90 (an improved version of NHC83) for the 1990 and 1991 hurricane seasons are compared in Figure 5.22. The QLM errors are similar up to 24 hours and are much smaller after 24 hours, compared to the NHC90 errors. The CLIPER errors are larger than the other two models.

#### 5.8.3.3.2 EUROPEAN CENTRE FOR MEDIUM RANGE WEATHER FORECASTS (ECMWF), UNITED KINGDOM

Currently, the operational ECMWF global model has a T213 L31 resolution (equivalent to about 100 km horizontal resolution). The operational data assimilation system does not make use of any bogus observations for the representation of tropical cyclones. However, Andersson and Hollingsworth (1988) performed some experiments to study the impact of bogusing in the prediction of tropical cyclone movement by the ECMWF global spectral model.

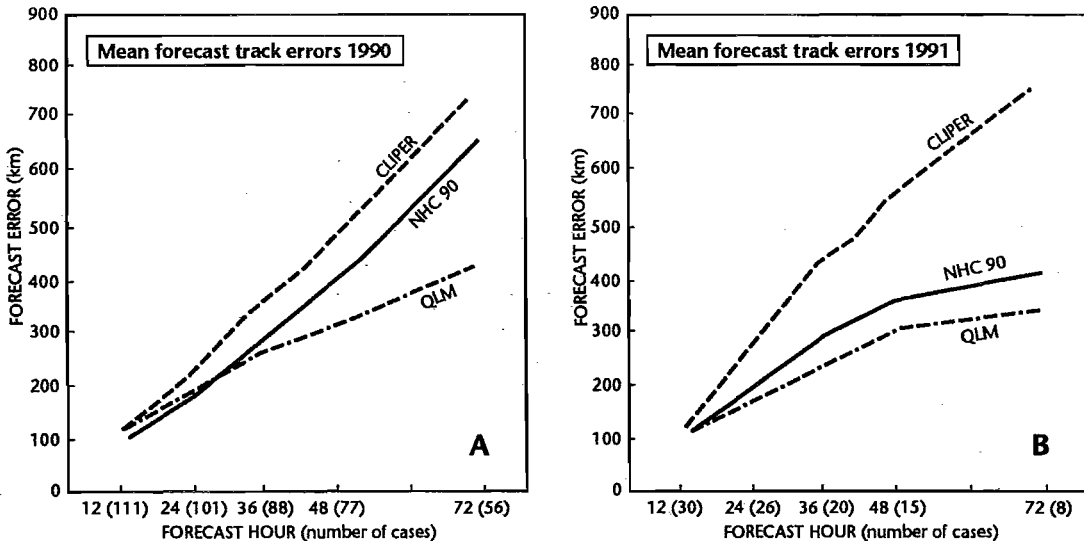


Figure 5.22 — Mean forecast track errors from the QLM, NHC90 and CLIPER during the (a) 1990; and (b) 1991 North Atlantic hurricane seasons (Adapted from Mathur, 1991).

The bogus observations are generated with a simple idealized tropical cyclone model which consists of two parts: an idealized symmetric vortex, and a background field. The two parts are superimposed. The symmetrical wind field at all levels is modelled by a Rankine vortex. In a Rankine vortex, the tangential velocity  $v$  as a function of radial distance  $r$  is given by:

$$\begin{aligned} V &= V_m(r/r_m) ; r < r_m \\ V &= V_m(r/r_m)^{-\alpha} ; r > r_m \end{aligned}$$

where  $V_m$  is the maximum tangential wind speed and  $r_m$  is the radius of maximum wind,  $\alpha$  is a parameter with a value normally between 0.5 and 1. The gradient wind relation is used to relate wind to geopotential  $\phi$ :

$$\partial\phi/\partial r = fV + V^2/r$$

The above equation is integrated to compute  $\phi$ . The strength of the vortex is decreased with increasing height by a composite wind shear factor given by McBride (1981a, b). Wind bogus is provided between 850 and 300 hPa, while mass bogus is provided at 1 000 hPa. No humidity or thickness bogus data is used in order not to upset the convection. The observations enter the analysis system as if they are conventional radiosonde observations.

Andersson and Hollingsworth (1988) report two case studies of cyclone prediction by using bogus data. For a tropical cyclone in the Gulf of Carpentaria in the Australian region, predictions using bogus observations only — that is, excluding any observations within a certain area of the tropical cyclone — were virtually the same as those using only observed data. In this case, large amounts of data were available since cyclone Jason occurred during the Australian Monsoon Experiment (AMEX). In another case in the western North Pacific, bogus observations did improve the forecasts significantly.

#### 5.8.3.3.3 UNITED KINGDOM METEOROLOGICAL OFFICE (UKMO)

The general characteristics of the UKMO global NWP model are described in Bell and Dickinson (1987). The horizontal resolution of the model in the tropics is around 200 km. According to Morris and Hall (1987), the analysis of tropical cyclones in the UKMO is done by inserting bogus winds at four positions around the centre at each level between 850 and 500 hPa. The bogus winds are usually symmetric but could be made slightly stronger in the direction of movement of the cyclone if the translation speed is significant. No attempt is made to model the horizontal structure of the cyclone. However, a warm core is maintained in the vertical. The objective is only to correct the position of the circulation centre or to create a circulation if none is present in the analysis.

The UKMO has been applying the above method of bogusing tropical cyclones in its global model since 1986. While the 24-hour forecast position errors are rather large as compared to manual forecasts at 48 hours and beyond, the model shows considerable skill in predicting the position of cyclones (Chan, 1990).

#### 5.8.3.4 JAPAN METEOROLOGICAL AGENCY (JMA)

The JMA runs a global spectral model (T106 L21) for medium-range forecasts, an Asia spectral model with 16 levels in the vertical for 48-hour forecasts, a Japan spectral model (23L) for 24-hour forecasts, and a typhoon forecast model (TYM) for typhoon predictions. The initialization of the typhoon is accomplished through a scheme of bogusing in which, based on position, size and intensity of the tropical cyclone, an asymmetric surface pressure field is built around the cyclone centre by using Fujita's formula (JMA, 1990) as follows:

$$P(r) = P_E - \Delta P [1 + (r/R_o)^2]^{1/2}$$

$$\Delta P = P_E - P_{cm}$$

where  $P_E$  and  $P_{cm}$  are the environmental values of mean sea-level pressure and manually-analysed central pressure, respectively.  $R_o$  is a parameter which governs the shape of the profile.  $R_o$  is determined to get 15 m/s gradient winds at the reported gale wind radius. D-values are calculated for the upper troposphere to incorporate the anti-cyclonic flow. Relative humidity is prescribed as 90 per cent in the troposphere around the cyclone centre, so as to enhance the spin-up of the vortex through a convection scheme. The bogus typhoon is superposed onto the objectively-analysed fields through the following weighted mean formula:

$$f(r, \theta) = f_m(r, \theta) \cdot W(r) + f_g(\theta) \cdot [1 - w(r)]$$

$$= 1 ; r \leq R_{cl} \text{ (inner area)}$$

$$= (R_{co} - r)/(R_{co} - R_{cl}) ; \text{(transition area)}$$

$$= 0 \text{ (Outer area)}$$

where  $R_{cl}$  and  $R_{co}$  are bound radii of the transition annulus and  $f_m$  and  $f_g$  are field variables in the model typhoon and objective analysis, respectively.

After the bogus typhoon is embedded into the analysis fields, a non-linear normal mode initialization is applied to the fields to reduce the excitation of the gravity-inertia oscillation. Finally asymmetric flow field of wave number 1 with respect to typhoon centre is superposed onto the entire wind field including the bogus typhoon to get a reasonable initial movement of the model typhoon.

#### 5.8.4 Tropical cyclone probability forecasts

Several forecast centres use the concept of probability to describe uncertainties in the spatial and temporal occurrence of tropical cyclones. The most common uses of forecast probability in relation to the occurrence of severe cyclonic effects, such as the distribution of hurricane-force winds, the height of sea waves and the elevation of storm surges, are:

- (a) To extend the usable length of forecasts despite their increasing uncertainty as the forecast period increases;
- (b) To provide a quantitative assessment of the threat posed by a cyclone approaching possible landfall;
- (c) To compare the relative threat to different places at the same time, or at different times as a threat develops;
- (d) To cause a consistent response to the same or similar set of circumstances;
- (e) As a tool in risk analysis in respect to both long-term protective measures as well as for contemporary warning purposes.

Jarrell and Brand (1983) provide a fairly comprehensive overview of the types of probabilities presently available. The most common application of probability has been to express the uncertainty in forecasts of cyclone motion through the construction of percentage probability ellipses. The occurrence data may have been provided by selected analogue tracks for a particular time of the year by tracks generated by other means — such as by varying the speed or direction of a cyclone to take into account all reasonable variations — or by the characteristic official track forecast errors. Probability ellipses may be constructed to enclose selected percentages (usually 25, 50, or 75 per cent) of all cyclone locations. In general, the dimensions of the ellipses (uncertainties) increase as the forecast interval increases. Further details are provided by Southern (1985) and Jarrell and Brand (1983).

#### 5.8.5 Verification of tropical cyclone forecasts

The tropical cyclone track forecasts that are released to the public are based on consideration of all available guidance. The multiple objective aids available in an operational situation invariably produce conflicting tracks. It is necessary for a forecaster to have a good knowledge of the skill and performance characteristics of the various aids. The objectives of the verification studies are to promote better utilization of this guidance and to provide the developers of various aids with a basis for improvement. Another type of verification study is the characterization of official forecast errors, which are helpful in understanding the utility of these forecasts by the users.

##### 5.8.5.1 MEASURES OF TRACK FORECAST ERRORS

The most widely reported measure of the tropical cyclone track forecast error is the displacement error, which is the great circle distance between the forecast and the observed positions (also referred to as vector error). This measure has the shortcoming that it does not include any information on the direction of error. One way to include the direction of error is to measure the latitudinal and longitudinal components separately. However, in this approach, the interpretation of systematic errors that may be present, for example in the dynamical models, becomes difficult when the sample indicates a wide variety of track directions, for example, storm tracks before and after recurvature. An alternative is to verify the forecasts in a coordinate system that is oriented along the storm track. The error components in this framework are the along-track and cross-track. The cross-track component represents the skill in forecasting turning motion. The along-track error represents the speed error, though it is not equal to the speed error. Even if a storm is forecast to move at the correct speed, the along-track error will be negative if the direction is incorrect. Shapiro and Neumann (1984) and Shapiro (1984) note that the correlation coefficients between the along-track and cross-track errors are near

zero, so that these errors are essentially independent. In contrast, meridional and zonal error components in the geographic coordinate system are not independent. Peak and Elsberry (1986) and Chan, *et al.* (1987) define cross-track and along-track error components relative to a persistence or a CLIPER track, respectively. These simple no-skill track forecast techniques are used to normalize the forecast positions, which make an intercomparison of the forecast performance of different techniques easy to comprehend. Skill in forecasting is said to exist if the accuracy of forecast exceeds the levels achieved by such basic methods as climatology and persistence. Neumann and Pelissier (1981) used the CLIPER model as a benchmark to judge the skill of other objective aids. Pike (1985) also used the CLIPER-type models in each tropical cyclone region to assess the difficulty of forecasting in each region. The author used best-track information to define a relative forecast difficulty. Pike ranked the regions in terms of decreasing difficulty as south-west Pacific, Australia, Atlantic, western North Pacific, south-west Indian Ocean, eastern North Pacific, and north Indian Ocean.

The verification statistics may be evaluated with inclusion or exclusion of the initial positioning errors. The positioning error is the distance between the operationally-determined initial storm position and the position which is determined from a post-analysis or best-track. A dual verification of all official forecasts issued by NHC during 1970–1979 indicates that inclusion of the initial positioning error increased the average forecast error by 11, 6, 2 and 1 per cent for the 12-, 24-, 48- and 72-hour projections, respectively. These results may not be representative of other ocean basins.

In order for a comparison of the performance characteristics of two or more models to be meaningful, it must be based on homogeneous samples. Stratification of the samples by latitude is often useful because the track characteristics are different between the easterlies and the westerlies. The track characteristics as well as the forecast error characteristics depend on the synoptic regime.

#### 5.8.5.2 COMPARISON OF VARIOUS OBJECTIVE AIDS

Neumann and Pelissier (1981) provide a comprehensive review of the performance of objective aids at the National Hurricane Center. Figure 5.23 shows the performance of several models, SANBAR, MFM, NHC67, NHC72, NHC73, and the NHC official forecasts, normalized with reference to CLIPER. It would be seen that the performance of the MFM is poor at 12 hours and excellent at 48 hours. In the Atlantic, the statistical models (NHC67, NHC72 and NHC73) generally provide the best overall guidance, and the analogue model (HURRAN) is the worst (Elsberry, 1985). In a survey of forecast centres, Holland (1985) reports that the average forecast errors for Australia, Guam and Hong Kong were quoted as being around 200–250 km at 24 hours, 400–450 km at 48 hours and 600–700 km at 72 hours. Neumann and McAdie (1991) report the comparison of average forecast errors of the models NHC83, CLIPER, NHC72, NHC73 and the official forecasts for the period 1983–1988, which are presented in Table 5.2. According to these comparisons, the NHC83 outperforms all other models at all the forecast ranges. Mathur (1991) gives a comparison of the NMC, Washington dynamic model QLM, the NHC83, and CLIPER for the years 1988 and 1989 (Table 5.3). In this case, NHC83 outperforms QL in all the three forecast ranges, 24, 48, and 72 hours.

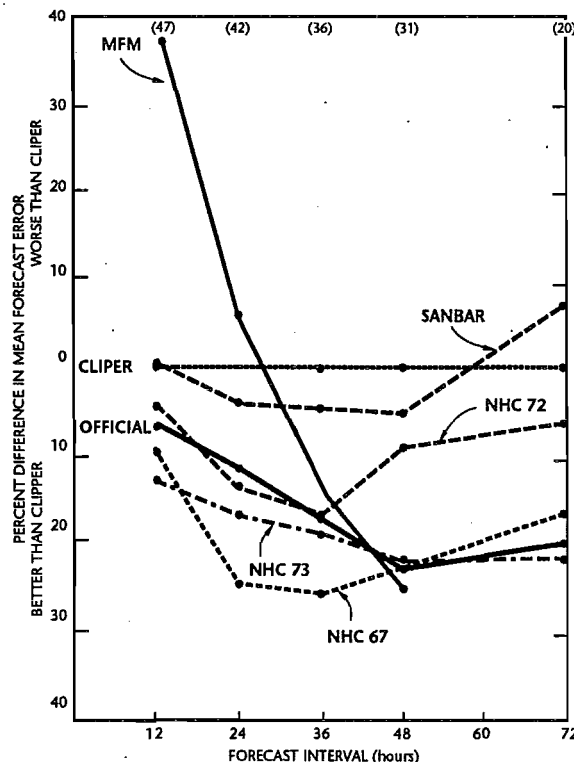


Figure 5.23 — Forecast errors relative to CLIPER for a homogeneous sample of Atlantic storms during 1976–1979 (After Neumann and Pelissier, 1981).

Table 5.2  
Average forecast errors (operational) of specified models for each year 1983–1988,  
and over the entire six-year period

AVERAGE FORECAST ERRORS (NAUTICAL MILES) FOR EACH YEAR, (1983–1988)						
	NHC83	CLIPER	NHC72	OFFICIAL	NHC73	SAMPLE SIZE
1983	12h	26*	30	32	39	32
	24h	49*	63	67	81	90
	48h	166	140*	149	223	213
	72h	374*	441	666	397	417
1984	12h	48*	53	50	53	50
	24h	96*	119	104	116	119
	48h	217*	260	252	224	243
	72h	324*	332	422	341	419
1985	12h	48*	53	57	48*	50
	24h	88*	117	128	100	107
	48h	168*	271	290	222	242
	72h	288*	399	367	333	466
1986	12h	43	47	42*	44	43
	24h	88*	109	95	101	99
	48h	173*	241	210	230	228
	72h	294*	377	405	387	429
1987	12h	47	52	51	47	41*
	24h	103*	140	147	114	109
	48h	222*	391	365	233	293
	72h	313*	638	556	365	466
1988	12h	35*	38	-	36	-
	24h	58*	74	-	62	-
	48h	129*	175	-	138	-
	72h	193*	282	-	222	-
1983– 1988†	12h	43.6*	48.1	50.6	45.5	46.8
	24h	84.3*	108.9	117.0	97.0	109.3
	48h	177.4*	252.9	276.9	201.9	249.0
	72h	274.4*	377.7	436.9	311.5	442.4

† Summary for NHC72 and NHC73 models does not include 1988 season.

NOTE: An asterisk designates the minimum error for a specified model for a given forecast period. The sample is homogeneous and combines 0000 and 1200 UTC forecasts. The CLIPER, NHC72 (statistical-synoptic) and NHC73 (statistical-dynamical) models are described by Neumann and Pelissier (1981) and NHC83 is described by Neumann (1988).

Table 5.3  
A comparison of QLM, NHC83, and CLIPER operational mean track forecast errors  
(kilometres) for the 1988 and 1989 hurricane season

	24h	48h	72h
<b>1988</b>			
QLM	182	367	539
NHC83	104	218	326
CLIPER	122	272	457
Number of cases	42	36	27
<b>1989</b>			
QLM	180	357	564
NHC83	146	287	500
CLIPER	183	431	668
Number of cases	66	51	42

Based on Mathur, 1991.

No single model can satisfy the forecast guidance needs. A combination of different models may be needed. Neumann and Pelissier (1981) suggest that the statistical-dynamical approach for the extended ranges should be combined with the statistical-synoptic approach for shorter ranges, except that the CLIPER should be the primary guidance within the easterly wind regime. Tsui (1984) has proposed an optimum weighting scheme for combining all of the objective aids. The periodic updating of prediction models may be required to ensure an optimum balance between the various factors which dictate the choice of prediction model.

### **5.8.6      *Storm surge prediction***

The storm surge — an abnormal rise in sea elevation due to a tropical cyclone — is an oceanic event responding to meteorological driving forces. Potentially disastrous surges occur along coasts with low-lying terrain that allow inland flooding or across inland water bodies, such as bays, estuaries, lakes and rivers. It has been estimated that there are 40 to 50 countries in the tropics which are affected by cyclones. Many of these countries frequently suffer major catastrophes on account of storm surges. In earlier years, there were no satisfactory methods for predicting the sudden rise in sea level when a storm struck the coast. Consequently, damage due to coastal flooding was often substantial. More recently, encouraging results have been obtained in surge prediction with the aid of computer-oriented mathematical models.

It is recognized that there are a number of parameters which contribute to the elevation in sea level during the passage of a storm. The important parameters are:

- (a) The lowest central pressure, maximum wind and its distance from the storm centre, inflow angle (cross-isobar flow), and speed of propagation of the storm;
- (b) The topography of the sea bed;
- (c) The angle between the storm track and the coastline;
- (d) The geometry and configuration of the coastline;
- (e) The phase of the astronomical tide with respect to the time of storm landfall.

#### **5.8.6.1    SURGE PREDICTION BY MATHEMATICAL MODELS**

Although statistical surge forecasting techniques exist, these methods are often impractical because of the lack of surge data from past events. Mathematical models are therefore used for surge forecasting. Mathematical models for surge prediction generally express the propagation of long waves in shallow water. Two main assumptions are made in modelling experiments: the amplitude of the surge is small, and the horizontal dimensions of the surge is large in comparison with the depth of the sea. These conditions are generally satisfied, except in very shallow regions where the surge amplitude is comparable with the depth of the sea. Examples of such exceptions are the north-eastern sector of the Bay of Bengal — where over a large area, the sea depth is just five metres — the areas surrounding off-shore islands, and in the vicinity of river estuaries. In such regions, modelling experiments become more difficult because the prediction equations are no longer linear and water flow may not be sub-critical.

The mathematical modelling of storm surges requires the solution of hyperbolic, partial differential equations in two horizontal dimensions. In addition to the initial and boundary conditions, the driving forces must be specified in terms of surface stress and pressure gradient body force. Adapting a surge model to a given region requires laborious data acquisition to specify the bathymetry of water areas and the land surface topography for each model grid square. All of these data must be carefully adjusted to a common datum or reference level.

The following are the main factors which are taken into consideration for storm surge forecasting.

##### **5.8.6.1.1    DATUM**

All elevations of terrain, bathymetry, barriers, and surface water heights must refer to the same datum, such as mean sea level.

##### **5.8.6.1.2    INITIALIZATION**

A surge model has to be initialized with a pre-storm water level. The initialization can be performed with the observations on quiescent, coastal sea levels before the storm, or the computed steady-state level for a stationary storm far out at sea.

##### **5.8.6.1.3    STORM MODELLING**

For tropical storm surge prediction, information is required on the storm parameters just before, during, and after landfall, when surge generation is most pronounced. The surge prediction depends critically on the quality of input storm data. Usually a storm model is specified using simple meteorological parameters. For operational forecasting, the storm is assumed to be well behaved, with a single eye and an analytical wind structure. Input to surge models requires the storm track, the intensity of the storm, and the size of the storm. The storm intensity may be specified by the difference between the central pressure and the ambient pressure outside the storm. Estimates of the central pressure of the storm may be obtained from satellite pictures and Dvorak's (1973, 1975, 1984) nomograms. But storms are known to change in intensity fairly rapidly as they approach the coast and, on such occasions, the predicted sea-level elevation could be incorrect. The storm size is parameterized by a scaling radius, usually the radius of maximum winds. A major uncertainty lies in the accurate track and landfall prediction of the storm. The average error in a 24-hour prediction of the point of landfall is in the order of 100 nautical miles. Sudden changes in the propagation speed or recurvature near the coastline are difficult to simulate in modelling experiments.

The wind stress per unit mass on the sea surface is formulated as a function of the drag coefficient, water and air densities, and vector wind. As the surface stress applies specifically to the sea surface, the wind observations available from different platforms need to be converted to a constant level. Alternately, it is useful to design a storm surge model dependent on simple meteorological parameters and to compute directly a vector wind at or near the surface level.

#### 5.8.6.1.4 SURGE MODELLING

Several types of numerical surge models have been designed varying from simple one-dimensional models to complex ones. A typical operational surge model is two dimensional in the horizontal. A rule-of-thumb for determining the maximum allowable grid size (in the area of interest) is that the numerical differencing scheme should resolve accurately a wavelength that is four times the radius of maximum winds.

A description of the basin is necessary when running a surge model in a given area. This includes inland terrain, inland water bodies such as lakes, bays and estuaries, and a segment of the continental shelf.

The specification of the boundary conditions is a difficult problem in surge forecast models. Very little is known, for example, of the nature of sea bed friction or the transfer of momentum from air to sea during high winds. Complicated input boundary values may be required as a function of time to compute surges with a surge model. An exception is for surges over an isolated lake that is unconnected to, and unaffected by, events in any other water body. Boundary inputs are not required in deep water or along coasts with high terrain. If the core of a storm crosses (or exits) the basin through a deep water boundary, or exits (or crosses) through high terrain, simple boundary conditions may be adequate.

The following types of models are generally designed for forecasting storm surges:

- (a) Some storm surge models are restricted to the continental shelf only (Jelesnianski, 1972; Wanstrath, *et al.*, 1976) and the coastline is represented as an impenetrable vertical wall. Such a model does not consider flooding across terrain, nor surges across inland water bodies;
- (b) A simple shelf model with a large basin and a coarse mesh or even a one-dimensional surge model is used to compute the necessary input boundary values for a limited-area, fine-mesh, bay model. If these two models are dynamically uncoupled, the specification of the interface conditions can be troublesome. An alternative is to have a coarse-mesh model to cover the entire region from deep water, through a bay, and over inland terrain. The numerical solution in inland areas is on a coarse grid, but the dynamic feedback effects from the bay onto the shelf are approximated. A coarse mesh does not give a detailed description of the inland surges across terrain that may be complicated by obstructions and small inland water bodies. However, it can give seaward detail along coastlines bordering the ocean. Such a model can be useful for supplying approximate boundary values for a fine-mesh, limited-area, surge model;
- (c) Rather than limiting the fine mesh to a small region or small basin, a stretched coordinate system may be used with a fine mesh in a limited area and a continuous transition to a coarse mesh on distant boundaries of a large basin. In this manner, a large geographical area can be resolved with a detailed description over the fine-mesh region. In many cases, simple boundary conditions in the outer region are sufficient. Although there are advantages to this stretched-grid coordinate system, Lewis, *et al.* (1982) point out some serious pitfalls. Most importantly, this type of grid system tends to trap energy in the finer grid mesh, and thus may overestimate surge levels at the points of greatest interest.

Astronomical tides can be treated crudely by superposition with the computed surge. From a forecasting standpoint, it is difficult to predict a storm's landfall time and have the proper phase for the astronomical tide. Small errors in timing on storm track positions will invalidate the superposition with the astronomical tide.

As with all models, it is necessary to resist the temptation to treat undetermined coefficients as tuning parameters that are to be arbitrarily specified for a single historical storm event. Such a procedure will give an excellent validation of the computed surge for one storm event. However, there is no guarantee that the same coefficients will be appropriate for other storms or for different regions. Large errors are inherent in both surge and meteorological observations. Thus, coefficient values must be determined from many storm events. One school of thought suggests that more generalized coefficients to serve all storms in all regions should be used, even if computed results are not ideal for a particular storm event.

Despite uncertainties, mathematical models of storm surge predictions have produced realistic results. A model developed by Jelesnianski (1967, 1972), with meteorological parameters as input, provides the coastal surge envelope of high waters, including the peak surge along a straight coast, for the Gulf of Mexico and east coast of the United States (Jelesnianski, 1965, 1974; Jelesnianski and Taylor, 1973). Coastal irregularities, such as a shallow bay, were considered in a model by Miyazaki (1965). For the Bay of Bengal, surge prediction diagrams have been prepared by Das, *et al.* (1974) and Robinson and Flierl (1972). Their models compute the peak surge generated at the time of landfall by an idealized storm striking different sectors of the coast with uniform speed. Peak surges were computed for different values of storm intensity, maximum wind, and speed of propagation. Sea-bed friction was not included in Robinson and Flierl's model and predicted surges were higher than those of Das, *et al.* An interesting fact, however, was that in spite of uncertainties about storm parameters, the predicted values were essentially correct;

#### 5.8.6.1.5 TIDE SURGE INTERACTIONS

The accuracy of surge prediction depends on the time at which the storm is likely to cross the coast because of tide surge interactions. Generally, on account of friction, the surge is largest at the time of low water (Proudman, 1953), but a simple superposition of the predicted surge on the astronomical tide does not always need to provide a realistic estimate of the total sea-level elevation. This is true if the astronomical tide is of the same magnitude as the surge. In the United States, for instance, the astronomical tide is usually an order of magnitude smaller than the surge. Hence the interaction is small, but there are other regions, notably the northern sector of the Bay of Bengal, where tidal effects are considerable;

#### 5.8.6.1.6 SURGE PREDICTIONS

It is most useful to provide a coastal surface envelope (Jelesnianski, 1972) of high waters for the entire storm without respect to time. At each grid point of a basin, the highest computed surge is stored for output. The potential surge conditions can be specified by a careful consideration of the tropical storm characteristics from climatology. An adequate description of potential flooding along a real segment of coast may require several hundred integrations with storms varying in track direction, landfall locations, translation speed, intensity and size. With surge information from model simulations, an atlas of events can be compiled to depict flooding from hypothetical storms. The forecaster can match an approaching storm with one from the atlas to assess the flooding potential. With the aid of an atlas, the forecaster can run the surge model in real-time to finalize a more detailed surge forecast after refining his best estimate of storm track, size and intensity.

The storm surge forecast can also be given in terms of probability. Each of the storm scenarios that comprise the atlas mentioned above is a set of conditions whose occurrence probability can be calculated based on the current forecast. If these scenarios can be considered to be exhaustive and mutually exclusive, then the probability of a surge exceeding a specific application is simply the sum of the occurrence probabilities of all scenarios that would cause the surge to exceed that elevation. An example of such a methodology can be found in Jarrell and Brand (1983).

#### 5.8.6.2 SURGE PREDICTION WITH THE HELP OF NOMOGRAMS

Ghosh (1977) has prepared nomograms to estimate peak storm surges by tropical cyclones impinging on the east coast of India using Jelesnianski's (1972) SPLASH model. The pre-computed nomograms accommodate fixed values for pressure drop, radius of maximum wind, vector motion of storms, and offshore bathymetry. Two sets of nomograms are presented — one for the north-east coast of India where the slope of the continental shelf is extremely shallow — the other for the remaining east coast where the slope in general is extremely steep. A nomogram to correct the magnitude of the peak surge for tidal effects is also prepared for the north-east coast of India where the semi-diurnal tide range is large. A method to estimate total sea elevation along a coastal stretch by means of nomograms is given for the north-east coast of India.

Crawford (1979) discusses hurricane surge potentials over south-east Louisiana, United States as revealed by a storm surge forecast model. In addition, the WMO publication *Present Techniques of Tropical Storm Surge Prediction* (WMO-No. 500) describes, in detail, present techniques for the prediction of storm surges associated with tropical storms.

### 5.9 Mesoscale phenomena in the tropics

Most of the weather phenomena occurring in the atmosphere, which have a damaging potential, occur in association with mesoscale processes, such as severe thunderstorms, squalls, extremely heavy precipitation, severe turbulence, etc. The class of atmospheric motions which qualify to be called mesoscale systems include organized convection, tropical cyclones, explosive cyclogenesis in extratropical latitudes, and some types of orographically-induced circulations such as mountain lee waves.

Mesoscale can be defined as having a temporal and horizontal spatial scale smaller than the conventional rawinsonde network, but significantly larger than individual cumulus clouds. This implies that the horizontal scale is in the order of a few kilometres to several hundred kilometres or so, with a time scale of about one to 12 hours. The vertical scale extends from tens of metres to the depth of the troposphere. The shorter scales correspond to atmospheric features that, for forecasting purposes, can only be described statistically, whereas the longer scales correspond to the smallest features we can generally distinguish on a synoptic weather map. Mesoscale can also be applied to those atmospheric systems that have a horizontal extent large enough for the hydrostatic approximation to the vertical pressure distribution to be valid, yet small enough for the geostrophic and gradient winds to be inappropriate as approximations to the actual wind circulations above the planetary boundary layer.

The different scale classifications of the atmospheric motions and the classification of the mesoscale part of a spectrum, as suggested by Orlanski (1975) are found in section 3.1.1 as well as in WMO (1987b) and in Collier (1989).

According to their genesis, the mesoscale atmospheric systems can be divided into two groups (Pielke, 1984):

- (a) Those that are primarily forced by surface inhomogeneities (terrain-induced mesoscale systems);
- (b) Those that are primarily forced by instabilities in travelling large-scale disturbances (synoptically-induced mesoscale systems).

In the first category are features such as sea and land breezes, mountain-valley winds, urban circulations, and forced airflow over rough terrain. Examples of the second include squall lines, hurricanes, and travelling mesoscale cloud clusters. Prediction of the first category of systems is relatively easier as they occur in association with geographically fixed features with time scales of 12 hours or so, and they are repetitive in nature. These systems do not also move far from their point of origin.

The occurrence of the second type of mesoscale systems is irregular with reference to a given location. These are not forced by well defined geographical features. The data requirements for identification and prognoses of these systems are much higher than those in the first case. These systems are initiated by some kind of atmospheric instability, for example, the conditional instability of the second kind (CISK). A large percentage of the rainfall over the earth results from such synoptically-induced mesoscale-sized precipitating cloud systems.

For the prediction of mesoscale systems and its associated weather it is imperative to obtain good quality observational data at closely spaced points over a large domain. Until recent times, such data were hardly available, and it was not possible to identify the mesoscale atmospheric systems and to predict them numerically. With the development of satellite, radar and other methods of remote sensing with a high resolution in both time and space, as also the availability of dense ground-based observational network (radars) in some regions, it is now possible to identify mesoscale atmospheric perturbations with the use of data on clouds, precipitation, and humidity. Most of these are qualitative in nature and cannot be used directly in numerical weather prediction, but the progress in remote sensing in infrared and microwave ranges, and the development of the Doppler technique indicate that the initial database for very fine-mesh mesoscale numerical models are now available and are continuously on the increase. Satellites and radars, by far, constitute the most important source of mesoscale observations. The geostationary satellites provide cloud imageries in quick session over a broad range of meteorological scales from the synoptic scale down to the cloud scale, which is very helpful in mesoscale forecasting. The expansion of a database, the improvement of numerical weather prediction models in terms of resolution and physical parameterization, and the availability of faster computer systems has made it possible to develop mesoscale numerical models which can resolve mesoscale circulations on very fine meshes and thus help in the more detailed prediction of weather elements in a limited area.

Some important characteristics of different mesoscale systems are briefly described below. Further details are provided by Atkinson (1981), Pielke (1984), and WMO (1989, 1990).

### 5.9.1 *Terrain-induced mesoscale systems\**

#### 5.9.1.1 SEA AND LAND BREEZES OVER FLAT TERRAIN

The sea and land breezes over flat terrain are the result of horizontal temperature gradients set up by the differential heating of large water bodies and land, located contiguously. The sea breeze is defined to occur when the wind is onshore, whereas land-breeze occurs when the opposite flow exists. The occurrence of sea breeze is strongly influenced by the prevailing synoptic flow. The evolution of the sea breeze is more complicated when the synoptic scale flow is present than when it is absent. Using observational data, Biggs and Graves (1962), and Lyons (1972) developed indices to estimate whether or not sea breeze will occur. Lyons, for example, has shown that when  $V_g^2 / C_p \Delta T$  is greater than 10 (where  $V_g$  is the surface geostrophic wind speed and  $\Delta T$  the maximum temperature difference between the inland air temperature and the mean lake surface temperature), a sea breeze will not occur at the Chicago shore line. A sea breeze does not develop when this ratio is large because the horizontal pressure gradient generated by the differential heating between the land and the lake is insufficient to overcome the kinetic energy of the large-scale flow.

Studies have demonstrated that land and sea breezes (and other similar mesoscale circulations) are poorly resolved in conventional weather-observing network systems. Such a lack of resolution creates serious problems in developing routine operational forecasts of these phenomena.

Several numerical simulation studies conducted since the 1970s have thrown various new insights into the sea-breeze phenomenon. Anthes (1978) showed, using a two dimensional model, that with a zero large-scale prevailing flow, the return flow of the sea breeze occurs entirely above the boundary layer whereas the onshore winds are confined below that level. Abe and Yoshida (1982) examined the influence of peninsula width on the intensity of the sea breeze and found that a width of 30 to 50 km produces the strongest upward vertical velocities. Several other studies have shown that, along the shorelines, under undisturbed synoptic conditions during the summer in the tropics and subtropics, the sea breeze exerts a dominant influence on the sites of formation and the movement of thunderstorm complexes. The sea breeze may also be responsible for generating severe local weather.

#### 5.9.1.2 MOUNTAIN-VALLEY WINDS

In a region with irregular terrain, local wind patterns can develop because of the differential heating between the ground surface and the free atmosphere of the same elevation some distance away. A large diurnal temperature variation usually occurs at the ground, so that during the day the higher terrain becomes an elevated heat source, whereas at night it is an elevated heat sink. Two categories of mountain-valley winds are generally recognized — slope flow, and valley winds.

\* This section is based on Pielke (1984).

These types are easiest to recognize when the prevailing large-scale flow is light. Slope flow refers to cool, dense air flowing down elevated terrain at night, with warm, less dense air moving toward higher elevations during the day. Such air movement is often referred to as nocturnal drainage flow and daytime upslope, respectively. The nocturnal drainage flow is also called katabatic wind and the daytime upslope anabatic wind.

Valley winds, the second category of mountain-valley flow are up and down valley circulations that develop from along valley horizontal pressure gradients in one segment of a valley, which occur because of the input into that part of the valley by the slope flow of air of a different temperature structure than occurs adjacent to that segment.

During sunny days, slope winds tend to be deeper than at night, as with the sea breeze, because the heating of the ground by the sun is mixed upward effectively by turbulent heat flux. At night radiational cooling predominates if the winds are light and the resultant perturbation flow field is more shallow.

When either a large-scale flow — often including a vertical shear of the horizontal wind — variable surface characteristics, and/or three-dimensional topographic features are present, the resultant mesoscale flow can become very complex. The diurnal variations in winds in such situations can be predicted only with an extensive network of observations and accurate three-dimensional mesoscale models.

#### 5.9.1.3 FORCED AIRFLOW OVER AND AROUND ROUGH TERRAIN

When air flows over terrain features that have horizontal scales of 25–100 km or so another type of mesoscale system develops, which is different from the sea and land breezes, and mountain-valley winds, because forced ascent of air in a prevailing stably stratified air mass, rather than differential heating of the ground by the sun, generates the mesoscale perturbation. The intensity of this mesoscale perturbation is directly proportional to the pressure gradient generated by this forced movement of air.

According to linear theory, in the absence of Coriolis effect, two types of wave motions are induced as air flows over rough terrain: forced waves, which are colocated with the underlying topography, and lee waves, which propagate downstream. Trapped lee waves, which propagate indefinitely downstream in the absence of friction but which decay in amplitude rapidly with height, are a commonly seen type of air motion to the lee of the mountain barriers when the Scorer parameter decreases rapidly with height. Linear theory predicts that the vertical wavelength of lee waves induced by a single ridge is given by:

$$L_z = 2\pi S_o^{1/2} = 2\pi V_g / [(g/\theta_o)(\partial\theta_o/\partial z)]^{1/2}$$

where  $S_o$  is called the Scorer parameter. According to linear theory, for well-developed waves to develop, the Scorer parameter must be less in the upper troposphere than at lower levels. This requires that if  $\partial\theta_o/\partial z$  is constant,  $V_g$  must increase with height, whereas if  $V_g$  is constant,  $\partial\theta_o/\partial z$  must be less stable in the higher levels. When the Coriolis effect and boundary layer dynamics are included, the response of the atmosphere to terrain is more complicated. The following are some important effects on the weather and atmospheric structure associated with the forced airflow over mountains.

Strong downslope winds occur in the lee side of the mountains. These winds are strongest when an inversion is present near a mountain top level upstream and if the temperature and wind profiles are such that the wave induced by the terrain approximately reverses the phases between the surface and the tropopause.

When the air is too stable and cannot go over or around the mountain breeze and when the terrain feature is too elongated, the influence of the mountain propagates rapidly upwind — a process called blocking. This blocking causes a deformation of the potential temperature surfaces so as to create an unstable layer upstream of the mountain. This blocking can result in the formation of mountain parallel low-level jets.

The blocking and the resultant deformation of the upstream isentropes could also create regions of convective instability even if no such instability were present in the upwind synoptic flow, thereby enhancing precipitation immediately upstream of the mountains, as well as increasing the spatial irregularity of precipitation.

Because of the increase in potential temperature that results from the release of latent heat and of the potentially warmer air from above the planetary boundary layer, comparatively dry and even arid regions often occur in the lee of the mountains, particularly when the prevailing flow is persistently from one direction.

The precipitation and cloud shadowing can effect the intensity of airflow over the mountains. The latent heat release can substantially alter the structure of internal waves over mountain terrain.

#### 5.9.2 *Synoptically-induced mesoscale phenomena*

##### 5.9.2.1 CONVECTIVE STORMS\*

Convective storms are composed of individual convective cells which are defined as regions of strong updraft having a horizontal cross-section of 10–100 km<sup>2</sup>, and extending in the vertical through most of the troposphere. Convection plays a part in most large-scale weather systems, but there also exist systems of mesoscale dimensions within which convective cells form a disturbance which is isolated and not part of a larger disturbance containing atmospheric mechanisms other than near vertical convection. There is a notable tendency for convective storms to be organized into lines. The classification of convective storms is described below:

\*This section is based on Doswell (1989a) and Collier (1989).

#### 5.9.2.1.1 **SHORT-LIVED SINGLE CELL STORMS**

A single updraft extending through the troposphere and producing liquid water and ice. When the raindrops or ice particles become too heavy to be supported by the updraft they fall creating a downdraft within which mixing of drier air occurs causing evaporative cooling. This cooling accelerates the downdraft, and if the downdraft becomes strong enough it spreads horizontally near the surface producing a cold surge referred to as a gust front.

#### 5.9.2.1.2 **SUPERCELL STORM**

A single, quasi-steady, rotating updraft having a life time of several hours. The storm propagates to the right, or occasionally to the left of the mean winds, and often evolves from multicell storm systems. It represents a high positive correlation between vertical velocity and the vertical component of vorticity. In more colloquial terms it is a rotating thunderstorm (Doswell, 1989b). Although supercells are relatively rare, accounting for less than 10 per cent of all severe-weather producing convective storms (the fraction of supercells varies geographically), they account for a disproportionate share (perhaps approaching 50 per cent in some areas) of the damage and casualties associated with severe thunderstorms. This is generally a reflection of the intensity of the phenomena associated with supercells. Severe events in supercells tend toward the high end of the intensity scale for all forms of severe weather, with the possible exception of precipitation intensity. Supercells can produce virtually all forms of severe weather (hail, damaging straight winds, tornadoes, heavy precipitation, and frequent lightning) at one time or another during their existence.

Supercell storms typically have life cycles measured in hours, rather than tens of minutes as do the component cells in non-supercellular convection. It is, therefore, common to consider supercells as having attained a steady state structure. This is though somewhat misleading, as supercells generally exhibit a characteristic evolution taking place over a period of about 45 minutes, and many supercells go through this evolution more than once, qualifying as so-called cyclic supercells.

For reasons that are as yet unclear, there can be low-precipitation supercells, high-precipitation supercells, and so-called classical supercells, depending on the amount and storm-relative distribution of precipitation. Since many supercells move relatively slowly, the classical and high-precipitation versions of the supercell can produce flash flooding. Large hail may be produced even in the low-precipitation version of the supercell.

#### 5.9.2.1.3 **MULTICELL STORMS**

A cluster of short-lived single cells, the cold outflow from which may combine to form a large gust front. Convergence at the leading edge of the gust front triggers new updrafts and new cells develop. These can be divided into multicell line structures and multicell cluster structures, as follows:

(a) **Multicell line structures (squall lines)**

A multicellular thunderstorm structure in which the cells are aligned laterally over a distance that is large compared to the dimensions of a single cell and where the spacing between cells is comparable to or less than those single cell dimensions. The above definition implies that the cells within the line interact strongly. The mutual interaction among cells in a squall line tends to limit the local intensity of the severe weather. In fact the more the cells interact, the less likely is the severe weather, with some rare exceptions.

Studies indicate that squall lines apparently propagate as waves with particularly intense convective activity occurring where two or more of these waves constructively re-inforce one another and where the atmosphere is convectively unstable (Raymond, 1975). Sun and Ogura (1979) suggested that squall lines may also be initiated through differential temperature gradients in the boundary layer interacting with the synoptic flow. Uccellini and Johnson (1979) examined the role of tropospheric jet streaks in squall line development. Emanuel (1982) discussed the possibility that squall lines are self exciting and involve a CISK-like co-operative interaction between the cumulus and the mesoscale. Squall lines that become stagnant over one geographic location can produce devastating floods. Squall lines also often produce devastating tornado outbreaks;

(b) **Multicell cluster structure: mesoscale convective complexes**

Maddox (1980a, b) identified mesoscale convective complexes (MCCs) or mesoscale convective clusters, which are characterized by the intensification of areas or bands of cumulonimbus which together with a region of stratiform rain may extend laterally over hundreds of kilometres. Maddox gives the following definition of an MCC:

- (i) Size: Contiguous cloud shield with temperatures less than or equal to  $-32^{\circ}\text{C}$  covering an area of more than  $100\,000\,\text{km}^2$ , and an interior cloud region with temperatures less than or equal to  $-52^{\circ}\text{C}$  covering an area of more than  $50\,000\,\text{km}^2$ ;
- (ii) Duration: The above two conditions must last for at least six hours. The MCC is then defined as an entity until the two conditions listed above no longer apply;
- (iii) Shape: The eccentricity (i.e. ratio of minor to major axis) must be greater than or equal to 0.7 at the time of its maximum extent. The convective cells that make up such a system go through many life cycles during such a long-lasting episode. In fact, such MCC-type systems can be comparable to tropical cyclones in terms of size and/or duration, but the

convection within them can exceed tropical cyclonic convection in intensity. A composite model of MCCs has been suggested recently by Cotton, *et al.* (1989). Systems failing to meet the MCC criteria can still be important mesoscale convective systems (MCSs) (Doswell, 1989a).

The process that usually is responsible for most of the convective systems is the merged outflow from the constituent convective cells. The system is persistent simply because so much rain-cooled outflow air is produced by the many convective cells. Further, along the outflow's leading edge, new convection is being initiated constantly during the life time of the system. Strong winds, heat, and tornadoes are most likely during the development of such a system, while individual cells are not interacting strongly. Later, the typical MCSs produce mostly moderate to heavy rain, so that the threat shifts to flash flooding. Occasionally, some systems produce widespread episodes of severe weather, consisting mostly of damaging winds. It is not yet entirely clear why a few MCSs develop this character. When they do, such systems are called derechos (Doswell, 1989a).

MCCs are a major component of the tropical atmosphere and in the past have been referred to as cloud clusters (Pielke, 1984). A cloud cluster appears on a satellite picture as an organized solid white mass. Sometimes large cirrus canopies are associated with these cloud clusters. An analysis of the characteristics of cloud clusters was presented by Williams (1970), who found that clusters were usually associated with a weak form of wave motion. Cyclonic shear rather than curvature was the main feature of these waves. The vertical divergence patterns revealed inflow below 400 hPa, with a compensating outflow concentrated around 200 hPa. Many studies have been in progress on the development and movement of cloud clusters. Mention may be made of an objective technique which was suggested by Sikdar and Suomi (1971) for estimating the energy exchange in tropical convection systems. This was done by measuring the change in the area of cirrus outflow from successive geosynchronous cloud photographs. Sikdar and Suomi proposed different models of tropical convection. These models suggest a lower layer of inflow in which moist air is drawn into the cloud region by convergence in the planetary boundary layer. Above this lies a layer of vertical motion in the form of a funnel. The vertical motion is maximum at the core and decreases rapidly towards the periphery of the cloud. Lastly, the models suggest a layer of outflow between the layer of vertical motion and the tropopause. It is believed that this form of convection transports heat from the boundary layer in the tropics to the tropical upper troposphere. The main uncertainty lies in the mechanism of entrainment or mixing between a rising cloud tower and its environment, which inhibits the growth of the cloud. The work of Riehl and Malkus (1958) discusses hot towers and their role in the dynamics of forecasting in the tropics.

Leary and Houze (1979) discuss the structure and evolution of convection in a tropical cloud cluster. Their data show that virtually all of the precipitation in the tropical cloud cluster studied was associated with six identifiable mesoscale precipitation features, which appear to be the primary entities within which deep tropical convection occurs. This study describes the importance and interaction of these features during the formative, intensifying, mature, and dissipating stages of the cloud cluster. The results of other research presented in recent literature concern the structure and dynamics of a tropical squall line system (Houze, 1977), and the mesoscale and convective-scale downdrafts as distinct components of a squall line structure (Zipser, 1977). Observational studies of these tropical systems include those of Houze and Cheng (1981), Houze (1982), and Zipser, *et al.* (1981). The comprehensive review of the studies on convective storms and cloud dynamics can be found in Cotton and Anthes (1989).

#### 5.9.2.2 ENVIRONMENTAL CONDITIONS FAVOURABLE FOR THE OCCURRENCE OF CONVECTIVE STORMS

- (a) Broadly, the character of convective storms is determined primarily by the strength of the updrafts and vertical wind shear. It has long been recognized that severe convective storms have a direct association with subtropical latitude jet streams. Figure 5.24 shows the close relation between the seasonal positions of upper-level jet streams and the severe weather-prone areas around the world;

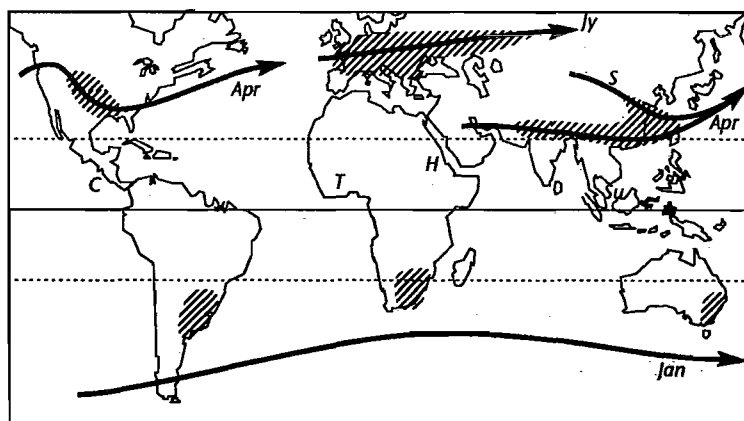


Figure 5.24 — Schematic illustration of the relation between seasonal positions of upper-level jet streams (arrows) and the severe weather-prone areas around the world (slanted hatching). Vertical hatching shows tropical regions prone to strong thunderstorms (After Doswell, 1989a).

- (b) The supercell storms tend to occur at the extreme ends of the buoyancy-shear distribution. Supercells mostly occur in situations with strong convective instability (very low static stability, copious low-level moisture) that is kept from premature release by a capping inversion. The loaded gun sounding that characterizes most supercell events evolves as moisture at low levels and is transported under an elevated mixed layer characterized by nearly neutral static stability (i.e. dry adiabatic lapse rate). This type of sounding development often favours the creation of low-level jet streams and increasing wind shear;
- (c) For squall lines, the most favourable shear structure is one in which the shear tends to be confined to relatively low levels in the environment. The linear character of squall lines is promoted by the processes that favour development of substantial outflow, i.e. dry air impinging on the storm from the rear in mid-troposphere;
- (d) Severe multicell storms occur with moderate instability, many different ranges of moisture and moderate vertical wind shear.

#### 5.9.2.2.1 USE OF A HODOGRAPH FOR THE DIAGNOSIS OF VERTICAL WIND SHEAR

The diagnosis of vertical wind shear can be carried out with the help of a hodograph. A hodograph is a line connecting the tips of the wind vectors in a vertical wind profile, and all the vectors are plotted to a common origin. Any segment of the hodograph between any two wind vectors represents the shear in the layer between them. Typical hodographs for environments favouring the occurrence of weak, unorganized convection, multicell storms and supercell storms are depicted in Figure 5.25.

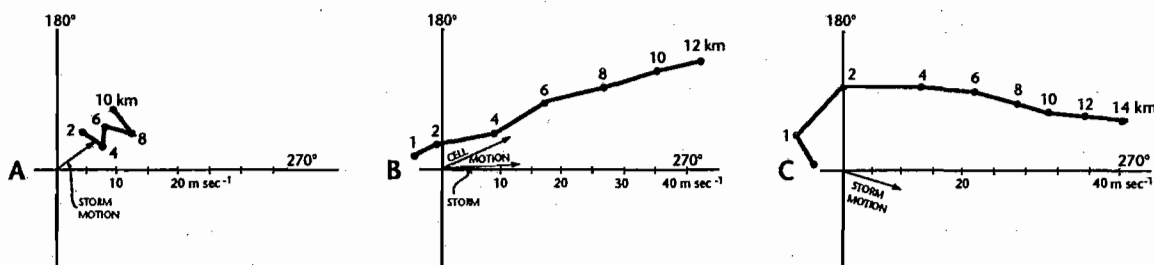


Figure 5.25 — Characteristic hodographs for (a) weak, unorganized convection; (b) multicell storms; and (c) supercell storms (After Doswell, 1989b).

#### 5.9.3 Operational diagnostic tools for mesoscale forecasting

##### (a) Surface observations

With the exception of some of the remote sensing tools, it is the surface data network that comes closest to providing the forecaster with mesoscale data. The special code groups (e.g., pressure change) are extremely important data. Ideally, analysis of surface data on an hourly basis are needed for accurate mesoscale forecasting;

##### (b) Satellite images

The ideal way to view a satellite imagery is in a looping system because the added dimension of motion makes interpretation vastly easier than looking at static images. Though the satellite images give only qualitative information, it is an extremely useful source of information and is, in fact, the only source of data over remote data void regions. The satellite images enable the forecaster to identify the extent of clouds, the height of cloud tops, the movement of clouds, the type of clouds (e.g., convective or stratiform) and the characteristic patterns associated with atmospheric phenomena;

##### (c) Satellite soundings

The TOVS temperature soundings available globally from the National Oceanic and Atmospheric Administration (NOAA) polar orbiters are leading to improvements in the definition of synoptic-scale systems, especially in data-sparse regions. These are expected to provide a better synoptic-scale background field for mesoscale forecasting. However, the sounders need to be on a geostationary platform. The geostationary satellite GOES carries a VISSR atmospheric sounder (VAS) which produces hourly a number of products that are useful in mesoscale forecasting especially for thunderstorm prediction;

##### (d) Radar data

Since the 1950s, the radar has played a central role in mesoscale forecasting and research. Radar echo reflectivity data from various atmospheric targets, the shape and evolution of the echo, the associated Doppler velocity, and polarization characteristics, all provide information about the target themselves and about the convection and mesoscale air motions affecting them. More details on the analysis of radar information are discussed in section 4.3.1.2.5.

For mesoscale forecasting purposes, it is important to achieve good-quality observations over large portions of synoptic-scale precipitation systems and to obtain such observations over considerable distances upwind of the forecast area. This calls for the use of networks of radars.

A typical resolution for weather radar data is one kilometre and five minutes (Browning, 1989). Since this resolution is difficult to achieve in operational practice, a compromise could be five kilometres and 15 minutes. This could be adequate for mapping and tracking most precipitation systems. However, the five kilometre resolution is not adequate in areas where severe convection is common, because it would not resolve important details of individual convective storm cells and convergence lines.

Increasing numbers of weather radars nowadays are capable of measuring line-of-sight velocity from the Doppler shift. It is possible to derive mean wind velocity by conical scans at different elevation angles. A possible method for obtaining a complete three-dimensional field of both temperature and wind through the analysis of a time series of volume scans from a single Doppler radar has been suggested by Wolfsberg (1987).

Wind profiler systems are being implemented in some countries, such as in the United States, to measure wind in the atmosphere. The network is capable of providing detailed and almost continuous time/height wind records of particular value for diagnosing the progression of mesoscale features and for initializing numerical weather prediction models.

A network of Doppler sound detecting and ranging (SODAR) radars for measuring boundary layer winds and, perhaps, combined with a radio-acoustic sounding system (RASS) for measuring detailed low-level temperature profiles might be contemplated in the future.

#### **5.9.4 Mesoscale forecasting methods\***

##### **5.9.4.1 LINEAR EXTRAPOLATION**

This approach, suited to situations with isolated storm cells, is used to extrapolate a linear least-squares fit through successive positions of the centre of the storm cell (Wilk and Gray, 1970). Clustering techniques can be used to deal with more complex and evolving patterns (Blackmer, *et al.*, 1973). A simpler, more robust, and for many purposes more effective approach, is to extrapolate using motions estimated by a cross-correlation technique either in an overall sense (Austin and Bellon, 1974) or within a number of sub-areas to enable different motions to be applied in different regions (Bellon, *et al.*, 1980). The skill of extrapolation forecasts of rainfall patterns derived from radars and satellite, however, falls off dramatically due to fresh developments and decay.

The linear extrapolation approach can be applied to other phenomena besides precipitation, for example, for cloud areas as seen by satellite and thunderstorm areas as detected by lightning detection systems. Other phenomena, such as microbursts, tornado vortex signatures, and wind-shift lines detectable by Doppler radar, are more evanescent and extrapolation may be valid for only minutes or tens of minutes ahead. Because of the severity of the associated weather, however, even this can be valuable, given the appropriate means of disseminating the information.

##### **5.9.4.2 CONCEPTUAL MODELS**

Conceptual models encapsulating an understanding of the structure, mechanism and life cycle of an observed phenomenon (Browning, 1986) may be used to enhance the extrapolation forecasts in many situations. Thus, it is possible, on the basis of conceptual models, to interpret the satellite imagery or the pattern of radar reflectivity or Doppler velocity in terms of a particular category of mesoscale phenomenon, its detailed structure, and the stage in its life cycle. An example is the case just mentioned of a tornado vortex signature detectable by Doppler radar. It is known that as early as 40 minutes before the tornado touches down, the tornado vortex signature may be detected aloft in the middle or upper troposphere (Donaldson, 1975; Brown, *et al.*, 1975), thereby giving the potential for useful advance warning (Hennington and Burgess, 1981).

Zipser (1982) described the application of a life cycle model of a mesoscale convective system (MCS) for enhancing the extrapolation of observed MCSs. The model, from Leary and Houze (1979) shows the varying mixture of convective and stratiform precipitation during the evolution of a class of MCSs common in both the tropics and mid-latitudes. During the formative stage  $t$  and the intensifying state  $t + 3$  hours, cells of heavy convective precipitation predominate. During the mature state  $t + 6$  hours, there is a mixture of convective precipitation and lighter, more widespread, stratiform precipitation. During the decaying stage  $t + 9$  hours, light stratiform precipitation predominates. The decaying stage is often characterized by extensive high cloud, prominent in the satellite imagery, and there may also be widespread lightning. Thus, a forecaster may wrongly predict continuing outbreaks of severe weather unless he keeps the life cycle model in mind.

##### **5.9.4.3 RULES OF THUMB**

Although objective extrapolation and numerical models are playing an increasing role in mesoscale forecasting, rules of thumb are still needed, the application of which require an appreciation on the part of the forecaster of the mesoscale behaviour of the atmosphere. Unfortunately, rules of thumb tend not to be intellectually satisfying and so there is not much well-organized literature on the subject.

One area where rules of thumb need to be applied is that of forecasting thunderstorm outbreaks. McGinley (1986) summarized some of the key steps the forecaster should take based mainly upon experience in the United States:

- (a) Analyse accurately the morning radiosondes in the region of interest to determine the stability and amount of lift necessary to break any capping inversion;

---

\* This section is based on Browning (1989).

- (b) Watch the evolution of sea breezes and urban heating which may locally enhance or suppress the capping layer;
- (c) Look for evidence of increasing boundary-layer moisture;
- (d) Note the formation and distribution of the first convective clouds to determine if there is a forcing mechanism on the mesoscale, evident from either satellite or upper-air data. Also watch outflow boundaries as sources of destabilization;
- (e) Be alert to the likely patterns of uplift associated with fronts and jet streaks;
- (f) Watch for indications of the establishment of a low-level jet.

The preconditions for severe storms are similar to those for ordinary thunderstorms but with two notable additions — a source of dry air above the moist layer, and vertical wind shear. Colquhoun (1987) proposed a decision-tree approach to forecasting thunderstorms and their severity. At each decision point, the forecaster uses a rule of thumb which needs to be appropriately tuned for his particular region.

#### 5.9.4.4 MESOSCALE CLIMATOLOGY

Topography plays an important part in generating mesoscale phenomena and in localizing the resulting weather effects in ways that depend on the low-level wind and stability. There is therefore considerable benefit to be gained from the derivation of conditional mesoscale climatologies. The forecast problem is then a matter of combining the climatological information with the identification and tracking of the present situations.

#### 5.9.4.5 SPECIAL PURPOSE ONE-DIMENSIONAL MODELS

For a reliable site-specific forecast of mesoscale phenomena, such as boundary-layer cloud amount and the occurrence of fog, it is necessary to go beyond the mere extrapolation of observed cloud areas and mesoscale climatology. An estimation must also be made of the daily cycle of the boundary-layer structure. Because of the importance of representing the turbulent processes, the boundary layer needs to be modelled using many levels in the vertical. This can be done either by means of a nested approach in which extra layers are introduced within a limited-area NWP model or, more simply, by means of an air mass transformation (AMT) model in which a one-dimensional boundary-layer model is applied to trajectories calculated by the NWP model (Reiff, 1987).

#### 5.9.4.6 MESOSCALE NUMERICAL WEATHER PREDICTION

Good progress has been made recently in the development of mesoscale NWP models. Some are being used solely for research but one or two are in use semi-operational. One of these is the United Kingdom Meteorological Office mesoscale model, derived from the model first described by Tapp and White (1976), which is a three-dimensional, non-hydrostatic primitive equation model now operating with 16 levels and a horizontal grid of 15 km (Golding, 1987).

In view of the advances in mesoscale observational techniques described above, it would be tempting to imagine that an immediate way forward would be to incorporate the new data as input into a mesoscale model. Unfortunately, it is not as easy as that. A problem where existing mesoscale observations are concerned is that they tend to be of parameters such as cloud, rain and lightning which, though important in themselves are not easily converted into the dynamically-relevant variables, temperature, humidity and wind. Moreover, although networks of wind profilers will provide the wanted input when they come into operation, great care will be needed to ensure that the model and the observations are combined in an optimal way to produce initial conditions that are consistent with both the models and the observations (Gal-Chen, 1988).

Whether or not mesoscale input data are crucial for obtaining useful forecasts from mesoscale models depends on the meteorological situation. When the predominant forcing is by terrain features, such as land/water temperature contrasts, the initial state of the atmosphere need not be specified in great detail. Indeed, it may be sufficient to rely solely on a background field from a large-scale model as initial data. This approach can lead to useful forecasts of sea breezes, especially where there is a well-defined peninsula as in the case of Florida (Pielke, 1984), and of the distribution of boundary-layer convergence and resulting precipitation when a cold air stream encounters land after crossing either a relatively warm lake (Lavoie, 1972) or warm sea (Monk, 1987). In the case of mesoscale phenomena driven by their own internal dynamics, such as mesoscale convective systems and mesoscale frontal rainbands, however, there can be no escaping the need for detailed observations to depict the mesoscale phenomena, or their precursors, within the initial data. It may be that the synoptic-scale forcing represented in the background field will lead to the development of these phenomena in the model, but in the absence of mesoscale input data it will not necessarily lead to a reliable mesoscale forecast of precisely when or where the development will occur.

Radar and satellite imagery are the only observational data presently available that can match the resolution of the mesoscale model. Although the imagery depicts variables that are of little direct use in a NWP model, the patterns in the imagery contain valuable information about the processes that produced them. Hence, it is the interpretation by an analyst, or eventually to some extent by expert systems, of the patterns seen in the imagery that provides the key to producing the initial mesoscale analyses. This will call for the development over the next decade of a variety of indirect approaches.

## REFERENCES

- Abe, S. and T. Yoshida, 1982: The effect of the width of a peninsula on the sea breeze. *Journal of the Meteorological Society of Japan*, 60, pp. 1074–1084.
- Albignat, J. P. and R. J. Reed, 1980: The origin of African wave disturbances during Phase III of GATE. *Monthly Weather Review*, 108, pp. 1827–1839.
- Allen, L. R., Jr., 1984: COSMOS, CYCLOPS objective steering model output statistics. *Fifteenth conference on hurricanes and tropical meteorology*, 9–13 January 1984, Miami, Florida, American Meteorological Society, pp. 14–20.
- Anderson, A., A. Hollingsworth, S. Uppala and P. Woiceshyn, 1987: *A study of the feasibility of using sea and wind information from the ERS-1 satellite, Part 1: Wind scatterometer data*. European Space Agency, Contract Report.
- Anderson, J. R., 1984: Slow motions in the tropical troposphere. *Paper No. 381*, Department of Atmospheric Science, Colorado State University, Ft. Collins, Colorado.
- Andersson, E. and A. Hollingsworth, 1988: Typhoon bogus observations in the ECMWF data assimilation system. *ECMWF Research Development Technical Memorandum No. 148*, ECMWF, United Kingdom.
- Annette, P., 1978: Cyclone-analogue prediction of the course of tropical cyclones by the National Meteorological Analysis Centre, Melbourne. *Technical Report 28*, Bureau of Meteorology, Australia.
- Anthes, R. A., 1978: The height of the planetary boundary layer and the production of circulation in a sea breeze model. *Journal of the Atmospheric Sciences*, 35, pp. 1231–1239.
- Arnold, C. P., 1977: Tropical cyclone and intensity relationships. *Paper No. 277*, Department of Atmospheric Science, Colorado State University, Ft. Collins Colorado.
- Arnold, J. E., 1966: Easterly wave activity over Africa and in the Atlantic with a note on the intertropical convergence zone during early July 1961. *SMRP Research Paper No. 65*, University of Chicago, Chicago.
- Askue, C. and Cheng Shang Lee, 1984: A study of the genesis and intensification of two 1979 northwest Pacific supertyphoons. *Fifteenth conference on hurricanes and tropical meteorology*, 9–13 January 1984, Miami, Florida, American Meteorological Society, pp. 243–248.
- Aspliden, C. I., G. A. Dean and H. Landers, 1965–1967: *Satellite study, tropical North Atlantic, 1963: Six reports dated from September 1965–December 1967*. Research Reports, Department of Meteorology, Florida State University, Tallahassee, Florida.
- Atkinson, B. W., 1981: *Meso-scale Atmospheric Circulations*. Academic Press, London.
- Atkinson, G. D., 1971: Forecaster's guide to tropical meteorology. *Technical Report 240*, U.S. Air Weather Service.
- Austin, G. L. and A. Bellon, 1974: The use of digital weather records for short-term precipitation forecasting. *Quarterly Journal of the Royal Meteorological Society*, 100, pp. 658–664.
- Bell, G. J., 1962: Predicting the movement of tropical cyclones in the region of the China Sea. *Proceedings of the inter-regional seminar on tropical cyclones*, 18–31 January 1962, Tokyo, pp. 195–198.
- Bell, R. S. and A. Dickinson, 1987: The Meteorological Office operational numerical weather prediction system. *Meteorological Scientific Paper No. 41*, published by HMSO.
- Bellon, A., S. Lovejoy and G. L. Austin, 1980: Combining satellite and radar data for the short-range forecasting of precipitation. *Monthly Weather Review*, 108, pp. 1554–1566.
- Bengtsson, L., H. Bottger and M. Kanamitsu, 1982: Simulation of hurricane-type vortices in a general circulation model. *Tellus*, 34, pp. 440–457.
- Bengtsson, L. and A. J. Simmons, 1983: Medium-range weather prediction: Operational experience at ECMWF. In: *Large-Scale Dynamical Processes in the Atmosphere* (B. J. Hoskins and R. P. Pearce, eds.), Academic Press, New York, pp. 337–363.
- Bengtsson, L., 1985: *Medium-range Forecasting at the ECMWF: Issues in Atmospheric and Oceanic Modelling, Advances in Geophysics*. Part B: Weather Dynamics, Volume 28, Academic Press, New York, pp. 3–51.
- Betts, A. K., 1986: A new convective adjustment scheme, Part I: Observational and theoretical basis. *Quarterly Journal of the Royal Meteorological Society*, 112, pp. 677–691.
- Betts, A. K. and M. J. Miller, 1986: A new convective adjustment scheme, Part II : Single column tests using GATE — Wave, BOMEX, ATEX, and Arctic airmass data sets. *Quarterly Journal of the Royal Meteorological Society*, 112, pp. 693–709.
- Biggs, W. G. and M. E. Graves, 1962: A lake breeze index. *Journal of Applied Meteorology*, 1, pp. 474–480.
- Blackmer, R. H., Jr. and R. O. Duda, 1973: Application of pattern recognition techniques to digitized weather radar data. *Final Report*, Contract 1-36072, Stanford Research Institute, Menlo Park, California.
- Borneman, R., 1978: Verification of satellite derived cloud tops. *National Weather Digest*, 3, pp. 5–9.
- Bradford, R. E., W. B. Waltham and M. M. Kazmierczak, 1975: The man-machine interactive processing system. *Technical Memorandum*, NESS-64, National Oceanic and Atmospheric Administration, U.S. Department of Commerce, Washington, D.C., pp. 83–93.
- Brier, G. W. and J. Simpson, 1969: Tropical cloudiness and rainfall related to pressure and tidal variations. *Quarterly Journal of the Royal Meteorological Society*, 95, pp. 120–147.
- Brown, R. A., D. W. Burgess, J. K. Carter, L. R. Lemon and D. Sirmans, 1975: NSSL dual-Doppler radar measurements in tornadic storms: A preview. *Bulletin of the American Meteorological Society*, 56, pp. 524–526.
- Browning, K. A., 1986: Conceptual models of precipitation systems. *Weather and Forecasting*, 1, pp. 23–41.
- Browning, K. A., 1989: The database and physical basis of mesoscale forecasting: Mesoscale forecasting and its applications. *Lectures presented at the fortieth session of the WMO Executive Council*, 1–20 June 1989, Geneva, WMO-No. 712.

- Burpee, R. W., 1972: The origin and structure of easterly waves in the lower atmosphere of north Africa. *Journal of the Atmospheric Sciences*, 29, pp. 77-89.
- Cadet, D. L., 1990: Synoptic disturbances in the tropics. *Proceedings of the seminar on tropical extratropical interactions*, 10-14 September 1990, ECMWF, United Kingdom, pp. 117-146.
- Carlson, T. N., 1967: Structure of a steady-state cold low. *Monthly Weather Review*, 95, pp. 763-777.
- Carlson, T. N., 1969a: Synoptic histories of three African disturbances that developed into Atlantic hurricanes. *Monthly Weather Review*, 97, pp. 256-276.
- Carlson, T. N., 1969b: Some remarks on African disturbances and their progress over tropical Africa. *Monthly Weather Review*, 97, pp. 716-726.
- Chan, J. C. L., B. J. Williams and R. L. Elsberry, 1987: Performance of the nested tropical cyclone model as a function of five storm related parameters. *Monthly Weather Review*, 115, pp. 1238-1252.
- Chan, J. C. L. and R. T. Williams, 1987: Analytical and numerical studies of the beta-effect in tropical cyclone motion, Part I: Zero mean flow. *Journal of the Atmospheric Sciences*, 44, pp. 1257-1264.
- Chan, J. C. L., 1990: Tropical forecasting with global models. *Proceedings of the seminar on tropical extratropical interactions*, 10-14 September 1990, ECMWF, United Kingdom.
- Chang, C., 1970: Westward propagating cloud patterns in the tropical Pacific as seen from time-composite satellite photographs. *Journal of the Atmospheric Sciences*, 27, pp. 133-138.
- Chang, C. P. and K. M. W. Lau, 1980: Northeasterly cold surges and near-equatorial disturbances over the winter Monex area during December 1974, Part II: Planetary scale aspect. *Monthly Weather Review*, 108, pp. 298-312.
- Charney, J. G. and A. Eliassen, 1964: On the growth of the hurricane depression. *Journal of the Atmospheric Sciences*, 21, pp. 68-75.
- Charney, J. G., 1970: Maintenance of the ITCZ. *Proceedings of the symposium on tropical meteorology*, 2-11 June 1970, University of Hawaii, Honolulu, Hawaii (unpublished).
- Cheang, B. K. L. and T. N. Krishnamurti, 1980: Middle latitude interactions during the winter monsoon. *Report No. 80-8*, Department of Meteorology, Florida State University, Tallahassee, Florida.
- Chelam, E. V., 1977: Forecasting techniques for west Africa. *Lectures on forecasting of tropical weather, including tropical cyclones with particular relevance to Africa*. Proceedings of the WMO Seminar, 15-26 November 1976, Senegal, Dakar, WMO-No. 492, pp. 105-125.
- Chen, L. and W. M. Gray, 1984: Global view of the upper-level outflow patterns associated with tropical cyclone intensity change during FGGE. *Fifteenth conference on hurricanes and tropical meteorology*, 9-13 January 1984, Miami, Florida, American Meteorological Society, pp. 224-231.
- Choudhury, A., P. S. Urrankar and C. U. Upadhye, 1985: Cloud patterns of monsoon depressions as viewed by meteorological satellites. *Mausam*, 36, pp. 491-498.
- Collier, C. G., 1989: Mesoscale analysis of mid-latitude convective and frontal systems: Programme on short- and medium-range weather prediction research. *PSMP Report Series*, No. 30, World Meteorological Organization, Geneva, pp. 119-140.
- Colquhoun, J. R., 1987: A decision tree method of forecasting thunderstorms, severe thunderstorms and tornadoes. *Weather and Forecasting*, 2, pp. 337-345.
- Cotton, W. R. and R. A. Anthes, 1989: *Storm and Cloud Dynamics*, Academic Press, New York.
- Cotton, W. R., M. S. Lin, R. L. McAnelly and C. I. Trembeck, 1989: A composite-model of mesoscale convective complexes. *Monthly Weather Review*, 117, pp. 765-783.
- Crawford, K. C., 1979: Hurricane surge potentials over southeast Louisiana as revealed by a storm surge forecast model: A preliminary study. *Bulletin of the American Meteorological Society*, 60, pp. 422-429.
- Crutcher, H. L. and R. L. Joiner, 1977: Separation of mixed data sets into homogeneous sets. *Technical Report*, EDS 19, National Oceanic and Atmospheric Administration, Environmental Data Service, Washington, D.C.
- Das, P. K., M. C. Sinha and V. Balasubrammyam, 1974: Storm surges in the Bay of Bengal. *Quarterly Journal of the Royal Meteorological Society*, 100, pp. 437-449.
- Das, P. K., 1986: Monsoons, Chapter 2: Planetary aspects of monsoons. *Fifth IMO Lecture*, Ninth Congress, 2-27 May 1983, World Meteorological Organization, Geneva WMO-No. 613, pp. 11-28.
- Davidson, N. E. and G. J. Holland, 1987: A diagnostic analysis of two intense monsoon depressions over Australia. *Monthly Weather Review*, 115, pp. 380-392.
- De las Alas, J.G. and R. A. Guzman, 1976: Numerical weather analysis and prediction. *Technical Report*, Typhoon Research Project, NSDB PAG 7206En.
- Dell'Osso, L. and L. Bengtsson, 1985: Prediction of a typhoon using a fine-mesh NWP model. *Tellus*, 37A, pp. 97-105.
- Donaldson, R. J., Jr., 1975: History of a tornado vortex traced by plan shear indicator. *Preprints of the sixteenth radar meteorological conference*, Boston, American Meteorological Society, pp. 80-82.
- Dong, K. and C. D. Neumann, 1983: On the relative motion of binary tropical cyclones. *Monthly Weather Review*, 111, pp. 945-953.
- Doswell, C. A., 1989a: Fundamental concepts of operational mesoscale analysis and forecasting for severe convective storms: Programme on short- and medium-range weather prediction research, *PSMP Report Series*, No. 30, World Meteorological Organization, Geneva, pp. 81-117.
- Doswell, C. A., 1989b: Recent research findings on the role of vertical wind shear, applications to forecasting: Programme on short- and medium-range weather prediction research, *PSMP Report Series*, No. 30, World Meteorological Organization, Geneva, pp. 141-156.

- Douglas, M. W., 1987: The structure and dynamics of monsoon depressions. *FSU Report*, No. 86-15, Florida State University, Tallahassee, Florida.
- Dugdale, G., 1977: Streamline and isotach analysis. *Lectures on forecasting of tropical weather, including tropical cyclones with particular reference to Africa*. Proceeding of the WMO Seminar, 15–26 November 1976, Senegal, Dakar, WMO-No. 492.
- Dunn, G. E., 1940: Cyclogenesis in the tropical Atlantic. *Bulletin of the American Meteorological Society*, 21, pp. 215–229.
- Dunn, G. E. and B. I. Miller, 1964: *Atlantic Hurricanes* (revised edition), Louisiana State University Press, Baton Rouge, Louisiana.
- Dvorak, V. F., 1973: A technique for the analysis and forecasting of tropical cyclone intensities from satellite pictures. *Technical Memorandum*, NESS 45, National Oceanic and Atmospheric Administration, Washington, D.C.
- Dvorak, V. F., 1975: Tropical cyclone intensity analysis and forecasting from satellite imagery. *Monthly Weather Review*, 103, pp. 420–430.
- Dvorak, V. F., 1984: Tropical cyclone intensity analysis using satellite data. *NOAA Technical Report*, NESDIS 11, U.S. Department of Commerce, Washington, D.C.
- Elsberry, R. L., 1985: Tropical cyclone motion: A global view of tropical cyclones, Chapter 4. *International workshop on tropical cyclones*, 25 November–5 December 1985, Bangkok, Thailand.
- Emanuel, K. A., 1982: Inertial instability and mesoscale convective systems, Part II: Symmetric CISL in a baroclinic flow. *Journal of the Atmospheric Sciences*, 39, pp. 1080–1097.
- Erickson, C. O., 1974: Use of geostationary satellite cloud vectors to estimate tropical cyclone intensity. *Technical Memorandum*, NESS-59, National Oceanic and Atmospheric Administration, U.S. Department of Commerce, National Environmental Satellite Service, Washington, D.C.
- Erickson, S., 1977: Comparison of developing vs. nondeveloping tropical disturbances. *Atmospheric Science Paper*, No. 274, Colorado State University, Ft. Collins, Colorado.
- Estoque, M. A., 1975: Structure of the mid-oceanic intertropical convergence zone. *Journal of the Meteorological Society of Japan*, 53, pp. 317–322.
- Estoque, M. A. and M. Douglas, 1978: Structure of intertropical convergence zone over the GATE area. *Tellus*, 30, pp. 55–61.
- Estoque, M. A., 1982: African wave disturbances in a general circulation model. *Extended abstracts of the papers presented at the MSJ/JMA/WMO/AMS regional scientific conference on tropical meteorology*, 18–22 October 1982, Tsukuba, Japan, WMO Programme on Research in Tropical Meteorology, Report No. 7, TM-7, pp. 63–64.
- Fett, R. W., 1966: Upper level structure of the formative tropical cyclone. *Monthly Weather Review*, 94, pp. 9–18.
- Fett, R. W. and S. Brand, 1975: Tropical cyclone movement forecasts based on observations from satellites. *Journal of Applied Meteorology*, 14, pp. 452–465.
- Frank, N. L., 1969: The inverted V cloud pattern: An easterly wave? *Monthly Weather Review*, 97, pp. 130–140.
- Frank, N. L., 1970: On the energetics of cold lows. *Proceedings of the symposium on tropical meteorology*, 2–11 June 1970, University of Hawaii, Honolulu, Hawaii, pp. IV-1-E-IV-6.
- Frank, W. M., 1985: A global view of tropical cyclones, Chapter 3. *International workshop on tropical cyclones*, 25 November–5 December 1985, Bangkok, Thailand.
- Fujita, T. T., K. Watanabe and T. Izawa, 1969: Formation and structure of equatorial anticyclones caused by large-scale cross-equatorial flows determined by ATS-I photographs. *Journal of Applied Meteorology*, 8, pp. 649–667.
- Gal-Chen, T., 1988: A theory for the retrieval of virtual temperature from remote measurements of horizontal winds and thermal radiation. *Monthly Weather Review*, 116, pp. 1302–1319.
- Ghosh, S. K., 1977: Prediction of storm surges on the east coast of India. *Indian Journal of Meteorology, Hydrology and Geophysics*, 28, 2, pp. 157–168.
- Giraud, M., 1977: Use of climatology as a forecasting aid — II. *Lectures on forecasting of tropical weather, including tropical cyclones with particular reference to Africa*. Proceedings of the WMO Seminar, 15–26 November 1976, Senegal, Dakar, WMO-No. 492, pp. 220–223.
- Godbole, R. V. and S. K. Ghosh, 1975: The structure of the inter-tropical convergence zone and equatorial westerlies during MONEX-1973. *Tellus*, 27, pp. 123–131.
- Golding, B. W., 1987: Short-range forecasting over the United Kingdom using a mesoscale forecasting system. In: *Short and Medium Range Weather Prediction* (T. Matsuno, ed.), Tokyo, Meteorological Society of Japan, pp. 563–572.
- Gray, W. M., 1968: Global view of the origin of tropical disturbances and storms. *Monthly Weather Review*, 96, pp. 669–770.
- Gray, W. M., 1975: Tropical cyclone genesis. *Atmospheric Science Paper*, No. 234, Colorado State University, Ft. Collins, Colorado.
- Gray, W. M., 1979: Hurricanes: Their formation, structure and likely role in the tropical circulation. *Meteorology over the Tropical Oceans* (D. B. Shaw, ed.), RMS Publisher, Bracknell, United Kingdom, pp. 155–218.
- Gray, W. M., 1981: *Recent advances in tropical cyclone research from rawinsonde composite analysis*, WMO Programme on Research in Tropical Meteorology, Report No. 2, TMP-2.
- He, S. W. and Z. F. Yang, 1981: The relationship between the intensity of summer southwest monsoon over the northwest Pacific and the circulation patterns of the southern hemisphere. *Scientia Atmospheric Sinica*, 5, pp. 50–59.

- Hebert, P. J., 1973: Subtropical cyclone. *Mariners Weather Log*, 17, pp. 203–207.
- Heckley, W. A., M. J. Miller and A. K. Betts, 1987: An example of hurricane tracking and forecasting with a global analysis forecasting system. *Bulletin of the American Meteorological Society*, 68, pp. 226–229.
- Heckley, W. A., 1990: Data assimilation in the tropics. *Proceedings of the seminar on tropical extratropical interations*, 10–14 September 1990, ECMWF, United Kingdom, pp. 303–352.
- Hennington, L. and D. W. Burgess, 1981: Automatic recognition of mesocyclones from single Doppler radar data. *Preprints of the twenty-second conference on radar meteorology*, Boston, American Meteorological Society, pp. 704–706.
- Herbert, P. H. and K. O. Poteat, 1975: A satellite classification technique for subtropical cyclones. *Technical Memorandum*, NWS SR-83, National Oceanic Atmospheric Administration, National Weather Service, Scientific Service Division, Southern Region, Fort Worth, Texas.
- Holland, G. J., 1985: A global view of tropical cyclones. Chapter 2, *International workshop on tropical cyclones*, 25 November–5 December 1985, Bangkok, Thailand.
- Holton, J., 1971: A diagnostic model for equatorial wave disturbances: The role of vertical shear of the mean zonal wind. *Journal of the Atmospheric Sciences*, 28, pp. 55–64.
- Holton, J., 1979: *An Introduction to Dynamic Meteorology*. Chapter 12: Tropical motion systems, Academic Press, New York, pp. 324–361.
- Hope J. R. and C. J. Neumann, 1970: An operational technique for relating the movement of existing tropical cyclones to past tracks. *Monthly Weather Review*, 98, pp. 925–933.
- Houze, R. A., Jr., 1977: Structure and dynamics of a tropical squall-line system. *Monthly Weather Review*, 105, pp. 1540–1567.
- Houze, R. A., Jr., and C-P. Cheng, 1981: Convection in GATE. *Review of Geophysics and Space Physics*, 19, pp. 541–576.
- Houze, R. A., Jr., 1982: Cloud clusters and large-scale vertical motions in the tropics. *Journal of the Meteorological Society of Japan*. Ser. II, 60, pp. 396–410.
- Hubert, L. F., A. F. Krueger and J. S. Winston, 1969: The double intertropical convergence zone: Fact or fiction? *Journal of the Atmospheric Sciences*, 26, pp. 771–773.
- Hubert, L. F. and L. F. Whitney, Jr., 1971: Wind estimation from geostationary satellite pictures. *Monthly Weather Review*, 99, pp. 665–672.
- Japan Meteorological Agency, 1990: Outline of Operational Numerical Weather Prediction at the Japan Meteorological Agency. *Annex to WMO Progress Report on Numerical Weather Prediction of 1990*, Tokyo, WMO/TD No. 403.
- Jarrell, J. D. and W. L. Somervell, 1970: A computer technique for using typhoon analogues as a forecast aid. *Technical Paper No. 6–70*, U.S. Navy Weather Research Facility, Norfolk, Virginia.
- Jarrell, J. D., C. J. Mauck and R. J. Renard, 1975: *Navy's analog scheme for forecasting tropical cyclone motion over the northeastern Pacific Ocean*. ENVPREDRSCHFAC Technical Paper No. 6–75, U.S. Environmental Prediction Research Facility, Naval Postgraduate School, Monterey, California.
- Jarrell, J. D. and S. Brand, 1983: Tropical cyclone strike and wind probability applications. *Bulletin of the American Meteorological Society*, 64, pp. 1050–1056.
- Jelesnianski, C. P., 1965: A numerical calculation of storm tides induced by a tropical storm impinging on a continental shelf. *Monthly Weather Review*, 93, pp. 343–358.
- Jelesnianski, C. P., 1967: Numerical computations of storm surges with bottom stress. *Monthly Weather Review*, 95, pp. 740–756.
- Jelesnianski, C. P., 1972: SPLASH special program to list amplitudes of surges from hurricanes, Part I: Landfall storms. *Technical Memorandum*, NWS TDL-46, National Oceanic and Atmospheric Administration, National Weather Service Techniques Development Laboratory, Silver Spring, Maryland.
- Jelesnianski, C. P. and A. D. Taylor, 1973: A preliminary view of storm surges, before and after storm modification. *Technical Memorandum*, ERL WMPO-3, National Oceanic and Atmospheric Administration, U.S. Department of Commerce, National Hurricane Research Laboratory, Miami, Florida.
- Jelesnianski, C. P., 1974: SPLASH Part II: General track and variant storm conditions. *Technical Memorandum*, NWS TDL-52, National Oceanic and Atmospheric Administration, National Weather Service, Techniques Development Laboratory, Silver Spring, Maryland.
- Johnson, D. R., M. Yanai and T. K. Schaack, 1987: *Monsoon Meteorology*. Chapter 10: Global and regional distributions of atmospheric heat sources and sinks during the GWE, Part III: Heating, topography and clouds, Oxford University Press, New York, pp. 271–297.
- Joint Typhoon Warning Centre, 1979: *Annual Typhoon Report, 1979*, Naval Oceanography Command Centre, Guam, Marianas Islands.
- Jordan, C. L., 1952: On the low-level structure of the typhoon eye. *Journal of Meteorology*, 9, pp. 285–290.
- Jordan, C. L., 1958: The thermal structure of the core of tropical cyclones. *Geophysica (Helsinki)*, 6, pp. 281–297.
- Joung, C. H. and M. H. Hitchman, 1982: On the role of successive downstream development in east Asian polar outbreak. *Monthly Weather Review*, 110, pp. 1224–1237.
- Kallberg, P., 1985: On the use of cloud track and wind data from FGGE in the upper troposphere. *Technical Memorandum No. 111*, ECMWF Research Department, ECMWF United Kingdom.
- Kanamitsu, M., 1985: A study of the predictability of the ECMWF operational forecast model in the tropics. *Journal of the Meteorological Society of Japan*, 63, No. 5, pp. 779–804.

- Katz, A. L., 1972: *Appearance and Vertical Structure of the Intertropical Convergence Zone in Summer*. Trudy, Hydro-meteorological Centre of the U.S.S.R., Moscow, pp. 60–71.
- Keenan, T. D. and F. Woodcock, 1981: Objective tropical cyclone movement forecasts using synoptic and track analogue information. *Meteorological Note 121*, Bureau of Meteorology, Australia.
- Keenan, T. D., 1984: Statistical tropical cyclone forecasting technique for the southern hemisphere. *Technical Report TR 84-07*, Naval Environmental Prediction Research Facility.
- Keenan, T. D., 1986: Forecasting tropical cyclone motion using a discriminant analysis procedure. *Monthly Weather Review*, 114, pp. 434–441.
- Khromov, S. P., 1957: Die geographische Verbreitung der Monsune. *Petermanns geographische Mittellungen*, 101(3), pp. 234–237.
- Klein, W. H. and H. R. Glahn, 1974: Forecasting local weather by means of model output statistics. *Bulletin of the American Meteorological Society*, 55, pp. 1217–1227.
- Koteswaram, P. and C. A. George, 1960: A case study of a monsoon depression in the Bay of Bengal. *Symposium on monsoons of the world*, 19–21 February 1958, New Delhi, pp. 145–156.
- Koteswaram, P. and N. S. Bhaskar Rao, 1963: Formation and structure of Indian summer monsoon depressions. *Australian Meteorological Magazine*, 41, pp. 62–75.
- Krishnamurti, T. N. and R. S. Hawkins, 1970: Mid-tropospheric cyclones of the southwest monsoon. *Journal of Applied Meteorology*, 9, pp. 442–458.
- Krishnamurti, T. N. and M. Kanamitsu, 1973: A study of a coasting easterly wave. *Tellus*, 37, pp. 568–585.
- Krishnamurti, T. N., M. Kanamitsu, W. J. Koss and J. D. Lee, 1973: Tropical east-west circulation during the northern winter. *Journal of the Atmospheric Sciences*, 30, pp. 780–787.
- Krishnamurti, T. N., M. Kanamitsu, R. Godbole, Chia-Bo Chang, F. Carr and J. H. Chow, 1975: Study of a monsoon depression, I: Synoptic structure. *Journal of the Meteorological Society of Japan*, Vol. 53, No. 4, pp. 227–239.
- Krishnamurti, T. N., M. Kanamitsu, R. Godbole, Chia-Bo Chang, F. Carr and J. H. Chow, 1976: Study of a monsoon depression, II: Dynamical structure. *Journal of the Meteorological Society of Japan*, Vol. 54, No. 4, pp. 208–224.
- Krishnamurti, T. N. and D. Subrahmanyam, 1982: The 30–50 day mode at 850 mb during MONEX. *Journal of the Atmospheric Sciences*, 39, pp. 2088–2095.
- Krishnamurti, T. N., 1985: Summer monsoon experiment: A review. *Monthly Weather Review*, 113, pp. 1590–1626.
- Krishnamurti, T. N. and S. Gadgil, 1985: On the structure of 30 to 50 day mode over the globe during FGGE. *Tellus*, 37, pp. 336–360.
- Krishnamurti, T. N., P. K. Jayakumar, J. Sheang, N. Surgi, A. Kumar and S. Gadgil, 1985: Divergent circulations on the 30 to 50 day time scale. *Journal of the Atmospheric Sciences*, 42, pp. 364–375.
- Krishnamurti, T. N., D. Oosterhof and N. Dignon, 1988: Hurricane prediction with a high resolution global model. *FSU Report*, No. 88-8, Department of Meteorology, Florida State University, Tallahassee, Florida.
- Krishnamurti, T. N., 1990: Simulation of low frequency aspects of monsoons. *Proceedings of the seminar on tropical extratropical interactions*, 10–14 September 1990, ECMWF, United Kingdom, pp. 221–251.
- Krishnamurti, T. N., A. Kumar, K. S. Yap, A. P. Dastoor, N. Davidson and J. Sheang 1990: Performance of a high resolution mesoscale tropical prediction model. *Advances in Geophysics*, Vol. 32, Academic Press, New York, pp. 133–286.
- Kruzhkova, T. S., and A. P. Kryzhanovskaya, 1971: *Intertropical convergence zone and principal cyclone routes in the tropics*. Trudy, Hydrometeorological Centre of the U.S.S.R., Moscow, 87, pp. 15–31.
- Kumar, S. and K. Prasad 1973: An objective method for the prediction of tropical storm movement in Indian seas. *Indian Journal of Meteorological Geophysics*, 24, pp. 31–34.
- Kumar, S. and K. Sethumadhavan, 1980: The structure of the intertropical convergence over the Arabian Sea during MONEX-1979, GARP. *FGGE Operations Report*, Vol. 9, World Meteorological Organization, Geneva.
- Kuo, H. L., 1974: Further studies of the parameterization of the influence of cumulus convection on large scale flow. *Journal of the Atmospheric Sciences*, 31, pp. 1232–1240.
- Kurihara, Y. and R. E. Tuleya, 1981: A numerical simulation study of the genesis of a tropical storm. *Monthly Weather Review*, 109, pp. 1629–1653.
- Kurihara, Y. and R. E. Tuleya, 1982: *Influence on Environmental Conditions on the Genesis of a Tropical Storm Intense Atmospheric Vortices* (L. Bengtsson and J. L. Hill, eds.) Springer Verlag, Berlin and New York, pp. 71–79.
- Kurihara, Y., 1985: Numerical modelling of tropical cyclones (Syukuro Manabe, ed.), Vol. 28: Issues in Atmospheric and Oceanic Modelling, Part B: Weather Dynamics. *Advances in Geophysics*, Academic Press, New York.
- Kuuse, J., 1979: Statistical synoptic predictions of tropical cyclone motion. *Australian conference on tropical meteorology*, 24–25 March 1983, Melbourne, Bureau of Meteorology, Australia.
- Lajoie, F. A. and N. Nicholls, 1974: A relationship between the direction of movement of tropical cyclones and the structure of their cloud systems. *Technical Report II*, Department of Science, Bureau of Meteorology, Australia.
- LaSeur, N. W., 1964: Synoptic models in the tropics. *Proceeding of the symposium on tropical meteorology*, 5–13 November 1953, Rotorua, New Zealand, New Zealand Meteorological Service, pp. 319–328.
- Lau, H. and L. Peng, 1987: Origin of low frequency (intraseasonal) oscillations in the tropical atmosphere, Part I: The basic theory. *Journal of the Atmospheric Sciences*, 44, pp. 950–972.

- Lavoie, R. L., 1972: A mesoscale numerical model of lake-effect storms. *Journal of the Atmospheric Sciences*, 29, pp. 1025–1040.
- Leary, C. A. and R. A. Houze, Jr., 1979: The structure and evolution of convection in a tropical cloud cluster. *Journal of the Atmospheric Sciences*, 36, pp. 437–457.
- Lee, C. S., 1986: An observational study of tropical cloud cluster evolution and cyclogenesis in the western North Pacific. Report No. 403, Department of Atmospheric Science, Colorado State University, Ft. Collins, Colorado.
- Leftwich, P. W. and C. J. Neumann, 1977: Statistical guidance for the prediction of eastern North Pacific tropical cyclone motion — Part 2. *Technical Memorandum*, NWS WR 125, National Oceanic and Atmospheric Administration, Salt Lake City, Utah.
- Lewis, J. K., R. E. Whitaker and W. D. Merrell, Jr., 1982: The effects of a stretched-grid coordinate system on long-wave dispersion and energy characteristics. *Journal of Geophysical Research*, 97, pp. 4265–4266.
- Lindzen, R. S. and J. R. Holton, 1968: A theory of quasi-biennial oscillation. *Journal of the Atmospheric Sciences*, 25, pp. 1095–1107.
- Lindzen, R. S., 1987: On the development of the theory of the QBO. *Bulletin of the American Meteorological Society*, 68, pp. 329–336.
- Lorenc, A. C., R. S. Bell and B. Macpherson, 1991: The Meteorological Office analysis correction data assimilation scheme. *Quarterly Journal of the Royal Meteorological Society*, 117, pp. 59–89.
- Lorenc, D., 1984: The evolution of planetary scale 200 mb divergences during the FGGE year. *Technical Note*, No. II/210, Meteorological Office, pp. 1–23.
- Love, G. and G. Garden, 1983: The monsoon low of January 1974. *Extended abstracts of the Australian Conference on tropical meteorology*, 24–25 March 1983, Melbourne, Bureau of Meteorology, Australia.
- Lyons, W. A. 1972: The climatology and prediction of the Chicago lake breeze. *Journal of Applied Meteorology*, 11, pp. 1259–1270.
- Lu, Mong-Ming and M. Yanai, 1984: Equatorially trapped waves at the 200 mb level and their association with meridional wave energy flux and cloud activity. *Fifteenth conference on hurricanes and tropical meteorology*, 9–13 January 1984, Miami, Florida, American Meteorological Society, pp. 514–521.
- Madden, R. A. and P. R. Julian, 1971: Detection of a 40–50 day oscillation in the zonal wind in the tropical Pacific. *Journal of the Atmospheric Sciences*, 28, pp. 702–708.
- Madden, R. A. and P. R. Julian, 1972: Description of global-scale circulation cells in the tropics with a 40–50 period. *Journal of the Atmospheric Sciences*, 29, pp. 1109–1123.
- Maddox, R. A., 1980a: Mesoscale convective cluster. *Bulletin of the American Meteorological Society*, 61, pp. 1374–1387.
- Maddox, R. A., 1980b: A satellite based study of midlatitude, mesoscale convective complexes. *Preprint of the eighth AMS conference on weather forecasting and analysis*, 1–13 June 1980, Denver, Colorado, pp. 329–338.
- Manabe, S., J. L. Holloway and H. M. Stone, 1974: Tropical circulation in a time integration of a global model of the atmosphere. *Journal of the Atmospheric Sciences*, 27, pp. 580–613.
- Mandal, G. S., S. K. Saha and S. C. Gupta, 1987: Diagnostic studies of a Bay of Bengal monsoon depression. *Mausam*, 38, 2, pp. 245–250.
- Mandal, G. S., 1990: *Various aspects of cyclonic storms over the Bay of Bengal and Arabian Sea*. Ph.D. thesis, Jadavpur University, Calcutta.
- Maruyama, T., 1967: Large scale disturbances in the equatorial lower stratosphere. *Journal of the Meteorological Society of Japan*, 46, pp. 391–408.
- Maruyama, T., 1982: Equatorial waves observed during the FGGE period. *Extended abstracts of papers presented at the MSJ/JMA/WMO/AMS regional scientific conference on tropical meteorology*, 18–22 October 1982, Tsukuba, Japan, WMO Programme on Research in Tropical Meteorology, Report No. 7, TM-7, pp. 105–106.
- Mathur, M. B., 1991: The National Meteorological Centre's quasi-Lagrangian model for hurricane prediction. *Monthly Weather Review*, 119, pp. 1419–1447.
- Matsumoto, C. R., 1984: On predicting three-day tropical cyclone motion: An improved statistical scheme. *Fifteenth conference on hurricanes and tropical meteorology*, 9–13 January 1984, Miami, Florida, American Meteorological Society, pp. 21–27.
- McBride, J. L. and W. M. Gray, 1980: Mass divergence in tropical weather system; Paper II: Large scale controls on convection. *Quarterly Journal of the Royal Meteorological Society*, 106, pp. 517–538.
- McBride, J. L., 1981a: Observational analysis of tropical cyclone formation, Part I: Basic definition of data sets. *Journal of the Atmospheric Sciences*, 38, pp. 1117–1131.
- McBride, J. L., 1981b: Observational analysis of tropical cyclone formation, Part III: Budget analysis. *Journal of the Atmospheric Sciences*, 38, pp. 1152–1166.
- McBride, J. L. and R. Zehr, 1981: Observational analysis of tropical cyclone formation, Part II: Comparison of non-developing versus developing systems. *Journal of the Atmospheric Sciences*, 38, pp. 1132–1151.
- McBride, J. L. and T. D. Keenan, 1982: Climatology of tropical cyclone genesis in the Australian region. *Journal of Climatology*, Vol. 2, No. 1, pp. 13–33.
- McBride, J. L., 1984: Observational studies of the Australian northwest monsoon. *Fifteenth conference on hurricanes and tropical meteorology*, 9–13 January 1984, Miami, Florida, American Meteorological Society, pp. 406–409.
- McGinley, J., 1986: Nowcasting mesoscale phenomena. In: *Mesoscale Meteorology and Forecasting*, (P. S. Ray, ed.) American Meteorological Society, Boston, pp. 657–688.

- Merrill, R. T., 1984: A comparison of large and small tropical cyclones. *Monthly Weather Review*, 112, pp. 1408–1418.
- Merrill, R. T., 1985: Environmental influences on hurricane intensification Paper No. 394, Department of Atmospheric Sciences, Colorado State University, Ft. Collins, Colorado.
- Merritt, E. S., 1964: Easterly waves and perturbations. *Journal of Meteorology*, 3, pp. 367–382.
- Miller, B. I., E. C. Hill and P. P. Chase, 1968: Revised technique for hurricane motion by statistical methods. *Monthly Weather Review*, 96, pp. 540–548.
- Miller, F. R. and R. N. Keshavamurthy, 1968: Structure of an Arabian Sea summer monsoon system. *International Indian Ocean Expedition Meteorological Monographs*, No. 1, East-West Centre Press, Honolulu, Hawaii.
- Miyakoda, K., T. Gordon, R. Caverly, W. Stern, J. Sirutis and W. Bourke, 1983: Simulation of a blocking event in January 1977. *Monthly Weather Review*, 111, pp. 846–869.
- Miyakoda, K. and J. Sirutis, 1985: Extended Range Forecasting (Syukuro Manabe, ed.), Vol. 28: Issues in Atmospheric Modelling, Part B: Weather Dynamics. *Advances in Geophysics*, Academic Press, New York, pp. 55–83.
- Miyazaki, M., 1965: A numerical computation of the storm surge of hurricane Carla in the Gulf of Mexico. *Oceanographical Magazine*, 17, pp. 109–140.
- Monk, G. A., 1987: Topographically related convection over the British Isles. In: *Satellite and radar imagery interpretation* (M. Bader and A. Waters, eds.), EUMETSAT, Darmstadt, Federal Republic of Germany, pp. 305–324.
- Mooley, D. A., 1973: Some aspects of Indian monsoon depressions and the associated rainfall. *Monthly Weather Review*, 101, pp. 271–280.
- Morris, R. M. and C. D. Hall, 1987: Forecasting of the tracks of tropical cyclones with the UK operational global model. *ESCAP/WMO Typhoon Committee annual review, 1987*, Typhoon Committee Secretariat, UNDP, Manila, Philippines, pp. 102–105.
- Neumann, C. J., 1972: An alternate to the HURRAN tropical cyclone forecast system. *Technical Memorandum*, NWS SR-62, National Oceanic and Atmospheric Administration, National Weather Service, Southern Region Headquarters, Fort Worth, Texas.
- Neumann, C. J. and J. R. Hope, 1972: A performance analysis of the HURRAN tropical forecast system. *Monthly Weather Review*, 100, pp. 245–255.
- Neumann, C. J., J. R. Hope and B. I. Miller, 1972: A statistical method of combining synoptic and empirical tropical cyclone prediction systems. *NOAA Technical Memorandum*, NWS SR-63.
- Neumann, C. J. and M. B. Lawrence, 1975: An operational experiment in the statistical-dynamical prediction of tropical cyclone motion. *Monthly Weather Review*, 103, pp. 665–673.
- Neumann, C. J. and E. A. Randrianarison, 1976: Statistical prediction of tropical cyclone motion over the southwest Indian Ocean. *Monthly Weather Review*, 104, pp. 76–85.
- Neumann, C. J. and P. W. Leftwich, 1977: Statistical guidance for the prediction of eastern North Pacific tropical cyclone motion — Part I. *Technical Memorandum*, NWS-124, National Oceanic and Atmospheric Administration, National Weather Service, Salt Lake City, Utah.
- Neumann, C. J. and G. S. Mandal, 1977: Statistical prediction of tropical storm motion over the Bay of Bengal and Arabian Sea. *Indian Journal of Meteorological and Hydrological Geophysics*, 29, pp. 487–500.
- Neumann, C. J., 1979: On the use of deep-layer-mean geopotential height fields in statistical prediction of tropical cyclone motion. *Sixth conference on probability and statistics in atmospheric sciences*, Boston, American Meteorological Society, pp. 32–38.
- Neumann, C. J. and J. M. Pelissier, 1981: Models for the prediction of tropical cyclone motion over the North Atlantic: An operational evaluation. *Monthly Weather Review*, 109, pp. 522–538.
- Neumann, C. J., 1983: What should be done to improve the percent? Review of federal research and data collection programme for improving tropical cyclone forecasting. *Federal Coordinator for Meteorological Services and Supporting Research Document FCM-R2-1982*, pp. E-1–E-10.
- Neumann, C. J., 1988: The National Hurricane Centre NHC83 model. *NOAA Technical Memorandum*, NWS NHC 41, National Hurricane Centre, Coral Gables, Florida.
- Neumann, C. J. and C. J. McAdie, 1991: A revised National Hurricane Centre NHC83 model (NHC90). *NOAA Technical Memorandum*, NWS NHC 44, National Oceanic and Atmospheric Administration, Washington, D.C.
- Norquist, D. C., E. E. Recker and R. J. Reed, 1977: The energetics of African wave disturbances as observed during Phase II of GATE. *Monthly Weather Review*, 105, pp. 334–342.
- Novak, C. and M. Young, 1976: The operational processing of wind estimates from cloud motions: Past, present and future. *Proceedings of the symposium on meteorological observations from space: their contribution to the FGGE*, Nineteenth COSPAR (Committee on Space Research, NASA), 7–10 June 1976, Philadelphia, Pennsylvania.
- Obasi, G. O. P., 1977: Forecasting techniques in east Africa. In: *Lectures on forecasting of tropical weather, including tropical cyclones with particular relevance to Africa*. Proceedings of the WMO Seminar, 15–26 November 1976, Senegal, Dakar, WMO-No. 492, pp. 72–101.
- Ooyama, K., 1964: A dynamical model for the study of tropical cyclone development. *Geofísica Internacional* (Mexico), 4, pp. 187–198.
- Orlanski, I., 1975: A national sub-division of scales for atmospheric processes. *Bulletin of the American Meteorological Society*, 56, pp. 520–527.

- Pallmann, A. J., 1968: The synoptics, dynamics and energetics of the temporal using satellite radiation data. *Second Year's Report No. 2*, WBG-89, Department of Geophysics, St. Louis University, St. Louis, Missouri.
- Palmen, E. and C. W. Newton, 1969: *Atmospheric Circulation Systems: Their Structure and Physical Interpretation*, Chapter 14: Circulation and disturbances of the tropics, Academic Press, New York, pp. 427–470.
- Palmer, C. E., 1952: Tropical meteorology. *Quarterly Journal of the Royal Meteorological Society*, 78, pp. 126–164.
- Palmer, C. E., C. W. Wise, L. J. Stempson and G. H. Duncan, 1955: The practical aspect of tropical meteorology. *AWS Manual*, Vol. 1, pp. 105–148.
- Pan, Hua-lu, 1984: 10–20 day tropical-midlatitude interaction during the winter monsoon. *Fifteenth conference on hurricanes and tropical meteorology*, 9–13 January 1984, Miami, Florida, American Meteorological Society.
- Parker, D. E., 1973: Equatorial kelvin waves at 100 millibars. *Quarterly Journal of the Royal Meteorological Society*, 99, No. 1, pp. 116–129.
- Peak, J. E. and R. L. Elsberry, 1986: Prediction of tropical cyclone turning and acceleration using empirical orthogonal function representations. *Monthly Weather Review*, 114, pp. 156–164.
- Pielke, R. A., 1984: *Mesoscale Meteorological Modelling*, Academic Press, Orlando.
- Pike, A. C., 1971: Intertropical convergence zone studied with an interacting atmosphere and ocean model. *Monthly Weather Review*, 99, pp. 469–477.
- Pike, A. C., 1972: Improved barotropic hurricane track prediction by adjustment of the initial wind field. *Technical Memorandum*. NWS SR-66, National Oceanic and Atmospheric Administration, National Weather Service, Southern Region Headquarters, Fort Worth, Texas.
- Pike, A. C., 1984: Geopotential thickness vs. heights as predictors of Atlantic tropical cyclone motion and intensity. *Fifteenth conference on hurricanes and tropical meteorology*, 9–13 January 1984, Miami, Florida, American Meteorological Society, pp. 145–150.
- Pike, A. C., 1985: The variation of track forecast difficulty among tropical cyclone basins. *Extended abstracts of the sixth conference on hurricanes and tropical meteorology*, 14–17 May 1985, Houston, Texas, American Meteorological Society, pp. 76–77.
- Pisharoty, P. R. and G. C. Asnani, 1957: Rainfall around monsoon depressions over India. *Indian Journal of Meteorology and Geophysics*, 8, pp. 15–20.
- Prasad, K. and D. K. Rao, 1974: Case studies of westerly waves in the development of monsoon depressions. *Indian Journal of Meteorology and Geophysics*, 25, 2, pp. 265–268.
- Prasad, K., 1990: Synthetic observations for representation of tropical cyclones in NWP data assimilation systems. *Proceedings of the international symposium on assimilation of observations in meteorology and oceanography*, 9–13 July, 1990, Clermont-Ferrand, France, pp. 581–587.
- Prasad, K., S. R. Kalsi and R. K. Datta, 1990: Wind and cloud structure of monsoon depressions. *Mausam*, 41, 3, pp. 365–370.
- Proudman, J., 1953: *Dynamical Oceanography*, Methuen & Co., Ltd. London.
- Puri, K. and P. Lonnberg, 1991: Use of high-resolution structure functions and modified quality control in the analysis of tropical cyclones. *Monthly Weather Review*, 119, pp. 1151–1167.
- Ramage, C. S., 1961: The subtropical cyclone. *Report No. 15*, Hawaii Institute of Geophysics.
- Ramage, C. S., 1971: *Monsoon Meteorology*, Academic Press, New York.
- Rao, Y. P., 1976: *Southwest Monsoon*. Meteorological Monograph Synoptic Meteorology No. 1/1976, India Meteorological Department, New Delhi.
- Rasmusson, E. M., 1990: Development of our knowledge of the general circulation of the tropics. *Proceedings of the seminar on tropical extratropical interactions*, 10–14 September 1990, ECMWF, United Kingdom.
- Raymond, D. J., 1975: A model for predicting the movement of continuously propagating convective storms. *Journal of the Atmospheric Sciences*, 32, pp. 1308–1317.
- Reed, R. J., 1960: The circulation of the stratosphere. *Paper presented at the fortieth anniversary meeting of the American Meteorological Society*, 19–22 January 1960, Boston, Massachusetts.
- Reed, R. J., D. C. Norquist and E. E. Recker, 1977: The structure and properties of African wave disturbances as observed during phase III of GATE. *Monthly Weather Review*, 105, pp. 317–333.
- Reiff, J., 1987: Forecasting boundary layer clouds and fog: A review on operational numerical models. *Proceedings of an international symposium on mesoscale analysis and forecasting*, 17–19 August 1987, Vancouver, ESA-SP 282, pp. 407–414.
- Riehl, H., 1945: Waves in the easterlies and the polar front in the tropics. *Miscellaneous Reports*, No. 17, Department of Meteorology, University of Chicago, Chicago, Illinois.
- Riehl, H., 1950: On the role of the tropics in the general circulation of the atmosphere. *Tellus*, 2, pp. 1–17.
- Riehl, H., 1954: *Tropical Meteorology*. McGraw Hill Book Company, Inc., New York.
- Riehl, H. and J. S. Malkus, 1958: On the heat balance in the equatorial trough zone. *Geophysics*, 6, pp. 503–538.
- Riehl, H., 1967: Varying structure of waves in the easterlies. *Proceedings of the international symposium on dynamics of large-scale processes in the atmosphere*, 23–30 June 1965, Moscow, pp. 411–417.
- Riehl, H., 1979: *Climate and the Weather in the Tropics*, Academic Press, London, pp. 395–515.
- Robinson, A. R. and G. R. Flierl, 1972: Deadly surges in the Bay of Bengal: Dynamics and storm-tide tables. *Nature*, 239, pp. 213–215.

- Rodgers, E. B., W. E. Shenk, A. C. Gentry and V. J. Oliver, 1977: The benefits of using short interval satellite imagery to derive winds for tropical cyclones. *Paper presented at the eleventh technical conference on hurricanes and tropical meteorology*, 13–16 December 1977, Miami Beach, Florida, American Meteorological Society, pp. 653–660.
- Rodgers, E. B., 1984: The justification for using VAS data to improve tropical cyclone forecasting. *Fifteenth conference on hurricanes and tropical meteorology*, 9–13 January 1984, Miami, Florida, American Meteorological Society, pp. 151–158.
- Sadler, J. C., 1964: Tropical cyclones of the eastern North Pacific as revealed by TIROS observations. *Journal of Applied Meteorology*, 3, pp. 347–366.
- Sadler, J. C., 1967a: On the origin of tropical vortices. *Proceedings of the working panel on tropical dynamic meteorology*, August 1967, Monterey, California, NWRF 12-1167-132, U.S. Naval Weather Research Facility, pp. 39–67.
- Sadler, J. C., 1967b: The tropical upper tropospheric trough as a secondary source of typhoons and a primary source of trade wind disturbances. *Final Report*, Contract No. AF 19(628)-3860, HIG Report 67-12, Hawaii Institute of Geophysics.
- Sadler, J. C., 1969: Average cloudiness in the tropics from satellite observations. *International Indian Ocean Expedition Meteorological Monographs*, No. 2, East-West, Press Honolulu, Hawaii.
- Sadler, J. C., 1976: A role of the tropical upper tropospheric trough in early season typhoon development. *Monthly Weather Review*, 104, pp. 1266–1278.
- Sadler, J. C., 1978: Mid-season typhoon development and intensity changes and the tropical upper tropospheric trough. *Monthly Weather Review*, 106, pp. 1137–1152.
- Sanders, F. A. and R. W. Burpee, 1968: Experiments in barotropic hurricane forecasting. *Journal of Applied Meteorology*, 7, pp. 313–323.
- Sanders, F. A., A. C. Pike and J. P. Gaertner, 1975: A barotropic model for operational prediction of tracks of tropical storms. *Journal of Applied Meteorology*, 14, pp. 265–280.
- Sanders, F. A., L. Adams, N. J. B. Gordon and W. D. Jenson, 1980: Further development of a barotropic operational model for predicting paths of tropical storms. *Monthly Weather Review*, 108, pp. 642–654.
- Sarker, R. P. and A. Choudhury, 1988: A diagnostic structure of monsoon depressions. *Mausam*, 39, 1, pp. 9–18.
- Saucier, W. J., 1955: *Principles of Meteorological Analysis*. The University of Chicago Press, Chicago, Illinois.
- Shaffer, A. R. and R. L. Elsberry, 1982: A statistical climatological tropical cyclone track prediction technique using an EOF representation of the synoptic forcing. *Monthly Weather Review*, 110, pp. 1945–1954.
- Shaffer, A. R., C. P. Chang and R. L. Elsberry, 1984: Long-wave forcing of equatorial penetrating winter monsoon cold surges. *Fifteenth conference on hurricanes and tropical meteorology*, 9–13 January 1984, Miami, Florida, American Meteorological Society.
- Shapiro, L. J., 1984: Sampling errors in statistical models of tropical cyclone motion: A comparison of predictor screening and EOF techniques. *Monthly Weather Review*, 112, pp. 1378–1388.
- Shapiro, L. J. and C. J. Neumann, 1984: On the orientation of grid systems for the statistical prediction of tropical cyclone motion. *Monthly Weather Review*, 112, pp. 188–199.
- Shapiro, L. J., 1986: The three-dimensional structure of synoptic-scale disturbances in the tropical Atlantic. *Monthly Weather Review*, 114, pp. 1876–1891.
- Shapiro, L. J., D. E. Stevens and P. E. Cieselski, 1988: A comparison of observed and model-derived structures of Caribbean easterly waves. *Monthly Weather Review*, 116, pp. 921–938.
- Sheets, R. C. and G. J. Holland, 1981: Australian tropical cyclones Kerry and Rosa, February–March 1979. *Technical Memorandum*, ERL AOML 46, Hurricane Research Division, 4301, Rickenbacker Cause.
- Shimuzu, N., 1982: Some aspects of formation of typhoon Ellis as revealed in satellite imageries. *Extended abstracts of papers presented at the MSJ/JMA/WMO/AMS regional scientific conference on tropical meteorology*, 18–22 October 1982, Tsukuba, Japan, WMO Programme on Research in Tropical Meteorology, Report No. 7, TM-7, pp. 33–34.
- Shukla, J., 1976: *On the dynamics of monsoon disturbances*. D.Sc. Dissertation, Department of Meteorology, Massachusetts Institute of Technology, Cambridge.
- Shukla, J., 1984: Predictability of time averages. In: *Problems and Prospects in Long and Medium Range Weather Forecasting* (D. M. Burridge and E. Kallen, eds.), Springer-Verlag, Berlin and New York, pp. 109–206.
- Shukla, J., 1985: Predictability (Syukuro Manabe, ed.), Vol.28: Issues in Atmospheric and Oceanic Modelling, Part B: Weather Dynamics. *Advances in Geophysics*, Academic Press, New York, pp. 87–121.
- Sikdar, D. N. and V. Suomi, 1971: Time variation of tropical energetics. *Journal of the Atmospheric Sciences*, 28, pp. 170–180.
- Sikka, D. R. and S. Gadgil, 1975: Large-scale rainfall over India during the summer monsoon and its relations to lower and upper tropospheric vorticity. *Geophysical fluid dynamics workshop*, Monsoon meteorology, I.I. Sc., pp. 1–31.
- Sikka, D. R., 1977: Some aspects of the life history, structure and movement of monsoon depressions. *Pure and Applied Geophysics: PAGEOPH*, 115, pp. 1501–1529.
- Simpson, R. H., 1952: Evolution of the Kona storm: A subtropical cyclone. *Journal of Meteorology*, 9, pp. 24–35.
- Simpson, R. H. and H. Riehl, 1981: *The Hurricane and its Impact*. Louisiana State University Press, Baton Rouge, Louisiana.

- Smagorinsky, J., 1969: Problems and promises of deterministic extended range forecasting. *Bulletin of the American Meteorological Society*, 50, pp. 286-311.
- Snitkovsky, A. I., 1973: *Intertropical Convergence Zone and Weather in the Equatorial Part of the East Pacific*. Trudy, Hydrometeorological Centre of the U.S.S.R., Moscow, 105, pp. 3-35.
- Southern, R. L., 1985: Tropical cyclone warning and mitigation systems: A global view of tropical cyclones. *International workshop on tropical cyclones*, 25 November-5 December 1985, Bangkok, Thailand, pp. 147-155.
- Srinivasan V., S. Raman and A. R. Ramakrishnan, 1971: Monsoon depressions as seen in satellite pictures. *Indian Journal of Meteorology and Geophysics*, Vol. 22, No. 3, pp. 337-346.
- Srinivasan, V. and K. Ramamurthy, 1973: Northeast monsoon. *Forecasting Manual*. Part IV, FMU Report No. IV-184, India Meteorological Department.
- Sun, W. Y. and T. Ogura, 1979: Boundary layer forcing as a possible trigger to a squall line formation. *Journal of the Atmospheric Sciences*, 37, pp. 1558-1572.
- Tai, K. S. and Y. Ogura, 1987: An observational study of easterly waves over the eastern Pacific in the northern summer using FGGE data. *Journal of the Atmospheric Sciences*, 44, pp. 339-361.
- Tapp, M. C. and P. W. White, 1976: A non-hydrostatic mesoscale model. *Quarterly Journal of the Royal Meteorological Society*, 102, pp. 277-296.
- Thompson, R. M., S. W. Payne, E. E. Recker and R. J. Reed, 1979: Structure and properties of synoptic scale wave disturbances in the intertropical convergence zone of the eastern Atlantic. *Journal of the Atmospheric Sciences*, 36, pp. 53-72.
- Tsay, C. Y. and S. T. Wang, 1981: Nonlinear energy exchanges among waves and cold-air outbreaks. *National Science Council Monthly* (People's Republic of China), 9, pp. 891-905.
- Tsui, T. L., 1984: A selection technique for tropical cyclone objective forecast aids. *Fifteenth conference on hurricanes and tropical meteorology*, 9-13 January 1984, Miami, Florida, American Meteorological Society, pp. 40-44.
- Tuleya, R. E. and Y. Kurihara, 1981: A numerical study on the effects of environmental flow on tropical storm genesis. *Monthly Weather Review*, 109, pp. 2487-2506.
- Tuleya, R. E. and Y. Kurihara, 1982: A note on the sea surface temperature sensitivity of a numerical model of tropical storm genesis. *Monthly Weather Review*, 110, pp. 2063-2069.
- Tuleya, R. E. and Y. Kurihara, 1984: The formation of comma vortices in a tropical numerical simulation model. *Monthly Weather Review*, 112, pp. 491-502.
- Uccellini, L. W. and D. R. Johnson, 1979: The coupling of upper and lower tropospheric jet streaks and implications for the development of severe convective storms. *Monthly Weather Review*, 107, pp. 682-703.
- Vasic, R. S., 1977: Use of climatology as a forecasting aid - I. In: *Lectures on forecasting of tropical weather including tropical cyclones, with particular relevance to Africa*. Proceeding of the WMO Seminar, 15-26 November 1976, Senegal, Dakar, WMO-No. 492, pp. 215-219.
- Wallace, J. M. and V. E. Kousky, 1968: Observational evidence of Kelvin waves in the tropical stratosphere. *Journal of the Atmospheric Sciences*, 25, pp. 900-907.
- Wallace, J. M., 1969: Some recent developments in the study of tropical wave disturbances. *Bulletin of the American Meteorological Society*, 50, pp. 792-799.
- Wallace, J. M. and C. P. Chang, 1969: Spectrum analysis of large scale wave disturbances in the tropical lower troposphere. *Journal of the Atmospheric Sciences*, 26, pp. 1010-1025.
- Wallace, J. M., 1971: Spectral studies of tropospheric wave disturbances in the tropical western Pacific. *Review of Geophysics and Space Physics*, 9, pp. 557-612.
- Wanstrath, J. J., R. E. Whitaker, R. O. Reid and A. C. Vastomo, 1976: Storm surge simulation in transformal coordinates, Volume 1: Theory and application. *Technical Report No. 76-3*, U.S. Army Coastal Engineering Research Centre.
- Warner, C. and R. H. Grumm, 1984: Cloud distributions in a Bay of Bengal monsoon depression. *Monthly Weather Review*, 112, 1, pp. 153-172.
- Weatherford, C. and W. M. Gray, 1984: Relating typhoon intensity to outer 1-3 radius circulation as measured by reconnaissance aircraft. *Fifteenth conference on hurricanes and tropical meteorology*, 9-13 January 1984, Miami, Florida, American Meteorological Society, pp. 238-242.
- Weatherford, C. and W. M. Gray, 1988: Typhoon structure as revealed by aircraft reconnaissance, Part II: Structural variability. *Monthly Weather Review*, 116, pp. 1044-1056.
- Wilk, K. E. and K. C. Gray, 1970: Processing and analysis techniques used with the NSSL weather radar system. *Proceedings of the fourteenth weather radar conference*, Boston, American Meteorological Society, pp. 369-374.
- Williams, K., 1970: Characteristics of the wind, thermal and moisture fields surrounding satellite-observed mesoscale trade wind cloud clusters of the western North Pacific. *Proceedings of the symposium on tropical meteorology*, 2-11 June 1970, Honolulu, Hawaii, pp. D IV-1-D IV-8.
- Willoughby, H. E., J. A. Clos and M. G. Shoreibah, 1982: Concentric eye wall, secondary wind maxima and the evolution of the hurricane vortex. *Journal of the Atmospheric Sciences*, 39, pp. 395-411.
- Wolfsberg, D. G., 1987: Retrieval of three-dimensional wind and temperature fields from single Doppler radar data. *Report No. 84*, Cooperative Institute for Mesoscale Meteorological Studies, Norman, Oklahoma.
- Woodcock, F., 1980: On the use of analogues to improve regression forecasts. *Monthly Weather Review*, 108, pp. 292-297.

- World Meteorological Organization, 1979: *WWW WMO Tropical Cyclone Project — Sub-project No. 6: Operational Techniques for Forecasting Tropical Cyclone Intensity and Movement*, WMO-No. 528, Geneva.
- World Meteorological Organization, 1987a: *The World Weather Watch Programme, 1988–1997, Second WMO Long-term Plan*, Part II, Vol.1, WMO-No. 691, Geneva.
- World Meteorological Organization, 1987b: Programme on Short- and Medium-Range Weather Prediction Research. *PSMP Report Series*, No. 23, Geneva.
- World Meteorological Organization, 1989: Programme on Short- and Medium-Range Weather Prediction Research. *PSMP Report Series*, No. 30, Geneva.
- World Meteorological Organization, 1990: *Mesometeorology and Short-Range Forecasting Lecture Notes and Students' Workbook for Training Class I and Class II Meteorological Personnel*, by N. F. Veltishchev, WMO-No. 701, Geneva.
- World Meteorological Organization, 1991: *Numerical Weather Prediction Report for 1990*, WMO/TD No. 403, Geneva.
- Xu, Y. and C. J. Neuman, 1985: A statistical model for the prediction of western North Pacific tropical cyclone motion (WPCLPR). *NOAA Technical Memorandum*, NWS-NHC 28, National Hurricane Center, Miami, Florida.
- Yanai, M. and T. Maruyama, 1966: Stratospheric wave disturbances propagating over the equatorial Pacific. *Journal of the Meteorological Society of Japan*, 44, pp. 291–294.
- Yanai, M. and Y. Hayashi, 1969: Large-scale equatorial waves penetrating from the upper troposphere into the lower stratosphere. *Journal of the Meteorological Society of Japan*, 47, pp. 167–182.
- Yanai, M. and M. Murakami, 1970: A further study of tropical wave disturbances by the use of spectrum analysis. *Journal of the Meteorological Society of Japan*, 48, pp. 185–197.
- Yap, Kok-Seng, 1987: *Documentation on two simple tropical models*. WMO Tropical Meteorology Programme Report Series No. 26.
- Yasunari, T., 1981: Structure of an Indian summer monsoon system with around 40-day. *Journal of the Meteorological Society of Japan*, 59, pp. 336–354.
- Young, M. T., R. C. Doolittle and L. M. Mace, 1972: Operational procedure for estimating wind vectors from geostationary satellite data. *Technical Memorandum*, NESS 39, National Oceanic and Atmospheric Administration, U.S. Department of Commerce, Washington, D.C.
- Zangvil, A. and M. Yanai, 1980: Upper tropospheric waves in the tropics, Part I: Dynamical analysis in the wave number frequency domain. *Journal of the Atmospheric Sciences*, 37, pp. 283–298.
- Zangvil, A. and M. Yanai, 1981: Upper tropospheric waves in the tropics, Part II: Association with clouds in the wave number frequency domain. *Journal of the Atmospheric Sciences*, 38, pp. 939–953.
- Zipser, E. J., 1977: Mesoscale and convective-scale downdrafts as distinct components of squall-line structure. *Monthly Weather Review*, 105, pp. 1568–1589.
- Zipser, E. J., R. J. Meiting and M. A. Le Mone, 1981: Mesoscale motion fields associated with a slowly moving GATE convective band. *Journal of the Atmospheric Sciences*, 38, pp. 1725–1750.
- Zipser, E. J., 1982: Use of a conceptual model of life cycle of mesoscale convective systems to improve very-short-range forecasts, Part 3: Simple forecasting methods. In: *Nowcasting* (K. A. Browning, ed.), Academic Press, New York, pp. 191–204.

## ANNEX 5.A

**GUIDELINES FOR DETERMINING THE TYPE OF CYCLONE AND ORIGIN  
OF SUBTROPICAL CYCLONES**

**A. Determining type:**

	Subtropical	Tropical
1. Main convection	Poleward and eastward from centre	Equatorward and eastward from centre
2. Cloud system size	Width 15° latitude or more	Width usually less than 10° latitude
3. Interaction with the environment	Convective cloud system remains connected to other synoptic systems (with the exception of some cold lows)	Cloud system becomes isolated

**B. Determining origin:**

1. Frontal band – typical cloud structure.
2. East of upper trough – amorphous convective cloud mass.
3. Cold low – circular cloud pattern with limited convection near the centre.

## ANNEX 5.B

**GUIDELINES FOR ESTIMATING THE INTENSITY OF SUBTROPICAL CYCLONES**

1. ST 1.5 (25–30 knots)
  - (a) Low-level circulation centre  $\geq 1/2^\circ \leq 2^\circ$  latitude from poorly organized convection (not necessarily dense);
  - (b) For cold lows, convection may not be connected to other systems and a small area ( $<3^\circ$  latitude) of deep-layer convection exists near the centre.
2. ST 2.5 (35–40 knots)
  - (a) Low-level circulation centre  $\geq 1/2^\circ \leq 2^\circ$  latitude from increased deep-layered convection with greater curvature than previous day (not necessarily dense);
  - (b) Outer convective band  $5\text{--}10^\circ$  of latitude east of the centre and possibly another convection band  $2\text{--}4^\circ$  north-west of the centre.
3. ST 3.0 (45–50 knots)
  - (a) Same criteria as (2) above except greater curvature and better organized convection than previous day. Overcast may become dense;
  - (b) Evidence of banding near the centre ( $<1^\circ$  latitude).
4. ST 3.5 (55–65 knots)
  - (a) Deep-layer convection (frequently dense overcast) in band(s)  $1\text{--}3^\circ$  latitude from the centre (no central dense overcast);
  - (b) Outer convective band  $5\text{--}10^\circ$  to the east weaker than previous day, but new band may form  $5\text{--}10^\circ$  latitude to the west;
  - (c) For systems moving rapidly eastward there may be only a dense overcast ( $\geq 3^\circ$  latitude) about  $2\text{--}4^\circ$  east of the centre.

NOTES: (1) ST numbers are analogous to the T numbers developed in Dvorak's (1973) technique.

(2) In (3) and (4) above, if the forward speed of the system at picture (classification) time is greater than 20 knots, then the excess should be added to the maximum wind speed obtained by the cloud feature criteria.

## ANNEX 5.C

**SIMILARITIES AND DIFFERENCES BETWEEN THE DVORAK TECHNIQUE FOR TROPICAL CYCLONES (T) AND THE SUBTROPICAL CYCLONE (ST) TECHNIQUE**

**A. Similarities**

1. Both use convective overcast.
2. Both use distance of the circulation centre from the overcast.
3. ST number features are selected to correspond with observed current intensity (CI) numbers so that ST numbers merge to Dvorak's T number when systems become tropical.

**B. Differences****The ST technique:**

1. Considers environment in determining type.
2. Cannot have a centre under central dense overcast.
3. Translational speed excess above 20 knots added to cloud feature wind estimate.
4. Does not require dense overcast.
5. Does not require bands.
6. Uses curvature of convective features for all ST numbers in the absence of bands.
7. Intensity estimates (i.e. ST numbers) are for wind-speed ranges.

NOTE: For a more complete discussion, see the original paper prepared by Herbert, P. H. and K. O. Poteat, 1975: A satellite classification technique for subtropical cyclones. *NOAA Technical Memorandum, NWS SR-83*, National Weather Service, Scientific Services Division, Southern Region, Fort Worth, Texas.

## CHAPTER 6

# QUALITY CONTROL PROCEDURES

### 6.1 General description

The purpose of quality control is to detect errors in the information content of observations used in the GDPS and, if possible, to correct them. Telecommunication checks are made as well as the verification of the meteorological text and content. At some centres these checks may be separated and the telecommunication control is carried out at the RTH while the checking of the meteorological content is made at the RMC or NMC. At centres where only the meteorological content is to be checked, the irrelevant part concerning telecommunication and the text format of the message may be excluded. For this purpose, some effort is made to separate the two areas in the following description.

The reports of the different data types are divided into two main parts. One contains the identification elements and the other contains the physical elements of the current observation. Although the checking of the physical elements may be the main task, it should be realized that the validity checks of the identification elements are equally important. Therefore, in operational work, the best way of proceeding is to apply the validity checks of identification elements first and then to continue by checking the physical elements. The choice of control methods depends very much on the way in which the check is made and on the data available at the time of checking. In manual checking, simple, fairly straightforward methods should be used, while in automatic checking, the techniques can be more complex and perhaps more thorough. The structure of the checking procedure may then take the form described below.

#### 6.1.1 *Pre-processing checks*

The validity check of identification elements contains checks of format, date and time in the message, block number and station number, positions for ships and buoys and duplicate checks. All these control methods are called pre-processing checks, as the control is usually performed during the decoding of the message. If the report is erroneous in any of the identification elements and if it is impossible to correct the value, then there is no point in continuing the quality control. The report is then either rejected or sent back to the data source. A report with correct identification elements is subsequently checked physically.

#### 6.1.2 *Physical elements*

The quality control of the physical elements can be divided into several steps depending on how far the checking is to proceed and on the facilities available. It is suggested that the different steps in the physical control should include a gross error check, internal consistency check, time consistency check, and space/time consistency check. Finally, some kind of a combined control can be performed.

#### 6.1.3 *Building a quality control system*

The aim of this presentation is to build a quality checking system by adding different control methods. It is necessary to start with the basic pre-processing checks, which are usually made during the decoding procedure. These control methods are suitable for both manual and automatic handling. The subsequent gross error control, in which the data is checked against certain limits, can be used in both manual and automatic systems. The methods for internal consistency and time consistency checking are sometimes complicated. Therefore, these methods start with simple descriptions that can be used both manually and automatically followed by methods that should preferably be used in an automatic system. The space/time consistency checks that are described here are only suitable for automatic handling. In the last section on combined checks, examples are given where automatic methods are to be used. The chapters on checks of physical elements contain a description of the methods to be used for each data type.

#### 6.1.4 *Flagging*

The result of checking determines the different ways of continuing, depending on the system that is used. In the case of manual checking, the erroneous values can be either rejected or corrected, and if there are too many errors in the report, the whole report should be discarded or sent back to the data source. With automatic handling, it is necessary to define a system for flagging the errors. The computer program should identify and log all reports that do not pass the control criteria. The flagging system makes it possible to decide on the further handling of the report. The erroneous values may be substituted either by automatically computed values or by manual corrections. Alternatively, the errors may be so serious that the whole report should be excluded. The report can also be accepted with the errors flagged and the flagging can be considered in the further handling of the observations.

The flagging system can also be used to assess the quality of the whole report, which can be useful in choosing between duplicates. Normally when the reports received are duplicates in date, time and position, only the last report is saved, but sometimes a duplicate arrives after both decoding and quality control have been performed. Then the quality assessment of the report can make it easier to decide which report should be kept.

## 6.2 Pre-processing checks

Although each type of message has a unique international transmission format, errors occur during transmission owing to reasons such as human error, machine fault, etc. If the telecommunications operator detects an error while sending the message, he can use a standard procedure of correction by introducing the characters E E E and repeating the last correct group, and then continuing with the message.

Some other fairly common types of errors in messages are alpha characters instead of numeric characters, and errors in grouping. Most meteorological messages contain groups of five numeric characters separated by a blank, but sometimes this blank character disappears or an extra blank appears in the group. The check of adherence to data format specification is generally carried out simultaneously with the decoding of information from the coded message. The possibility of carrying out data format checks depends on the characteristics of the various data format specifications.

### 6.2.1 Checks within the telecommunication area

The heading to identify a message is examined first. It contains information on data type, data source and the time of the message. The reports of the most common data types start by providing information on the date, time and identification, such as the block number and station number or the position of a ship or a buoy. The date and time can be checked against the information in the heading, the station number can be checked against an index, and the position is checked to ensure, for example, that ships are not situated on land.

Duplicate reports occur frequently and a decision must be taken on how to deal with them. Usually the latest report is kept but sometimes other rules have to be applied in order to keep the report with the most data available.

#### 6.2.1.1 HEADING CHECKS

Bulletins with improper headings are automatically rejected and undergo manual inspection. The type of message in the abbreviated heading can be checked against the type of message given in the text of the bulletin.

#### 6.2.1.2 CHECKING E E E REPORTS

If errors are detected during transmission, it is possible to correct the message immediately by sending the letter "E" and "space" repeated alternatively three times and then repeating the last correct group. Often these regulations are not followed strictly, but in a manual check the irregularities are usually easy to find. In an automatic check, however, it is necessary to set up rules to detect and handle the error, otherwise there can be problems in obtaining the correct physical parameters. The following rules are suggested:

- (a) When the message is corrected according to the regulations, the group following E E E is regarded as a reference group. The part of the message that precedes the E E E group is searched for the reference group and when it is found all groups from then on, up to and including the E E E are rejected. For example, if the original message is:

TTAA 62001 06610 99996 01307 01005 00312 // 85320 523 E E 85320 12310  
36010 70890 18520 36015...

the underlined groups are rejected.

- (b) When the last correct group before the E E E group has not been repeated, only the E E E group and the group preceding it should be rejected, as for example, in:

TTAA 62001 06610 99996 01307 01005 00312 // 85320 523 E E 12310 66010  
70890 18520 36015...

the underlined groups are rejected.

#### 6.2.1.3 CHECKING THE SYNTAX AND FIVE-CHARACTER GROUPS

Often alphabetic characters appear in a text that ought to be numerical. This error is usually due to a missing shift and, in such a case, the alpha characters are changed to the corresponding numeric characters. Most reports contain information given in five-character groups. In SYNOP and satellite data reports, there are also section identification groups containing three characters. If any illegal characters are found in a five-character data group, then the parameters in the group are considered to be missing.

Many messages have some kind of grouping error, which, if not corrected, can create confusion in the decoding process. The most common errors are:

- (a) Two or more groups may not have blank separators. Proposed action: a blank character is inserted after every fifth numeric character;
- (b) Two groups may be separated by a special character. Proposed action: the special character is replaced by a blank;
- (c) Groups may not consist of a standard number of characters:
  - (i) A group consists of three characters and is followed by a group of five characters. Proposed action: if the data type is SYNOP or satellite, the three-character group is kept, otherwise it is replaced by a group of five slashes;
  - (ii) A group consists of three characters and is followed by a group of two characters, or vice versa. Proposed action: the blank between the two groups is removed;
  - (iii) A group consists of N (i.e. not three or five) numbers and is followed by a group containing five numbers. Proposed action: if N is less than eight then the group is replaced by

one group of five slashes. If N is larger than eight but less than 12 it is replaced by two such groups, otherwise the group is deleted;

- (iv) A group consists of N (i.e. not three or five) numbers and is followed by a group containing M (i.e. not three or five) numbers. Proposed action: both groups are replaced by groups of five slashes.

## 6.2.2 Control of the WMO code part

### 6.2.2.1 CHECKING THE DATE AND TIME

The abbreviated heading of a message contains a group YYGGgg, which gives the information on date YY and time GGgg. The report itself usually contains information on the date and time as well. The most simple rule to apply is to require that the date be less than or equal to the maximum day for the current month and that the hour of the report be less than or equal to 24. If the hour is 24, then it can be changed to zero and the date can be increased by one.

The date and time information in the heading and in the report should be compatible, but the time can be permitted to differ somewhat. The difference depends on the type of data and on the base hour of the data collection. It is up to the user to define the limits. As a guideline, the following values are suggested. If the difference between heading time and report time is greater than three hours for SYNOP, the report should be rejected. Corresponding limits are 12 hours for TEMP and PILOT and 18 hours for AIREP reports.

### 6.2.2.2 CHECKING THE BLOCK/STATION NUMBER AND THE POSITION

The geographical designator in the abbreviated heading combined with the WMO station list gives information on which block numbers are allowed for the current area. The block number from the report is checked against this information and, if the block number is improper, the report is rejected. The station number should be a non-zero, three-digit number. In most countries, selections of the WMO stations are used. A comprehensive station index, which is valid for the relevant country, is recommended. A search can be made in this index to find the block and station number. If the station does not appear in the index, then the report is either flagged or rejected. One purpose of flagging is to keep track of stations that appear frequently but are not in the index. The index should thus be updated at regular intervals.

A ship report contains information on the quadrant of the Earth in which the ship is positioned as well as its latitude and longitude. The first check is to decide whether the quadrant notation is equal to any of the allowed numbers one, three, five or seven. Furthermore, the latitude should be in the range of 0° to 90° and the longitude should be in the range of 0° to 180°. Reports with latitude and longitude missing are rejected as are SYNOP reports with an improper quadrant.

Ship upper-air data contain an additional group giving the Marsden square of the ship's position. If the quadrant is in some way improper, a correct value may be found from the Marsden-square information.

An important check to be made is to determine whether the ship is at sea. One way of doing so is to look at a table drawn from a map, either manually or automatically, where a notation for land or sea is made for every one-degree square. The latitude and longitude of the ship's position is then compared with information given in the table.

### 6.2.2.3 CHECKS DURING THE DECODING PROCEDURE

Several easy checks can be made during the decoding procedure to make sure that the decoded values are reasonable for the expected parameters. In certain types of reports, such as SYNOP, each group begins with a unique number, indicating both the contents of the subsequent numbers and the relative position of the group within the report. This group identification should be used in the decoding to make sure that correct parameters are extracted. If groups are found in the wrong order, the extra care is needed to ascertain that the group is correctly identified and decoded.

The different meteorological parameters extracted from a SYNOP report should be checked against reasonable limits:

- (a) The pressure, PPPP, in units of 0.1 hPa is given in four digits, with the 1 000 hPa digit removed for pressure above 999.9 hPa. The following rules apply:
  - (i)  $8700 \leq PPPP \leq 9999$  divide by 10 and accept;
  - (ii)  $0000 \leq PPPP \leq 1000$  divide by 10, add 1000.0, and accept;
  - (iii)  $1000 \leq PPPP \leq 8700$  reject;
- (b) The direction of the wind is only accepted if it is in the range of 0° to 360° and the wind speed is not to exceed  $100 \text{ m s}^{-1}$ ;
- (c) Very high or very low values of temperature may be erroneous but may also imply extreme conditions. The temperature should normally be in the range -50° to 50°C. In extreme cases, a temperature check can be made during the decoding phase in the gross-error limit check. Sometimes it is better to perform the temperature control as early as possible and, when extreme cases appear, to try to decide whether there are sufficient conditions to justify the extreme temperature value. One way of doing this is to define certain areas or WMO blocks and certain seasons when temperatures below -50°C are acceptable. A similar definition can be made for conditions when temperatures warmer than 50°C are permissible;
- (d) The dew-point temperature must not exceed the air temperature.

For upper-air data the following checks can be performed during the decoding phase:

- (a) The direction of the wind is only permissible in the range of  $0^\circ$  to  $360^\circ$ ;
- (b) The pressure level indicator, consisting of two characters, in the reports of significant level is checked to ensure that it is in proper sequence. If a discrepancy is found, a search is made for the next proper indicator, and all the groups, beginning from the one with the incorrect indicator up to the next one with the proper indicator, are eliminated. In some cases, the indicator can be restored, but this should be done with great care. The significant levels should also be checked to ensure that the pressure decreases between two successive levels;
- (c) The reports of standard pressure level data also have two-character level indicators, which should be checked to ensure that they are in proper order. In the case where a discrepancy is found, the pressure indicator can be changed, provided that the next standard pressure level indicator can be recognized. Otherwise, all the decoded parameter values for the suspect level should be set as missing;
- (d) Another decision to be made during the decoding procedure is how to find the proper height for the 850 hPa and 700 hPa levels. When coded in the report, the one-thousand digit is omitted from both these levels. It is necessary to restore this before the values are used. One thousand geopotential metres are added to the decoded value of 850 hPa and this new value is accepted as correct unless there is a 500 hPa height available which is less than 5 100 gpm, and unless the decoded 850 hPa value is larger than 650. Two thousand geopotential metres are added to the decoded value of 700 hPa and this value is accepted provided it is not less than 2 300 gpm. If it is less, the height value is increased by another 1 000 gpm.

#### 6.2.2.4 DUPLICATE CHECKS

The methods used to detect and eliminate duplicates differ greatly and depend on the procedures used for collection and decoding. If reports, received in the same collection, are duplicates in date, time and station number, ship call-sign, ship position or aircraft identification/position, then only the latest report is kept. If a report is a duplicate of a report already decoded, then the report with the largest amount of information should be kept. If the old report has already been checked, then the new one should also be decoded and checked. The report with the best quality should be chosen. The quality rating for the reports can be a combination of the amount of data available and the quality of the data. In upper-air reports where data from one station arrive in different parts, it may sometimes be hard to decide on a method to eliminate duplicates. Each part can first be checked for duplicates within the same collection in a similar way to that mentioned above. The different parts are usually combined to form one report after the decoding phase.

If a duplicate of one part arrives after this combination has been made, the problem of how to handle the new information arises. There are many different ways of proceeding. One way is to decode the new report and to compare it, level by level, with the old one. If information is missing on any level in the old report and if the new report provides the information, then the whole level is replaced by information from the new report. When the old information is in some way considered to be erroneous, then the new information replaces it, and the whole observation has to be checked again.

### 6.3 Quality control techniques

The possibility of checking meteorological observations is based upon the redundancy of the information. A simple example of redundancy is the reporting of heights as well as temperatures in the TEMP message. The hydrostatic equation together with this redundancy of data content can be used to construct a very powerful, quality control algorithm ("the hydrostatic control"). In most cases, the redundancy is not as complete as in the TEMP message and, in general, it will only be possible to determine the likelihood of a certain observed value. In this sense almost all methods of quality control of meteorological observations will have a statistical nature. Most algorithms for the rejection of erroneous observations will therefore be based on a compromise between the risk of accepting erroneous values and the risk of rejecting correct values. This problem is illustrated by the following simplified example.

Let us assume that every 10th report from a certain SYNOP station is contaminated by a + 20 hPa error in the surface pressure observation  $Ps_{OBS}$ . For quality control purposes the surface pressure at the station is estimated by horizontal interpolation. Let  $Ps_{INT}$  denote the interpolated value and  $Ps_{TRUE}$  the true surface pressure value. For simplicity, it is further assumed that the interpolation error ( $Ps_{TRUE} - Ps_{INT}$ ) is normally distributed with zero mean and a standard deviation,  $\sigma = 5$  hPa:

$$(Ps_{TRUE} - Ps_{INT}) \sim N(0, 5)$$

To reject the contaminated observations the following checking algorithm is applied:

$$\text{Accept } Ps_{OBS} \text{ if } |Ps_{OBS} - Ps_{INT}| < K \cdot \sigma$$

$$\text{Reject } Ps_{OBS} \text{ if } |Ps_{OBS} - Ps_{INT}| > K \cdot \sigma$$

The constant  $K$  of the checking algorithm is discussed below.

In this simplified case, the probability distribution of  $(Ps_{OBS} - Ps_{INT})$  for the correct observations is  $N(0, 5)$ , while the probability distribution of  $(Ps_{OBS} - Ps_{INT})$  for the erroneous observations is  $N(20, 5)$ . Also taking into account, the probability for an error to occur the total probability distribution for  $(Ps_{OBS} - Ps_{INT})$  will be as illustrated in Figure 6.1.

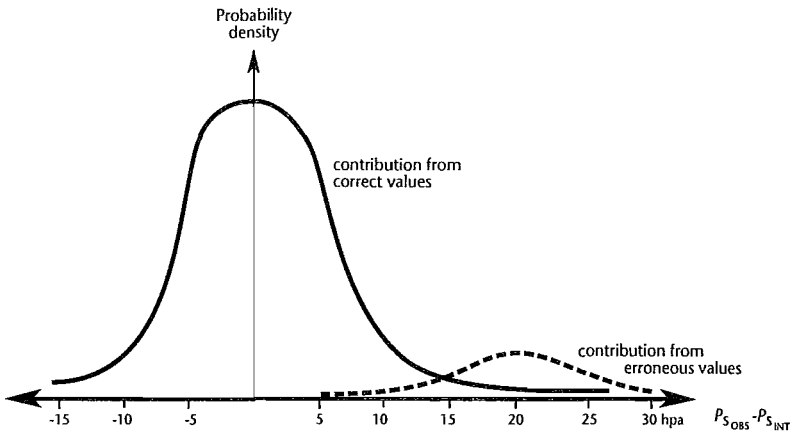


Figure 6.1 — The total probability distribution for  $(Ps_{OBS} - Ps_{INT})$ .

It is evident from the figure that the probability distributions for correct and erroneous values will overlap. Thus, for any value of  $K$  in the checking algorithm, there will be a certain risk of rejecting correct values as well as a risk of accepting erroneous values. The selection of  $K$  will always be a compromise between these two risks. In Table 6.1, these risks are calculated for the simplified case discussed above.

Table 6.1  
Probability of rejecting a correct value or accepting an erroneous value

<i>K</i>	Probability of rejecting a correct value	Probability of accepting an erroneous value
1	$0.90 \cdot 0.1587 \approx 14.3\%$	$0.10 \cdot 0.5 \cdot 0.0013 \approx 0.0\%$
2	$0.90 \cdot 0.0228 \approx 2.1\%$	$0.10 \cdot 0.5 \cdot 0.0228 \approx 0.1\%$
3	$0.90 \cdot 0.0013 \approx 0.1\%$	$0.10 \cdot 0.5 \cdot 0.1587 \approx 0.8\%$
4	$\approx 0.0\%$	$0.10 \cdot 0.5 = 5\%$

From this simple example it is evident that there is a risk of failure for any quality control algorithm. It should also be noted that risks of failure are largest for the most valuable information, for example when extreme values occur in data-sparse areas.

In the practical application of quality control algorithms, it is not always easy to analyse their behaviour. The main reason is that the characteristics of the gross error occurrence are not known. As a result, many operational quality control algorithms have an *ad hoc* formulation with empirical constants which have to be tuned by operational application.

### 6.3.1 Gross-error limit checks

Checks against physical and climatological limits can be performed for many types of data both manually and automatically. These limit checks will only have the ability to detect very crude observational errors. It is an advantage, however, that only a limited amount of resources are needed to apply these checks. The following types of check can be applied:

- (a) Checks against certain fixed-limit values. These checks are mainly applied to variables containing coded information and should only give a classification of the values as correct or erroneous;
- (b) Checks against limits which are functions of area and season (or month). These checks are mainly applied to variables containing information in physical units. The result of these checks can give a classification of the values as correct, suspect or erroneous.

#### 6.3.1.1 LIMIT CHECKS FOR SURFACE DATA

The check against fixed limits in (a) above is only used for data which is given in code form. Normally the WMO code form does not admit values outside these limits, but the decoding procedure can in some way go wrong, resulting in erroneous values which should be detected. The conditions for the values to be considered erroneous are given in Tables 6.2 and 6.3.

Checks against limits which depend on area and time of year can be performed for wind speed, air temperature, dew-point temperature, station-level pressure, sea-level pressure, three-hour pressure tendency, and sea-surface temperature. Suggested limits are presented for each parameter in Tables 6.4–6.10. The limits can be changed and perhaps be made narrower on the basis of improved climatological statistics or experience. The tables suggest the limits to be used for winter and summer.

Table 6.2

Fixed limits for parameters in coded form (in case of indicator  $i_x = 1-4$ )

(The parameters are considered to be erroneous outside the limits.

The denotations are the same as those used in the *Manual on Codes*, WMO-No. 306)

Valid parameter intervals	Valid parameter intervals
$0 \leq h \leq 9$ and / $00 \leq VV \leq 50$ or $56 \leq VV \leq 99$ $0 \leq N \leq 9$ and / $0 \leq a \leq 8$ $00 \leq ww \leq 99$ $0 \leq W_1 \leq 9$ and / $0 \leq W_2 \leq 9$ and / $0 \leq N_h \leq 9$ and / $0 \leq C_L \leq 9$ and / $0 \leq C_M \leq 9$ and / $0 \leq C_H \leq 9$ and / $00 \leq dd \leq 36$ and 99 $00 \leq ff \leq 99$ $s_n = 0, 1, /, 9$ $i_R = 0-4$ $i_x = 1-7$	$00 \leq P_w P_{w'} \leq 99$ and // $00 \leq H_w H_{w'} \leq 99$ and // $00 \leq d_w d_{w'} \leq 36$ and 99 $0 \leq E \leq 9$ and / $0 \leq E' \leq 9$ $0 \leq S \leq 9$ $0 \leq N_s \leq 9$ $0 \leq C \leq 9$ and / $00 \leq h_s h_{s'} \leq 50$ or $56 \leq h_s h_{s'} \leq 99$ $0 \leq D_s \leq 9$ and / $0 \leq v_s \leq 9$ and /

Table 6.3

Fixed limits for parameters in coded form (in case of indicator  $i_x = 5-7$ )

(The parameters are considered to be erroneous outside the limits.

The denotations are the same as those used in the *Manual on Codes*, WMO-No. 306)

Valid parameter intervals	Valid parameter intervals
$0 \leq h \leq 9$ and / $00 \leq VV \leq 50$ or $56 \leq VV \leq 99$ or // $0 \leq N \leq 9$ and / $0 \leq a \leq 8$ and / $00 \leq ww \leq 05$ or $10 \leq ww \leq 12$ or $18 \leq ww \leq 35$ or $40 \leq ww \leq 99$ and // $0 \leq W_1 \leq 9$ and / $0 \leq W_2 \leq 9$ and / $0 \leq N_h \leq 9$ and / $0 \leq C_L \leq 9$ and / $0 \leq C_M \leq 9$ and / $0 \leq C_H \leq 9$ and / $00 \leq dd \leq 36$ and 99 $00 \leq ff \leq 99$ $s_n = 0, 1, /, 9$ $i_R = 0-4$ $i_x = 5-7$	$00 \leq P_w P_{w'} \leq 99$ and // $00 \leq H_w H_{w'} \leq 99$ and // $00 \leq d_w d_{w'} \leq 36$ and 99 and // $0 \leq E \leq 9$ and / $0 \leq E' \leq 9$ and / $0 \leq S \leq 9$ and / $0 \leq N_s \leq 9$ and / $0 \leq C \leq 9$ and / $00 \leq h_s h_{s'} \leq 50$ or $56 \leq h_s h_{s'} \leq 99$ or // $00 \leq D_s \leq 9$ and / $0 \leq v_s \leq 9$ and /

Table 6.4

Limit values for surface wind speed

(The value is considered suspect when  $\text{MAX 1} < ff < \text{MAX 2}$ ;the value is considered erroneous when  $ff > \text{MAX 2}$ )

Area	Winter		Summer	
	MAX 1	MAX 2	MAX 1	MAX 2
45°S – 45°N	60 m s <sup>-1</sup>	125 m s <sup>-1</sup>	90 m s <sup>-1</sup>	150 m s <sup>-1</sup>
45°N – 90°N and 45°S–90°S	50 m s <sup>-1</sup>	100 m s <sup>-1</sup>	40 m s <sup>-1</sup>	75 m s <sup>-1</sup>

Table 6.5

Limit values for surface temperature

(The value is considered suspect when  $\text{MIN } 2 \leq T < \text{MIN } 1$  or  $\text{MAX } 1 < T \leq \text{MAX } 2$ ;  
the value is considered erroneous when  $T < \text{MIN } 2$  or  $T > \text{MAX } 2$ )

Area	Winter				Summer			
	MIN 2	MIN 1	MAX 1	MAX 2	MIN 2	MIN 1	MAX 1	MAX 2
45°S – 45°N	-40°C	-30°C	+50°C	+55°C	-30°C	-20°C	+50°C	+60°C
45°N – 90°N and 45°S – 90°S	-90°C	-80°C	+35°C	+40°C	-40°C	-30°C	+40°C	+50°C

Table 6.6

Limit values for surface dew-point temperature

(The value is considered suspect when  $\text{MIN } 2 \leq T_d < \text{MIN } 1$  or  $\text{MAX } 1 < T_d \leq \text{MAX } 2$ ;  
the value is considered erroneous when  $T_d < \text{MIN } 2$  or  $T_d > \text{MAX } 2$ )

Area	Winter				Summer			
	MIN 2	MIN 1	MAX 1	MAX 2	MIN 2	MIN 1	MAX 1	MAX 2
45°S – 45°N	-45°C	-35°C	+35°C	+40°C	-35°C	-25°C	+35°C	+40°C
45°N – 90°N and 45°S – 90°S	-99°C	-85°C	+30°C	+35°C	-45°C	-35°C	+35°C	+40°C

Table 6.7

Limit values for station pressure

(The value is considered suspect when  $\text{MIN } 2 \leq p \text{ (station)} < \text{MIN } 1$  or  
 $\text{MAX } 1 < p \text{ (station)} \leq \text{MAX } 2$ ; the value is considered erroneous when  
 $p \text{ (station)} < \text{MIN } 2$  or  $p \text{ (station)} > \text{MAX } 2$ )

Area	All year			
	MIN 2	MIN 1	MAX 1	MAX 2
45°S – 45°N	300 hPa	400 hPa	1 080 hPa	1 100 hPa
45°N – 90°N and 45°S – 90°S	300 hPa	400 hPa	1 080 hPa	1 100 hPa

Table 6.8

Limit values for mean sea-level pressure

(The value is considered suspect when  $\text{MIN } 2 \leq p < \text{MIN } 1$  or  $\text{MAX } 1 < p \leq \text{MAX } 2$ ;  
the value is considered erroneous when  $p < \text{MIN } 2$  or  $p > \text{MAX } 2$ )

Area	Winter				Summer			
	MIN 2	MIN 1	MAX 1	MAX 2	MIN 2	MIN 1	MAX 1	MAX 2
45°S – 45°N	870 hPa	910 hPa	1 080 hPa	1 100 hPa	850 hPa	900 hPa	1 080 hPa	1 100 hPa
45°N – 90°N and 45°S – 90°S	910 hPa	940 hPa	1 080 hPa	1 100 hPa	920 hPa	950 hPa	1 080 hPa	1 100 hPa

Table 6.9

Limit values for the three-hour mean sea-level pressure tendency  
 (The value is considered suspect when  $\text{MAX } 1 \leq p_{pp} \leq \text{MAX } 2$ ;  
 the value is considered erroneous when  $p_{pp} > \text{MAX } 2$ )

Area	All year	
	MAX 1	MAX 2
45°S – 45°N	40 hPa	50 hPa
45°N – 90°N and 45°S – 90°S	40 hPa	50 hPa

Table 6.10

Limit values for sea-surface temperature  
 (The value is considered suspect when  $\text{MIN } 2 \leq T_s < \text{MIN } 1$  or  $\text{MAX } 1 < T_s \leq \text{MAX } 2$ ;  
 the value is considered erroneous when  $T_s < \text{MIN } 2$  or  $T_s > \text{MAX } 2$ )

Area	Winter				Summer			
	MIN 2	MIN 1	MAX 1	MAX 2	MIN 2	MIN 1	MAX 1	MAX 2
45°S – 45°N	0°C	+2°C	+32°C	+35°C	0°C	+2°C	+32°C	+35°C
45°N – 90°N and 45°S – 90°S	-2.1°C	-1.0°C	+27°C	+30°C	-2.1°C	-1.0°C	+30°C	+35°C

### 6.3.1.2 LIMIT CHECKS FOR UPPER-AIR DATA (TEMP, PILOT, TEMP SHIP, PILOT SHIP)

The check against limits, which are functions of area and possibly season, is performed for data on the different levels in an upper-air report. The parameters to be checked are geopotential height, temperature and wind speed. Suggested limits for the standard pressure/height levels are given in Tables 6.11–6.13. Limits for intermediate levels may be obtained from the table limits by linear interpolation. The tables do not give limits for different seasons.

Table 6.11

Limit values for geopotential height at different levels  
 (The value is considered suspect when  $\text{MIN } 2 \leq Z < \text{MIN } 1$  or  $\text{MAX } 1 < Z \leq \text{MAX } 2$ ;  
 the value is considered erroneous when  $Z < \text{MIN } 2$  or  $Z > \text{MAX } 2$ ; units are in gpm)

Vertical level	Area 45°S – 45°N				Area 45°N – 90°N and 45°S – 90°S			
	MIN 2	MIN 1	MAX 1	MAX 2	MIN 2	MIN 1	MAX 1	MAX 2
1 000 hPa	-1 000	-800	600	800	-700	-550	650	800
850 hPa	0	200	2 000	2 000	200	400	2 000	2 200
700 hPa	2 200	2 350	3 450	3 600	2 300	2 450	3 450	3 600
500 hPa	4 500	4 700	6 100	6 300				
400 hPa	6 100	6 300	7 800	8 000				
300 hPa	7 300	7 550	9 800	10 100				
250 hPa	8 500	8 800	11 100	11 400				
200 hPa	10 000	10 300	12 900	13 200				
150 hPa	12 000	12 300	14 900	15 200				
100 hPa	14 000	14 400	17 700	18 100				
70 hPa	15 500	16 100	20 900	21 500				
50 hPa	17 700	18 300	23 100	23 700				
30 hPa	20 500	21 100	25 900	26 500				
20 hPa	23 300	23 900	29 700	30 300				
10 hPa	26 000	26 800	33 200	34 000				
7 hPa	30 700	31 300	35 800	36 400				
5 hPa	33 300	33 800	37 800	38 300				
3 hPa	36 600	37 100	41 600	42 100				
2 hPa	39 400	39 800	44 400	44 900				
1 hPa	44 900	45 500	50 100	50 700				

See values for 45°S – 45°N

**Table 6.12**  
**Limit values for temperature at different levels**  
 (The value is considered suspect when  $\text{MIN } 2 \leq T \leq \text{MIN } 1$  or  $\text{MAX } 1 < T \leq \text{MAX } 2$ ;  
 the value is considered erroneous when  $T < \text{MIN } 2$  or  $T > \text{MAX } 2$ )

Vertical level	Area $45^{\circ}\text{S} - 45^{\circ}\text{N}$				Area $45^{\circ}\text{N} - 90^{\circ}\text{N}$ and $45^{\circ}\text{S} - 90^{\circ}\text{S}$			
	MIN 2	MIN 1	MAX 1	MAX 2	MIN 2	MIN 1	MAX 1	MAX 2
1 000 hPa	- 50°C	-30°C	+50°C	+60°C	- 90°C	-70°C	+40°C	+50°C
850 hPa	- 65°C	-50°C	+30°C	+40°C	- 90°C	-70°C	+20°C	+30°C
700 hPa	- 80°C	-70°C	+20°C	+30°C	- 90°C	-70°C	+10°C	+20°C
500 hPa	- 95°C	-80°C	+ 5°C	+10°C	-100°C	-80°C	- 5°C	+ 5°C
400 hPa	-100°C	-85°C	- 5°C	+ 0°C	-100°C	-85°C	-10°C	- 5°C
300–100 hPa	-100°C	-85°C	-10°C	- 5°C	See values for $45^{\circ}\text{S} - 45^{\circ}\text{N}$			
70–10 hPa	-100°C	-85°C	- 5°C	+ 5°C				
7 hPa	- 90°C	-80°C	+10°C	+20°C				
5 hPa	- 80°C	-70°C	+15°C	+30°C				
3 hPa	- 70°C	-60°C	+25°C	+35°C				
2 hPa	- 70°C	-60°C	+30°C	+40°C				
1 hPa	- 70°C	-60°C	+30°C	+40°C				

**Table 6.13**  
**Limit values for wind speed in metres per second at different levels**  
 (The value is considered suspect when  $\text{MAX } 1 < ff \leq \text{MAX } 2$ ;  
 the value is considered erroneous when  $ff > \text{MAX } 2$ )

Vertical level		Area $90^{\circ}\text{S} - 90^{\circ}\text{N}$	
Pressure	Height	MAX 1	MAX 2
1 000 hPa	300 m	60	100
850 hPa	1 500 m	65	100
700 hPa	3 000 m	70	100
500 hPa	5 500 m	100	120
400 hPa	7 000 m	130	150
300–200 hPa	9 000–12 000 m	160	180
150–50 hPa	14 000–20 000 m	150	170
30–20 hPa	22 000–26 000 m	90	110
10 hPa	30 000 m	75	95
7 hPa	—	80	100
5 hPa	—	120	140
3 hPa	—	150	170
2–1 hPa	—	200	220

### 6.3.1.3 LIMIT CHECKS FOR SINGLE LEVEL WIND AND TEMPERATURE DATA (AIRCRAFT, SATOB)

The data in an aircraft report concerning wind and temperature can be checked against limits which are functions of area and level in the same way as the upper-air data. The limits can be obtained from the data in Tables 6.12 and 6.13.

Another way of setting limits for aircraft data is to use the following equations, where the height indicator  $Z_p$  is the height in thousands of feet. The range for  $Z_p$  values is 0 to 61. Suggested lower limits for temperature are:

$$\begin{aligned} \text{MIN} &= -65 + 0.15 \cdot Z_p && \text{when } Z_p \leq 20 \\ \text{MIN} &= -42 - Z_p && \text{when } 20 \leq Z_p < 54 \\ \text{MIN} &= -96 && \text{when } 54 \leq Z_p \leq 61 \end{aligned}$$

Suggested upper limits for temperature are:

$$\begin{aligned} \text{MAX} &= 60 - 3 \cdot Z_p && \text{when } Z_p < 20 \\ \text{MAX} &= 32 - 1.6 \cdot Z_p && \text{when } 20 \leq Z_p < 40 \\ \text{MAX} &= -30 && \text{when } 40 \leq Z_p < 51 \\ \text{MAX} &= -81 + Z_p && \text{when } 51 \leq Z_p \leq 61 \end{aligned}$$

The upper limits which can be used for wind speed are:

$$\begin{aligned} \text{MAX} &= 225 \text{ knots} && \text{when } Z_p \leq 39 \\ \text{MAX} &= 225 - 10 \cdot (Z_p - 39)/3 \text{ knots} && \text{when } 39 < Z_p \leq 61 \end{aligned}$$

### 6.3.1.4 LIMIT CHECKS FOR SATELLITE-SOUNDING DATA (SATEM)

The limit checks for conventional upper-air data can also be used for satellite-sounding data.

### 6.3.2 Internal consistency checks

The checks that are made to control the internal consistency of a report are reasonably straightforward. Most of the checks can be performed either manually or automatically. The different parameters in SYNOP reports are checked against each other and parameters which do not agree with the rest of the information are considered to be either suspect or erroneous. The SYNOP reports may contain station-level pressure observations in addition to pressure reduced to mean sea level or any other standard level. This redundancy of information enables a check to be made of the pressure reduction procedure. The different kinds of upper-air reports are checked for vertical consistency. Thus the temperature profile is checked for superadiabatic layers, the wind profile is checked for extreme wind shear and the geopotentials, together with the temperatures at the standard pressure levels, are checked hydrostatically. The hydrostatic check is rather laborious and should preferably be performed in an automatic system.

Satellite sounding data can, to some extent, be checked in the same way as upper-air data. For example, the temperatures can be checked for superadiabatic lapse rates.

#### 6.3.2.1 CONSISTENCY CHECKS FOR SURFACE DATA

##### 6.3.2.1.1 IN CASE OF INDICATOR $i_x = 1-4$

The different parameters in SYNOP reports are checked against each other. In the description below, the suggested checking algorithms have been divided into areas where the physical parameters are closely connected:

(a) Wind  $dd/ff$

The wind information is considered to be erroneous in the following cases:

$$dd = 00 \text{ and } ff \neq 00;$$

$$dd \neq 00 \text{ and } ff = 00;$$

$$dd = 99 \text{ and } ff = 00 \text{ or } ff \geq 05 \text{ m s}^{-1};$$

(b) Visibility  $VV$  and weather  $ww$

The values of visibility and weather are considered suspect when:

$$42 \leq ww \leq 49 \text{ and } \{10 \leq VV \leq 89 \text{ or } 94 \leq VV \leq 99\};$$

$$ww = 10 \text{ and } \{00 \leq VV \leq 09 \text{ or } 90 \leq VV \leq 93\};$$

$$VV < 10 \text{ and } \{ww < 04 \text{ or } ww = 05 \text{ or } 10 \leq ww \leq 16 \text{ or } 20 \leq ww \leq 29 \text{ or } ww = 40\};$$

$$\{VV < 60 \text{ or } 90 \leq VV \leq 96\} \text{ and } ww \leq 03;$$

$$\{60 \leq VV \leq 89 \text{ or } 97 \leq VV \leq 99\} \text{ and } \{04 \leq ww \leq 07 \text{ or } 38 \leq ww \leq 39\};$$

$$\{ww = 11 \text{ or } ww = 12 \text{ or } ww = 28 \text{ or } ww = 40\} \text{ and } \{00 \leq VV \leq 09 \text{ or } 90 \leq VV \leq 93\};$$

(c) Visibility  $VV$  and cloud information

The values of visibility and cloud cover are considered suspect when:

$$0 \leq h \leq 1 \text{ and } \{70 \leq VV \leq 89 \text{ or } 98 \leq VV \leq 99\};$$

(d) Cloud information

The values of cloud cover are considered erroneous when:

$$N < N_h;$$

$$N_h = 0 \text{ and } \{C_L \neq 0 \text{ or } C_M \neq 0 \text{ or } h \neq 9\};$$

$$1 \leq N_h \leq 8 \text{ and } \{C_L = 0 \text{ and } C_M = 0\};$$

$$N_h = 9 \text{ and } \{C_L \geq 0 \text{ or } C_M \geq 0 \text{ or } C_H \geq 0\};$$

$$N_h = 9 \text{ and } h \geq 0;$$

$$N = 0 \text{ and } \{C_H > 0 \text{ or } C_M > 0 \text{ or } C_L > 0\};$$

$$N \geq 1 \text{ and } N_h = 0 \text{ and } C_H = 0;$$

$$1 \leq N \leq 8 \text{ and } N_h = /;$$

$$1 \leq N_h \leq 8 \text{ and } \{C_L = 0 \text{ and } C_M = 0 \text{ or } C_L = /\};$$

$$\{N_h = 8 \text{ and } 1 \leq C_L \leq 9\} \text{ and } \{C_M \geq 0 \text{ or } C_H \geq 0\};$$

$$N_h = 8 \text{ and } C_L = 0 \text{ and } C_H \geq 0;$$

$$N_h = 0 \text{ and } \{C_H = / \text{ or } C_H = 0\};$$

$$0 < N < 9 \text{ and } N_h = C_L = C_M = C_H = 0;$$

$$N = 0 \text{ and } h \neq 9;$$

$$N = 9 \text{ and } h \neq /;$$

$$N = 9 \text{ and } 0 \leq N_h \leq 8;$$

$$N = 9 \text{ and } N_s \neq 9;$$

$$C_L = 0 \text{ and } C_H = 0 \text{ and } N_h \neq N;$$

$$C_M = 0 \text{ and } C_H = 0 \text{ and } N_h \neq N;$$

$$C_L > 0 \text{ and } \{N_h = 0 \text{ or } N_h = /\};$$

$$C_M > 0 \text{ and } \{N_h = 0 \text{ or } N_h = /\};$$

$$C_L = 0 \text{ and } C_M = /;$$

$$C_M = 0 \text{ and } C_H = /;$$

$$C_M = / \text{ and } C_H \neq /;$$

$$C_L = 0 \text{ and } C \geq 6;$$

$$C_L > 0 \text{ and } C < 6 \text{ in the 1st group } 8N_sCh_sh_s;$$

$$C_L = 3, 9 \text{ and } C \neq 9 \text{ in all groups } 8N_sCh_sh_s;$$

$$C_L \neq 3, 9 \text{ and } C = 9;$$

$$\{C_M = / \text{ or } C_M = 0\} \text{ and } 3 \leq C \leq 5;$$

$$\{C_M = 1 \text{ or } C_M = 2\} \text{ and } C = 3;$$

$\{3 \leq C_M \leq 6 \text{ or } C_M = 8\} \text{ and } 4 \leq C \leq 5;$   
 $1 \leq C_H \leq 4 \text{ and } C = 2;$   
 $7 \leq C_H \leq 8 \text{ and } C = 0;$   
 $0 \leq C_H \leq 8 \text{ and } C = 1;$   
 $C_H = 7 \text{ and } N \neq 8;$   
 $N_s = 9 \text{ and } C \neq /;$   
 $N_s = 9 \text{ and } N \neq 9;$   
 $N_s > N;$   
 $1 \leq N_s \leq 8 \text{ and } C = /;$   
 $0 \leq C \leq 2 \text{ and } \{C_H = / \text{ or } C_H = 0\};$   
 $3 \leq C \leq 4 \text{ and } \{C_M = / \text{ or } C_M = 0\};$   
 $C = 5 \text{ and } C_M \neq 2, 7;$   
 $C_L > 0 \text{ and } N_h < N_s \text{ in group } 8N_sCh_sh_s \text{ with } C \geq 6;$   
 $C_L = 0 \text{ and } N_h < N_s \text{ in group } 8N_sCh_sh_s \text{ with } 3 \leq C \leq 5;$   
 $C \neq 9 \text{ and } N_s < 1 \text{ in 1st group } 8N_sCh_sh_s;$   
 $C \neq 9 \text{ and } N_s < 3 \text{ in 2nd group } 8N_sCh_sh_s;$   
 $C \neq 9 \text{ and } N_s < 5 \text{ in 3rd group } 8N_sCh_sh_s;$   
 $h_sh_s \text{ in 2nd group } 8N_sCh_sh_s < h_sh_s \text{ in 1st group } 8N_sCh_sh_s;$   
 $h_sh_s \text{ in 3rd group } 8N_sCh_sh_s < h_sh_s \text{ in 2nd group } 8N_sCh_sh_s;$

(e) Cloud information and weather *ww*

Clouds and weather are considered suspect when:

$N = 9 \text{ and } \{ww < 16 \text{ or } 18 < ww < 29 \text{ or } ww = 36 \text{ or } ww = 37 \text{ or } ww = 40 \text{ or } ww = 41$   
 $\text{or } ww = 42 \text{ or } ww = 44 \text{ or } ww = 46 \text{ or } ww = 48\};$   
 $N \neq 9 \text{ and } \{ww = 43 \text{ or } ww = 45 \text{ or } ww = 47 \text{ or } ww = 49\};$   
 $N = 0 \text{ and } \{ww = 03 \text{ or } 14 \leq ww \leq 17 \text{ or } 80 \leq ww \leq 99\};$   
 $N < 5 \text{ and } 50 \leq ww \leq 59;$   
 $N < 3 \text{ and } \{60 \leq ww \leq 69 \text{ or } 72 \leq ww \leq 75 \text{ or } 77 \leq ww \leq 79\};$   
 $N_h = 0 \text{ and } \{50 \leq ww \leq 75 \text{ or } 77 \leq ww \leq 99\};$   
 $95 \leq ww \leq 99 \text{ and } C \neq 9;$

(f) Temperature *T* and weather *ww*

Both elements are considered suspect when:

$T > +5^\circ\text{C} \text{ and } \{70 \leq ww \leq 79 \text{ or } 85 \leq ww \leq 88\};$   
 $T < -2^\circ\text{C} \text{ and } \{50 \leq ww \leq 55 \text{ or } 58 \leq ww \leq 65 \text{ or } 80 \leq ww \leq 82\};$   
 $T > +12^\circ\text{C} \text{ and } \{68 \leq ww \leq 69 \text{ or } 83 \leq ww \leq 84\};$   
 $T < -5^\circ\text{C} \text{ and } \{68 \leq ww \leq 69 \text{ or } 83 \leq ww \leq 84\};$   
 $T > +3^\circ\text{C} \text{ and } \{56 \leq ww \leq 57 \text{ or } 66 \leq ww \leq 67\};$   
 $T < -10^\circ\text{C} \text{ and } \{56 \leq ww \leq 57 \text{ or } 66 \leq ww \leq 67\};$   
 $T > +3^\circ\text{C} \text{ and } 48 \leq ww \leq 49;$

(g) Temperature *T* and dew-point temperature *T<sub>d</sub>*

Both values are considered suspect when:

$T - T_d > 5^\circ\text{C} \text{ and } 40 \leq ww \leq 49;$   
 $T_d > T;$

(h) Pressure tendency *app*

The values of *a* and *ppp* are considered erroneous when:

$a = / \text{ and } ppp \geq 0;$   
 $a \geq 0 \text{ and } ppp = /;$   
 $a = 4 \text{ and } ppp > 0;$   
 $ppp = 000 \text{ and } 1 \leq a \leq 3;$   
 $ppp = 000 \text{ and } 6 \leq a \leq 8;$

(i) Weather *ww*, *W<sub>1</sub>*, *W<sub>2</sub>*

The values of *ww* and *W<sub>1</sub>*, *W<sub>2</sub>* are considered erroneous when:

$00 \leq ww \leq 03 \text{ and } 0 \leq W_1 \leq 2;$

(j) Past weather *W<sub>1</sub>*, *W<sub>2</sub>*

The values of *W<sub>1</sub>*, *W<sub>2</sub>* are considered erroneous when:

$W_1 < W_2;$   
 $0 \leq W_1 \leq 2 \text{ and } W_1 \neq W_2;$

(k) Past weather *W<sub>2</sub>* and cloud cover *N*

The values of *W<sub>2</sub>* and cloud cover are considered suspect when:

$W_2 = 0 \text{ and } 5 \leq N \leq 8;$   
 $W_2 = 2 \text{ and } 0 \leq N \leq 4;$

(l) Weather *ww* and wind speed

The values of *ww* and *ff* are considered suspect when:

$\{31 \leq ww \leq 35 \text{ or } ww = 37 \text{ or } ww = 39 \text{ or } ww = 98\} \text{ and } ff < 10 \text{ m s}^{-1};$

- (m) Temperature  $T$  and minimum/maximum temperature  $T_n/T_x$   
 The values of  $T$  and  $T_n, T_x$  are considered erroneous when:  
 $T < T_n;$   
 $T_x < T;$
- (n) Precipitation  $RRR$  and past weather  $W_1, W_2$   
 The values of  $RRR$  and  $W_1, W_2$  are considered erroneous when:  
 $\{5 \leq W_1 \leq 8 \text{ or } (W_1 = 9 \text{ and } 5 \leq W_2 \leq 8)\} \text{ and } RRR = 000;$
- (o) Indicator  $i_R$  and precipitation  $RRR$   
 The values of  $i_R$  and  $RRR$  are considered erroneous when:  
 $i_R = 0-2 \text{ and } \{RRR = 000 \text{ or } RRR = //\};$   
 $i_R = 3 \text{ and } \{RRR \neq 000 \text{ or } RRR \neq //\};$   
 $i_R = 4 \text{ and } RRR = //\};$
- (p) Indicator  $i_x$  and weather  $ww, W_1, W_2$   
 The values of  $i_x$  and  $W_1, W_2$  are considered erroneous when:  
 $i_x = 1, 4 \text{ and } ww \neq 00-99;$   
 $i_x = 2, 3 \text{ and } ww = 00-99;$
- (q) Check on station pressure reduction

A relation between the reduced height and reduced pressure can be derived by using the hydrostatic equation and by assuming a linear temperature variation with respect to height ( $dT = dZ^{-1} = 0.0065^\circ\text{C m}^{-1}$ ):

$$Z_{red} - Z_{stn} = \frac{R}{g} \cdot T_m \cdot \ln\left(\frac{p_{stn}}{p_{red}}\right)$$

where  $R = 0.287 \text{ J g}^{-1} \text{ }^\circ\text{C}^{-1}$  and  $g = 9.808 \text{ m s}^{-2}$

$$T_m = T_{stn} - \frac{\gamma(Z_{red} - Z_{stn})}{2}$$

where  $\gamma = 0.0065^\circ\text{C m}^{-1}$

In these expressions, the index STN indicates station level, and the index RED indicates the level to which data are reduced;

(i) Reduction to standard height level  $Z_{red}$  (= 0 for mean sea level)

$$\alpha = \frac{g(Z_{stn} - Z_{red})}{R \cdot T_m}$$

$$P_{red} = P_{stn} \cdot e^\alpha$$

where  $T_m = \frac{T_{stn} + \gamma(Z_{stn} - Z_{red})}{2}$  and

$\gamma = 0.0065^\circ\text{C m}^{-1}$

The checking tolerance can be derived from possible deviations from the temperature profile assumptions. The tolerances suggested are  $\pm 0.4 \text{ hPa}$  for stations where  $|Z_{red} - Z_{stn}| \leq 100 \text{ metres}$  and  $\pm 0.004 \cdot |Z_{red} - Z_{stn}|$  for other stations;

(ii) Reduction to standard pressure level  $P_{red}$ .

$$Z_{red} = \frac{Z_{stn} + \frac{R}{g} \ln\left(\frac{p_{stn}}{p_{red}}\right) \cdot \left(T_{stn} + \frac{\gamma}{2} \cdot Z_{stn}\right)}{1 + \frac{R}{g} \ln\left(\frac{p_{stn}}{p_{red}}\right) \cdot \frac{\gamma}{2}}$$

where  $\gamma = 0.0065^\circ\text{C m}^{-1}$

The tolerances suggested are  $\pm 5 \text{ m}$  for stations where  $|P_{red} - P_{stn}| \leq 20 \text{ hPa}$  and  $\pm 0.25 \cdot (P_{red} - P_{stn})$  metres for other stations;

(r) State of ground

The values of state of ground are considered suspect when:

$E > 0$  and  $E' > 0$ ;

$E = 4$  and  $T_g T_g > 0^\circ\text{C}$ ;

$E' = 0$  and  $T_g T_g > +3^\circ\text{C}$ ;

$5 \leq E' \leq 8$  and  $T_g T_g > 0^\circ\text{C}$ ;

$E = 0$  and  $1 \leq t_R \leq 2$  and  $RRR > 3 \text{ mm}$ ;

$E \geq 0$  and  $sss > 0$ ;

$\{E' = 1 \text{ or } E' = 5\} \text{ and } sss \neq 998$ ;

$\{2 \leq E' \leq 4 \text{ or } 6 \leq E' \leq 8\} \text{ and } sss = 998$ ;

$E' = 9$  and  $sss < 15 \text{ cm}$ ;

$E = 5$  and  $\{S_p S_p = 35 \text{ or } S_p S_p = 37 \text{ or } S_p S_p = \Delta\}$ ;

## (s) Supplementary information

The supplementary information are considered suspect when:

- $ww = 8$  and  $\{M_w \leq 6 \text{ or } M_w = /\}$  (group 919 $s_ps_p$ );
- $ww = 19$  and  $\{7 \geq M_w \text{ or } M_w = /\}$  (group 919 $s_ps_p$ );
- $ww = 38$  and  $S_8 \neq 8$  (group 929 $s_ps_p$ );
- $ww = 39$  and  $S_8 \neq 9$  (group 929 $s_ps_p$ );
- $S'_8 = 0$  and  $36 \leq ww \leq 39$  (group 929 $s_ps_p$ );
- $S'_8 = 5$  and  $38 \leq ww \leq 39$  (group 929 $s_ps_p$ );
- $S'_8 > 1$  and  $\{16 \leq ww \text{ or } 18 \leq ww \leq 35 \text{ or } 40 \leq ww \leq 69 \text{ or } 79 \leq ww \leq 84\}$  (group 929 $s_ps_p$ );
- $8 \leq S_8 \leq 9$  and  $S'_8 = /$  (group 929 $s_ps_p$ );
- $S_ps_p = 32$  and  $W_1 < 8$  and  $ww \neq 27$ ;
- $48 \leq ww \leq 49$  and  $\{S_ps_p \neq 35 \text{ or } S_ps_p \neq 36\}$ ;
- $\{56 \leq ww \leq 57 \text{ or } 66 \leq ww \leq 67\}$  and  $\{S_ps_p \neq 34 \text{ or } S_ps_p \neq 36\}$ ;
- $ss > 05$  and  $\{16 \leq ww \text{ or } 18 \leq ww \leq 21 \text{ or } ww = 25 \text{ or } 28 \leq ww \leq 35 \text{ or } 41 \leq ww \leq 67 \text{ or } 80 \leq ww \leq 82 \text{ or } 91 \leq ww \leq 92 \text{ or } ww = 98 \text{ or } W_1 \leq 6\}$  (group 931 $s_ps_p$ ).

6.3.2.1.2 IN CASE OF INDICATOR  $i_x = 5-7$ 

The different parameters in SYNOP reports are checked against each other. In the description below, the suggested checking algorithms have been divided into areas where the physical parameters are closely connected:

(a) Wind  $dd/ff$ 

The wind information is considered to be erroneous in the following cases:

- $dd = 00$  and  $ff \neq 00$ ;
- $dd \neq 00$  and  $ff = 00$ ;
- $dd = 99$  and  $ff = 00$  or  $ff \geq 05 \text{ m s}^{-1}$ ;

(b) Visibility  $VV$  and weather  $ww$ 

The values of visibility and weather are considered suspect when:

- $\{ww = 5 \text{ or } 29 \leq ww \leq 35\}$  and  $\{10 \leq VV \leq 89 \text{ or } 94 \leq VV \leq 99\}$ ;
- $VV < 10$  and  $\{00 \leq ww \leq 04 \text{ or } 06 \leq ww \leq 17 \text{ or } 19 \leq ww \leq 28\}$ ;
- $\{VV < 60 \text{ or } 90 \leq VV \leq 96\}$  and  $ww \leq 03$ ;
- $\{ww = 10 \text{ or } ww = 20\}$  and  $\{00 \leq VV \leq 09 \text{ or } 90 \leq VV \leq 93\}$ ;

(c) Visibility  $VV$  and cloud information

No proposed algorithm

## (d) Cloud information

The values of cloud cover are considered erroneous when:

- $N = 0$  and  $h \neq 9$ ;
- $N = 9$  and  $h \neq /$ ;
- $N = 9$  and  $N_s \neq 9$ ;
- $N = /$  and  $h \neq /$ ;
- $N_s = 9$  and  $C \neq /$ ;
- $N_s = 9$  and  $N \neq 9$ ;
- $N_s > N$ ;
- $C \neq 9$  and  $N_s < 1$  in 1st group  $8N_sCh_sh_s$ ;
- $C \neq 9$  and  $N_s < 3$  in 2nd group  $8N_sCh_sh_s$ ;
- $C \neq 9$  and  $N_s < 5$  in 3rd group  $8N_sCh_sh_s$ ;
- $h_sh_s$  in 2nd group  $8N_sCh_sh_s < h_sh_s$  in 1st group  $8N_sCh_sh_s$ ;
- $h_sh_s$  in 3rd group  $8N_sCh_sh_s < h_sh_s$  in 2nd group  $8N_sCh_sh_s$ ;

(e) Cloud information and weather  $ww$ 

Clouds and weather are considered suspect when:

- $N = 9$  and  $00 < ww < 25$ ;
- $N = 0$  and  $\{ww = 03 \text{ or } ww = 18 \text{ or } \{40 \leq ww \leq 49\}$ ;
- $1 \leq N \leq 3$  and  $\{50 \leq ww \leq 69 \text{ or } 72 \leq ww \leq 76\}$ ;

(f) Temperature  $T$  and weather  $ww$ 

Both elements are considered suspect when:

- $T > +5^\circ\text{C}$  and  $\{45 \leq ww \leq 46 \text{ or } 70 \leq ww \leq 79 \text{ or } 85 \leq ww \leq 87\}$ ;
- $T < -2^\circ\text{C}$  and  $\{43 \leq ww \leq 44 \text{ or } 50 \leq ww \leq 53 \text{ or } 57 \leq ww \leq 63 \text{ or } 81 \leq ww \leq 84\}$ ;
- $T > +3^\circ\text{C}$  and  $\{47 \leq ww \leq 48 \text{ or } 54 \leq ww \leq 56 \text{ or } 64 \leq ww \leq 66\}$ ;
- $T < -10^\circ\text{C}$  and  $\{47 \leq ww \leq 48 \text{ or } 54 \leq ww \leq 56 \text{ or } 64 \leq ww \leq 66\}$ ;
- $T > +3^\circ\text{C}$  and  $ww = 35$ ;

(g) Temperature  $T$  and dew-point temperature  $T_d$ 

Both values are considered suspect when:

- $T - T_d > 5^\circ\text{C}$  and  $30 \leq ww \leq 35$ ;
- $T_d > T$ ;

(h) Pressure tendency *appp*

The values of *a* and *ppp* are considered erroneous when:

- a* = / and *ppp* ≥ 0;
- a* ≥ 0 and *ppp* = /;
- a* = 4 and *ppp* > 0;
- ppp* = 000 and 1 ≤ *a* ≤ 3;
- ppp* = 000 and 6 ≤ *a* ≤ 8;

(i) Weather *ww*, *W<sub>1</sub>*, *W<sub>2</sub>*

The values of *ww* and *W<sub>1</sub>*, *W<sub>2</sub>* are considered erroneous when:

$$00 \leq \text{ww} \leq 03 \text{ and } 0 \leq W_1 \leq 2;$$

(j) Past weather *W<sub>1</sub>*, *W<sub>2</sub>*

The values of *W<sub>1</sub>*, *W<sub>2</sub>* are considered erroneous when:

$$\begin{aligned} W_1 &< W_2; \\ 0 \leq W_1 \leq 2 \text{ and } W_1 &\neq W_2; \end{aligned}$$

(k) Past weather *W<sub>2</sub>* and cloud cover *N*

The values of *W<sub>2</sub>* and cloud cover are considered suspect when:

$$\begin{aligned} W_2 &= 0 \text{ and } 5 \leq N \leq 8; \\ W_2 &= 2 \text{ and } 0 \leq N \leq 4; \end{aligned}$$

(l) Weather *ww* and wind speed

The values of *ww* and *ff* are considered suspect when:

$$\{27 \leq \text{ww} \leq 29\} \text{ and } ff < 10 \text{ m s}^{-1};$$

(m) Temperature *T* and minimum/maximum temperature *T<sub>n</sub>*/*T<sub>x</sub>*

The values of *T* and *T<sub>n</sub>*, *T<sub>x</sub>* are considered erroneous when:

$$\begin{aligned} T &< T_n; \\ T_x &< T; \end{aligned}$$

(n) Precipitation *RRR* and past weather *W<sub>1</sub>*, *W<sub>2</sub>*

The values of *RRR* and *W<sub>1</sub>*, *W<sub>2</sub>* are considered erroneous when:

$$\{4 \leq W_1 \leq 8 \text{ or } (W_1 = 9 \text{ and } 4 \leq W_2 \leq 8)\} \text{ and } RRR = 000;$$

(o) Indicator *i<sub>R</sub>* and precipitation *RRR*

The values of *i<sub>R</sub>* and *RRR* are considered erroneous when:

$$\begin{aligned} i_R &= 0-2 \text{ and } \{RRR = 000 \text{ or } RRR = //\}; \\ i_R &= 3 \text{ and } \{RRR \neq 000 \text{ or } RRR \neq //\}; \\ i_R &= 4 \text{ and } RRR = //; \end{aligned}$$

(p) Indicator *i<sub>x</sub>* and weather *ww*, *W<sub>j</sub>*, *W<sub>2</sub>*

The values of *i<sub>x</sub>* and *W<sub>1</sub>*, *W<sub>2</sub>* are considered erroneous when:

$$\begin{aligned} i_x &= 7 \text{ and } \text{ww} \neq 00-99; \\ i_x &= 5, 6 \text{ and } \text{ww} = 00-99; \end{aligned}$$

## (q) Check on station pressure reduction

A relation between the reduced height and reduced pressure can be derived by using the hydrostatic equation and by assuming a linear temperature variation with respect to height ( $dT = dZ^{-1} = 0.0065^\circ\text{C m}^{-1}$ ):

$$Z_{red} - Z_{stn} = \frac{R}{g} \cdot T_m \cdot \ln\left(\frac{p_{stn}}{p_{red}}\right)$$

where  $R = 0.287 \text{ J g}^{-1} \text{ }^\circ\text{C}^{-1}$  and  $g = 9.808 \text{ m s}^{-2}$

$$T_m = T_{stn} - \frac{\gamma(Z_{red} - Z_{stn})}{2}$$

where  $\gamma = 0.0065^\circ\text{C m}^{-1}$

In these expressions, the index STN indicates station level, and the index RED indicates the level to which data are reduced;

(i) Reduction to standard height level *Z<sub>red</sub>* (= 0 for mean sea level)

$$\alpha = \frac{g(Z_{stn} - Z_{red})}{R \cdot T_m}$$

$$P_{red} = P_{stn} \cdot e^\alpha$$

$$\text{where } T_m = \frac{T_{stn} + \gamma(Z_{stn} - Z_{red})}{2} \text{ and}$$

$$\gamma = 0.0065^\circ\text{C m}^{-1}$$

The checking tolerance can be derived from possible deviations from the temperature profile assumptions. The tolerances suggested are ±0.4 hPa for stations where  $|Z_{red} - Z_{stn}| \leq 100$  metres and  $\pm 0.004 \cdot |Z_{red} - Z_{stn}|$  for other stations;

(ii) Reduction to standard pressure level  $P_{red}$ 

$$Z_{red} = \frac{Z_{std} + \frac{R}{g} \ln\left(\frac{p_{std}}{p_{red}}\right) \cdot \left(T_{std} + \frac{\gamma}{2} \cdot Z_{std}\right)}{1 + \frac{R}{g} \ln\left(\frac{p_{std}}{p_{red}}\right) \cdot \frac{\gamma}{2}}$$

where  $\gamma = 0.0065^{\circ}\text{C m}^{-1}$

The tolerances suggested are  $\pm 5$  m for stations where  $|P_{red} - P_{std}| \leq 20$  hPa and  $\pm 0.25 \cdot (P_{red} - P_{std})$  metres for other stations.

## (r) State of ground

The values of state of ground are considered suspect when:

- $E > 0$  and  $E' > 0$ ;
- $E = 4$  and  $T_g T_g > 0^{\circ}\text{C}$ ;
- $E' = 0$  and  $T_g T_g > +3^{\circ}\text{C}$ ;
- $5 \leq E' \leq 8$  and  $T_g T_g > 0^{\circ}\text{C}$ ;
- $E = 0$  and  $1 \leq t_R \leq 2$  and  $RRR > 3$  mm;
- $E \geq 0$  and  $sss > 0$ ;
- $\{E' = 1 \text{ or } E' = 5\} \text{ and } sss \neq 998$ ;
- $\{2 \leq E' \leq 4 \text{ or } 6 \leq E' \leq 8\} \text{ and } sss = 998$ ;
- $E = 5$  and  $\{S_p S_p = 35 \text{ or } S_p S_p = 37 \text{ or } S_p S_p = \Delta\}$ ;

## (s) Supplementary information

The supplementary information are considered suspect when:

- $\{47 \leq ww \leq 48 \text{ or } 54 \leq ww \leq 56 \text{ or } 64 \leq ww \leq 66\} \text{ and } \{S_p S_p \neq 34 \text{ or } S_p S_p \neq 36\}$ ;

## 6.3.2.2 CONSISTENCY CHECKS FOR UPPER-AIR DATA

The TEMP/TEMP SHIP and PILOT/PILOT SHIP messages contain a large amount of redundant information which can be used to construct an efficient scheme for internal (vertical) consistency control.

The following methods can be used separately or in combination:

- (a) Lapse-rate check of vertical temperature profiles;
- (b) Check for consistency between significant level data and standard level data;
- (c) Check for hydrostatic balance between standard level height and standard level temperature data;
- (d) Check for vertical wind shear.

Depending on which parts of the message (A, B, C and/or D) are available, different methods are applied. Methods (a), (b) and (d) above can be used in manual handling, preferably by drawing the sounding in the thermodynamic diagram (tephigram or other). Method (c) is somewhat more complicated and should be used in an automatic system. For PILOT messages, the consistency control is restricted to the check of vertical wind shear. During the check, suspected or erroneous values can be flagged and if possible corrected. The four methods applied sequentially with little or no interaction between them will work satisfactorily for most types of errors. The interaction in this case can be that values are marked correct or suspect as each method is applied. Then this information together with the result from the next control method will either confirm the flagging or mark the value as erroneous. Sometimes, however, the errors are not appropriately identified and corrected. In these cases, combined quality control, as presented in section 6.5, can be applied. The methods for the different vertical checks are described in the following paragraphs.

## 6.3.2.2.1 LAPSE-RATE CHECK OF VERTICAL TEMPERATURE PROFILES

In the lapse-rate check, the vertical temperature profile is searched layer by layer to examine whether there is a superadiabatic lapse rate or any unreasonable inversion in the layer. For each layer, the following procedures apply:

## (a) Check for unreasonable inversions

If the difference between the temperature at the level above the current level  $T_{i+1}$  and the temperature at the current level  $T_i$  is larger than a certain limit, then at least one of the temperatures  $T_i$  or  $T_{i+1}$  is considered to be erroneous. The limit can be given a fixed value or can be a function of layer position and layer thickness and, if necessary, also a function of season and latitude. Limits are suggested in Table 6.14.

## (b) Check for superadiabatic lapse rates

The temperature  $T_i$  at a pressure level  $p_i$  is used to compute a temperature  $NT_{i+1}$  at the next pressure level  $p_{i+1}$  by the dry adiabatic lapse rate. The formula used is:

$$NT_{i+1} = T_i \left( \frac{p_{i+1}}{p_i} \right) \mu$$

where  $\mu = R/Cp$  and  $p_i > p_{i+1}$ .

If  $NT_{i+1} - T_{i+1} < \epsilon$ , where  $\epsilon$  is zero or a small positive limit value, the temperature profile is considered not to be superadiabatic. If the difference is, however, larger than the chosen limit

Table 6.14  
Suggested limits in checking for unreasonable inversions

Position of vertical layer	Thickness of vertical layer	Limit of maximum inversion $T_{i+1} - T_i$		
		Winter		
		0°N – 30°N 0°S – 30°S	30°N – 60°N 30°S – 60°S	60°N – 90°N 60°S – 90°S
$p_i > 850 \text{ hPa}$	< 20 hPa ≥ 20 hPa	1.0°/hPa 20°	1.5°/hPa 30°	1.7°/hPa 34°
$850 \text{ hPa} \geq p_i > 200 \text{ hPa}$	< 10 hPa ≥ 10 hPa	0.8°/hPa 8°	1.0°/hPa 10°	1.2°/hPa 12°
$200 \text{ hPa} \geq p_i > 70 \text{ hPa}$	< 10 hPa ≥ 10 hPa	2.0°/hPa 25°	2.0°/hPa 25°	2.0°/hPa 25°
$p_i \leq 70 \text{ hPa}$	< 10 hPa ≥ 10 hPa	2.5°/hPa 25°	2.5°/hPa 25°	2.5°/hPa 25°

Position of vertical layer	Thickness of vertical layer	Limit of maximum inversion $T_{i+1} - T_i$		
		Summer		
		0°N – 30°N 0°S – 30°S	30°N – 60°N 30°S – 60°S	60°N – 90°N 60°S – 90°S
$p_i > 850 \text{ hPa}$	< 20 hPa ≥ 20 hPa	0.8°/hPa 16°	1.0°/hPa 20°	1.2°/hPa 24°
$850 \text{ hPa} \geq p_i > 200 \text{ hPa}$	< 10 hPa ≥ 10 hPa	0.8°/hPa 8°	1.0°/hPa 8°	1.2°/hPa 8°
$200 \text{ hPa} \geq p_i > 70 \text{ hPa}$	< 10 hPa ≥ 10 hPa	2.0°/hPa 20°	2.0°/hPa 20°	2.0°/hPa 20°
$p_i \leq 70 \text{ hPa}$	< 10 hPa ≥ 10 hPa	2.5°/hPa 25°	2.5°/hPa 25°	2.5°/hPa 25°

value, the temperature profile is considered superadiabatic. For a complete report with significant temperatures the limits should be fairly close to zero. The following values are considered:

- (i) For layers above 850 hPa, if  $p_i \leq 850 \text{ hPa}$  — the limit value should be 0°C;
  - (ii) For layers below 850 hPa, if  $p_i > 850 \text{ hPa}$  — the limit value can vary depending on the season, the latitude, and the thickness of the layer.
- If the layer is superadiabatic or the inversion is too strong, at least one of the temperatures  $T_i$  or  $T_{i+1}$  is considered to be erroneous. In order to determine which temperature is erroneous and, if possible, to correct the error, it is necessary to use data from layers in the vicinity;
- (c) If it is considered that a temperature which is erroneous will be corrected by the lapse-rate check simply by changing sign, this correction should be applied.

#### 6.3.2.2.2 CHECKING THE CONSISTENCY BETWEEN SIGNIFICANT LEVEL DATA AND STANDARD LEVEL DATA

The standard level data are recomputed from the significant level data and are compared with the reported standard level data. The following methods can be applied for recomputation of standard pressure level data:

- (a) Temperatures and dew-point temperatures are interpolated assuming a linear variation in  $(\ln p)$  between the significant levels:

$$T_s = T_i + \frac{\ln(p_s) - \ln(p_i)}{\ln(p_{i+1}) - \ln(p_i)} (T_{i+1} - T_i)$$

$$T_{ds} = T_{di} + \frac{\ln(p_s) - \ln(p_i)}{\ln(p_{i+1}) - \ln(p_i)} (T_{di+1} - T_{di})$$

Here the index  $s$  is used for a standard pressure level and indices  $i$  and  $i+1$  are used for significant levels in the vicinity of this standard pressure level.

The formulae are only applied when  $p_i > p_s > p_{i+1}$  and the thickness of the layer  $p_i$  to  $p_s$  and the layer  $p_s$  to  $p_{i+1}$  are less than or equal to a certain limit. Suggested values for this limit are:

- (i) 150 hPa for the standard pressure levels 1 000 – 700 hPa
- (ii) 100 hPa for the standard pressure levels 500 – 300 hPa

- (iii) 75 hPa for the standard pressure levels      250 – 100 hPa
- (iv) 20 hPa for the standard pressure levels      70 – 30 hPa
- (v) 10 hPa for the standard pressure levels      20 – 1 hPa
- (b) Heights of standard pressure levels are obtained by the integration of the hydrostatic equation from the station level to the standard pressure level. If possible, the virtual temperatures,  $T_i^*$ , are used for the height integration:

$$Z_s = Z_{std} + \sum_{i=1}^{N-1} \frac{R_d}{g} \frac{T_i^* + T_{i+1}^*}{2} \ln\left(\frac{p_i}{p_{i+1}}\right) + \frac{R_d}{g} \frac{T_N^* + T_s^*}{2} \ln\left(\frac{p_N}{p_s}\right)$$

and  $N$  is the number of significant levels below the level calculated.

Significant temperature levels are also needed to fulfil the requirement for computation of temperatures at all standard levels up to  $p_s$ :

- (c) Winds at standard pressure levels are interpolated from significant level winds by assuming a linear variation of wind components ( $u$  and  $v$ ) in  $(\ln p)$  between the significant wind levels. Interpolation formulae and requirements of maximum thickness for vertical interpolation are the same as those in (a) above.

The recomputed standard level data are compared with the reported standard level data and if the height difference is larger than 15 gpm for levels below 400 hPa or larger than 30 gpm for levels above 400 hPa then the standard level height is erroneous or any utilized significant level data is erroneous. The same conclusion is drawn for temperature if the difference is greater than 1.5°C for levels below 300 hPa and below the tropopause or the difference is greater than 3°C for levels above 300 hPa or above the tropopause. The dew-point temperature is considered suspect if the difference between the recomputed value and the reported value is greater than 1.5°C.

If the difference in wind speed is greater than 5 m s<sup>-1</sup> or the difference in wind direction is greater than 10° then the standard level wind is considered to be erroneous or any of the significant level winds in the vicinity is erroneous.

If a standard level temperature has been considered erroneous by the checking procedure then an attempt to correct the reported temperature can be made by changing its sign. If this correction gives a temperature within the limits of the recomputed temperature and if the numerical value of the correction is larger than 6°C, the corrected value is kept and the temperature can be flagged as "changed during vertical check". When any standard level parameter or all data from a standard level are missing in the original message, the corresponding values from the recomputed standard level data can be inserted and marked as "original data missing—reconstituted value inserted".

#### 6.3.2.2.3 CHECKING THE HYDROSTATIC BALANCE BETWEEN STANDARD LEVEL HEIGHT AND STANDARD LEVEL TEMPERATURE DATA

The hydrostatic equation can be used to check the vertical consistency between temperature and geopotential data at standard pressure levels. Several algorithms, founded on this principle, have been developed. The following algorithm is based on Hinkelmann (1969).

Consider a layer between two consecutive standard pressure levels  $p_i$  and  $p_{i+1}$  (Figure 6.2):

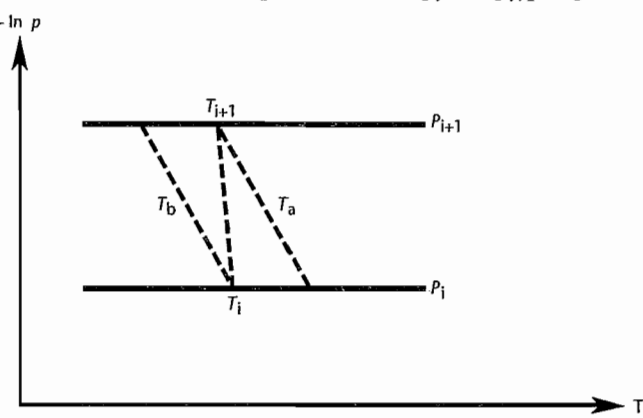


Figure 6.2 — Schematic diagram for checking  $T_i$  and  $T_{i+1}$ .

If only part A of the TEMP message is available, then the details of the temperature profile in the layer from  $p_i$  to  $p_{i+1}$  are not known. By assuming that temperature has a linear variation in  $\ln p$  in the layer it is possible to compute the approximate thickness  $D_i$  of the layer. If possible, the virtual temperature should be used in the computation of the thickness:

$$D_i = \frac{R_d}{g} \frac{T_i^* + T_{i+1}^*}{2} \ln\left(\frac{p_i}{p_{i+1}}\right)$$

where  $T^*$  denotes virtual temperature.

A tropopause located between levels  $p_i$  and  $p_{i+1}$  is taken into consideration for computing thickness. A modified temperature  $T'_{i+1}$  is obtained with the aid of the tropopause temperature and is used for the thickness computation:

$$T'_{i+1} = T_{i+1} + T_{trop} - T_{int}$$

$$\text{where } T_{int} = T_i + \frac{\ln(p_i) - \ln(p_{trop})}{\ln(p_i) - \ln(p_{i+1})}$$

and  $T_{trop}$ ,  $p_{trop}$  denote tropopause temperature and tropopause pressure.

The computed thickness,  $D_i$ , generally deviates from the reported thickness,  $Z_{i+1} - Z_i$ , since the reported thickness has been computed from a more detailed temperature profile in the layer. In order to establish a tolerance for this deviation, we can compute two extreme thicknesses from the possible temperature variations in the layer.

$D_a$ : We assume that we have an inversion at level  $p_i$  and a dry adiabatic lapse rate between levels  $p_i$  and  $p_{i+1}$  (the temperature profile  $T_a$  is plotted in the figure).

$$D_a = \frac{R_d}{2g} \left\{ I + \left( \frac{p_{i+1}}{p_i} \right)^{R/C_p} T_i \ln \left( \frac{p_i}{p_{i+1}} \right) \right\}$$

$D_b$ : We assume that we have an inversion at level  $p_{i+1}$  and a dry adiabatic lapse rate between levels  $p_i$  and  $p_{i+1}$  (the temperature profile  $T_b$  is plotted in the figure).

$$D_b = \frac{R_d}{2g} \left\{ I + \left( \frac{p_i}{p_{i+1}} \right)^{R/C_p} T_{i+1} \ln \left( \frac{p_i}{p_{i+1}} \right) \right\}$$

The maximum deviation between the reported and the computed thicknesses is then given approximately by:

$$|Z_{i+1} - Z_i - D_i| < 1/2 \cdot |D_a - D_b|$$

From experience it has been found that it is possible to use a smaller tolerance, which means that the extreme temperature profiles  $T_a$  and  $T_b$  are highly unlikely:

$$|Z_{i+1} - Z_i - D_i| < 3/4 \cdot 1/2 \cdot |D_a - D_b| = TOL$$

This checking algorithm is used with a minimum value of TOL taken as 20 gpm and a maximum value taken as 50 gpm for layers below 400 hPa and as 80 gpm for layers above 400 hPa. If the checking algorithm is not fulfilled, one or some of the reported values  $Z_i$ ,  $T^*_i$ ,  $Z_{i+1}$  or  $T^*_{i+1}$  are erroneous. In order to decide which value is wrong, information from adjacent layers must be used.

Let us assume that we have computed the deviation  $E_i = Z_{i+1} - Z_i - D_i$  and that the absolute value of one of the deviations is larger than the corresponding tolerance. It is then possible to compute the index  $F_i = E_i/E_{i+1}$ . From the value of this index it is then possible to decide which value has the smallest likelihood. We shall examine the value of index  $F_i$  at different intervals.

(a)  $0.5 < F_i < 2.0$ :

The temperature  $T_{i+1}$  is probably erroneous since  $E_{i+1}$  has a large value of the same sign as  $E_i$ . For example:

$$\begin{array}{r} p_{i+3} \\ \hline E_{i+2} = 2 \\ p_{i+2} \\ \hline E_{i+1} = -85 \\ p_{i+1} \quad F_i = 1.05 \\ \hline E_i = -90 \\ p_i \\ \hline E_{i-1} = 3 \\ p_{i-1} \end{array}$$

(b)  $-2.0 < F_i < -0.5$ :

The height  $Z_{i+1}$  is probably erroneous since  $E_{i+1}$  has a large value of the opposite sign as  $E_i$ . For example:

$$\begin{array}{r} p_{i+3} \\ \hline E_{i+2} = -1 \\ p_{i+2} \\ \hline E_{i+1} = 105 \\ p_{i+1} \quad F_i = -0.93 \\ \hline E_i = -98 \\ p_i \\ \hline E_{i-1} = 2 \\ p_{i-1} \end{array}$$

(c)  $F_i \geq 2.0$ :

All heights at and above level  $i+1$  are probably erroneous:

$$\begin{aligned} \frac{p_{i+2}}{E_{i+1}} &= 2 \\ \frac{p_{i+1}}{E_i} &= 104 \quad F_i = 52 \\ \frac{p_i}{E_{i-1}} &= 3 \\ \frac{p_{i-1}}{E_i} &= 1 \end{aligned}$$

(d)  $F_i \leq 0.5$ :

With a value of  $F_i$  in this interval it is more difficult to find a unique error. Probably several of the values involved are erroneous.

The element which is considered to be erroneous can be recomputed using data from surrounding levels. The recomputed value is checked hydrostatically and, if this gives a good result, the new value can be inserted and marked as "changed during vertical check". If the new value also fails in the checking, the original value is kept and considered erroneous.

There are many different methods of computing missing and error-marked heights or temperatures. Only values from standard levels are used in the methods described below.

The following methods can be used to compute the temperature:

(a)  $T_i$  is missing or erroneous and all the surrounding data are available.

The hydrostatic equation for the height difference in the layer  $i$  to  $i+1$  is used to give one expression for  $T_i$  and then the equation for the layer  $i-1$  to  $i$  is used to give another expression for the temperature at level  $i$ :

$$T_i(1) = \frac{2g(z_{i+1} - z_i)}{R \ln\left(\frac{P_i}{P_{i+1}}\right)} T_{i+1} \text{ in the layer } i \text{ to } i+1$$

$$T_i(2) = \frac{2g(z_i - z_{i-1})}{R \ln\left(\frac{P_{i-1}}{P_i}\right)} T_{i-1} \text{ in the layer } i \text{ to } i+1$$

Both temperatures are checked for lapse rate and if both are correct and the difference between them is less than  $5^\circ\text{C}$ , an average temperature of  $T_i(1)$  and  $T_i(2)$  is used for  $T_i$ . If one of the computed temperatures is considered to be erroneous, then the other one is used for  $T_i$ . When both of the temperatures are considered to be erroneous a new expression for  $T_i$  is computed by assuming that the temperature is linear in  $\ln p$  between  $T_{i-1}$  and  $T_{i+1}$ :

$$T_i = T_{i-1} + \frac{\ln\left(\frac{p_{i-1}}{p_i}\right)}{\ln\left(\frac{p_{i-1}}{p_{i+1}}\right)} (T_{i+1} - T_{i-1})$$

If this temperature, when checked for the lapse rate, is also erroneous, then temperature  $T_i$  cannot be completed.

(b)  $T_i$  and  $Z_i$  are missing or both are erroneous

A temperature for level  $i$  is computed from:

$$T_i = \frac{\frac{2(Z_{i+1} - Z_{i-1})}{R \ln\left(\frac{p_{i-1}}{p_{i+1}}\right)} - \frac{T_{i-1} \ln\left(\frac{p_{i-1}}{p_i}\right) + T_{i+1} \ln\left(\frac{p_i}{p_{i+1}}\right)}{\ln\left(\frac{p_{i-1}}{p_{i+1}}\right)}}{2g}$$

If  $T_i$  is considered erroneous in the lapse-rate check, then the equation for  $T_i$  in (a) above is used to compute the temperature. If this temperature is also erroneous in the lapse-rate check, no temperature at level  $i$  can be computed.

(c)  $T_i$  and  $Z_i$  as well as  $Z_{i-1}$  or  $Z_{i+1}$  are missing or erroneous

The equation for  $T_i$  in (a) above is used to compute the temperature.

(d)  $T_i$ ,  $Z_i$  and  $T_{i+1}$  are missing or erroneous

The temperature at level  $i+1$  is computed by:

$$T_{i+1} = \frac{Z_{i+1} - Z_{i-1}}{\frac{R}{2g} \ln\left(\frac{p_{i-1}}{p_{i+1}}\right)} - T_{i-1}$$

and the temperature at level  $i$  is then computed as in (b) above.

- (e)  $T_i$  and  $T_{i-1}$  are missing or erroneous

$$T_i = \frac{Z_{i+1} - Z_i}{\frac{R}{2g} \ln\left(\frac{p_i}{p_{i+1}}\right)} - T_{i+1}$$

If  $T_i$  is considered to be erroneous and the level  $i-2$  is complete and correct, then a new effort is made to compute the temperature at level  $i$  by:

$$T_i = \frac{Z_i - Z_{i-2}}{\frac{R}{2g} \ln\left(\frac{p_{i-2}}{p_i}\right)} - T_{i-2}$$

If this value is also erroneous, then a new temperature is not computed.

- (f)  $T_i$  and  $Z_{i-1}$  are missing or erroneous

$$T_i = \frac{Z_{i+1} - Z_i}{\frac{R}{2g} \ln\left(\frac{p_i}{p_{i+1}}\right)} - T_{i+1}$$

The temperature is checked and if it is considered to be erroneous a new temperature is computed by using the equation for  $T_i$  in (a) above. No further computations are made.

- (g)  $T$  and  $Z_{i+1}$  are missing or erroneous

$$T_i = \frac{Z_i - Z_{i-1}}{\frac{R}{2g} \ln\left(\frac{p_{i-1}}{p_i}\right)} - T_{i-1}$$

If the temperature is found to be erroneous in the lapse-rate check, a new temperature is computed by using the equation for  $T_i$  in (a) above.

- (h)  $T_i$  and  $T_{i+1}$  are missing or erroneous

$$T_i = \frac{Z_i - Z_{i-1}}{\frac{R}{2g} \ln\left(\frac{p_{i-1}}{p_i}\right)} - T_{i-1}$$

If  $T_i$  is considered erroneous and the values of  $T_{i+2}$  and  $Z_{i+2}$  are correct, then a new value is computed by:

$$T_i = \frac{Z_{i+2} - Z_i}{\frac{R}{2g} \ln\left(\frac{p_i}{p_{i+2}}\right)} - T_{i+2}$$

- (i)  $T_i$ ,  $T_{i+1}$  and  $Z_{i-1}$  are missing or erroneous

The computations are the same as those in (h) above.

- (j)  $T_i$ ,  $T_{i-1}$  and  $Z_{i-1}$  are missing or erroneous

The computations are the same as those in (e) above.

If a larger number of elements are missing or erroneous, no reliable computation of the temperature at level  $i$  can be performed.

The hydrostatic equation is also used to recompute a height that is missing or considered erroneous. The following conditions are considered:

If only  $Z_i$  is missing or erroneous, then:

$$Z_a = Z_{i+1} - \frac{R_d}{g} \frac{T_i^* + T_{i+1}^*}{2} \cdot \ln\left(\frac{p_i}{p_{i+1}}\right)$$

$$Z_b = Z_{i-1} - \frac{R_d}{g} \frac{T_i^* + T_{i+1}^*}{2} \cdot \ln\left(\frac{p_{i-1}}{p_i}\right)$$

The new height  $Z_i$  is computed from  $Z_a$  and  $Z_b$  according to the following conditions:

- (a) When  $|Z_a - Z_b| \leq 30$  gpm, then  $Z_i = \frac{Z_a + Z_b}{2}$ ;

- (b) When  $|Z_a - Z_b| > 30$  gpm and both  $Z_a$  and  $Z_b$  are accepted by a hydrostatic tolerance check, then  $Z_i = \frac{Z_a + Z_b}{2}$ . Otherwise, if only one value of  $Z_a$  and  $Z_b$  is accepted by the hydrostatic check, this value is used for  $Z_i$ ;

- (c) When  $Z_i$  is missing or is erroneous and the values from level  $i-1$  cannot be used, then  $Z_i = Z_a$ ;  
 (d) When  $Z_i$  is missing or is erroneous and the values from level  $i+1$  cannot be used, then  $Z_i = Z_b$ .

### 6.3.2.2.4 CHECKING THE VERTICAL WIND SHEAR

The vertical wind shear control described below can be applied to check the wind data at standard levels. The wind shear is verified layer by layer and the check is terminated as soon as two levels are found not to be adjacent because of a missing level between them.

The shear is checked in two ways:

- (a) A check on the wind speed shear;
- (b) A check on a combination of directional shear and the sum of the wind speeds.

The layer  $i$  to  $i + 1$  where  $p_i > p_{i+1}$  is checked and the speed is given in  $\text{m s}^{-1}$ .

- (i) The maximum wind speed shear permitted is  $ff_i - ff_{i+1} = (\alpha) + (\beta)(ff_i + ff_{i+1})$ , with the suggested values  $\alpha = 20.6$  and  $\beta = 0.275$ .
- (ii) The directional shear is  $D = dd_i - dd_{i+1}$  and if the shear  $D$  is greater than  $180^\circ$ , then  $D = (360 - D)$  is chosen. Suggested values for the maximum permitted sum of speeds in relation to the directional shear and to the different levels is given in Table 6.15.

It is to be noted that real vertical wind shears can occur, which are close to the limits in the checking algorithm. Therefore, the check on vertical wind shear should be applied with great care.

Table 6.15

Suggested values for the maximum permitted sum of speed in relation to the directional shear

$p_i$ vertical level in hPa	Tolerance for $ff_i + ff_{i+1}$ as a function of directional shear							
	<30°	30°–39°	40°–49°	50°–59°	60°–69°	70°–79°	80°–89°	>90°
1 000–700	100	72	61	57	53	49	46	41
500–150	120	110	84	77	70	63	52	50
100–1	100	72	61	57	53	49	46	41

### 6.3.3 Time consistency checks

Time consistency checks utilize the redundancy of information in consecutive reports from the same geographical location. For some types of data, such as observed tendencies and pressures, the time consistency checks are a simple but efficient means of detecting even fairly small observational errors. Time consistency checks are also important in verifying the positions in consecutive ship and buoy reports. Position checks can also be made for aircraft reports along flight tracks and sequences of reports along satellite tracks.

#### 6.3.3.1 CHECKING THE SURFACE DATA

The different temperature measurements as well as the mean sea-level pressure and pressure tendencies are checked against previous reports. The time difference between the observation time  $t_o$ , and the preceding observation time is noted as  $dt$ . Different checking tolerances are used for different time periods and parameters (Table 6.16). The temperatures at time  $t_o$  as well as at time  $(t_o - dt)$  are considered suspect when:

$$| T(t_o) - T(t_o - dt) | > T \text{TOL}(dt)$$

For the dew-point temperature  $T_d$  the check is similar:

$$| T_d(t_o) - T_d(t_o - dt) | > T_d \text{TOL}(dt)$$

The pressure tendency is checked in an algorithm using an expression  $p_{tend}$  where:

$$\begin{aligned} p_{tend}(t_o) &= -pp(t_o) && \text{if } 5 \leq a(t_o) \leq 8, \text{ and} \\ p_{tend}(t_o) &= pp(t_o) && \text{if } 0 \leq a(t_o) \leq 4 \end{aligned}$$

The pressure tendencies at time  $t_o$  and  $(t_o - dt)$  are considered suspect when:

$$| p_{tend}(t_o) - p_{tend}(t_o - dt) | > pp \text{TOL}(dt)$$

The pressure is checked against the pressure tendency as described hereafter.

Table 6.16  
Suggested tolerances for the temperatures and the tendency as a function of time period between consecutive reports

Parameter	$dt = 1$ hour	$dt = 2$ hours	$dt = 3$ hours	$dt = 6$ hours	$dt = 12$ hours
$T \text{TOL}$	4°C	7°C	9°C	15°C	25°C
$T_d \text{TOL}$	4°C	6°C	8°C	12°C	20°C
$pp \text{TOL}$	3 hPa	6 hPa	9 hPa	18 hPa	36 hPa

The pressure values, in hPa, at time  $t_0$  and at time  $(t_0 - dt)$  as well as the pressure tendency at time  $t_0$  are suspect in two cases:

- (a) If  $|p(t_0) - p(t_0 - dt) - p_{tend}(t_0)| > 1.5$  hPa for  $dt = 3$  hours;
- (b) If  $|p(t_0) - p(t_0 - dt) - 0.5 \cdot p_{tend}(t_0 - dt) - 1.5 p_{tend}(t_0)| > 2.5$  hPa for  $dt = 6$  hours.

In case (b), possible non-linear variations of  $p$  have been taken into account.

The station level pressure can be checked in the same way, but the tolerance value should be smaller, 0.5 hPa for  $dt = 3$  hours and 1.5 hPa for  $dt = 6$  hours. When checking pressures and pressure tendencies, the diurnal variation of pressure should be taken into account.

Observed precipitation amounts may be checked against the *ww* code figures for the preceding time interval. If no precipitation amount is given, but the code indicates that some precipitation has fallen, both the precipitation amount and the *ww* code should be considered suspect. This check can also be made against past weather  $W_1$  and  $W_2$ .

#### 6.3.3.2 GPCC PROCEDURES FOR PRECIPITATION QUALITY MONITORING

Data which arrived at GPCC are partly affected by reading or coding errors and other modifications happening during the transmission from the originator to the archive. In many questionable cases it is not possible to get replies from the data originator. The following problems occur:

- (a) Important metadata (station identifications, format descriptions) are missing and have to be procured;
- (b) Delivered datasets are irregularly formatted;
- (c) Delivered station coordinates are erroneous (occurs frequently);
- (d) Doublets of stations have to be eliminated;
- (e) Missing precipitation is not clearly indicated in the data;
- (f) Recorded precipitation depths are affected by coding/decoding errors;
- (g) Temporal misplacement of data in time-series.

##### 6.3.3.2.1 TREATMENT OF ERRORS

Area means of precipitation derived from raingauge data are contaminated by errors of different origin:

- (a) Systematic measuring errors depend on the characteristics of the instrument type, size and exposition and on the meteorological conditions during the individual event. Any correction will not result in the true individual local precipitation amount, but will put the data closer to the truth in a statistical sense. Corrected data are still contaminated by stochastic errors from approximative corrections;
- (b) Erroneous individual data which are not discovered by quality control cause a stochastic error of a data collective;
- (c) The sampling error is area-related and depends on the number of observations per area and on the regional precipitation variability;
- (d) The methodical error represents approximations of the used interpolation scheme or the method for calculation of area mean precipitation.

These error types must be treated and quantified separately and the results need to be merged to a total error of the area mean precipitation (Rudolf, *et al.*, 1994).

A central part of the GPCC operational data-processing system, which is described in Rudolf (1993), is the precipitation point data bank (PDB) consisting of three major parts:

- (a) The continuous monthly precipitation data of the different sources (for each station data from up to five sources are stored separately, as there are monthly precipitation totals from CLIMAT reports, totals calculated from synoptic reports at the CPC and the GPCC and additional regional as well as national datasets);
- (b) The climatological normals for different base periods; and
- (c) A station catalogue containing the station-related information, such as geographical coordinates, elevation above mean sea level, station name and WMO and/or national station number.

Another important part of the data-processing system is the quality control of the gauge-measured monthly precipitation data and station metadata. First of all, the station metadata (identification, geographical location) have to be checked, corrected (geographical coordinates are partly erroneous) or complemented. If monthly precipitation data at a station are available from more than one source, then an "optimal" value is selected automatically based on statistically-predefined random errors of the data from the different sources and intercomparisons between them. The quality control of the precipitation data at the GPCC is semi-automatic. In the automatic check of the full raingauge dataset, the precipitation data at a station are checked against the climatological normal and for spatial homogeneity and questionable data are flagged.

Data marked as questionable in the automatic quality-control process can be subsequently manually reviewed by a trained expert using an interactive programme on a graphics workstation. This software shows all relevant information of the station being checked as well as the precipitation data of the neighbouring stations

and background fields such as gridded climatologies or a three dimension orography (the data source is displayed by symbol, stations with data flagged as questionable are marked by colour). Obvious errors in the precipitation data are corrected, if possible. Otherwise incorrect data are set to the code for missing values or, if available, the monthly precipitation from another source can be selected for the analysis. If a station is misplaced, its geographical location can also be corrected. All these corrections are then archived in the PDB.

The automatic part of the control procedure has not been designed to correct data, but rather to reduce the number of data for which a visual control is necessary. A fully automatic quality control would eliminate all questionable data and, with regard to the high variability of precipitation, also remove a large amount of true data, in particular extreme values. These data, however, are very important to describe the real structure of the spatial distribution and the variability within the gridded precipitation analysis. In order to keep the true extreme data and also to remove obviously wrong data from the analysis system, a visual check of the questionable data, although very time-consuming, seems to be inalienable (Rudolf, *et al.*, 1994).

The final analysis of gridded area-average precipitation is performed on the basis of the quality-controlled data by using the objective analysis method Spheremap, which is based on an inverse distance and directional weighting scheme.

### 6.3.3.3 CHECKING THE POSITIONS IN CONSECUTIVE REPORTS

A method for checking the consecutive positions of ship and buoy reports is described in detail below, while the position check of aircraft reports is only outlined. The prime condition for these types of position checks is that there is a unique identifier in each of the consecutive reports.

The parameters needed for an efficient check of position in ship or buoy reports are the latitude and longitude of the position (LAT, LON) and the mean course and mean speed of the vessel or platform for the last three hours (DS, VS).

If the spherical surface of the sea is approximated with a plane in the vicinity of the position at time  $t_0$ , the following approximative position of the ship or buoy  $dt$  hours earlier holds:

$$\begin{aligned} ELAT(t_0 - dt) &= LAT(t_0) + \frac{\bar{v}}{60} \cdot dt \cdot \cos(\bar{D}) \\ ELO(t_0 - dt) &= LON(t_0) + \frac{\bar{v}}{60} \cdot dt \cdot \frac{\sin(\bar{D})}{\cos(LAT(t_0))} \end{aligned}$$

where LAT, LON are given in degrees, the mean speed  $\bar{v}$  of the ship is given in knots, the mean course  $\bar{D}$  of the ship is given in degrees, and the time increment,  $dt$ , is given in hours.

Most commercial ships send SHIP messages only every sixth hour or less. The changes in a ship's course and speed are generally very small over time periods of three to 12 hours, at least for ship routes over ocean areas. Therefore, it is reasonable to approximate the mean motion of the ship over time periods of six to 12 hours by averaging the mean motions at the start and the end of this period. Mean motions will thus be obtained by the following formula:

$$\bar{V} = \sqrt{\bar{u}^2 + \bar{v}^2} \text{ and } \bar{D} = \arctg \frac{\bar{v}}{\bar{u}}$$

where  $\bar{u} = \alpha(dt) \cdot u(t_0 - dt) + \beta(dt) \cdot u(t_0)$

$\bar{v} = \alpha(dt) \cdot v(t_0 - dt) + \beta(dt) \cdot v(t_0)$  and

$u(t) = V(t) \cdot \cos(D(t))$ ,  $v(t) = V(t) \cdot \sin(D(t))$ .

Table 6.17 gives the values of the coefficients  $\alpha(dt)$  and  $\beta(dt)$  for different time periods.

Table 6.17  
Values of coefficients  $\alpha(dt)$  and  $\beta(dt)$  for different time periods

$dt$	$\alpha(dt)$	$\beta(dt)$
3 hours	0.0	1.0
6 hours	0.25	0.75
9 hours	0.34	0.66
12 hours	0.37	0.63

The conversion of the coded values DS and VS in ship and buoy reports to  $D(t)$  and  $V(t)$  can be done with the help of Table 6.18.

Table 6.18  
Conversion of the coded values DS and VS in ship or buoy reports to  $D(t)$  and  $V(t)$

<i>(a)</i>			<i>(b)</i>		
<i>VS</i>	<i>Interval (knots)</i>	<i>V(t)</i>	<i>DS</i>	<i>Course</i>	<i>D(t)</i>
0	No motion	0	0	No motion	0
1	1–5	3	1	NE	45
2	6–10	8	2	E	90
3	11–15	13	3	SE	135
4	16–20	18	4	S	180
5	21–25	23	5	SW	225
6	26–30	28	6	W	270
7	31–35	33	7	NW	315
8	36–40	38	8	N	360
9	40	43			

Upper limits of the allowed difference between the reported position (LAT, LON) and the estimated position (ELAT, ELON) at time  $t_0 - dt$  may be defined as:

$$\begin{aligned} \text{LATMAX} &= 0.2 + 0.05 \cdot dt - 0.007 \cdot V \cdot dt \\ \text{LONMAX} &= 0.2 + (0.05 \cdot dt - 0.007 \cdot V \cdot dt) \\ &\quad / \cos(\text{LAT}(t_0)) \end{aligned}$$

where the accuracy of the reported parameters has been taken into account.

Both the position and the mean course and speed at times  $t_0$  and  $(t_0 - dt)$  should be considered suspect if:

$$\begin{aligned} |\text{LAT}(t_0 - dt) - \text{ELAT}(t_0 - dt)| &> \text{LATMAX} \text{ or} \\ |\text{LON}(t_0 - dt) - \text{ELON}(t_0 - dt)| &> \text{LONMAX} \end{aligned}$$

For aircraft reports with unique identifiers, the position sequence can be checked by using a criterion which is inferred from the requirement that along the track the basic speed should vary within a given range. This check is rather coarse since the basic speed may vary considerably owing to wind or air traffic operations.

Another method of detecting errors in aircraft positions is the so-called predictor-corrector method. It can roughly be described in the following way. Look at two consecutive points  $i$  and  $j$  along the flight track which have already been checked and found correct. In view of the continuity of the basic speed, the next observation point,  $k$ , should be found within a ring bounded by circles around the point  $j$  with the radii  $r_1$  and  $r_2$ .

The expressions for the radii are:

$$\begin{aligned} r_1 &= \frac{t(k) - t(j)}{t(j) - t(i)} (1 - \delta) d(i, j) \text{ and} \\ r_2 &= \frac{t(k) - t(j)}{t(j) - t(i)} (1 + \delta) d(i, j) \end{aligned}$$

where  $d(i, j)$  denotes the arc distance between points  $i$  and  $j$ ,  $t(i)$ ,  $t(j)$  and  $t(k)$  denote the times, and  $\delta$  is the appropriate constant ( $\delta = 0.2$ ). When point  $k$  is not found within the ring something may be wrong either in the position or in the time. In case of course changes the method must be refined.

#### 6.3.3.4 CHECK AGAINST NUMERICAL FORECASTS

In modern data assimilation systems where good first guess forecasts are available, comparison with forecasts, valid at the time of the observation, constitutes a powerful technique for checking observations. There are several ways of doing a first guess check. The one described below is used at ECMWF and is fairly typical.

The observed data, usually height, temperature, wind or surface pressure, denoted by the symbol  $A^o$ , are transformed into deviations from the first guess field,  $A^p$ , interpolated to the point of observation. The deviation is then normalized by an estimated accuracy of the first guess forecast itself,  $E^p$ :

$$\delta^o = (A^o - A^p)/E^p$$

This is necessary, since the first guess forecast may be less accurate in data-sparse areas, such as oceans, and observations should not be deemed bad because they do not agree with an uncertain forecast. Each observation also has its own estimated error,  $E^o$ , which is normalized in the same way:

$$\varepsilon^o = E^o/E^p$$

The observed deviations may now be compared with a predetermined multiple, ERRLIM, of its estimated variance. Thus, if  $\delta^o 2 > (1 + \varepsilon^o 2)^* \text{ERRLIM}^2$  the observation is considered suspect.

Wind components should be checked together. If:

$$\frac{1}{2}(\delta_u^o)^2 + \delta_v^o > (1 + \frac{1}{2}(\varepsilon_u^o)^2 + \varepsilon_v^o)^2 \cdot ERRLIM^2$$

both wind components should be considered suspect.

It may be advantageous to classify the magnitude of the deviation by using a sequence of error limits,  $ERRLIM_j$ . The observed value is then appended by a quality flag,  $j$ , determined in the following way. If

$$\delta^o > (1 + \varepsilon^o)^2 \cdot ERRLIM_j$$

the flag is set to  $j$ . The observations can then be treated differently in the continued processing depending on their quality flags. Table 6.19 is an example of such a flagging system.

Table 6.19  
Example of a flagging system

<i>Flag</i> $j$	<i>ERRLIM</i> $_j$	<i>Observation quality</i>
1		"Correct"
2	4	"Probably correct"
3	6	"Probably erroneous"
4	8	"Erroneous"

### 6.3.4 Space/time consistency check

The methods used for ascertaining the space/time consistency of the observations are usually the same as those used for the objective analysis itself (section 3.3). This may either be done as a separate step or may be integrated into the objective analysis. In either case, the same statistical interpolation procedures are used both for the space/time consistency checks and the actual analysis.

Indeed it may be most satisfactory to incorporate these checks into the objective analysis scheme. This has the added advantage that improvements made to the objective analysis scheme will automatically result in improvements in the quality control procedures. The advantages of using the statistical interpolation technique for quality control are the same as those obtained in using it in objective analysis. In particular, the distribution of observations in relation to the statistical structure of the variable being checked is taken into account. The disadvantage is that it is necessary to specify carefully a number of statistical parameters related to observational errors and the structure of the meteorological variable concerned. Details of the multivariate statistical interpolation method are described by Lorenc (1981).

#### 6.3.4.1 SPACE CONSISTENCY OR NEIGHBOUR TEST

Redundant information in nearby observations can be used to compare the observations using the statistical methods of the objective analysis scheme. Each pair of neighbouring observations is compared. If they agree, they are both likely to be either correct or erroneous. If they disagree, one of them is likely to be correct, the other to be erroneous.

By intercomparison of all neighbouring pairs in a local area, it is possible to filter out the erroneous ones. One method of selection is to employ the flagging system described in section 6.3.3.4. This is essentially the method employed at the ECMWF.

The check is again performed on the normalized deviations from the first guess prediction at observation  $i$ :

$$\delta_i^o = (A_i^o - A_i^p)/E_i^p$$

and a similar deviation  $\delta_j^o$  at observation  $j$ .

It may be shown that the estimated variance of the difference between two such deviations,  $\delta_i^o$  and  $\delta_j^o$ , depends both on the observation errors and the spatial and temporal correlation of the prediction error. The two observations can be deemed to disagree if they do not pass a criterion of the following type:

$$(\delta_i^o - \delta_j^o)^2 > LIM^* (\varepsilon_i^o)^2 + (\varepsilon_j^o)^2 + r_{ij}^2/b^2 + t_{ij}^2/c^2$$

In this expression,  $LIM$  is an acceptance limit,  $\varepsilon_i^o$  and  $\varepsilon_j^o$  are the normalized observation errors, which are assumed to be uncorrelated,  $r_{ij}$  and  $t_{ij}$  are the spatial and temporal separations between  $i$  and  $j$ , respectively, and  $b$  and  $c$  are estimated space and time-scales of the prediction error correlation. If a pair of observations fails the test, a special flag attached to each observed datum is increased by one for both observations. If the observations pass the test, and have a flag value greater than one, the flag is reduced by one unit.

#### 6.3.4.2 COMPARISON WITH ANALYSIS

In statistical interpolation methods it is possible to interpolate, or analyse, all observations in a local area to the position of a certain observation that is to be checked. In the interpolation procedure, this particular observation is excluded. The preliminary interpolated value should then be a good approximation of the

observation. If it is not, the observation is most likely to be erroneous and should not be used for the final interpolation to the grid points of the analysis field. The checking criterion is:

$$(\delta_i^o - \delta_i^j)^2 / \epsilon_i^2 > ALIM^2$$

where  $\delta_i^o$  is the deviation of the observation from the first guess,  $\delta_i^j$  is the deviation of the preliminary interpolated value at  $i$  from the first guess, and  $\epsilon_i$  is the interpolation error, which is determined from the optimum interpolation procedure.

An observed value is deemed to have failed the check if it does not pass the criterion. If more than one observed value fails in a local area, the worst failure is excluded and all other failures are retested. This procedure can be repeated until all doubtful data have been excluded from the final interpolation.

#### 6.4 Flagging and design of computer programs

In a checking system, it is necessary to take care of all information from the different quality control techniques. The manual or automatic decisions made in the different checking procedures can be expressed by quality control indicators, or flags, which characterize the status of the individual system. The construction depends very much on how and at what stage in the GDPS procedures the different checking methods are applied.

##### 6.4.1 Example of a flagging system

An example of a flagging system that can be used in the checking of meteorological data is described below.

For each observed parameter in the various types of data records, a number of quality control algorithms can be applied. The results of these quality control algorithms are then given by a number of quality control flags. Each parameter is associated with a number of quality control flags stored in a temporary quality control vector. For the user of the data it is, however, inconvenient to inspect several quality control flags before making a decision on whether to use a certain observed value or not. Therefore, the content of the temporary quality control vector should be summarized into a final quality control flag to be retained in the archived data record. The temporary quality control vector should be retained until all quality control processing has been finalized for a certain dataset. Table 6.20 gives the standard of quality control indicators which can be used.

Table 6.20  
Quality control indicators which can be used in a man/machine mixed control system

<i>Quality control indicator</i>	<i>Description</i>
0	The parameter is not expected to be observed.
1	Quality control has not been made.
2	Observed value was found correct during quality control.
3	Observed value was found correct by manual inspection; computerized method indicated suspect/erroneous value.
4	Observed value was found suspect during quality control.
5	Observed value was found erroneous during quality control.
6	Observed value was found suspect during quality control, and the most likely value, estimated by a computerized method, was entered.
7	Observed value was found erroneous during quality control, and the most likely value, estimated by a computerized method, was entered.
8	Observed value was found suspect during quality control, and the most likely value, estimated by a manual method, was entered.
9	Observed value was found erroneous during quality control, and the most likely value, estimated by a manual method, was entered.
10	Observed value was missing, and the most likely value, estimated by a computerized method, was entered.
11	Observed value was missing, and the most likely value, estimated by a manual method, was entered.

##### 6.4.2 Design of computer programs

The computer programs used in an automatic system can be of three main types:

- (a) Programs for the preliminary checking of data (such as check against physical and climatological limits, internal-consistency checks, and time-consistency checks);
- (b) Programs for space/time consistency checks and combined quality control;
- (c) Programs for support to manual intervention in the quality control process.

A full set of these programs should provide a very efficient checking system, but even with programs from the first type a very good standard of quality control is achieved.

The computer program design for the preliminary check is a rather straightforward task, since the checking algorithms are simple and since the need for reference information is small. It is, however, advisable to program all checking subroutines in small independent modules, which can be used easily in any programmed system of quality control.

The space/time consistency check of data is a more laborious task from a computer programming point of view. The total amount of data involved is large and all data cannot be kept simultaneously in the computer memory. Therefore, it is necessary to structure the computations and the input/output flow of data carefully in order to ensure that the calculations are carried out efficiently. Furthermore, the search for influencing information during the space/time interpolation requires a careful housekeeping of reference information. This type of checking is normally integrated into an objective analysis system, for instance in statistical interpolation. It is important to feed quality control results within such programs into the observation database, so as to be included in a final quality flag.

## 6.5 Combined quality control

A part of the system of combined quality control can comprise the procedure for summarizing the content of the temporary quality control vectors into the final quality control flag.

The general objective of a system of combined quality control is to obtain a more reliable quality control result by simultaneously applying several checking methods and algorithms. Besides summarizing the result of the temporary quality control vectors, systems for combined quality control may include:

- (a) Selection of alternative quality control algorithms on the basis of the results of some previous quality control algorithms;
- (b) Repeated application of quality control algorithms with alternative corrections to some observed parameters.

The design of systems and methods for combined quality control is a laborious task. It is necessary to analyse carefully the nature and likelihood of various types of errors together with the possibilities for various types of checking algorithms to detect such errors. It is often useful to construct two-dimensional tables with entries corresponding to the reaction of each selected quality control method to each type of error. The following principles should be applied when determining the final quality control flag to be assigned to the various elements of an observation:

- (a) If all the elements stored in the temporary quality control vectors indicate that the observed value is correct, then the value of the final quality control flag should correspond to "correct";
- (b) If one or several elements stored in the temporary quality control vectors indicate that the observed value is suspect, but the rest of the elements indicate that the value is correct, then the final quality control flag should correspond to "suspect";
- (c) If at least one element stored in the temporary quality-control vector indicates that the value is erroneous, then the value of the final quality control flag should be shown as "erroneous";
- (d) If one element of an observation is found to be clearly erroneous, algorithms for previous internal consistency checks should be re-applied in order to eliminate the large number of "suspect" flags in the surrounding elements due to an error in the reference information.

## REFERENCES

- Belousov, S. L., L. S. Gandin and S. A. Mashkovich, 1971: *Computer Processing of Meteorological Data*. Israel Program for Scientific Translations, Jerusalem.
- Bergman, K. H., 1979: Multivariate analysis of temperatures and winds using optimum interpolation. *Monthly Weather Review*, 107, pp. 1423–1444.
- De Jong, H. M., 1976: *Study on the system mix of radiosonde aircraft and satellite observations in the North Atlantic region. Observational characteristics and data processing*. Scientific Report W.R. 76-5, Koninklijk Nederlands Meteorologisch Instituut.
- Gandin, L. S., 1963: *Objective Analysis of Meteorological Fields*. Israel Program for Scientific Translations, Jerusalem.
- Gustafsson, N., 1981: A review of methods for objective analysis. In: *Dynamic Meteorology Data Assimilation Methods. Applied Mathematical Sciences*, Vol. 36, Springer Verlag, 1981, New York, pp. 17–76.
- Hinkelmann, K. H., 1969: Automatic data processing of synoptic and upper-air reports. *Lectures on Numerical Short-range Weather Prediction*, WMO Regional Training Seminar, Moscow, 17 November–14 December 1965, WMO/TP 297, pp. 542–612.
- Lorenc, A. C., 1981: A global three-dimensional multivariate statistical interpolation scheme. *Monthly Weather Review*, 109, pp. 701–721.
- Parfiniewicz, J., 1981: On the complex control method. In: Nowcasting: Mesoscale observations and short-range prediction. *Proceedings of an international IAMAP symposium*, 25–28 August 1981, Hamburg, pp. 109–110.
- Rudolf, B., 1993: Management and analysis of precipitation data on a routine basis. *Proceedings of the International Symposium on Precipitation and Evaporation* (B. Sevruk and M. Lapin, eds.), ETH Zurich, Volume 1, pp. 69–76.
- Rudolf, B., H. Hauschild, W. Rueth and U. Schnieder, 1994: Terrestrial precipitation analysis: operational method and required density of point measurements. NATO ASI I/26, *Global Precipitations and Climate Change* (M. Desbois and F. Desalmand, eds.), Springer Verlag Berlin, pp. 173–186.

(

(

(

(

## CHAPTER 7

### NON-REAL-TIME FUNCTIONS OF WMCs, RSMCs AND NMCs

#### 7.1 Major non-real-time functions of WMCs, RSMCs and NMCs

The non-real-time functions of WMCs, RSMCs and NMCs are given in Volume I of the *Manual on the Global Data-processing System* (WMO-No. 485) which is Annex IV to the WMO Technical Regulations.

#### 7.2 Collection, quality control, storage and retrieval of data in the GDPS

##### 7.2.1 Collection of data to be stored

Data for non-real-time use may be collected via the GTS or by any other means which are appropriate.

##### 7.2.2 Quality control of data to be stored

The purpose of non-real-time quality control is to ensure the highest possible standard of basic meteorological data, as well as for climatological, hydrological and other purposes, before they are stored and subsequently delivered to users.

The non-real-time quality control should be applied to all basic observational data, even those having been subjected to real-time quality control in connection with the distribution of the data over the Global Telecommunication System. The primary responsibility for non-real-time quality control rests with the centres which store the data (see Volume I, Attachment III.2 to the *Manual on the GDPS*). The control should be performed on a routine basis and begin as soon as possible after the data to be stored have been received at the data centre. Minimum standards of non-real-time quality control are being developed and will be given in Volume I, Attachment II.1 to the *Manual on the GDPS*.

Methods for detecting errors in data being stored by WMCs, RSMCs and NMCs may involve:

- (a) Testing the identification elements of all reports (e.g. testing marine reports to ensure that they are not landlocked);
- (b) Testing the various parameters against upper and lower limits in order to delete obviously erroneous data at an early stage;
- (c) Testing the various parameters against statistically-determined limits which are normally functions of geographical position and time of the year, and in some cases, also depend on the values of other elements;
- (d) Checking the *physical* consistency between different elements in the same observation (e.g. that high relative humidity is observed in connection with such weather phenomena as rain, snow, sleet, fog, dense mist and drizzle);
- (e) Testing the *horizontal* consistency by comparison with simultaneous observations at adjacent stations or analysed fields;
- (f) Testing the *vertical* consistency (e.g. hydrostatic control) of certain upper-air and oceanographic data;
- (g) Testing the *time* consistency using both preceding and subsequent observations from the same stations.

Examples associated with the various methods of detection can be found in Chapter 6. When detected by quality control procedures, meaningless data should be eliminated and erroneous data should be corrected and marked, as appropriate.

It is desirable for all WWW centres to use the methods indicated above when performing non-real-time quality control. However, it is recognized that all centres may not be able to carry out the complete programme. Therefore, when data are exchanged internationally, information regarding the quality control procedures used should accompany the exchanged data.

#### 7.3 Data to be stored at each level of the GDPS

Types of material designed for storage at WMCs, RSMCs and NMCs are given in Volume I of the *Manual on the GDPS*.

#### 7.4 Media and formats for storage and exchange

Information on media and formats for storage and exchange of data are found in Volume I of the *Manual on the GDPS*.

#### 7.5 Classification, cataloguing and exchange of data

Procedures for classification, cataloguing and exchange of stored data are found in Volume I of the *Manual on the GDPS*.

(

(

(

(

## CHAPTER 8

### **EXCHANGE OF PERSONNEL ENGAGED IN DATA-PROCESSING ACTIVITIES**

The exchange of personnel engaged in data-processing activities can take many forms, for example:

- (a) The exchange of experts by bilateral agreement between two countries to discuss new technical or operational developments:
  - (i) In automatic processing of raw meteorological data;
  - (ii) In analysis and forecasting by manual or computer techniques; or
  - (iii) To train new computer personnel and meteorologists in NWP techniques;
- (b) The provision of expert assistance to the national Meteorological Service of a country through the Voluntary Assistance Programme;
- (c) The holding of symposia or workshops among several Member countries on techniques used in meteorology and on meteorological data processing to acquaint meteorologists in one country with the techniques being tested and applied in another country or countries. These symposia should be concerned with a wide range of methods for automatic data processing so that Members can exchange detailed knowledge on the most relevant and latest methods in using computer technology in an operational forecast system.

Such exchange programmes should first of all aim at assisting Members in developing or improving automatic data-processing procedures at their meteorological centres. In addition, the programmes should aim at facilitating exchange of knowledge in operational data processing between Members, thus avoiding duplication of effort.

---